

# **Birla Central Library**

**BILANI (Rajasthan)**

**Class No: 621.353**

**Book No Z 991 P**

**Accession No: 37506**

Acc. No. ....

**ISSUE LABEL**

**Not later than the latest date stamped below.**

--	--	--





**PHOTOELECTRICITY  
AND ITS APPLICATION**

**BOOKS BY V. K. ZWORYKIN  
AND COLLABORATORS**

**PHOTOELECTRICITY AND ITS APPLICATION**

By V. K. Zworykin and E. G. Ramberg

**ELECTRON OPTICS AND THE ELECTRON MICROSCOPE**

By V. K. Zworykin, G. A. Morton, E. G. Ramberg,  
J. Hillier, and A. W. Vance

**TELEVISION: THE ELECTRONICS OF IMAGE TRANSMISSION**

By V. K. Zworykin and G. A. Morton

# PHOTOELECTRICITY AND ITS APPLICATION

BY

V. K. ZWORYKIN, E.E., Ph.D.

*Director of Electronic Research  
Vice President and Technical Consultant  
Radio Corporation of America*

AND


E. G. RAMBERG, Ph.D.

*Research Physicist  
R.C.A. Laboratories Division, Princeton, N. J.*

NEW YORK

JOHN WILEY & SONS, INC.

LONDON · CHAPMAN & HALL, LIMITED

COPYRIGHT, 1930, 1932, 1934  
BY  
VLADIMIR KOSMA ZWORYKIN  
AND  
EARL DEWITT WILSON  
under the title  
*Photocells and Their Application* 

---

COPYRIGHT, 1949  
BY  
JOHN WILEY & SONS, INC.

---

*All Rights Reserved*

*This book or any part thereof must not  
be reproduced in any form without  
the written permission of the publisher.*

SECOND PRINTING, JULY, 1950

PRINTED IN THE UNITED STATES OF AMERICA

## PREFACE

At the time of the appearance, in 1934, of the second edition of *Photocells and Their Application*, by Zworykin and Wilson, the antimonycesium phototube was unknown, the high-gain secondary-emission multiplier and the image tube were yet to be developed, and electronic television was in its infancy. This statement epitomizes the gap that had to be filled when we were approached to prepare a revision of the book. It soon became apparent that a completely new treatment was required, sharing with *Photocells and Their Application* little more than its aim and the general arrangement of the material.

The purpose of this book, as of the older book, is to familiarize the reader with the properties, preparation, and use of photoelectric devices. The emphasis is, throughout, on the practical aspects of the subject. Theory is presented largely for its mnemonic value. Mathematical developments are restricted to footnotes so as not to interrupt the reader's train of thought.

The book is divided into two roughly equal parts. The first eleven chapters deal with the principles and the preparation of photosensitive devices, the remainder of the book with their application. A brief account of earlier developments in the field of photoelectricity is followed by a discussion of light sources and the basic principles of the photoemissive effect. Compound photocathodes are treated largely from the point of view familiarized by de Boer and his coworkers. Modern materials and techniques for preparing phototubes receive detailed attention. The chapters on vacuum phototubes, gas-filled phototubes, multiplier phototubes, and image tubes present, along with the operating characteristics of these devices, the fundamentals of gas amplification, secondary electron emission, and electron optics. The succeeding chapters on photoconductive cells and photovoltaic cells, finally, collect recent findings in these important branches of the field of photoelectricity.

The portion of the book dealing with the application of photoelectric devices begins with a detailed discussion of circuits suitable for the amplification of photocurrents and the actuation of relays. The ultimate limits in the measurement of small photocurrents are examined, and the preeminent position of the multiplier phototube in this field is pointed out. The great value of this relatively new scientific tool becomes once

more evident in the chapter on photoelectric measuring devices which indicates a wide range of application of phototubes, barrier layer cells, and photomultipliers. Motion picture sound, facsimile, television, and infrared detection techniques receive individual attention as direct outgrowths of the photoelectric art. Finally, manifold uses of the phototube, particularly as a control organ, are gathered together under the heading "Miscellaneous Applications." The book closes with a brief discussion of the range available for future improvements in the photoelectric field. Tables of constants in MKS units—the system employed throughout the book—and of conversion factors are added for the convenience of the diligent reader; the copious references at the end of each chapter serve the same purpose.

We hope that this book may help to broaden the appreciation of the field of photoelectricity and prove a useful tool in the hands of student and engineer. If it does, much credit is due our colleagues in the RCA organization who liberally contributed their suggestions and criticisms. We also wish to acknowledge our indebtedness to the many generous contributors of illustrative material. The work of Earl DeWitt Wilson in the older *Photocells and Their Application* lives on in this book, even though he did not share directly in its preparation.

Figures 3.2, 3.5, 3.17, 3.18, 8.9, and 9.9 of this book are based on figures appearing in two German periodicals, *Zeitschrift für Physik* (1928, 1929, 1935, 1936, 1938), published by Julius Springer, of Berlin, and *Zeitschrift für technische Physik* (1936), published by Johann Ambrosius Barth, of Leipzig. The German interests in the U. S. Copyright in these periodicals were vested in 1946 by the Alien Property Custodian. The use of this material in this book is by permission of the Attorney General of the United States in the public interest under License No. JA-1351.

V. K. ZWORYKIN  
E. G. RAMBERG

*Princeton, N. J.*  
*January, 1949*

# CONTENTS

## CHAPTER

### 1. HISTORICAL INTRODUCTION

The Photovoltaic Effect . . . . .	1
The Photoconductive Effect . . . . .	2
The Photoemissive Effect . . . . .	3
Hertz's Discovery . . . . .	3
Further Studies of the Photoelectric Process . . . . .	4
The First Alkali Phototubes . . . . .	5
The Photoelectric Carrier . . . . .	6
Empirical Laws . . . . .	7
The First Practical Phototubes . . . . .	8
References . . . . .	9

### 2. GENERAL THEORY

#### I. Radiant Energy

Spectrum of Radiant Energy . . . . .	10
Sources of Radiant Energy . . . . .	13
Black-Body Radiation . . . . .	14
Thermal Sources . . . . .	17
Gaseous Sources . . . . .	20
Luminescent Sources . . . . .	22
Photometric Measurements . . . . .	23

#### II. Photoemissive Effect

Einstein's Equation . . . . .	25
Structure of Matter . . . . .	30
Color Sensitivity . . . . .	32
References . . . . .	34

### 3. PHOTSENSITIVE SURFACES

Alkali Films on a Metal Base . . . . .	37
The Effect of Adsorbed Oxygen . . . . .	43
Potassium Hydride Phototubes . . . . .	44
Photocathodes with Intermediate Oxide Layers; the Silver-Cesium Oxide-Cesium Phototube . . . . .	46
Photocathodes with Electronegative Components Other than Oxygen . . . . .	55
"Alloy Surfaces" . . . . .	55
References . . . . .	60

### 4. MATERIALS AND APPARATUS FOR MAKING PHOTOTUBES

Choice of Glass . . . . .	62
Glass-to-Metal Seals . . . . .	63
Pre-treatment of Metals . . . . .	66



## CHAPTER

Vacuum Pumps . . . . .	67
Production of High Vacuum . . . . .	71
Techniques for Metal Tubes . . . . .	73
Measurement of Low Pressures . . . . .	74
Gases Used in Phototubes . . . . .	79
Gas Dosage . . . . .	80
The Alkali Metals . . . . .	82
References . . . . .	83
5. GENERAL METHODS OF PREPARING PHOTOTUBES	
Geometrical Arrangement of Phototubes . . . . .	85
Electric Leakage . . . . .	87
Introduction of Active Metals . . . . .	88
Sensitizing with Hydrogen . . . . .	92
Preparation of the Silver-Cesium Oxide-Cesium Phototube . . . . .	93
Preparation of the Antimony-Cesium Phototube . . . . .	96
Preparation of Phototubes for the Ultraviolet . . . . .	99
References . . . . .	102
6. THE VACUUM PHOTOTUBE	
Propagation of Photoelectrons in Vacuum . . . . .	103
The Effect of Electrostatic and Magnetic Fields . . . . .	105
Current-Voltage Relation . . . . .	108
Current-Light Flux Relations . . . . .	112
Dynamic Characteristics . . . . .	113
Spectral Response Curves and Sensitivity Standards . . . . .	114
Properties of Commercial Vacuum Phototubes . . . . .	116
Vacuum Phototubes for the Ultraviolet . . . . .	118
References . . . . .	119
7. THE GAS-FILLED PHOTOTUBE	
Kinetic Theory of Gases . . . . .	120
Mean Free Path . . . . .	121
Ionization in Gases . . . . .	122
Limitation of Gas Amplification . . . . .	124
Current-Voltage Curves . . . . .	125
Current-Light Characteristics . . . . .	126
Dynamic Characteristics . . . . .	127
Properties of Standard Gas-Filled Phototubes . . . . .	132
References . . . . .	135
8. THE MULTIPLIER PHOTOTUBE	
Secondary Electron Emission . . . . .	136
Preparation of Secondary-Emissive Surfaces . . . . .	140
Magnetic Secondary-Emission Multiplier . . . . .	142
Electrostatic Secondary-Emission Multiplier . . . . .	144
Dark Currents . . . . .	148
Dynamic Secondary-Emission Multiplier . . . . .	150

# CONTENTS

ix

## CHAPTER

Standard Types of Multiplier Phototubes . . . . .	152
References . . . . .	154
<b>9. THE IMAGE TUBE</b>	
Accelerating-Field Tube . . . . .	155
Electron Optics . . . . .	156
Electrostatic Lenses . . . . .	157
Magnetic Lenses . . . . .	162
Image Tubes Employing Long Magnetic Focusing Fields . . . . .	164
Image Tubes Employing Short Lenses . . . . .	166
Image Tubes Employing Cylindrical Fields . . . . .	172
References . . . . .	174
<b>10. PHOTOCONDUCTIVE CELLS</b>	
The Element Selenium . . . . .	175
The Selenium Cell . . . . .	176
Mechanism of Conduction . . . . .	177
Photoconductivity . . . . .	180
Properties of Selenium Photoconductive Cells . . . . .	181
The Thallous Sulfide or "Thalofide" Cell . . . . .	184
The Lead Sulfide Cell . . . . .	189
The Silicon Cell . . . . .	191
Photoconductive Effect in Cadmium Sulfide . . . . .	193
References . . . . .	195
<b>11. PHOTOVOLTAIC CELLS</b>	
Wet Photovoltaic Cells . . . . .	196
The Cuprous Oxide Barrier-Layer Cell . . . . .	197
Origin of Photocurrent . . . . .	199
The Selenium Barrier-Layer Cell . . . . .	201
Power Conversion by Barrier-Layer Cells . . . . .	209
Dynamic Response; Fatigue and Temperature Effects . . . . .	211
Commercial Selenium Barrier-Layer Cells . . . . .	214
References . . . . .	214
<b>12. PHOTOCELL CIRCUITS AND AMPLIFICATION</b>	
Basic Circuits for Light Measurements . . . . .	216
The Operation of Relays by Photocells . . . . .	219
The Need for Amplification . . . . .	220
Thermionic Vacuum Tubes and Their Operation . . . . .	220
Direct-Current Amplifying Circuits for Phototubes; Inverse Feedback . . . . .	227
Vacuum-Tube Circuits for Photovoltaic and Photoconductive Cells . . . . .	231
Relay Circuits; the Thyatron . . . . .	233
Alternating Currents . . . . .	236
Wide-Band Alternating-Current Amplifiers . . . . .	239
Periodically Interrupted Signals; Narrow-Band Alternating-Current Amplification . . . . .	242
Voltage and Current Regulation . . . . .	246
References . . . . .	249

## CHAPTER

## 13. THE MEASUREMENT OF SMALL PHOTOCURRENTS

Shot Noise . . . . .	250
Thermal Noise . . . . .	252
Noise Sources in Thermionic Amplifiers . . . . .	252
Electrometers and Electrometer Tubes . . . . .	253
Noise Reduction by Secondary-Emission Amplification . . . . .	258
Multiplier Phototube Circuits . . . . .	259
Measurement of Very Low Light Levels with a Multiplier Phototube . . . . .	261
Gas-Discharge Counters . . . . .	263
Noise in Photoconductive Cells . . . . .	265
References . . . . .	268

## 14. PHOTOELECTRIC MEASURING DEVICES

Phototube and Barrier-Layer Cell in Photometry . . . . .	269
Measurement of Light Sources and Illumination . . . . .	270
Reflectometers, Fluorometers, and Refractometers . . . . .	277
Colorimetry and Pyrometry . . . . .	283
The Measurement of Photographic Exposure . . . . .	292
Photoelectric Spectrophotometry . . . . .	297
Spectrochemical Analysis . . . . .	306
The Measurement of Corpuscular Radiations and X-Rays by Photocells . . . . .	313
References . . . . .	319

## 15. PHOTOTUBES IN SOUND REPRODUCTION

The Recording of Sound on Film . . . . .	323
Phototube Monitoring of Sound Recorders . . . . .	327
Rerecording . . . . .	329
The Sound Track on the Projected Film . . . . .	331
Sound-Reproduction Equipment: Requirements . . . . .	333
The Optical System of the Reproducer . . . . .	334
Complete Sound-Reproducer Systems . . . . .	338
Sound Reproduction from Dye Tracks . . . . .	342
Photoconductive Cells in Sound Reproduction . . . . .	347
References . . . . .	347

## 16. PHOTOTUBES IN PICTURE TRANSMISSION

The Scanning Principle . . . . .	349
Facsimile Scanners . . . . .	352
The Transmission System . . . . .	354
Facsimile Recorders . . . . .	357
Facsimile Synchronization . . . . .	361
Tape Facsimile . . . . .	362
Copying by Facsimile . . . . .	363
Facsimile of Color Pictures . . . . .	363
The Requirements of Television . . . . .	365
Mechanical Television Systems . . . . .	366
Electronic Flying-Spot Scanning . . . . .	369
Electronic Viewing Tubes or Kinescopes . . . . .	375
Color Transmission System for Slides and Film . . . . .	377

CHAPTER

Ultrafax . . . . .	378
Flying-Spot Microscope . . . . .	381
References . . . . .	383
17. PHOTOSENSITIVE CAMERA TUBES IN TELEVISION	
The Image Dissector . . . . .	385
The Iconoscope . . . . .	386
The Image Iconoscope . . . . .	390
The Orthicon . . . . .	391
The Image Orthicon . . . . .	393
Television Pickup Cameras . . . . .	398
The Complete Electronic Television System . . . . .	400
Special Applications of Television Equipment . . . . .	403
References . . . . .	405
18. LIGHT BEAM SIGNALING AND INFRARED DETECTION	
Infrared Transmission of the Atmosphere . . . . .	407
Infrared Light Sources . . . . .	408
Detection of Code and Voice Signals Transmitted on an Infrared Beam . . . . .	412
The Detection of Hot Bodies . . . . .	414
Infrared-Sensitive Image Tube . . . . .	415
Attempts at Extending the Wave-Length Range of Infrared Viewing Devices . . . . .	418
Photovision . . . . .	419
References . . . . .	420
19. MISCELLANEOUS APPLICATIONS OF PHOTOELECTRICITY	
Illumination Control . . . . .	421
Light Relays . . . . .	424
Traffic Control . . . . .	427
Photoelectric Safety Devices . . . . .	429
Photoelectric Controls for Industrial Processes . . . . .	434
Automatic Inspection . . . . .	441
Photoelectric Gages . . . . .	443
Phototubes in Astronomy . . . . .	450
Photoelectric Organ . . . . .	455
Photoelectric Aids for the Blind . . . . .	456
References . . . . .	461
20. PHOTOCELLS IN THE FUTURE	
Retrospect . . . . .	464
Scope for Future Advances . . . . .	465
Ultimate Limits in the Enhancement of Vision . . . . .	466
Compact Photocells of High Output . . . . .	469
Conversion of Solar Energy into Electric Power . . . . .	469
New Materials for Phototubes . . . . .	470
References . . . . .	471

## APPENDIX

The Chemical Elements by Atomic Number . . . . .	473
Periodic Table of the Elements . . . . .	474
Units and Conversion Factors . . . . .	474
Physical Constants in MKS Units . . . . .	477
Relative Luminosity Factors . . . . .	478
AUTHOR INDEX . . . . .	479
SUBJECT INDEX . . . . .	485

## Chapter 1

# HISTORICAL INTRODUCTION

The energy which sustains life on the earth is radiant energy. The sun not only provides us with necessary warmth, but, in addition, stores up energy, through the chemical action of light, in plant life for our use as food and fuel and, through the evaporation of surface water, in rivers and lakes as a source of power. Beyond this, light, by making vision possible, is the most effective means of acquainting us with our environment. It is hence obvious that the objective measurement and detection of light are of great importance. The phenomenon of photoelectricity has provided us with means for accomplishing them which exceed in sensitivity and speed of response any others known at the present time.

More precisely, the science of photoelectricity deals with the effect of light on electrical phenomena. The three most important manifestations of this effect are (1) the generation of an electromotive force between two electrodes when either of them or the intervening medium is illuminated, (2) the reduction of the electrical resistance of materials by illumination, and (3) the emission of charged particles (electrons) from illuminated surfaces. These phenomena are commonly designated as the *photovoltaic*, the *photoconductive*, and the *photoemissive effect*, respectively.

**The Photovoltaic Effect.** Edmond Becquerel<sup>1</sup> appears to have been the first person to observe the action of light in generating an electric current or voltage. In his experiments, carried out as early as 1839, a pair of electrodes was immersed in a liquid electrolyte, or two layers of electrolytes, such as ferric chloride solution and alcohol, capable of reacting with each other. The current generated when the cell was illuminated with sunlight was measured by a galvanometer connected between the two electrodes. Becquerel eliminated the possibility that the observed currents might be the result of the differential heating of the two electrodes by observing the effect of color filters placed in the

<sup>1</sup> See reference 1.

path of the illuminating beam. It was then found that the electrical effect of the light did not in any way parallel its heating effect, as measured by a thermocouple. Blue light, of equal energy, proved far more effective as current generator than yellow or red light. Although the current of many cells became negligible after a relatively short exposure, this did not apply in every case. In particular, cells with platinum or gold electrodes coated with silver chloride and with water acidified with nitric acid as electrolyte exhibited steady currents over periods of about two hours. Becquerel suggested their use for the measurement of the actinic component of light—in effect, as photographic exposure meters.<sup>2</sup>

Becquerel's studies remained for a long time isolated observations. Much of the work of later authors, particularly in the first part of the twentieth century, added to the accumulation of experimental data without clarifying the fundamental processes involved. A certain degree of understanding of the photovoltaic effect—or, at least, of its most important manifestations—was eventually achieved after the dry photovoltaic cells, or barrier-layer cells, had attained great practical importance.<sup>3</sup>

**The Photoconductive Effect.** The discovery that selenium increases in conductivity upon illumination was made by Willoughby Smith <sup>4</sup> in 1873. Smith employed the selenium bars, 5 to 10 centimeters in length and 1 to 1.5 millimeters in diameter, hermetically sealed in glass tubes, as high resistances (1400 megohms) in testing and signaling at a shore station during the submersion of long submarine cables. It was found that the resistance of the bars dropped by 15 to 100 per cent when they were exposed to sunlight. Placing the rods in water to cool them did not diminish the effect of exposure, so that Smith correctly concluded that the reduction in resistance was an effect of the light rather than simply a thermal change in resistance.

Smith's discovery was immediately seized upon by numerous inventors and researchers who investigated the complex properties of selenium and, eventually, discovered similar properties in a number of other materials. For several decades the selenium photoconductive cell played a dominant role in the field of photoelectricity. It lost ground, however, to the photoemissive cells or *phototubes* and the new types of photovoltaic cells in the 1920's and 1930's. Photoconductive cells attained renewed importance, however (in particular as high-sensitivity infrared detectors), in the war years after 1940.<sup>5</sup>

<sup>2</sup> See Becquerel, reference 2.

<sup>3</sup> See Chapter 11.

<sup>4</sup> See reference 3.

<sup>5</sup> See Chapter 10.

**The Photoemissive Effect.** The photoemissive effect was the last to appear on the scene; yet it has contributed most to our understanding of the interaction of light and matter and has outstripped both the other photoelectric effects in the importance of its applications. It will, accordingly, form the subject matter of the remainder of this introductory discussion.

**Hertz's Discovery.** The photoemissive effect was discovered by Hertz in 1887, as a by-product of his classical researches on electric waves and oscillations.<sup>6</sup> Hertz employed the length of gap across which a spark would jump as a measure of the amplitude of electrical oscillations excited in a secondary circuit. He noted that this length was increased when the secondary gap was in line of sight of the spark across the gap in the primary, inducing, circuit. To investigate the phenomenon more closely, Hertz adopted the modified arrangement shown in Fig. 1.1.<sup>7</sup> The primary circuits of two Ruhmkorff coils *a* and *e* were placed in series with a battery *b* and an interrupter *c*. The first Ruhmkorff coil was provided with a fixed gap *d* in the secondary circuit, the second,

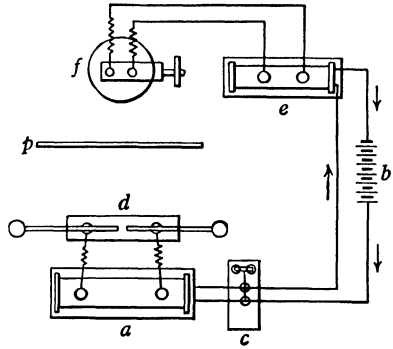


FIG. 1.1. Apparatus with Which Hertz Demonstrated the Existence of a Photoemissive Effect.

with a variable, micrometer, gap *f*. Hertz found that longer sparks could be obtained across *f* when it was exposed to the spark across *d* than when it was shielded from it. Placing the micrometer gap in an insulating or conducting box or simply placing a sheet of glass between the fixed gap and the micrometer gap reduced the length of spark across the latter. Hertz observed, however, that when the direct path between the two gaps was blocked and a mirror was provided to reflect radiation from the fixed gap to the micrometer gap, the spark length in the second gap was increased. These observations led Hertz to suspect that the ultraviolet component of the radiation from the main spark falling on the terminals of the micrometer gap was responsible for the phenomenon. He confirmed his suspicion by passing the light from the main spark through a quartz spectrometer and letting its output fall on the terminals of the micrometer spark gap. The spark length was increased when, and only when, the ultraviolet portion of the spectrum fell on

<sup>6</sup> See Hertz, reference 4.

<sup>7</sup> See Hertz, reference 5.



the terminals. Other sources of ultraviolet radiation, such as a magnesium flare, were found to have the same effect on the spark length. Hertz established, in addition, that the effect of the ultraviolet radiation was greatest when it was incident on the negative terminal of the gap, that a large sphere or plate terminal yielded a greater effect than a small pointed one, and that freshly polished surfaces responded more to the ultraviolet radiation than tarnished surfaces.

**Further Studies of the Photoelectric Process.** Hertz left to other researchers further investigation of the photoelectric effect which he had discovered. Wiedemann and Ebert <sup>8</sup> promptly confirmed his results and

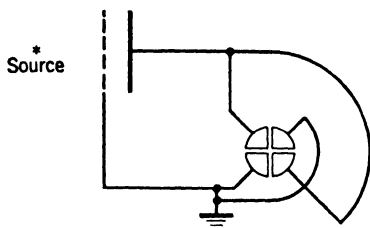


FIG. 1.2. Circuit Used by Righi to Measure the Charge Acquired by a Photosensitive Body

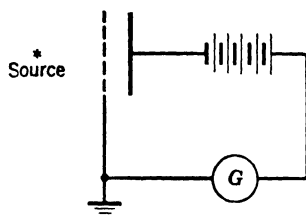


FIG. 1.3. Circuit Used by Stoletow to Measure Photoelectric Currents.

found that the ultraviolet radiation affected the discharge *only* when it was incident on the negative terminal. Wilhelm Hallwachs <sup>9</sup> simplified the experimental conditions for observing the effect so as to bring out clearly its principal physical properties. He connected a polished zinc sphere to a gold-leaf electroscope and observed these effects: When the sphere was charged negatively and then irradiated with ultraviolet radiation it lost its charge quickly; irradiation produced no effect when the sphere was charged positively; finally, a positively charged body, placed close to an irradiated negatively charged sphere, lost its charge. From these and additional, more detailed, observations, Hallwachs could conclude definitely that, *under the influence of ultraviolet radiation, negative electricity leaves a body and follows electrostatic lines of force in its passage*. This phenomenon came to be known as the *Hallwachs effect*.

Righi altered Hallwachs's arrangement by employing a coarse-mesh grid in front of a polished plate, thus illuminating the plate through the grid.<sup>10</sup> The plate was connected to one pair of quadrants of an electrometer; the grid to the other pair and to the ground (Fig. 1.2). Irradia-

<sup>8</sup> See reference 6.

<sup>9</sup> See reference 7.

<sup>10</sup> See Righi, reference 8.

tion was found to cause a deflection of the electrometer, indicating a change in the potential of the plate. Righi regarded the deflection as a measure of the original potential difference—the “contact potential difference”—between the two electrodes, a conclusion which cannot be upheld in the light of later findings. However, he also showed that such an arrangement is capable of producing current under the action of ultraviolet radiation and denoted it, hence, as a “photoelectric cell.” Placing two similar cells in series was found to double the electrometer deflection on irradiation of both; this then constituted a “photoelectric battery.” Stoletow<sup>11</sup> replaced the electrometer by a high-resistance galvanometer and put a voltaic pile (battery) in series with it, approaching closely present-day methods of investigating the photoemissive effect (Fig. 1.3).

**The First Alkali Phototubes.** The transition from these early beginnings to phototubes in the modern sense of the word, sensitive to visible light as well as to ultraviolet radiation, resulted chiefly from an extended series of researches carried out jointly by Julius Elster and Hans Geitel. Their starting point was the observation that the electrochemically positive elements, such as aluminum, magnesium, and zinc, exhibited

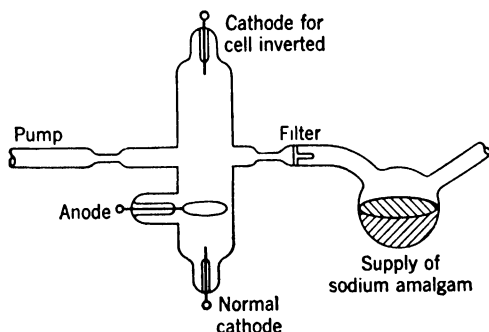


FIG. 1.4. Sodium-Amalgam Phototube of Elster and Geitel.

the photoemissive effect most strikingly. It appeared probable, therefore, that the still more electropositive alkali metals, of which sodium and potassium are the most common, would be even more effective. Unfortunately, these very active metals could not be used directly, since their surfaces reacted almost instantly with the air and water vapor to form heavy coatings of oxides and hydroxides. However, by amalgamating them with mercury and thus slowing up the reaction, Elster and Geitel<sup>12</sup> obtained surfaces which, when freshly prepared,

<sup>11</sup> See reference 9.

<sup>12</sup> See reference 10.

were more sensitive than any that preceded them. More important, these sodium and potassium amalgam surfaces were discharged by irradiation even when a glass plate absorbing the ultraviolet component was placed between the source and the surface. They were thus photoelectrically active to visible light.

Shortly afterwards, in 1890, Elster and Geitel<sup>13</sup> took the important step of enclosing the sensitive alkali-amalgam surface in an evacuated glass envelope, preserving its freshness. This was the first true phototube (Fig. 1.4).

**The Photoelectric Carrier.** Although Hallwachs had established that the photoemissive effect consisted in the liberation of negative electricity which followed electrostatic lines of force, it was unknown in what form this electricity was liberated. Work which was carried on concurrently on discharges in evacuated tubes helped to clarify this question. If a high voltage is supplied between two electrodes sealed into a tube which is being evacuated, a luminous discharge appears which disappears again as the pressure drops below a certain value. Beyond this point a beam is found to proceed in straight lines from the negative electrode or cathode in the general direction of the anode, revealing its presence by the fluorescence excited at the point of incidence on the glass envelope. This beam is found to be capable of deflection by an electric or magnetic field and hence must consist of charged material particles; the direction of the deflection indicates the charge to be negative. J. J. Thomson<sup>14</sup> was able to determine the ratio of the charge and mass of the particles constituting the beam from the magnitude of the magnetic deflecting field required to nullify the deflection produced by a given electrostatic field at right angles to it. Independent measurements of the charge of the particles led him to conclude that their mass was less than a thousandth of the mass of a hydrogen atom. This new, and lightest, material particle came to be designated as an *electron*. Thomson noted that the electrons obtained from all metal cathodes were identical in charge and in mass.

The first step in determining the nature of the electricity liberated in the photoelectric effect was taken by Elster and Geitel,<sup>15</sup> who showed that the current in a phototube, subjected to a magnetic field at right angles to the path from cathode to anode, was reduced by as much as 50 per cent. This observation established the fact that the carriers of the liberated electricity were negatively charged material particles. Lenard<sup>16</sup> eliminated the possibility that they might be negatively

<sup>13</sup> See reference 11.

<sup>14</sup> See reference 12.

<sup>15</sup> See reference 13.

<sup>16</sup> See reference 14.

charged atoms of the cathode by permitting sufficient current to flow between a sodium-amalgam cathode and a platinum wire anode to deposit on the platinum wire an amount of sodium that could be readily detected by the Bunsen flame test. Actually no trace of sodium was detected on the wire. He next built a tube with an aluminum cathode, to be illuminated with ultraviolet radiation, and an anode with a central aperture which limited the photoelectric carriers transmitted by it to a narrow beam (Fig. 1.5). Two terminals were provided at the opposite end of the tube. The ratio of charge to mass of the particles could thus be determined by measuring the strength of the magnetic field required

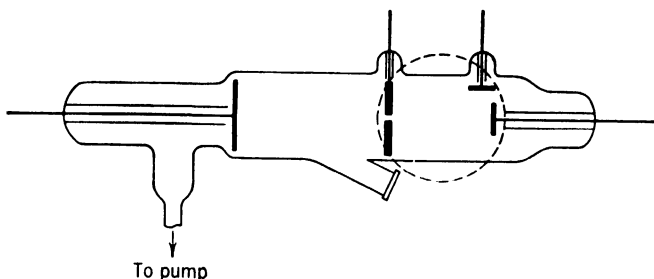


FIG. 1.5. Lenard's Tube for Measuring  $e/m$  for Photoelectric Carrier.

to deflect the beam from the first terminal to the second. This ratio was found to be identical with that determined by Thomson for electrons.

More accurate measurements, made by Merritt and Stewart<sup>17</sup> in 1900 and especially by Alberti<sup>18</sup> in 1912, prove beyond question that *the photoelectric carriers are, indeed, negative electrons*. The most recently accepted values for the constants of the electron are:<sup>19</sup>

$$\frac{e}{m} = 1.76 \cdot 10^{11} \text{ coulomb per kilogram}$$

$$e = 1.60 \cdot 10^{-19} \text{ coulomb}$$

$$m = 9.11 \cdot 10^{-31} \text{ kilogram}$$

**Empirical Laws.** Out of the experimental work of the early investigators there gradually crystallized two fundamental laws of photoelectric action, their statement developing from crude approximation to confident precision as more and more accurate research eliminated disturbing errors which confused preliminary results. The *First Law*

<sup>17</sup> See reference 15.

<sup>18</sup> See reference 16.

<sup>19</sup> For more accurate values, see Appendix, p. 477.

may be worded: *The number of electrons released per unit time at a photoelectric surface is directly proportional to the intensity of the incident light.*

This law has been tested for a range of intensities varying from values so low that the finite size of the electronic charge introduces appreciable statistical fluctuations<sup>20</sup> to full sunlight. Wherever deviations have been reported, the discrepancy could always be accounted for by errors in measurement, imperfect collection of the emitted photoelectrons, modification of the emitting surface, or other faults in phototube construction or operation.

The *Second Law* is more surprising. *The maximum energy of the electrons released at a photoelectric surface is independent of the intensity of the incident light, but increases linearly with the frequency of the light.*

In other words, although the electrons emitted under the influence of radiation possess various velocities, the highest velocity represented is determined solely by the highest frequency of the radiation. No matter how greatly the intensity of the radiation is increased, this highest velocity remains the same. The more intense beam does not act on the individual atoms or electrons of the metal more strongly; it just affects a larger number of them. The basic theory of the photoemissive effect, which conforms to these laws—both of which are based on experiments by Lenard—will be given in the next chapter.

**The First Practical Phototubes.** The earliest photoelectric devices, employing polished metal surfaces in air, were unsuited for photometric measurements, since they tarnished rapidly and simultaneously lost their sensitivity. The first photometric device was, probably, Elster and Geitel's amalgamated zinc sphere, described in 1889.<sup>21</sup> It remained constant in response sufficiently long to permit a set of comparison readings to be taken and could be easily restored by fresh amalgamation. The vacuum-enclosed sodium-amalgam photocathode, developed shortly afterward, had the added advantage of being sensitive to visible radiation; even it was not truly permanent, but had to be renewed occasionally by a crude filtering process.

In 1904 Hallwachs<sup>22</sup> devised a phototube for photometric purposes, sensitive to the ultraviolet only. It had a copper plate coated with black oxide as cathode. With the electrodes mounted in an evacuated enclosure, the response remained constant over a period of several months.

Elster and Geitel, continuing their work with the alkali phototubes, found presently that the hydride crystals of sodium and potassium were

<sup>20</sup> See, for example, Chapter 13, p. 250.

<sup>21</sup> See Elster and Geitel, reference 10.

<sup>22</sup> See reference 17.

more photosensitive than the pure metals. The most important step in this development, which increased the sensitivity of the phototubes by two orders of magnitude, was, however, the following. When a glow discharge was passed through hydrogen gas in the alkali phototube a highly colored colloidal layer was formed on the cathode which was some hundred times as sensitive as the pure metal. These hydrogenated alkali phototubes of Elster and Geitel,<sup>23</sup> dating back to 1912, mark the beginning of modern phototube development, which forms the subject of later chapters.

## REFERENCES

1. E. BECQUEREL, "Studies of the effect of actinic radiation of sunlight by means of electric currents," *Compt. rend.*, Vol. 9, pp. 145-149, 1839.
2. E. BECQUEREL, "Note on the electric effects produced under the influence of sunlight," *Compt. rend.*, Vol. 9, pp. 561-567, 1839.
3. W. SMITH, "Effect of light on selenium during the passage of an electric current," *Am. J. Sci.*, Vol. 5, p. 301, 1873.
4. H. HERTZ, "On very rapid electrical oscillations," *Ann. Physik*, Vol. 31, pp. 421-448, 1887.
5. H. HERTZ, "Ultra-violet light and electric discharge," *Ann. Physik*, Vol. 31, pp. 983-1000, 1887.
6. E. WIEDEMANN and H. EBERT, "On the effect of light on electric discharge," *Ann. Physik*, Vol. 33, pp. 241-264, 1888.
7. W. HALLWACHS, "On the effect of light on electrostatically charged bodies," *Ann. Physik*, Vol. 33, pp. 301-312, 1888.
8. A. RIGHI, "On some electrical phenomena provoked by radiation," *Phil. Mag.*, Vol. 25, pp. 314-316, 1888.
9. A. STOLETOW, "On photoelectric currents in rarefied air," *J. phys.*, Vol. 9, pp. 468-473, 1890.
10. J. ELSTER and H. GEITEL, "On the discharge of negative electric bodies by sun and daylight," *Ann. Physik*, Vol. 38, pp. 497-514, 1889.
11. J. ELSTER and H. GEITEL, "The use of sodium amalgam in photoelectric experiments," *Ann. Physik*, Vol. 41, pp. 161-165, 1890.
12. J. J. THOMSON, "On the masses of the ions in gases at low pressures," *Phil. Mag.*, Vol. 48, pp. 547-567, 1899.
13. J. ELSTER and H. GEITEL, "On the inhibiting effect of magnetism on photoelectric discharge in rarefied gases," *Ann. Physik*, Vol. 41, pp. 166-176, 1890.
14. P. LENARD, "Production of cathode rays by ultraviolet light," *Ann. Physik*, Vol. 2, pp. 359-375, 1900.
15. E. MERRITT and O. M. STEWART, "The development of cathode rays by ultraviolet light," *Phys. Rev.*, Vol. 11, pp. 230-250, 1900.
16. E. ALBERTI, "New determination of the specific charge of photoelectrons," *Ann. Physik*, Vol. 39, pp. 1133-1164, 1912.
17. W. HALLWACHS, "Photoelectric fatigue and photometry," *Physik. Z.*, Vol. 5, pp. 489-499, 1904.
18. J. ELSTER and H. GEITEL, "Proportionality of light intensity and photocurrent in alkali metal cells," *Physik. Z.*, Vol. 14, pp. 741-752, 1913.

<sup>23</sup> See reference 18.

## Chapter 2

# GENERAL THEORY

## I. RADIANT ENERGY

It is impossible to have clear notions of the photoelectric effect without understanding certain fundamental characteristics of radiation and of the sources of radiant energy. Radiant energy may be defined as the energy associated with electromagnetic oscillations propagated through space. The frequencies of these oscillations may have practically any value, ranging from zero upward. Any given type of radiation is characterized by a corresponding range of frequencies, determining the effect of the radiation upon matter, by which it is reflected, absorbed, or transmitted.

**Spectrum of Radiant Energy.** Figure 2.1 pictures the conventional classification of radiation into frequency intervals, set apart by different normal methods of detection and different origins. It must be emphasized that all types of radiant energy differ from each other only in frequency or wave length. Thus most of the consecutive ranges overlap to a greater or smaller extent. The simple relation between frequency  $\nu$  and wave length  $\lambda$ , both indicated on the chart, is  $\nu = c/\lambda$ , where  $c$  is the velocity of light, which is very nearly equal to  $3 \cdot 10^8$  meters per second.

It will be noted that the octave of frequencies which constitutes visible light forms but the tiniest fraction of the entire gamut. A frequency of approximately  $7.5 \cdot 10^{14}$  vibrations per second, corresponding to a wave length of 4000 Angstrom units,<sup>1</sup> produces a sensation of violet color when incident on the retina. Radiation of about half that frequency or twice that wave length produces the sensation of red.

Radiations immediately beyond the violet constitute the ultraviolet. By use of a vacuum spark spectrograph Millikan and Bowen <sup>2</sup> have been able to detect ultraviolet waves as short as 136 Angstrom units. Since the human eye may be considered as just failing to detect radiations

<sup>1</sup> An Angstrom unit (A.U. or Å) or "tenth-meter" is  $10^{-10}$  meter.

<sup>2</sup> See reference 1.

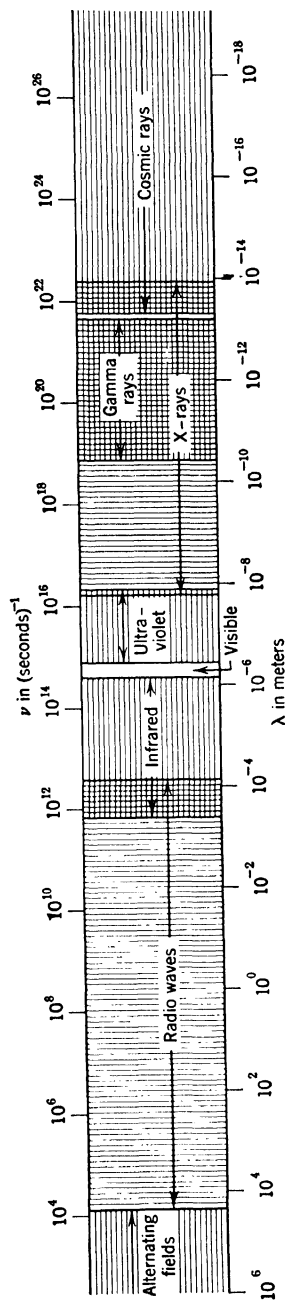


Fig. 2.1. The Spectrum of Electromagnetic Radiation. The different types of radiation are distinguished by their method of generation and detection. The limits of the several ranges correspond to available empirical data.



beyond 3800 Angstrom units, it may be concluded that ultraviolet radiations occupy about five octaves in the frequency spectrum.

Osgood <sup>3</sup> has succeeded in detecting and recording long x-ray waves at least 167 Angstrom units in length. On the other extreme, characteristic x-rays from the heaviest element occurring in nature, uranium, have been produced and measured by Dessauer and Back.<sup>4</sup> The shortest wave length of these radiations is only 0.108 Angstrom unit.<sup>5</sup> X-rays with a continuous, rather than a discrete, or line, spectrum may be produced by the bombardment of any kind of target (or *anticathode*) by electrons of high velocity, such as may be attained through acceleration by a strong electrostatic field. Duane and Hunt <sup>6</sup> have found that the equation  $V \cdot \lambda = 12.35$  <sup>7</sup> may be used for calculating precisely the shortest wave length (in Angstrom units) of the radiation emitted by a target bombarded by electrons which have been accelerated through a potential drop of  $V$  kilovolts. X-ray tubes are now in use which operate continuously at 2000 kilovolts.<sup>8</sup> By the formula the most penetrating radiations so produced have a wave length of only 0.0062 Angstrom unit. In the 100-million volt betatron,<sup>9</sup> in which electrons strike a target after acquiring enormous energies through acceleration by a changing magnetic field, x-rays are generated with wave lengths as short as 0.00012 Angstrom unit.

The so-called  $\gamma$ -rays emitted by radioactive materials, either natural or artificial, fall in the same range. A table of radioactive disintegrations <sup>10</sup> yields  $\gamma$ -ray wave lengths lying between 0.0007 and 0.39 Angstrom unit.

Electromagnetic radiations of wave lengths shorter than the wave length of any x-rays and  $\gamma$ -rays recorded so far have been found to be associated with the cosmic rays reaching the Earth from outer space. If the cosmic rays incident on the Earth's atmosphere consist, in part, of electrons with an energy of 10,000 million electron volts,<sup>11</sup> their interaction with atmospheric matter may result in the emission of electromagnetic radiation with a wave length of the order of  $10^{-6}$  Angstrom unit. Since more recent estimates assign energies as high as  $10^{17}$  electron volts to the primary cosmic ray particles, these are without ques-

<sup>3</sup> See reference 2.

<sup>4</sup> See reference 3.

<sup>5</sup> See Rechou, reference 4.

<sup>6</sup> See reference 5.

<sup>7</sup> A more recent value of the constant in this equation is 12.395.

<sup>8</sup> See Goodman, reference 6.

<sup>9</sup> See Westendorp and Charlton, reference 7.

<sup>10</sup> See Livingston and Bethe, reference 8.

<sup>11</sup> See Neddermeyer and Anderson, reference 9.

tion the source of electromagnetic radiations with the highest frequencies known to us.

Immediately on the opposite side of the visible region lies the infrared. The human eye generally ceases to register above about 7600 Angstrom units. In 1911 Rubens and von Baeyer,<sup>12</sup> by a method of focal isolation, detected infrared radiations with wave lengths as great as  $3.2 \cdot 10^{-4}$  meter. This limit was later extended by Nichols and Tear<sup>13</sup> to at least  $4.2 \cdot 10^{-4}$  meter. The last two investigators separated the long waves from a mercury arc by transmission through a thick plate of quartz and several layers of black paper.

The same men succeeded in generating and receiving damped radio waves only  $2.2 \cdot 10^{-4}$  meter in length, or shorter than the long infrared waves. Their results have been bettered by Arkadiewa,<sup>14</sup> who obtained damped oscillations of the unbelievably short length  $8.2 \cdot 10^{-5}$  meter. Continuous radio waves capable of modulation, a few millimeters in length, may be generated by vacuum-tube transmitters of appropriate design.<sup>15</sup> At the other end of the range, 22.5-kilometer waves have been sent out regularly by the Lafayette broadcasting station near Bordeaux, in France. In fact, any oscillation of electricity in a circuit, no matter how small the frequency, is capable of radiating electromagnetic energy into space. Thus there is no actual limit to the length of radiant waves. Usually, we think of frequencies lower than those of the broadcast range as being associated simply with alternating or pulsating currents.

**Sources of Radiant Energy.** The frequency range of radiations which normally cause the emission of electrons extends upward from the near infrared. In the normal applications of photocells, however, frequencies beyond the near ultraviolet do not come into play, permitting us to restrict our attention to emitters of infrared, visible, and ultraviolet radiations. Such sources may be divided conveniently into three general classes: thermal radiators, excited gases and vapors, and luminescent materials or phosphors.

The thermal radiators comprise the oldest, most familiar, and most widely distributed light sources, including the sun itself. In them light is emitted by matter rendered incandescent by being raised to a high temperature. The necessary energy may be supplied by chemical reaction, as in the case of the minute carbon particles suspended in the flame of a candle or gas jet, rendering it luminous; it may be provided by an electric current passing through a resistive material such as a

<sup>12</sup> See reference 10.

<sup>13</sup> See reference 11.

<sup>14</sup> See reference 12.

<sup>15</sup> See Mueller, reference 13.

carbon or tungsten filament, as in the incandescent lamp; or it may be derived from the kinetic energy of electrons or charged atoms (*ions*) bombarding the light-giving surfaces, forming, for example, the craters in the electrodes of a carbon arc.

The spectral distribution of the radiation of all these sources is continuous over a broad band of wave lengths, rising from a low value at very long wave lengths to a maximum at a wave length  $\lambda_m$  and declining as the wave length is reduced further. In fact, the emissive powers of any of these sources, at a given temperature and wave length, must differ from each other only by a factor equal to the ratio of their absorptive powers for radiation of that wave length.<sup>16</sup> Hence, if the emissive properties of a truly black body, that is, a body absorbing all radiation incident on it, are known and the spectral variation of absorptivity of a given surface (at the temperature in question) is available, the emissive properties of that surface are also known.

**Black-Body Radiation.** The nearest approach to a black body is a small opening in the enveloping walls of a cavity. If the opening is small enough, practically all the light entering it will be absorbed, eventually after many reflections at the wall surfaces, and a negligible proportion will return through the opening or be "reflected" by it. If, now, the inner walls of the cavity are heated, so that a uniform temperature  $T^\circ \text{ K}$ <sup>17</sup> is established within it, radiation issues from the opening. In fact, Stefan,<sup>18</sup> from an analysis of empirical data for incandescent platinum, found that the total radiation emitted by a surface is proportional to the fourth power of its absolute temperature:

$$E = \sigma T^4 \quad (2.1)$$

This law was verified by Lummer and Pringsheim for the radiation issuing from a heated cavity<sup>19</sup> and derived by Boltzmann<sup>20</sup> from the second law of thermodynamics. The value of the Stefan-Boltzmann constant  $\sigma$  is  $5.672 \cdot 10^{-8} \text{ joule} \cdot \text{meter}^{-2} \cdot \text{deg}^{-4} \text{ sec}^{-1}$ .

Lummer and Pringsheim<sup>21</sup> began an investigation of the spectral distribution of the radiation from a heated enclosure in 1899. Their observations formed the basis for a careful experimental check of a

<sup>16</sup> See, for example, Richtmyer and Kennard, reference 14, p. 162. Chapter 5 of this book treats the subject matter of the next section in detail.

<sup>17</sup> The zero point of the absolute temperature scale ( $^\circ \text{K}$  or  $^\circ \text{A}$ ) lies at  $-273.16^\circ \text{C}$ . The absolute scale and the centigrade scale differ simply by an additive constant 273.16.

<sup>18</sup> See reference 15.

<sup>19</sup> See Lummer and Pringsheim, reference 16.

<sup>20</sup> See reference 17.

<sup>21</sup> See reference 18.

number of formulas which had been derived from theoretical considerations. The nature of the curves obtained is shown in Fig. 2.2. Figure 2.3

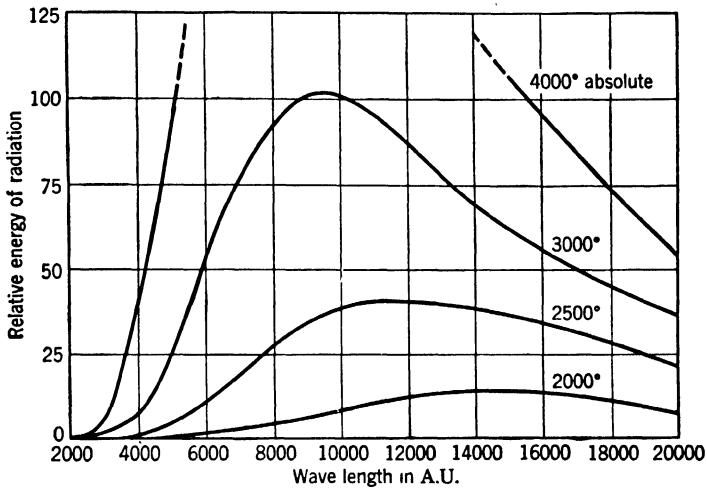


FIG. 2.2. Spectral Distribution of the Emission from a Heated Enclosure at Various Absolute Temperatures.

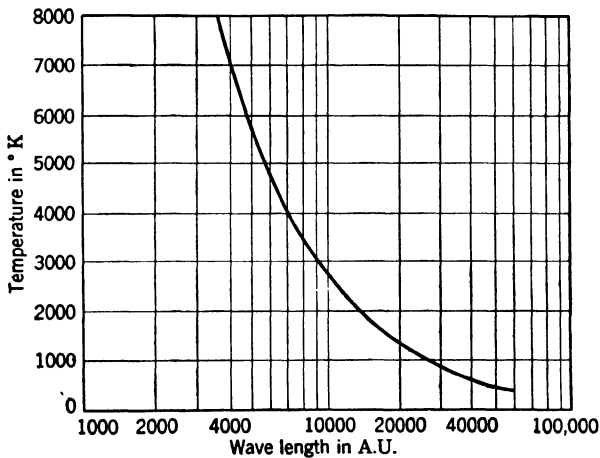


FIG. 2.3. Variation of Wave Length  $\lambda_m$  Corresponding to Maximum Emission with Temperature.

shows the decrease with increasing temperature of the wave length  $\lambda_m$  corresponding to maximum emission. Thermodynamic reasoning shows that this displacement of the maximum must obey the relation

$$\lambda_m T = A \quad (2.2)$$

Here  $A$  is a constant. This is known as Wien's displacement law.<sup>22</sup> The value of the constant  $A$  is  $2.8971 \cdot 10^{-3}$  meter·degree.<sup>23</sup> The relation was fully confirmed by the observations of Lummer and Pringsheim.

The formulas first advanced for the spectral distribution of black-body radiation were less fortunate. Thus Wien's formula<sup>24</sup>

$$E = a\lambda^{-5}e^{-h/kT} \quad (2.3)$$

derived by making certain special assumptions regarding the properties of the emitting molecules, fitted the experimental curves closely at short wave lengths, but failed to do so at the longer wave lengths. A formula advanced by Rayleigh,<sup>25</sup> based on an application of statistical mechanics to the electromagnetic oscillations in the cavity,

$$E = cT\lambda^{-4} \quad (2.4)$$

was verified for long wave lengths, but was completely at variance with experiment at short wave lengths. Its failure to hold good at all wave lengths indicated definitely that classical statistics did not apply to electromagnetic radiation.

Max Planck<sup>26</sup> came to the rescue with a revolutionary proposal that perhaps bodies do not, after all, radiate and absorb energy continuously, but rather discontinuously. By considering mathematically a simple linear oscillator as representing a molecule or atom emitting radiation, he was led to suggest that its energy at any moment might be made up of a number of submultiple energies, each one of which is proportional to the frequency of vibration of the oscillator. Thus the unit of energy or quantum<sup>27</sup> of any perfect radiator he took to be  $h\nu$ , where  $h$  is a constant of proportionality, now known as Planck's constant. Beginning with this assumption and making use of the laws of probability, he arrived at a definite expression for the energy distribution curves:

$$E = \frac{8\pi h\nu}{\lambda^4(e^{h\nu/kT} - 1)} = \frac{8\pi hc}{\lambda^5(e^{hc/\lambda kT} - 1)} \quad (2.5)$$

This formula fits the curves perfectly for all wave lengths and temperatures. Here  $k$ , the Boltzmann constant or the general gas constant evaluated for one molecule, is numerically equal to  $1.380 \cdot 10^{-23}$  joule·

<sup>22</sup> See Wien, reference 19.

<sup>23</sup> See Birge, reference 20.

<sup>24</sup> See Wien, reference 21.

<sup>25</sup> See reference 22.

<sup>26</sup> See reference 23.

<sup>27</sup> A quantum of electromagnetic radiation is frequently called a photon.

degree<sup>-1</sup>. The value of  $h$  itself is  $6.624 \cdot 10^{-34}$  joule·second.<sup>28</sup> The symbol  $c$  is the velocity of light ( $2.99776 \cdot 10^8$  meters per second). It is seen that for large values of  $\nu$  (short wave lengths) Planck's law reduces to Wien's law (Eq. 2.3); for long wave lengths it takes on the form of Rayleigh's law.

**Thermal Sources.** Since the absorption of all physical bodies is less than that of the perfect black body, their emission is correspondingly less than that of a black body at the same temperature. Figure 2.4 compares the emission of a tungsten surface with that of a black body, as given by Eq. 2.5, for a temperature of 2870 °K. The ratio of the two ordinates for any one wave length indicates the spectral emissivity (and absorptivity) of tungsten at the given temperature and wave length. Figure 2.5 shows how the spectral emissivity varies with these two parameters. If the spectral emissivity of an incandescent surface over a range of wave lengths and temperatures and Planck's law, as well, are known, it is possible to infer its true temperature ( $T$ ) from the intensity and color of its radiation. This fact is utilized in the optical pyrometers,<sup>29</sup> which measure the temperature of incandescent materials, employing the emission of a calibrated lamp as the standard of comparison. It is customary to define the temperature of a black body having the same light emission per unit area as a given source as the brightness temperature ( $T_B$ ) of that source. The temperature of a black body whose emission has the same color as the source, on the other hand, is known as its color temperature ( $T_C$ ). Figure 2.4 shows that the brightness temperature of tungsten at 2870° K is considerably lower than its true temperature, its color temperature slightly higher.

As shown in Table 2.1, the color temperatures of tungsten filament lamps, under normal conditions of operation, range from 2500° K to 3200° K. The maximum of their spectral distribution falls thus, as indicated by Eq. 2.2, in the near infrared. The earlier filament lamps and flame sources have considerably lower color temperatures and correspondingly low efficiencies as light emitters.

Higher temperatures and surface brightnesses are attained in the anode crater of the carbon arc. Here—particularly in the cored and impregnated types—the emission of the gaseous arc atmosphere is superposed on the thermal radiation of the electrodes, modifying the spectral distribution of the arc.

A source having somewhat similar characteristics, but great advantages in compactness and steadiness of operation, is the Western Union

<sup>28</sup> See Birge, reference 20. To yield the radiation per unit area per unit wave-length range, Eq. 2.5 must be multiplied by  $c/4$ .

<sup>29</sup> For a discussion of photocell pyrometers, see Chapter 14, p. 291.

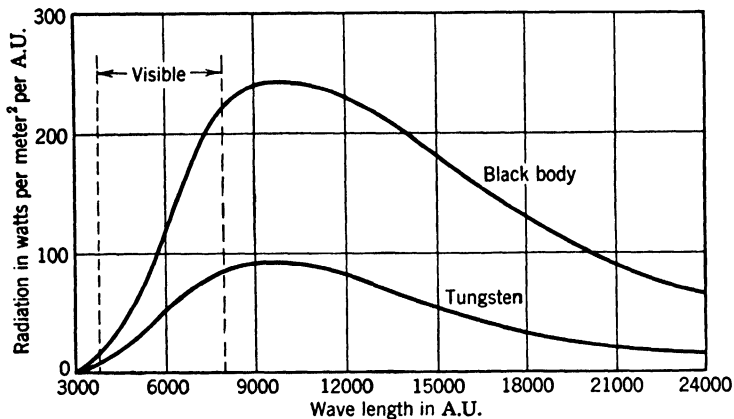


FIG. 2.4. Comparison between the Spectral Distribution of the Emission from an Ideal Black Body and a Tungsten Surface, Both at 2870 °K.

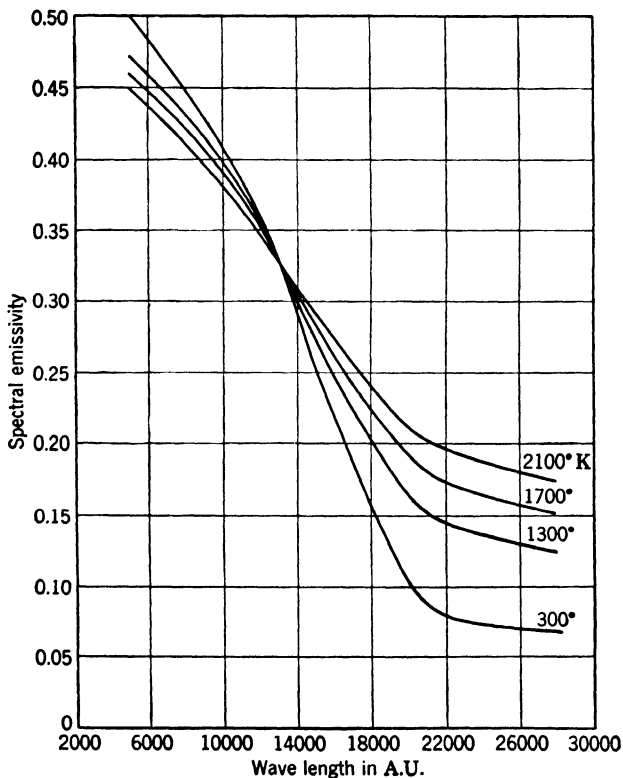


FIG. 2.5. Variation of the Spectral Emissivity of Tungsten with Wave Length and with Temperature. (After Forsythe and Worthing, by courtesy of the *Astrophysical Journal*.)

TABLE 2.1. TEMPERATURE, BRIGHTNESS, AND EFFICIENCY OF SELECTED SOURCES OF ILLUMINATION

 $T$ ,  $T_B$ ,  $T_C$  = true, brightness, and color temperature in degrees Kelvin $E$  = efficiency in lumens per watt $B$  = intrinsic brightness in candles/cm<sup>2</sup> (10<sup>-4</sup> candle/m<sup>2</sup>)

Source	$T$	$T_B$	$T_C$	$E$	$B$	Reference	Remarks
Thermal sources							
Candle; sperm			1,930		1.0	27	bright spot
Hefner lamp			1,880		0.7	27	bright spot
Pentane lamp			1,920			27	10 cp standard
Gas flame			2,160			27	bat's wing
Incandescent lamps							
C, 50-w	2,130		2,195	4.0	78.0	27	vacuum
Ta, 50-w	2,180		2,260	6.3	53.0	27	vacuum
W, 60-w	2,465		2,509	10.1	211.0	27	vacuum
W, 50-w	2,685		2,670	10.0	469	27	gas-filled
W, 1000-w	3,185		3,175	24.2	2,065	27	gas-filled
W, 50-w	2,650			10.0	7.8	27	gas-filled, frosted bulb
Carbon arc							
solid		3,385	3,780		9,200	27	anode crater
solid	3,925-3,970	3,810				28	anode crater
high-intensity					90,000	30	rotating anode
cored		3,075	3,420		4,130	27	
Concentrated arc, 10-w	3,480				4,000-10,000	24	ZrO cathode
Gaseous sources							
Neon, 90-w tube				14.0		25	220-volt, 0.95 amp
Neon crater lamp					100	29	50 ma
Neon crater lamp					500	29	8 amp
Mercury							
500-w, 50 in., 0.002 atm				16.0	2.1	33	110 volts a.c.
400-w, 1 atm				45.0	100	25, 31	130 volts, 2.4 amp
800-w, 120 atm				55.5	91,000	25	600 volts, 1.3 amp, water-cooled
1,400-w, 200 atm					180,000	32	water-cooled
Sodium arc							
197-w				61	5.5	26	
Luminescent sources							
Gas mantle					6.2	27	bright spot
Fluorescent lamps							
daylight				29.8		33	phosphor coating on glass, low-pressure mercury discharge
white (1½-in. tube)			2,500	36.7	0.6	33	
blue				18.8		33	
green				53.0		33	
gold				22.0		33	
red				2.4		33	
Zinc sulfide, excited by electrons				35		34	55 kv, 78 $\mu$ a
Light sources in nature							
Clear sky					0.8	27	average
Moon					0.25	27	bright spot
Sun					165,000	27	at earth's surface
					224,000	27	above atmosphere



concentrated-arc lamp.<sup>30</sup> Here the zirconium-oxide cathode and the anode are sealed in a glass bulb containing argon at atmospheric pressure. In operation the discharge fuses the zirconium oxide and forms a zirconium metal film at its surface. This film, together with a cloud of vapor extending a few thousandths of an inch in front of it, emits a brilliant white light. The effective size of the source in the smallest lamp is only 0.003 inch in diameter, so that this arc lamp approximates a point source. The emission of the fused zirconium has a maximum near 10,000 Angstrom units, that is, in the near infrared. It is supplemented by the emission of the vapor, which is rich in ultraviolet and visible radiations of wave length less than 5000 Angstrom units.

**Gaseous Sources.** When the molecules of a gas collide with other particles, such as electrons or ions, traveling at high velocities, they may be excited or ionized; in other words, their electronic structure may be disarranged, storing up as potential energy some of the kinetic energy of the incident particles. This energy may be emitted as radiant energy as the electrons drop back into place and the normal state of the atom is restored. The frequencies of the radiation obtained in this manner are characteristic of the substance of the gas. Hence, if the emission of an excited gas is analyzed with the spectroscope, it is found to consist of a series of discrete frequencies; a line spectrum of the gas is obtained.

The most important gaseous sources are the neon lamp and the mercury and sodium arcs. The cesium arc lamp, similar in construction to the sodium arc lamp, finds special application as a source of infrared radiation since it emits primarily the cesium resonance lines at 8521 and 8943 Angstrom units.<sup>31</sup> In the neon lamp, widely used in advertising, the discharge takes place between two metallic electrodes in the rare gas neon at a pressure of 1 to 2 millimeters of mercury. The emission lines are largely concentrated in the red and orange parts of the spectrum. Neon lamps with small electrode separations—in particular the neon crater lamp—have played an important part in early television developments, since they provided an intense small source capable of rapid modulation.

The modern low-pressure mercury arc consists of a glass or quartz tube containing, in addition to a small amount of liquid mercury, a noble gas such as argon or neon. The noble gas initiates the discharge, heating up the tube until enough mercury evaporates to determine the nature of the emission. The emission in the visible consists primarily of the green line at 5461 Angstrom units with an admixture of yellow (5770 and 5790 A.U.) and blue (4358 A.U.) light. Most of the energy

<sup>30</sup> See Buckingham and Deibert, reference 24.

<sup>31</sup> See Chapter 18, p. 411.

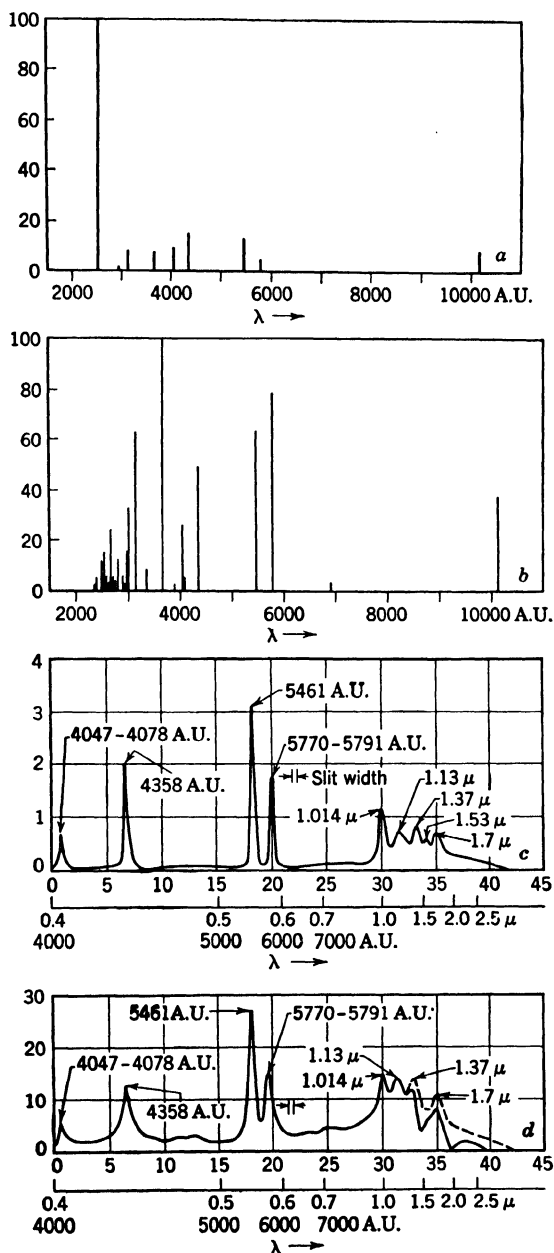


FIG. 2.6. Variation of Spectral Distribution of Emission of Mercury Vapor Lamp with Pressure of Mercury Vapor: (a) at  $10^{-2}$  mm Hg, (b) at 1 atmosphere, (c) at 20 atmospheres, and (d) at 130 atmospheres. (Uyterhoeven, reference 25.)

of the emission is concentrated in the resonance line at 2537 Angstrom units, in the ultraviolet.

Much greater luminous efficiencies are obtained with high-pressure mercury arcs. Here the discharge tube consists of a small tube of quartz or hard glass containing two oxide-coated electrodes and an amount of mercury sufficient to build up the desired pressure when fully evaporated. The discharge takes place along a narrow channel in the center of the tube, where temperatures of several thousand degrees are built up—far in excess of the tube-wall temperatures. The pressures in commercial tubes range from 1 to 100 atmospheres. The advantage over low-pressure mercury arcs rests primarily in the fact that, as the pressure is increased, a progressively larger proportion of the emission is concentrated at longer wave lengths. At very high pressures a continuous spectrum is superposed on a spectrum of broadened lines. The change in the energy distribution in the spectrum with the pressure of the mercury vapor is illustrated in Fig. 2.6.<sup>32</sup>

The operation of the sodium arc is essentially similar to that of the low-pressure mercury vapor lamp. The tube contains, in addition to a small amount of sodium metal, neon at a pressure of 1.5 mm Hg.<sup>33</sup> This gas initiates and determines the nature of the discharge. However, as the temperature of the tube rises to a value corresponding to its normal operating condition (about 270° C) enough sodium metal vaporizes to change the emission from neon red to the characteristic yellow of sodium (5890 and 5896 A.U.), yielding a practically monochromatic source of high luminous efficiency. The interior of the lamp walls is given a special borosilicate glaze to prevent discoloration by the sodium.

**Luminescent Sources.** Certain solid substances will emit light when properly excited without being raised to a high temperature. Such substances are known as luminescent materials or phosphors. The most important exciting agents are ultraviolet radiation and high-velocity electrons. An example of thermally excited, or cando-, luminescence is the Welsbach gas mantle, composed of the oxides of thorium and cerium.

The spectral emission of phosphors is concentrated in bands of frequencies which are determined by their chemical composition and preparation. Slight admixtures of metallic impurities, or activators, play a particularly important role in determining both the intensity and the color of their emission. The sulfides of the alkaline earths, zinc, and cadmium, zinc orthosilicate or willemite, and calcium tungstate

<sup>32</sup> See Uyterhoeven, reference 25.

<sup>33</sup> See Fonda and Young, reference 26.

are some of the most widely employed phosphors. Coating the inner wall surface of low-pressure mercury discharge tubes, they make possible the highly efficient fluorescent lamps, providing illumination of practically any color desired. In them the conditions of discharge are such that about half the energy emitted by the mercury vapor is concentrated in the resonance line (2537 A.U.) in the ultraviolet, which is very effective as an exciter of luminescence; whatever ultraviolet radiation is not absorbed by the phosphor is absorbed subsequently by the glass envelope of the tube.

The excitation of phosphors by electron bombardment finds application in cathode ray tubes and television viewing tubes. Here also high efficiencies of energy conversion into light are attained, particularly in tubes operating with high voltages or very high electron velocities. This is shown in Table 2.1, which summarizes the properties of the light sources discussed here. The employment of phosphors for rendering electron images visible is described in Chapter 9.

**Photometric Measurements.** The eye is not equally sensitive to all colors. If a yellow light and a red light of equal radiant energy were compared by a person with normal color vision, the yellow light would seem to be brighter. For any one individual a curve may be plotted

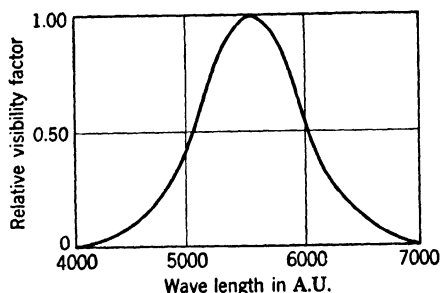


FIG. 2.7. The Visual Sensitivity Curve of the Human Eye.

showing the variation of the reciprocal of the radiant energy, required to create a fixed impression of brightness, with the wave length of the light observed. The average of a large number of such curves, obtained for different normal-sighted individuals, is the normal visual sensitivity (or sensibility) curve shown in Fig. 2.7. This curve has a maximum in the green, at 5550 Angstrom units, and drops off almost symmetrically on either side of the maximum, toward the red and toward the blue. It is obvious that, in the comparison of light sources with different spectral distributions of emission, it is important to distinguish between total

radiant energy in the visible range and total luminous flux as visually determined.

The original unit of luminous intensity was one candlepower, defined as the light output of a candle made of spermaceti weighing  $2\frac{2}{3}$  ounces and burning at the rate of 120 grains per hour. This unit has been superseded by the Vernon-Harcourt pentane lamp of 10 candlepower and the German Hefner lamp of 0.9 candlepower; the Hefner lamp uses amyl acetate as fuel. More recently, the average light emission of a group of 45 carbon filament lamps, preserved at the National Bureau of Standards and operated at specified current, functions as primary standard in the United States. The emission of a black body at the freezing temperature of platinum, specified to have a brightness of 60 candles per square centimeter, has now become the standard. For most purposes secondary and tertiary standards are employed; these are tungsten filament lamps calibrated from primary sources by recognized experts. Accurate comparisons of the luminous intensities of two sources can be made only when the sources are of the same color or are effectively reduced to the same color by means of compensating filters.

For investigating the sensitivity of photocells to white light, it is customary to employ a tungsten lamp with concentrated filament. The temperature of the filament is measured to gain information with respect to the spectral distribution of energy, and the corresponding candlepower is determined by comparison with a secondary standard. However, the amount of light from the lamp that passes into the cell through an aperture of definite area depends also on the distance of the lamp from the cell. A new quantity, the intensity of illumination at the cell, must be introduced. If the source has a luminous intensity of one candlepower and the cell is placed a distance of one meter from it, the intensity of illumination at the cell will be one meter candle or lux; a screen a square meter in area, placed at the cell,<sup>34</sup> will intercept a quantity of light or luminous flux equal to one lumen, the emission of a one-candlepower source into unit solid angle. If the distance between the source and the cell or screen is doubled, the amount of light received by either is only one-fourth as great; the illumination is one-fourth lux. Generally, if the extent of the source is small in comparison with the distance between the source and the receiving surface, the intensity of illumination at the receiving surface in lux is given by the ratio of the candlepower of the source and the square of the separation between the source and the surface in meters. The light flux in lumens received by

<sup>34</sup> This screen should, in all strictness, be a section of a sphere about the source as center, so that the radiation is incident at right angles on it throughout.

the surface is given by the product of the intensity of illumination in lux by the area of the surface in square meters.

It has already been seen that there is no general relationship between the radiant energy and the luminous flux emitted by a light source. It is possible, however, to define as the least mechanical equivalent of light the flux of radiant energy in watts corresponding to one lumen of green light with the wave length of 5550 Angstrom units, to which the eye is most sensitive. Measurements by Ives<sup>35</sup> yield a value of 0.0016 watt per lumen for the least mechanical equivalent.

The sensitivity of the eye to radiant energy is extraordinarily great. Measurements by Tumlriz<sup>36</sup> indicate that the total emission of the Hefner candle into unit solid angle in a horizontal direction is 0.1483 gram-calorie per second. Since 2.4 per cent of the emission falls into the visible range and the gram-calorie is equivalent to 4.2 joules of energy, the luminous energy emitted per unit solid angle per second is 0.015 joule.<sup>37</sup> If the diameter of the pupil is taken to be 3 millimeters, an eye placed a distance of one meter from a Hefner candle will hence receive luminous energy at a rate of  $1.1 \cdot 10^{-7}$  joule per second—just about enough energy to heat 1 gram of water  $1^\circ \text{C}$  in a year and a month. Very much smaller quantities of light are, of course, still perceived by the eye. Observations by Barnes and Czerny<sup>38</sup> led them to the conclusion that the human eye may be able to detect a light flux as small as 40 to 90 photons per second or a radiant flux of the order of  $10^{-17}$  watt!

## II. PHOTOEMISSIVE EFFECT

The preceding considerations regarding the properties of electromagnetic radiation and light sources find application in the study of the photoconductive and photovoltaic effects as well as in the study of the photoemissive effect. In the following paragraphs the theory of the photoemissive effect alone will be considered, a discussion of the two other types of photoelectric effect being reserved for later chapters.

**Einstein's Equation.** Just as classical physics was inadequate for explaining the spectral distribution of energy radiation by a black body, so it failed to account satisfactorily for the release of electrons by radiation. Thus Marx<sup>39</sup> showed that an electron, treated as a classical linear oscillator in resonance with the incident radiation, could acquire the

<sup>35</sup> See reference 35.

<sup>36</sup> See reference 36.

<sup>37</sup> See Drude, reference 37.

<sup>38</sup> See reference 38.

<sup>39</sup> See reference 39.

quantum of energy necessary for its release only if the radiation field was  $5 \cdot 10^{11}$  times as strong as radiation fields ( $6 \cdot 10^{-11}$  watt/meter<sup>2</sup>) which had been observed to yield photoemission. In 1905 Albert Einstein<sup>40</sup> proposed that photoemissive phenomena could be accounted for by adopting Planck's quantum theory of radiation and assuming that, when a quantum of energy  $h\nu$  reacted with an electron, the latter would

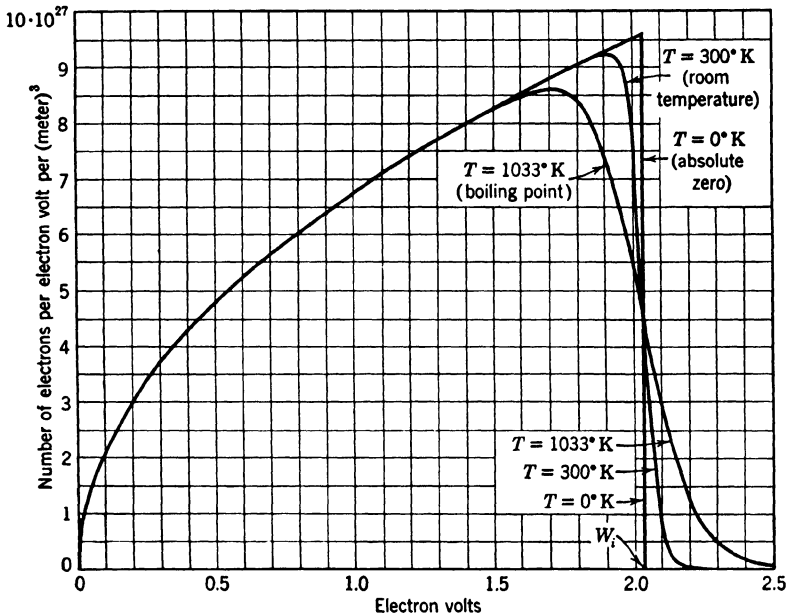


FIG. 2.8. Energy Distribution of Conduction Electrons in Potassium, on the Basis of the Elementary Sommerfeld Theory.

acquire the total quantum and be released in possession of an equivalent amount of kinetic energy. Einstein's equation for the kinetic energy of the photoelectron is

$$\frac{mv^2}{2} = h\nu - W \quad (2.6)$$

Here  $W$  represents the excess of the energy which the electron has to expend to free itself from the body of the emitting substance over the energy which it possessed originally, before its reaction with the quantum. For any one electron of the substance,  $W$  is a constant. Hence Eq. 2.6 expresses the second empirical law, given on page 8, to the

<sup>40</sup> See reference 40.

effect that the energy of emission increases linearly with the exciting radiation. It is plain that the quantum hypothesis is also in harmony with the first empirical law, stating that the number of electrons released is proportional to the intensity of the light, since the intensity is a measure of the number of quanta incident on the electron emitter.

It is obvious from the definition of  $W$  that  $W$  will have a certain minimum value  $w$  provided that the energy of the electrons within the emitter has a definite upper limit. This upper limit, which may be

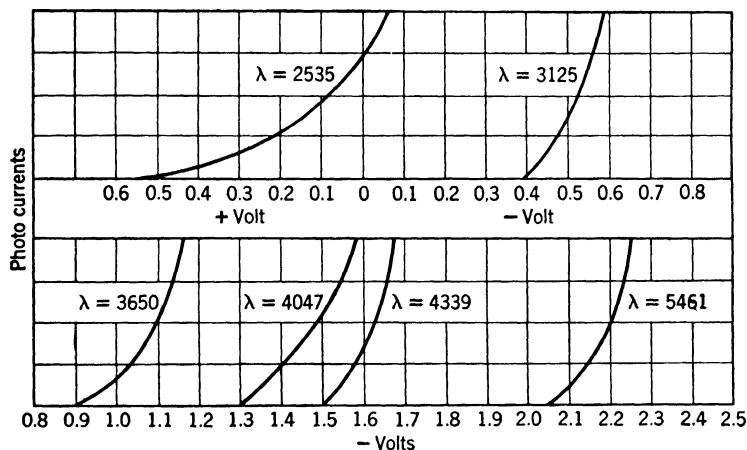


FIG. 2.9. Retarding Potential Curves for Photocurrents from Sodium Illuminated by Monochromatic Radiation of Different Frequencies. (Millikan, reference 42.)

denoted by  $W_i$ , does in fact exist. The energy distribution of the least tightly bound electrons—the “free” or conduction electrons, which are responsible for the photoeffect in the visible range—in a metal such as potassium is represented in Fig. 2.8.<sup>41</sup> It is seen that at  $0^\circ$  K the distribution cuts off sharply at the value  $W = W_i = 2.028$  electron volts,<sup>42</sup> which is calculated from theory. At room temperature ( $300^\circ$  K) a very small proportion of the electrons has energies in excess of  $W_i$ , so that the limit is not perfectly sharp. At much higher temperatures the right-hand tail of the distribution curve extends even beyond  $W_a$ , the difference in the mean potential energy of an electron outside the metal and within it. Electrons with energies in excess of  $W_a$  may leave the metal without being given additional energy. They give rise to the thermionic emission of the metal.

<sup>41</sup> See Reimann, reference 41, pp. 13–20.

<sup>42</sup> An electron volt is the kinetic energy acquired by an electron in being accelerated through a difference of potential of 1 volt. It is equal to  $1.60203 \cdot 10^{-19}$  joule.



In the study of photoemission, the existence of the tail of the distribution curve plays a minor role; in many of the earlier researches its effects remained unnoticed altogether. Thus, effectively, the minimum value of  $W$ , which by Eq. 2.6 must equal a quantum of the lowest frequency ( $\nu_o$ ) giving rise to photoemission from the given surface, is related to  $W_i$  and  $W_a$  as follows:

$$w = h\nu_o = W_a - W_i \quad (2.7)$$

It is customary to designate  $w = W_a - W_i$  as the work function of the substance,  $\nu_o$  as the threshold frequency, and  $\lambda_o = c/\nu_o$  as the threshold wave length.

Einstein's equation (2.6) has received repeated experimental confirmation. Figure 2.9 records measurements by Millikan<sup>43</sup> of the varia-

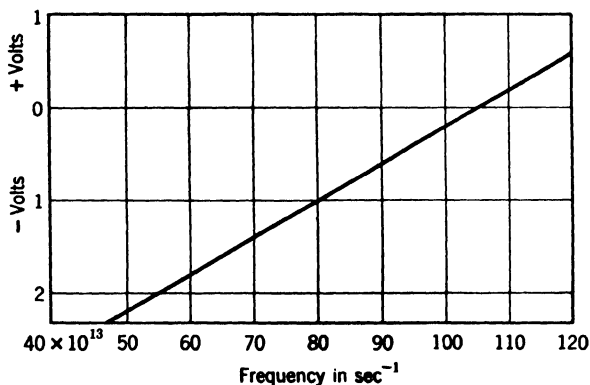


FIG. 2.10. The Voltage Intercepts in Fig. 2.9 Plotted as Function of the Frequency of the Exciting Radiation. The Slope of the Curve is  $h/e$ . (Millikan, reference 42.)

tion of photocurrents from sodium metal, collected by a cylindrical electrode to which a retarding potential was applied, with the magnitude of this potential. The sodium was kept bright by means of a paring tool enclosed in the vacuum vessel and operated electromagnetically. The extrapolated intercept<sup>44</sup> on the axis of abscissas indicates the voltage for which even the fastest electrons are forced back into the sodium. In Fig. 2.10 these intercepts are plotted against the frequency of the

<sup>43</sup> See reference 42.

<sup>44</sup> In view of the tail of the distribution in Fig. 2.8 the curves actually approach the axis of abscissas asymptotically. Even so, knowing the shape of the distribution curve near the upper limit, it is possible to determine the intercepts corresponding to  $w = W_a - W_i$ . See Fowler, reference 43.

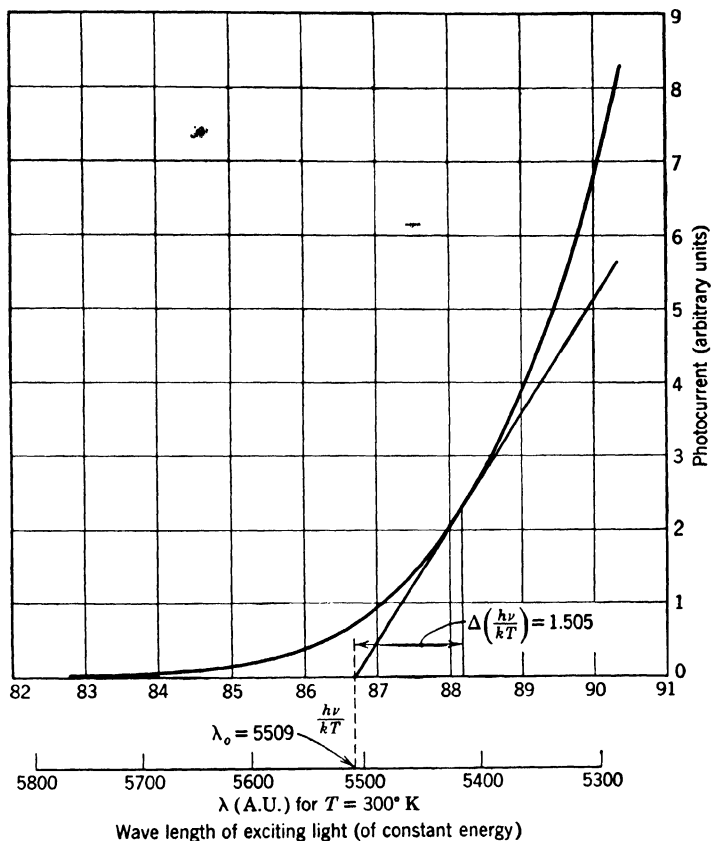


FIG. 2.11. Determination of Threshold Wave Length from Variation of Photocurrent with Wave Length of Exciting Light. If the photocurrent is plotted as function of  $h\nu/kT$ , the tangent to the curve drawn through the point for which the tangent intercept is 1.505 intersects the axis at the value  $h\nu/kT$  corresponding to the threshold wave length  $\lambda_0$ .

light giving rise to the photoemission. The result is an exact straight line, in accord with the relation

$$eV = \frac{mv^2}{2} = h\nu - w \quad (2.8)$$

where  $V$  is the retarding potential required to stop the fastest photoelectrons. Furthermore, the value of  $h/e$  determined from the slope  $dV/d\nu$  of the line has been found to agree, within a fraction of one per cent, with the best value of this quantity obtained by other methods. Millikan's research thus affords a precise check of Einstein's equation and the quantum theory of the photoelectric effect.

It should be noted that the potential difference plotted in Fig. 2.10 differs from the true retarding potential required to stop the fastest electrons by an additive constant, the contact difference of potential between the collector and the source. This contact difference, multiplied by the electronic charge, is equal to the difference in the work functions of the two surfaces in question. Hence the measured retarding potential corresponding to the intercepts of the curves in Fig. 2.9 is determined by the difference in energy of the light quantum and the work function of the collector, not that of the emitter. The work function of the emitter is found most readily by plotting the photocurrent as a function of the wave length or frequency of the exciting radiation, both the light intensity and the collector potential being maintained at a constant value. The effective intercept<sup>44</sup> of the curve on the axis of abscissas represents the threshold wave length or frequency, to which the work function is related by Eq. 2.7. In such measurements the collector potential is adjusted to a value sufficiently high so that none of the photoelectrons returns to the emitting surface. An example of a curve from which the threshold wave length can be determined—it is here approximately 5500 Angstrom units—is shown in Fig. 2.11.

The value of  $W_a$ , the difference in the mean potential within the emitter and outside of it, and hence that of the work function, is very sensitive to the condition of the surface. The absorption of traces of gas may alter the photoelectric properties completely. Even so it is possible, by taking special precautions, to obtain reproducible values for the photoelectric work functions of the pure metals. Table 2.2 lists, in particular, those of the alkalis and some of the alkaline earths, both of which play a considerable role in phototubes in practical use. The values for magnesium, calcium, and barium are most reliable.

TABLE 2.2. SELECTED PHOTOELECTRIC WORK FUNCTIONS OF PURE METALS

<i>Element</i>	<i>Volts</i>	<i>Reference</i>	<i>Element</i>	<i>Volts</i>	<i>Reference</i>
Lithium	2.28	41	Cesium	1.87-1.96	41
Sodium	2.46	41	Magnesium	3.61	44
Potassium	2.24	41	Calcium	2.706	45
Rubidium	2.16-2.19	41	Barium	2.51-2.52	45

**Structure of Matter.** It has already been noted that the pioneering investigations of J. J. Thomson revealed the existence of the negatively charged electron as a constituent of all matter. It remained for Ernest Rutherford<sup>45</sup> and Niels Bohr<sup>46</sup> to postulate a structure of the atom which, in its basic outline, continues to be accepted today. According to it, almost all the mass of the atom is concentrated in a minute, posi-

<sup>45</sup> See reference 46.

<sup>46</sup> See reference 47.

tively charged core or nucleus, with a diameter of the order of  $10^{-14}$  meter. Its charge is exactly balanced by the negative charge of the electrons, which course about the nucleus in planetary orbits. The nuclei themselves are now believed to be made up of *protons*, particles with a positive charge numerically equal to the charge of the electron and a mass 1837 times as great as that of the electron, and of *neutrons*, which have practically the same mass as the protons, but no charge. The number of electrons in the atom—which is equal to the number of protons in the nucleus—is known as the atomic number of the element to which it belongs. It is this number which determines the chemical properties of the element. For the majority of the elements the total number of particles in the nucleus—the mass number, which is also very nearly equal to the atomic weight—is approximately twice as large as the atomic number. In other words, most nuclei contain about as many neutrons as protons. Atoms with the same number of protons but different numbers of neutrons in the nucleus exhibit the same chemical behavior and are known as *isotopes*. Elements with a number of common isotopes have atomic weights deviating considerably from integer values, since the conventional atomic weight of an element represents an average of the atomic weights of the isotopes weighted by the frequency of their occurrence.

The lightest and simplest of the atoms is the atom of ordinary (light) hydrogen, consisting of a proton as nucleus and an electron traveling about it in a planetary orbit; the electrostatic attraction between the particles plays the role of gravitation. An atom of the rarer, heavy, hydrogen differs from an atom of light hydrogen only in having a neutron added to the proton in the nucleus. The next element, helium, has a nucleus consisting of two protons and two neutrons and a pair of electrons at an equal mean separation from the nucleus. Since they are subject to the attraction of a positive charge twice as great as the charge of the hydrogen nucleus, they are bound more tightly than the electron in hydrogen.

The next element, lithium, has 3 electrons coursing about a triply charged nucleus. Two of them form an inner “shell” of charge, similar to the 2 electrons of helium; the third electron travels in an orbit lying largely outside this shell, which reduces the attraction exerted upon the electron by the nucleus. This electron is more readily detached from the atom than either the electron of hydrogen or one of the electrons in helium. As the nuclear charge, and hence the number of electrons in the atom, is increased, a second shell of 8 electrons is gradually built up, leading to the very stable and chemically inactive gas neon. The addition of a further charge to the nucleus, making the total 11, leads

to a stable system in which 10 electrons are tightly bound in closed shells and one, peripheral, electron is attached loosely to the remainder. The resulting element, sodium, resembles lithium chemically, with the distinction that it enters even more readily into reactions with other elements, corresponding to the weaker binding of its peripheral electron. Generally, when a system of closed shells is built up (with 2, 10, 18, 36, 54, and 86 electrons) an extremely stable element, in the form of a rare gas, results. The addition of one more charge leads to one of the highly active alkali metals: lithium (3), sodium (11), potassium (19), rubidium (37), and cesium (55). The element with atomic number 87 has been obtained only as a product of artificial nuclear disintegrations. The looseness of binding of the peripheral electron and the chemical activity of these elements increase with increasing atomic number.

The alkaline earth metals—beryllium (4), magnesium (12), calcium (20), strontium (38), and barium (56)—differ from the alkali metals in having two in place of one peripheral electron. These electrons are, in view of the greater nuclear charge, bound somewhat more strongly than the outermost electrons of the alkali metals. Several of them, in particular barium and strontium, have found application in phototubes.

Electromagnetic radiations of sufficiently high frequencies, such as x-rays, are capable of ejecting electrons from the inner, tightly bound, electron shells of the atoms. In the photoeffect initiated by the infrared, visible, and near ultraviolet, however, only the most loosely bound electrons play a role. It is these electrons which provide the conduction electrons in a compact metal. An example of their energy distribution has already been given in Fig. 2.8.

**Color Sensitivity.** Early work already described indicated definitely that some photoemissive surfaces are sensitive to longer wave lengths than others. For example, the alkali metals are caused to emit electrons by visible radiations, whereas a surface of copper oxide is responsive only to the ultraviolet. Pohl and Pringsheim<sup>47</sup> showed that for a liquid alloy of sodium and potassium the number of electrons released by unit energy of incident radiation increases from zero at the red end of the spectrum to a maximum in the blue or near ultraviolet and then decreases to a low value again, only to start rising again at still higher frequencies. This variation is represented in Fig. 2.12. A similar behavior of the photoemission from pure alkali metal surfaces is predicted by modern theories of the photoelectric effect.<sup>48</sup> According to

<sup>47</sup> See reference 48.

<sup>48</sup> See, for example, Mitchell, reference 49, and Tamm and Schubin, reference 50. The results apply strictly for oblique light with the electric vector parallel to the plane of incidence. The effect of polarization is discussed briefly in Chapter 3.

them, practically all the photoemission in the visible range arises from the interaction of the incident radiation with the conduction electrons of the emitter at the surface (surface photoelectric effect). Starting from the threshold wave length, the initial rise in emission stems from the rapid increase in the number of electrons capable of escaping, provided that a quantum of energy is added to their original energy, with the magnitude of the quantum. The eventual reaching of a maximum

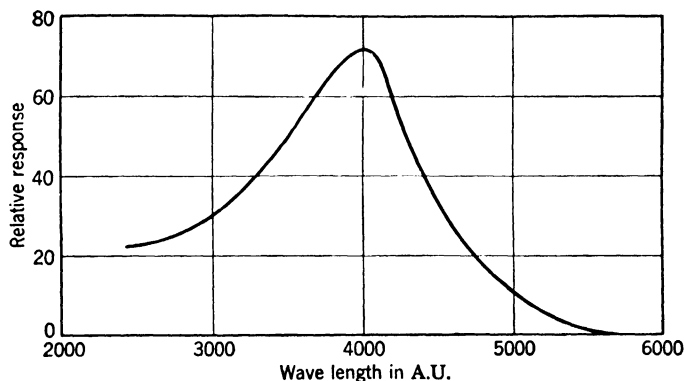


FIG. 2.12. Spectral Sensitivity Curve for a Liquid Alloy of Sodium and Potassium. (Pohl and Pringsheim, reference 48.)

and the subsequent decline of the curve follow from the rapid decrease in the efficiency of interaction between the radiation and the conduction electrons with the frequency of the radiation. This behavior corresponds roughly to the rapid decline in photoelectric absorption with frequency which is observed in the x-ray region. Finally, the second rise in the color sensitivity curve of a homogeneous metal may be ascribed to the interaction of the radiation with the more tightly bound conduction electrons in the body of the emitter.<sup>49</sup> In view of the smaller energy of these electrons, the "volume photoeffect" has a shorter wave-length threshold than the surface photoeffect, and hence becomes significant only in the near ultraviolet.

A fitting close to the general considerations of this chapter is formed by the series of color sensitivity curves shown in Fig. 2.13. They were

<sup>49</sup> Excitation of electrons in the interior of the metal is restricted by "selection rules" which prevent the electrons in the higher occupied energy levels (near the Fermi level) from being given just enough energy to escape. The volume effect, which corresponds to the excitation of electrons in harmony with these selection rules, does not depend on the polarization of the exciting light. More recent work by Fan (reference 51) suggests that the volume effect contributes materially even to the first maximum of the photosensitivity curve of the alkalis.

obtained by Miss Seiler<sup>50</sup> for phototubes employing the five different alkali metals as cathodes. The phototubes were glass tubes containing argon and all were prepared in identical manner; it was not intended that they should indicate the photoelectric behavior of the pure metals. A comparison of the curves yields two interesting conclusions. First, the wave length of maximum sensitivity increases in the same order as the atomic numbers of the alkali elements; second, the number of elec-

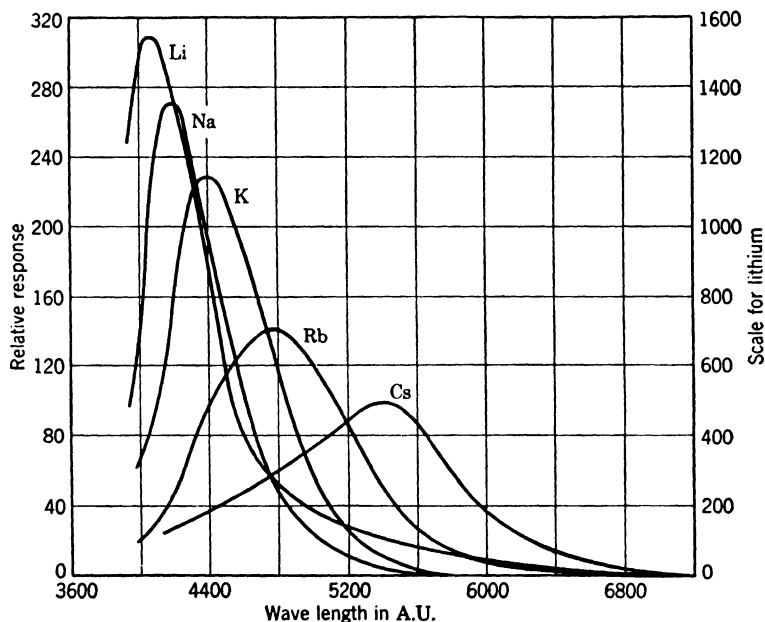


FIG. 2.13. Spectral Sensitivity Curves for the Alkali Metals. (Seiler, reference 51.)

trons released at the maximum decreases and the breadth of the spectral response increases from lithium to cesium. A similar behavior is encountered in many of the practical phototubes described in later chapters. One of the major objectives in phototube design must be the matching of the spectral response of the phototube to the output of the most common light sources. The fact that the maximum of the radiation of these sources lies in the near infrared points to cesium as a material of great utility in photocathode preparation.

## REFERENCES

1. R. A. MILLIKAN and I. S. BOWEN, "Extreme ultraviolet spectra," *Phys. Rev.* Vol. 23, pp. 1-34, 1924.

<sup>50</sup> See reference 52.

2. T. H. Osgood, "Soft x-ray spectra," *Nature*, Vol. 119, p. 817, 1927.
3. F. DESSAUER and E. BACK, "On x-ray excitation with very high voltages," *Verhandl. deut. physik. Ges.*, Vol. 21, pp. 168-200, 1919.
4. G. RECHOU, "Spectrographic study of the K-series of the heavy elements," *Compt. rend.*, Vol. 180, p. 1107, 1925.
5. W. DUANE and F. L. HUNT, "On x-ray wave lengths," *Phys. Rev.*, Vol. 6, pp. 166-171, 1915.
6. D. GOODMAN, "Production control with 2,000,000 volt x-rays," *Electronics*, Vol. 19, pp. 146-149, 1946.
7. W. F. WESTENDORP and E. E. CHARLTON, "A 100-million volt induction electron accelerator," *J. Applied Phys.*, Vol. 16, pp. 581-593, 1945.
8. M. S. LIVINGSTON and H. A. BETHE, "Nuclear dynamics, experimental," *Rev. Mod. Phys.*, Vol. 9, pp. 245-390, 1937.
9. S. H. NEDDERMEYER and C. D. ANDERSON, "Nature of cosmic-ray particles," *Rev. Mod. Phys.*, Vol. 11, pp. 191-207, 1939.
10. H. RUBENS and O. VON BAEYER, "On the energy distribution in the long-wave radiation emitted by the quartz-mercury lamp," *Preuss. Akad. Wiss., Berlin, Ber.*, pp. 666-677, 1911, and "On a very long wave radiation of mercury vapor," *Berlin, Ber.*, pp. 339-345, 1911.
11. E. F. NICHOLS and J. D. TEAR, "Joining the infrared and electric wave spectra," *Astrophys. J.*, Vol. 61, pp. 17-37, 1925.
12. A. GLAGOLEWA-ARKADIEWA, "Short electromagnetic waves of wave length up to 82 microns," *Nature*, Vol. 113, p. 640, 1924.
13. G. E. MUELLER, "Propagation of 6 mm waves," *Proc. Inst. Radio Engrs.*, Vol. 34, pp. 181-183, 1946.
14. F. K. RICHTMYER and E. H. KENNARD, *Introduction to Modern Physics*, McGraw-Hill Book Company, New York, 1942.
15. J. STEFAN, "On the relation between thermal radiation and temperature," *Sitz. d. k. Ges. d. Wiss. zu Wien*, II. Abt., Vol. 79, p. 391, 1879.
16. O. LUMMER and E. PRINGSHEIM, "The radiation of a black body between 100° and 1300° C.," *Ann. Physik*, Vol. 63, pp. 395-410, 1897.
17. L. BOLTZMANN, "On a relation of heat radiation to the Second Law discovered by Mr. Bartoli," *Ann. Physik*, Vol. 22, pp. 31-39, 1884.
18. O. LUMMER and E. PRINGSHEIM, "The distribution of energy in the spectrum of the black body," *Verhandl. deut. physik. Ges.*, Vol. 1, pp. 23-41, 1899.
19. W. WIEN, "Temperature and entropy of radiation," *Ann. Physik*, Vol. 52, pp. 132-165, 1894.
20. R. T. BIRGE, "New table of values of the general physical constants (as of August, 1941)," *Rev. Mod. Phys.*, Vol. 13, pp. 233-239, 1941.
21. W. WIEN, "On the energy distribution in the emission spectrum of a black body," *Ann. Physik*, Vol. 58, pp. 662-669, 1896.
22. LORD RAYLEIGH, "Remarks upon the law of complete radiation," *Phil. Mag.*, Vol. 49, pp. 539-540, 1900.
23. M. PLANCK, "On the theory of the law of energy distribution in the normal spectrum," *Verhandl. deut. physik. Ges.*, Vol. 2, pp. 237-245, 1900.
24. W. D. BUCKINGHAM and C. R. DEIBERT, "The concentrated-arc lamp," *J. Optical Soc. Am.*, Vol. 36, pp. 245-250, 1946.
25. W. UYTERHOEVEN, *Elektrische Gasentladungslampen*, Springer, Berlin, 1938.
26. G. R. FONDA and A. H. YOUNG, "The a-c sodium vapor lamp," *Gen. Elec. Rev.*, Vol. 37, pp. 331-338, 1934.



27. *International Critical Tables*, Vol. 5, McGraw-Hill Book Company, New York, 1926-1930.
28. N. K. CHANEY, V. C. HAMISTER, and S. W. GLASS, "Properties of carbon at arc temperature," *Trans. Am. Electrochem. Soc.*, Vol. 57, pp. 107-148, 1935.
29. D. D. KNOWLES, Westinghouse Research Laboratories (private communication).
30. W. E. FORSYTHE, "Arcs—their operation and light output," *Trans. Illum. Eng. Soc.*, Vol. 35, p. 127, 1940.
31. J. W. MARDEN, N. C. BEESE, and G. MEISTER, "Brightness of the mercury arc," *Trans. Illum. Eng. Soc.*, Vol. 33, pp. 147-158, 1939.
32. W. ELENBAAS, "On the brightness attainable with super-high pressure mercury arcs," *Z. tech. Physik.*, Vol. 17, pp. 61-63, 1936.
33. A. E. KNOWLTON, *Standard Handbook for Electrical Engineers*, McGraw-Hill Book Company, New York, 1941 (Section 16).
34. W. ROGOWSKI and E. RÜHLEMAN, "The Braun tube as light source," *Arch. Elektrotech.*, Vol. 24, pp. 691-692, 1930.
35. H. E. IVES, "The luminous properties of the black body," *J. Optical Soc. Am. and Rev. Sci. Instr.*, Vol. 12, pp. 75-78, 1926.
36. O. TUMLIRZ, "The mechanical equivalent of light," *Ann. Physik*, Vol. 38, pp. 640-662, 1889.
37. P. DRUDE, *The Theory of Optics*, translated by C. R. MANN and R. A. MILLIKAN, Longmans, Green, and Co., London, 1902.
38. R. B. BARNES and M. CZERNY, "Observations with the eye of a shot effect for photons," *Z. Physik*, Vol. 79, pp. 436-449, 1932.
39. E. MARX, "Theory of the accumulation of energy with intermittent illumination and the basis of the law of black-body radiation," *Ann. Physik*, Vol. 41, pp. 161-190, 1913.
40. A. EINSTEIN, "A heuristic standpoint concerning the production and transformation of light," *Ann. Physik*, Vol. 17, pp. 132-148, 1905.
41. A. L. REIMANN, *Thermionic Emission*, Chapman & Hall, Ltd., London, 1934.
42. R. A. MILLIKAN, "A direct photoelectric determination of Planck's 'h'," *Phys. Rev.*, Vol. 7, pp. 355-388, 1916.
43. R. H. FOWLER, "The analysis of photoelectric sensitivity curves for clean metals at various temperatures," *Phys. Rev.*, Vol. 38, pp. 45-56, 1931.
44. R. J. CASHMAN and W. S. HUXFORD, "Photoelectric properties of pure and gas-contaminated magnesium," *Phys. Rev.*, Vol. 48, pp. 734-741, 1938.
45. N. C. JAMISON and R. J. CASHMAN, "Photoelectric properties of barium and calcium," *Phys. Rev.*, Vol. 50, pp. 624-631, 1936.
46. E. RUTHERFORD, "The scattering of  $\alpha$  and  $\beta$  particles by matter and the structure of the atom," *Phil. Mag.*, Vol. 21, pp. 669-688, 1911.
47. N. BOHR, "On the constitution of atoms and molecules," *Phil. Mag.*, Vol. 26, pp. 1-25, 476-502, 857-875, 1913.
48. R. POHL and P. PRINGSHEIM, "The photoelectric sensitivity of alkali metals as function of wave length," *Verhandl. deut. physik. Ges.*, Vol. 12, pp. 215-228, 1910.
49. K. MITCHELL, "Theory of the surface photoelectric effect in metals," *Proc. Roy. Soc. (London)*, Vol. A 146, pp. 442-464, 1934; Vol. 153, pp. 513-533, 1936.
50. I. TAMM and S. SCHUBIN, "Theory of the photoeffect of metals," *Z. Physik*, Vol. 68, pp. 97-113, 1931.
51. H. Y. FAN, "Theory of photoelectric emission from metals," *Phys. Rev.*, Vol. 68, pp. 43-52, 1945.
52. E. F. SEILER, "Color-sensitiveness of photoelectric cells," *Astrophys. J.*, Vol. 52, pp. 129-153, 1920.

## Chapter 3

# PHOTOSENSITIVE SURFACES

Normally the photoemissive process takes place in a thin surface layer of the emitter. This fact might be expected to follow from the relative opacity of the metals—which constitute many of our photoemitters—for the exciting light. It is even to a greater extent a consequence of the very small penetration of the electrons which have acquired energy from the light within the emitter. The attainment of desirable photoemissive characteristics depends, therefore, on the suitable physical and chemical treatment of the emissive surface.

**Alkali Films on a Metal Base.** It has already been noted that, of all the metals in bulk, the alkali metals exhibit the greatest sensitivity to visible radiation. Geitel<sup>1</sup> found a platinum anode in a potassium phototube to be similarly photosensitive, although pure platinum metal was known to respond only to ultraviolet radiation. Heating the anode caused the photosensitivity to vanish; after cooling it gradually returned to its original point. Geitel correctly attributed this effect to the deposition on the anode of potassium atoms from the vapor present in the tube. Heating evaporated the absorbed potassium and destroyed the photosensitivity of the surface.

The effect described has a close relation to experiments carried out by Taylor and Langmuir<sup>2</sup> and Becker<sup>3</sup> on the thermionic emission of tungsten surfaces which had been exposed to cesium vapor. These and earlier studies resulted in the following findings.

1. A tungsten wire exposed for a short time to cesium vapor gives off, when heated, only positively charged cesium ions, *not* cesium atoms. From the known pressure of the cesium vapor the rate of deposition, and hence the coverage, of the cesium on the tungsten can be inferred. The evaporation of the cesium in the form of ions takes place only up to the time when approximately one-

<sup>1</sup> See reference 1.

<sup>2</sup> See reference 2.

<sup>3</sup> See reference 3.

eighth of the tungsten surface is covered with cesium atoms. For greater coverages an increasing fraction of the cesium leaves the tungsten wire as neutral atoms.

2. The work function of the tungsten surface decreases from the value for pure tungsten (4.54 electron volts) with increasing coverage of the tungsten by the cesium atoms, reaching a minimum (1.54 electron volts) when the coverage is nearly complete. As more than a monatomic layer of cesium is deposited it begins to increase again, approaching eventually the value for cesium in bulk (1.81 electron volts). A monatomic layer of cesium corresponds to about  $4 \cdot 10^{18}$  atoms per square meter of the surface.

On the basis of these observations it is possible to construct a picture of the adsorption process. Because the tungsten surface has high elec-

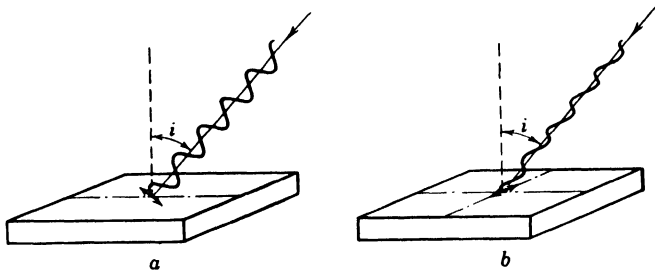


FIG. 3.1. Illumination of a Surface with Polarized Light: (a) with the Electric Vector in the Plane of Incidence and (b) with the Electric Vector Normal to the Plane of Incidence ( $i$  = angle of incidence).

tron affinity, reflected in its high work function, the peripheral or valence electrons of the first cesium atoms are drawn into the metal, their cores remaining bound tightly to the surface by electrostatic forces as positively charged ions. These charged ions, together with the electron cloud at the metal surface, form an electric double layer with the positive charge on the outside. This layer facilitates the escape of electrons from the metal and reduces the work function of the surface. The presence of the adsorbed ions reduces the polarizing force of the surface on cesium atoms which arrive later and are deposited between the ions; these atoms, therefore, retain their complete structure. However, the electron cloud surrounding the nucleus is displaced toward the surface, so that these adsorbed atoms also contribute to the electric double layer, resulting in a further decrease in the work function. This situation holds until the tungsten surface is practically blanketed by a single layer of cesium ions and atoms. The addition of more cesium atoms

actually decreases the effective strength of the electric double layer, so that a slow increase of the work function takes place until the surface has assumed the properties of the adsorbed metal in bulk.

This model accounts satisfactorily for the observed variation of the photoelectric threshold for metallic cathodes on which alkali metals are deposited, just as it explains the change in thermionic emission with the thickness of the adsorbed layer. The selective maximum of the spectral response curve remains to be accounted for. This maximum is observed if the electric vector of the light incident on the surface has a component normal to it. This is always the case for a rough surface or a surface illuminated obliquely by unpolarized light or light polarized so that its electric vector is parallel to the plane of incidence. The selective effect is *not* observed for a microscopically smooth surface illuminated perpendicularly or, generally, by light polarized so that its electric vector is normal to its plane of incidence (Fig. 3.1). It has this property in common with the very much smaller surface photoelectric effect of pure metals, mentioned on page 33.<sup>4</sup>

Figure 3.2<sup>5</sup> shows the spectral response curves for an obliquely illuminated platinum mirror on which films of potassium were deposited. A very thin film has a normal response curve similar to that of pure platinum with the threshold shifted to longer wave lengths. For an approximately monatomic layer (curve I) the maximum excursion of the threshold is observed and the selective maximum is just noticeable. As the thickness is increased beyond this point the threshold wanders back toward shorter wave lengths and the selective maximum becomes very pronounced (curves II and III), eventually declining once more. By the time the potassium film has become barely visible, the photo-emission of the surface has again become relatively small (curve IV).

Brady,<sup>6</sup> building up alkali films by letting an atomic beam impinge on a cooled, freshly evaporated silver surface, found values for the

<sup>4</sup> The periodic regularity of the surface film, as well as the pure metal surface, in its plane restricts the excitation of electrons by electric fields in this plane (electric vector normal to the plane of incidence) to higher frequencies in the same manner as the three-dimensional periodicity in the interior of the crystal lattice of the metal restricts the excitation of electrons to such frequencies (volume effect) for any orientation of the exciting field. However, the work of Ives and Briggs, discussed on page 42, shows that such selectivity with regard to the polarization of the incident light is to be expected for any thin alkali film deposited on a mirror surface, irrespective of the regularity of the surface film. It is simply a consequence of the fact that, at the surface of a perfect conductor, the electric field component parallel to the surface must vanish.

<sup>5</sup> See Suhrmann and Theissing, reference 4.

<sup>6</sup> See reference 5.

maximum excursion of the threshold ( $\lambda_{o \max}$ ), the corresponding number of layers of alkali atoms ( $n_o$ ), the number of layers leading to the greatest total photoemission (most pronounced selective maximum— $n_1$ ), and

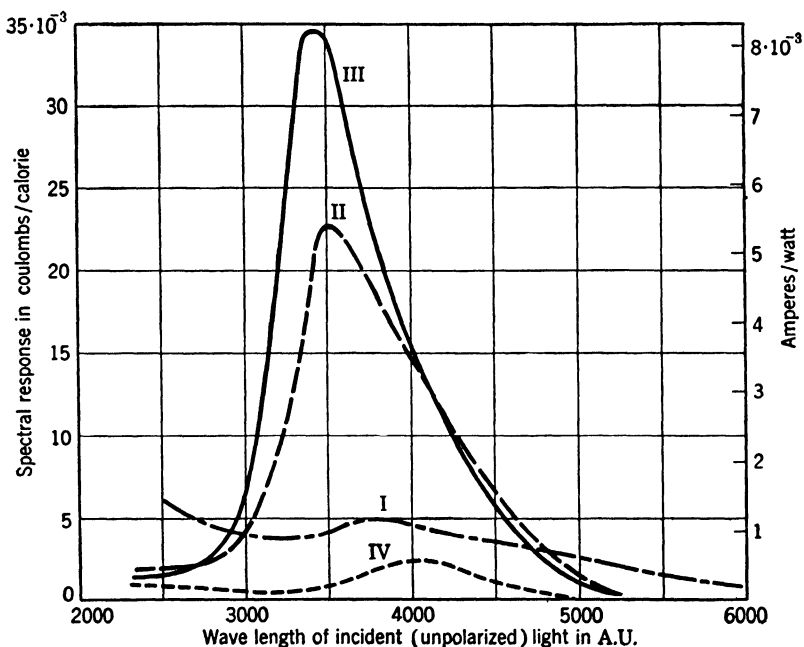


FIG. 3.2. Spectral Response of Potassium Films of Increasing Thickness (I-IV) Deposited on a Platinum Mirror. (Suhrmann and Theissing, reference 4.) I: Nearly monatomic film. II, III: Invisible films of greater thickness. IV: Film thick enough to be visible as a clouding of the mirror (unpolarized light, incident at 60 to 70° to the normal). (By permission of the Attorney General in the public interest under License No. JA-1351.)

the number of layers ( $n_2$ ), and the threshold ( $\lambda_{o2}$ ) for which the photoemission was stabilized, that is, exhibited the properties of the alkali metal in bulk. These values are shown here in tabular form.

Element	$\lambda_{o \max}$ A.U.	$n_o$	$n_1$	$\lambda_{o2}$	$n_2$
Potassium	5800	3	12.4	5500	19
Rubidium	6200	1.5	5.0	5900	12
Cesium	6600	1.5	5.0	6300	10

As de Boer <sup>7</sup> points out, the number of monatomic layers ( $n_o$ ,  $n_1$ ,  $n_2$ ) given by Brady are probably too large, since Brady did not correct for the roughness of the silver surface. He raises the further objection that, at the low temperature of the cathode, the surface mobility of the adsorbed alkali atoms was probably too small to establish uniform

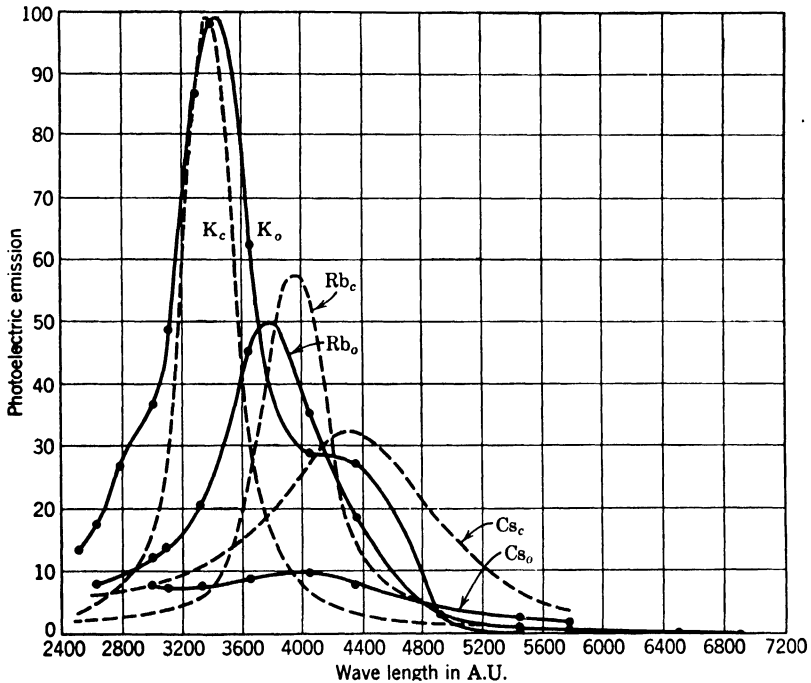


FIG. 3.3. Light Absorption (subscript  $c$ ) and Spectral Response (subscript  $o$ ) of Alkali Films Deposited on Platinum-Iridium Mirrors. (Ives and Briggs, reference 8.) (Courtesy of the *Journal of the Optical Society of America*.)

layers. Nevertheless, the conclusion is almost certainly justified that the spectral selective maximum reaches its greatest value for film thicknesses several times (3 to 4) as great as those leading to the lowest work function.

The findings described above suggest that the selective photoeffect has its origin in the adsorbed film rather than in the base metal. This point of view received strong support from the interesting observation of Fleischmann <sup>8</sup> that thin films of alkali metals deposited on quartz plates were scarcely visible in light incident on them perpendicularly or,

<sup>7</sup> See reference 6.

<sup>8</sup> See reference 7.

generally, light polarized so that the electric vector was normal to the plane of incidence. In oblique illumination with the electric vector parallel to the plane of incidence they exhibited lively colors which were complementary to the colors for which the selective response of the films is a maximum. There is, thus, perfect correspondence between the conditions for the absorption of light by thin alkali films and the conditions for the selective photoeffect.

The recent studies of Ives and Briggs<sup>9</sup> on the spectral response of platinum-iridium surfaces on which films of potassium, rubidium, and cesium were deposited go considerably further. The measurements were made on cathodes at room temperature, in thermal equilibrium with the walls of the vacuum tube, on which there was an excess of the alkali metal. Figure 3.3 compares the measured spectral response curves with the light absorption in the alkali film, as determined by the optical constants of both the base metal and the alkali metal. The effect of the thin alkali film on the standing wave pattern above the platinum-iridium surface was neglected. When it was taken into account, both the positions and the width of the absorption maxima were shifted so as to improve the correspondence. In fact, assuming an emission probability of the excited photoelectrons proportional to  $\nu - \nu_0$  ( $\nu_0$  = threshold frequency) and subtracting from the experimental curves minor peaks which could be attributed to contaminations, Ives and Briggs attained a practically perfect coincidence of their experimental and theoretical curves.

The various observations described in the preceding section lead to the following conclusions, accepted by the majority of the workers in the field:

1. The normal photoeffect, excited by light in any state of polarization, arises from the excitation of the electrons of the base metal, whose escape may be facilitated by the surface film. It is responsible, in general, for photoemission at the threshold.
2. The selective photoeffect, excited by light polarized parallel to the plane of incidence and incident obliquely on the surface, results from the photoionization of the adsorbed atoms. The base metal will affect the position of the selective maximum only insofar as it modifies the binding force of the peripheral electrons to the adsorbed atoms. It also serves the purpose of supplying electrons to the adsorbed atoms after ionization, restoring the surface to its original condition.

The above interpretation of the origin of the selective photoeffect applies not only to a film of active metal adsorbed on a more passive

<sup>9</sup> See reference 8.

metallic base but also to many of the more complex surface structures considered in the following sections.

**The Effect of Adsorbed Oxygen.** Metallic electrodes in vacuum tubes almost always have a certain amount of oxygen adsorbed on their surface. The adsorbed negative oxygen ions form an electrical double layer whose polarity is such as to impede electron emission and to increase the work function. If the surface is heated to a sufficiently high temperature the oxygen may be driven off and the thermionic emission

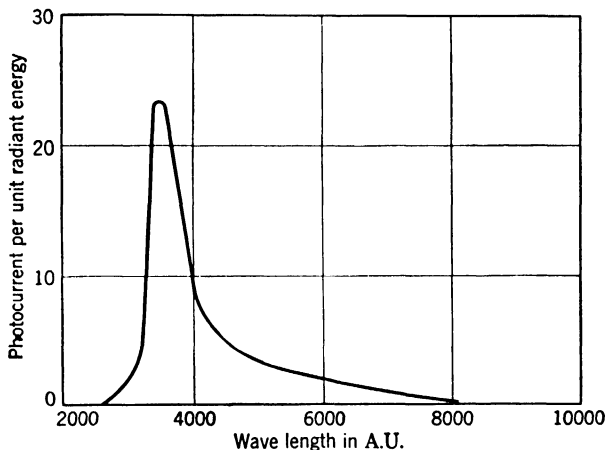


FIG. 3.4. Spectral Response of [Ag]-O-Cs Surface. (Koller, reference 10.)  
(Courtesy of the *Physical Review*.)

and photosensitivity may increase. However, unless precautions are taken, oxygen will quickly be readsorbed as the surface cools.

Under certain circumstances the adsorbed oxygen may, however, perform a useful purpose. Thus Kingdon<sup>10</sup> found that if tungsten, oxidized by being briefly heated to 1900° K in oxygen at a pressure of 0.02 millimeter of mercury, was exposed to cesium vapor, a thermionic emitter was formed which was more stable than the tungsten-cesium surface, and yet had an even lower work function (0.71 electron volt). This condition was attained after the surface was "flashed" at 1600° K, this final heat treatment making it possible for the oxygen atoms and cesium atoms to assume their most favorable positions. The adsorbed layer of oxygen and cesium was distinctly less than monatomic, and the spectral response curve, whose threshold wave length was shifted well into the infrared, exhibited no selective maximum. A similar experiment, carried out with silver as the base metal and with a lower-tempera-

<sup>10</sup> See reference 9.



ture thermal treatment (at 300° C), led to a response curve with a decided selective maximum. This lay, however, far toward the violet end of the spectrum <sup>11</sup> (Fig. 3.4).

More recent work by Rentschler and Henry <sup>12</sup> on the photoemission of extremely clean, sputtered metal surfaces, on which small amounts of potassium were distilled, even suggests that the presence of oxygen or some other contaminant capable of reacting with the alkali metal is essential for the formation of a surface whose threshold is shifted toward longer wave lengths relative to that of the alkali metal in bulk.

**Potassium Hydride Phototubes.** It has already been seen in Chapter I that the first phototubes which showed a high and constant emission in the visible did not apply oxygen, but hydrogen, as sensitizing agent. Hydrogen, like oxygen, is readily adsorbed by many metals. Unlike oxygen, it generally decreases, rather than increases, the work function, being adsorbed in the form of positive rather than negative ions.

This adsorption of hydrogen is not, however, responsible for the great increase in sensitivity which Elster and Geitel observed in the treatment of potassium with hydrogen. In fact, Elster and Geitel <sup>13</sup> found that the admission of hydrogen into their potassium phototubes destroyed the photosensitivity. Only after a glow discharge in the hydrogen atmosphere did the light response take on a high value, exhibiting a prominent selective maximum in the blue.

Later researches established definitely that in these phototubes the hydrogen is not adsorbed in the form of positive ions, but combines with the potassium to form the photoelectrically insensitive, colorless salt potassium hydride. It is the formation of an adsorbed layer of potassium metal on the surface of the potassium hydride which is responsible for the pronounced selective photoeffect observed.

Highly purified (molecular) hydrogen gas does not react with potassium in bulk, nor does it affect its photosensitivity, even if a glow discharge is passed through the tube.<sup>14</sup> The essential component for the reaction is hydrogen in the atomic form; it may be provided directly by the emission of hydrogen ions from a heated tungsten filament in hydrogen at a low pressure <sup>15</sup> or by the reaction of the potassium with water vapor which may be present in the hydrogen gas as an impurity. The final stage of activation, namely, the formation of a potassium film adsorbed on the surface of the hydride, may occur by the sputtering of

<sup>11</sup> See Koller, reference 10.

<sup>12</sup> See reference 11.

<sup>13</sup> See reference 12.

<sup>14</sup> See Suhrmann and Theissing, reference 13.

<sup>15</sup> See Rijnoff, reference 14.

potassium metal (in the glow discharge), the migration of potassium atoms over the surface of the hydride crystals (if the surface temperature is not too low), or by direct evaporation of potassium on the hydride layer. The last process was employed by Lukirsky and Rijanoff,<sup>16</sup> who systematically built up layers of potassium hydride and potassium films and observed the effect of this procedure on the photoemission. In a notation introduced by J. H. de Boer and M. C. Teves

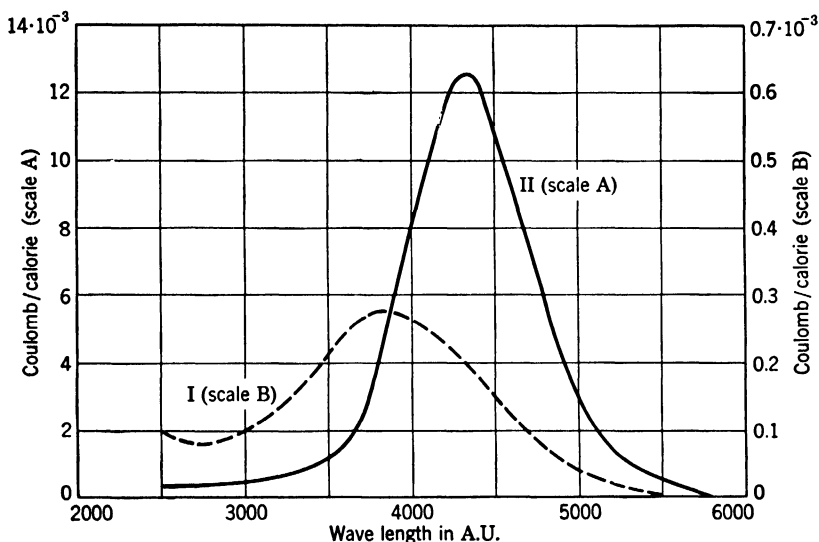


FIG. 3.5. Spectral Response Curves of a Compact Potassium Surface. I: Directly after Distillation. II: After Passage of Glow Discharge in Hydrogen. (Suhrmann and Theissing, reference 13.) (By permission of the Attorney General in the public interest under License No. JA-1351.)

photoemissive surfaces of this type may be represented by the symbol [K]-KH-K. The symbol in brackets represents the base; the components of the several layers are separated by hyphens.

A typical response curve for a sensitized potassium hydride surface ([K]-KH-K) is shown in Fig. 3.5. The selective maximum lies near 4350 Angstrom units, the long-wave threshold at 5900 Angstrom units. The behavior of the [K]-KH-K surface is quite analogous to that of surfaces with intermediate salt layers studied by de Boer and Teves.<sup>17</sup> A thin layer of calcium fluoride was deposited by evaporation on a silver base and exposed to a steady supply of cesium. The resulting surface acted as a photocathode. As the deposition of cesium on the surface increased, the photoemission first increased linearly, rose to a

<sup>16</sup> See reference 15.

<sup>17</sup> See reference 16.

maximum at a diminishing rate, and eventually fell again to a constant value corresponding to a compact layer of cesium (Fig. 3.6). Beginning with the point of maximum response, the surface takes on an increasingly deep blue coloration.

De Boer and Teves interpret the variation in the following manner. The initial increase in response corresponds to the binding of the incident cesium atoms on the most active points, such as projecting corners

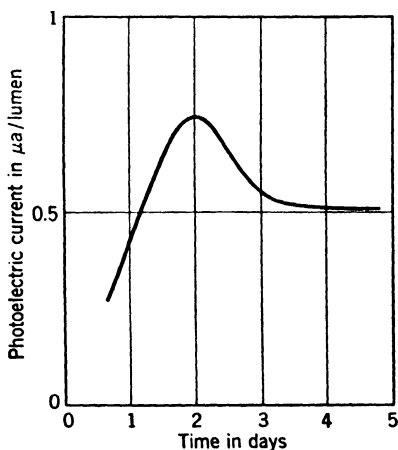


FIG. 3.6. Variation of Photoemission with Time of Deposition of Cesium on a Calcium Fluoride Layer on Silver. (de Boer and Teves, reference 16.)

and edges, of the calcium fluoride lattice. The binding here reduces the energy required for the ionization of the adsorbed atoms to the point that the absorption is primarily in the infrared. As the most active spots are occupied and the binding of the cesium atoms decreases, the absorption shifts to the visible, giving rise to the observed blue color. Eventually the atoms form a continuous layer over the surface. As this condition is approached, a reduction in the photocurrent is to be expected. Whereas for individual adsorbed atoms one electron is emitted for every absorbed light quantum, and half of these may be expected to leave the surface, only a fraction of the con-

duction electrons excited by the absorbed light will escape from a continuous surface layer, the remainder being held back by the potential barrier. It should be noted that in the experiment described here the layer of salt was so thin that the adsorbed cesium atoms, when ionized by light, could draw electrons from the base metal through the salt layer by virtue of their strong electrostatic fields ("cold emission"), resulting in their neutralization and the restoration of the original state.

**Photocathodes with Intermediate Oxide Layers; the Silver-Cesium Oxide-Cesium Phototube.** The possibility of sensitizing alkali surfaces with oxygen instead of hydrogen was realized by Pohl and Pringsheim<sup>18</sup> as early as 1913. It was found that the introduction of dry oxygen in the evacuated potassium phototube caused the formation of a colored layer accompanied by the appearance of a selective response maximum at 4050 Angstrom units. The surface so obtained may be described by

<sup>18</sup> See reference 17.

the symbol  $[K]-K_2O-K$ , the colloidal potassium metal giving rise to the coloration being adsorbed on a layer of an oxide of potassium. The same phenomenon does not, however, take place with cesium.<sup>19</sup> Here the oxide, as soon as formed, dissolves in the remaining cesium. Hence the emission properties are not materially affected until the cesium is almost completely oxidized. If the cesium is originally deposited on a metallic base such as silver and if, after complete oxidation, a slight amount of cesium is sublimed onto the surface, a photocathode is

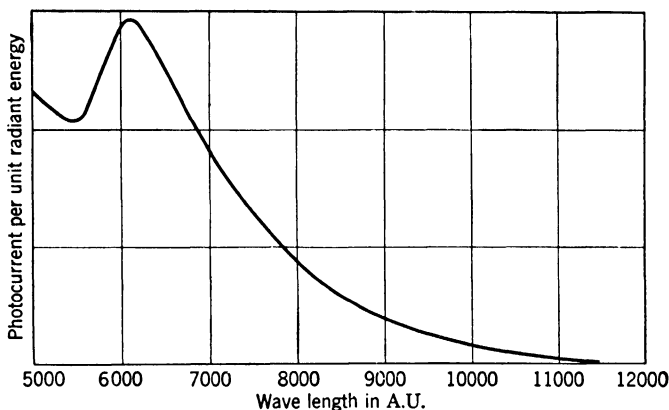


FIG. 3.7. Spectral Response Curve of a  $[Ag]-Cs_2O-Cs$  Surface. (de Boer and Teves, reference 16.)

obtained with a threshold in the neighborhood of 11,500 Angstrom units and a pronounced selective maximum at 6070 Angstrom units. A typical response curve is shown in Fig. 3.7.<sup>20</sup> In the notation of de Boer and Teves a surface prepared as described may be represented by  $[Ag]-Cs_2O-Cs$ .

In order to have a photocathode with a cesium-on-oxide layer highly sensitive in the infrared and visible, two conditions must be fulfilled. (1) A large number of highly active places must exist in the oxide lattice which will adsorb cesium atoms so that they can be ionized by light quanta of low energy, and (2) the intermediate layer must be sufficiently conductive that ionized adsorbed atoms may be readily neutralized by electrons from the base metal. The first condition demands, patently, relatively thick, porous, oxide layers and techniques which will promote the adsorption of cesium throughout the layer. The second would most readily be fulfilled by very thin layers; in any case its

<sup>19</sup> See Koller, reference 10.

<sup>20</sup> See de Boer and Teves, reference 16.

fulfilment may be approached more closely by dispersing metal atoms in the oxide layer. For this reason the technique introduced by Koller<sup>21</sup> of first oxidizing the silver, then admitting cesium and baking the photocathode at about 200° C, leads both to a higher response and to a longer wave-length threshold (arising from the greater number and strength of the active centers within the layer) than any procedure described so far. The cesium reacts with the silver oxide to form

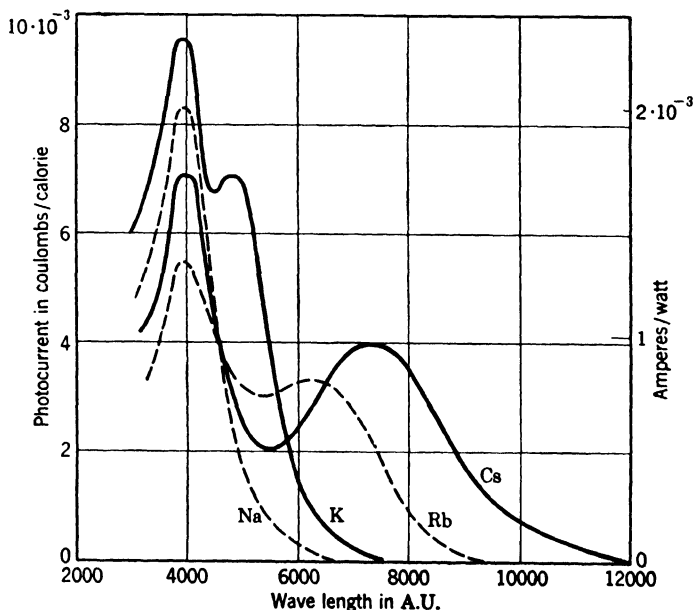


FIG. 3.8. Spectral Response Curves for [Ag]—Cs<sub>2</sub>O, Ag—Cs, [Ag]—Rb<sub>2</sub>O, Ag—Rb, [Ag]—K<sub>2</sub>O, Ag—K, and [Ag]—Na<sub>2</sub>O, Ag—Na Photocathodes. (Kluge, reference 18.)

cesium oxide with the freed silver dispersed through the layer and the cesium atoms adsorbed on the active places. This surface is thus appropriately designated by [Ag]—Cs<sub>2</sub>O, Ag—Cs.

Essentially the same technique is applicable to all the alkalis. Figure 3.8 shows a series of curves obtained by Kluge<sup>22</sup> for cathodes activated in this manner with cesium, rubidium, potassium, and sodium. The interesting point is the existence of two characteristic maxima (which coincide for sodium). The short-wave-length maximum, whose position does not vary appreciably with the atomic number of the alkali, has been attributed to light absorption by alkali atoms adsorbed

<sup>21</sup> See reference 10.

<sup>22</sup> See reference 18.

next to alkali ions. The long-wave maximum, which shifts toward shorter wave lengths as the atomic number is decreased, is ascribed to light absorption by alkali atoms adsorbed on the neutral surface of the oxide.

A further increase in sensitivity has been attained by evaporating a great variety of metal atoms, in particular gold and silver,<sup>23</sup> on the

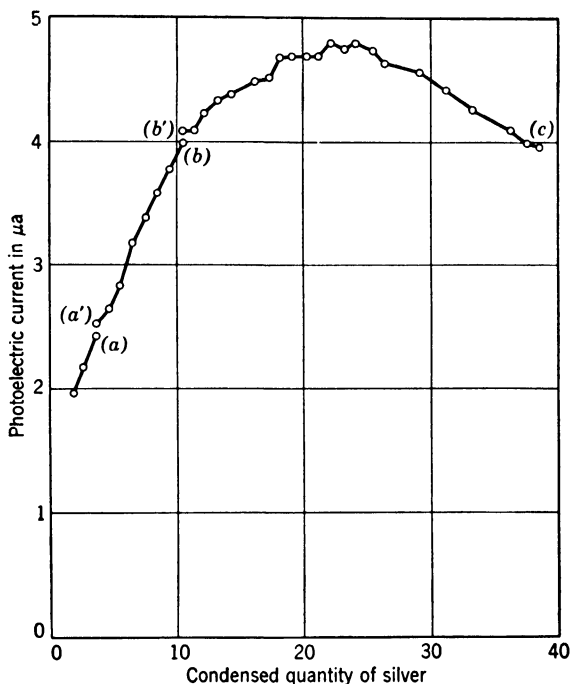


FIG. 3.9. Effect of Treating Thin-Layer [Ag]— $\text{Cs}_2\text{O}$ , Ag, Cs—Cs Surface with Evaporated Silver. Points *a*, *b*, and *c* indicate the instant at which curves 2, 3, and 4, respectively, in Fig. 3.10, were obtained. (Asao, reference 20.)

prepared cathode and subjecting the cathode to a second thermal treatment. Figure 3.9 shows the effect of treating a relatively thin layer cathode (having originally seventy molecular layers of silver oxide) with evaporated silver.<sup>24</sup> The original cathode, which had absorbed enough cesium to replace all the silver in the  $\text{Ag}_2\text{O}$ , leaving one free cesium atom to every ten molecules of  $\text{Cs}_2\text{O}$  (and twenty dispersed silver atoms), had a sensitivity of 7 to 10 microamperes per lumen, measured with a tungsten filament source having a color temperature

<sup>23</sup> See Asao and Suzuki, reference 19.

<sup>24</sup> See Asao, reference 20.

of  $2700^{\circ}\text{K}$ . The maximum increase—to 50 microamperes per lumen—was obtained when two-thirds as many additional silver atoms had been deposited as there were  $\text{Cs}_2\text{O}$  molecules. The increase in total

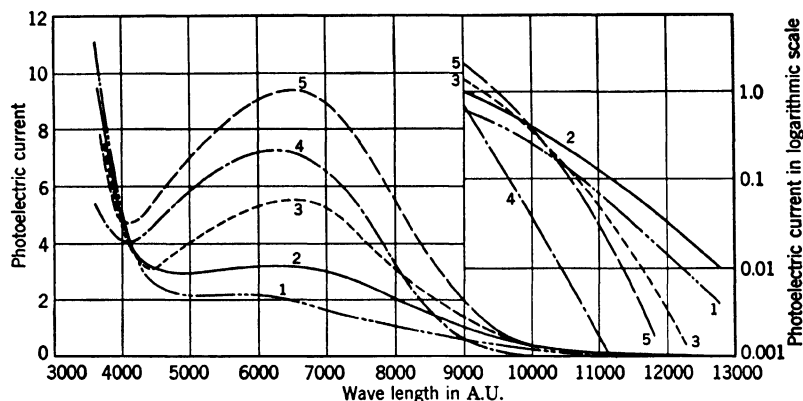


FIG. 3.10. Effect of Evaporation of Silver on Spectral Response of Thin-Layer  $[\text{Ag}]-\text{Cs}_2\text{O}$ ,  $\text{Ag}$ ,  $\text{Cs}-\text{Cs}$  Cathode. (1) Untreated Cathode. (2-4). Response after Deposition of Different Amounts of Silver (see Fig. 3.9). (5) Response after Heat Treatment of Cathode with Response 4. (Asao, reference 20.)

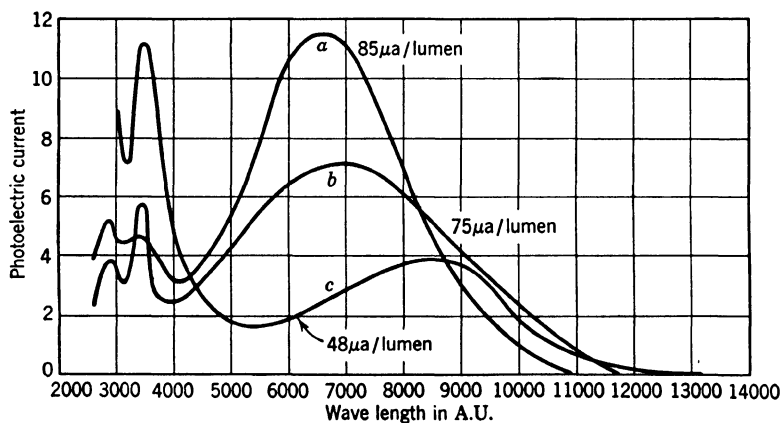


FIG. 3.11. Spectral Response of Thick-Layer  $[\text{Ag}]-\text{Cs}_2\text{O}$ ,  $\text{Ag}$ ,  $\text{Cs}-\text{Cs}$  Cathodes (a and b) Treated with Evaporated Silver Compared with That of a Thin-Layer Cathode (c) Similarly Treated. (Asao, reference 20.)

emission is accompanied by a decrease in the long-wave threshold and, hence, in thermionic emission (Fig. 3.10). Asao was also able to increase the photoemission of thicker cathodes, having initially 150 to 200 layers of silver oxide on a specular base, from 20 to 30 microamperes

per lumen up to 95 microamperes per lumen. This enhancement was accompanied by a shift of the long-wave maximum from the infrared into the visible (Fig. 3.11) and reduced photoelectric fatigue.<sup>25</sup> Two further observations of interest were made by Asao.

1. The activation with cesium of a fully oxidized silver layer on quartz resulted in a film with metallic conduction (normal temperature coefficient of resistance).
2. The activation of a  $\text{Cs}_2\text{O-Cs}$  layer on quartz with evaporated silver resulted in a semiconducting film (negative temperature coefficient of resistance).

These observations suggest that, although the original, reduced, silver tends to form larger aggregates and metal bridges parallel to the sur-

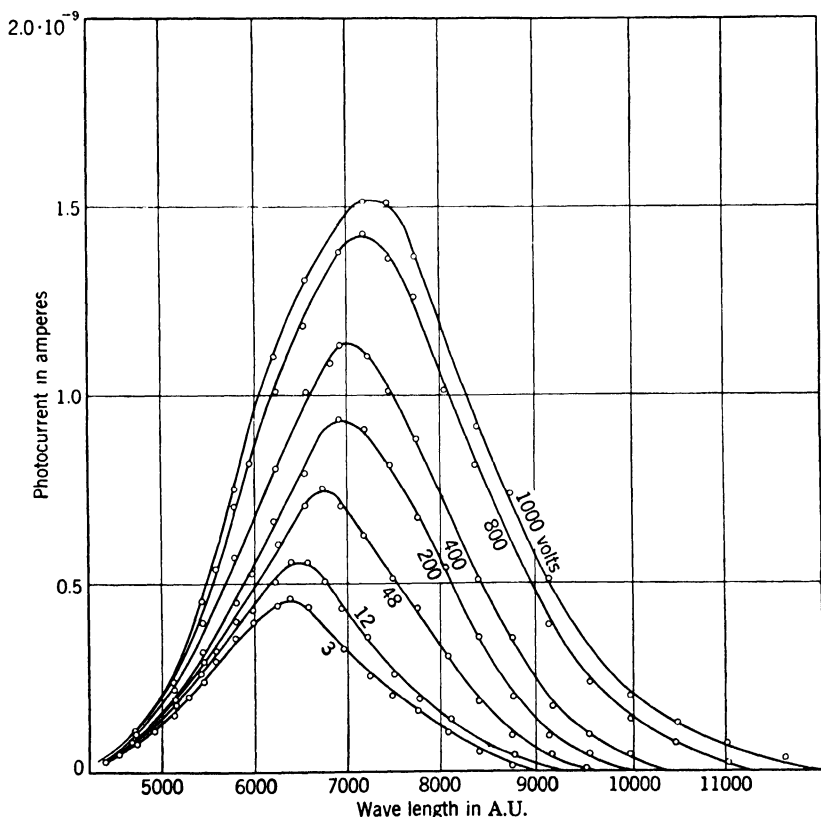


FIG. 3.12. Spectral Response of Barium-Strontium Oxide Cathode for Different Accelerating Potentials. (Huxford, reference 23.) (Courtesy of the *Physical Review*.)

<sup>25</sup> See p. 53.



face, the silver evaporated subsequently does not. Asao attributes the increase in work function resulting from the evaporation of the silver to the adsorption of silver atoms to the cesium oxide close to the adsorbed cesium atoms, resulting in a weakening of the binding of the cesium atoms to the cesium oxide.

The very high sensitivities attained by Asao by the subsequent deposition of silver atoms are not unique. Comparable results have

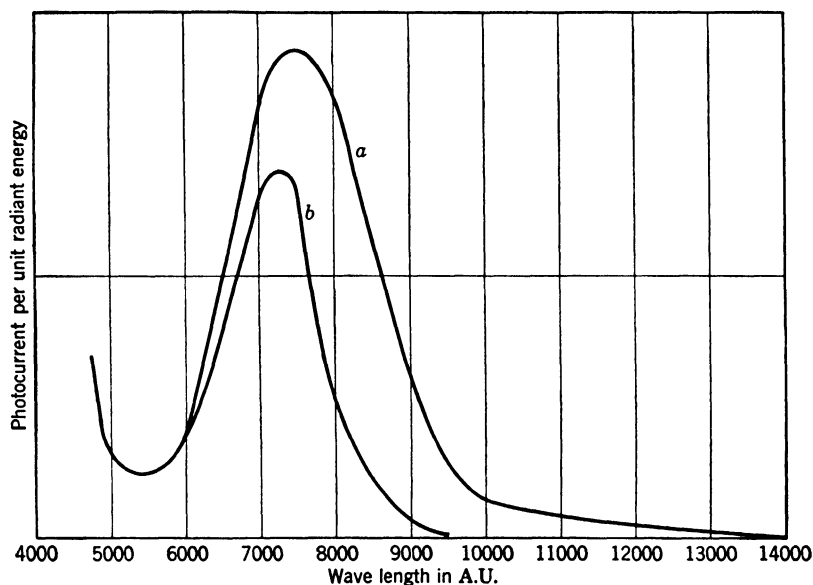


FIG. 3.13. Spectral Response of [Ag]—Cs<sub>2</sub>O, Cs, Ag—Cs Photocathode (a) before and (b) after Prolonged Exposure. (de Boer and Teves, reference 24.)

been achieved in other laboratories by different methods. Various refinements in procedure, furthermore, have been used to obtain special effects, such as pushing the threshold out as far as 17,000 Angstrom units.<sup>26</sup> Prolonged heating in cesium vapor, partial reduction of the silver oxide layer with hydrogen before activation, and bombarding the surface with cesium ions represent some of the techniques applied.

Quite analogous to the thick-layer alkali oxide-alkali surfaces are the barium and strontium photocathodes first introduced by Case.<sup>27</sup> Some measurements by Huxford on the type of barium-strontium cathode widely employed as thermionic source in vacuum tubes are shown in Fig. 3.12.<sup>28</sup> The increase in photoemission with applied field arises

<sup>26</sup> See de Boer, reference 6, pp. 330–333, and Fleischer and Goerlich, reference 21.

<sup>27</sup> See reference 22.

<sup>28</sup> See Huxford, reference 23.

from the fact that relatively high fields are required to draw electrons from the base metal so as to neutralize adsorbed barium and strontium atoms that have been photoionized.

Thick-layer photocathodes exhibit, furthermore, certain fatigue phenomena which must be attributed to the delayed refurbishing of electrons to ionized adsorbed atoms. If the charge of a number of adsorbed ions is not neutralized, the number of atoms which can be photoionized is decreased on the one hand and the magnitude of the quanta required to ionize the remaining adsorbed atoms is increased on the other. Thus prolonged exposure causes the selective maximum both to become less pronounced and to shift toward shorter wave lengths (Fig. 3.13).<sup>29</sup> The reduced supplementation of electrons results largely from the building up of a space charge in the interior of the oxide layer. Part of the electrons drawn out of the base metal by the field of the adsorbed ions are trapped at various points within the oxide lattice, forming there negatively charged "excitation centers." The resulting space charge screens the field from the base metal and thus prevents the further emission of electrons from the metal. The electrons may be dislodged again by the thermal motion of the lattice, so that eventually the charges are again neutralized. The process may be accelerated by heating or illumination with infrared light. Figure 3.14 shows, for a particular photocathode, the effect of the type of illumination on the fatigue. For the infrared the freeing of the electrons from excitation centers in the semiconducting layer is, in the case examined, sufficient to compensate completely the accumulation of charge by the photoionization of the adsorbed atoms.

A final fatigue effect, most pronounced with high applied voltages, is the drift of the adsorbed alkali ions to the base metal under the influence of the applied field. This drift leads to an impoverishment of the sur-

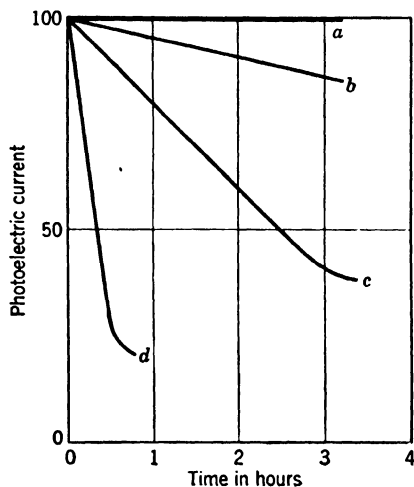


FIG. 3.14. Decrease in Photocurrent from a Particular [Ag]—Cs<sub>2</sub>O, Cs, Ag—Cs Cathode with Exposure to (a) Infrared, (b) Red, (c) Green, and (d) Blue Radiation. (de Boer and Teves, reference 24.)

<sup>29</sup> See de Boer and Teves, reference 24.

face and, hence, to a diminution of the response—especially to long-wave light—with time. After neutralization at the base metal the alkali atoms diffuse again toward the surface, restoring the original condition.

All these effects are least for layers containing large numbers of neutral metal atoms and adsorbed cesium atoms in the interior. The role of the supplementation of electrons in the response characteristics of thick-layer cathodes is well illustrated by the finding of Ramadanoff <sup>30</sup> that

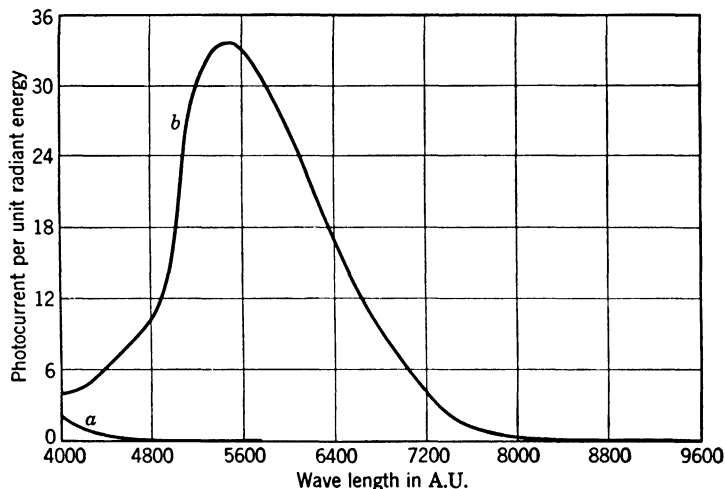


FIG. 3.15. Spectral Response of Sodium Surface: (a) Distilled in Vacuum and (b) Distilled in Air at a Pressure of 1.5 mm Hg. (Reimert, reference 26.) (Courtesy of the *Journal of the Optical Society of America*.)

oxide cathodes exhibited a photoelectric effect (measured by intermittent light) at high temperatures which was sixteen times as large as at room temperature.

It may be mentioned that sensitive photocathodes which are probably fundamentally similar to those described in the preceding paragraphs have been prepared by the distillation of metals onto a cooled surface in air at low pressure (1.5 mm Hg). Thus Reimert <sup>31</sup> found that a gray sodium cathode prepared in this manner had a response threshold near 10,000 Angstrom units (as compared with 5800 Angstrom units for pure sodium) and a selective maximum at 5500 Angstrom units (Fig. 3.15). It is reasonable to assume that the composition of this surface may be represented by  $[M]-Na_2O, Na-Na$ .

<sup>30</sup> See reference 25.

<sup>31</sup> See reference 26.

**Photocathodes with Electronegative Components Other than Oxygen.**

Olpin<sup>32</sup> and Kluge<sup>33</sup> have shown that sulfur, selenium, or tellurium may be substituted for oxygen in alkali photocathodes, leading to only slight changes in the response curves. Their investigations covered the surfaces [K]-K<sub>2</sub>S-K, [K]-K<sub>2</sub>Se-K, [K]-K<sub>2</sub>Te-K, and [Na]-Na<sub>2</sub>S-Na. A small increase in the wave length of the selective maximum with the atomic number of the electronegative component was demonstrated. Olpin obtained a much more pronounced effect by letting both sulfur and oxygen act on a sodium surface. In this manner a selective maximum near 5000 Angstrom units was obtained in addition to the usual one at 3600 Angstrom units. Some of Olpin's curves are shown in Fig. 3.16. Olpin investigated, in addition, the influence of a large number of dyes and organic compounds on the response. Their effect may, in general, be attributed either to their action as light filters or to the sensitizing action of water, present as a component.

**"Alloy Surfaces."** A new type of photosensitive surface was developed by P. Goerlich<sup>34</sup> in an effort to find a highly sensitive semitransparent photocathode. A semitransparent photocathode may be defined as a cathode in which the incidence of the light and the collection of the photocurrent takes place on opposite sides of the sensitive layer. The silver-cesium oxide-cesium phototubes known to Goerlich<sup>35</sup> had the drawback that the metal base layer deposited on glass absorbed and reflected an excessive proportion of the incident light, leading to a low sensitivity, particularly in the red and infrared range. A base metal would be unnecessary if a sensitive film consisting of a conducting alloy rather than a semiconducting oxide or salt layer were employed. Since high sensitivity throughout the visible was required, cesium was logically chosen as one component of the alloy. Of the several metals investigated for red sensitivity, bismuth, as second component, gave the best results, with antimony, thallium, and lead following in sequence. Two typical response curves for a Bi, Cs cathode are shown in Fig. 3.17. The cathodes were prepared by evaporating first a relatively thin layer of bismuth and then exposing it to cesium. The subsequent exposure of the cathode to oxygen at a low pressure may produce shifts of the maximum toward the red, for instance, from 4300 to 6000 Angstrom units; more commonly the shift is small or nonexistent.

<sup>32</sup> See reference 27.

<sup>33</sup> See reference 28.

<sup>34</sup> See reference 29.

<sup>35</sup> As the same author mentions in a later paper (reference 30), semitransparent cathodes of the type [Ag]-Cs<sub>2</sub>O, Ag-Cs can, in fact, be prepared to have sensitivities and spectral response curves similar to those obtained for opaque cathodes.

An extension of the investigation to other combinations of resistive metals and alkalis emphasized the difference in the nature of the "alloy" photosurfaces and the cathodes described in the preceding sec-

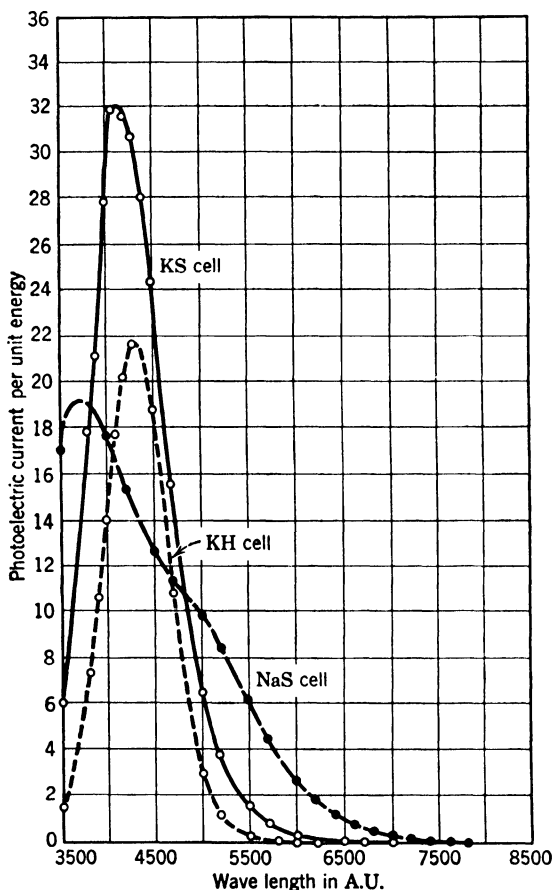


FIG. 3.16. Spectral Response of Potassium Sulfur and Sodium Sulfur Phototubes Compared with That of Potassium Hydride Phototube. (Olpin, reference 27.) (Courtesy of the *Physical Review*.)

tions.<sup>36</sup> One of the most striking factors is the slight dependence of the response of the phototubes on the atomic number of the alkali metals employed. Thus Goerlich found that antimony and bismuth "alloys" with the several alkali metals had response maxima located at the following wave lengths:

<sup>36</sup> See Goerlich, reference 31.

M	Cs	Rb	K	Na	Li
Sb, M	4300-4600	4200-4600	4000	4000-4250	4200-4300
Bi, M	4300	4400	4000-4200	4000 4200	4450 4500

The sensitivity of these photocathodes decreases in the order Cs-Rb-K-Na. The Li cathodes, however, have as great sensitivity as the Rb cathodes and possess the added advantage of very low thermionic emis-

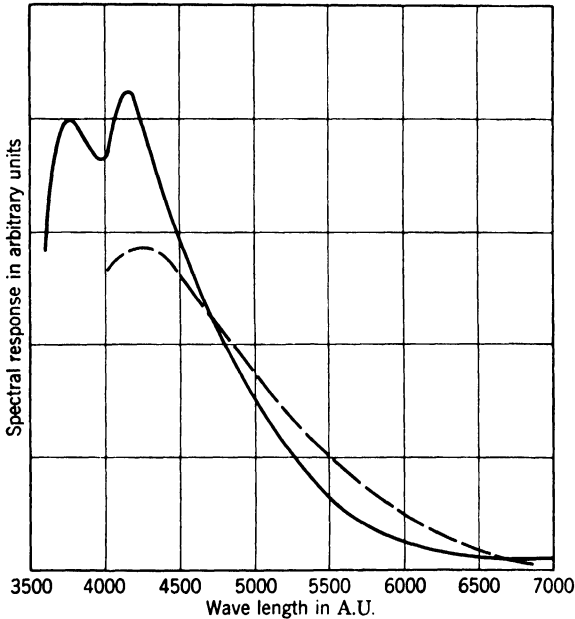


FIG. 3.17. Typical Response Curves for Bi, Cs Photocathodes. (Goerlich, reference 29.) (By permission of the Attorney General in the public interest under License No. JA-1351.)

sion. In absolute measure the sensitivities of the "alloy" cathodes are very high. Goerlich compares the response of antimony-cesium and antimony-lithium cathodes with that of a cesium oxide-cesium cathode to a source of color temperature  $2180^{\circ}\text{K}$  and one with uniform spectral distribution within the indicated ranges as follows:

Range, A.U. [Ag]-	Source with Color Temp. $2180^{\circ}\text{K}$			Uniform Spectral Distribution		
	Sb, Cs	Sb, Li	Cs <sub>2</sub> O, Ag-Cs	Sb, Cs	Sb, Li	Cs <sub>2</sub> O, Ag-Cs
4800-8000	118	34.8	66.0	95.4	39.2	9.5
4000-7000	117.7	34.7	22.1	95.4	39.2	5.5
4150-7150	115.6	32.5	40.4	82.6	33.8	7.2

The absolute sensitivity in the visible exceeds, thus, that of the silver-cesium oxide-cesium phototubes. Hopshtein and Khorosh<sup>37</sup> find for the integral sensitivity of antimony, arsenic, and bismuth "alloys" with cesium maximum values of 70, 40, and 15 microamperes per lumen respectively. N. S. Khlebnikov,<sup>38</sup> who noted the striking absence of fatigue and saturation phenomena in these photocathodes, obtained, for Sb, Cs phototubes and light with a color temperature of 2848° K, sensitivities of 60 to 100 microamperes per lumen. Values as high as 110 microamperes per lumen of 2870° K radiation have been reported from the laboratories of the RCA-Victor Division in Lancaster.

If an Sb, Cs or Bi, Cs cathode of appropriate thickness is evaporated on a silver-cesium oxide-cesium cathode, a response is obtained which is quite flat throughout the visible. Some spectral distribution curves for photosurfaces prepared by Goerlich in this manner are shown in Fig. 3.18.<sup>39</sup>

More recent studies of antimony-cesium and related photosurfaces suggest that the term "alloy photocathode" is a misnomer.<sup>40</sup> The active substance in the antimony-cesium photosurface appears to be not an alloy, but an intermetallic compound  $\text{Cs}_3\text{Sb}$ . As indicated by the measurements of J. A. Burton,<sup>41</sup> of the Bell Laboratories, on thin antimony-cesium films formed on quartz, they have the properties of an intrinsic semiconductor.<sup>42</sup> Burton found (1) that the spectral photoelectric response of the films paralleled their light absorption, as shown in Fig. 3.19,<sup>43</sup> and (2) that the mean depth of origin of the photoelectrons, as determined by the relative photocurrent yield for light incident on the quartz side and the vacuum side of the films, was 250 Angstrom units. The response to polarized light and the high quantum efficiency of the photoeffect (of the order of 23 per cent!) could best be accounted for by assuming a volume photoelectric effect with a quantum efficiency unity and a ready escape of the photoelectrons into vacuum.

The emphasis, in the present chapter, has been placed on the mechanism of photoemission from various types of photoemitters. The conclusions reached are not final. Thus, it is quite conceivable that an internal photoeffect in the semiconducting oxide layer, rather than the photoionization of the adsorbed alkali atoms, may constitute the essen-

<sup>37</sup> See reference 32.

<sup>38</sup> See reference 33.

<sup>39</sup> See Goerlich, reference 30.

<sup>40</sup> See, e.g., Sommer, reference 34.

<sup>41</sup> See reference 35.

<sup>42</sup> See Chapter 10, p. 180.

<sup>43</sup> It may be noted that a minor, secondary peak near 2500 Angstrom units, suggested by the experimental points, has been repeatedly noted by other observers.

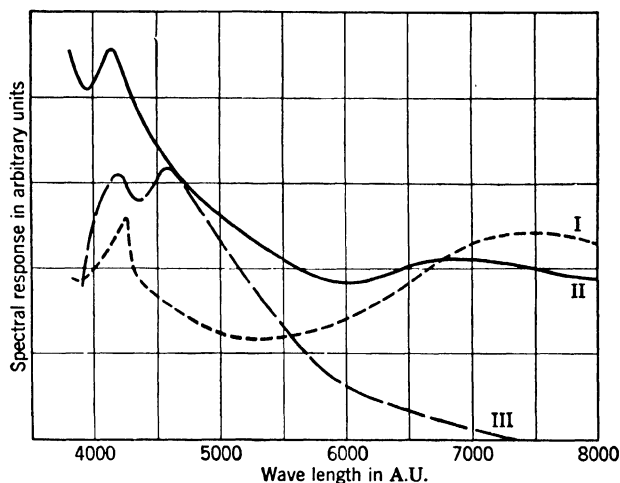


FIG. 3.18. Spectral Response of Composite Photocathodes (Bi, Cs on [Ag]—Cs<sub>2</sub>O, Ag—Cs). I: Very Thin Bi, Cs Film. II: Somewhat Thicker Bi, Cs Film. III: Very Thick Bi, Cs Film on [Ag]—Cs<sub>2</sub>O, Ag—Cs Base. (Goerlich, reference 30.) (By permission of the Attorney General in the public interest under License No. JA-1351.)

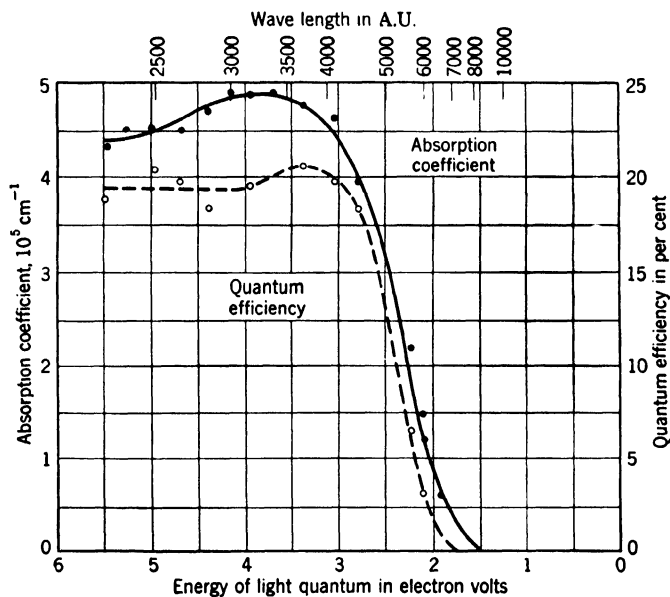


FIG. 3.19. Quantum Yield and Light Absorption of an Antimony-Cesium Film on Quartz. (Courtesy of Dr. J. A. Burton, Bell Laboratories.)



tial feature of the silver-oxy-cesium photocathode. Furthermore, no attempt has been made to list the sensitive surfaces which have achieved practical importance. Data regarding a number of such photocathodes will be found in Chapters 5 and 6.

### REFERENCES

1. H. GEITEL, "Proportionality of photocurrent and illumination for very thin potassium films," *Ann. Phys.*, Vol. 67, pp. 420-427, 1922.
2. J. B. TAYLOR and I. LANGMUIR, "The evaporation of atoms, ions, and electrons from cesium films on tungsten," *Phys. Rev.*, Vol. 44, pp. 423-458, 1933.
3. J. A. BECKER, "Thermionic and adsorption characteristics of cesium on tungsten and oxidized tungsten," *Phys. Rev.*, Vol. 28, p. 341, 1926.
4. R. SUHRMANN and H. THEISSING, "Selective photoelectric effect," *Z. Physik*, Vol. 55, pp. 701-716, 1929.
5. J. J. BRADY, "Photoelectric properties of alkali metal films as a function of their thickness," *Phys. Rev.*, Vol. 41, pp. 613-626, 1932.
6. J. H. DE BOER, *Electron Emission and Adsorption Phenomena*, Cambridge University Press, London, 1935.
7. R. FLEISCHMANN, "Selective photoeffect and light absorption," *Naturwissenschaften*, Vol. 19, p. 826, 1931.
8. H. E. IVES and H. B. BRIGGS, "Correlation of optical properties and photoelectric emission in the films of alkali metals," *J. Optical Soc. Am.*, Vol. 28, pp. 330-338, 1938.
9. K. H. KINGDON, "Electron emission from adsorbed films on tungsten," *Phys. Rev.*, Vol. 24, pp. 510-522, 1924.
10. L. R. KOLLER, "Photoelectric emission from thin films of cesium," *Phys. Rev.*, Vol. 36, pp. 1640-1647, 1930.
11. H. C. RENTSCHLER and D. E. HENRY, "Photoelectric emission," *J. Franklin Inst.*, Vol. 223, pp. 135-145, 1937.
12. J. ELSTER and H. GEITEL, "On colored hydrides of alkali metals and their photosensitivity," *Physik. Z.*, Vol. 11, pp. 257-262 and pp. 1082-1083, 1910; Vol. 12, pp. 609-614, 1911.
13. R. SUHRMANN and H. THEISSING, "Influence of hydrogen on the photoelectric emission of potassium," *Z. Physik*, Vol. 52, pp. 453-463, 1928.
14. S. RIJANOFF, "Photoelectric properties of a potassium surface changed by the action of hydrogen atoms," *Z. Physik*, Vol. 71, pp. 325-338, 1931.
15. P. I. LUKIRSKY and S. RIJANOFF, "Dependence of photoemission of potassium on arrangement of atomic hydrogen and potassium layers on its surface," *Z. Physik*, Vol. 75, pp. 249-257, 1932.
16. J. H. DE BOER and M. C. TEVES, "The influencing of the photoelectric properties of cesium by adsorption on salt layers," *Z. Physik*, Vol. 65, pp. 489-505, 1930.
17. R. POHL and P. PRINGSHEIM, "The effect of oxygen on the selective photoeffect of potassium," *Verhandl. deut. physik. Ges.*, Vol. 15, pp. 625-636, 1913.
18. W. KLUGE, "Selective photoelectric emission from compound alkali cathodes," *Physik. Z.*, Vol. 34, pp. 115-126, 1933.
19. S. ASAO and M. SUZUKI, "Improvement of thin film cesium photoelectric tube," *Proc. Phys.-Math. Soc. Japan*, Vol. 12, pp. 247-250, 1930.

20. S. ASAO, "Behavior of the foreign metal particles in the composite photocathode," *Proc. Phys.-Math. Soc. Japan*, Vol. 22, pp. 448-486, 1940.
21. R. FLEISCHER and P. GOERLICH, "On composite photocathodes," *Physik. Z.* Vol. 35, pp. 289-292, 1934.
22. T. W. CASE, "New strontium and barium photoelectric cells," *Phys. Rev.*, Vol. 17, pp. 398-399, 1921.
23. W. S. HUXFORD, "Effect of electric field on emission of photoelectrons from oxide cathodes," *Phys. Rev.*, Vol. 38, pp. 379-395, 1931.
24. J. H. DE BOER and M. C. TEVES, "Secondary phenomena of the primary photoeffect of cesium atoms adsorbed on salt layers," *Z. Physik*, Vol. 74, pp. 604-623, 1932.
25. D. RAMADANOFF, "Photoelectric properties of composite surfaces at various temperatures and potentials," *Phys. Rev.*, Vol. 37, pp. 884-896, 1931.
26. L. J. REIMERT, "Photoelectric properties of metals in a finely divided state," *J. Optical Soc. Am.*, Vol. 36, pp. 278-283, 1946.
27. A. R. OLPIN, "Methods of enhancing the sensitivities of alkali photoelectric cells," *Phys. Rev.*, Vol. 36, pp. 251-295, 1930.
28. W. KLUGE, "The photosensitization of potassium by sulfur, selenium, and tellurium," *Z. Physik*, Vol. 67, pp. 497-506, 1931.
29. P. GOERLICH, "On composite transparent photocathodes," *Z. Physik*, Vol. 101, pp. 335-342, 1936.
30. P. GOERLICH, "Measurements on composite photocathodes," *Z. Physik*, Vol. 109, pp. 374-386, 1938.
31. P. GOERLICH, "Photoelectric cells for the visible spectral range," *J. Optical Soc. Am.*, Vol. 31, pp. 504-505, 1941.
32. N. M. HOPSHTEIN and D. M. KHOROSH, "Photoeffect and secondary emission of alloy cathodes," *J. Tech. Phys. (USSR)*, Vol. 8, pp. 2103-2106, 1938.
33. N. S. KHLEBNIKOV, "The volt-ampere and light characteristics of antimony-cesium cells," *J. Tech. Phys. (USSR)*, Vol. 10, pp. 1908-1912, 1940.
34. A. SOMMER, "Photoelectric alloys of alkali metals," *Proc. Phys. Soc. (London)*, Vol. 55, pp. 145-154, 1943.
35. J. A. BURTON, "Photoelectric and optical properties of cesium-antimony films," *Phys. Rev.*, Vol. 72, pp. 531-532, 1947.

## Chapter 4

# MATERIALS AND APPARATUS FOR MAKING PHOTOTUBES

In making phototubes, it is essential to have a certain amount of knowledge of the nature of materials entering into their construction and likewise of the apparatus employed in the exhaust and treatment of the phototubes after assembly. It is the intent of this chapter to discuss these practical matters from the point of view of common physical experience rather than of theoretical design.

**Choice of Glass.** For phototubes intended to respond to ordinary light, including the near ultraviolet and the near infrared, just common kinds of glass are quite satisfactory for the bulb and for the press or stem through which the wires are led out. For small tubes a soft glass is used chiefly because it is easy to fuse in the glass-working flame. The bulb of the phototube is usually made of *lime glass*, because this is resistant to the chemical action of hot alkali vapors. Lead glass is readily attacked by alkalies, the lead being displaced to produce a dark brown coloration. Hence it cannot be used for the bulb since it would cause absorption of the incident light. However, lead glass, which is less brittle than lime glass, is commonly used for the press where any degree of opacity is of no moment. As a matter of fact, lead glass in the press serves as a practical means of eliminating excess alkali in some types of phototubes.

In larger tubes, in which mechanical strains are greater and in which thermal expansions might be more serious, especially because the walls are thicker, a hard glass is commonly employed. *Pyrex*<sup>1</sup> has come to be a favorite material because of its unusually low thermal expansion. It can be heated and cooled quickly without danger of cracking. If Pyrex is to be sealed to ordinary hard glass, there should be an intermediate gradation of yellow Pyrex, uranium, or cobalt glass to minimize strains at the junction.

<sup>1</sup> Trademark of Corning Glass Works.

All ordinary kinds of glass, both soft and hard, are quite transparent to infrared radiations to which the photoemissive surfaces known at present respond and hence do not limit the effectiveness of phototubes in this portion of the spectrum. However, in the ultraviolet there is a rather sharp cut-off in transmission near 3200 Angstrom units. Beyond this limit ordinary phototubes are quite ineffective. Tubes which are to operate in the spectral range beyond 3200 Angstrom units are provided with envelopes of quartz or some special ultraviolet transmissive hard glass, such as Corex and, more recently, Corning 9741.

**Glass-to-Metal Seals.** When wires are sealed into a press or into the wall of a bulb, it is of course necessary that glass and metal have the same effective coefficient of thermal expansion in order that intimate contact be maintained to insure a hermetically tight seal. For lead and lime glass, platinum makes an excellent seal, but it is used seldom because of the expense involved. A cheaper wire, which makes a satisfactory seal, consists of a core of nickel-iron alloy coated with copper. Commonly known as *Dumet*, it is used almost exclusively in all soft-glass tubes manufactured in appreciable quantities.

Neither platinum wire nor Dumet can be sealed in hard glasses. It is universal practice to employ tungsten. Since this metal is very brittle, as well as expensive, only a short length is used, where the wire actually passes through the glass. The remaining length consists of some other metal, such as nickel or copper, securely welded to the tungsten. Although nickel does not seal vacuum-tight into glass, the nickel part of a *pressweld*, as these composite wires are called, is often embedded part way into the glass to increase rigidity and to remove strain from the welded joint. Sometimes molybdenum wire is substituted for the nickel. This wire seals fairly well into hard glass and is at the same time tough and rigid. Figure 4.1 shows a typical machine-made press with three presswelds.

Glass-to-metal seals are by no means limited to the sealing of wires into glass envelopes. At a relatively early date a technique was developed for sealing copper tubing to either hard or soft glass.<sup>2</sup> For this purpose the tubing is gradually tapered at the end to be sealed so that at the extremity the metal is as thin as paper. The glass can then be

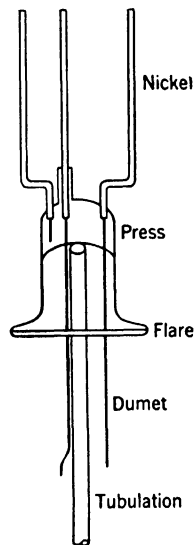


FIG. 4.1. Machine-Made Press with Three Presswelds, Tubulation, and Insulating Glass Sleeve.

<sup>2</sup> See Houskeeper, reference 1.

fused to the copper, which yields sufficiently during changes of temperature to conform to the dimensions of the more rigid glass. By this means it is possible to make a reliable seal between hard and soft glass by using a coupling tube of copper which is tapered at both ends.

The development of certain cobalt-nickel-iron alloys such as Fernico and Kovar and of special seal glasses with matching coefficients of expansion has greatly simplified the preparation of glass-to-metal seals, making possible the application of machine processes as in the manufacture of metal vacuum tubes. The metal portion of the seal may be joined to other metal parts of the assembly by welding or soldering; the glass portion requires a graded seal if it is to be attached to Pyrex or other types of glasses.

There is no difficulty in forming glass seals to Fernico or Kovar in sizes up to 8 inches in diameter. Proper annealing is required as in other types of glass seals, and precautions must be taken in the tube design to prevent other metal structures attached to the Kovar or Fernico from introducing distortions at the seal as a consequence of differences between the expansion coefficients of these attached members and the expansion coefficient of the Kovar or Fernico.

In the great majority of applications in the field of photoelectricity Fernico and Kovar seals are entirely satisfactory. However, in applications where radio-frequency currents are required to flow on the surface of the Kovar, considerable power losses may result from the relatively large electrical resistance of the Kovar. Processing and glassing techniques have been developed which permit coating the Kovar with films, up to 0.005 inch thick, of any of the high-conductivity metals, copper, silver, gold, or chromium, so that glass seals may be made to the coating.<sup>3</sup> Such an arrangement provides a high-conductivity metal film to conduct the radio-frequency currents with low loss, and consequent small temperature rise, and permits the use of the specially developed seal glasses matching the expansion coefficient of the Kovar, which acts as main structural member. The Kovar or Fernico is first formed, polished, and fired in hydrogen and is then electroplated to the desired thickness, which is usually greater than the depth of penetration of the radio-frequency currents. The coating materials are usually silver and copper. A very thin film (less than 0.0001 inch) of chromium is electroplated over the first coating, covering only the area to be glassed plus approximately  $\frac{1}{2}$  inch or less on either side of the seal, provided that this area is subject to the glass-working fires. The Kovar piece is then fired in wet hydrogen to form the first electroplated film into a homogeneous tightly bonded layer and to oxidize the thin chromium film com-

<sup>3</sup> See Smith and Hegbar, reference 2.

pletely. Oxygen-gas fires are then used to make the seal to the chromium oxide, and the finished seal is annealed in the conventional manner. The chromium-oxide layer provides some protection to the metal film from the glass-working fires and yields a surface with good thermal radiating properties which prevents overheating of the metal film and consequent blistering and cracking.

Low-loss glass-to-metal seals are also made to silver-plated chrome-iron alloys with special glasses developed to match the expansion coeffi-

TABLE 4.1. CONSTANTS OF VARIOUS GLASSES AND METALS

Material	Density	Coefficient of Expansion	Softening Point, °C	Annealing Point, °C	Melting Point, °C
Lead glass	3.04	$8.7 \cdot 10^{-6}$	630	431	
Lime glass	2.47	$9.2 \cdot 10^{-6}$	696	510	
Fernico or Kovar seal					
glass: 704	2.24	$4.7 \cdot 10^{-6}$	697	484	
7052	2.29	$4.7 \cdot 10^{-6}$	708	480	
Nonex (hard)	2.35	$3.6 \cdot 10^{-6}$	756	521	
Pyrex (hard)	2.23	$3.2 \cdot 10^{-6}$	818	553	
Corex D		$3.8 \cdot 10^{-6}$	804	558	
Fused silica	2.2	$0.4 \cdot 10^{-6}$			1700
Tungsten	19.3	$4.5 \cdot 10^{-6}$			3380
Molybdenum	10.1	$5.1 \cdot 10^{-6}$			2470
Dumet		$9.8 \cdot 10^{-6}$			
Platinum	21.45	$9.0 \cdot 10^{-6}$			1773
Nickel	8.8	$13.9 \cdot 10^{-6}$			1452

cient of the alloy. These glasses are, however, of a lower softening temperature than those used with Fernico and Kovar. No chromium-oxide layer is required, since the heating for sealing is obtained by induction at radio frequencies and not by glass-working fires.

Since no metal can even approximately match the exceedingly low coefficient of expansion of fused silica or quartz, the sealing of wires into quartz envelopes presents a special problem. It is solved, in general, by making the metal so thin that the forces of adhesion to the quartz exceed the stresses tending to contract the metal on cooling. Molybdenum strips less than 20 microns thick may satisfactorily be fused into quartz at its melting temperature (1700° C).<sup>4</sup> Leads prepared in this manner have been employed to carry currents of the order of 10 am-

<sup>4</sup> See Lauster, reference 3.

peres. Thicker, tungsten, leads may be fused into quartz tubes with the aid of a special intermediate glass which seals to both tungsten and quartz.<sup>5</sup>

Table 4.1 gives a list of coefficients of expansion and other pertinent data for various kinds of glass and metal. A simple, tight seal can be made only when the effective coefficient for the metal is approximately the same as for the glass. If there is any deviation, it should be in such a direction that the outer component has the higher coefficient. If wires are sealed into glass, the glass should have greater thermal expansion; if a glass window is sealed into a metal frame, the metal should be more sensitive to temperature. A method of preparing presses which is gaining increasing acceptance consists in placing powdered glass in suitably shaped carbon molds, with the press wires held in position by jigs, and sintering the glass by high-frequency heating.

**Pre-treatment of Metals.** Metal parts which enter into the construction of phototubes and other types of evacuated devices are originally contaminated with grease, various mineral salts, and adsorbed films of gas molecules. Foreign atoms remain attached to the surface even after careful cleaning by mechanical means and with such solvents as benzol, alcohol, or carbon tetrachloride. Furthermore, foreign atoms are distributed throughout the whole volume of the metal, either forming definite chemical compounds or adhering to crystal boundaries, crevices, or pores of the metal. If these impurities are not removed, they may gradually disengage themselves when in the evacuated envelope and produce harmful effects. Although the metal parts are often treated after assembly, during evacuation of the envelope, a pre-treatment or outgassing before assembly is generally advisable.

Two common methods of outgassing are heating the parts in hydrogen and heating them in a vacuum. The following is a simple procedure for "hydrogen firing". The metal parts are placed in the central part of a fused-quartz tube on which an electric heating coil is wound. Hydrogen is flushed continuously through the tube, finding exit through a quartz jet at whose tip it is ignited and burns harmlessly. The central part of the tube is heated to a good yellow glow for a period of 10 to 30 minutes. The heat drives out the impurities, which either combine with the hydrogen or are driven out with it through the jet. Hydrogen, being a powerful reducing agent, breaks down oxides at the surface and leaves the metal bright and clean. The furnace is allowed to cool with the gas flowing, after which the parts may be removed and stored temporarily in a closed jar.

Some metals, such as tantalum, cannot be cleaned in a hydrogen furnace, since they absorb this gas in large quantities and are rendered

<sup>5</sup> See Noel, reference 4.

brittle thereby. In such cases treatment in a vacuum furnace is recommended.

Heat treatment in a vacuum differs from the hydrogen process in that the quartz tube is hermetically sealed and is exhausted to a pressure preferably less than  $10^{-3}$  mm Hg. When a vacuum has been established, the temperature is raised to a point appreciably below the sublimation point of the metal being treated. For metals such as nickel, iron, and molybdenum, temperatures less than  $1000^{\circ}\text{C}$  are found to be satisfactory. It is essential that vacuum is maintained while the furnace is cooling. Heating of metals in a vacuum by induction will be described later in the chapter.

The gases which are most copiously driven out of metals during heat treatment are carbon dioxide, carbon monoxide, water vapor, hydrogen, and nitrogen. The relative proportions depend on the metal and its previous history of treatment.

Parts which have been cleaned should by no means be touched with the fingers, but should be handled only with bright tweezers or with gloved hands.

**Vacuum Pumps.** The press with its structure of metal parts, mounted either by welding or by crimping, is sealed into an appropriately shaped bulb. A small tubulation attached at some point to the bulb or press serves as a connecting artery between the glass vessel and the system used for removing the air from it. Electronic tubes should be exhausted to a pressure not higher than about  $10^{-6}$  mm Hg. To obtain this degree of vacuum, an exhaust system comprising three stages may be employed. The great bulk of the air is first drawn out into an exhaust pipe line connected to a heavy-duty pump capable of maintaining a reduced pressure of about 10 mm Hg. This part of the system is designated as the "house vacuum." Although not absolutely essential, it shortens the total time of exhaust and saves the more delicate equipment from handling such great quantities of air. Since normal atmospheric pressure is 760 mm Hg, it is apparent that the house vacuum removes about 98 per cent of the total quantity.

A two-way stopcock serves to switch the exhaust action to a small rotary oil pump, which is capable of reducing the pressure to less than 0.1 mm Hg. Mechanical oil pumps have, in fact, been designed to exhaust clean and perfectly air-tight systems to less than 0.001 mm Hg. However, even this pressure is not nearly low enough for vacuum tubes. The final stage of pressure reduction, to a value less than the smaller figure by a factor of a thousand, requires the services either of a molecular pump of the type developed by Holweck and Gaede or of a diffusion or condensation pump. The reader is referred to other sources for a



fuller discussion of the various types of high-vacuum pumps.<sup>6</sup> It will suffice here to describe briefly the operation of the mercury and oil condensation systems which, combining ruggedness and simplicity, are widely used in laboratory and factory.

Figure 4.2 is a diagram of an original glass form of Langmuir's mercury condensation pump. The mercury in the boiler *A* is heated electrically to about 110° C. Vapor ascends from the boiler, passes through

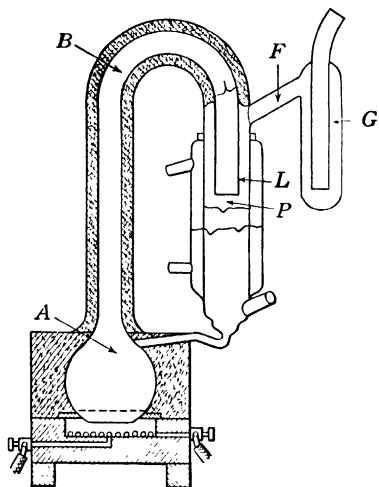


FIG. 4.2. Langmuir's Mercury Condensation Pump (Original Glass Type). (After S. Dushman, *General Electric Review*.)

the insulated tubing *B*, and discharges with appreciable velocity from the nozzle *L* into the chamber *P*, which is directly connected through the trap *G* to the system to be exhausted. Gas molecules arriving through *F* at the mouth of the nozzle are accelerated downward by physical collision with the mercury atoms and enter the forevacuum space. The mercury vapor itself is almost completely condensed on the walls of *P*, which are kept cool by a water jacket. The condensed mercury finds its way back to the boiler by gravity. An external refrigerant surrounding the freezing-out trap *G* serves to condense any mercury vapor which diffuses out through *F*. The process is continuous. For an input of 300 watts in

the boiler, it has a speed of about 5000 cubic centimeters per second, which means that the pressure in a 5-liter system would be reduced to about one-third its original value in 1 second.

A pump of this type requires a forevacuum pressure of roughly 0.05 mm Hg for effective operation. It is customary, in order to permit a higher forevacuum pressure, to use two condensation pumps in series, the one next to the forepump discharging mercury vapor through a larger nozzle at relatively low speed, while the other discharges the vapor at high speed through a smaller nozzle. For a two-stage condensation pump, the forevacuum does not need to be lower than 1 mm Hg. A rugged all-metal two-stage mercury condensation pump manufac-

<sup>6</sup> See Dushman, reference 5. In some cases the final vacuum is obtained with "getters," that is, active substances which remove residual gases by absorption or chemical reaction.

tured by the General Electric Company is shown in cross section in Fig. 4.3.

High-vacuum pumps with considerably greater pumping speeds have resulted from the utilization of low-boiling organic oils as working fluids. Since the vapor pressures at room temperature of several of

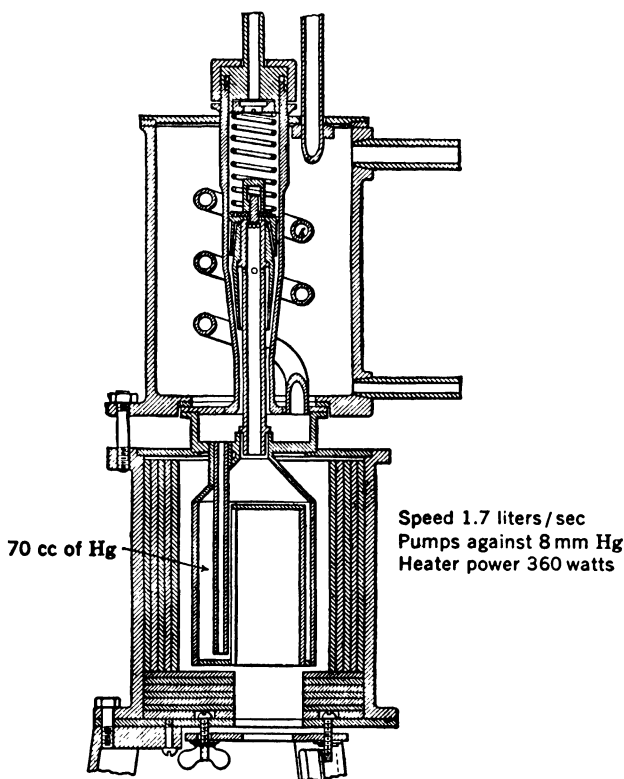


FIG. 4.3. Two-Stage All-Metal Mercury Diffusion Pump. (Courtesy of General Electric Company.)

these oils, in particular the phthalates and sebacates, marketed under the trade names Octoil and Amoil, are of the order of  $10^{-6}$  mm Hg or less—as compared with  $3 \cdot 10^{-3}$  mm Hg for mercury—oil diffusion pumps require no freezing-out traps except where extreme cleanliness is needed. In addition, the boiling of the oil takes place without the “bumping” or mechanical concussion characteristic of the boiling of mercury. On the other hand, oil diffusion pumps require particularly careful design to prevent the accumulation of high-vapor-pressure fractions in the high-

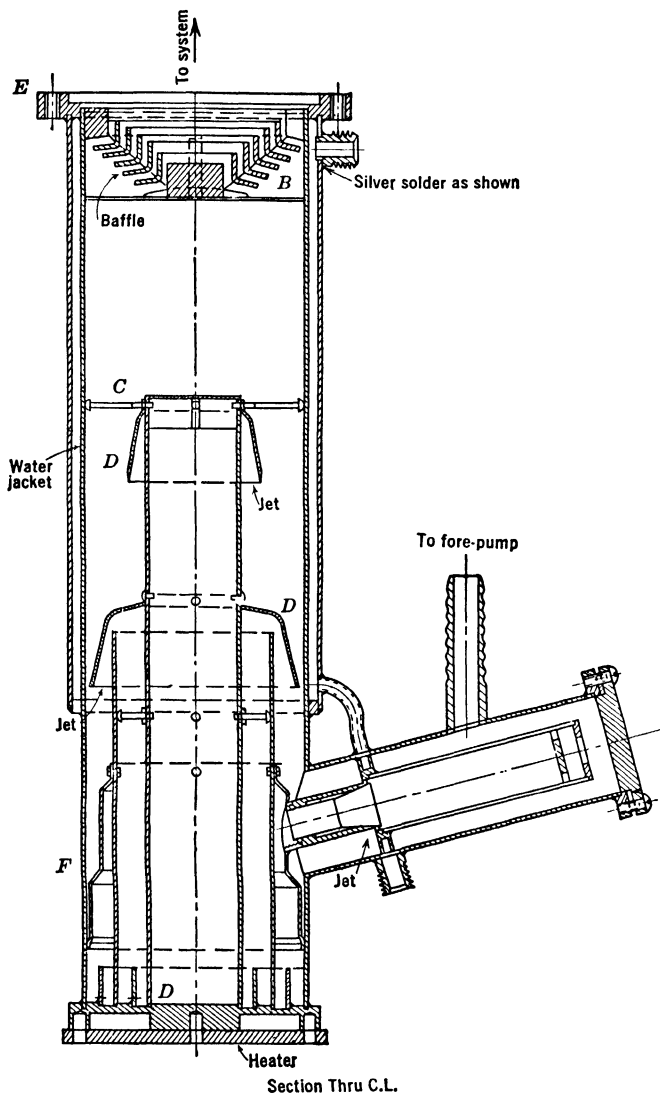


FIG. 4.4. Oil Diffusion Pump. (Zworykin and Morton, *Television*, John Wiley and Sons, New York, 1940.)

vacuum portion of the pump. Figure 4.4 shows a three-stage oil diffusion pump which meets this requirement and has given satisfactory service. Hickman, who has played an important role in the development of these pumps,<sup>7</sup> quotes a pumping speed of 250 liters per second

<sup>7</sup> See Hickman, reference 6.

—over a hundred times as great as that of the mercury pump shown in Fig. 4.3—for a particular oil diffusion pump 4 inches in diameter.<sup>8</sup>

Another drawback of these oils as pump fluids is their relatively great sensitivity to oxidation. If a considerable amount of air is admitted into a hot diffusion pump, its rate of recovery is much smaller when the working fluid is oil than when it is mercury. It has been found that with Dow-Corning Silicone pump oils, in which carbon is replaced by silicon, the sensitivity of the boiling oil to oxygen is materially reduced. Pressures of the order of  $5 \cdot 10^{-7}$  mm Hg have been reached with Dow-Corning Silicone oils 702 and 703 in standard Distillation Products VMF pumps.

**Production of High Vacuum.** Good results demand, in addition to satisfactory pumping equipment, a suitable technique for carrying out the exhaust schedule. The laboratory exhaust procedure described below may serve as an example.

All tubes to be exhausted are provided with a short length of tubing communicating with the interior of the bulb. The free end of this tubulation is sealed, by means of a gas-air or gas-oxygen torch, to similar tubulations extending from the glass manifold which leads through a freezing-out trap to the diffusion pump. The system is then opened to the house vacuum for removing the bulk of the gas. In order to make sure that all glass joints are perfect, the high-tension terminal of a special type of spark coil is passed over all doubtful places. If the joints are tight, the potential of several thousand volts causes a diffuse glow of the air inside the manifold. If, on the other hand, there is a pinhole or crack, the discharge is concentrated at the place of leakage, indicating its exact location by a bright spot. If such a leak is found, air is let into the system and the place repaired.<sup>9</sup>

If no leak is found, the system is switched to the intermediate fore-pump and the heater or heaters of the diffusion pumps are turned on. The circulation of water through the jackets should be carefully checked.

The pressure should drop to less than  $10^{-5}$  mm Hg within 15 minutes. To accelerate the exhaust procedure, the tubes—and, for systems employing oil diffusion pumps, the freezing-out trap and vacuum gage as well—may now be given a preliminary bake before the refrigerant is applied so as to remove condensable vapors from the whole system.

<sup>8</sup> See Hickman, reference 7.

<sup>9</sup> A highly effective procedure for detecting small leaks in vacuum systems employs a helium jet to explore suspicious points. The system is exhausted through a mass spectrometer, which indicates minute traces of the rare gas whenever the jet strikes a vacuum leak. See Nier, Stevens, Hustrulid, and Abbott, reference 8. Instead, a hydrogen jet may also be utilized in conjunction with the palladium-window gage shown in Fig. 4.8d.

The most common refrigerants are liquid air and liquid nitrogen; the latter is to be preferred because it produces a lower temperature in the trap ( $-195^{\circ}\text{C}$ ) and does not constitute a fire hazard when it comes into contact with organic matter. The refrigerant is applied to the trap in a Dewar flask, one filling lasting approximately a day. A mixture of carbon dioxide snow and ether, or simply a coating of alkali metal on the inner walls of the trap, may serve as substitute.

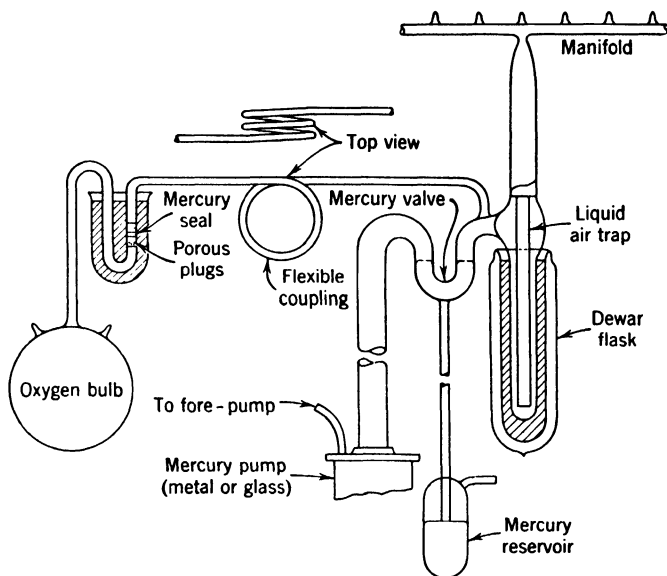


FIG. 4.5. Vacuum System Suitable for the Preparation of Phototubes. (Courtesy of S. Essig.)

During the final bake the refrigerant, in place, prevents the diffusion of pumping fluids into the manifold and condenses volatile substances, such as water vapor, in the trap. A portable cylindrical oven may be placed over a manifold of radial structure with the tubes pendent from the extremities of short "spokes"; or a rectangular oven in a fixed frame may be lowered over a linear manifold bearing the tubes like twigs on a branch, as shown in Fig. 4.5.

Tubes of soft glass are baked at a temperature not exceeding  $400^{\circ}\text{C}$ , and tubes of hard glass at a temperature not exceeding  $500^{\circ}\text{C}$ , for a period of 15 to 30 minutes. This treatment drives out from the glass adsorbed water vapor and gases which would otherwise soon destroy the final vacuum produced in the finished tube.

During the bake of the manifold and tubes the remaining parts of the glass system between the oven and the freezing-out trap may profitably

be heated with a soft Bunsen flame. This "torching" accelerates the removal of adsorbed vapors, in particular mercury and water, which otherwise would diffuse away slowly, in an asymptotic manner.

After baking and torching, the oven is removed and the tubes are permitted to cool. A vacuum heat treatment of metal structures that can tolerate high temperatures is generally given at this point. A favorite procedure is to heat the metal elements by means of an induction coil excited by a high-frequency oscillator. The eddy currents induced raise the parts in question to any desired temperature. A red heat corresponding to about 900° C is generally sufficient. Large masses of metal may liberate so much gas that the heat treatment must be given intermittently to allow the pumps to remove the accumulated gas.

Metals may also be outgassed by introducing an inert gas such as argon and letting an ionizing discharge take place between two electrodes in the tube. Alternatively, positively connected elements may be heated by bombardment with high-speed electrons from a thermionic cathode. Filaments themselves can be outgassed, of course, by heating them to abnormally high temperatures by means of excessive conduction currents.

After this treatment the pressure within the tubes should not exceed  $10^{-6}$  mm Hg. They are now ready to be subjected to the sensitization schedule described, before being sealed off from the manifold. Sensitizing procedures for phototubes are described in Chapter 5.

**Techniques for Metal Tubes.** Metal may supplant glass in vacuum tubes at all points except where the glass is required for electrical insulation or as a member permeable to light or other radiation. When the parts are adequately processed and cleaned before assembly, firing in a hydrogen or, preferably, a vacuum furnace being a common method, metal envelopes are capable of sustaining a vacuum fully as well as a glass envelope and possess some advantages of shock resistance and adaptability to demountable structures. The final vacuum closure for the metal envelope may be a welded joint, a compression gasket joint, a gold diffusion seal between two metal elements, a soldered joint or a glass seal. The copper gasket between polished steel surfaces gives a vacuum-tight joint entirely satisfactory for sealed-off tubes and provides rapid demountability.<sup>10</sup>

The metal tube is often exhausted by a metal vacuum system containing a metal oil diffusion vacuum pump, metal liquid air trap, and metal connecting tubing. The development of the metal cold-weld type of vacuum seal-off has made such all-metal systems practical.<sup>11</sup>

<sup>10</sup> See Smith and Hegbar, reference 2.

<sup>11</sup> See Garner and Bricker, U. S. Patent Application 417424.

Instead of removing the tube from the vacuum system by heating the usual connecting glass pumping lead until its walls soften and collapse, a tube of metal, such as copper, is used as the pumping lead and is squeezed between two cylindrical members until the tubing is literally pinched off. A vacuum-tight diffusion weld is produced at the area of maximum pressure. Such seal-off welds are made on copper tubing from diameters less than  $\frac{1}{16}$  inch to greater than 1 inch. This cold weld has been applied successfully in the laboratory to disk seals over 3 inches in diameter. The cold-weld seal-off is superior to the glass tubulation seal-off insofar as it occurs without the liberation of gas or vapor.

**Measurement of Low Pressures.** To avoid confusion, any mention of auxiliary equipment for measuring the degree of vacuum obtained at any stage of the exhaust schedule has been purposely omitted so far. However, such measurements are extremely important, and hence the common devices employed for the purpose will be described briefly.

For pressures greater than a few millimeters of mercury, a simple mercury manometer, such as that shown in Fig. 4.6, is convenient. The U-shaped glass appendage is about half full of mercury when sealed to a fully evacuated system. The level in both sides is then precisely the same. When a gas pressure exists at the open end, the difference in level of the two arms is a direct measure of the pressure. Since there is a good vacuum in the closed arm, the column may ascend to the top of the enclosure. The purpose of the constriction is to prevent too rapid a rise in case of a sudden increase in pressure.

FIG. 4.6. A Simple Mercury Manometer.

Here also organic liquids with low vapor pressures may be substituted for mercury. Butyl benzyl phthalate has a specific gravity slightly greater than unity as compared to 13.6 for mercury. Hence, for the same pressure, the phthalate would show a difference of level thirteen times as great as mercury.

An instrument capable of indicating absolute pressures ranging from a few millimeters down to  $10^{-5}$  millimeter of mercury is the familiar McLeod gage. By depressing a mercury column communicating with the reservoir at the bottom of the gage a definite volume of gas is trapped off from the system at the pressure prevailing in the system. The mercury is made to rise farther in the system until this volume has been compressed to a known small decimal fraction of its original value, whereby, in accordance with Boyle's law, its pressure is increased in the

same proportion. Then the difference in level between the top of the compressed column and that of a neighboring uncompressed column must simply be multiplied by the above-mentioned decimal fraction to yield the absolute pressure of the gas in the system. Figure 4.7 shows a typical McLeod gage.

The McLeod gage has the advantages of covering a wide range of pressures and of being fully calibrated by geometrical measurements. At the same time, it has the serious drawback of not giving continuous pressure readings; the column must be raised and lowered for each observation. Furthermore, it does not register the pressures arising from condensable vapors.

A convenient substitute for the range from 1 to about  $10^{-3}$  mm Hg is the thermocouple. It may be made as shown in Fig. 4.8a, where one leg of the X-shaped filament assembly consists of one kind of metal and the other leg of a different metal. Pairs of metal frequently used for this purpose are copper-advance, chromel-alumel, and silver-bismuth. A small electric current is sent along one wire to the welded junction at the center and out again through the adjacent wire of the second metal. The remaining two terminals are connected to a low-resistance millivoltmeter.

The temperature of the junction, and hence the voltage output, depends on the value of the heating current and also on the rate at which heat is convected away by gas molecules. Thus, if the couple is sealed into a bulb and attached to the system, the reading of the meter for a fixed heating current will be a definite function of the gas pressure.

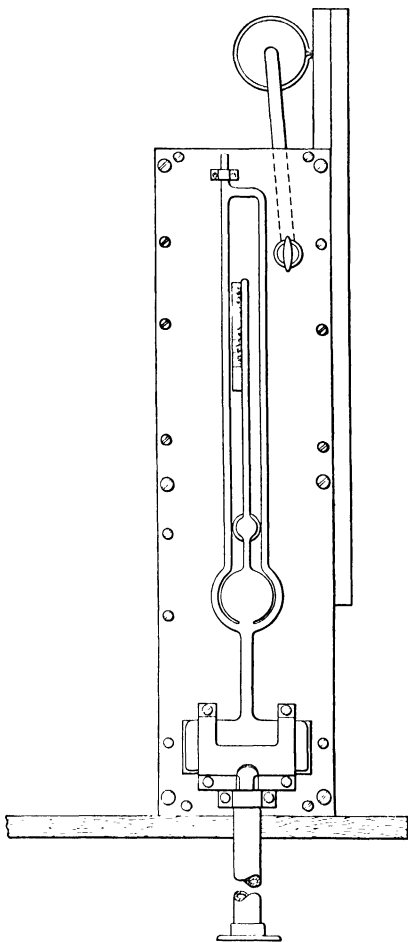


FIG. 4.7. A McLeod Gage.



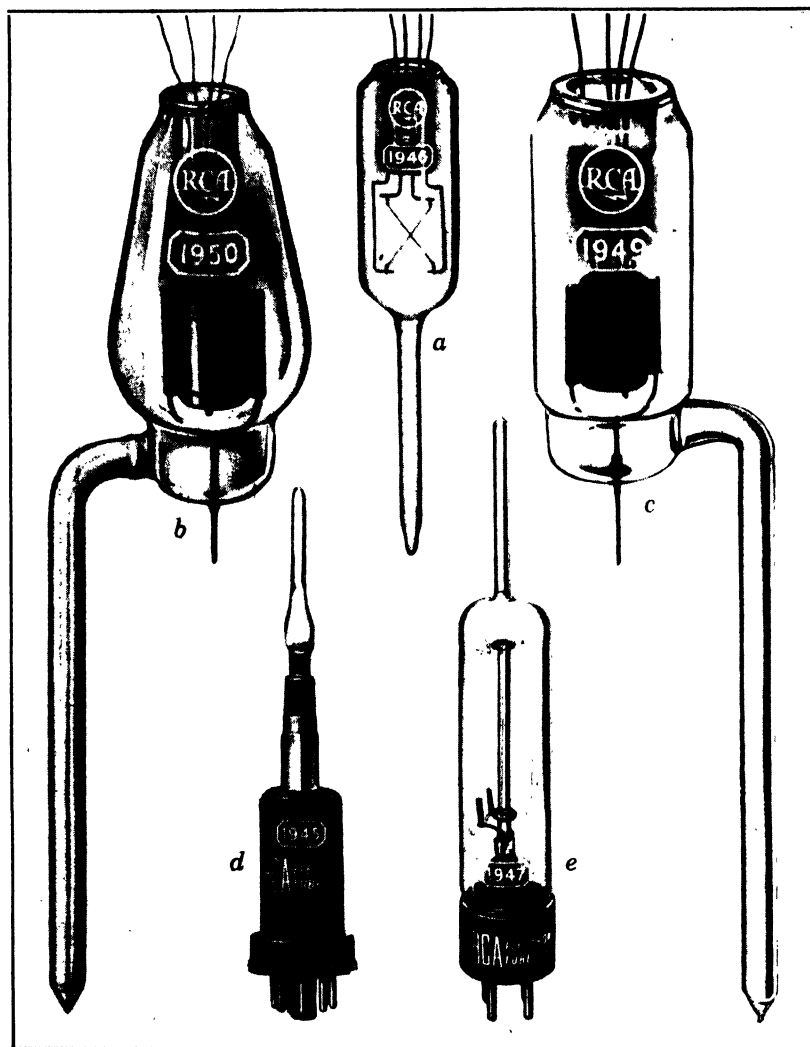


FIG. 4.8. Various Vacuum Gages: (a) Thermocouple Gage. (b) Ionization Gage (soft glass). (c) Ionization Gage (hard glass). (d) Ionization Gage for Leak Testing with Hydrogen Jet (tube volume separated from vacuum vessel by palladium window which, on heating by electron bombardment, admits hydrogen into gage). (e) Pirani Gage.

An accurate, continuous-reading device for measuring the lowest pressures is the *ionization gage*.<sup>12</sup> It is a three-electrode thermionic tube<sup>13</sup> in which the grid element is used to collect the thermionic electron current from the filament, while the plate element is made negative in order to collect positive ions produced by electrons colliding with the molecules of residual gas in the intervening space. The tube, like the thermocouple, is attached directly to the system and is subject to the same pressure as the manifold. For pressures below  $10^{-3}$  mm Hg the positive-ion current is practically proportional to the pressure. The lowest pressure which can be measured is normally determined by the sensitivity of the meter employed to measure the ion current. With a sensitive, portable microammeter, pressures of  $10^{-6}$  mm Hg can readily be detected; much greater sensitivities may be attained with vacuum-tube amplification. In practice, the device is calibrated for some definite ionizing current between filament and grid. For a given pressure, the ion current is roughly proportional to the electron current. Vacuum-tube circuits are available for automatically adjusting the filament current so as to keep the emission current to the grid constant.<sup>14</sup> In this manner changes in grid current arising from supply line voltage variations and poisoning of the filament by oxygen or other gases are prevented. It is important to outgas the ionization gage thoroughly before use, by baking or torching the envelope and high-frequency heating the metal parts and glowing the filament. Failure to do this will, on the one hand, lead to a pollution of the vacuum when the gage is first put into use and, on the other, yield a false indication of the vacuum in the attached system.

The principal drawback of the normal ionization gage is the presence of an incandescent filament whose lifetime is limited and which, in particular, will burn out if air is inadvertently admitted into the system. This difficulty is avoided in the Philips gage and the Alphatron.

The Philips gage<sup>15</sup> (Fig. 4.9) consists of a ring anode placed between two cathode plates of thorium or zirconium and a strong magnetic field aligned with the axis of the ring. A difference of potential of 2000 volts is applied between the cathode and the anode. The magnetic field causes electrons which leave the cathode plates as a result of positive-ion bombardment to travel along helical paths about magnetic field lines and prevents their collection by the anode ring. They are hence capable of causing many more ionizations of gas atoms than in the

<sup>12</sup> See Dushman and Found, reference 9.

<sup>13</sup> See Chapter 12.

<sup>14</sup> See Nelson and Wing, reference 10.

<sup>15</sup> See Penning, reference 11.

absence of the magnetic field, maintaining a self-sustained discharge even at very low pressures. The discharge current is a measure of the gas pressure in the tube; it is a nonlinear function of the pressure, which furthermore depends, as for all ionization gages, on the nature of the residual gas. The choice of the cathode material is such as to provide copious electron emission under ion bombardment and as to minimize the sputtering of the cathode metal. The Philips gage is a satisfactory pressure meter for the range of  $10^{-2}$  to  $10^{-5}$  mm Hg.

The Alphatron<sup>16</sup> (Fig. 4.10) employs the alpha rays emitted by a radioactive source to ionize the gas in a chamber communicating with

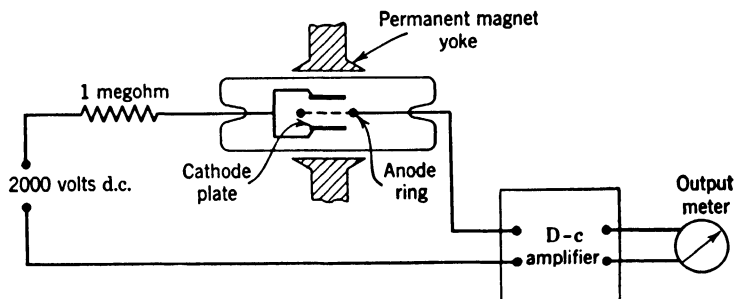


FIG. 4.9. The Philips Gage (Schematic). (After Penning, reference 11.)

the space in which the pressure is to be measured. In the example shown the source *a* is gold-radium alloy covering an area of approximately 1 square centimeter and containing about 0.2 milligram of radium. It is electroplated with nickel to prevent the loss of radioactive disintegration products, which contribute to the alpha emission, and reaction of traces of mercury in the vacuum vessel with the gold. The four-wire positive-ion collector *b* is supported by a lead entering a cage *c* maintained at a positive potential of 30 to 40 volts through an insulator *e*. It is electrically connected to the input of a high-gain meter amplifier. Since the collector currents are much smaller than for the normal ionization gage—about  $3 \cdot 10^{-10}$  ampere for a pressure of 1 mm Hg—the Alphatron is less sensitive than the thermionic ionization gage. On the other hand, it has a perfectly linear response throughout its range of utility, for instance, from 0.001 to 10 mm Hg.

One other useful high-vacuum gage is the Pirani gage.<sup>17</sup> It consists of a filament heated by a constant current in a tube communicating with the vacuum vessel. This filament constitutes one of the resistance branches of a Wheatstone bridge. Since the resistance of the filament

<sup>16</sup> See Downing and Mellen, reference 12.

<sup>17</sup> See Pirani, reference 13, Hale, reference 14, and Campbell, reference 15.

depends on the rate of cooling by the residual gas in the tube, the unbalance current through the bridge galvanometer is a measure of the pressure in the tube. The useful range of the Pirani gage is approximately  $10^{-4}$  to 1 mm Hg. The comparison resistance in the Wheatstone bridge usually is a second, identical, gage, sealed off in a high vacuum. Pressure indications may also be obtained from a Pirani gage by adjusting

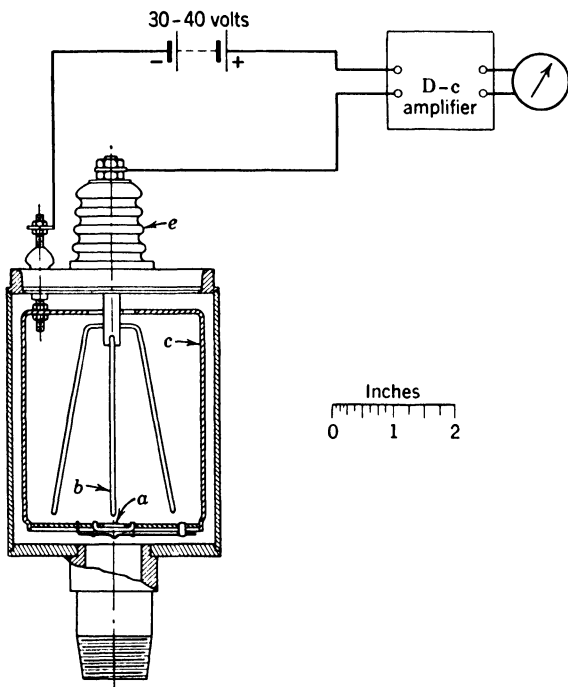


FIG. 4.10. The Alphatron Ionization Gage. (Downing and Mellen, reference 12.)  
(Courtesy of *Review of Scientific Instruments*.)

the current to keep the resistance or the voltage drop constant, or by adjusting the voltage drop to keep the resistance or current constant.

**Gases Used in Phototubes.** Since the alkali metals are highly active chemically, only inert gases may be employed for amplification by ionization.<sup>18</sup> There are only five truly inactive gases: helium, neon, argon, krypton, and xenon. All these gases were actually separated and identified within the brief space of four years during the last decade of the nineteenth century. Helium, which is only one-fourth as heavy as oxygen and is now familiar as filler for American dirigibles, is not fre-

<sup>18</sup> See Chapter 7.

quently employed in gas phototubes because of its high ionization potential.<sup>19</sup> This gas, which was first detected spectroscopically in the solar spectrum by Lockyer<sup>20</sup> in 1868, obtained its name from the Greek word for sun. It was first physically separated from a mineral in 1895 by Ramsay.<sup>21</sup> Its principal source at the present time is the natural gas wells in the United States.

Neon, brought to public notice by its use in brilliant red electric signs, serves satisfactorily in phototubes. However, it is fairly expensive since it constitutes only about 0.002 per cent by volume of the air from which it is obtained. Neon was formerly used quite extensively in glow tubes for television receivers. It is somewhat heavier than oxygen.

Argon comprises as much as 1 per cent of the air, from which it is separated with relative ease. Because of its abundance and, more especially, because of its low ionization potential, it is almost universally employed in phototubes. Argon was isolated, as the first of the inert gases, by Rayleigh and Ramsay in 1894.<sup>22</sup> Argon's only drawback is its great atomic mass, which is over twice that of oxygen. This great mass is partly responsible for the decreasing dynamic sensitivity of gas phototubes.

In 1898 Ramsay and Travers<sup>23</sup> identified successively, from residues of the evaporation of liquid air, the gases krypton, xenon, and neon. They were all detected through the observation of new spectral lines. Xenon, the heaviest of these gases, has since found application in certain gas-discharge control tubes (thyratrons).

Helium, argon, and neon may be conveniently purified to the extent required for admission into phototubes by storing in a glass container provided with calcium electrodes. If an arc is formed between the electrodes, the calcium reacts with any impurities which may be present.

In addition to the inert gases, which generally form the final atmosphere in gas phototubes, other active gases like oxygen and hydrogen commonly find application in the sensitization schedule.

**Gas Dosage.** All these gases can easily be admitted to the vacuum system in more or less controllable quantities by simply joining the gas bottle to the system through two high-quality stopcocks in series. The coupling tube between the cocks should be relatively small to avoid wasting the gas. To admit the gas, the cock nearest the bottle is opened to fill the coupling tube and is then securely closed. Then the second

<sup>19</sup> See Table 7.2 on p. 122.

<sup>20</sup> See reference 16.

<sup>21</sup> See reference 17.

<sup>22</sup> See reference 18.

<sup>23</sup> See reference 19.

cock is opened very slightly so that the gas enters the system as slowly as possible. The increasing pressure can be read on a thermocouple meter or on a mercury or phthalate manometer or, if a low pressure is to be established within a specified tolerance, on a Pirani or ionization gage. When the desired pressure has been obtained, the cock is closed. Needless to say, the pump must be shut off from the manifold during this procedure. This may be done by means of a large-bore stockcock or, preferably, a Y-shaped mercury trap in which a rising column of mercury closes off a bend in the tubing between the pump and liquid air trap. The gas enters the system just ahead of the liquid air trap.

The series stopcock method of dosage is conveniently rapid; however, a stopcock is always a potential source of leakage and contamination. At times a mercury-sealed glass valve seat with an iron plunger is provided. If the plunger is raised momentarily by an external solenoid, the gas bubbles through the mercury into the manifold.

A more elegant method has been adapted from the Bauer valve for "softening" x-ray tubes. The connecting tube from the gas bottle is cut, and the open ends are closed with unglazed porcelain or fired soapstone plugs, which are slightly permeable to gases. Normally the plugs are separated a fraction of an inch by means of a small well of mercury. However, a portion of the tubing is wound into a helix to provide extensibility. Thus, when desired, the movable end can be brought into contact with the fixed end, squeezing out the mercury between the plugs and permitting gas to penetrate through both plugs from the bottle into the system. Instantaneous cut-off is obtained by simply allowing the helix to retract. The scheme has the advantage of slow dosage, perfect hermetical insulation, absolute cleanness, and easy manipulation.

Oxygen is conveniently introduced into the system by heating a small mass of pure mercuric oxide contained in a bulb of hard glass connected directly to the system. At room temperature the oxide emits practically no gas, so that a high vacuum may be obtained in its presence; however, when the bulb is heated by a Bunsen burner to about 400° C, pure oxygen is liberated freely. Mercury vapor escaping at the same time is condensed in the trap. Care must be taken not to overheat the oxide to avoid sublimation and actual physical spouting into adjacent parts of the system. A helpful preventive is a wadding of out-gassed glass wool in the neck of the bulb.

Hydrogen may also be introduced in a distinctive manner. Hot palladium is known to be permeable to hydrogen, but not to any other gas. Hence a tiny hollow cylinder of the metal, closed at one end, may be sealed into the system. If the protruding portion of the tubing is heated in a Bunsen flame, hydrogen from the fuel gas will pass through

into the system. When cool, the palladium again becomes impermeable.

**The Alkali Metals.** The atomic structure of the alkali metals and their place in the periodic table of elements have already been discussed.<sup>24</sup> It remains to give a brief account of their discovery and their principal physical properties.

Sodium and potassium occur most abundantly in nature and were the first alkali metals to be isolated. Chemists had long been familiar with their hydroxides, known as caustic soda and caustic potash, but were under the impression that the compounds themselves were elements. It remained for Humphry Davy,<sup>25</sup> in 1807, to separate these now familiar alkali elements from their hydroxides by electrolysis. Sodium and potassium can now be purchased in the metallic state, preserved from reaction with the atmosphere by immersion in an inactive medium such as water-free kerosene. They are also available in many cheap compounds. The names sodium and potassium are merely Latinized derivatives of the English words soda and potash.

The next alkali metal to be separated was lithium. It was discovered in 1817 by Arfvedson,<sup>26</sup> who separated it from the alkali residue of the minerals lepidolite and spodumene by virtue of the relative insolubility of its carbonate and by other chemical properties. The name lithium was given to the new element from the Greek word for "stone" because it was thought to exist only in mineral as distinct from organic sources. Lithium is the lightest of all metals. It is available both in the pure state and in compounds.

The other alkalies, cesium and rubidium, were discovered spectroscopically by Bunsen and Kirchhoff<sup>27</sup> in 1860 and 1861, respectively. Cesium was so named because of its distinctive sky-blue spectral lines, rubidium, for its prominent doublet of deep red lines, the Latin words signifying "blue" and "red," respectively. Although both elements are very scarce, they can be secured, either pure or in compounds, for a reasonable price.

All the alkali metals, in their purest form, are silvery white in color. Cesium usually appears as a golden yellow because of slight traces of nitrogen. All are very active chemically, the activity increasing from lithium, which tarnishes rather slowly in air, to cesium, which reacts so quickly with air as to melt and ignite. A number of the physical constants of the alkali metals are listed in Table 4.2. The meth-

<sup>24</sup> See Chapter 2, p. 31.

<sup>25</sup> See reference 20.

<sup>26</sup> See reference 21.

<sup>27</sup> See reference 21.

ods employed for handling these active elements are described in Chapter 5.

TABLE 4.2. PROPERTIES OF THE ALKALI METALS  
(Hopkins, *Chemistry of the Rarer Elements*, D. C. Heath & Co., New York, 1923)

	Lithium	Sodium	Potassium	Rubidium	Cesium
Atomic weight	6.94	23.0	39.1	85.45	132.81
Specific gravity	0.534	0.9712	0.8621	1.532	1.87
Atomic volume	13.1	23.7	45.4	55.8	71.0
Melting point	186.0°	97.0°	62.5°	38.5°	26.5°
Boiling point	1400.0°	877.5°	700.0°	696.0°	670.0°
Specific heat	0.941	0.293	0.166	0.0792	0.0482
Color of flame	Crimson	Yellow	Violet	Violet	Blue

## REFERENCES

1. W. G. HOUSKEEPER, "The art of sealing base metals through glass," *J. Am. Inst. Elec. Engrs.*, Vol. 42, pp. 954-960, 1923.
2. P. T. SMITH and H. R. HEGBAR, "Duplex tetrode UHF power tubes," *Proc. Inst. Radio Engrs.*, Vol. 36, pp. 1348-1353, 1948.
3. F. LAUSTER, "Foil fusion as an advance in quartz lamp construction," *Elektrotech. Z.*, Vol. 57, pp. 517-519, 1936.
4. E. B. NOEL, "Development of water-cooled quartz mercury lamps," *J. Applied Phys.*, Vol. 11, pp. 325-336, 1940.
5. S. DUSHMAN, "Recent advances in the production and measurement of high vacua," *J. Franklin Inst.*, Vol. 211, pp. 689-750, 1931.
6. K. C. D. HICKMAN, "Vacuum pumps and pump oils," *J. Franklin Inst.*, Vol. 221, p. 215-235; 383-402, 1936.
7. K. C. D. HICKMAN, "Trends in design of fractionating pumps," *J. Applied Phys.*, Vol. 11, pp. 303-313, 1940.
8. A. O. NIER, C. M. STEVENS, A. HUSTRULID, and T. A. ABBOTT, "Mass spectrometer for leak detection," *J. Applied Phys.*, Vol. 18, pp. 30-33, 1947.
9. S. DUSHMAN and C. G. FOUND, "Studies with the ionization gauge," *Phys. Rev.*, Vol. 17, pp. 7-19, 1921.
10. R. B. NELSON and A. K. WING, "Emission-regulating circuit for an ionization gauge," *Rev. Sci. Instruments*, Vol. 13, pp. 215-217, 1942.
11. F. M. PENNING, "High-vacuum gauges," *Philips Tech. Rev.*, Vol. 2, pp. 201-208, 1937.
12. J. R. DOWNING and G. MELLE, "Sensitive vacuum gauge with linear response," *Rev. Sci. Instruments*, Vol. 17, pp. 218-223, 1946.
13. M. V. PIRANI, "Self-indicating vacuum meter," *Verhandl. deut. physik. Ges.*, Vol. 4, pp. 686-694, 1906.
14. C. F. HALE, "The measurement of very small gas pressures," *Trans. Am. Chem. Soc.*, Vol. 20, p. 243, 1911.
15. N. R. CAMPBELL, "A method for the micro-analysis of gases by the use of the Pirani pressure gauge," *Proc. Phys. Soc. (London)*, Vol. 33, pp. 287-296, 1921.



16. N. LOCKYER, "Notice of an observation of the spectrum of a solar prominence," *Phil. Mag.*, Vol. 37, pp. 143-145, 1869.
17. W. RAMSAY, "On a gas showing the spectrum of helium, the reputed source of  $D_3$ , one of the lines in the spectrum of the sun's chromosphere," *Nature*, Vol. 52, p. 7, 1895.
18. LORD RAYLEIGH and W. RAMSAY, "Argon, a new constituent of the atmosphere," *Proc. Roy. Soc. (London)*, Vol. A 57, p. 265, 1895.
19. W. RAMSAY and M. W. TRAVERS, "New gases of atmospheric air," *Compt. rend.*, Vol. 126, pp. 1762-1763, 1898.
20. H. DAVY, "Electrochemical researches on the decomposition of the earths; with observations on the metals obtained from the alkaline earths, and on the amalgam procured from ammonia," *Phil. Trans. Roy. Soc. (London)*, Vol. 98, pp. 333-370, 1808.
21. G. KIRCHHOFF and R. BUNSEN, "Chemical analysis by spectrum observation," *Phil. Mag.*, Vol. 22, pp. 330-349, 1861.

## Chapter 5

# GENERAL METHODS OF PREPARING PHOTOTUBES

It can probably be stated with safety that no two laboratories of phototube manufacturers employ identical methods in the preparation of phototubes. All that will be attempted in this chapter will be an elucidation of some general principles to be observed in phototube preparation and a description of a few procedures which have led to successful results.

**Geometrical Arrangement of Phototubes.** The method of preparation depends, to some extent, on the disposition of the cathode and anode within the tube. Figure 5.1 shows a series of electrode configurations meeting different requirements. The first form (*a*), with a small central cathode surrounded by a large spherical anode provided with a window for the admission of light to the cathode, finds application only in research. It is suitable for the study of the velocity distribution of the photoelectrons, since the electric field between the anode and the cathode is such as to assure the collection of all photoelectrons whose kinetic energy of emission exceeds the difference in potential between points at the surface of the cathode and of the anode. As a phototube this arrangement is inefficient, since only a small portion of the light flux which may be intercepted by the tube as a whole reaches the cathode. The light which is reflected by the cathode and returns to it as the result of a second reflection at a mirror anode generally plays a negligible role. In effect, the total photoemission is determined by the amount of light originally incident on the cathode.

In practical general-purpose phototubes, therefore, the cathode and the window are made comparable in size with the cross section area presented by the tube to the incoming light, and the anode is arranged as so to obstruct this light as little as possible. It is furthermore placed so that the collecting field at the cathode is approximately uniform over the surface. All these requirements are fulfilled, to a reasonable extent, in the configurations represented in Fig. 5.1, *b-f*. In this figure

*b* shows an earlier tube type in which the cathode is deposited directly on the glass envelope; the light is admitted through a window cleared by torching the glass, and the electrons are collected by a central ring electrode. This arrangement has now been largely replaced by that shown in *c*, with a semicylindrical metal cathode and a coaxial, straight-

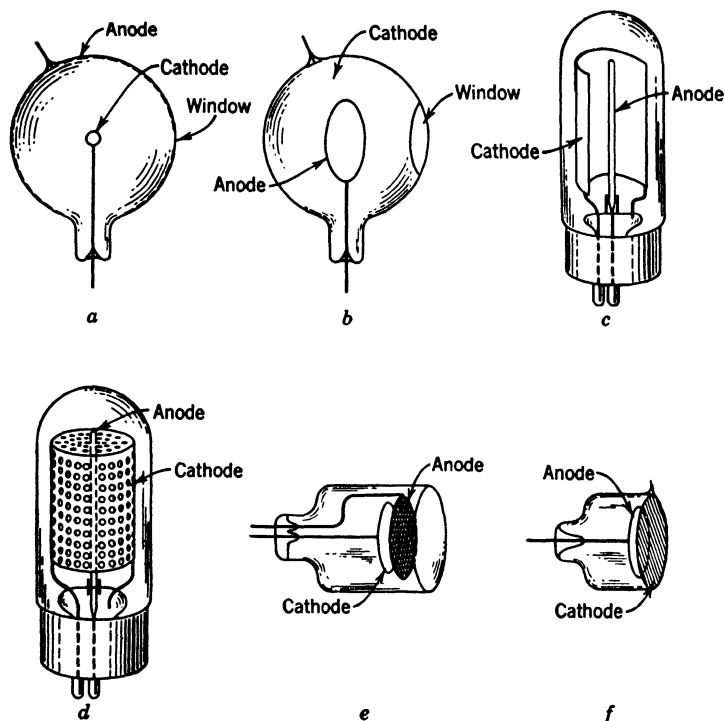


FIG. 5.1. Geometrical Arrangement of Phototubes: (*a*) Central cathode type. (*b*) Cathode deposited on envelope. (*c*) Semicylindrical cathode and rod anode. (*d*) Perforated-cylinder cathode and rod anode. (*e*) Flat cathode and mesh anode. (*f*) Transparent cathode.

wire anode. It is advantageous, in particular, in reducing electric leakage and in rendering the preparation of the base of the photosensitive surface more flexible. If the tube is to respond equally to light coming from all azimuthal directions, the half-cylinder cathode may be replaced by a full-cylinder, perforated cathode as shown in *d*.

The arrangement *e*, consisting of a circular cathode disk and a high-transmission screen anode, is to be preferred if the light beam has a circular cross section and if the tube is to offer minimal obstruction in the plane of the cathode. It is also suitable for low-voltage operation in

applications in which the tube capacity is immaterial. For gas tubes the disk may profitably be replaced by a shallow cup and the anode screen by a ring of comparable diameter; in this manner the path traveled by the photoelectrons is increased.

In *f*, where a transparent cathode is deposited directly on the flat glass window of the tube, no part of the cathode is obstructed by the anode. This arrangement is ideal where the tube must take up as little space in the plane of the cathode as possible.

It is to be noted that a small anode, well separated from the cathode, is quite generally desirable since it makes the tube capacity small and hence permits the employment of the tube in high-frequency applications. At the same time, reducing the size of the anode (for instance, the thickness of the anode wire) also reduces the collecting field at the surface of the cathode and increases the required operating potential. In practice the anode wires are of the order of 0.030 inch in thickness.

Tubes with very large exposed cathode surfaces are advantageous if they are to respond to light coming from different directions. If the direction of incidence of the light is fixed, on the other hand, it is generally more profitable to use a phototube of moderate size together with a large-diameter lens or mirror which concentrates the light on the photocathode.

**Electric Leakage.** How serious electric leakage between electrodes may be depends on the relative magnitude of the electronic current generated by the radiation incident on the photocathode. In early phototubes the photocurrents were small enough, even for strong illumination, to require the use of sensitive galvanometers for their measurement; hence very small leakage currents could lead to serious error. With very sensitive phototubes precautions against leakage become necessary only in measurements of very small light intensities. An effective method for shunting the small leakage current out of the galvanometer circuit is to introduce, somewhere in the high-resistance path, a conducting ring which is connected to ground. Furthermore, leakage may be minimized by increasing the length of the leakage path by placing the terminals at opposite ends of the tube or by enclosing either or both wires at the seals by long enveloping insulating sleeves. The insulation may be further improved by coating the envelope with ceresin or a suitable silicone lacquer.

The rate at which an alkali metal will distribute itself over insulating parts of a phototube depends mainly on its vapor pressure in the tube. In general, the vapor pressures of the alkali metals increase with atomic weight in somewhat the same manner as the melting points decrease.<sup>1</sup>

<sup>1</sup> See Table 4.2, p. 83.

The melting points of pure lithium and sodium are high enough for their vapor pressures to be almost negligible at ordinary temperatures, and no appreciable distillation and subsequent condensation take place even over indefinitely long periods of time. However, if a phototube contains an excess of an alkali metal as volatile as cesium or even potassium, it is almost impossible to prevent the eventual deposition of a conducting layer between terminals. One practical precaution is to enclose the anode support wire in a glass sleeve provided at the free end with a metal cap which covers and encircles the sleeve but does not touch it. A practical remedy, in the presence of leakage, is to apply local heating continuously so as to evaporate the condensed alkali metal.

Recent methods in the manufacture of phototubes with complex cathodes make it possible to use even cesium in tubes with both leads in a single press and still have an ohmic resistance between terminals of many thousands of megohms. It is done by using an extremely small amount of free alkali metal which is bound to the cathode surface during the process of formation. Very small amounts of excess cesium may also be absorbed by the lead glass constituting the tube press. This process, in which cesium chemically replaces the lead in the glass, freeing the lead, results in a darkening of the glass surface.

**Introduction of Active Metals.** All phototubes which respond to visible radiations have for their sensitive material one of the alkali metals, lithium, sodium, potassium, rubidium, cesium, or one of the alkaline earth metals, calcium, strontium, barium, or some physical or chemical compound of an alkali or alkaline earth. The metals most frequently used are sodium, potassium, rubidium, cesium, and barium. They may be deposited on the photocathode from *solution*, by *distillation*, by *electrolysis*, or by the *reduction of compounds* of the alkali or alkaline earth metals.

The method of solution was applied by J. Kunz<sup>2</sup> to lithium, which requires an inconveniently high temperature for distillation. The lithium metal was dissolved in ethylamine in the presence of ammonia and the resulting blue solution placed in the phototube bulb. When the ethylamine was pumped out, a grayish-blue lithium deposit was left on the glass. Its spectral response is shown in Fig. 2-13 on page 34.

Distillation of the alkali metals, sodium to cesium, may be carried out either from an external supply through a connecting glass system to the phototube or by direct evaporation from a reservoir of pure metal introduced into the tube before evacuation. Because of its relatively high melting point, 186° C, lithium cannot be distilled through glass systems, but it can be evaporated from a solid portion properly prepared

<sup>2</sup> See Seiler, reference 1.

and mounted within the tube. Ives and Olpin<sup>3</sup> have suggested a practical way of preparing the lithium. A small hollow cylinder of steel is driven through a block of the solid alkali metal; in this manner a protected core, with only the ends oxidized, is obtained. The cylinder with its core is mounted in a bulb and is fitted with a fairly heavy plunger which bears down on the lithium with its weight. When the cylinder is heated by a high-frequency electromagnetic field, the molten lithium, ordinarily unable to seep through its oxide crust, is forced to do so by the plunger and at once evaporates to condense on the walls of the bulb.

The other alkali metals may, rather inconveniently, be distilled from an original supply in a remote part of a glass appendage through a series of condensing chambers, as shown in Fig. 5.2. The metal becomes purer at each stage, until ultimately the vapor is driven into the phototube, after which the whole appendage with its chambers is sealed off. Within the phototube, the alkali metal may be permitted to condense directly upon the glass walls or else upon a conducting metallic coating, such as silver, previously deposited. The successive distillations may be effected by the simple expedient of applying a Bunsen flame.

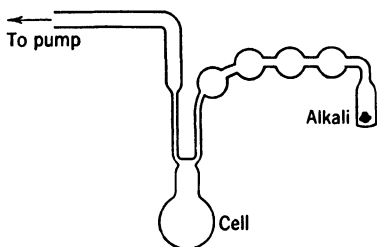


FIG. 5.2. Distilling Alkali Metal into Phototube through a Number of Condensing Chambers.

One novel method of introducing alkali metals into phototubes takes advantage of the reduced activity of these elements at low temperatures. For example, a lump of potassium is melted at low pressure in a glass bulb, and the molten metal is then decanted into a side tube and sealed off. When cool, the tube is immersed in liquid air. Any portion of the tube with its potassium core may then be snapped off and quickly inserted into a distillation appendage leading to the phototube. The appendage may be sealed off and the entire manifold evacuated before the alkali becomes warm enough to oxidize appreciably.

Electrolysis through the glass walls of the tube may be employed to deposit alkali metals on its interior walls. R. C. Burt<sup>4</sup> has developed and described a process by which pure sodium can be introduced into an evacuated bulb by this method. The bulb into which the sodium is to be introduced, for instance, a 60-watt lamp, must be made of soda glass. It is placed in a bath of molten sodium nitrate ( $\text{NaNO}_3$ , melting

<sup>3</sup> See reference 2.

<sup>4</sup> See reference 3.

point  $312^{\circ}\text{C}$ ) which also contains a heavy copper wire as anode. When the filament is incandescent, electrons travel to the glass, charging up its inner surface negatively. The resulting electric field between the melt, which is at a positive potential relative to the filament, and the inner surface of the bulb causes a drift of the sodium ions in the glass toward the inner surface. Those which arrive there are neutralized by the electrons from the filament and evaporate as free sodium atoms to condense on the cooler parts of the bulb. Phototubes prepared by this

process are quite permanent. Unfortunately their sensitivity is low compared to that of more modern types of phototubes.

It was demonstrated by one of the authors<sup>5</sup> that potassium phototubes could be prepared in like manner, employing pure potash glass and a potassium nitrate ( $\text{KNO}_3$ ) melt. Earlier attempts by Burt to send potassium ions through soda glass had failed since the replacement of the sodium ions by dissimilar potassium ions caused molecular strains which ultimately resulted in fracture. However, Forró and Patai<sup>6</sup> have shown since that potassium, as well as cesium and rubidium, phototubes may be produced by electrolysis in soda glass bulbs. For this purpose the bulbs, filled with a melt of the nitrate of the desired alkali, are placed in a sodium

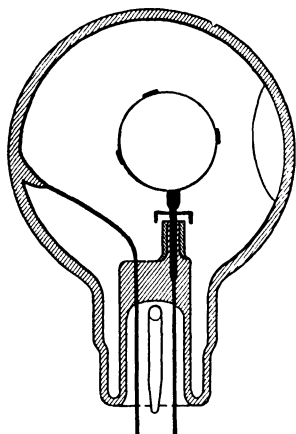


FIG. 5.3. A Cross Section of the Structure of a Cesium-Magnesium Phototube.

nitrate bath, and a reversed electrolytic current is passed through the glass walls. This process stores the desired alkali metal in the inner walls of the tube. After removal of the excess nitrate a filament may be sealed in and the bulb may be evacuated. Electrolysis in a sodium nitrate melt will now result in the deposition of a film of the desired alkali metal, released from the inner walls.

The most generally useful method of introducing active metals, however, is the thermal disintegration of chemical compounds. This method was used successfully in the Zworykin cesium-magnesium phototube.<sup>7</sup> Its mechanical structure can be clearly understood from Fig. 5.3. The press contains two wires; one of them is sealed to the inner wall of the tube, the other is centrally located, with a ring of metallic ribbon

<sup>5</sup> See Zworykin, reference 4.

<sup>6</sup> See reference 5.

<sup>7</sup> See Zworykin and Wilson, reference 6.

mounted on it. A glass sleeve, topped but not touched by a metal cap, surrounds the central wire and insures effective insulation. A few bits of magnesium are welded to the ring, which is painted, in addition, with a small quantity of an aqueous solution of cesium trinitride ( $\text{CsN}_3$ ). After the tube has been exhausted and baked out in the usual manner, it is at once sealed off from the manifold. When, subsequently, the ring is heated by a high-frequency field, the magnesium evaporates and

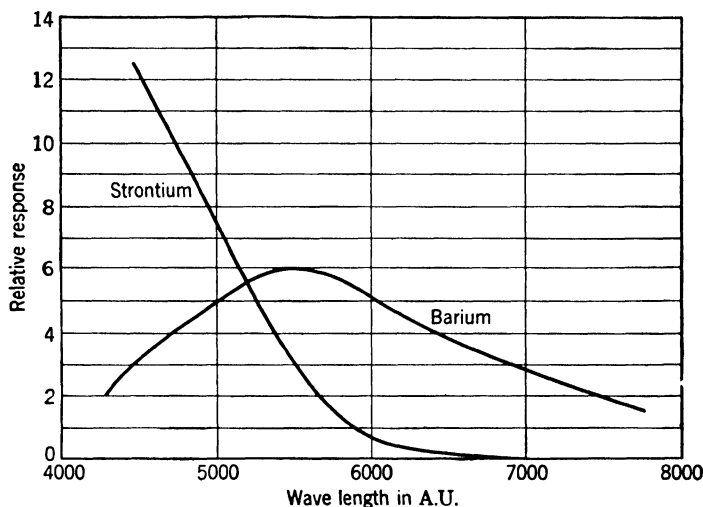


FIG. 5.4. Spectral Response of Barium and Strontium Phototubes Made by Case.

condenses on the walls of the bulb. At the same time the trinitride is thermally decomposed and the free nitrogen is chemically bound by the active magnesium. Thus, ultimately, the cesium vapor condenses in an invisibly thin film upon the silvery magnesium coating. A window is made in an appropriate position by applying a Bunsen flame externally, and the phototube is finished.

Case<sup>8</sup> employed the thermal disintegration of the oxides of strontium and barium on a platinum-iridium filament to form barium and strontium photoemitters on sheet nickel. The filament was impregnated with a paste of barium and strontium nitrates, heated in air to change the nitrates into oxides, and mounted, together with the nickel plate, in a tube. After evacuation and baking the nickel plate was outgassed by electron bombardment from the filament. When, thereafter, the difference of potential between the electrodes was reduced to zero and the filament raised to an orange heat, barium (and barium suboxide)

<sup>8</sup> See reference 7.



were liberated and deposited on the plate, forming a sensitive photocathode. Strontium was given off when the filament was white hot. Figure 5.4 indicates the spectral response of photosurfaces prepared in this manner. Case mentions that the photocurrent of the strontium phototube, with a photocathode area of the order of 7 square inches, is 100 to 150 microamperes in average sunlight.

The most common source of the alkali metals cesium and rubidium is an intimate mixture of the alkali chromate with a reducing agent such as powdered silicon. It is compressed into a pellet and sealed into a

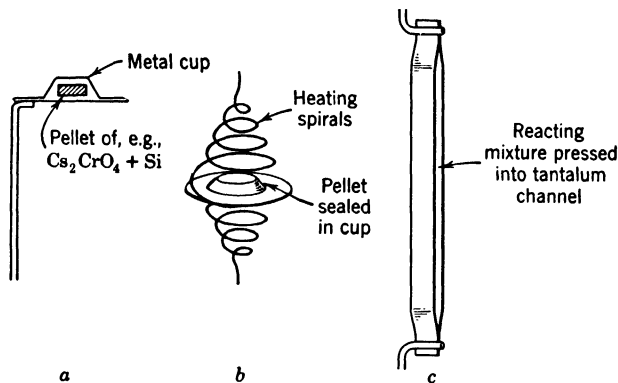


FIG. 5.5. Liberation of Alkali Metals by Chemical Reaction in (a) High-Frequency-Heated Metal Cup, (b) Metal Cup Heated by Conduction and Radiation, and (c) Tantalum Channel Heated by Conduction.

flat nickel or tantalum cup. Welded either to the anode wire or on a stem in a side tube, the alkali metal may be liberated from the cup by heating with a high-frequency coil. Alternatively, the mixture may be pressed into a narrow tantalum "channel," formed by folding a narrow strip of tantalum sheet, which may be welded to two press wires and heated by conduction. It is found that with the second source the evolution of contaminating gases accompanying the liberation of the cesium is minimized. Figure 5.5 shows these alkali metal sources. In the figure *b* indicates how the advantages of heating by conduction may be utilized with the circular pellet sealed in a metal cup; the cup is welded between two helical tungsten filaments which heat it primarily by radiation.

**Sensitizing with Hydrogen.** Elster and Geitel's method of sensitizing alkali surfaces by a glow discharge in hydrogen has already been mentioned in Chapter 1. In this process, which is quite simple, different types of tubes require, for best results, different gas pressures and voltages. As an example, a potassium phototube may be sensitized in the

following manner. After the alkali has been introduced into the tube, dry hydrogen is admitted to a pressure of 2 or 3 millimeters of mercury. As a direct voltage of approximately 300 volts is applied, with an external series resistance of about 3000 ohms between the tube terminals, a glow discharge takes place which immediately colors the surface of the potassium. The discharge is continued for a few seconds, until the surface assumes a peacock blue coloration. At this point the sensitivity of the phototube, for the light of a tungsten lamp, should have risen to approximately a hundred times its initial value. A still more reliable procedure consists of alternately applying the discharge voltage and measuring the photoelectric response until maximum sensitivity is attained.

There is a tendency for the potassium hydride and adsorbed potassium formed by the glow discharge to be submerged in the alkali metal, so that the coloration gradually disappears and the augmented sensitivity along with it. Campbell<sup>9</sup> describes a phototube in which an invisibly thin film of alkali metal is deposited on a metal plate. This film is sensitized by a hydrogen discharge and, being so thin, is completely converted into the hydride, with potassium adsorbed on it, in a reasonably short period. The tube, which is ultimately filled with a definite pressure of hydrogen, is reported to have a long dependable life.

Unlike the remaining alkali metals, cesium is not effectively sensitized by the action of hydrogen in a glow discharge.

**Preparation of the Silver-Cesium Oxide-Cesium Phototube.** This phototube, pre-eminent in its red and infrared sensitivity, was introduced by Koller<sup>10</sup> of the General Electric Company in 1929. Since then a large number of different preparation procedures have been worked out, leading to different spectral responses and sensitivities. Prescott and Kelly<sup>11</sup> of the Bell Laboratories have given a detailed account of one standardized preparation technique and the results so obtained. The procedure outlined below, which differs from it in several respects, should produce phototubes with an integral sensitivity (for a tungsten lamp with a color temperature of 2870° C) of 10 to 30 microamperes per lumen.

A piece of sheet nickel is bent into a semicylinder and welded to two wires of the press, electroplated lightly with copper to improve the adhesion of the silver, and then electroplated with silver, forming a matte surface.<sup>12</sup> A third press wire serves as anode. A nickel cup containing a

<sup>9</sup> See reference 8.

<sup>10</sup> See reference 9.

<sup>11</sup> See reference 10.

<sup>12</sup> More commonly, the semicylindrical cathode is shaped out of pure silver sheet.

pellet of cesium chromate and silicon is welded to the top or bottom of this wire in such a manner that it can be heated with a high-frequency coil without overheating the cathode. The press is now sealed into a lime glass bulb, and the bulb, in turn, is sealed to a vacuum system. After the tube has been evacuated and baked at about  $350^{\circ}\text{C}$  until the pressure has dropped below  $10^{-5}$  mm Hg, the oven is removed and the metal parts are raised to a dull red heat with a high-frequency coil to free them of gas. After they are cooled, oxygen is admitted to a

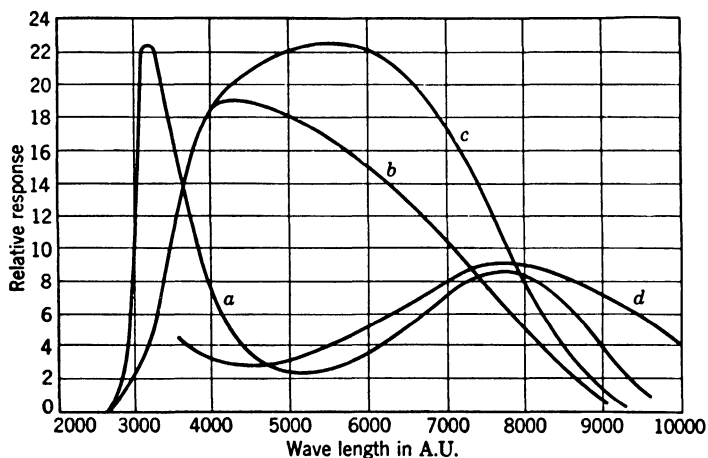


FIG. 5.6. Spectral Response of Different Silver-Cesium Oxide-Cesium Phototubes.

pressure of about 2 mm Hg and a high-frequency glow discharge is passed between the cathode and anode. As the silver layer becomes oxidized it changes in color, becoming in turn yellow, red, blue, yellow, red, blue-green, and green; at this point the discharge is stopped and the oxygen pumped out. The cesium pellet in the nickel cup is now heated with a high-frequency coil until the cesium chromate and the silicon react, liberating cesium, which condenses largely on the glass parts of the tube. The tube is now baked at about  $200^{\circ}\text{C}$  until the edges of the cathode, which becomes dark gray during the bake, turn light. If there is considerable excess of cesium, it may be absorbed by a coating of a mixture of lead oxide or tin oxide, which, suspended in amyl acetate, is painted on the back of the cathode or on the press. At the end of the bake the tube is sealed off. Curve *a* in Fig. 5.6 indicates the spectral response of a tube prepared in this manner.

If the tube is baked too long, the cathode will turn an ivory color and the photosensitivity will drop to a low value. If, then, argon is intro-

duced into the tube and a glow discharge is established between the electrodes, the original sensitivity will be recovered, the argon may be pumped out, and the tube may be sealed off.

The several curves shown in Fig. 5.6 were obtained from phototubes subjected to slightly different sensitizing procedures. The high infrared sensitivity indicated by curve *d* may be attained consistently by paying careful attention to the purity of the ingredients and a precisely

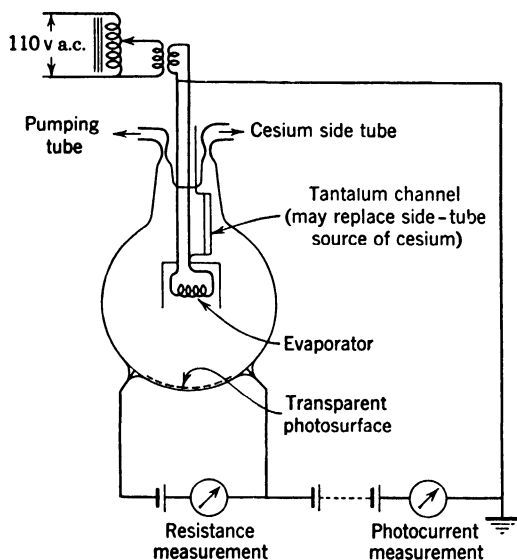


Fig. 5.7. Tube Structure and Circuit Employed in Preparation of Transparent Silver-Cesium Oxide-Cesium, or Antimony-Cesium Photosurface.

controlled baking schedule. Exact control of the sensitization is facilitated in the procedure for preparing transparent silver-cesium oxide-cesium phototubes described below.

A suitable tube structure for this purpose is shown in Fig. 5.7. The original bulb is provided with a metal contact sealed through the glass at the edge of the projected cathode area; the region of the inner wall adjacent to the contact is painted with silver paste. A silver evaporator, consisting of a silver bead fused on a helical tungsten filament, is mounted in a suitable shield between two press wires. The cesium pellet is not mounted in the bulb, but in a side tube (not shown in Fig. 5.7) so arranged that the main bulb and the side tube can be heated in two separate ovens. After evacuation, baking (of both tubes), and outgassing of the metal parts, silver is evaporated until the silver film

deposited on the tube wall transmits 50 per cent of the incident light. It is then fully oxidized by a glow discharge in oxygen. After the oxygen has been pumped out, silver is again evaporated over the oxidized layer (which is relatively transparent) until the light transmission once more drops to 50 per cent. A microammeter and battery are then connected in series with the cathode contact and the evaporator (functioning as anode), making possible the measurement of the thermionic currents from the cathode. The oven, at 200° C, is placed over the main bulb and the pellet in the side tube is exploded. With the side tube oven, adjusted to a lower temperature such as 150° C, placed over the side tube, cesium slowly distills into the main bulb and reacts with the oxidized silver. As the reaction proceeds a thermionic current, as indicated by the microammeter, is observed. As soon as this current has passed its peak, the side tube is immersed in liquid air and may be sealed off. The main bulb may similarly be removed from the system after the main oven has been raised. The grayish transparent photocathode prepared in this manner has a specific surface resistance of some hundred ohms and a sensitivity comparable to that of an opaque photocathode sensitized in similar fashion.

Other sensitization techniques, such as the evaporation of silver on the finished silver-cesium photocathode, have already been discussed in Chapter 3.

**Preparation of the Antimony-Cesium Phototube.** The antimony-cesium phototube is the most sensitive of a family of phototubes whose sensitive surface consists of an intermetallic compound of an alkali metal with bismuth, antimony, and related metals. The method of preparation given below applies to a transparent cathode phototube<sup>13</sup> of the form shown in Fig. 5.7. The modifications required for forming an opaque photocathode are sufficiently obvious to render separate treatment superfluous.

As shown in Fig. 5.7, the antimony<sup>14</sup> is placed in a tungsten spiral in the evaporator. An additional press wire is provided as current lead for heating a tantalum channel containing the mixture of cesium chromate and silicon which serves as cesium source. After the tube has been evacuated and baked at a temperature not exceeding 350° C (a higher temperature would cause sublimation of the antimony) antimony is evaporated to a thickness—checked by observing the light transmission of the deposited film—which has, by previous tests, been found to give the most favorable result. The tube is then raised to a temperature of

<sup>13</sup> Transparent molybdenum-cesium phototubes were prepared by a similar method as early as 1926 by one of the authors (see Zworykin, reference 11).

<sup>14</sup> Or alloy of antimony with palladium or silver (see below).

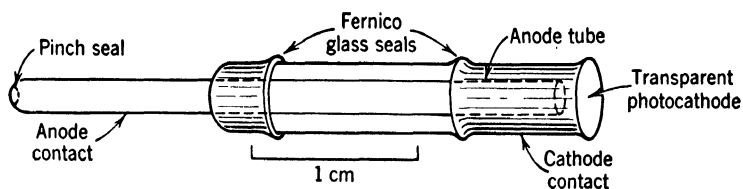


FIG. 5.8. Construction of Miniature Phototube with Antimony-Cesium Photocathode (Type 1P42).

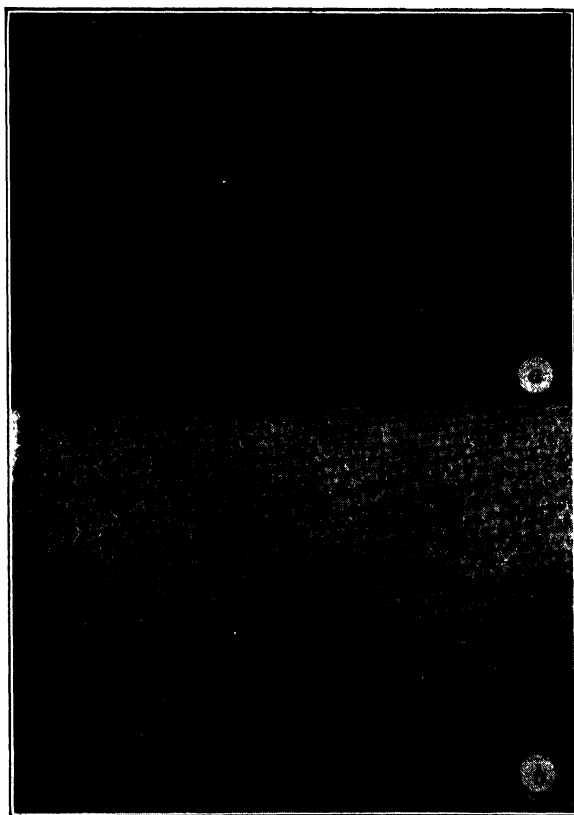


FIG. 5.9. Electron Micrographs of Evaporated Film of (a) Pure Antimony and (b) Silver-Antimony Alloy. Magnification: 50,000. The films (somewhat less than 100 Å.U. thick) were condensed on thin quartz films which, in turn, were formed by condensation on rock salt. (Preparation by J. E. Ruedy. Micrographs by J. Hillier.)

150° C in the oven and the cesium is admitted gradually by heating the tantalum channel until the photosensitivity reaches a broad maximum. The tube is then cooled. After being cooled, it is subjected to a series of brief liberations of cesium and subsequent bakes until the sensitivity ceases to rise farther. The photocathode appears reddish by transmission. The average photosensitivity of tubes prepared in this manner is,

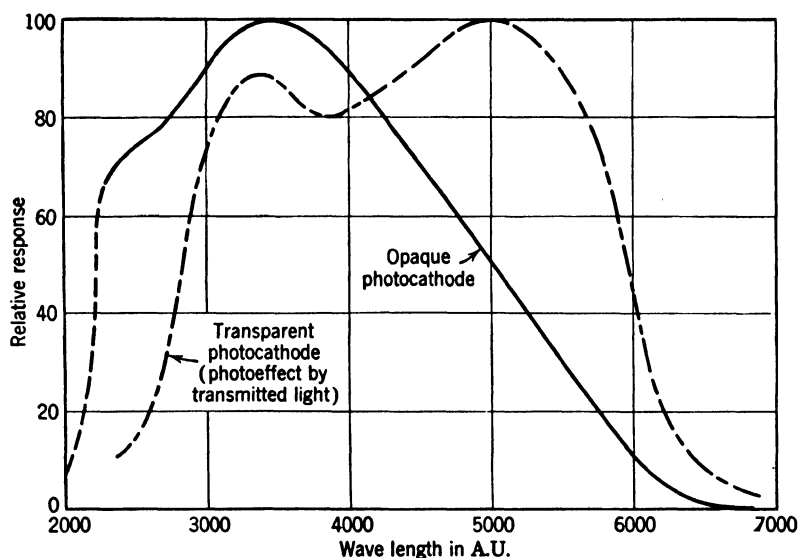


FIG. 5.10. Spectral Response of an Opaque and a Transparent Antimony-Cesium Photocathode.

for a tungsten source with a color temperature of 2870° C, 45 micro-amperes per lumen.

In very small tubes the antimony film is generally deposited in a separate evaporating chamber. In this case special precautions must be taken to prevent the overheating and oxidation of the antimony when the tube is sealed together. Figure 5.8 shows a cross section of a diminutive tube of this type. The transparent cathode is sealed into a Fernico cylinder, which provides the cathode contact. A glass cylinder separates it from the anode tube, through which the phototube is evacuated and through which cesium is admitted. After activation the anode tube is closed by a pinch seal.

In practice, palladium and silver alloys of antimony, rather than pure antimony, are used in the formation of transparent photocathodes. They have several advantages; they form beads on the tungsten filament

quite readily—pure antimony does not—and show less tendency to sublime during the bake. More important, it is found that, for instance, an antimony-palladium alloy containing 41 per cent antimony ( $\text{Sb}_3\text{Pd}_5$ ) will form a film having a surface resistance of only some hundred ohms, whereas a film of comparable thickness evaporated from pure antimony or from an alloy containing more than 69 per cent of antimony ( $\text{Sb}_2\text{Pd}$ ) will measure many megohms. Electron micrographs of films of pure antimony and of silver-antimony alloy show marked differences in structure which may provide a key to the observed differences in conductivity (Fig. 5.9). It should be noted that the spectral response of the alloy cathodes is relatively insensitive to processing procedure. However, there is a marked difference in the response curves for transparent and opaque, front-surface, cathodes. Differential light absorption in the sensitive film causes the transparent cathodes to exhibit relatively greater sensitivity at longer wave lengths (Fig. 5.10).

**Preparation of Phototubes for the Ultraviolet.** In the ultraviolet the pure metals form satisfactory photoemissive materials. The threshold wave length of the metal yields the upper limit of the spectral range, the ultraviolet absorption of the envelope, in general, the lower limit. Long-wave thresholds of a number of suitable metals are given in Table 5.1.<sup>15</sup>

TABLE 5.1. PHOTOELECTRIC THRESHOLDS OF PURE METALS

<i>Element</i>	<i>Threshold, A.U.</i>	<i>Element</i>	<i>Threshold, A.U.</i>
Cerium	4300	Bismuth	2870
Calcium	3850	Molybdenum	2850
Thorium	3650	Chromium	2840
Uranium	3400	Tungsten	2700
Zirconium	3300	Iron	2680
Titanium	3150	Nickel	2550
Tantalum	3010	Platinum	2000
Cadmium	2920		

The envelope material most commonly used for phototubes, lime glass, absorbs strongly below 3000 Angstrom units. Greater transmission in the near ultraviolet is obtained with Corex D, which may be employed for radiation down to 2800 Angstrom units. A specially thin, blown window of Corex D will even transmit 70 per cent of the incident radiation at 2500 Angstrom units.<sup>16</sup> The combined effect of the position

<sup>15</sup> See Rentschler and coworkers, references 12–14.

<sup>16</sup> See Rentschler, Henry, and Smith, reference 12.



of the threshold and the absorption of a Corex D envelope in creating a relatively narrow spectral response is shown, for a series of pure metal surfaces, in Fig. 5.11. The greatest integral sensitivity in the ultraviolet is obtained, however, by enclosing a photocathode activated with cesium in an envelope of a modern ultraviolet transmitting glass

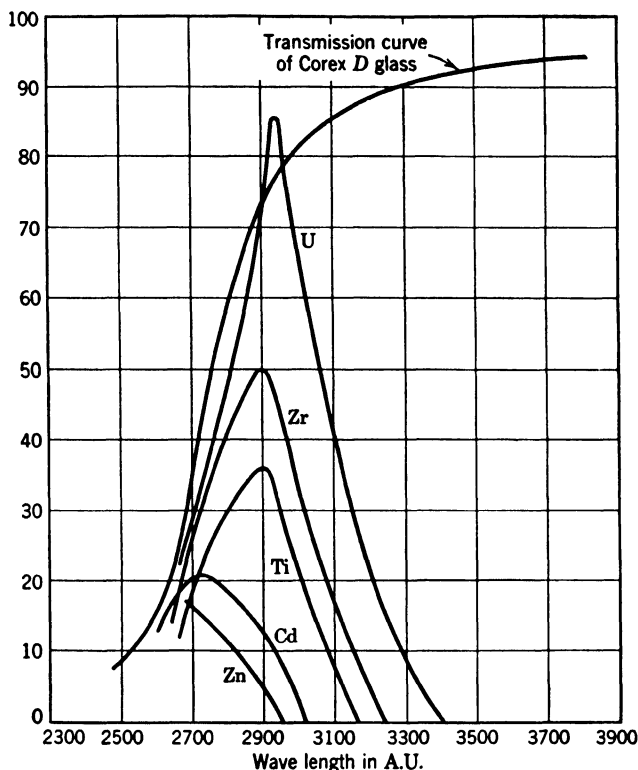


FIG. 5.11. Spectral Response of Various Pure Metal Surfaces Enclosed in Corex D Envelope. (After Rentschler.)

such as Corning 9741, whose spectral transmission in the ultraviolet approaches that of fused quartz.<sup>17</sup>

A technique for preparing very clean surfaces of any base metal that can be formed into a wire has been developed by H. C. Rentschler of the Westinghouse Lamp Division Laboratories and his coworkers.<sup>18</sup> Since relatively small contaminations may give rise to considerable shifts of the threshold (toward longer wave lengths) and, in addition,

<sup>17</sup> The spectral response S-5, shown in Fig. 6.10, on p. 115, is obtained with an antimony-cesium surface in a Corning 9741 envelope.

<sup>18</sup> See Rentschler and Henry, reference 13.

may influence the sensitivity of the surface adversely, the precautions taken are necessary to assure perfectly reproducible results.

The construction of the phototube is shown in Fig. 5.12. The photosensitive metal which is to be deposited on the cathode is in the form of a wire *w*, mounted in front of the semicylindrical nickel electrode *d*, which is welded to the two-wire frame *b*. The lower parts of *w* and its lead are shielded by the ceramic insulator *s* and the glass sleeve *a*. A nickel cylinder *f*, which shields the glass envelope during the deposition of the active metal, slides on the frame *b*. After the tube has been exhausted and baked at 400° C and the metal parts have been out-gassed, argon is introduced and the tube is sealed off. Now, with the nickel cylinder *f* surrounding the electrode *d* and the wire *w*, a discharge, with *w* as cathode, is passed through the tube, so that the metal of *w* is sputtered on the electrode *d*. When a sufficiently thick layer has been deposited, the tube *g* is sealed to a vacuum system and the thin glass bubble *h* is broken by raising the iron plunger *p* with a magnet and allowing it to drop. The argon then is pumped out and the tube sealed off at *m*.

Phototubes which combine relatively high sensitivity in the visible with a good response in the ultraviolet may be obtained by enclosing any alkali-activated photocathode in an ultraviolet transmissive envelope. Apart from the familiar cesium phototubes, sodium photocathodes have, in particular, found application for this purpose.<sup>19</sup> The effect of the envelope material—lime glass, Corex D, and fused quartz—on the response of a silver-cesium oxide-cesium phototube is brought out strikingly in Fig. 5.13.

<sup>19</sup> The spectral response of an ultraviolet-sensitive sodium phototube is given by S-6 in Fig. 6.10 on p. 115.

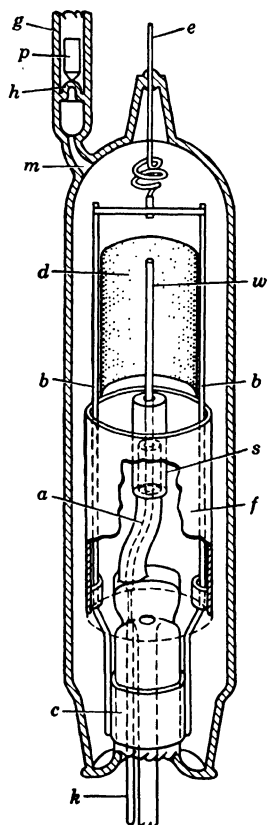


FIG. 5.12. Structure of Ultraviolet-Sensitive Phototube with Pure-Metal Cathode: (a) Glass Sleeve. (b) Wire Frame. (c) Structure-Supporting Metal Collar. (d) Cathode. (e) Cathode Lead. (f) Movable Shield. (g) Exhausting Tube. (h) Glass Bubble. (k) Anode Lead. (m) Sealing Constriction. (p) Iron Plunger. (s) Ceramic Insulator. (v) Anode Rod of Cathode-Surface Material. (Rentschler, Henry, and Smith, reference 12.) (Courtesy of *Review of Scientific Instruments*.)

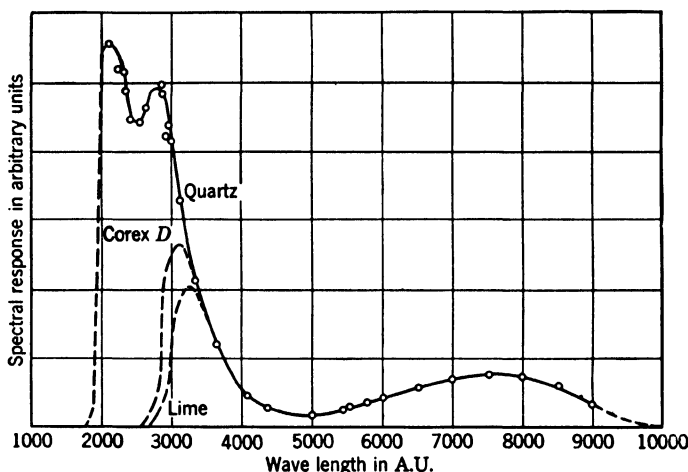


FIG. 5.13. Effect of Envelope Material on Spectral Response of Silver-Cesium Oxide-Cesium Surface.

#### REFERENCES

1. E. F. SEILER, "Color-sensitiveness of photoelectric cells," *Astrophys. J.*, Vol. 52, pp. 129-153, 1920.
2. H. E. IVES and A. R. OLPIN, "Maximum excursion of the photoelectric long-wave limit of the alkali metals," *Phys. Rev.*, Vol. 34, pp. 117-128, 1929.
3. R. C. BURT, "Sodium by electrolysis through glass," *J. Optical Soc. Am.*, Vol. 11, pp. 87-91, 1925.
4. V. K. ZWORYKIN, "Electrolytic conduction of potassium through glass," *Phys. Rev.*, Vol. 27, p. 813, 1926.
5. M. FORBÓ and E. PATAI, "An electrolytic method of preparing alkali metals in discharge tubes," *Z. tech. Physik*, Vol. 12, pp. 256-262, 1931.
6. V. K. ZWORYKIN and E. D. WILSON, "The cesium-magnesium photocell," *J. Optical Soc. Am.*, Vol. 19, pp. 81-89, 1929.
7. T. W. CASE, "A photoelectric effect in audion bulbs of the oxide-coated filament type," *Trans. Am. Electrochem. Soc.*, Vol. 39, pp. 423-428, 1921.
8. N. R. CAMPBELL, "The photoelectric emission of thin films," *Phil. Mag.*, Vol. 12, pp. 173-185, 1931.
9. L. R. KOLLER, "Some characteristics of photoelectric tubes," *J. Optical Soc. Am.*, Vol. 19, pp. 135-145, 1929.
10. C. H. PRESCOTT, JR., and M. J. KELLY, "The cesium-oxygen-silver photoelectric cell," *Bell System Tech. J.*, Vol. 11, pp. 334-367, 1932.
11. V. K. ZWORYKIN, "A study of photoelectric cells and their improvement," *University of Pittsburgh Bulletin*, Vol. 22, No. 31, 1926.
12. H. C. RENTSCHLER, D. E. HENRY, and K. O. SMITH, "Photoelectric emission from different metals," *Rev. Sci. Instruments*, Vol. 3, pp. 794-802, 1932.
13. H. C. RENTSCHLER and D. E. HENRY, "Effect of oxygen upon the photoelectric threshold of metals," *J. Optical Soc. Am.*, Vol. 26, pp. 30-34, 1936.
14. H. C. RENTSCHLER and D. E. HENRY, "Photoelectric emission," *J. Franklin Inst.*, Vol. 223, pp. 135-145, 1937.

## Chapter 6

# THE VACUUM PHOTOTUBE

The electron emission of a photocathode exposed to light may be utilized in a number of different ways within the tube of its origin. In the ordinary vacuum phototube it is simply collected by the anode, a second electrode at a positive potential with respect to the cathode. The characteristics of such tubes are the subject of this chapter. The utilization of the photocurrent in the circuit connecting the anode and cathode will be dealt with at a later point.

**Propagation of Photoelectrons in Vacuum.** Measurements by Ives and his coworkers<sup>1</sup> indicate that the photoelectrons emitted by a surface are distributed symmetrically about the normal to the surface and that the emission per unit solid angle in any direction is proportional, approximately, to the cosine of the angle which the direction in question makes with the normal (Fig. 6.1). This statement applies for any angle of incidence, spectral distribution, and polarization of the exciting light. The cosine distribution holds, of course, only in the neighborhood of the point of origin. Since the electrons are accelerated, by the electrostatic field between the anode and the cathode, in the direction of the electrostatic lines of force, and since these lines are normal to the cathode surface, the motion of the electrons at a small distance from the cathode is predominantly normal to the cathode. The exact path of any electron depends on its point of origin on the cathode, its velocity and direction of emission, and the electrostatic field distribution between the cathode and the anode.

The upper limit of the initial kinetic energy of the photoelectrons is given, as has been seen in Chapter 2, by the difference in the energy of the incident light quantum ( $12,395/\lambda_{A.U.}$  electron volts) and the work function of the emitter. Most measurements of the energy distribution of the electrons have yielded curves which ascend fairly uniformly from zero to a maximum lying somewhere in the upper half of the energy range and then drop relatively sharply to a point near the upper energy

<sup>1</sup> See Ives, Olpin, and Johnsrud, reference 1.

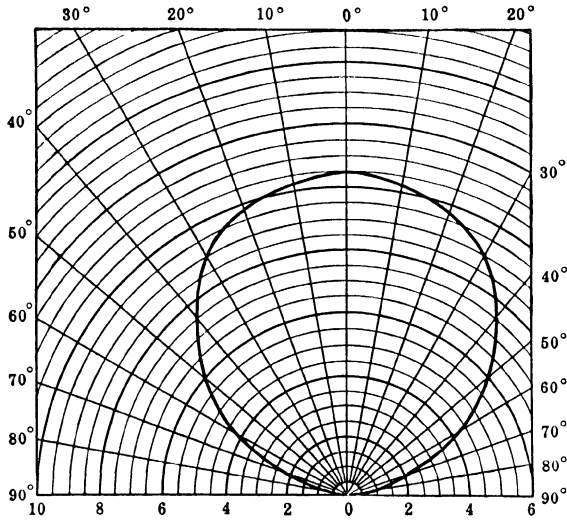


FIG. 6.1. Polar Diagram of Angular Distribution of Photoelectrons. (Ives, Olpin, and Johnsrud, reference 1.) (Courtesy of the *Physical Review*.)

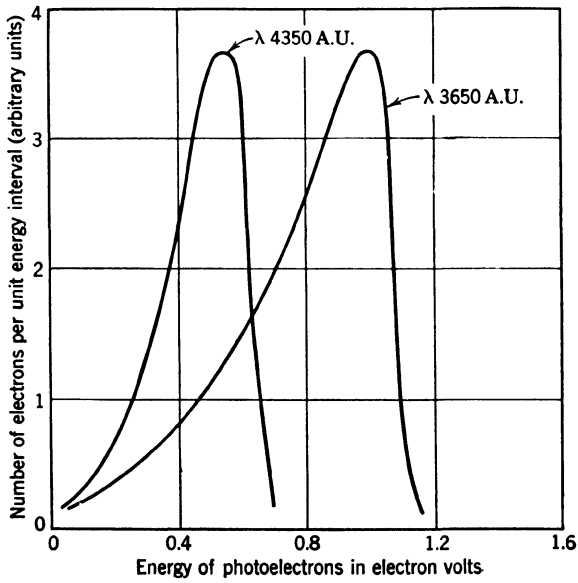


FIG. 6.2. Energy Distribution of Photoelectrons from a Potassium Film of 30 Molecular Layers on Silver for Two Different Wave Lengths of the Incident Radiation. (Brady, reference 2.) (Courtesy of the *Physical Review*.)

limit. Figure 6.2 shows measurements by Brady<sup>2</sup> on potassium irradiated by two different lines of the mercury spectrum. The variation shown is characteristic for a pure metal; it is predicted by theories of the surface photoeffect developed by Mitchell<sup>3</sup> and other authors. The energy distributions of the photoelectrons emitted by compound and semiconductor photocathodes, by contrast, may exhibit pronounced irregularities.<sup>4</sup>

**The Effect of Electrostatic and Magnetic Fields.** If the strength of the electrostatic field at any point is  $E$ , the force acting on an electron (charge,  $-e$ , and mass,  $m$ ) at the point in the direction of the field is  $-eE$ . The energy supplied to the electron in traveling from a point of the field  $A$  to another point of the same field  $B$  is always the same, irrespective of its route. It is equal to  $e(V_B - V_A)$ , where  $V_A$  and  $V_B$  are the electrostatic potentials at the two points in question. In particular, the energy given the electron in traveling from the cathode to the anode is  $eV$ , where  $V$  is the potential of the anode relative to that of the cathode. If the initial velocity of the electron is  $v_o$ , it will arrive at the anode with a velocity  $v$  given by  $mv^2/2 = mv_o^2/2 + eV$  or  $v = (v_o^2 + 2eV/m)^{1/2}$ . If, between the cathode and anode, the electron encounters a retarding field—as is always the case if the anode is negative with respect to the cathode—the electron may be turned back toward the cathode, reaching it with its original energy of emission. This may also result, at very low positive anode voltages, from the modification of the field distribution between the electrodes by the presence of a large number of negatively charged electrons in front of the emitting cathode. The repulsion of this negative “space charge” may return the electrons, leaving the cathode with low initial velocities and thus reducing the total photocurrent. However, normally, the electronic space charge in phototubes is much too small to have an appreciable effect.

Magnetic fields, other than the weak earth’s magnetic field, are not present in the usual vacuum phototube. They do play a role, however, in a number of more complex photosensitive devices which will be described later. The actions of magnetic fields and electrostatic fields on electrons are quite different. In the first place, a magnetic field has no effect whatsoever on a charge not in motion. Second, the force acting on a moving charge is directly proportional to the velocity of motion and has a direction at right angles both to the line of motion and to the

<sup>2</sup> See reference 2.

<sup>3</sup> See reference 3.

<sup>4</sup> Thus Kollath (reference 4) found three maxima in the energy distribution curve for photoelectrons emitted from an antimony-cesium photocathode at a specific angle with respect to the normal.

direction of the field. The magnitude of the force on an electron moving with a velocity  $v$  in a direction at an angle  $\theta$  with the lines of induction of a magnetic field of flux density  $B$  is

$$F = eBv \sin \theta \quad (6.1)$$

Thus, when the electron travels at right angles to the field, the force reduces simply to  $eBv$ . Furthermore, when it travels parallel to the field ( $\theta = 0$ ), the force is zero. The direction of the force corresponds to that of the middle finger of the right hand, bent forward so as to be perpendicular to the plane of the palm, if the thumb and the forefinger, both in the plane of the palm, point in the direction of the magnetic field and that of the motion of the electron, respectively. For a positive charge the direction of the force exerted by the magnetic field is opposite to that for a negative charge or, specifically, for an electron.

The path of an electron moving at right angles to a magnetic field is bent into a circle whose radius of curvature  $R$  is proportional to the velocity of the electron and inversely proportional to the magnetic flux density.<sup>5</sup> If the motion of the electron is not at right angles to the magnetic field, but forms an arbitrary angle with the field lines, it may be resolved into two components, one in the direction of the field and one at right angles thereto. Accordingly the electron describes a helix whose radius is determined by the ratio of the perpendicular component of velocity to the magnetic induction, and whose pitch depends on the ratio of the parallel component to the induction.<sup>6</sup> It follows that, in

<sup>5</sup> Since the acceleration of a particle at right angles to its direction of motion is given by  $v^2/R$ , where  $v$  is the velocity of the particle, Newton's second law of motion leads to

$$\frac{mv^2}{R} = eBv \quad R = \frac{mv}{eB} \quad (6.2)$$

In terms of the accelerating potential  $V$  required to give the electron the velocity  $v$ , this becomes

$$R = \frac{1}{B} \left( \frac{2mV}{e} \right)^{1/2} = 3.37 \cdot 10^{-6} \frac{V^{1/2}}{B} \text{ meter} \quad (6.3)$$

if  $V$  is measured in volts and  $B$  in webers per square meter ( $1 \text{ weber/meter}^2 = 10^4 \text{ gauss}$ ).

<sup>6</sup> If the angle between the field lines and the direction of motion of the electron is  $\theta$ , the velocity component parallel to the field lines is  $v \cos \theta$ , that in a direction at right angles to the field lines,  $v \sin \theta$ . Accordingly, the radius of the helix is

$$R = 3.37 \cdot 10^{-6} \frac{V^{1/2}}{B} \sin \theta \text{ meter} \quad (6.4)$$

and its pitch

$$d = \frac{2\pi R v \cos \theta}{v \sin \theta} = 2\pi R \cot \theta = 2.108 \cdot 10^{-5} \frac{V^{1/2}}{B} \cos \theta \text{ meter} \quad (6.5)$$

strong magnetic fields, electrons travel along helices about the magnetic lines of induction, the helix being "tighter" in proportion as the magnetic field is stronger (Fig. 6.3).

Consider next the simultaneous action of a uniform electrostatic field  $E$  and a uniform magnetic field  $B$  on an electron. If the two fields are parallel, each field affects the electron in a manner essentially the same as if the other field were absent, and the resulting displacements

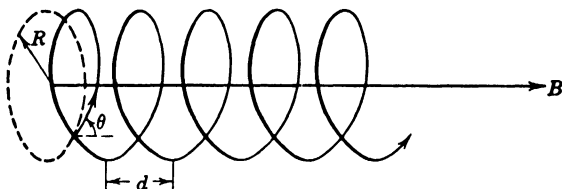


FIG. 6.3. Path of Electron in Uniform Magnetic Field.

and velocities may be added vectorially. The deflections produced by each field are at right angles to each other. If the electron starts from rest, its path is a helix with increasing pitch (Fig. 6.4).

If the electric and the magnetic fields are crossed (perpendicular to each other) there is one velocity of an electron traveling at right angles to both fields for which no deflection occurs.<sup>7</sup> In all other cases the motion becomes fairly complex. For an electron starting from rest the

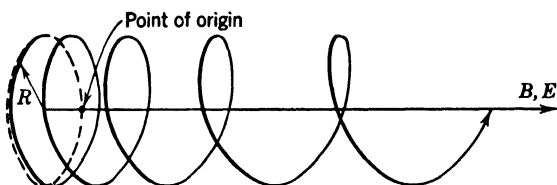


FIG. 6.4. Path of Electron in Superposed Uniform Electric and Magnetic Fields with the Same Direction.

combined action of the accelerating field and the magnetic field causes the electron to travel along a cycloidal path, described by a point on the rim of a wheel running along a track which passes through the point of origin and is normal to both fields. The velocity of the wheel is that of the undeflected electron (Eq. 6.6), and its radius is the radius of curvature of the path of an electron traveling with this velocity at right angles

<sup>7</sup> This velocity is given by

$$-eE + eBv = 0 \quad v = \frac{E}{B} \quad \text{or} \quad V = \frac{mE^2}{2eB^2} = 2.84 \cdot 10^{-12} \frac{E^2}{B^2} \text{ volts} \quad (6.6)$$



to the magnetic field in the absence of the electric field.<sup>8</sup> Initial velocity components of the electron normal to the magnetic field have the effect of moving the generating point on the wheel up or down a spoke without modifying its radius or velocity. A velocity component of the electron in the direction of the magnetic field simply causes a uniform translation of the electron in this direction; this translation has to be added vectorially to the cycloidal motion normal to the magnetic field. Figure 6.5

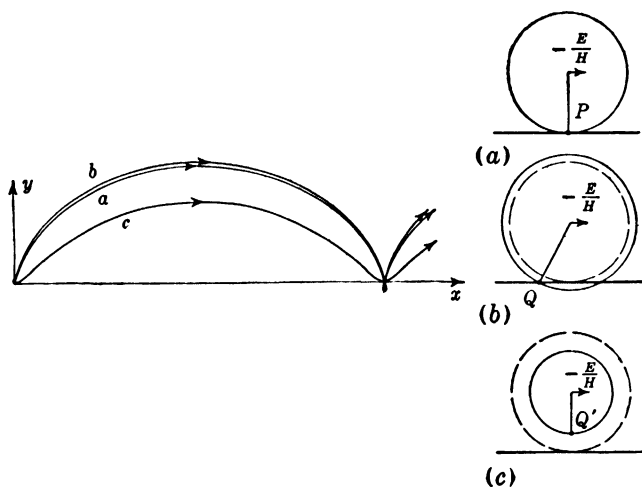


FIG. 6.5. (a) Paths of Electrons in Crossed Uniform Fields for Zero Initial Velocity, (b) an Initial Velocity in the  $y$ -Direction, and (c) an Initial Velocity in the  $x$ -Direction. The points  $P$ ,  $Q$ , and  $Q'$  represent the initial position of the electron. (Zworykin, Morton, Ramberg, Hillier, and Vance, *Electron Optics and the Electron Microscope*, John Wiley and Sons, New York, 1945.)

shows electron paths in crossed electric and magnetic fields for different initial velocities.

**Current-Voltage Relation.** The proper utilization of a phototube requires a knowledge of the variation of the anode-cathode current with applied voltage for fixed values of the illumination. In an ideal phototube, current would begin to flow for a difference in potential between cathode and anode  $V_{\min}$  such that

$$V_{\min} = V_c - 12,395 \left( \frac{1}{\lambda_{\min}} - \frac{1}{\lambda_0} \right) \text{volts} \quad (6.8)$$

where  $V_c$  is the contact difference of potential of the cathode relative to

<sup>8</sup> This radius is

$$R = \frac{mE}{eB^2} = 5.68 \cdot 10^{-12} \frac{E}{B^2} \text{meter} \quad (6.7)$$

the anode,  $\lambda_o$  is the long-wave threshold of the photocathode, and  $\lambda_{\min}$  is the shortest wave length represented in the illumination of the

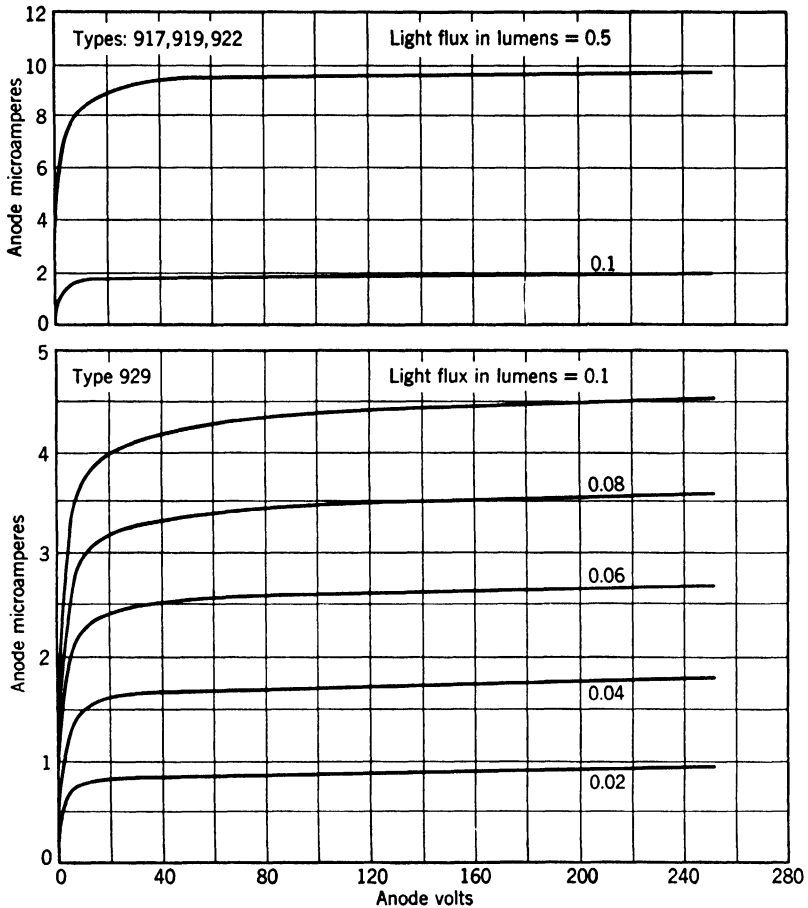


FIG. 6.6. Current-Voltage Curves for (a) a Silver-Cesium Oxide-Cesium Tube (Types 917, 919, 922) and (b) an Antimony-Cesium Tube (Type 929) (RCA Victor Division).

phototube. The tube current would increase as the anode was made more positive until the tube voltage reached the value  $V_{\text{sat}}$ :

$$V_{\text{sat}} = V_c \quad (6.9)$$

Beyond this point the current would remain constant. Thus, for  $\lambda_o = 6600$  Angstrom units,  $\lambda_{\min} = 3700$  Angstrom units, the current would rise from zero to its maximum value in an interval of only 1.5 volts.

An examination of current-voltage curves for actual phototubes, such as those shown in Fig. 6.6, reveals a relatively rapid variation in current in a range of the order of 20 volts and appreciable deviations from constancy even for collecting voltages of the order of 100 volts. Two fac-

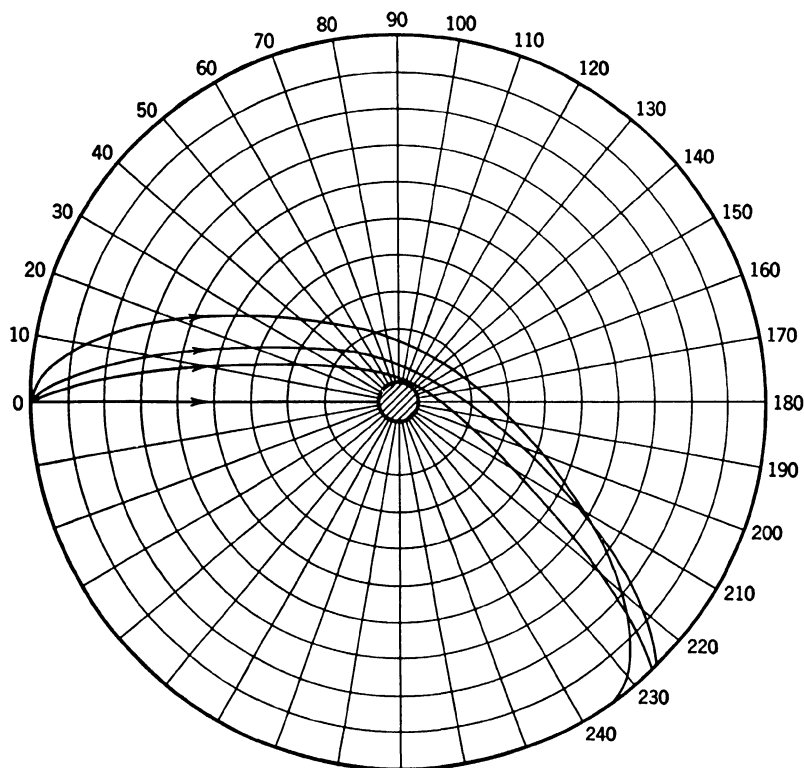


Fig. 6.7. Paths of Photoelectrons in Tube with Cylindrical Cathode and Rod Anode for Constant Initial Kinetic Energy (0.016 V) and Different Angles of Emission ( $0^\circ$ ,  $30^\circ$ ,  $45^\circ$ , and  $90^\circ$  with respect to normal).  $V$  = anode voltage.

tors are responsible for this behavior. First of all, the photoemission itself of complex surfaces may be dependent on the applied field. This "Schottky effect" is known to be negligible in the range of electric fields normally encountered in phototubes both for pure metallic surfaces and for thin alkali metal films bound on a slightly oxidized substrate.<sup>9</sup> It may be appreciable for the thick silver-cesium oxide-cesium surfaces and the semiconducting films of intermetallic compounds of cesium which play the major role in phototubes.

<sup>9</sup> See Lawrence and Linford, reference 5.

The magnitude of the other factor is more readily estimated. Since, in most phototubes, the anode is made small, so as to obstruct as little of the cathode surface as possible, a certain fraction of the electrons which leave the cathode return to it without striking the anode (Fig. 6.7). This fraction is considerable for small applied voltages and may vanish altogether for very high voltages. Figure 6.8 shows the variation of anode current with applied voltage for a particular phototube, the emission process being assumed to be uninfluenced by the applied voltage.

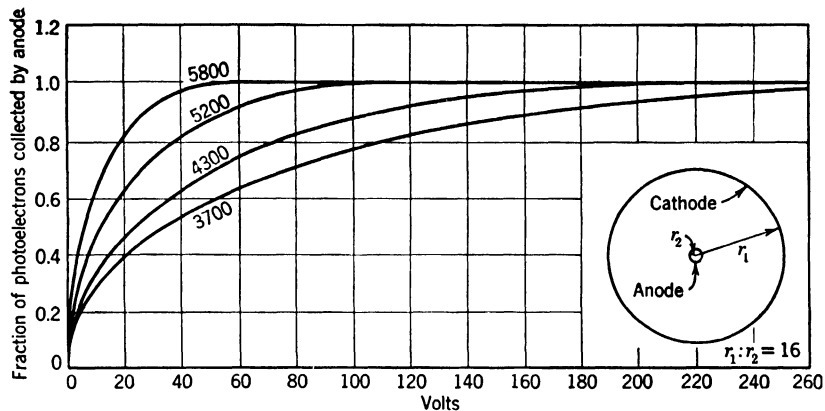


Fig. 6.8. Calculated Current-Voltage Curves of Phototube with Cylindrical Cathode and Rod Anode for Different Monochromatic Radiations. (Consideration of back scattering of electrons incident on cathode would make these curves somewhat steeper.)

Each curve corresponds to monochromatic illumination with a particular wave length. The model of the phototube chosen for the calculation consists of a cylindrical cathode, 1 inch in diameter, with a wire anode,  $\frac{1}{16}$  inch thick, along its axis. The long-wave threshold of the photocathode is assumed to be  $\lambda_0 = 6600$  Angstrom units and the energy distribution of the photoelectrons to increase linearly from zero at zero electron volts to a maximum at  $12,395 (1/\lambda - 1/\lambda_0)$  electron volts. This energy distribution corresponds quite closely to the distribution shown in Fig. 6.2. The angular distribution of the electrons is assumed to obey the cosine law.

The theoretical curves in Fig. 6.8 and the experimental curves in Fig. 6.6 show sufficient points of agreement to attribute a large share of the difference between the current-voltage characteristics of real phototubes and ideal phototubes to the geometrical factors considered here. The ascent of the curves is seen to become more gradual as the wave length of the exciting light is decreased, since this decrease cor-

responds to an increase in the spread of the initial velocities of the photoelectrons. This trend, also, is confirmed by observation.

In the majority of actual phototubes the cathode is approximately semicylindrical. The tube wall through which the light falls on the cathode may then, in principle, assume either a potential close to cathode potential or one close to anode potential. If the anode is small in dimension, it is most likely that the wall takes on cathode potential, in this case the potential distribution and the electron paths resemble quite closely those assumed in the derivation of the curves in Fig. 6.8. On the other hand, if the tube wall takes on anode potential, which may happen if the secondary-emission coefficient of the glass<sup>10</sup> is relatively high, an electron must reach the anode for every photoelectron which strikes the wall. Under these circumstances the anode current would be very nearly saturated, that is, equal to the total photoemission, even for an applied potential of a few volts. Actually, the first condition is more likely to prevail at low operating voltages, the second at high operating voltages.

**Current-Light Flux Relations.** Ideally, the photocurrent, and hence the number of electrons released by the incident light, should be exactly proportional to the light flux received by the photocathode. Factors

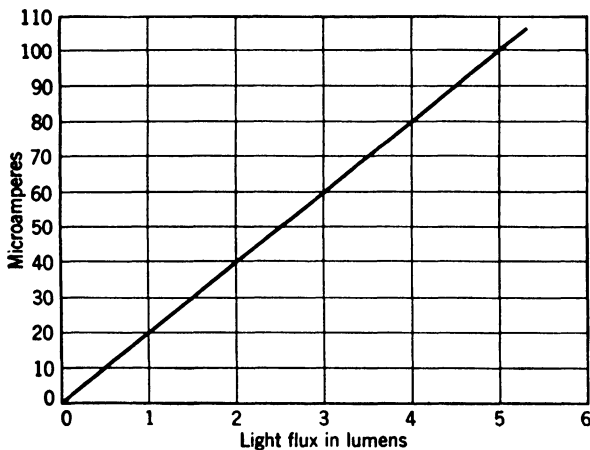


FIG. 6.9. Variation of Photocurrent with Light Flux for a Vacuum (Silver-Cesium Oxide-Cesium) Phototube.

which lead to a deviation from this proportionality have been discussed in Chapter 3, page 53. Practical vacuum phototubes employ photosensitive surfaces for which these factors are negligible over a wide oper-

<sup>10</sup> See Chapter 8.

ating range. Figure 6.9 illustrates the linearity of the relation between photocurrent and light flux for a particular phototube for a range from 0 to 5 lumens, the latter corresponding to an illumination of approximately 6000 lux. The upper limit of the operating range of any tube is set both by photoelectric fatigue phenomena and the partial decomposition of the sensitive surface by the thermal action of the intense illumination.

**Dynamic Characteristics.** The response of a vacuum phototube to incident light signals is exceedingly rapid. This fact arises from two circumstances. First, the time which elapses between the incidence of a light quantum and the ejection of a photoelectron has been found to be too brief for measurement.<sup>11</sup> Second, the time of transit of the electron between cathode and anode is exceedingly short; this is a consequence of the fact that the electron has a much larger ratio of charge to mass than any other known object, so that even a relatively weak electric field imparts an enormous acceleration to it. For two flat electrodes spaced a distance  $d$  apart, the time of transit  $T$  is simply equal to the ratio of the separation of the two electrodes and the average velocity of the electron or one half its final velocity:

$$T = 2d \left( \frac{2eV}{m} \right)^{-1/2} \quad (6.10)$$

Here  $V$  is the voltage applied between the two electrodes. For  $d = 10^{-2}$  meter (1 cm),  $V = 100$  volts, and  $e/m = 1.758 \cdot 10^{11}$  coulombs/kilogram, the time of transit, therefore, becomes  $3.4 \cdot 10^{-9}$  second. For a cylindrical cathode and wire anode, such as is represented in Fig. 6.7, the transit time is larger since the accelerating field in the initial portions of the electron paths is weaker.<sup>12</sup> Thus, for a cathode radius  $r_1 = 10^{-2}$  meter, and a ratio of the cathode radius  $r_1$  to the anode radius  $r_2$  equal to 10, the transit time  $T$  becomes, for  $V = 100$  volts,  $4 \cdot 10^{-9}$  second. Even if the anode radius should be made only a tenth of a millimeter ( $r_2/r_1 = 1/100$ ),  $T = 6.4 \cdot 10^{-9}$  second. It follows that, with

<sup>11</sup> See Lawrence and Beams, reference 6.

<sup>12</sup> For an electron leaving the cathode with zero initial velocity

$$\begin{aligned} T &= r_1 \left( \frac{2eV}{m} \right)^{-1/2} \left[ \pi \log_e \frac{r_1}{r_2} \right]^{1/2} \Phi \left\{ \left[ \log_e \frac{r_1}{r_2} \right]^{1/2} \right\} \\ &= r_1 \left( \frac{2eV}{m} \right)^{-1/2} \left[ \pi \log_e \frac{r_1}{r_2} \right]^{1/2} \\ &\quad - r_2 \left( \frac{2eV}{m} \right)^{-1/2} \left\{ 1 - \frac{1}{2} \left[ \log_e \frac{r_1}{r_2} \right]^{-1} + \frac{3}{4} \left[ \log_e \frac{r_1}{r_2} \right]^{-2} - \dots \right\} \quad (6.11) \end{aligned}$$

$r_1$  and  $r_2$  are the radii of the cathode and anode, respectively, and  $\Phi$  denotes the "error function."

proper external circuit connections, photocurrents from vacuum phototubes should be able to reflect faithfully fluctuations in the incident light flux taking place in a small fraction of a millionth of a second. This property is of importance in numerous applications, particularly in the field of television.

The dynamic response of a phototube refers to the variation of the output of the tube with the frequency of an incident light signal. If, instead, the illumination is kept constant and an alternating voltage is applied to the tube, the phototube acts as a rectifier, yielding unidirectional current pulses. A simultaneous variation in the light intensity is expressed as a modulation of the pulse amplitude.<sup>13</sup> For frequencies of the applied voltage in excess of 50,000 cycles per second an appreciable capacitative current through the phototube will generally be added to the modulated photocurrent.

**Spectral Response Curves and Sensitivity Standards.** The Radio Manufacturers' Association and the National Electrical Manufacturers' Association have jointly adopted a classification of commercial phototubes on the basis of their spectral response characteristics. Figure 6.10 shows the response curves for sensitive-surface types S-1, S-3, S-4, S-5, S-6, and S-8, all of which are represented in commercial phototubes. S-1 corresponds to a silver-cesium oxide-cesium surface in a lime-glass bulb, exhibiting high sensitivity in the infrared. S-3 is a silver-rubidium oxide-rubidium surface with a response maximum near 4200 Angstrom units in lime glass. It has high sensitivity throughout the visible, approximating relatively closely the response of the human eye. S-4 represents an antimony-cesium surface in lime glass, with a maximum response in the blue. A similar surface, enclosed in an envelope of ultraviolet-transmitting glass, yields the response of S-5, with high sensitivity near the mercury resonance line at 2537 Angstrom units. S-6 represents a sodium surface, also predominantly ultraviolet sensitive. S-8, finally, is a bismuth-cesium surface, whose response extends toward longer wave lengths than the response of the antimony-cesium surface S-4.

Because of their greater sensitivity, these types have almost completely replaced earlier types, such as the potassium hydride-potassium phototube, whose spectral response is shown in Fig. 3.5, page 45, and the more sensitive cesium-magnesium phototube (Fig. 6.11). It is interesting to note the similarity in the spectral responses of the cesium-magnesium phototube and the antimony-cesium phototube (S-4 in Fig. 6.10).

The spectral response curves given indicate merely the relative sensitivity of the phototube to radiations of different wave length.

<sup>13</sup> See Chapter 12, p. 242.

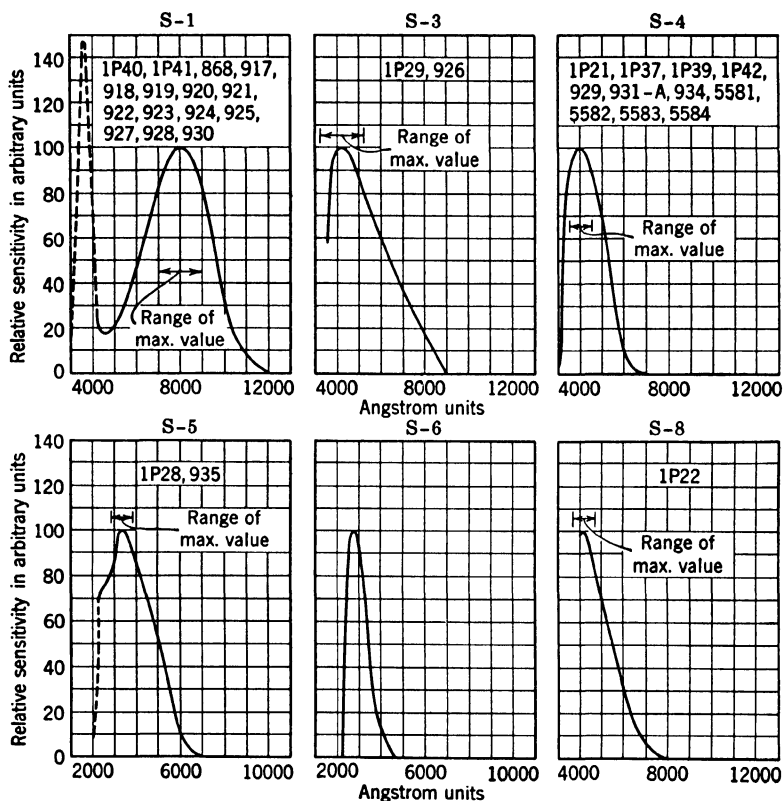


Fig. 6.10. Standard Spectral Response Characteristics of Phototubes.

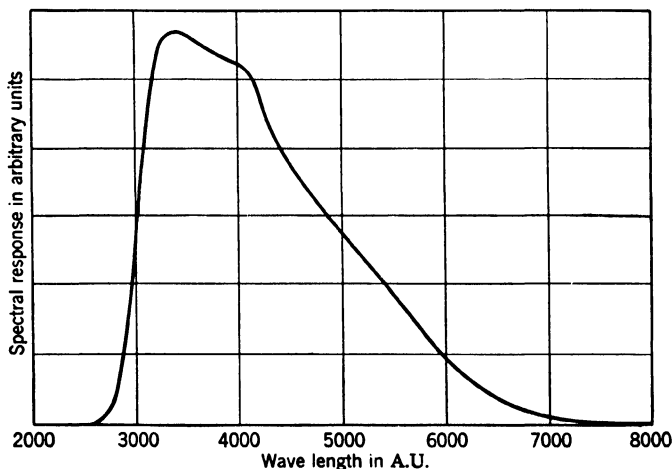


Fig. 6.11. Spectral Response of the Cesium-Magnesium Phototube.



The absolute luminous sensitivity is generally given in microamperes per lumen, an incandescent tungsten filament at a color temperature of 2870° K serving as light source. On this basis the sensitivity of the cesium-magnesium phototube is about 2 microamperes per lumen, that of the potassium hydride-potassium tube, one-tenth as much.

**Properties of Commercial Vacuum Phototubes.** Since new and improved types of phototubes are continually being introduced by phototube manufacturers, any tabulation of their characteristics is subject to

TABLE 6.1. PROPERTIES OF RCA PHOTOTUBES FOR THE VISIBLE  
(Mean Values)

Type	Cathode		Physical Structure	Sensitivity		Maximum Current Density		Maximum Voltage, volts	Inter-electrode Capacity, $\mu\text{f}$
	Surface	Area, sq in.		$\mu\text{a}/\mu\text{watt}$ at Response Peak	$\mu\text{a}/\text{lumen}$ , 2870° K Source	Peak, $\mu\text{a}/\text{sq in.}$	Average, $\mu\text{a}$		
917	S-1	1	A	0.002	20	100	10	500	2
919									
922	S-1	0.4	B	0.002	20	100	5	500	0.5
925	S-1	0.4	C	0.0015	15	100	5	250	1.5
926	S-3	0.4	B	0.0016	6.5	100	5	500	0.5
929	S-4	0.5	D	0.042	45	100	5	250	2.6
1P39									
934	S-4	0.3	E	0.028	30	100	4	250	1.5
1P42	S-4	0.03	F	0.02	25	100	0.4	150	1.7

a degree of obsolescence. Nevertheless, Table 6.1, indicating the principal properties of a series of RCA vacuum phototubes, may serve a useful purpose in acquainting the prospective user with the characteristics of some of the more common types. In addition, the information given may render more significant references to phototubes by type number in the discussion of their applications. More complete and up-to-date information may be obtained from the manufacturers.<sup>14</sup>

Figure 6.12 shows outline drawings to scale of the several tube types listed; Fig. 6.13 shows their external appearance. All of them except

<sup>14</sup> The addresses of some of the principal manufacturers of phototubes are: Radio Corporation of America, Tube Department, Harrison, N. J.; General Electric Company, Schenectady, N. Y.; Westinghouse Electric Corporation, Pittsburgh, Pa.; The Rauland Corporation, Chicago, Ill.; and the Continental Electrical Company, Geneva, Ill. In comparing the sensitivity ratings given by different manufacturers, it is well to bear in mind that sources of lower color temperature than 2870° K are at times employed to determine the sensitivity of S-1 phototubes. This leads to higher apparent values of the tube sensitivity.

the 1P42 (*F*) have a semicylindrical cathode and all except the 922 and 926 (*B*), a rod anode. The 917 and 919 are provided with a grid cap to which the anode and the cathode, respectively, are connected. The

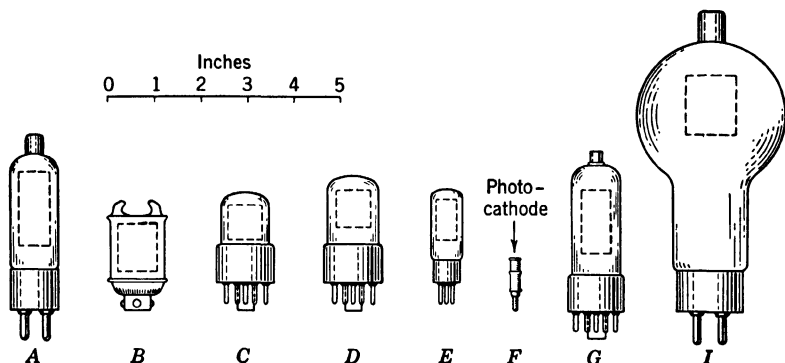


FIG. 6.12. Outline Drawings of Some Commercial Phototube Types. (Dotted rectangles indicate projected area of photocathodes.)

resulting wide separation of the leads increases the leakage path between the electrodes and therefore makes these tube types particularly suitable for measurements at low light levels. The cartridge-type tubes (*B*),

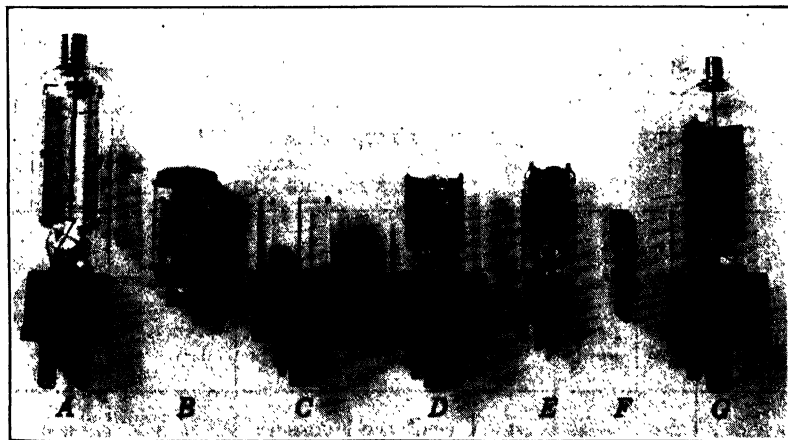


FIG. 6.13. A Selection of Commercial Phototubes.

similarly, have their electrode connections at opposite ends of the glass envelope, increasing the leakage path. The 925, 929, and 1P39 have standard octal bases, the only distinction between the 929 and 1P39

being that the latter is provided with a special nonhygroscopic base which minimizes leakage at high atmospheric humidity. The 1P42, finally, is a diminutive phototube with a maximum diameter of only one-fourth inch and a transparent cathode. It is designed especially for applications in which the phototube is to occupy a minimum amount of space.

The maximum ambient temperature which can be tolerated is 100° C for tubes with S-1 and S-3 (as well as S-8) surfaces and 75° C for those with S-4 (and S-5) surfaces. Although the maximum permissible anode voltage as given in the table is, in general, 250 or 500 volts, applications which demand extreme constancy of the sensitivity over prolonged periods make an operating voltage of 20 volts or less desirable. At higher voltages positive ions formed in the traces of residual gas in the tube cause, by their bombardment of the cathode, a gradual change in the response characteristics of the tube.

**Vacuum Phototubes for the Ultraviolet.** Among the ultraviolet-sensitive tubes listed in Table 6.2 are some, namely the RCA 935 and the General Electric FJ-405, which have considerable sensitivity in the visible (20  $\mu$ A/lumen and 12  $\mu$ A/lumen, respectively), and others whose response is limited to certain spectral bands in the ultraviolet. The spectral response of the latter, Westinghouse, tubes is shown in Fig. 6.14. Both the FJ-405 and the WL-789 have thin blown windows to extend the transmission of the envelope farther into the ultraviolet. The envelopes of all these tubes are made of special ultraviolet transmitting glasses. While the RCA-935 can tolerate ambient temperatures up to 75° C, the upper limit for the remaining tubes is 50° C.

TABLE 6.2. PHOTOTUBES FOR THE ULTRAVIOLET

Type	Cathode		Physical Structure	Spectral Range, A.U.	Maximum at A.U.	Maximum Voltage, volts	Inter-electrode Capacity, $\mu\mu$ f
	Surface	Area, sq in.					
RCA-935	S-5	0.8	<i>G</i>	2300-7000	3400	250	0.6
FJ-405	S-3	0.8	<i>H</i>	2300-4600	2800	200	5.0
WL-767	Zr	1.3	<i>I</i>	2000-3150	2340	500	0.35
WL-773	Th	1.3	<i>I</i>	2000-3675	2550	500	0.35
WL-775	Ta	1.3	<i>I</i>	2000-3000	2400	500	0.35
WL-789	Pt		<i>J</i>	2100	1700	500	0.35

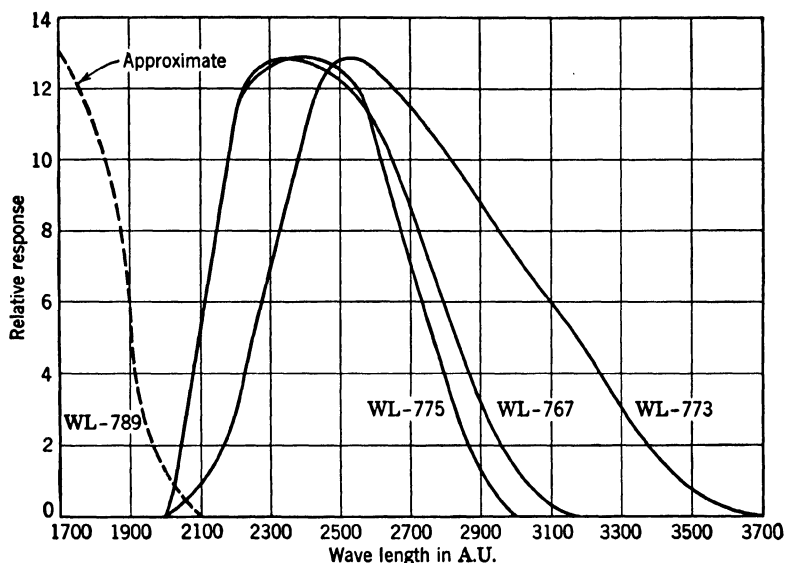


FIG. 6.14. Spectral Response of Westinghouse Ultraviolet-Sensitive Tubes. (Courtesy Westinghouse Electric Corporation.)

#### REFERENCES

1. H. E. IVES, A. R. OLPIN, and A. L. JOHNSRUD, "The distribution in direction of photoelectrons from alkali metal surfaces," *Phys. Rev.*, Vol. 32, pp. 57-80, 1928.
2. J. J. BRADY, "Energy distribution of photoelectrons as a function of the thickness of a potassium film," *Phys. Rev.*, Vol. 46, pp. 768-772, 1934.
3. K. MITCHELL, "The theory of the surface photoelectric effect in metals, II", *Proc. Roy. Soc. (London)*, Vol. A 153, pp. 513-533, 1935.
4. R. KOLLATH, "On the energy distribution of secondary electrons," *Ann. Physik*, Vol. 39, pp. 59-80, 1941.
5. E. O. LAWRENCE and L. B. LINFORD, "The effect of intense electric fields on the photoelectric properties of metals," *Phys. Rev.*, Vol. 36, pp. 482-497, 1930.
6. E. O. LAWRENCE and J. W. BEAMS, "The instantaneity of the photoeffect," *Phys. Rev.*, Vol. 29, pp. 903-904, 1927.

## Chapter 7

# THE GAS-FILLED PHOTOTUBE

A simple method of increasing the sensitivity of a phototube is to introduce into it an inert gas at a low pressure. The resulting *gas amplification* of the photocurrent may provide a gain by a factor of the order of 10. At the same time, the presence of the gas modifies the properties of the tube sufficiently to justify a detailed examination of the operation of a gas tube.

**Kinetic Theory of Gases.** The mechanical properties of the true gases—such as the noble gases and hydrogen, nitrogen, and oxygen at room temperature and atmospheric or lower pressures—can be deduced from the assumption that the average energy per degree of freedom of the molecules constituting them is  $kT/2$  and that their interactions are negligible except during collisions of exceedingly short duration.<sup>1</sup> The degrees of freedom of interest in this connection are the components of translation along three mutually perpendicular coordinates. From this assumption may be derived the general gas law

$$pV = RT \quad (7.1)$$

where  $p$  is the pressure of a body of gas,  $V$  is its volume, and  $R$  is a constant.<sup>2</sup> It follows, furthermore, that the number of molecules per unit volume depends only on the pressure and temperature and not on the gas:

$$n = \frac{p}{kT} \quad (7.2)$$

Thus, for atmospheric pressure<sup>3</sup> and room temperature<sup>4</sup> there are

<sup>1</sup>  $T$  is the temperature of the gas in °K,  $k$  is Boltzmann's constant ( $1.38 \cdot 10^{-23}$  joule/degree).

<sup>2</sup> If  $p$  is measured in newtons per square meter, and  $V$  is the volume, in cubic meters, of a number of kilograms of the gas equal to its molecular weight (a kilogram-mole),  $R$  is the universal constant  $N_0 k$ , where  $N_0$  is Avogadro's number ( $6.0 \cdot 10^{26}$  [kg-mole]<sup>-1</sup>), and  $k$  is, again, Boltzmann's constant.

<sup>3</sup> 760 mm Hg or  $1.014 \cdot 10^5$  newtons/meter<sup>2</sup>.

<sup>4</sup> 293° K.

$2.51 \cdot 10^{25}$  molecules in a cubic meter of gas. The number of molecules per unit volume,  $n$ , is directly proportional to the pressure and inversely proportional to the absolute temperature of the gas.

**Mean Free Path.** For the purpose of determining the mean distance of travel of the molecules between collisions (mean free path) they may conveniently be regarded as spheres of definite radius  $r$ . If a cylinder with radius  $2r$  is drawn about the path of a particular molecule, all other molecules whose centers lie within the cylinder will collide with it. The mean free path  $\lambda$  of the molecule is hence the length of the cylinder which, on the average, contains just one center of another molecule. Hence, if  $n$  is the number of molecules per unit volume, it might be expected that

$$\lambda = \frac{1}{4\pi nr^2} \quad (7.3)$$

This equation assumes, however, that the target molecules remain stationary during the transit of the one considered. If the displacement of the remaining molecules during the flight of the one in question is taken into proper account, the expression for the mean free path must be reduced by a factor  $\sqrt{2}$ :<sup>5</sup>

$$\lambda = \frac{1}{4\sqrt{2}\pi nr^2} \quad (7.4)$$

For electrons, with their much greater velocity and negligible dimensions, the motion of the molecules can be neglected and the radius of the cylinder to be drawn about the path of the electrons is simply the radius  $r$  of a molecule. Hence, the mean free path of an electron,  $\lambda_e$ , becomes

$$\lambda_e = \frac{1}{\pi nr^2} \quad (7.5)$$

The effective molecular radii of a few gases are listed in Table 7.1.<sup>6</sup>

TABLE 7.1. EFFECTIVE MOLECULAR RADII OF GASES

(E. H. Kennard, *Kinetic Theory of Gases*, McGraw-Hill Book Company, New York, 1938)

Gas	$r$ , A.U.	Gas	$r$ , A.U.	Gas	$r$ , A.U.
Hydrogen	1.37	Helium	1.09	Water vapor	2.30
Nitrogen	1.88	Neon	1.30	Carbon dioxide	2.30
Oxygen	1.80	Argon	1.82	Air	1.86
		Xenon	1.88		

<sup>5</sup> See Kennard, reference 1, pp. 107-113.

<sup>6</sup> See Kennard, reference 1, p. 149.

It follows that, in a high-vacuum phototube with a residual gas pressure of  $10^{-6}$  mm Hg, the mean free path for gas molecules is about 70 meters, that for electrons, 400 meters. The properties of high-vacuum devices arise not so much from the absence of gas molecules—even in the phototube just mentioned there are about  $3 \cdot 10^{16}$  molecules per cubic meter—but from the fact that electrons and ions traveling between the electrodes experience collisions only in rare cases (for instance, 1 in 10,000).

**Ionization in Gases.** If an electron of sufficiently great kinetic energy strikes a gas molecule it may liberate one of its atomic electrons. To do this it must have been accelerated through a potential drop at least

TABLE 7.2. IONIZATION POTENTIALS OF GASES

<i>Gas</i>	<i>Ionization Potential, volts</i>	<i>Source, reference</i>
Hydrogen	15.43	2
Helium	24.47	3
Neon	21.47	3
Argon	15.69	3
Krypton	13.94	3
Xenon	12.08	3
Nitrogen	15.58	2
Oxygen	15.5	4

equal to the ionization potential of the molecule. Table 7.2 gives the ionization potentials of a few gases. It is seen that a phototube filled with argon must be operated at a potential in excess of 15 volts if ionization is to take place.

Assume, now, that the applied voltage is greatly in excess of the ionization potential of argon, namely, 100 volts, and consider an electrode configuration in which both the cathode and the anode are plane and parallel to each other. After having traversed a distance greater than one-seventh of the interelectrode spacing, the photoelectrons are capable of ionizing the next gas atoms with which they may collide. In the collision an electron is liberated and begins to travel, along with the photoelectron, toward the anode. The positive ion formed in the process drifts back toward the cathode. After traveling an additional distance about one-seventh of the electrode separation, both the electrons are capable of liberating additional electrons in collisions, sending the corresponding number of positive ions back toward the cathode. In the end, for a single initial photoelectron,  $n$  electrons reach the anode and  $n - 1$  ions return to the cathode. Thus, within the limitations of the

above description of the collision processes involved, a gas amplification of the photoelectric current by the factor  $n$  takes place.

The factor  $n$  depends, obviously, both on the applied voltage and on the gas pressure. It can readily be seen that, for any applied voltage, there must be an optimum gas pressure, leading to a maximum value of  $n$ . For pressures so low that the number of collisions taking place in the transit between cathode and anode is negligible, the factor  $n$  approaches unity. Similarly, for pressures so high that a photoelectron loses so much energy in elastic collisions and collisions leading to excita-

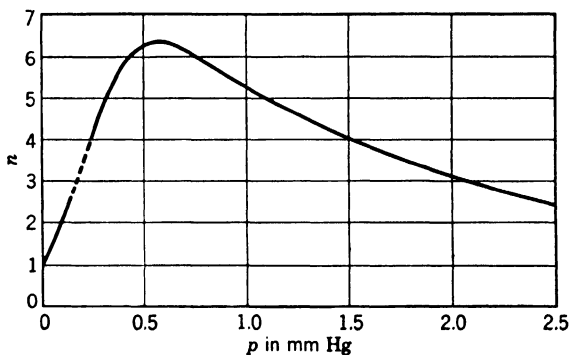


FIG. 7.1. Number of Electrons  $n$  Resulting from the Passage of One Photoelectron between Two Plane Electrodes One cm Apart in Argon at the Pressure  $p$  (accelerating voltage: 100 volts). (Kruithof, reference 5.) (Courtesy *Philips Technical Review*.)

tion of molecules without ionization that it reaches the anode without ever attaining sufficient energy to ionize,  $n$  must also approach unity. Even if, under similar circumstances, ionization does take place, the positive ion is likely to recombine with an electron from the cathode before reaching the cathode, so that the ionization does not enhance the tube current. The optimum pressure,  $p_{\text{opt}}$ , might be expected to be attained, roughly, when a collision takes place, on the average, in the time required for the electron to acquire a kinetic energy equal to the ionization potential of the gas. This would require that

$$\lambda_c = \frac{1}{\pi n r^2} = \frac{V_o}{V} d \quad (7.6)$$

Here  $V$  denotes the applied voltage,  $V_o$ , the ionization potential, and  $d$ , the interelectrode separation. Since  $n = (p_{\text{opt}}/p_o)n_o$ , where  $n_o$  is the number of molecules in unit volume at room temperature and atmospheric pressure  $p_o$ , it follows that

$$\frac{p_{\text{opt}}}{p_o} = \frac{V}{V_o \cdot \pi r^2 \cdot n_o \cdot d} \quad (7.7)$$



Substituting the appropriate numerical values— $V = 100$  volts,  $V_o = 15.7$  volts,  $r = 1.82 \cdot 10^{-10}$  meter,  $n_o = 2.51 \cdot 10^{25}$  meter $^{-3}$ ,  $d = 10^{-2}$  meter, and  $p_o = 760$  mm Hg—leads to

$$p_{\text{opt}} = 0.2 \text{ mm Hg}$$

Observation indicates that this value is somewhat low, but of the right order of magnitude. The observed variation of the factor  $n$  with the pressure  $p$  is shown in Fig. 7.1.<sup>7</sup> The larger value of the optimum pressure suggests that, as might be expected, most of the collisions at electron velocities below the ionization threshold are elastic and give rise to negligible energy losses. The validity of Stoletow's law, to the effect that the optimum pressure is proportional to the ratio of the field strength  $V/d$  to the ionization potential  $V_o$ , is confirmed experimentally.

**Limitation of Gas Amplification.** The picture given so far might lead one to expect an indefinite increase in amplification with voltage, especially if the gas pressure should be increased in proportion so as to be

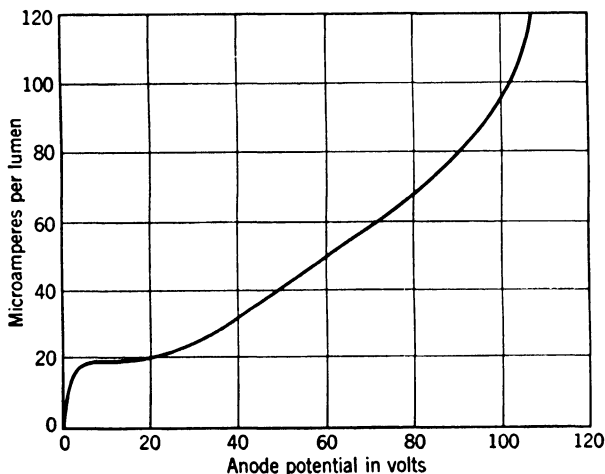


FIG. 7.2. Current-Voltage Curve for a Gas-Filled Phototube.

maintained at its optimum value. Actually, a limit is soon reached because a certain fraction  $\gamma$  of the ions formed in collision do not merely return to the cathode, but eject one or more electrons from it. If the ratio of the number of secondary electrons to the number of incident ions is  $\gamma$ , the number of elementary charges transferred from the cathode to the anode for each photoelectron becomes

<sup>7</sup> See Kruithof, reference 5.

$$\begin{aligned}
 N &= n + n(n-1)\gamma + n(n-1)^2\gamma^2 + \dots \\
 &= \frac{n}{1 - \gamma(n-1)}
 \end{aligned}
 \tag{7.8}$$

since the secondary-electron current is amplified by collisions with the gas molecules in the same manner as the primary photoelectron current. The value of  $\gamma$  depends both on the velocity of the ions and the surface properties of the cathode. For  $\gamma = 0.20$ ,  $N$  is seen to become infinite for  $n = 6$ . For voltages sufficiently high to make  $n = 6$  or greater, the discharge becomes self-sustaining, independent of external illumination, and limited either by external circuit parameters or the modification or destruction of the cathode surface by ion bombardment. In practice stable operation demands that the voltage be maintained at a value considerably lower than that required to cause such a "glow discharge."

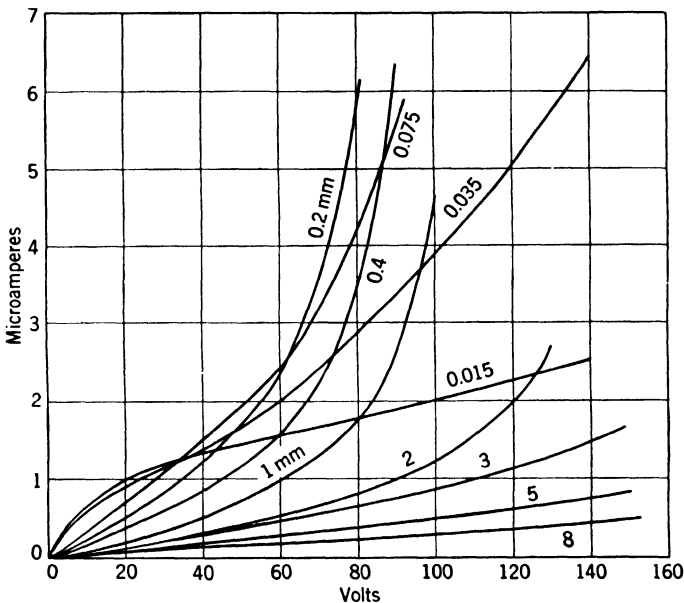


FIG. 7.3. The Effect of Gas Pressure on the Maximum Sensitivity of a Phototube. (Koller, reference 6.) (Courtesy of the *Journal of the Optical Society of America*.)

**Current-Voltage Curves.** The current-voltage curves for gas-filled phototubes exhibit the behavior which is to be expected on the basis of the above considerations. For voltages below the ionization potential of the gas filling ( $\sim 15$  volts) they do not differ appreciably from the

curves for vacuum phototubes. Beyond this point the current increases with increasing slope, ending in a sharp rise as the condition of glow discharge is approached (Fig. 7.2). Figure 7.3 shows a series of curves obtained by Koller<sup>8</sup> for a silver-cesium oxide-cesium tube filled with argon at pressures ranging from 0.015 to 8 mm Hg. The tube employed for the measurements had a semicircular cathode and a wire anode. It is seen that the optimum pressure for any given applied voltage increases with the voltage, in accord with Stoletow's law. For very high gas pressures the efficiency of the phototube is decreased because a considerable portion of the photoelectrons are returned, after a number of collisions, to the cathode.

**Current-Light Characteristics.** The current output of a gas phototube is not, strictly, a linear function of the light flux falling on the cathode (Fig. 7.4). Furthermore, this nonlinearity is, as brought out

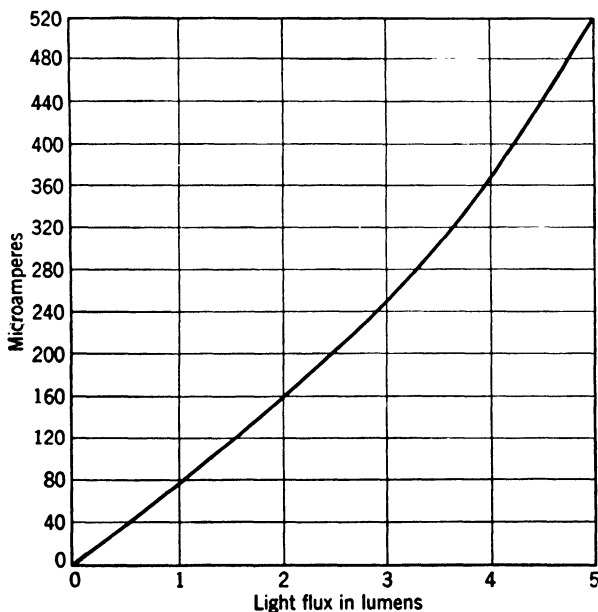


FIG. 7.4. Output Current as Function of Light Flux for a Gas-Filled Phototube.

particularly by Campbell and Ritchie,<sup>9</sup> strongly dependent on the geometrical structure of the tubes, being much greater for a spherical phototube than for a tube with plane electrodes. Huxford,<sup>10</sup> working

<sup>8</sup> See Koller, reference 6.

<sup>9</sup> See reference 7.

<sup>10</sup> See reference 8.

with a tube with plane electrodes with a silver-cesium oxide-cesium cathode, finds that (1) the response to light of a gas tube is increased if the cathode is simultaneously illuminated by a constant source and (2) the current enhancement by gas filling may be greater by 20 to 30 per cent for infrared light (9000 A.U.) than for red light (6600 A.U.). He ascribes these results to the fact that the positive ions returning to the cathode surface adhere to the surface in an unneutralized state for an extended period, reducing the work function of the surface and increasing both the photoemission and the secondary emission excited by the incident ions. It may be noted that the nonlinearity of the light response in the normal operating range is too small to prove objectionable except in precision light measurements, for which vacuum phototubes must be given preference.

**Dynamic Characteristics.** Since the current through a gas phototube is carried not only by electrons, but also by positive ions, it is reasonable to expect a time lag in the response of a gas tube which is not observed in a vacuum phototube. The velocity of ions and electrons, for equal energy, is inversely proportional to the square root of their masses. Thus an argon atom, with an atomic weight of 40, is slower than an electron by a factor  $(40 \cdot 1823)^{1/2} = 271$  and requires, for an energy of 25 electron volts, approximately 1 microsecond to cover a distance of 1 centimeter. In practice, collisions will tend to make the mean transit time of an argon ion much greater than this. Accordingly, an instantaneous light pulse falling on the cathode gives rise not simply to a correspondingly instantaneous pulse of photocurrent but, in addition, to an exponentially decreasing pulse, whose rate of decay is determined primarily by the mean time of transit of a positive ion and the secondary-emission ratio of the cathode for the incident ions,  $\gamma$ .

An ingenious method of measuring the response of a gas phototube to a brief light pulse has been developed by Huxford and Engstrom.<sup>11</sup> The current output of the gas phototube, illuminated by the periodically repeated light pulse, is made to provide the control bias of a grid-controlled vacuum phototube, which is illuminated by instantaneous light flashes, synchronized, with adjustable phase delay, with the illumination of the gas tube. A galvanometer measures the output of the second phototube, indicating, in this manner, the current output of the gas tube at fixed intervals after onset of the illumination. Figure 7.5 shows results obtained for a silver-cesium oxide-cesium phototube containing argon at a pressure of 0.15 mm Hg, with a number of different operating voltages. It is seen that, for voltages greater than 25 volts, one part of the photocurrent is practically instantaneous, while another

<sup>11</sup> See reference 3.

---presumably arising from the ion return to the cathode—builds up and decays quite gradually.

Consider now a light signal, fully modulated at the frequency  $\nu$ , so that its intensity varies as  $1 - \cos(2\pi\nu t)$ . If the frequency is sufficiently high that an appreciable fraction of the photocurrent excited at the peak of the signal passes through the tube at the time of the trough, it is obvious that the output current is no longer fully modulated and

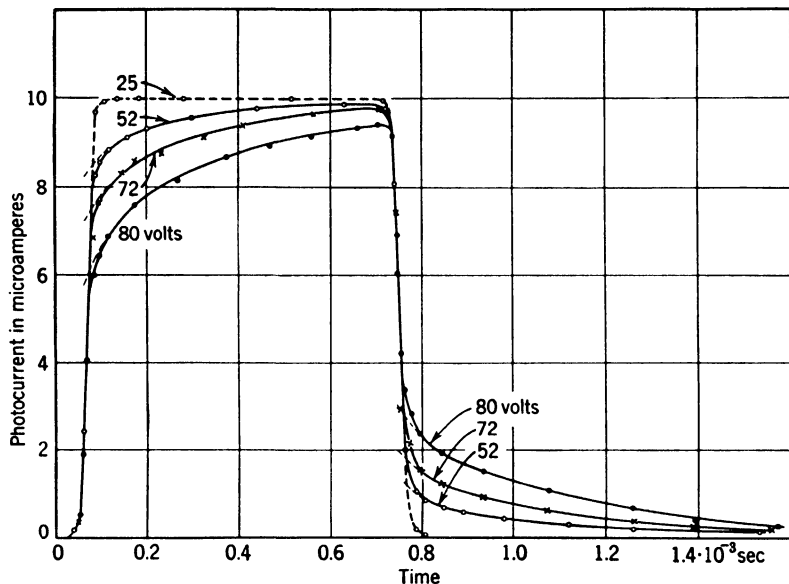


FIG. 7.5. Time Lag for an Argon-Filled Phototube ( $p = 0.15$  mm Hg). (Huxford and Engstrom, reference 9.) (Courtesy of Review of Scientific Instruments.)

that the response at the frequency is smaller than at zero frequency. In addition to this reduction in the response, which may be expressed by a factor  $\eta$ , the delay in the photocurrent will, in general, give rise to a phase delay  $\phi$ . Hence the output current may be expressed by

$$I = Ni_o[1 - \eta \cos(2\pi\nu t - \phi)] \quad (7.9)$$

where  $N$  is the gas amplification factor and  $i_o(1 - \cos(2\pi\nu t))$ , the primary photocurrent. Kruithof<sup>12</sup> has derived an expression for  $\eta$  on

<sup>12</sup> See reference 5. Assume that, on the average, a transport of  $N_1$  charges per primary photoelectron takes place instantaneously; then  $N_2 = N - N_1$  ( $N$  = gas amplification factor) charges make up the corresponding exponentially decaying

the basis of the mechanism of gas amplification described above. The top curve in Fig. 7.6 indicates the result for  $\eta$ , the modulation factor of the output, as function of frequency for a tube with a cylindrical cathode and rod anode, for the specific case that  $\gamma = 0.33$  and  $N = 10$ . For large frequencies the correspondence of the theoretical curve and the experimentally found variation (indicated by circles) is quite satisfactory. On the other hand, there is a considerable reduction in response in the range below 5000 cycles per second which is not reflected in the theoretical curve. This reduction is attributed to the excitation of the gas atoms to metastable states, that is, states of high potential energy from which the atom does not readily return to its normal state with the emission of the energy of excitation in the form of radiation. Such metastable atoms, having no charge, may drift about in the interelectrode space for a prolonged period before returning to the normal state or, eventually, striking the cathode surface. At the cathode surface, pulse. If  $i_o[1 - \cos(2\pi\nu t)]$  is the primary photocurrent, the instantaneous current arising from the modulated light signal is

$$I = N_1 i_o [1 - \cos(2\pi\nu t)] + \int_{-\infty}^t [1 - \cos(2\pi\nu t')] \cdot N_2 q e^{-q(t-t')} dt' \quad (7.10)$$

The second term represents the contribution to the current of the excitation that has taken place at the earlier time  $t'$ . The value of  $q$  follows from the requirement (Eq. 7.8)

$$e^{-q\tau_i} = \gamma(n-1) \quad (7.11)$$

where  $\tau_i$  is the average time of transit of an ion. This yields

$$q = -\frac{1}{\tau_i} \log_e [\gamma(n-1)] \quad (7.12)$$

$n$  being the number of electrons, per primary photoelectron, arriving at the anode for  $\gamma = 0$ .

Equation 7.10 yields for the total tube current

$$I = N_1 i_o [1 - \eta \cos(2\pi\nu t - \phi)] \quad (7.13)$$

with

$$\eta = \frac{1}{N} \left[ N_1^2 + \frac{N_2^2 + 2N_1 N_2}{1 + \frac{(2\pi\nu)^2}{q^2}} \right]^{\frac{1}{2}}$$

It follows that the relatively slow motion of the ions leads to both a reduction in the modulation factor,  $\eta$ , and a lag in phase,  $\phi$ . It should be noted that the value of  $N_1$  is not equal to  $n$ , but smaller, since part of the current excited is carried by positive ions even if  $\gamma = 0$ . Thus,

$$N_1 = 1 + Z(n-1) \quad (7.14)$$

For plane electrodes and an operating voltage of 100 volts, Kruithof finds  $Z = 0.4$ . It follows from Eq. 7.13 that for  $\gamma = 0.2$ ,  $n = 4$  the gas amplification at very high frequencies is  $N_1 = 2.2$  as compared with  $N = 10$  at low frequencies (Eq. 7.8). Thus  $\eta_{\min} = 0.22$ .

however, the potential energy of the metastable atoms may be utilized to eject an electron from the cathode, the work function of the cathode surface being much smaller than the ionization potential of a free gas atom. This electron emission adds a greatly delayed component to the photocurrent. Kruithof was able to support this explanation by introducing into the tubes, in place of pure argon, neon with a 10 per cent

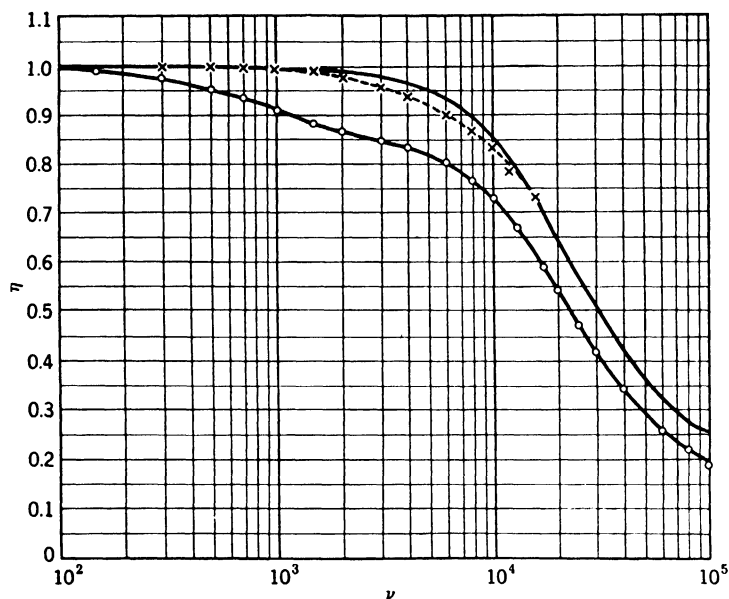


FIG. 7.6. Comparison of the Calculated and Measured Frequency Characteristic (measured points indicated by circles) of a Gas-Filled Phototube with Cylindrical Cathode and Rod Anode:  $N = 10$ ,  $\gamma = 0.33$ . The dotted line (measured points crosses) is measured with a gas filling of neon plus 10 per cent argon instead of pure argon. (Kruithof, reference 5.) (Courtesy of *Philips Technical Review*.)

admixture of argon. Since the ionization energy of argon is considerably lower than that of neon, metastable neon atoms could now give up their stored energy so as to ionize an argon atom with which they came into collision. The measured characteristic of such a tube (indicated by crosses in Fig. 7.6) corresponds quite closely to the theoretical curve, since the time delay occasioned by the long life of the metastable atoms is largely nullified.

The phase delay  $\phi$  of gas phototubes is of secondary importance in their applications. Figure 7.7 shows measurements by Wheateroft,<sup>13</sup> who compared the phase of the interruption of a light signal with that

<sup>13</sup> See reference 10.

of the current generated, on an oscillograph. He found, at an operating potential of 150 volts, a maximum phase lag of about 45 degrees at approximately 1500 cycles per second. The phase shift at higher frequencies is less because here the delayed current is spread over several cycles and hence has less effect in shifting the phase.

In the employment of gas tubes for sound reproduction, with a frequency range of 5000 to 10,000 cycles per second, the decline in ampli-

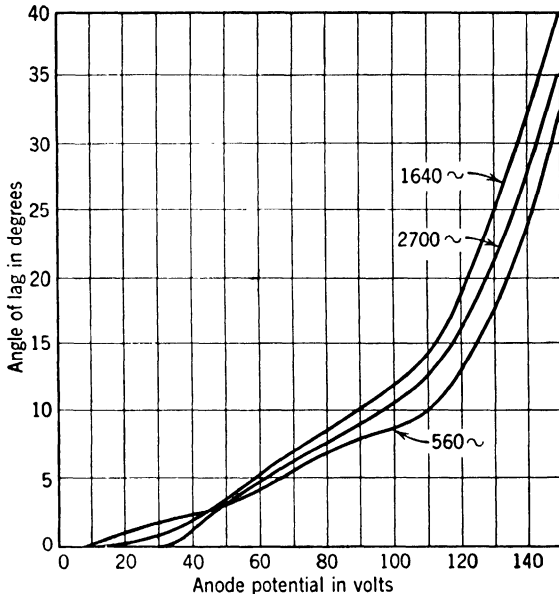


FIG. 7.7. Phase Delay of Output Current of Gas-Filled Phototube as Function of Applied Voltage for Several Frequencies of Light Pulsation. (Wheatcroft, reference 10.) (Courtesy of the *Philosophical Magazine*.)

cation at the high frequencies is in itself no serious objection, since it can be compensated by peaking circuits. In practice, however, it is inadvisable to permit a drop in response greater than about 25 per cent. This restriction is necessary to make the frequency response adequately insensitive to small voltage changes as well as to tube replacements. For this reason manufacturers generally recommend the operation of gas phototubes at voltages sufficiently low (for instance, 100 volts) to render the amplification factor less than 10. With certain photosensitive surfaces, such as the antimony-cesium surface S-4, maintenance of the cathode sensitivity sets a still lower limit to the permissible gas amplification.



**Properties of Standard Gas-Filled Phototubes.** Gas phototubes are available essentially with the same range of spectral characteristics in the visible and infrared (S-1, S-3, S-4) as vacuum phototubes. Their application is primarily in the field of relays and sound reproduction, where their slight nonlinearity and the decline of the dynamic characteristic at high frequencies play a minor role. In physical structure,

TABLE 7.3. PROPERTIES OF RCA GAS PHOTOTUBES  
(Mean Values)

Type	Cathode		Physical Structure	Sensitivity		Maximum Current Density		Maximum Voltage, volts	Maximum Gas Amplification Factor
	Surface	Area, sq in.		$\mu\text{a}/\mu\text{watt}$ at Response Peak	$\mu\text{a}/\text{lumen}$ , 2870° K Source	Peak, $\mu\text{a}/\text{sq in.}$	Average, $\mu\text{a}$		
1P29	S-3	0.78	N	0.010	40	100	5	100	9
1P37	S-4	0.78	N	0.11	120	100	5	100	5.5
868	S-1	0.78	N	0.009	90	100	5	90	8
918	S-1	0.78	N	0.015	150	100	5	90	10.5
1P40 } 930 }	S-1	0.5	D	0.0135	135	100	3	90	10
5581	S-4	0.5	D	0.125	135	100	3	100	5.5
921	S-1	0.44	B	0.0135	135	100	3	90	10
5582	S-4	0.44	B	0.11	120	100	2	100	5.5
927	S-1	0.3	E	0.0125	125	100	2	90	10
5583	S-4	0.3	E	0.125	135	100	2	100	5.5
1P41	S-1	0.25	K	0.0083	83	75	1.5	90	8.5
928	S-1	0.5	L	0.0065	65	100	3	90	10
920	S-1	2 × 0.3	M	0.010	100	50	2	90	9
5584	S-4	2 × 0.3	M	0.11	120	50	2	100	5.5

most gas tubes resemble corresponding vacuum phototube types (Figs. 6.12 and 6.13). Figure 7.8 shows, in addition, an end-on type tube with a ring anode (*K*) and a nondirectional tube with a perforated cathode cylinder with a rod anode along its axis (*L*), as well as a twin phototube, containing a pair of cylindrical-sector cathodes and rod anodes in a single envelope (*M*), and a tube of more conventional type (*N*). The principal properties of a series of RCA gas phototubes are given, for convenient reference, in Table 7.3. The significance of the symbols shown under "physical structure" will be apparent from Figs. 6.12, 6.13, and 7.8. For more complete and up-to-date information the reader is referred to the manufacturers of phototubes.<sup>14</sup>

Typical current-voltage characteristics for different values of the light flux incident on the cathode are shown, for a type 868 gas photo-

<sup>14</sup> See p. 116, footnote 14.

tube with S-1 cathode, in Fig. 7.9. The dynamic response for tubes with different spectral response is represented in Fig. 7.10. It will be

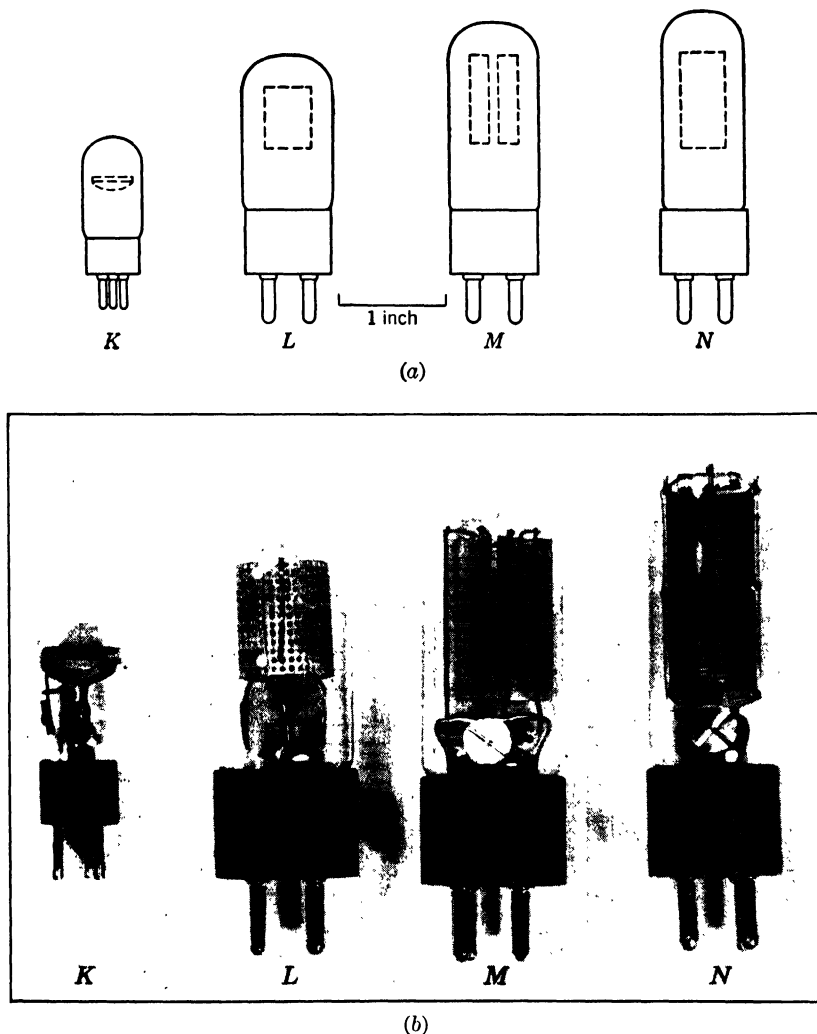


FIG. 7.8. Some RCA Gas Phototubes of Special Construction. (a) Outline. (b) External Appearance.

noted that the physical properties of the type 868 or type 918 (with an S-1 response) and the type 1P37 (with an S-4 response) are quite similar, so that they may be readily interchanged when a change in spectral response is desired. Other interchangeable pairs of tubes will be evi-

dent from the table. It may be noted that, if the operating voltage of the tubes is reduced by 20 volts below the maximum rating, it is permis-

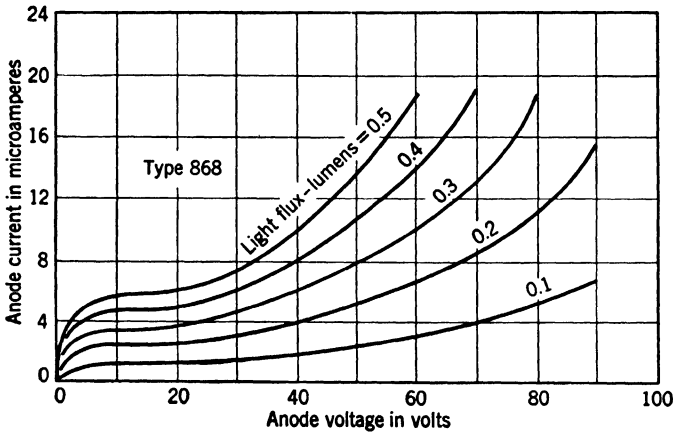


Fig. 7.9. Current-Voltage Curves of the Type 868 Gas Phototube with S-1 Spectral Response. (Courtesy RCA-Victor Division.)

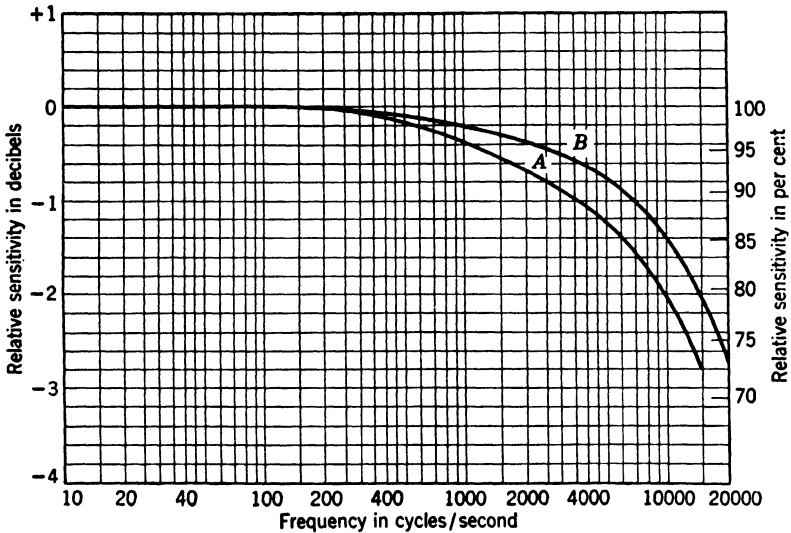


Fig. 7.10. Typical Dynamic Response Curves of Commercial Gas Phototubes with S-1 or S-3 Photocathode (A) and with S-4 Photocathode (B). (Courtesy RCA-Victor Division.)

sible to double the value of the maximum average cathode current given in the table. The upper limit of the ambient temperature is the same as for vacuum phototubes—75° C for tubes with S-4 response,

100° C for such with S-1 and S-3 response. Finally, the decline in the response with the frequency of the light signal is approximately the same for all gas tubes with a similar photosurface. For S-1 and S-3 surfaces it is approximately 15 per cent less than for a steady signal at 5000 cycles per second, 25 per cent less at 10,000 cycles per second; for a phototube with S-4 response the reduction is 8 and 20 per cent, respectively, at 5000 and 10,000 cycles per second.

## REFERENCES

1. E. H. KENNARD, *Kinetic Theory of Gases*, McGraw-Hill Book Company, New York, 1938.
2. G. HERTZBERG, *Molecular Spectra and Molecular Structure*, Vol. I, Prentice-Hall, Inc., New York, 1939.
3. R. F. BACHER and S. GOUDSMIT, *Atomic Energy States*, McGraw-Hill Book Company, New York, 1932.
4. F. L. MOHLER and P. D. FOOTE, "Ionization and resonance potentials of the non-metals," *Bureau of Standards Bulletin*, Vol. 16, pp. 669-700, 1920.
5. A. A. KRUTHOF, "Time lag phenomena in gas-filled photoelectric cells," *Philips Tech. Rev.*, Vol. 4, pp. 48-55, 1939.
6. I. R. KOLLER, "Some characteristics of photoelectric tubes," *J. Optical Soc. Am. and Rev. Sci. Instruments*, Vol. 19, pp. 135-145, 1929.
7. N. R. CAMPBELL and D. RITCHIE, *Photoelectric Cells*, Sir Isaac Pitman and Sons, London, 1934.
8. W. S. HUXFORD, "Townsend ionization coefficients in Cs-Ag-O phototubes filled with argon," *Phys. Rev.*, Vol. 55, pp. 754-762, 1939.
9. W. S. HUXFORD and R. W. ENGSTROM, "A photoelectric method of tracing current wave forms," *Rev. Sci. Instruments*, Vol. 8, pp. 385-390, 1937.
10. E. L. WHEATCROFT, "Experiments on time lag in gas-filled photoelectric cells," *Phil. Mag.*, Vol. 12, pp. 162-173, 1931.

## Chapter 8

# THE MULTIPLIER PHOTOTUBE

Secondary-emission multiplication offers a method of increasing the current output of a phototube without affecting adversely the dynamic characteristics of the tube. Since, furthermore, much greater gains can be attained in this manner than by gas amplification, it is not surprising that the multiplier phototube has, in a few years, become of great importance in the field of applied photoelectricity.

**Secondary Electron Emission.** When an electron with a kinetic energy of some hundred electron volts falls on a solid surface it may give up part of its energy to one or more electrons of the solid which, in turn, may escape from the surface as so-called secondary electrons. The average number of secondary electrons so formed depends strongly both on the nature of the solid and on the energy of the incident electrons. On the other hand, the velocity and angular distribution of the secondary electrons is only slightly dependent on the primary energy and varies relatively little from substance to substance.<sup>1</sup> The energy distribution has, in general, a rather pronounced maximum in the range between 1.4 and 2.2 electron volts—and is quite narrow for the familiar photoemitters. The distribution in angle, like that of photoelectrons, obeys the cosine law.

At very low primary energies (less than 10 volts) practically no secondary electrons are emitted; the electrons leaving the target are mainly elastically scattered primary electrons. However, the proportion of primary electrons in the electron emission of the target decreases rapidly with increasing primary electron energy, so that, in the range of 20 to 1000 electron volts, almost all the electrons leaving the target are secondary electrons. For most substances the ratio of the electron current leaving the target to the electron current incident on the target—the “secondary emission yield”<sup>2</sup>—increases with the accelerating voltage of the primary beam, passing the value unity in the neighbor-

<sup>1</sup> See Kollath, references 1 and 2.

<sup>2</sup> This definition of “secondary-emission yield” treats back-scattered primary electrons as part of the secondary electron current.

hood of 40 volts, and reaches a maximum at about 500 volts; for still higher voltages there is, generally, a slow decrease in the secondary emission ratio. The value of the maximum of the secondary-emission yield varies from a quantity of the order of 0.5 for soot and the *clean* surfaces of electropositive metals such as lithium, barium, or cesium<sup>3</sup> to 9 or 10 for properly sensitized silver-cesium oxide-cesium photo-surfaces.<sup>4</sup> Figure 8.1 shows a yield curve for a surface of the latter type, as well as one for a silver-antimony-cesium surface.

A final property of interest in the behavior of a secondary emitter is the dependence of the yield on the angle of incidence of the primary

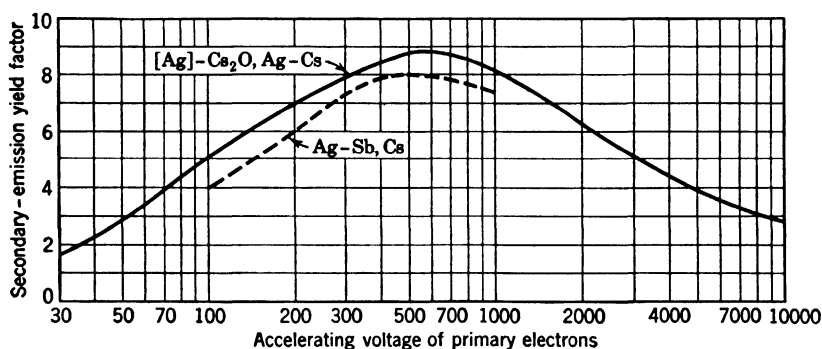


FIG. 8.1. Typical Secondary-Emission Yield Curves for Properly Sensitized Silver-Cesium Oxide-Cesium and Silver-Antimony-Cesium Photosurfaces.

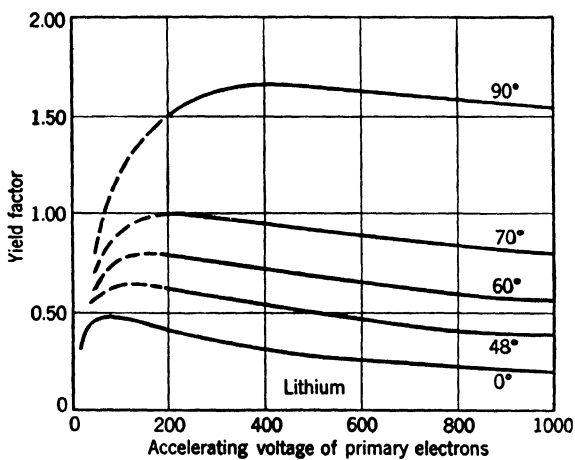
beam. It is found consistently (1) that the secondary-emission yield increases with increasingly oblique angle of incidence; and (2) that this effect is small at low accelerating voltages of the primary beam and becomes very pronounced at high voltages. For the highly electropositive elements (that is, elements with large atomic volume) the dependence on angle is greatest and becomes marked also at the lower voltages (Fig. 8.2).<sup>5</sup>

It may be noted that, although insulators such as the alkali halides and magnesium oxide exhibit very high secondary emission, impurity semiconductors such as cuprous oxide ( $\text{Cu}_2\text{O}$ ), silver oxide ( $\text{Ag}_2\text{O}$ ), and molybdenum sulfide ( $\text{MoS}_2$ ) have maximum yields of the order of

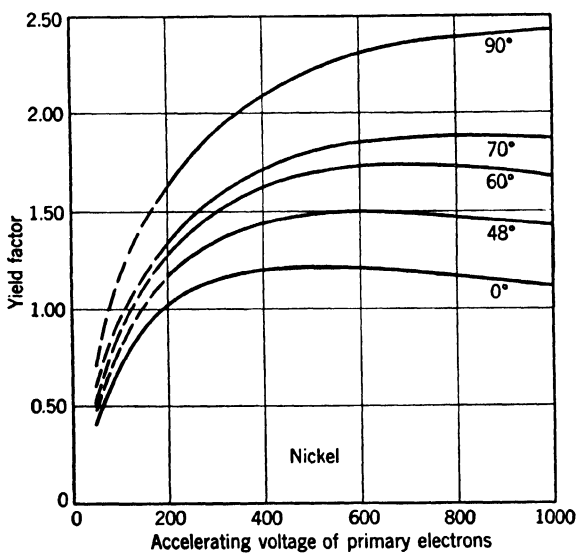
<sup>3</sup> See Bruining and de Boer, reference 3.

<sup>4</sup> Considerably higher values may be obtained from surfaces consisting of a layer of insulating material, such as an alkali halide or magnesium oxide, on a metal base. They, however, show pronounced fatigue phenomena arising from decomposition under bombardment and hence have little practical value. See, for example, Bruining and de Boer, reference 4.

<sup>5</sup> See Bruining, reference 5.



(a)



(b)

FIG 8.2. Secondary-Emission Yield Curves for (a) Lithium and (b) Nickel for Various Angles of Incidence. (Bruining, reference 5.) (Courtesy of *Physica*.)

unity.<sup>6</sup> On the other hand, certain intrinsic semiconductors, such as  $\text{Cs}_3\text{Sb}$ , which show an arrangement of energy levels similar to that of the insulators, have very high secondary-emission ratios (Fig. 8.1).

The following picture of the secondary-emission process results from these observations. The primary electron incident on the solid substance constituting the target gives some of the electrons of the target sufficient energy to escape. In metals the majority of these high-velocity secondary electrons lose sufficient energy in collisions with the conduction electrons of the metal on the way to the surface so that they are held back by the surface potential barrier and do not contribute to the secondary emission. In an insulator the secondary electrons formed in the interior cannot exchange energy and momentum with the electrons of the solid, since these completely fill the lower energy bands of the solid, leaving no free states to which either the secondary electron or the excited electron of the solid may transfer. Hence the number of electrons arriving at the surface with sufficient energy to escape is much greater than for metals. In intrinsic semiconductors such as  $\text{Cs}_3\text{Sb}$ , the concentration of conduction electrons with which the secondary electrons can exchange energy is much smaller than in metals, so that, here, electron-electron collisions do not greatly reduce the number of electrons arriving at the surface with sufficient energy to escape. This is especially true if the work function is low, so that the lower edge of the conduction band lies only slightly below the potential outside of the metal. Impurity semiconductors of the type cited above may be expected to have a lower secondary emission, since the impurity centers constitute traps of relatively large cross section to the secondary electrons in the conduction band.

At low primary energies the yield is low because the energy available for the excitation of the emitter electrons is low; at high primary energies it is low once more since here the excited electrons, formed most copiously when the primary electron has been slowed down to a velocity corresponding to a kinetic energy of some hundred electron volts, lose their excess energy on the way to the surface. This energy loss is minimized for a grazing angle of incidence of the primary electrons, explaining the dependence of the yield on the angle. The fact that this dependence is greatest for metals with large atomic volume must be ascribed to their low absorption cross section for fast electrons and their high absorption cross section for slow electrons. Finally, the relatively small dependence of the secondary-emission yield on the work function of a compound surface, in contrast with the much greater

<sup>6</sup> See Bruining and de Boer, reference 6. For a discussion of impurity and intrinsic semiconductors, see Chapter 10, p. 179.



dependence of the photoelectric response, must be attributed to the greater average initial velocity of the secondary electrons compared with that of the photoelectrons. The very low secondary-emission yield of spongy surfaces such as soot follows, of course, from the trapping of secondary electrons by projecting portions of the surface.<sup>7</sup>

For the purposes here considered, surfaces with very high secondary-emission ratios, preferably at low primary voltages, and exhibiting small fatigue and saturation effects are of greatest interest. The materials which have been found to be of greatest value are the photosensitive

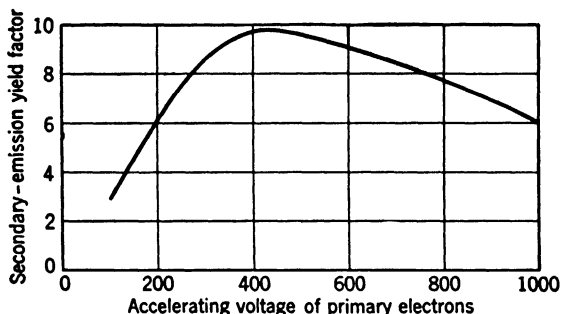


FIG. 8.3. Yield Curve for Silver-Magnesium Alloy. (Zworykin, Ruedy, and Pike, reference 7.) (Courtesy of *Journal of Applied Physics*.)

silver-cesium oxide-cesium and antimony-cesium surfaces and alloys of magnesium and beryllium with heavier metals. A typical yield curve of a silver-magnesium alloy surface is shown in Fig. 8.3. These alloy surfaces have the special advantage of very low thermionic emission (dark current) and high thermal stability.

**Preparation of Secondary-Emissive Surfaces.** Silver-cesium oxide-cesium and antimony-cesium surfaces which are to be employed as secondary emitters are prepared in the same manner as the photosensitive surfaces.<sup>8</sup> It is found, however, that the highest yields are obtained with silver-cesium oxide-cesium surfaces if the oxidation of the silver is carried only to the first blue surface coloration.

The following procedure is employed for forming a silver-magnesium secondary-emissive surface.<sup>9</sup> A known weight of silver is melted in a steel crucible in an electrically heated furnace. Then a piece of magnesium weighing 1 to 15 per cent of the weight of the silver is thrust,

<sup>7</sup> As distinguished from compound photocathodes of spongy consistency, this effect is not counterbalanced by the presence of an increased number of readily ionized adsorbed atoms.

<sup>8</sup> See pp. 93-99.

<sup>9</sup> See Zworykin, Ruedy, and Pike, reference 7.

with the aid of a steel wire, beneath the surface of the melt. After brief stirring the melt is cooled and the ingot is sawed or rolled to a convenient thickness. After it is cleaned, polished, and shaped, the alloy may be mounted in a vacuum-tube envelope, care being taken to prevent overheating during the sealing process. The yield at 200 electron volts primary energy is now found to be about 1.5. If, at this point, the tube is baked as in a normal outgassing routine, the yield rises to 4 or 6; it may be further increased by high-frequency heating in the presence of oxygen. The increase in yield is accompanied by a change from a silvery

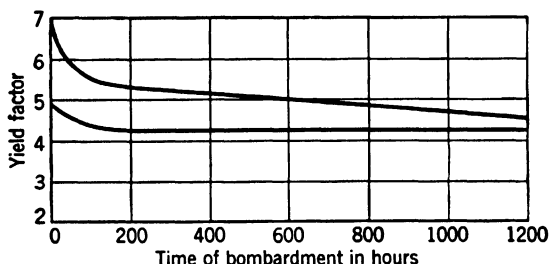


FIG. 8.4. Diminution of Yield with Time of Bombardment for Two Silver-Magnesium Alloy Surfaces (accelerating voltage of primary electrons: 200 volts; current density: 5 ma/cm<sup>2</sup>). (Zworykin, Ruedy, and Pike, reference 7.) (Courtesy of *Journal of Applied Physics*.)

to a golden or yellow appearance. Finally, the alloy as well as the remaining metal parts in the tube are heated, after the oxygen has been pumped out, once more with a high-frequency current, a barium-aluminum getter<sup>10</sup> is exploded, and the tube is sealed off.

Electron-diffraction studies of such surfaces indicate the presence of silver and of magnesium oxide. In view of the known high secondary-emission yield of magnesium oxide it seems likely that it is responsible for the high emission of the alloy surface, the silver forming a conducting substrate and being distributed so as to facilitate the neutralization of the positive charge left by the secondary-emission process in the oxide. Figure 8.4 shows the decay characteristics of two silver-magnesium surfaces subjected to slightly different activation schedules. During the life test the average primary current was maintained at 5 milliamperes per square centimeter. In both cases there is an initial decline during the first 100 hours. After this point the yield of the surface with the smaller initial yield remains stable, whereas that with

<sup>10</sup> A getter consists of a mixture of active metals which is deposited, in general, on a portion of the inner wall of the envelope and serves to bind traces of gas liberated from the wall and electrodes of the tube during operation, thus maintaining a high vacuum in a sealed-off tube.

the higher initial yield continues to become gradually less secondary-emissive.

**Magnetic Secondary-Emission Multiplier.** The basic operation of a multiplier phototube is shown in Fig. 8.5. It consists of a photocathode, a series of target electrodes or *dynodes* at increasing potential, and a collector. The photocurrent  $i_o$  is drawn from the cathode to the first target and ejects from it a secondary-electron current  $Ri_o$  ( $R$  being the secondary-emission ratio of the surface). This current, in turn, strikes the

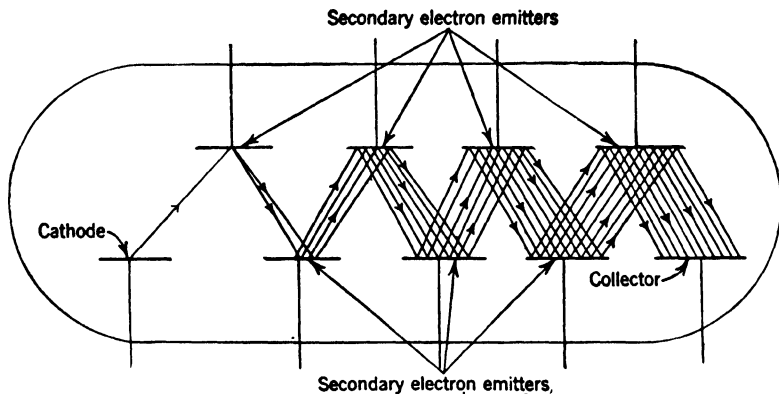


FIG. 8.5. Principle of the Secondary-Emission Multiplier. (Zworykin, Morton, Ramberg, Hillier, and Vance, *Electron Optics and the Electron Microscope*, John Wiley and Sons, New York, 1945.)

second target electrode and ejects from it a current  $R^2i_o$ . Thus, finally, if there are  $n$  target electrodes, a current  $R^n i_o$  reaches the collector. Thus a multiplier with 10 dynodes, each having a yield  $R = 4$ , has an output current which is a million times as great as the current leaving the photocathode.

The above considerations assume that all the secondary electrons leaving one target arrive at the succeeding one. The achievement of this condition constitutes the chief design problem of the multiplier phototube. It was first solved satisfactorily by subjecting the electrons emitted from the photocathode and the target electrodes to crossed electric and magnetic fields as shown in Fig. 8.6.<sup>11</sup> The photocathode and the nine dynodes are plates of equal size placed side by side in a common plane, faced by a similar set of field plates. Each field plate is connected electrically to the next succeeding dynode. A uniform magnetic field normal to the plane of the figure is maintained by a pair of soft-iron pole-piece plates, outside the tube envelope, polarized by per-

<sup>11</sup> See Zworykin, Morton, and Malter, reference 8.

manent magnets. Under the influence of the accelerating field from the target or photocathode to the field plate opposite, and the magnetic field, electrons leaving a point of the photocathode or target travel along approximately cycloidal paths to a corresponding point on the next target, provided that the following relation between the magnetic flux density  $B$ , the voltage per stage  $V$ , the distance between the centers of successive plates  $d$ , and the separation between the targets and field plates  $s$ , is fulfilled:

$$B = \left( \frac{2\pi m V}{eds} \right)^{1/2} = 6 \cdot 10^{-6} \left( \frac{V}{ds} \right)^{1/2} \text{ webers/meter}^2 \quad (8.1)$$

Thus, for a distance between plate centers of  $d = 0.01$  meter, a separation of targets and field plates  $s = 0.005$  meter, and  $V = 200$  volts,  $B = 0.012$

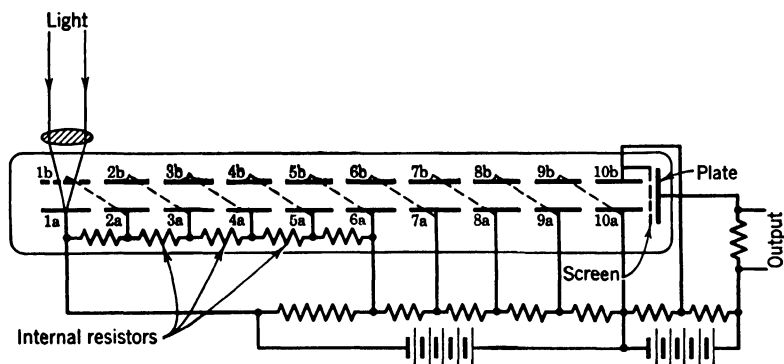


FIG. 8.6. Electrode Arrangement in the Magnetic Secondary-Emission Multiplier Phototube. (Zworykin, Morton, and Malter, reference 8.)

weber per meter<sup>2</sup> or 120 gauss, which can be attained with a small magnet.

The superposed fields have a focusing action on the electrons in the sense that electrons leaving a point a given distance from the edge nearest the photocathode of one target arrive at the next target an equal distance from the corresponding edge irrespective, within limits, of their initial velocities. Thus there is no serious spreading of the electrons in a forward direction. On the other hand, the fields do not influence velocity components in a lateral direction. Lateral spreading may be prevented, however, by mounting the plates between mica supports which charge up negatively and thus oppose an outward lateral drift of the electrons. Even with twelve or more stages, multipliers of this type do not exhibit appreciable electron losses.

In the magnetic-multiplier phototube shown in Fig. 8.6 the first few stages are connected by internal resistors forming part of a voltage di-

vider distributing voltage to the tube electrodes and thus reducing the total number of external leads required. A separate source is provided for the last target and the collector since they carry generally relatively high currents. Finally, a screen shields the remaining electrodes from voltage fluctuations of the collector or plate.

**Electrostatic Secondary-Emission Multiplier.** The magnetic multiplier phototube is entirely satisfactory in performance. However, the requirement of a magnetic field not only is an undesirable complication, but, in addition, in many applications interferes with the operation of neighboring equipment. For this reason the magnetic multiplier has,

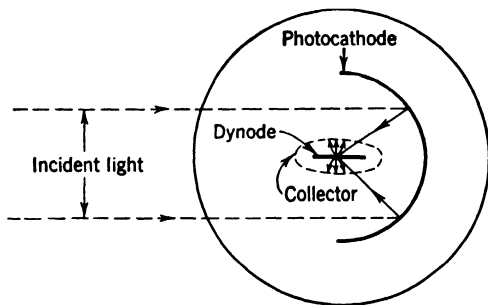


FIG. 8.7. Single-Stage Secondary-Emission Multiplier Phototube (Schematic). (Iams and Salzberg, reference 9.)

in practice, been quite generally replaced by purely electrostatic secondary-emission multipliers. The earliest multiplier phototubes, such as that of Iams and Salzberg<sup>12</sup> (Fig. 8.7), had a single stage of secondary-emission amplification. Photoelectrons leaving the concave cathode struck the strip dynode, ejecting therefrom secondary electrons which were collected by the flattened spiral collector grid surrounding the dynode. Iams and Salzberg obtained in this manner a secondary-emission amplification by a factor of 6.

An extremely simple electrostatic multiplier was devised by Weiss<sup>13</sup> of the German Post Office. It consists simply of a sequence of secondary-emission activated, fine-mesh screens at increasing potentials, a transparent cathode being provided at one end of the tube, a collector at the other (Fig. 8.8). In practice, the collector is usually a high-transmission screen in front of a solid-plate dynode, to take advantage of the greater efficiency of the solid dynode as a secondary emitter. Electrons striking the wires of any one target screen emit secondary electrons therefrom; these are drawn, by the accelerating field, through the meshes to

<sup>12</sup> See reference 9.

<sup>13</sup> See reference 10.

the next target. Since the electrons incident on the mesh openings are not multiplied, the current gain per stage of a screen multiplier is only about half as great as that for a multiplier with solid dynodes. Yield curves for a well-activated screen are shown in Fig. 8.9. Even so, ampli-

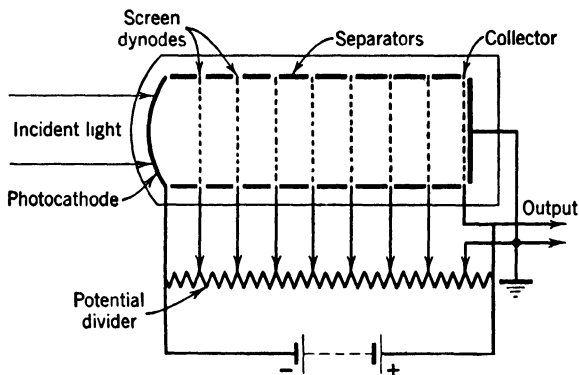


FIG. 8.8. Screen-Type Multiplier Phototube. (Weiss, reference 10.)

fications of the order of a million have been obtained in this manner in practical phototubes. Spreading of the electron current can be prevented by the employment of a solenoid providing a uniform magnetic field parallel to the axis of the tube. However, it was soon found that the insertion of glass rings separating the successive screens was equally

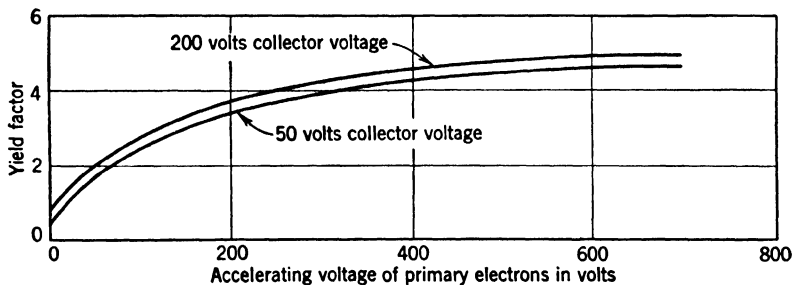


FIG. 8.9. Yield Curves for an Activated Screen Electrode (250 meshes per inch, transmission approximately 50 per cent). (Weiss, reference 10.) (By permission of the Attorney General in the public interest under License No. JA-1351.)

effective; the negative charge on the glass counteracts a drift of the electrons toward the periphery of the tube.

Electrostatic multiplier phototubes of greater efficiency and at least equal compactness may be achieved by dispensing with screens and relying entirely on the appropriate shaping of the electrodes for the proper guiding of the electrons from electrode to electrode. Figure 8.10<sup>14</sup>

<sup>14</sup> See Zworykin and Rajchman, reference 11.

illustrates a tube structure which fulfills the basic requirements for an effective electrostatic multiplier. The photocathode is separated from the secondary-emission target electrodes by a partition provided with an aperture, permitting the two portions of the tube to be activated individually. The dynodes are shaped so that the electrons leaving one target are guided to the next without loss. As in the magnetic and screen multipliers, the insulating mounting strips for the electrodes tend to charge negatively so as to prevent excessive sidewise spreading of the

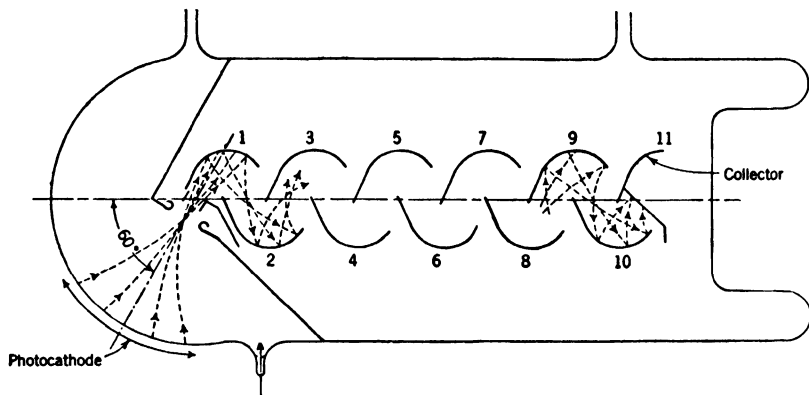


FIG. 8.10. Partition-Type Electron Multiplier. (Zworykin, Morton, Ramberg, Hillier, and Vance, *Electron Optics and the Electron Microscope*, John Wiley and Sons, New York, 1945.)

electron beam. Finally, bringing the electrodes up to the center line of the structure prevents positive ions formed in the neighborhood of the collector from traveling back toward the cathode. This is important at high multiplier gains. At a gain of a million, the formation of one positive ion which reaches the photocathode and ejects there an electron for every million electrons passing through the collector space is sufficient to render the multiplier phototube unstable.

A more compact multiplier phototube, having in common with the "linear" type just described the properties of good electron focusing between stages and the reduction to a minimum of ion feedback between collector and cathode, is obtained by arranging the dynodes in a circular array, as shown in Fig. 8.11. The electrode 0, illuminated through a wire grid, represents the photocathode; the grid 10, the collector. This structure is employed in standard commercial multiplier phototubes.

Numerous other secondary-emission multiplier structures have found application. Figure 8.12 shows a type in which the individual dynodes are in the form of small boxes, open on the two adjoining sides which

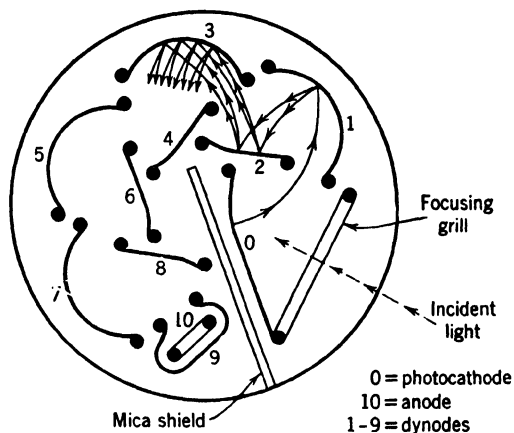


FIG. 8.11. Circular Electrostatic Multiplier Phototube (Horizontal Section). (Engstrom, reference 13.) (Courtesy of the *Journal of the Optical Society of America*.)

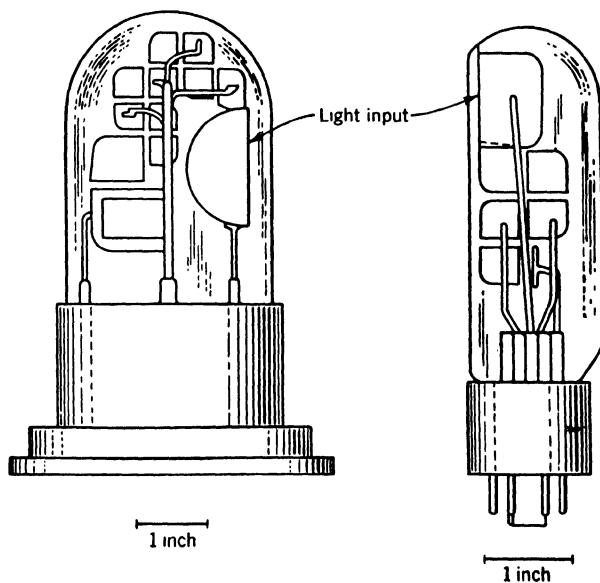


FIG. 8.12. Eleven- and Six-Stage Box-Type Electrostatic Multiplier Phototubes. (Larson and Salinger, reference 12.) (Courtesy of *Review of Scientific Instruments*.)



face the preceding and the succeeding stages, respectively.<sup>15</sup> Still other arrangements,<sup>16</sup> as well as multiplier phototubes with oversize photocathodes,<sup>17</sup> find application in television pickup systems.

**Dark Currents.** Any phototube to which voltage is applied will pass a certain amount of current even if the photocathode is unilluminated. Such dark currents are most significant in devices employed for the measurement or detection of very small amounts of light, a purpose for which multiplier phototubes are particularly well adapted. The relatively high potential differences present in these tubes may accentuate these dark currents.

There are, primarily, three sources of dark current in the electron multiplier. The first is ohmic leakage between the electrodes, both on the inside and on the outside of the tube envelope. The second is thermionic emission from the photocathode and the dynodes, which is multiplied, along with the light signal current, by the succeeding secondary emission stages. The third is the current generated by positive ion impact on the photocathode and dynodes, eventually augmented by field emission currents from projecting points of the electrodes. The currents arising from these several sources may be distinguished on the basis of their variation with voltage (Fig. 8.13). Ohmic leakage is proportional to applied voltage. Thermionic emission output currents, on the other hand, are approximately proportional to the gain of the tube and hence, in the normal range of operation of the multiplier, increase much more rapidly than the voltage.<sup>18</sup> At the upper end of the range, regenerative effects caused by the return to the cathode region of positive ions produced in residual traces of gas result in an abrupt increase in the dark current with applied voltage, which, furthermore, tends to be quite erratic. A multiplier phototube which exhibits appreciable feedback current in the normal operating range must be regarded as defective. Figure 8.13 shows the contribution of these three types of dark current as a function of applied voltage for a typical multiplier phototube with an antimony-cesium cathode.<sup>19</sup>

At the normal operating voltages of multiplier phototubes (and at room temperature) thermionic emission is the principal source of dark currents. Whereas ohmic leakage and ion feedback (as well as field

<sup>15</sup> See Larson and Salinger, reference 12.

<sup>16</sup> See Chapter 17, p. 395.

<sup>17</sup> See Chapter 16, p. 374.

<sup>18</sup> More precisely, if the photocathode and the  $n$  dynodes are similar in character and the gain per stage is  $R$ , the total dark current will be  $i_o(R^n + R^{n-1} + \dots + 1) = i_o G(1 - R^{-n-1})/(1 - R^{-1})$ . Here  $i_o$  is the thermionic emission from one electrode and  $G$  is the gain of the multiplier.

<sup>19</sup> See Engstrom, reference 13.

emission) may be minimized by careful attention to construction details, thermionic emission depends solely on the work function of the emitting surfaces and their temperature. The specific emission of a surface is given by the formula <sup>20</sup>

$$j = AT^2 e^{-w/kT} = AT^2 e^{-11,607w/T} \quad (8.2)$$

Here  $T$  is the absolute temperature of the surface,  $w$ , its work function in electron volts, and  $k$ , Boltzmann's constant. The constant  $A$  is, for

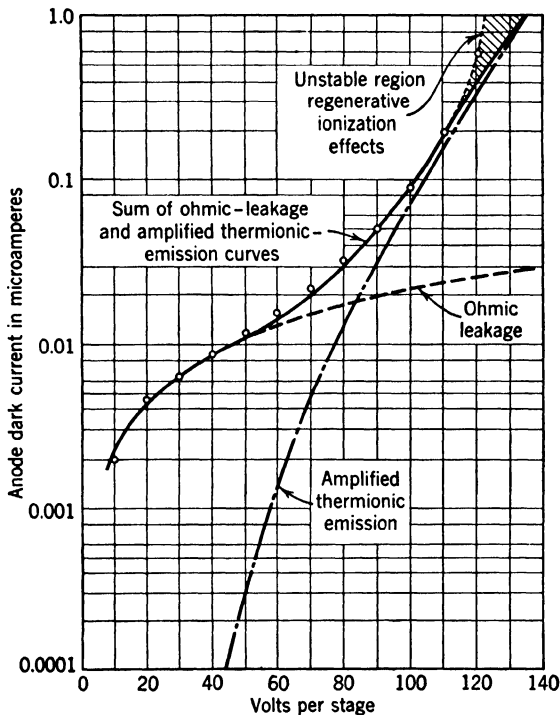


FIG. 8.13. Dark Current of a Multiplier Phototube with Antimony-Cesium Photocathode as Function of Applied Voltage. (Engstrom, reference 13.) (Courtesy of the *Journal of the Optical Society of America*.)

pure metals, of the order of  $1.2 \cdot 10^6$  amperes per square meter per degree squared. The exponential factor is, thus, very small and varies very rapidly with the temperature. This holds also for composite surfaces, although here the factor  $A$  is much smaller than the value given. It is hence possible to reduce greatly the dark current by cooling the multi-

<sup>20</sup> See Reimann, reference 14, Chapter 1.

plier phototube, for instance, by immersion in liquid air.<sup>21</sup> Figure 8.14 shows the dark current (referred back to the photocathode) of a multiplier phototube as function of temperature. Immersion in liquid air has made it possible to employ the electron multiplier for detecting a light flux of the order of one quantum per second, as described in greater

detail in Chapter 13.<sup>22</sup> The alternative method of employing electrodes with very low thermionic emission at room temperature (and corresponding lack of photosensitivity in the infrared and the visible) was employed by Bay,<sup>23</sup> who built linear electrostatic multipliers with magnesium alloy dynodes for the counting of photons as well as alpha, beta, and gamma rays from radioactive materials. Allen<sup>24</sup> has constructed similar multipliers for x-ray measurements, with a tantalum cathode and beryllium alloy dynodes.

**Dynamic Secondary-Emission Multiplier.** An ingenious method of obtaining the multiplication of photocurrents by secondary emission is employed in Farnsworth's<sup>25</sup> dynamic secondary-emission multiplier shown in Fig. 8.15. The electrodes in this tube are two flat activated cathodes and the cylindrical anode coating on the tube wall. The tube is surrounded by a solenoid producing an axial mag-

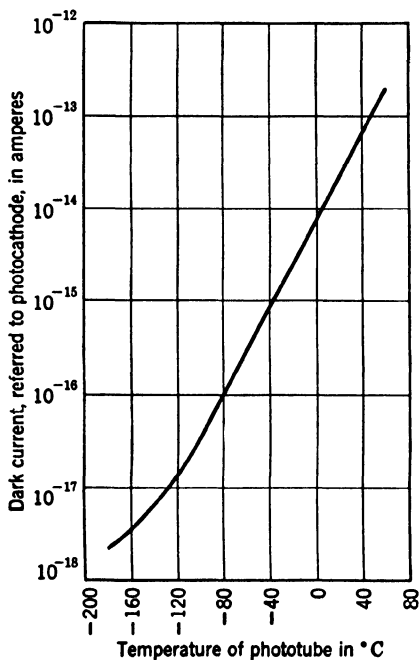


FIG. 8.14. Effective Cathode Dark Current of a Multiplier Phototube with Antimony-Cesium Photocathode as Function of Temperature. (After Engstrom, reference 13.) (Courtesy of the *Journal of the Optical Society of America*.)

netic field. If, now, in addition to a fixed positive voltage, an alternating voltage of the proper frequency (of the order of 50 megacycles per second) is applied to the anode, an electron leaving one of the cathodes in the proper phase of the alternation will be accelerated to an in-

<sup>21</sup> See Engstrom, reference 15.

<sup>22</sup> See Engstrom, reference 13.

<sup>23</sup> See reference 16.

<sup>24</sup> See reference 17.

<sup>25</sup> See reference 18.

creased extent during its passage from the cathode to the center of the anode and will be retarded to a reduced extent in its passage from the center of the anode to the second cathode. It may thus arrive at the second cathode with sufficient velocity to eject one or several secondary electrons, which again will gain energy in their passage to the original cathode as a result of the action of the alternating field. Hence they will eject

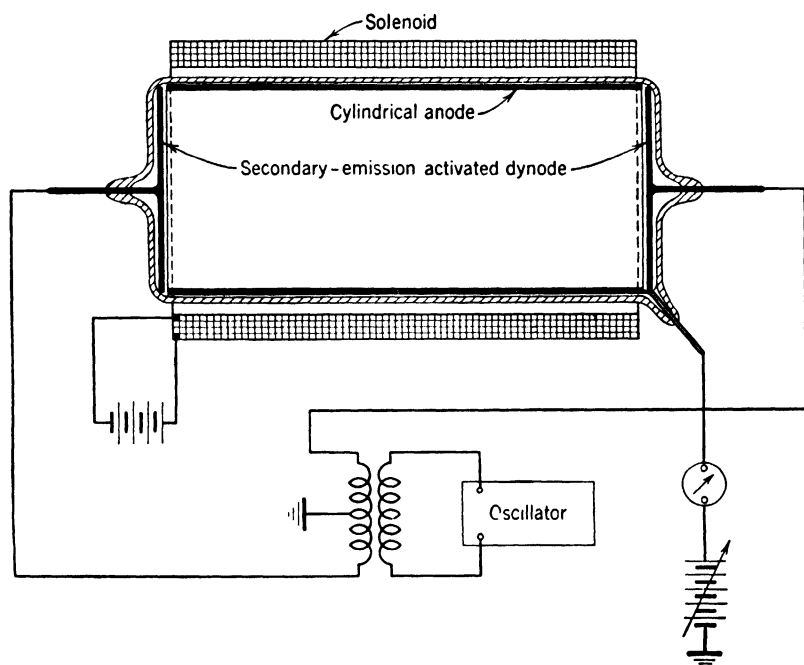


FIG. 8.15. Dynamic Secondary-Emission Multiplier Phototube. (Farnsworth, reference 18.)

still more secondary electrons, which will be multiplied after a further transit. Eventually all the secondary electrons will drift away from the center of the tube and be collected by the anode, or a self-maintained discharge will take place. The point of instability is determined by the strength and divergence of the magnetic field as well as by the amplitude of the alternating potential. Maximum amplification is obtained for a voltage amplitude just below that leading to a self-maintained discharge. The dynamic multiplier has been found to yield reproducible multiplications of several thousand. In practice it has been superseded by electrostatic multipliers, which are superior with respect to frequency response, stability, and equipment requirements.

**Standard Types of Multiplier Phototubes.** Multiplier phototubes are marketed with a spectral response primarily in the blue (S-4), in the blue, green, and red (S-8), and in the ultraviolet (S-5). The last-mentioned type is provided with an envelope of ultraviolet-transmitting glass having a spectral cut-off near 2000 Angstrom units. All the tubes listed in Table 8.1 are identical in physical structure, being of the circular electrostatic type (Fig. 8.11) with nine stages of multiplication.



FIG. 8.16. A Commercial Multiplier Phototube.

Figure 8.16 shows their external appearance. The projected area of the cathode is approximately 0.3 square inch, the region of maximum effective sensitivity lying closest to the first dynode. The capacity between the anode and dynode 9 is 4 micromicrofarads, that between the anode and all the remaining electrodes, 6.5 micromicrofarads.

The variation of gain with the voltage per stage is shown, for a particular type 931-A multiplier phototube, in Fig. 8.17. The normal operating voltage per stage is 75 to 100 volts; above 100 volts per stage instability may result from ion feedback. A difference of potential of 50 volts between the last dynode and the anode is found to be sufficient for the collection of the secondary emission from the dynode and is yet low enough to prevent undue damage of the dynode by ion bombardment. The dynamic characteristic of a multiplier phototube is flat up to limiting frequencies of many megacycles per second, as for an ordinary vacuum phototube. Irreversible fatigue effects are generally not observed unless the currents or voltages in the last stage exceed recommended values. The drawing of currents in excess of the maximum rating is likely to lead, however, to permanent damage. The light response of the multipliers is linear within a wide range: For a type 1P21 the deviation from linearity was found to be less than 3 per cent when the cathode illumination was varied from  $10^{-10}$  to  $10^{-4}$  lumen. At higher values nonlinearity results from space charge effects in the last stage. It may be noted that the type 1P21 tubes are similar to the 931-A tubes, being selected simply for very low dark current and high overall sensitivity. This selection makes them particularly suitable for the measurement of extremely small quantities of light.

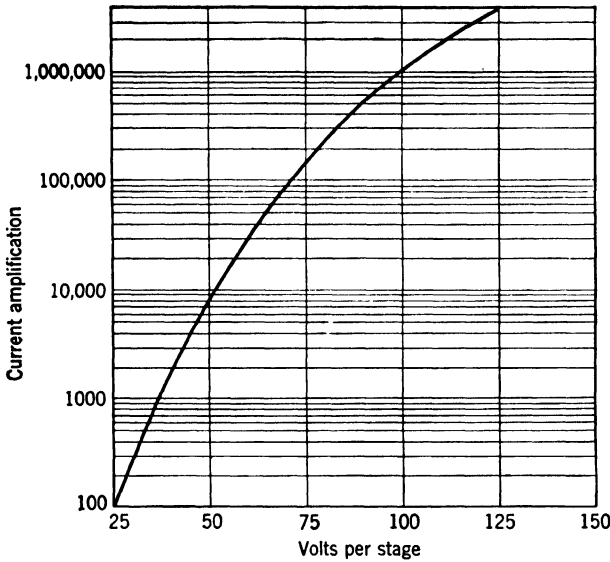


FIG. 8.17. Variation of Current Amplification with Voltage Applied between Stages for a Typical 931-A Multiplier Phototube. (Engstrom, reference 13.) (Courtesy of the *Journal of the Optical Society of America*.)

TABLE 8.1. PROPERTIES OF MULTIPLIER PHOTOTUBES  
(Mean Values)

Type	Sur- face	Sensitivity and Gain		Anode Cur- rent, maxi- mum, ma	Max. Voltage		Dark Cur- rent, maxi- mum, $\mu$ a	Tem- pera- ture, maxi- mum, $^{\circ}$ C
		at 75 volts per stage amp/lumen	at 100 volts per stage amp/lumen		Total, volts	Last Stage, volts		
RCA/GL/WL 931-A	S-4	1.5	10	1.0	1,250	250	0.25	75
		150,000 $\times$	1,000,000 $\times$					
RCA-1P21	S-4	6	40	0.1	1,250	250	0.1	75
		300,000 $\times$	2,000,000 $\times$					
RCA-1P22	S-8	0.09	0.6	1.0	1,250	250	0.25	50
		30,000 $\times$	200,000 $\times$					
RCA-1P28	S-5	0.45	3	0.5	1,250	250		75
		30,000 $\times$	200,000 $\times$					

RCA: Radio Corporation of America, Tube Department, Harrison, N. J.  
GL: General Electric Company, Schenectady, N. Y.  
WL: Westinghouse Electric Corporation, Pittsburgh, Pa.

## REFERENCES

1. R. KOLLATH, "Secondary emission of solid bodies," *Physik. Z.*, Vol. 38, pp. 202-224, 1937.
2. R. KOLLATH, "On the energy distribution of secondary electrons," *Ann. Physik*, Vol. 39, pp. 59-80, 1941; Vol. 1, pp. 357-380, 1947.
3. H. BRUINING and J. H. DE BOER, "Secondary electron emission of metals," *Physica*, Vol. 5, pp. 17-30, 1938.
4. H. BRUINING and J. H. DE BOER, "Secondary electron emission: compounds with a high capacity for secondary electron emission," *Physica*, Vol. 6, pp. 823-833, 1939.
5. H. BRUINING, "Absorption of secondary electrons," *Physica*, Vol. 5, pp. 901-917, 1938.
6. H. BRUINING and J. H. DE BOER, "The mechanism of secondary electron emission," *Physica*, Vol. 6, pp. 834-839, 1939.
7. V. K. ZWORYKIN, J. E. RUEDY, and E. W. PIKE, "Silver-magnesium alloy as a secondary electron emitting material," *J. Applied Phys.*, Vol. 12, pp. 696-698, 1941.
8. V. K. ZWORYKIN, G. A. MORTON, and L. MALTER, "The secondary emission multiplier—a new electronic device," *Proc. Inst. Radio Engrs.*, Vol. 24, pp. 351-375, 1936.
9. H. E. IAMS and B. SALZBERG, "The secondary emission phototube," *Proc. Inst. Radio Engrs.*, Vol. 23, pp. 55-64, 1935.
10. G. WEISS, "On secondary electron multipliers," *Z. tech. Physik*, Vol. 17, pp. 623-629, 1936.
11. V. K. ZWORYKIN and J. A. RAJCHMAN, "The electrostatic electron multiplier," *Proc. Inst. Radio Engrs.*, Vol. 27, pp. 558-566, 1939.
12. C. C. LARSON and H. SALINGER, "Photocell multiplier tube," *Rev. Sci. Instruments*, Vol. 11, p. 226, 1940.
13. R. W. ENGSTROM, "Multiplier phototube characteristics: application to low light levels," *J. Optical Soc. Am.*, Vol. 37, pp. 420-431, 1947.
14. A. L. REIMANN, *Thermionic Emission*, John Wiley and Sons, New York, 1934. (Out of print.)
15. R. W. ENGSTROM, "Refrigerator for multiplier phototube," *Rev. Sci. Instruments*, Vol. 18, p. 587, 1947.
16. Z. BAY, "Electron multiplier as an electron counting device," *Rev. Sci. Instruments*, Vol. 12, pp. 127-133, 1941.
17. J. S. ALLEN, "The x-ray photon efficiency of a multiplier phototube," *Rev. Sci. Instruments*, Vol. 12, pp. 484-488, 1941.
18. P. T. FARNSWORTH, "Television by electron image scanning," *J. Franklin Inst.*, Vol. 218, pp. 410-444, 1934.

## Chapter 9

# THE IMAGE TUBE

The various types of phototubes considered so far furnish a signal current which is a measure of the total amount of light falling on the photocathode. Their output gives no information on the spatial distribution of light in the incident beam. To gain this information it is necessary to separate the electron currents leaving different parts of the photocathode so that each can produce an effect corresponding to the light flux incident on that part. Tubes in which, in this manner, an electron image of the light distribution on the cathode is formed are known as image tubes. They will be met in later chapters as constituent parts of more complex electronic devices. In this chapter attention will be confined to the simplest image tubes, in which the electron image is formed on a luminescent screen, which renders it visible.

**Accelerating-Field Tube.** In the earliest form of image tube <sup>1</sup> (Fig. 9.1) a short, intense accelerating field prevents the electrons leaving a point

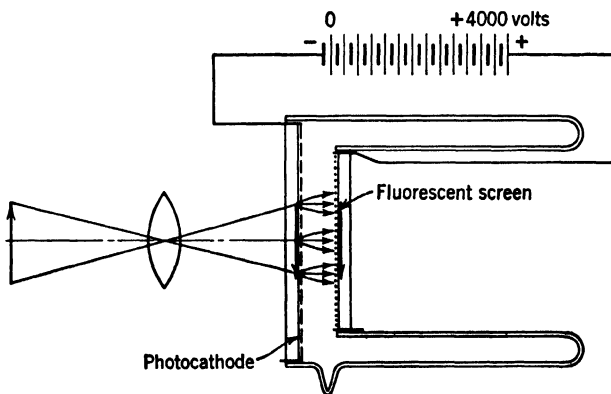


FIG. 9.1. Simple Accelerating-Field Image Tube. (Holst, de Boer, Teves, and Veenemans, reference 1.)

of the photocathode from spreading unduly before they reach the screen, which is deposited on a thin, transparent metallic film serving as anode.

<sup>1</sup> See Holst, de Boer, Teves, and Veenemans, reference 1.



The cathode itself is a transparent silver-cesium oxide-cesium film formed on a flat glass disk. The design of the envelope minimizes leakage currents between the cathode and the anode, between which a potential difference of the order of 4000 volts is established.

If the photoelectrons had zero initial velocity, all electrons leaving any point of the cathode would travel along identical paths and thus arrive at the same point of the anode. Actually, as has already been noted, they leave the cathode with small initial velocities in all forward directions. As a result, the electrons from one point fall on a limited area of the anode. The diameter  $D$  of this luminous *disk of confusion*, which corresponds to a single emitting point of the cathode, is proportional to the distance between cathode and anode and to the square root of the ratio of the initial to the final kinetic energy of the electrons.<sup>2</sup> For an accelerating potential of 4000 volts, a separation of electrodes equal to 1 centimeter (0.01 meter), and a maximum initial kinetic energy—as determined by the work function of the photocathode and the frequency of the exciting radiation—of 1 electron volt, the diameter of the disk of confusion becomes  $\frac{2}{3}$  millimeter or 0.025 inch ( $D = 0.00063$  meter). Since cold emission sets an upper limit to the voltage employed and activation requirements set a lower limit to the spacing between anode and cathode, it is not practicable to reduce this value of the diameter of the disk of confusion by a large factor.

**Electron Optics.** This difficulty may be overcome by employing more effective methods of bundling or *focusing* the electrons leaving individual points of the cathode. The existence of such methods may be deduced simply from the realization of William Rowan Hamilton<sup>3</sup> that the path of a particle in a potential field is subject to the same laws as the paths of light rays in a medium of variable refractive index. In particular, for an electron in an electrostatic field, the “index of refraction”

<sup>2</sup> Let  $v_r = (2eV_r/m)^{1/2}$  be the lateral component of the initial velocity of a particular electron;  $eV_r$ , the kinetic energy associated with this component;  $V$ , the accelerating potential; and  $L$ , the separation of cathode and anode. Since the lateral velocity component  $v_r$  is unaffected by the accelerating field of the tube, the lateral displacement  $r$  of the electron is given simply by the product of  $v_r$  and the time of transit  $T$ :

$$r = v_r T = \left( \frac{2eV_r}{m} \right)^{1/2} \cdot 2L \left( \frac{2eV}{m} \right)^{-1/2} = 2L \left( \frac{V_r}{V} \right)^{1/2} \quad (9.1)$$

Hence

$$D = 2r_{\max} = 4L \left( \frac{V_{r\max}}{V} \right)^{1/2} \quad (9.2)$$

$T$  is given simply by the ratio of the distance  $L$  and the average axial velocity of the electrons. The maximum value of  $eV_r$  is the difference of the energy of a quantum of the exciting radiation and the work function of the photocathode.

<sup>3</sup> See reference 2.

at any point in space is given by the square root of the electric potential at that point in space, measured relative to the potential at a point at which the velocity of the electron would be reduced to zero. Accordingly, the index is directly proportional to the velocity of the electron itself.<sup>4</sup> It follows that the well-known principles of light optics can be applied directly to electrons, electric (and magnetic) fields playing the role of the refracting elements. This is the basis of *electron optics*.

It is also possible to define an electron index of refraction for magnetic fields, although here, as in many crystalline materials, the index of refraction is a function not only of the location in space but also of the direction of the "electron ray" considered.<sup>5</sup> The most important consequence of this formal identity of the laws governing the motion of electrons in electrostatic and magnetic fields and the propagation of light rays in transparent media is that any axially symmetric electric and magnetic field acts on electrons in the same manner as an optical lens system acts on light rays. A few examples of this fact, which was first demonstrated by Hans Busch<sup>6</sup> in 1926, are given below.

**Electrostatic Lenses.** Perhaps the simplest electron lens is that formed between two coaxial cylinders at different potentials (Fig. 9.2). The properties of the electric field between them are most readily described by drawing the *equipotential surfaces* for a set of potential values differing by a fixed small fraction of the potential difference between the two electrodes. These equipotential surfaces are everywhere normal to the

<sup>4</sup> At velocities approaching the velocity of light this ceases to be true; see, for example, Zworykin, Morton, Ramberg, Hillier, and Vance, reference 3, Chapters 10 and 18. The approximation given here, however, is valid in all the applications considered in this book.

<sup>5</sup> The index, quite generally, may be written

$$n = V^{1/2} - \left( \frac{e}{2m} \right)^{1/2} A \cos \chi = V^{1/2} - 29.7A \cos \chi \quad (9.3)$$

Here  $A$  is the so-called vector potential of the magnetic field, related to the magnetic induction  $B$  by

$$B_x = \frac{\partial A_z}{\partial y} - \frac{\partial A_y}{\partial z} \quad B_y = \frac{\partial A_x}{\partial z} - \frac{\partial A_z}{\partial x} \quad B_z = \frac{\partial A_y}{\partial x} - \frac{\partial A_x}{\partial y} \quad (9.4)$$

and  $\chi$  is the angle between the vector potential  $A$  and the direction of motion of the electron. For the special case of an axially symmetric magnetic field, whose axis of symmetry coincides with the  $z$ -axis, the vector potential at any point a distance  $r$  from the axis, with the azimuth  $\phi$ , has an azimuthal direction and a magnitude

$$A = A_\phi = \frac{1}{r} \int_0^r r B_z dr = \frac{N}{2\pi r} \quad (9.5)$$

Here  $N$  is the magnetic flux through a circle about the axis passing through the point in question.

<sup>6</sup> See reference 4.

electric field lines. The path of an electron in such a lens field may be determined step by step, the electron being treated as though it moved with a constant, averaged velocity from one equipotential to the next.<sup>7</sup> If the intervals between equipotential surfaces are chosen small, this procedure leads to a close approximation to the true path.<sup>8</sup>

It is seen that the action of the electrostatic field on electron rays resembles that of a transparent onion, whose successive layers have

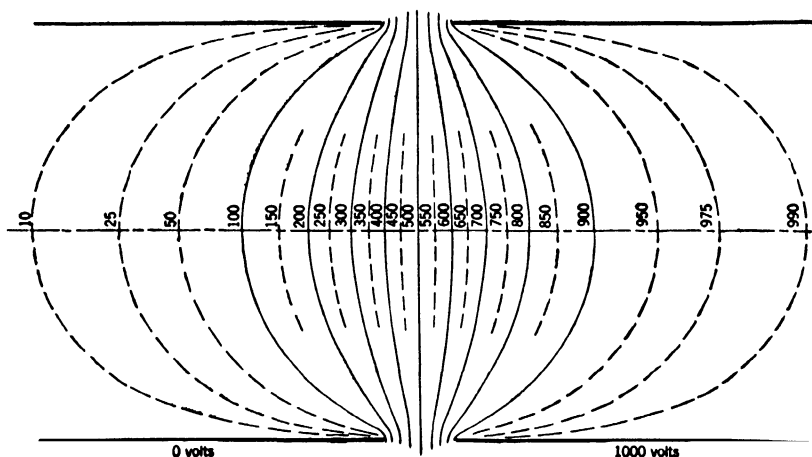


FIG. 9.2. Potential Distribution in Electrostatic Lens Formed between Two Equidiameter Cylinders at 0 and 1000 Volts, Respectively. (Zworykin, Morton, Ramberg, Hillier, and Vance, *Electron Optics and the Electron Microscope*, John Wiley and Sons, New York, 1945.)

increasing optical density, or, in fact, the crystalline lens of the human eye, on light rays. Electrons incident on the lens from any one point  $P_0$  on the axis, converge on, or appear to diverge from, a second point

<sup>7</sup> See Musson-Genon, reference 5, and Fig. 9.3. Let  $i$  be the angle of incidence of the electron on the equipotential  $V = V_n$ . Then its angular deflection in passing from equipotential  $V_n$  to equipotential  $V_{n+1}$  is assumed to be given by  $i' - i$ , where  $i'$  is the angle of refraction determined by Snell's law for a ray passing from a medium of index  $V_n^{1/2}$  into one of index  $V_{n+1}^{1/2}$ :

$$\sin i' = \left( \frac{V_n}{V_{n+1}} \right)^{1/2} \sin i \quad (9.6)$$

This establishes the direction of motion of the electron on leaving equipotential  $V_{n+1}$ ; the magnitude of its velocity at this point is, of course,  $(2eV_{n+1}/m)^{1/2}$ . The point of intersection  $B$  with the equipotential  $V_{n+1}$  is obtained by assuming that the electron travels from the intersection  $A$  with equipotential  $V_n$  through the region between the two equipotential surfaces with a velocity equal to the vector average of its initial and final velocities.

<sup>8</sup> For other methods of tracing electron paths, see Zworykin, Morton, Ramberg, Hillier, and Vance, reference 3, Chapter 12.

on the axis,  $P_i$ , after passing through the lens. Furthermore, those leaving other points near  $P_o$ , in the plane normal to the axis through  $P_o$ , are reunited in a set of points similarly disposed relative to each other in the normal plane through  $P_i$ , forming an image of the area about  $P_o$ . The position of the image and its magnification are given by the familiar lens

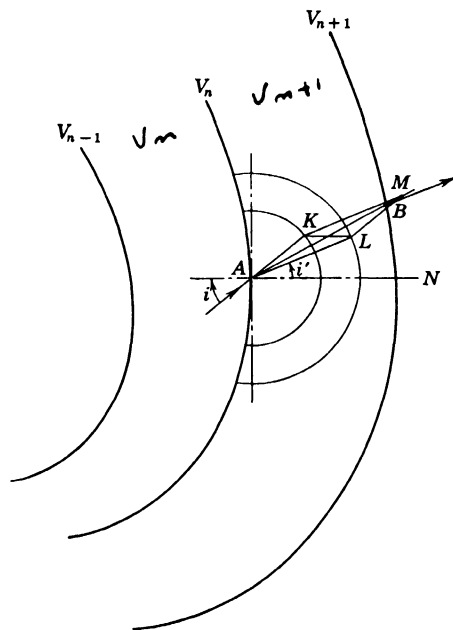


FIG. 9.3. Construction of Deflection and Displacement of Electron Path during Passage through the Region between Two Equipotential Surfaces. (Musson-Genon, reference 5):  $i$ , angle of incidence on equipotential  $V = V_n$ ;  $AK = V_n^{1/2}$ , in direction of incident ray;  $KL$  drawn parallel to perpendicular to equipotential  $V_n$  at  $A$ , to intersection with circle about  $A$  with radius  $V_{n+1}^{1/2}$ , establishing direction  $AL$  of ray leaving  $V_{n+1}$ .  $AM$  is vector resultant of  $AK$  and  $AL$ , giving direction of mean velocity. Its intersection with equipotential  $V_{n+1}$ ,  $B$ , indicates point of emergence of electron on equipotential  $V_{n+1}$ .

equation of light optics, with the square roots of the potentials at the object and image taking the place of the refractive indices in object space and in image space, respectively.<sup>9</sup> The lens equation is inter-

<sup>9</sup> The lens equation takes the form

$$\frac{V_o^{1/2}}{u} - \frac{V_i^{1/2}}{v} = \frac{V_o^{1/2}}{f_o} = \frac{V_i^{1/2}}{f_i} \quad M = \frac{v}{u} \left( \frac{V_o}{V_i} \right)^{1/2} \quad (9.7)$$

Here  $u$  is the distance of the object from the lens;  $v$ , the distance of the image from the lens;  $V_o$ , the potential in object space;  $V_i$ , the potential in image space;  $f_o$ , the object-space focal length;  $f_i$ , the image-space focal length; and  $M$ , the magnification.

preted most simply as relating the distance  $v$  of the image from the lens to the distance  $u$  of the object from the lens and a lens parameter, either the object-side focal length  $f_o$  or the image-side focal length  $f_i$ , characterizing the lens power. Such an interpretation is meaningful only if the extent of the lens field is negligible compared to the object and image distance. In this special case of a "thin lens" the focal lengths are given by simple expressions.<sup>10</sup>

In the more common case when the lens cannot be regarded as thin, it is necessary, just as in ordinary light optics, to introduce two auxiliary

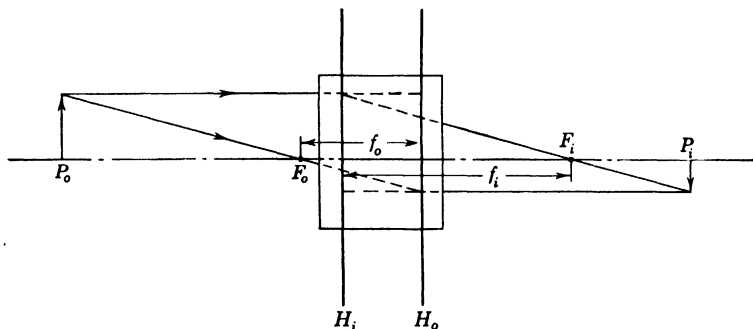


FIG. 9.4. Construction of the Image at  $P_i$  of an Object at  $P_o$  with the Aid of the Principal Planes  $H_o$ ,  $H_i$ , and Focal Points  $F_o$ ,  $F_i$  of a Thick Lens.

planes, the object-side principal plane  $H_o$  and the image-side principal plane  $H_i$ , which define the effective position of the "lens" for object space and image space, respectively (Fig. 9.4). These planes have the property of being imaged into each other by the lens with unity magnification. A ray aimed at a particular point of  $H_o$  from object space appears to come from a point of  $H_i$  which is equally distant from the axis after having passed through the lens. Knowing the positions of the principal planes,  $H_o$  and  $H_i$ , and those of the focal points,  $F_o$  and  $F_i$  (which lie on the axis, a distance  $f_o$  from  $H_o$  and a distance  $f_i$  from  $H_i$ , respectively), one may determine the magnitude and location of the image (at  $P_i$ ) of any object of known size and location (at  $P_o$ ), as indicated in Fig. 9.4. The image-side focal point  $F_i$  is the point in image space at which all rays incident parallel to the axis in object space converge. Similarly, the object-side focal point  $F_o$  is the source in object

<sup>10</sup> The focal lengths of a thin lens are given by

$$\left(\frac{V_i}{V_o}\right)^{1/2} \frac{1}{f_i} = \left(\frac{V_o}{V_i}\right)^{1/2} \frac{1}{f_o} = \frac{3}{16} \int_{z_o}^{z_i} \left(\frac{V'}{V}\right)^2 dz \quad (9.8)$$

Here  $V$  and  $V'$  are the value of the potential along the axis and its first derivative with respect to the axial coordinate  $z$ .

space of rays which emerge from the lens parallel to the axis in image space. This follows directly from the lens equation (Eq. 9.7).

The simple example considered serves to bring out not only the basic similarity of light lenses and electron lenses, but also some of the principal differences. They are:

1. The refractive media of electron lenses have a continuously variable index. The small permeability of matter for electrons renders impractical the employment of conductors in the path of the electron beam, which might introduce discontinuities in the refracting field. This circumstance restricts the properties of electron lenses so that (provided that object and image are in field-free space) (a) all electron lenses are positive or converging lenses and (b) the principal planes are always "crossed"—the object-side principal plane  $H_o$  is closer to image space than the image-side principal plane  $H_i$ . It also greatly limits the possibility of optically correcting lenses so as to minimize image defects.
2. The energy of the image-forming "radiation" is not a constant. Thus, in passing through an accelerating lens with a voltage ratio of 2:1 the energy of the electrons is doubled. In numerous devices, including image tubes, the initial energy of the image-forming electrons may be multiplied by a factor of several thousand. Similarly, the available range of the index of refraction (which in light optics is of the order of 2:1) is enormous, a circumstance which compensates to some extent for the limited possibilities of optical correction.
3. A final difference, which should be mentioned even though it plays no role in the present consideration, is that diffraction effects are much less important for electrons than for light since, for acceleration potentials of a few thousand volts, the wave length of electrons is less than that of light by a factor of the order of  $10^{-4}$  or  $10^{-5}$ .<sup>11</sup> This extraordinary shortness of the electron wave length is responsible for the possibility of constructing electron microscopes with resolving powers far exceeding that of any light microscopes.

Electron lenses similar to that described above may also be formed by pairs of apertures (Fig. 9.5c) or a cylinder and an aperture. If a third electrode is added between two electrodes at a common potential, a uni-

<sup>11</sup> According to de Broglie (reference 6) the electron wave length is given by

$$\lambda = \frac{h}{mv} = 12.3V^{-1/2} \cdot 10^{-10} \text{ meter} \quad (9.9)$$

Here  $h$  is Planck's constant,  $m$  the mass of the electron, and  $v$  its velocity, corresponding to the accelerating potential  $V$ .

potential lens is obtained which is a close approximation in behavior to the simple glass lens of light optics, for which both object and image lie in a medium of the same refractive index (air). On the other hand, a single electrode with an aperture between two regions of different field strength has a converging or diverging action, depending on whether the electron meets a stronger or a weaker field as it passes through the aper-

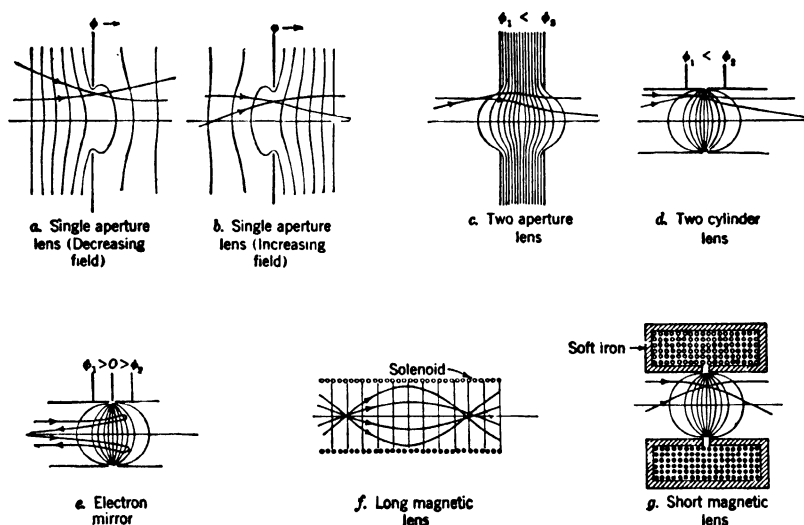


FIG. 9.5. Electron Paths in Various Types of Electron Lenses. (Courtesy *Journal of Applied Physics*, Vol. 10, p. 472, 1939.)

ture.<sup>12</sup> Figure 9.5, *a* and *b*, shows the action of such single-aperture lenses on the paths of electrons passing through the aperture.

**Magnetic Lenses.** Since, as brought out by Eq. 9.3, the index of refraction in a magnetic field depends on the direction of motion of the electron considered, the behavior of magnetic lenses is considerably more complex than that of electrostatic lenses. A ray incident parallel to the axis of a short magnetic lens will, in accord with the force law governing

<sup>12</sup> According to Davisson and Calbick (reference 7) the effective reciprocal focal length of an aperture is given by

$$\frac{1}{f} = \frac{4V}{V_i' - V_o'} \quad (9.10)$$

provided that the potential  $V$  of the apertured electrode is large compared to the product of the field strengths  $-V_i'$  and  $-V_o'$ , in image and object space respectively, with the diameter of the aperture.

the effect of a magnetic field on a moving electron,<sup>13</sup> first experience an azimuthal deflection, arising from the action of the radial component of the magnetic field on the electron. Only as it attains, in this manner, an azimuthal component of velocity will the axial component of the field affect its motion and bend its path toward the axis. A magnetic-lens field thus causes a rotation of the imaging electrons about the axis in addition to the focusing of the pencils leaving points in object space at conjugate points in image space. The total angle of rotation is proportional to the integral of the magnetic induction along the axis,<sup>14</sup> whereas the reciprocal focal length of the lens is proportional to the integral of the square of the magnetic induction.<sup>15</sup> As a result, a lens with a relatively concentrated field has a smaller image rotation than a lens of equal focal length with a relatively broad field. For the least concentrated magnetic-lens field, that is, a uniform magnetic field, the rotation is just 180 degrees ( $\pi$  radians) between an object and its nearest image. Hence the real images are here erect instead of inverted. It has already been seen that the images formed by such a field, which of course has no unique optic axis, have unity magnification.<sup>16</sup>

An approximately uniform magnetic field is most readily attained with the aid of a long solenoid (Fig. 9.5f).<sup>17</sup> A short magnetic lens may be realized by enclosing a coil in a shell of a ferromagnetic material, such as pure iron, which is provided with a narrow air gap, as shown in Fig. 9.5g. Since the magnetic-field integral about a closed loop is determined exclusively by the number of ampere turns linked by the loop and since, for a given magnetic induction, the field in the ferromagnetic material is less than that in free space by a factor equal to the permeability—approximately a 1000 for iron—very strong fields may be produced

<sup>13</sup> See Eq. 6.1 on p. 106.

<sup>14</sup> The total angle of rotation  $\chi$  is given by

$$\chi = \int_{z_0}^{z_1} \left( \frac{eB^2}{8mV} \right)^{1/2} dz = 1.48 \cdot 10^5 V^{-1/2} \int_{z_0}^{z_1} B dz \text{ radians} \quad (9.11)$$

where  $B$  is the magnetic induction along the axis in webers/meter<sup>2</sup>

<sup>15</sup> The reciprocal focal length of a short magnetic lens is

$$\frac{1}{f} = \int_{z_0}^{z_1} \frac{eB^2}{8mV} dz = 2.2 \cdot 10^{10} V^{-1} \int_{z_0}^{z_1} B^2 dz \text{ meter}^{-1} \quad (9.12)$$

<sup>16</sup> See Chapter 6, p. 106.

<sup>17</sup> The magnetic induction within a long solenoid is

$$B = 4\pi ni \cdot 10^{-7} \text{ weber/meter}^2 \quad (9.13)$$

where  $n$  is the number of turns per meter and  $i$  is the current passing through them in amperes.



in and near the gap with moderate currents.<sup>18</sup> In the special case where the permeability of the magnetic shell is so great that the "magnetic resistance" of the shell is negligible compared with that of the gap,<sup>19</sup> the magnetic-field distribution between the gap faces becomes identical with the electric-field distribution between two similarly shaped electrodes to which a difference in potential  $4\pi ni$  is applied.<sup>20</sup>

**Image Tubes Employing Long Magnetic Focusing Fields.** The simplest image tube employing electron focusing is obtained by superposing a uniform magnetic field on a uniform electrostatic accelerating field, as is shown schematically in Fig. 9.6. The uniform magnetic field is produced by a solenoid surrounding the tube, the uniform accelerating field, by providing a uniform resistive coating on the inner wall of the cylindrical envelope, connected at the two ends to the photocathode and the fluorescent-screen anode, respectively. In practice the resistive coating may be replaced by a series of equally spaced metal rings connected by equal resistances. The distance between cathode and screen, the accelerating voltage, and the magnetic induction are so adjusted that the time of flight of an electron from cathode to screen is just equal to the period in which an electron moving at right angles to the magnetic

<sup>18</sup> The magnetic induction along a line of induction surrounding the coil is related to the current  $i$  and the number of turns  $n$  in the coil by

$$\oint_{\mu} \frac{B}{\mu} ds = 4\pi ni \quad (9.14)$$

The integral is to be taken over a closed induction line linked with the coil;  $\mu$  is the permeability of the medium at any point of the line and is  $10^{-7}$  for vacuum, of the order of  $10^{-4}$  for iron. Hence, for a given value of  $ni$ ,  $B$  will be very high for an induction line passing almost entirely through the iron shell, as compared with its value for a line passing only through air, vacuum, and other nonferromagnetic materials. The induction lines are thus highly concentrated in the gap and bulge out into the neighboring region, forming the lens field.

<sup>19</sup> This condition may be written

$$\int_{\text{Shell}} \frac{ds}{\mu} \ll \int_{\text{Gap}} \frac{ds}{\mu} \quad (9.15)$$

<sup>20</sup> Under these circumstances the pole faces have constant scalar magnetic potentials  $\psi_1$  and  $\psi_2$ , related by

$$\psi_2 - \psi_1 = 4\pi ni \quad (9.16)$$

The components of the magnetic induction in the direction of the axis of symmetry ( $z$ -axis) and in a radial direction may be derived from the scalar potential  $\psi$  by

$$B_z = -\mu \frac{\partial \psi}{\partial z} \quad B_r = -\mu \frac{\partial \psi}{\partial r} \quad (9.17)$$

field would describe a complete circle.<sup>21</sup> If all the electrons left the cathode with the same component of velocity normal to the surface, electrons leaving a point of the cathode would, for proper adjustment of the coil current, be reunited exactly at the corresponding point of the screen. Actually, the kinetic energy associated with the normal component of the initial velocity may be expected to vary over a range of the order of an electron volt. As a result, the electrons leaving a point on the cathode are not reunited in a point, but in a disk of confusion whose diameter is proportional to the ratio of the distance between

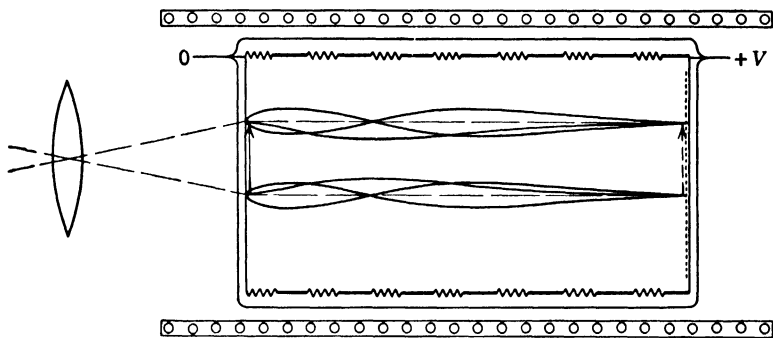


FIG. 9.6. Image Tube Employing Long Uniform Magnetic Field for Focusing.

cathode and screen and the accelerating potential.<sup>22</sup> If the cathode-screen separation is 10 centimeters (0.1 meter), the accelerating voltage is 4000 volts, and the initial energy spread of the photoelectrons is 1 electron volt, the diameter of the disk of confusion becomes 0.000025

<sup>21</sup> If  $d$  is the distance between cathode and screen,  $V$  is the accelerating potential, and  $B$  is the magnetic induction, we obtain

$$\frac{d}{\frac{1}{2} \left( \frac{2eV}{m} \right)^{1/2}} = \frac{2\pi m}{eB} \quad d = \frac{\pi}{B} \left( \frac{2mV}{e} \right)^{1/2} = 1.054 \cdot 10^{-5} \frac{V^{1/2}}{B} \quad (9.18)$$

<sup>22</sup> If the kinetic energy of the electrons associated with their initial axial velocity component ranges from 0 to  $eV_{z_{\max}}$ , the plane of focus varies by an axial distance

$$\Delta z = \left( \frac{V_{z_{\max}}}{V} \right)^{1/2} d \quad (9.19)$$

For a maximum kinetic energy of emission  $eV_{o_{\max}}$ , the maximum displacement in the midplane between extreme excursions of focus becomes

$$\Delta r_{\max} = \left[ \Delta z \left( \frac{V_o - V_z}{V} \right)^{1/2} \right]_{\max} = \frac{1}{2} \left( \frac{V_{o_{\max}}}{V} \right)^{1/2} \left( \frac{V_{o_{\max}}}{V} \right)^{1/2} \cdot d \quad (9.20)$$

This corresponds to a circle of confusion with a diameter  $D$ :

$$D = \frac{V_{o_{\max}}}{V} d \quad (9.21)$$

meter or, approximately, a thousandth of an inch. This is less by a factor of 25 than the value obtained for the simple accelerating-field tube.

It is frequently advantageous to operate with nonuniform accelerating fields. Figure 9.7 shows an example in which the electric-field lines diverge, so that the paths of the electrons leaving the cathode with zero

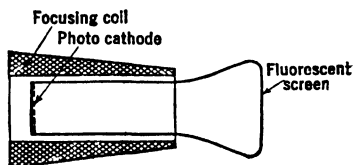


FIG. 9.7. Magnetic Image Tube with Focusing Coil Minimizing Aberrations (Iams, Morton, and Zworykin, reference 8). (From Zworykin and Morton, *Television*, John Wiley and Sons, 1940.)

initial velocity (the "principal" electron rays, constituting the central rays of the several imaging pencils) diverge also, though to a lesser extent. If, on the electric field, a magnetic field is superposed whose field lines everywhere coincide with the principal rays, the electrons traveling along them will not be influenced by the magnetic field. At the same time, the magnetic field focuses the electrons emitted with small lateral velocity components in the same manner as a

uniform field, so that a sharp and erect, *magnified*, image of the object is produced on the screen. The proper distortion of the magnetic-field lines is achieved by suitably distributing the turn density of the solenoid.<sup>23</sup>

**Image Tubes Employing Short Lenses.** Electron images which are either considerably larger or considerably smaller than the original

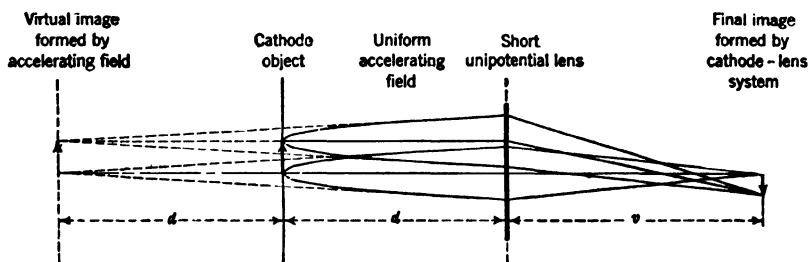


FIG. 9.8. Schematic Representation of the Operation of an Image Tube Employing a Short Lens. (Zworykin, Morton, Ramberg, Hillier, and Vance, *Electron Optics and the Electron Microscope*, John Wiley and Sons, New York, 1945.)

image on the cathode are most readily obtained with lens fields whose action is concentrated in a relatively short region of the electron paths. The general operation of such tubes is exemplified by Fig. 9.8. In the region between the cathode and the effective lens position the electrons are accelerated by a uniform electric field. They describe here parabolic

<sup>23</sup> See Iams, Morton, and Zworykin, reference 8.

paths with vertices close to the cathode plane. Since the tangent to a parabola intersects its axis at an axial distance behind the vertex equal to the axial distance of the point of tangency in front of the vertex, the rays falling on the lens, assumed to be at the potential  $V$  of the screen, appear to come from an apparent object at potential  $V$ , a distance  $2d$  from the lens. The strength of the lens must hence be such as to image an object at a distance  $2d$  on the screen, a distance  $v$  from the lens.<sup>24</sup>

The unsharpness of the image obtained with such a system arises from two sources: the fact that, for finite initial velocity, the apparent position of the object-cathode is displaced by an amount proportional to the ratio of the initial axial component of velocity to the final velocity, on the one hand, and that the focal length of the thin lens varies by an amount proportional to the ratio of the initial and final kinetic energies, on the other. The first factor normally has the greatest effect. It leads to an expression for the diameter of the circle of confusion which is the same as that obtained for the uniform-magnetic-field tube, multiplied by the magnification of the image.<sup>25</sup>

The magnification relation Eq. 9.22 has been found to apply to a number of different types of tubes, including such as appear to meet the conditions laid down in its derivation very imperfectly. In particular, it applies to image tubes similar to that shown in Fig. 9.9, provided with an accelerating field and a short magnetic focusing field,<sup>26</sup> and

<sup>24</sup> Accordingly the magnification is given by

$$M = \frac{v}{2d} \quad (9.22)$$

<sup>25</sup> The displacement of the apparent object plane is given by

$$\Delta z_o = 2d \left( \frac{V_z}{V} \right)^{1/2} \quad (9.23)$$

and the change in focal length of the thin lens by

$$\Delta f = kf \frac{V_o}{V} \quad (9.24)$$

Here  $eV_o$  and  $eV_z$  are the initial kinetic energy of the electron and the fraction thereof associated with motion in an axial direction,  $f$  is the focal length of the thin lens, and  $k$  is a numerical factor of the order of unity. For an initial radial kinetic energy  $e(V_o - V_z)$  the divergence angle at the image is  $\theta = [(V_o - V_z)/V]^{1/2}(2d/v)$ . Since, furthermore, the displacement along the axis  $\Delta z_o$  in object space corresponds to a displacement  $M^2 \Delta z_o$  in image space, the radial displacement and the diameter of the circle of confusion in the midplane between maximum excursions of focus are given by

$$\Delta r = \left( \Delta z_o - \frac{\Delta z_{o\max}}{2} \right) \theta M^2 \quad D = 2\Delta r_{\max} = M \frac{V_{o\max}}{V} d \quad (9.25)$$

<sup>26</sup> See Schaffernicht, reference 9, and Kluge, reference 10.

those represented in Figs. 9.10 and 9.11.<sup>27</sup> The tube in Fig. 9.10 consists simply of a cylinder of length  $u$ , at cathode potential, and a second cylinder of length  $v$ , at anode potential; the effective position of the lens is at the junction of the two cylinders. With this arrangement the position of the image is independent of the anode voltage, so that obtaining a sharp image is contingent on the accurate relative placement of the tube components. The dependence of the image distance  $v$  on the object distance  $u$ , both being measured in cylinder radii, is shown in Fig. 9.12. This tube suffers, furthermore, from very great "pincushion" distortion of the image and a falling off of sharpness toward the edge (Fig. 9.13a). Both drawbacks are removed in the arrangement shown in Fig. 9.11. First, the cathode cylinder is replaced by a set of rings connected by resistances, the connection of the ring nearest the anode cylinder being brought out through the tube envelope; by changing the voltage of this ring, the lens strength can be adjusted electrically until a sharp image is obtained on the screen. The variation of the image distance with the voltage  $V_1$  applied to this auxiliary electrode is shown in Fig. 9.14. A positive auxiliary voltage decreases the lens strength, a negative auxiliary voltage increases it.

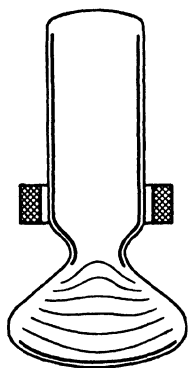


FIG. 9.9. Image Tube with Short Magnetic Lens. (Schaffernicht, reference 9.) (By permission of the Attorney General in the public interest under License No. JA-1351.)

Second, giving the cathode a curvature with a radius approximately equal to the cathode-to-lens distance minimizes the image distortion

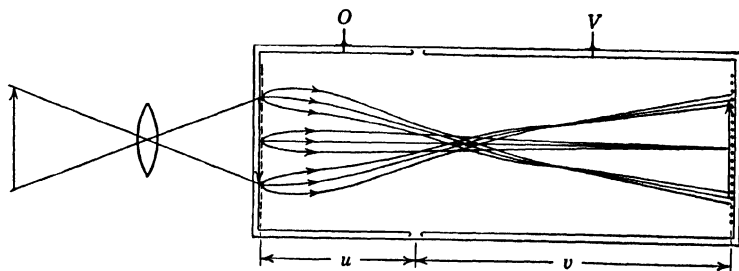


FIG. 9.10. Fixed-Focus Electrostatic Image Tube with Flat Cathode.

and the reduction in sharpness toward the edge (Fig. 9.13b). This improvement results from the fact that, in this manner, the field conditions surrounding any one "principal ray" closely approximate those surrounding the optic axis of the tube.

<sup>27</sup> See Zworykin and Morton, reference 11, and Morton and Ramberg, reference 12

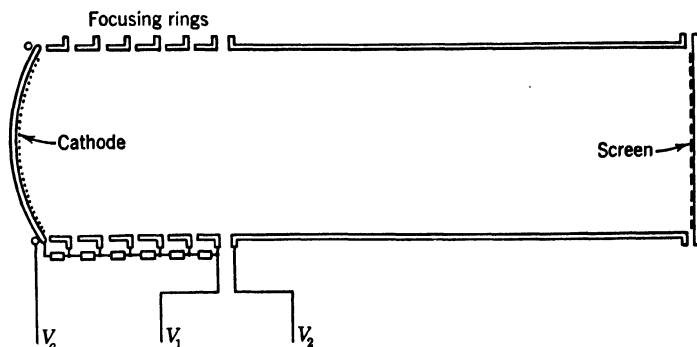


FIG. 9.11. Electrostatic Image Tube with Curved Cathode and Variable Focus. (Zworykin and Morton, reference 11.) (Courtesy of the *Journal of the Optical Society of America*.)

Figure 9.15 shows an image tube<sup>28</sup> basically similar to that just described in a form developed to yield very brilliant images with a very low level of illumination—eventually, by infrared radiation—of the photocathode. Focusing is accomplished by varying the voltage on the second or third ring electrode. The curvature of the cathode and the disposition of the electrodes are again made such as to reduce the defects in the marginal portions of the image to a minimum. The image on the screen is smaller than the image on the photocathode. In this manner the electron current per unit area and, hence, the brightness of the image on the screen are increased. The apparent dimensions of the image may then be increased with the aid of a magnifier without appreciable loss in apparent brightness. The glass hemisphere on which the screen is deposited forms a part of such a magnifier. The sharpness of the image near its center is sufficient to resolve a pattern of 1000 black and white lines of equal width projected on the useful portion of the photocathode.

With the tube shown, operating at 4000 volts, the light emitted from unit area of the screen equals approximately that inci-

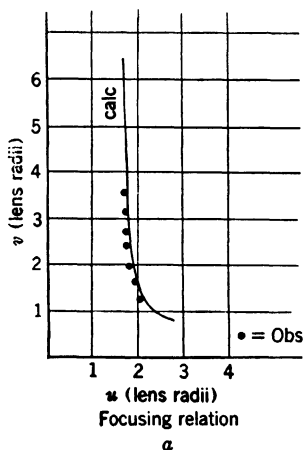


FIG. 9.12. Variation of Image Distance with Object Distance for Fixed-Focus Electrostatic Image Tube. (Zworykin and Morton, reference 11.) (From Zworykin *et al.*, *Electron Optics and the Electron Microscope*, John Wiley and Sons, New York, 1945.)

<sup>28</sup> See Morton and Flory, reference 13.

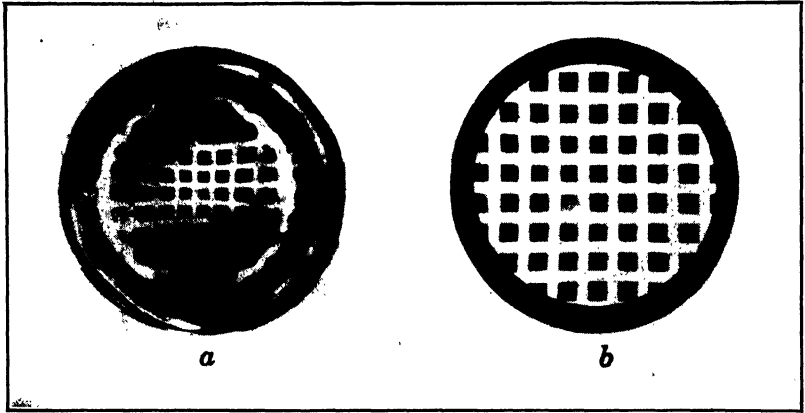


FIG. 9.13. Comparison of Images from Image Tubes with (a) Flat and (b) Curved Cathodes. (Morton and Ramberg, reference 12.) (Courtesy of *Physics*.)

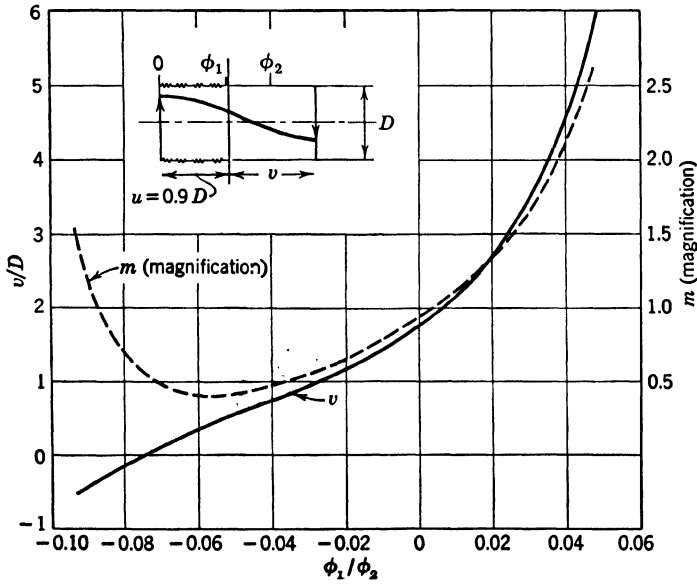


FIG. 9.14. Variation of Image Distance and Magnification with Ratio of Applied Voltages for a Variable-Focus Electrostatic Image Tube. (Zworykin *et al.*, *Electron Optics and the Electron Microscope*, John Wiley and Sons, New York, 1945.)

dent on unit area of the photocathode, provided that the photocathode is illuminated by a source with the color temperature  $2870^{\circ}\text{K}$ . The cathode is a transparent silver-cesium oxide-cesium film with a maximum sensitiv-

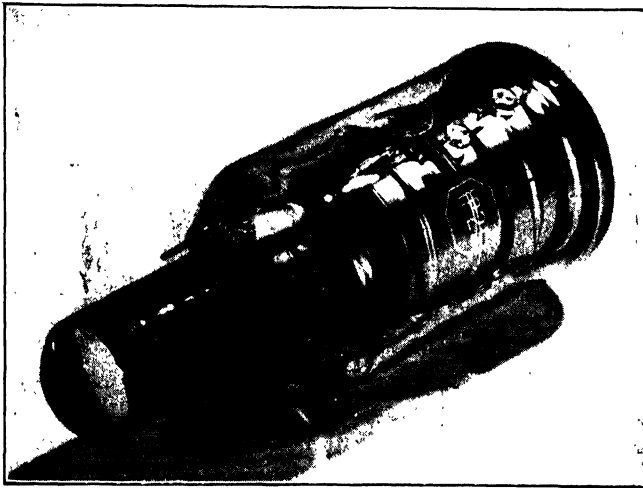
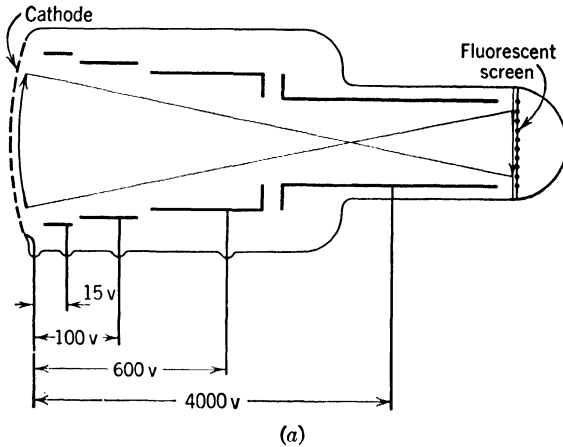


FIG. 9.15. The Type 1P25 Electrostatic Image Tube. (Morton and Flory, reference 13.) (a) Electrode arrangement. (b) External appearance. (Courtesy of *Electronics*.)

ity in the near infrared (8500 A.U.) and a threshold between 12,000 and 14,000 Angstrom units. Greater luminosities can be attained if the electrode arrangement is such as to permit a higher operating voltage. Thus, it is reported that a tube of the Allgemeine-Elektrizitäts-Gesellschaft in



Berlin, operating at 20 kilovolts, yielded ten times as much radiant energy as was incident on its photocathode.<sup>29</sup> A method of further enhancing the brightness of the observed image is shown schematically in Fig. 9.16. The image tube is divided into two or more sections, each operating at a voltage sufficiently high to lead to an output of radiant energy from the screen exceeding that incident on the photocathode. In tubes of this type<sup>29</sup> the intermediate screens had a blue-green emission matching the spectral region of maximum response of the antimony-cesium photocathodes here employed. Screen and cathode were deposited on opposite sides of partitions 30 microns in thickness. Light

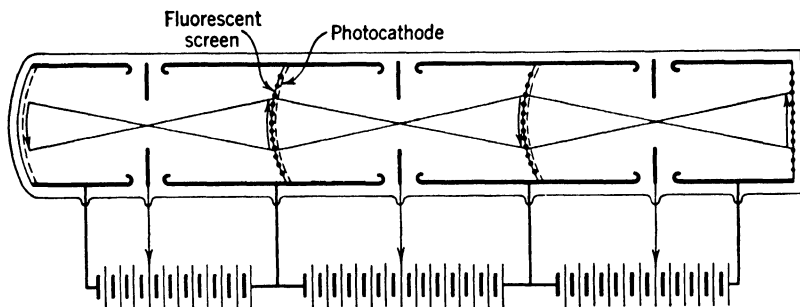


FIG. 9.16. Multiple-Image Tube (Schematic.)

feedback from the screens to the preceding cathodes may be prevented by the deposition of a thin film of aluminum over the screens, a procedure employed for increasing the efficiency and enhancing the contrast of the luminescent screens of television viewing tubes.<sup>30</sup> Such multiple-image tubes make it possible to increase the brightness of an image above that of the original scene—even with the same spectral distribution of light in both. This is a feat of which an ordinary optical system is fundamentally incapable.

**Image Tubes Employing Cylindrical Fields.** Under certain circumstances axial symmetry imposes inconvenient restrictions on the relative locations of the cathode and the fluorescent screen. It is then possible to utilize the imaging properties of superposed cylindrical electrical and magnetic fields.<sup>31</sup> An arrangement which accomplishes this is shown in Fig. 9.17. The two electrodes, as well as the two magnetic-pole faces, lie in the same plane. Both the magnetic-field and the electric-field lines are semicircles whose centers lie on the line separating the elec-

<sup>29</sup> See Krizek and Vand, reference 14.

<sup>30</sup> See Epstein and Pensak, reference 15.

<sup>31</sup> See Rose, reference 16.

trodes. If the magnetic field is sufficiently strong that an electron executes a complete loop while traveling along an arc of a line of force sufficiently short to be approximated by a straight line, its focusing action is practically the same as in the uniform-field image tube. Since the product of the magnetic induction along any field line and the length

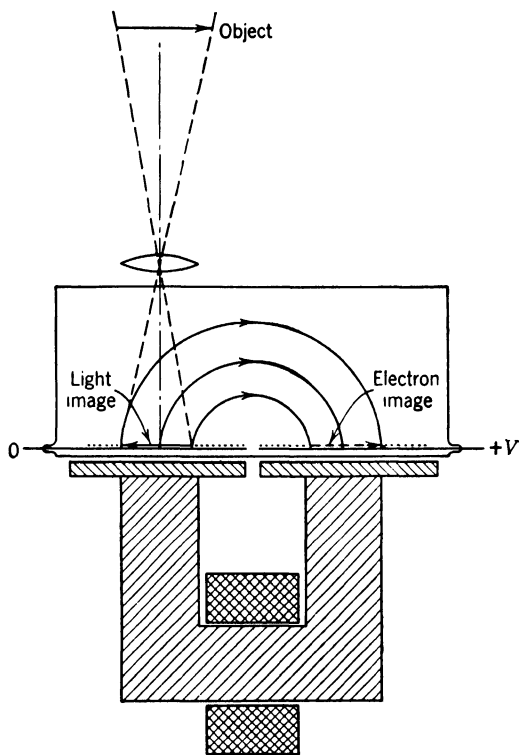


FIG. 9.17. Image Tube Employing Superposed Cylindrical Fields. (Zworykin, Morton, Ramberg, Hillier, and Vance, *Electron Optics and the Electron Microscope*, John Wiley and Sons, New York, 1945.)

of that field line is a constant, the focusing condition is fulfilled for all points of the image if it is fulfilled for one of them. As the total number of loops decreases, phenomena peculiar to the cylindrical field—namely, a shear distortion of the image in the direction of the common axis of the field lines and a dilatation normal thereto—become prominent and the definition deteriorates. These defects restrict the application of the cylindrical-field image tube to projects in which the axially symmetric types cannot be used.

## REFERENCES

1. G. HOLST, J. H. DE BOER, M. C. TEVES, and C. F. VEENEMANS, "An apparatus for the transformation of light of long wave length into light of short wave length," *Physica*, Vol. 1, pp. 297-305, 1934.
2. W. R. HAMILTON, "On a general method in dynamics," *Phil. Trans. Royal Soc.*, Vol. II, pp. 247-308, 1834.
3. V. K. ZWORYKIN, G. A. MORTON, E. G. RAMBERG, J. HILLIER, and A. W. VANCE, *Electron Optics and the Electron Microscope*, John Wiley and Sons, New York, 1945.
4. H. BUSCH, "On the operation of the concentrating coil in the Braun tube," *Arch. Elektrotech.*, Vol. 18, pp. 583-594, 1927.
5. R. MUSSON-GENON, "Graphic determination of electron trajectories in a given electric field," *Compt. rend.*, Vol. 222, pp. 858-860, 1946.
6. L. DE BROGLIE, *Thèse de doctorat*, Masson, Paris, 1924.
7. C. J. DAVISSON and C. J. CALBICK, "Electron lenses," *Phys. Rev.*, Vol. 38, pp. 585, 1931; Vol. 42, p. 580, 1932.
8. I. IAMS, G. A. MORTON, and V. K. ZWORYKIN, "The image iconoscope," *Proc. Inst. Radio Engrs.*, Vol. 27, pp. 541-547, 1939.
9. W. SCHAFFERNICHT, "Conversion of light images into electron images," *Z. Physik*, Vol. 93, pp. 762-768, 1935.
10. W. KLUGE, "Contribution on the 'transparent' photocathode and its applicability to electron-optical systems," *Z. Physik*, Vol. 93, pp. 789-791, 1935.
11. V. K. ZWORYKIN and G. A. MORTON, "Applied electron optics," *J. Optical Soc. Am.*, Vol. 26, pp. 181-189, 1936.
12. G. A. MORTON and E. G. RAMBERG, "Electron optics of an image tube," *Physics*, Vol. 7, pp. 451-459, 1936.
13. G. A. MORTON and L. E. FLORY, "Infra-red image tube," *Electronics*, Vol. 19, pp. 112-114, September, 1946.
14. V. KRIZEK and V. VAND, "The development of infra-red technique in Germany," *Electronic Eng.*, Vol. 18, pp. 316-317, 322, 1946.
15. D. W. EPSTEIN and L. PENSACK, "Improved cathode-ray tubes with metal-backed luminescent screens," *RCA Rev.*, Vol. 7, pp. 5-10, 1946.
16. A. ROSE, "Electron optics of cylindrical electric and magnetic fields," *Proc. Inst. Radio Engrs.*, Vol. 28, pp. 30-40, 1940.

## Chapter 10

# PHOTOCONDUCTIVE CELLS

Photoconductive cells contain materials whose electrical conductance changes under illumination. Their ohmic resistance changes in a definite manner with the intensity and the color of the light. The phenomenon of photoconduction was first intelligently observed by Willoughby Smith in 1873.<sup>1</sup> Small rods of selenium, which he was using as high-resistance elements in an experimental circuit set up at a transatlantic cable station, were found to become much better conductors of electricity when exposed to daylight or to any artificial illumination.

**The Element Selenium.** Selenium is a chemical element which lies in the borderland between conductors and insulators. Its place in the periodic table<sup>2</sup> is between the metal tellurium and the nonmetal sulfur. Selenium is a very poor conductor under any condition; however, its difference in conductivity in darkness and under illumination is both of scientific interest and of commercial importance.

Selenium was discovered by J. J. Berzelius<sup>3</sup> in 1817. This chemist succeeded in separating the element from the dregs which accumulate in a certain process of manufacturing sulfuric acid. Since that time all the properties of the "moon element" have been investigated. It is

TABLE 10.1. PHYSICAL CONSTANTS OF SELENIUM

Atomic weight	79.13
Melting point	220° C
Boiling point	688° C
Specific resistance (crystalline form)	$7 \cdot 10^2$ ohm-meter

known to exist in several allotropic forms. Of these, only the gray crystalline form has, in the past, been employed for photoconductive cells. Table 10.1 gives some of the more important physical constants of selenium.

<sup>1</sup> See reference 1.

<sup>2</sup> See Appendix.

<sup>3</sup> See reference 2.

Many different forms of selenium cells have been devised to take advantage of its photoconductive property. Since selenium is opaque, light cannot penetrate to any great depth; accordingly it is a chief object in design to expose as much surface as possible to irradiation without making the resistance too great. Apart from this, the essential structure of any photoconductive cell consists simply of two electrodes joined by a semiconducting element.

**The Selenium Cell.** Originally relatively crude methods were employed in the preparation of selenium "bridges." The electrodes commonly

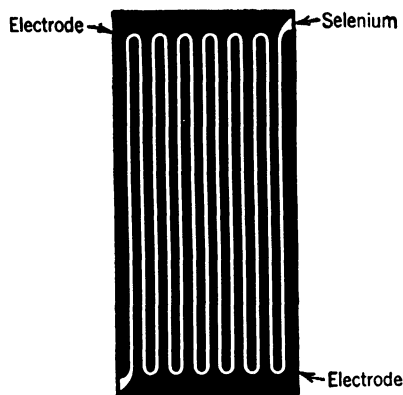


FIG. 10.1. One Form of Grid Used in Making Selenium Bridges.

took the form of two closely interpenetrating grids. This result can be attained, for example, by wrapping two wires with constant separation about an insulating cylinder or scratching a zigzag path in a conducting coating on a flat insulating surface (Fig. 10.1). This structure is then carefully coated with vitreous selenium, reduced to a thin, uniform layer by spreading with a spatula, scraping with a straight edge, or rolling with a cylindrical body. The vitreous selenium, cooling rapidly, forms a glossy, black surface over conductor and insulator alike.

If, thereafter, the whole unit is heated to a temperature not exceeding  $210^{\circ}\text{C}$  and is annealed at this or a slightly lower temperature for a period varying from a few minutes to several hours, the selenium is converted to the gray crystalline form which exhibits appreciable conductivity and possesses the desired property of being sensitive to light.

Selenium bridges made in this manner are subject to oxidation and to the attack of water vapor in the air. Also, there is generally a more or less indefinite volume of the selenium which is not completely penetrated by light and therefore reduces the ratio of light to dark conductance.

A more satisfactory method consists of distilling the selenium in a vacuum or in an atmosphere of inert gas onto a prepared grid of gold or platinum on glass. In this process the glass is maintained at a temperature high enough to cause the selenium to deposit in the gray crystalline form. The bridge is finished when a very thin film has been deposited. It may then be coated with paraffin or mounted in an evacuated tube to protect it from the air. The wattage rating of the cell

may be increased by filling the tube with helium, which serves to cool the selenium bridge by convection.

When a selenium bridge is connected in series with a potential supply and a meter, a small current will flow even when the cell is not illuminated. Admission of light will, however, result in a great increase in this current, the ratio of the increase to the dark current serving as criterion for the sensitivity of the device.

It may be noted that the effective sensitivity of a selenium cell is directly proportional to the applied voltage. For this reason the recommended operating voltage is usually close to the highest voltage which the cell will tolerate without deterioration.

**Mechanism of Conduction.** Selenium is only one of the many substances which exhibit photoconductivity. All practical photoconductors have the common property of being semiconductors, that is, of passing a small, but not negligible, current increasing with temperature when subjected to an electric field in the dark. The distinction between metals, semiconductors, and insulators becomes quite clear in terms of presently accepted models of their electronic structure.

According to the quantum theory, only one electron can occupy any one of a sequence of distinct quantum states of an individual atom. These quantum states are grouped into *shells*, the states within a particular shell differing but little in energy. In the normal atom the states of low energy are filled, leaving those of relatively high energy unoccupied (Fig. 10.2a). As many atoms are brought together in a crystal, these quantum states are modified by the interaction between atoms. Thus any one quantum state of the individual atom breaks up into a band of quantum states possessing as many individual quantum states as there are atoms in the crystal. For the very low energy states the interaction is small enough that the energy bands are exceedingly narrow. On the other hand, for the outermost, or valence, electrons they cover an energy range comparable with the potential energy of the electrons, and bands corresponding to different states of the same shell tend to overlap (Fig. 10.2b). The different electronic states in a single band may be considered as corresponding to different speeds and directions of motion of the electrons.

The distribution of the valence electrons over these bands determines whether the material in question is an insulator or a conductor. Either the band systems corresponding to quantum states in the same shell are completely occupied, or they are only partly occupied. The first happens, for instance, in ionic crystals, in which the electrons of the component ions are arranged in completed shells. The second condition is realized in metals, in which there may be only one or two electrons in

the valence shell of each atom, so that the valence energy bands are only partly occupied.

Consider, first, the case of the completely filled band. The different quantum states correspond to electrons moving in the lattice with different speeds and in different directions. If all states in the band are filled, there are just as many electrons moving in a given direction as

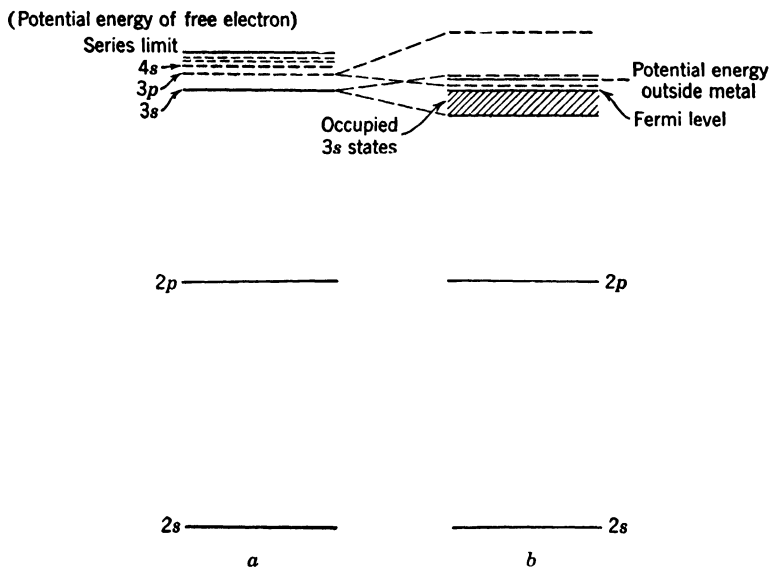


FIG. 10.2. Quantum Levels in (a) Isolated Atom and (b) Crystalline Solid of a Monovalent Metal Such as Sodium. Of the valence bands, only the 3s and 3p bands are indicated, of which the former is partly occupied by electrons. The empty portions of these overlapping bands extend above the energy value corresponding to an electron at rest outside the metal. Positions of lower edges of bands from Slater, reference 3.

in the opposite direction. In a perfect crystal at absolute zero this motion is unimpeded and the electrons are simply reflected at the crystal boundaries. At any realizable temperatures and in actual, imperfect, crystals the electrons are also scattered by the irregularities resulting from the thermal oscillations of the ions and by crystal faults. However, the thermal energies of vibration are too small for such collisions to impart sufficient energy to the electrons in the band considered to transfer them to the next higher, empty, band. Hence the electron distribution remains unaltered and, even in the presence of an electric field, the motion of the electrons in one direction is just balanced by the

motion of others in the opposite direction. Thus the material considered is an insulator (Fig. 10.3a).

If, on the other hand, only a fraction of the states in the band is occupied, the electrons in the filled levels are accelerated, between collisions with lattice irregularities, in the direction of the applied field (Fig. 10.3b). Thus a drift of the electrons results in the field direction which corresponds to metallic conduction. The charge displacement in this direction is proportional to the applied field. A decrease of conductivity with increasing temperature is to be expected since the amplitude of oscillation of the ions increases with temperature, presenting a greater

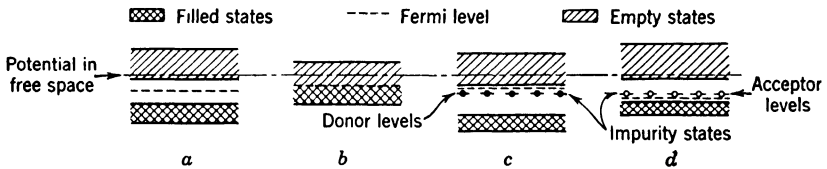


FIG. 10.3. Occupation of Quantum States in (a) Insulator, (b) Metal, (c) Excess (*n*-type) Semiconductor, and (d) Defect (*p*-type) Semiconductor.

obstacle to the conduction electrons and reducing the mean time of free flight.

A final possibility is that a lattice of the same general type as that of an insulator possesses a large number of faults. These faults may be atoms wedged between the ions of the lattice (interstitial atoms), vacancies in the lattice, or foreign ions substituted for the ions of the regular lattice. The electron distribution about such faults will adjust itself so as to maintain the electrical neutrality of the crystal region in question. Since the potential distribution differs here, however, from that in the remainder of the lattice, the energy levels of the electrons at the impurity will deviate from the band structure of the crystal as a whole. Figures 10.3c and 10.3d show two cases which are of particular interest. In the first the top occupied level of the impurity lies only slightly below the empty conduction band of the lattice. If the separation between this state and the conduction band is not too much greater than the mean thermal vibration energy of the ions, the impurity electron may occasionally be raised to the conduction band, leaving a vacancy at the impurity. Once in the conduction band it will experience a statistical drift in the direction of the applied field, between collisions, until it is trapped at some other crystal fault. A material exhibiting this type of conductivity is known as an excess or *n*-type (negative) semiconductor. Since the number of impurities is always small compared with that of normal ions and since, furthermore, the probability of thermal excita-



tion of impurity electrons to the conduction band is itself generally small, the conductivity of such a semiconductor is small compared with that of a metal. Furthermore, since the likelihood of thermal excitation increases exponentially with the temperature,<sup>4</sup> semiconductors exhibit a resistance which decreases with increasing temperature.

Figure 10.3*d* indicates the level arrangement of an impurity in a second type of semiconductor. Here the lowest unfilled impurity level lies slightly above the top filled band of the lattice. Thus one of the electrons of the band may be thermally excited so as to occupy the empty impurity level, leaving a vacancy behind in the band. Under the influence of an external field, electrons in states adjoining the vacant state, with a smaller velocity component in the direction of the field, pass over into it so that the vacancy or "hole" drifts back toward the cathode just as though it were an electron with positive charge. Eventually the hole is either trapped—that is, filled by an electron dropping into it from some other impurity state—or is neutralized by a cathode electron. Such a semiconductor is known as a defect or *p*-type (positive) semiconductor. The sign of the Hall effect<sup>5</sup> makes it possible to distinguish between the two types of semiconductors.

It should be noted that a pure substance with a closed-shell structure will behave as a semiconductor if the top filled band and the nearest conduction band are separated by a relatively small energy gap. In this case electrons from the filled band may be raised by thermal excitation to the empty band, and both the excited electrons and the residual holes will contribute to the conduction current. Their relative mobility will determine whether the substance acts as an excess or as a defect semiconductor. A semiconductor of this type is commonly denoted as an intrinsic semiconductor.

**Photoconductivity.** When a semiconductor of one of the above types is exposed to light, conduction may be initiated by the photoexcitation of an impurity or of an electron in the top filled band. The threshold wave length  $\lambda_0$  will be determined by the energy difference  $\Delta E$  between the original state of the electron and the excited state which may give rise to a mobile electron or a mobile hole.<sup>6</sup> However, this process is not sufficient to account for the continuous current under constant illumination which is observed in the practically useful photoconductors. In fact, the primary electrons (and holes) would be expected to drift a cer-

<sup>4</sup> That is, in proportion to  $e^{-\Delta E/2kT}$ , where  $\Delta E$  is the energy difference between the top impurity level and the conduction band,  $k$  is Boltzmann's constant, and  $T$  is the absolute temperature.

<sup>5</sup> That is, the direction of the transverse electric field observed on a strip of material traversed by current and subjected to a magnetic field perpendicular to the plane of the strip.

<sup>6</sup>  $\lambda_0 = hc/\Delta E = 12,395/\Delta E$  Angstrom units if  $\Delta E$  is measured in electron volts.

tain distance toward the anode and cathode, respectively, and then be trapped. This trapping would build up a negative space charge near the anode and a positive space charge near the cathode, eventually neutralizing the electric field in the photoconductor and preventing further drift of photoelectrically excited charges. Thus, under constant illumination, the current would presently drop to zero; this is in fact what happens in photosensitive insulators. Furthermore, under such circumstances, the duration of the photocurrent would be limited, except for the very brief life span of the mobile electrons and holes, to the actual period of illumination.

There are two primary factors which introduce both an enhancement of and a delay in the observed photocurrents in semiconductors: the release of trapped electrons or holes by thermal excitation and the drawing of additional electrons from the cathode and holes from the anode by the space-charge field set up within the semiconductor. The resulting *secondary* currents frequently exceed by a large factor the primary current and greatly complicate the study of the primary processes responsible for photoconduction. Both sources of secondary currents imply a time delay between the excitation by the incident light and the building up of the current. On the one hand, the lifetime of the trapped charges must be added to the time consumed in the drift toward the appropriate electrode; on the other hand, the establishment of equilibrium in the space-charge conditions within the photoconductor, both after the onset of the illumination and after its termination, must be expected to be a gradual process. The second factor must be held responsible for secondary currents which exceed one electron for every light quantum absorbed. In view of the complex origin of the observed photocurrents it is not surprising that a linear relation between photocurrent and illumination is the exception.

A great many substances—in particular sulfides, oxides, and halides, as well as transition elements between the metals and nonmetals—exhibit photoconductivity. Below only a few representatives of this long list—selenium, thallous sulfide, lead sulfide, silicon, and cadmium sulfide—will be considered in greater detail, in view of their proved usefulness in photoconductive cells.

**Properties of Selenium Photoconductive Cells.** Of the several cells to be considered, the selenium cells exhibit the most pronounced time-delay effects, indicating the predominant role played by the secondary currents. The precise characteristics are greatly dependent on processing techniques and cell construction. Figure 10.4 shows the response curve for two different selenium cells to a “square” light pulse. Even for the “hard” cell appreciable secondary current is seen to flow a minute after the illumination has been removed. The photocurrent, how-

ever, is reduced by 50 per cent 0.01 second after the light has been turned off. The alternating current response of a cell designed specifically for sound reproduction is shown in Fig. 10.5. Here, after an initial very rapid decline, the curve reaches a nearly level plateau for a considerable range beyond 1000 cycles per second. The spectral response of selenium photoconductive cells is generally broad with a fairly pronounced maximum near 7000 Angstrom units (Fig. 10.6). As expected,

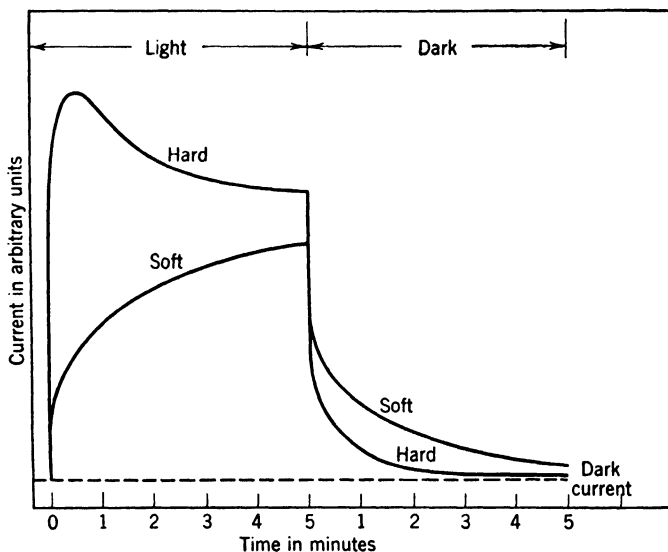


FIG. 10.4. Curves Showing Behavior of Extreme Types of Selenium Bridges with Respect to Rapidity of Response.

the relation between photocurrent and illumination is nonlinear; Fig. 10.7 gives an example. It should be stressed that different selenium cells exhibit response curves deviating greatly from the square-root relationship here represented. That selenium, in spite of the several undesirable characteristics described, has held its place for almost half a century as the most important photoconductive material is to be ascribed to its relatively high absolute sensitivity. A good selenium cell may yield approximately one electron per incident quantum of visible light. The dark resistances of such cells range from about 50,000 ohms to 10 megohms, the corresponding operating voltages from 9 to 500 volts. Considering a cell at the bottom end of the range, a luminous flux of 0.1 lumen may reduce the effective resistance of the cell by a factor of 3.

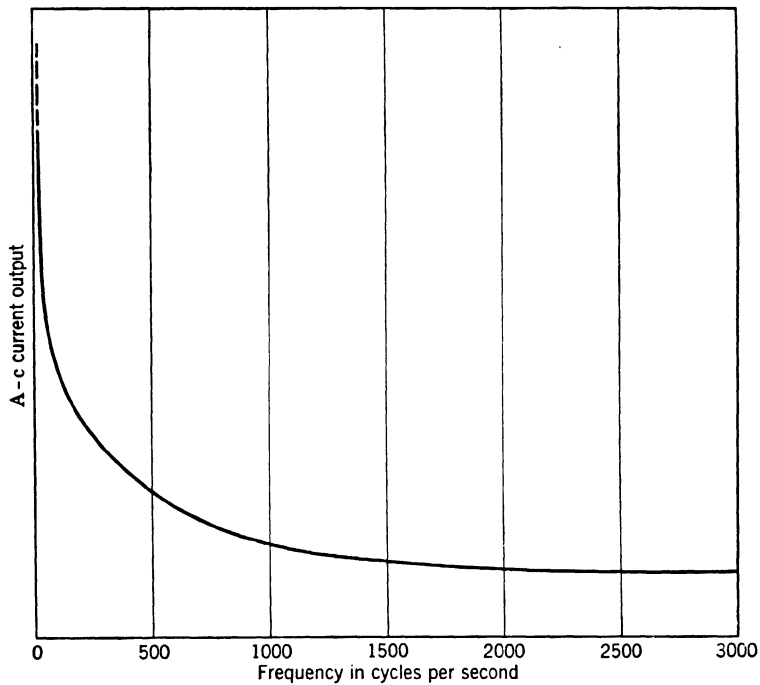


FIG. 10.5. Dynamic Response of a Typical Selenium Bridge.

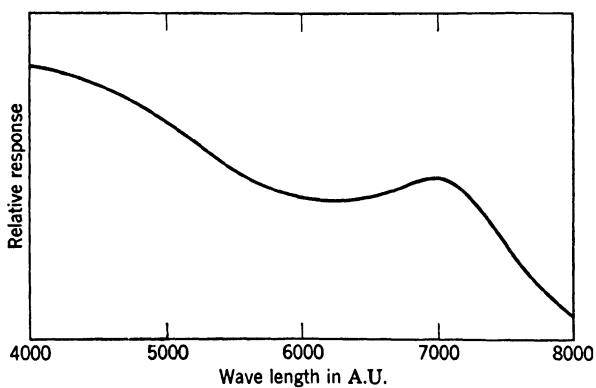


FIG. 10.6. Spectral Response Curve for Selenium Photoconductive Cell.

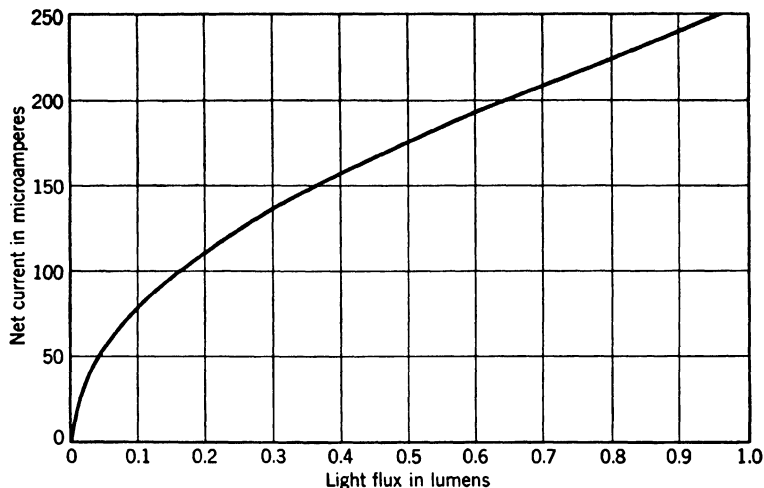


FIG. 10.7. Current-Light Curve for a Typical Selenium Photoconductive Cell.

**The Thallous Sulfide or "Thalofide" Cell.** More recently the selenium cell has been largely displaced by the thallous sulfide or "thalofide" cell, originally discovered by T. W. Case.<sup>7</sup> These cells are superior to selenium cells both in sensitivity and in dynamic response. They have been the subject of careful study,<sup>8</sup> leading to a relatively good understanding of the origin of the photocurrent. The cells employed in this study consisted of evacuated glass envelopes inscribed with a 16-line-per-inch aquadag grid (similar to that shown in Fig. 10.1) on whose surface a film of pure thallous sulfide ( $\text{Tl}_2\text{S}$ ) was deposited by evaporation. The dark gray film was of the order of 5000 Angstrom units in thickness. Then oxygen was introduced at a pressure of the order of a millimeter of mercury or less, depending on the cell volume, and was permitted to react with the thallous sulfide at a temperature of  $250^\circ$  or  $350^\circ$  C for several minutes. The thallous sulfide partly absorbs oxygen, partly reacts with it to form the yellow insulating compound  $\text{Tl}_2\text{SO}_2$ ; concurrently there is an increase in the photoresponse and a decrease in the dark conductance of the cell (Fig. 10.8). The photoresponse is here defined as the ratio of the current increase  $\Delta I$  under illumination to the dark current  $I_0$ , keeping the voltage across the cell constant.

An interpretation of the effect of the oxidation process on the photoconductivity has been given by von Hippel and Rittner.<sup>9</sup> Pure thallous

<sup>7</sup> See reference 4.

<sup>8</sup> See v. Hippel, Chesley, Denmark, Ulin, and Rittner, reference 5, and v. Hippel and Rittner, reference 6.

<sup>9</sup> See reference 6.

sulfide is an excess (*n*-type) semiconductor; electrons and holes freed in the lattice by thermal excitation wander, under the influence of an electric field, toward anode and cathode, respectively, being trapped and released repeatedly on their path; the mobility of the electrons exceeds that of the holes. Absorption of oxygen near the thallium atoms

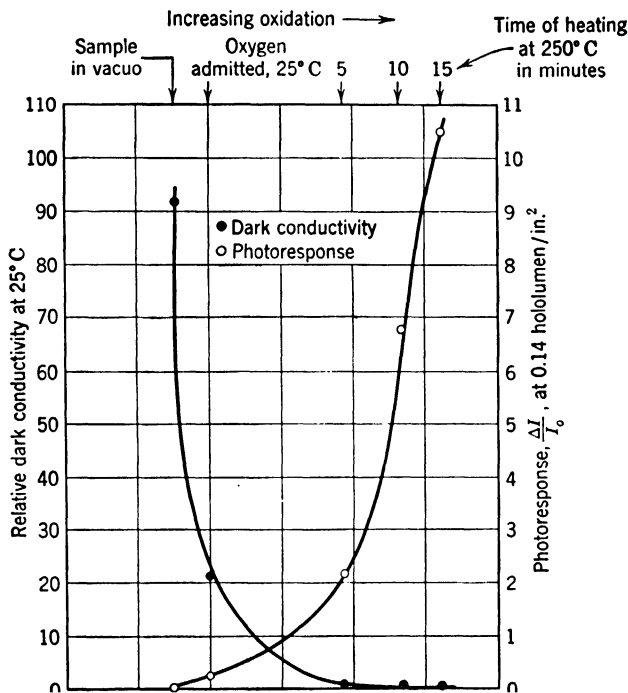


FIG. 10.8. Change of Photoresponse and Dark Conductivity of a Thallous Sulfide Cell with Increasing Oxidation. (v. Hippel, Chesley, Denmark, Ulin, and Rittner, reference 5.) (Courtesy of *Journal of Chemical Physics*.)

of the lattice will have two effects. (1) The oxygen, in view of its high electron affinity, will tend to trap electrons on their path to the anode, causing the hole conductivity to exceed the electron conductivity; oxidized thallous sulfide is a defect (*p*-type) rather than an excess semiconductor. (2) If thallous sulfide is excited by the absorption of a light quantum, the excited electron, instead of presently returning to its normal state, will tend to attach itself to an oxygen atom, forming a relatively stable  $O^-$  ion, while the hole will wander off toward the cathode. The presence of these low-mobility negatively charged centers will neutralize the positive space charge corresponding to a relatively large

current carried by holes, in the same manner as a small positive-ion current in a gas tube may neutralize the space charge of a much larger high-velocity electron current. As a result the semiconductor will, for a given externally applied field, pass a much larger current under illumination than in the dark.

As in the case of the selenium cells, there is a wide and uncontrollable variation in the response characteristics of thallous sulfide cells with

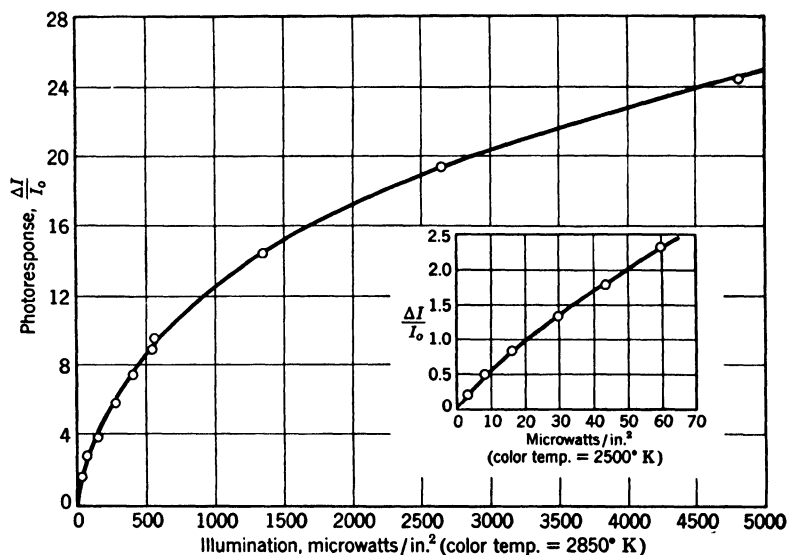


FIG. 10.9. Photoresponse of Thallous Sulfide Cell as Function of Intensity of Radiation. (v. Hippel, Chesley, Denmark, Ulin, and Rittner, reference 5.) (Courtesy of *Journal of Chemical Physics*.)

details of their preparation. Although both the photocurrent and the dark current are linear functions of the applied voltage, the variation of output with illumination is nonlinear (Fig. 10.9). Furthermore, the dynamic response varies greatly from cell to cell (Fig. 10.10). As the temperature increases, the photoresponse decreases (for instance, by a factor of 7 in the range from 27° to 75° C) and the relative dynamic response increases. For example, the time constant (the time in which the response to a flash of light drops to  $1/e = 0.37$  of its initial value) for a particular cell decreases, in the same temperature range, by a factor of the order of 40 (from about  $8 \cdot 10^{-3}$  to  $2 \cdot 10^{-4}$ ). Only the spectral response (Fig. 10.11) is fairly constant, having a cut-off near 13,000 Angstrom units and a maximum in the near infrared, close to 9000 Angstrom units. The quantum yield curves in Fig. 10.11 show that the passage

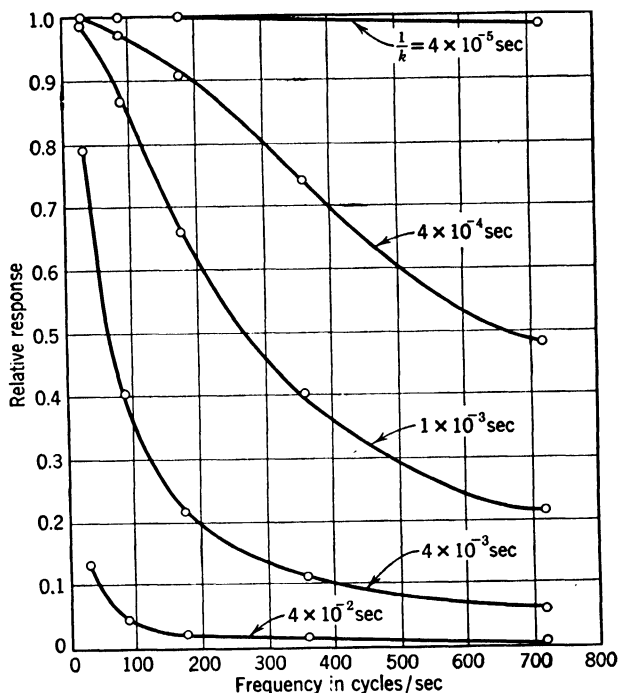


FIG. 10.10. Relative Response as Function of Frequency for Thallous Sulfide Cells with Different Time Constants (Calculated). (v. Hippel and Rittner, reference 6.) (Courtesy of *Journal of Chemical Physics*.)

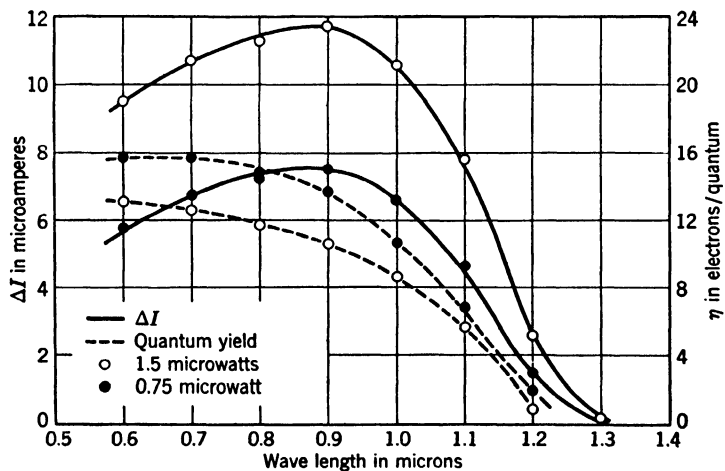


FIG. 10.11. Photocurrent and Quantum Yield as Function of Wave Length for Two Light Intensities (dark resistance 2.5 megohms; voltage 22.5 volts). (v. Hippel, Chesley, Denmark, Ulin, and Rittner, reference 5.) (Courtesy of *Journal of Chemical Physics*.)



of as many as sixteen electronic charges through the semiconductor may result, on the average, from the incidence of a single quantum of radiation. The photocurrent is thus, obviously, primarily a secondary current.

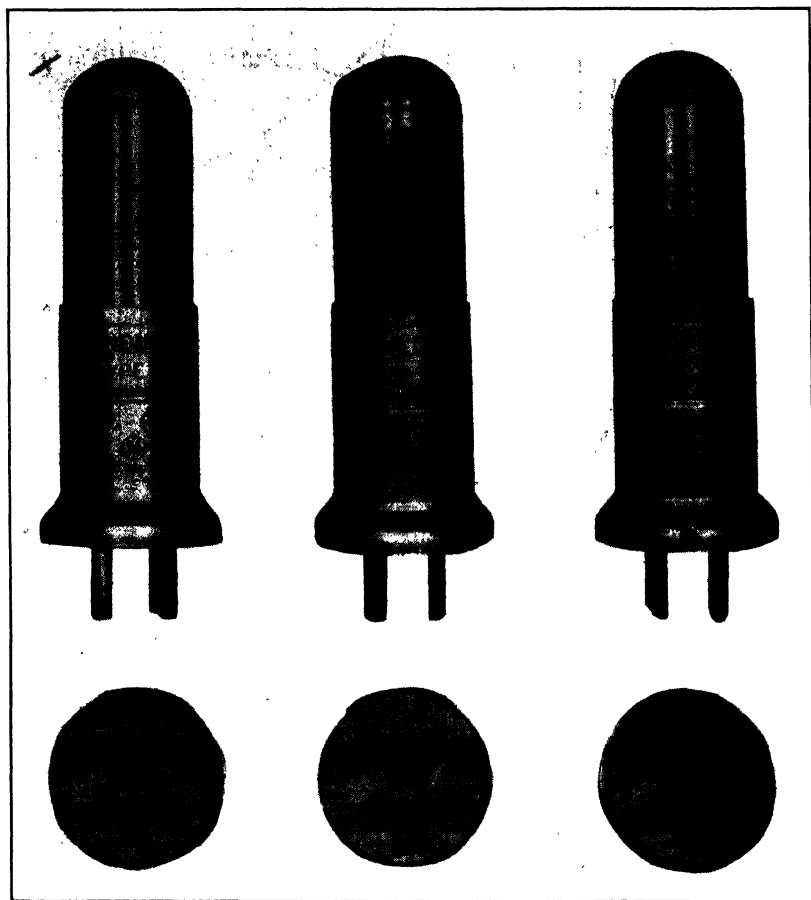


FIG. 10.12. Thallous Sulfide Photoconductive Cell. (Courtesy of Dr. C. W. Hewlett, General Electric Company.)

The development of the thallous sulfide cell into a radiation detector of extraordinary sensitivity has been carried out, primarily, by R. J. Cashman of Northwestern University. Figure 10.12 shows a commercial Cashman cell manufactured by the General Electric Company.<sup>10</sup> The cell responds both to radiation falling on the grid through the portion

<sup>10</sup> See Hewlett, reference 7.

of the envelope on which it is deposited and to that which reaches it through the window opposite.

**The Lead Sulfide Cell.** The fact that natural lead sulfide or galena crystals provided with a point contact at times exhibit photoconductivity was discovered as early as 1901 by the Indian physicist J. G. Bose.<sup>11</sup> However, the recent development of highly sensitive lead sul-

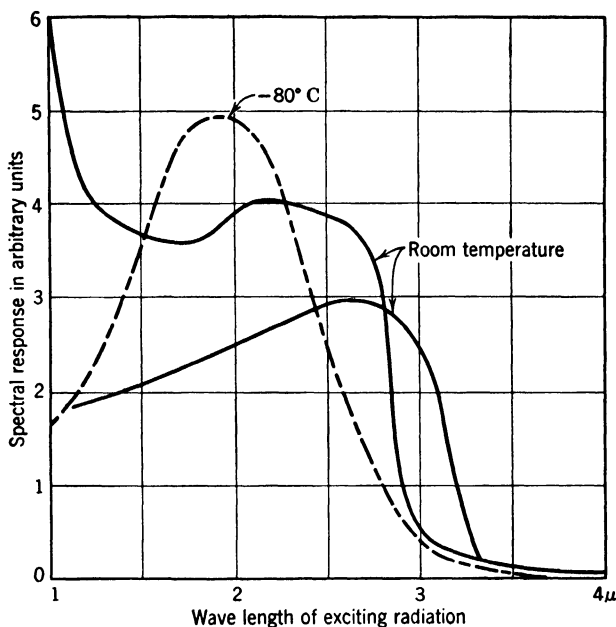


FIG. 10.13. Spectral Response of a Cooled and Two Uncooled Lead Sulfide Photoconductive Cells. (The ordinate scales for the cooled and uncooled cells differ.) (Cashman, reference 9.)

fide cells owes its impetus to the desire of the contesting forces in World War II to employ for signaling purposes the farther infrared, which could not be detected either by the image tube or the thallous sulfide cell.<sup>12</sup> The lead sulfide cells have a maximum sensitivity at a wave length of 2.5 microns and a cut-off near 3.6 microns (Fig. 10.13). They have a dark resistance between 0.1 and 10 megohms, are linear in response over a very great range of luminous flux,<sup>13</sup> and possess current

<sup>11</sup> See reference 8.

<sup>12</sup> See Cashman, reference 9.

<sup>13</sup> Lead sulfide cells have been found linear up to 0.01 hololumen, while, for thallous sulfide cells, the upper limit is about  $10^{-5}$  hololumen. A hololumen is defined as the total radiant flux from a tungsten lamp with a color temperature of 2848° K whose emission in the visible is one lumen.

sensitivities up to about 0.02 microampere per microholumen.<sup>12</sup> If cooled to dry-ice temperature ( $-80^{\circ}\text{C}$ ) they may detect bodies at ambient temperature from which as little as  $10^{-8}$  watt of radiant energy is incident on the cell surface.

Since the specific resistance of lead sulfide is lower than that of thallous sulfide or selenium, grid electrode structures are employed only for the larger-area cells. More commonly the sensitive surface is simply a square or rectangle of lead sulfide deposited between aquadag-strip electrodes;

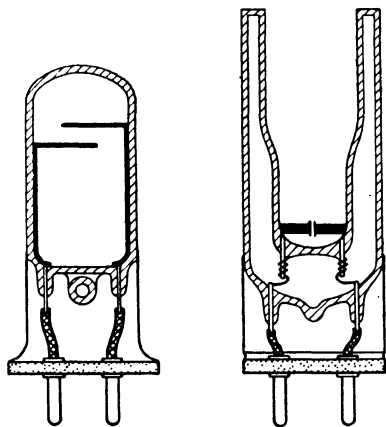


FIG. 10.14. Single-Walled and Double-Walled Lead Sulfide Cells. (Cashman, reference 9.)

its dimensions may be as little as 0.5 by 0.5 square millimeter. Depending on whether the cell is to be employed without or with cooling, the lead sulfide is deposited on the inner wall of a simple tubular envelope or of a double-walled cell (Fig. 10.14).

The lead sulfide deposited may be obtained either by a chemical reaction between lead acetate, thiourea, and sodium hydroxide in dilute solution or by the evaporation within the (hard-glass) cell of highly purified lead sulfide powder. The powder itself may be obtained by passing hydrogen sulfide through a pure, 30-gram-per-liter, lead nitrate solution and collecting the precipitate. In the evaporation process about 10 milligrams of lead sulfide powder are introduced into the cell, which is placed so that the baked-in overlapping electrode strips are at the top. The cell is evacuated and a vacuum leak adjusted so that a pressure of about 0.2 mm Hg of room air is maintained in the cell. Then the lead sulfide powder is evaporated by a broad gas-oxygen flame. The material is finally driven to the region between the electrodes, forming a not entirely opaque, blue-gray, layer. After this the cell is baked in an oven maintained at about  $400^{\circ}\text{C}$  for about 10 minutes. The oven is then removed and, after the cell has cooled down to room temperature, the vacuum leak is closed. As the cell is pumped for 10 to 30 minutes more, the cell resistance increases materially. If the cell is now sealed off it exhibits no further changes in characteristics.

The action of oxygen on the lead sulfide during and after deposition appears essential for the attainment of high sensitivity. Furthermore, maintaining a flow of gas through the tube during preparation seems to

serve the purpose of removing harmful reaction products, in particular sulfur dioxide. The net effect of the reaction of the oxygen with the lead sulfide evidently is to provide impurity centers in the lead sulfide to facilitate the photoconductive process. However, the details of this process in lead sulfide have not been worked out.



Fig. 10.15. Lead Sulfide Cell Suitable for Sound Reproduction. (Courtesy RCA-Victor Division, Lancaster, Pa.)

A lead sulfide cell employed experimentally for sound reproduction is shown in Fig. 10.15. Both the painted aquadag electrodes and some excess lead sulfide powder are clearly visible.

It may be noted that lead selenide has been found to be sensitive to even longer wave-length infrared radiation than lead sulfide. It has not been found possible, however, to prepare lead selenide cells of equal sensitivity.

**The Silicon Cell.**<sup>14</sup> Hard, smooth, high-purity silicon films may be deposited on a ceramic or quartz surface heated (by an internal conductor) to about 1100° C or higher, if the surface is placed in a current of silicon tetrachloride, hydrogen, and nitrogen gases in a glass reaction

<sup>14</sup> See Teal, Fisher, and Treptow, reference 10.

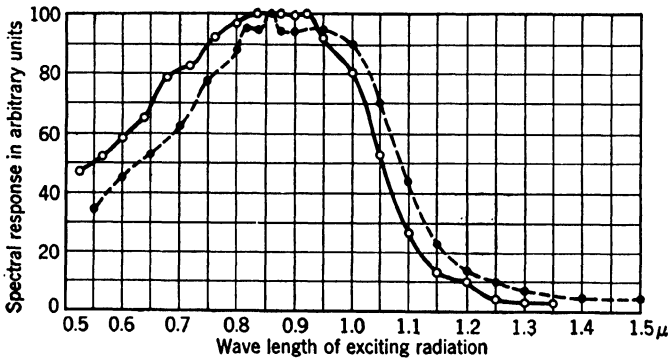


FIG. 10.16. Spectral Response of Two Silicon Photoconductive Cells. (Teal, Fisher, and Treptow, reference 10.) (Courtesy of *Journal of Applied Physics*.)

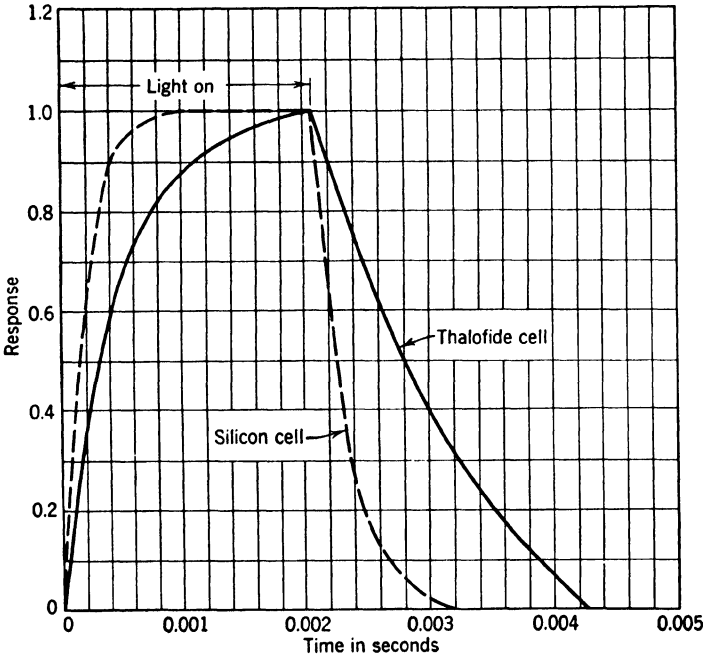


FIG. 10.17. Response of a Silicon and of a Thalofide Cell to a Light Flash. (Teal, Fisher, and Treptow, reference 10.) (Courtesy of *Journal of Applied Physics*.)

chamber provided with a water-cooled jacket. The silicon tetrachloride is reduced by the hydrogen at the hot surface, the silicon being deposited and the hydrogen chloride carried off with the gas stream. If electrodes are painted on the silicon surface with silver paste which is fired at 600° to 800° C, an effective photoconductive cell, intermediate in sensitivity between the thallos sulfide and the selenium cells, results. The unit may be either in the form of a rod, 0.095 inch in diameter and 0.75 inch long, or of a plate with a surface area of several square inches. The film thickness of a typical cell is 5 microns. The spectral response (Fig. 10.16) has a maximum near 9000 Angstrom units and decreases more sharply toward shorter wave lengths than either the selenium or the thallos sulfide cell. Since the variation of the conductivity with temperature for *pure* silicon indicates a separation of the filled and unfilled energy bands equal to 1.12 electron volts (corresponding to a wave length of 11,000 A.U.) the response curve shown supports the hypothesis that the photoconductive effect results from the raising of electrons from the filled band of the pure lattice to the empty conduction band. The relative dynamic response of typical silicon and thalofide cells is illustrated by Fig. 10.17, which shows the current induced by a light flash of constant intensity. The near-linearity of the relation between current and illumination makes a silicon cell much less sensitive to background illumination. A final advantage is its remarkable stability, which permits it to be heated to red heat by an oxygen-gas flame or to be exposed to strong sunlight without permanent effect on its response.

**Photoconductive Effect in Cadmium Sulfide.**<sup>15</sup> Ribbon-shaped crystals of cadmium sulfide, exhibiting a strong photoconductive effect, may be prepared in the following manner (Fig. 10.18). Cadmium metal in a

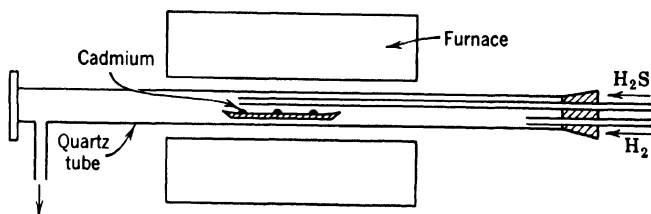


FIG. 10.18. Method of Preparing Photoconductive Cadmium Sulfide Crystals. (Frerichs, reference 11.) (Courtesy of *Physical Review*.)

porcelain boat placed in a quartz tube is heated in a slow current of hydrogen to 800° to 1000° C. The hydrogen gas brings the cadmium vapor into contact with a stream of hydrogen sulfide, with which it

<sup>15</sup> See Frerichs, reference 11.

reacts to form cadmium sulfide crystals on the walls of the reaction tube as the tube is cooled gradually. The yellow or yellowish-green crystals may be of the order of a centimeter in length, a millimeter in width, and a tenth of a millimeter in thickness. Their optical absorption (Fig. 10.19) begins just below 6000 Angstrom units and becomes virtually complete, even for crystals only 0.005 millimeter thick, for wave lengths below 5200 Angstrom units. Just above the latter wave length the pho-

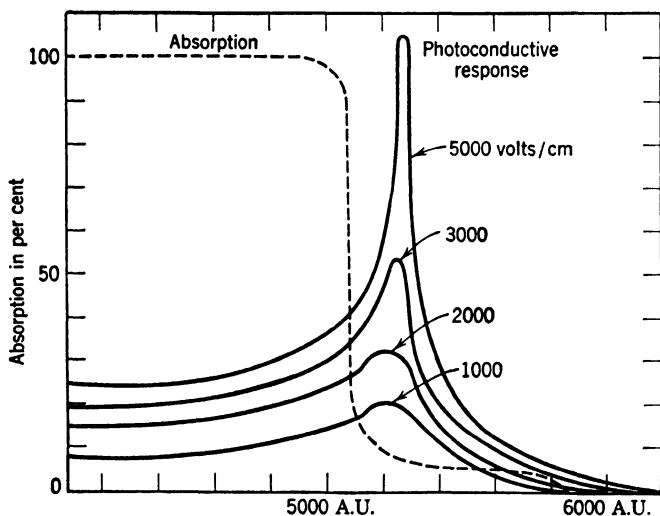


FIG. 10.19. Absorption of Cadmium Sulfide Crystals 0.1 mm in Thickness and Relative Photoconductive Response for Various Field Strengths. (Frerichs, reference 11.) (Courtesy of *Physical Review*.)

toconductivity has a maximum which increases rapidly with the strength of the applied field. Below 5000 Angstrom units the photoconductivity remains practically constant down to the shortest wave lengths for which it has been measured (2500 A.U.). While illumination with infrared radiation tends to quench the photoconductivity above 5200 Angstrom units, it has no effect on the conductivity induced by the shorter wave lengths. Furthermore, fatigue effects are much more pronounced above 5200 Angstrom units than below this absorption threshold. All this suggests that the short-wave-length photoconductivity is the result of excitations from the filled lattice band to the conduction band of the lattice, whereas that at the longer wave lengths results from the excitation of impurity centers.

The measured photocurrents are, in cadmium sulfide cells, of the same order as for thallous sulfide cells; at the same time, their dark resistance

is very much higher. A strip of cadmium sulfide 0.2 millimeter wide, 0.1 millimeter thick, and 1 centimeter long, between aluminum electrodes evaporated on the crystal on either side, may have a resistance of  $10^8$  ohms. The same cells are also remarkably sensitive detectors of x-rays and corpuscular radiation. A transport of  $10^6$  electrons has been observed for a single x-ray quantum, one of  $10^8$  to  $10^{10}$  electrons for a single alpha or beta particle.

## REFERENCES

1. W. SMITH, "Effect of light on selenium during the passage of an electric current," *Am. J. Sci.*, Vol. 5, p. 301, 1873.
2. J. J. BERZELIUS, "On selenium crystals and the preparation of selenium," *Ann. Physik*, Vol. 7, pp. 242-243, 1826.
3. J. C. SLATER, "Electronic structure of metals," *Revs. Modern Phys.*, Vol. 6, pp. 209-280, 1934.
4. T. W. CASE, "Thalofide cell—a new photoelectric substance," *Phys. Rev.*, Vol. 15, pp. 289-292, 1920.
5. A. VON HIPPEL, F. G. CHESLEY, H. S. DENMARK, P. B. ULIN, and E. S. RITTNER, "Thallous sulfide photoconductive cells. I. Experimental investigation," *J. Chem. Phys.*, Vol. 14, pp. 355-369, 1946.
6. A. VON HIPPEL and E. S. RITTNER, "Thallous sulfide photoconductive cells. II. Theoretical discussion," *J. Chem. Phys.*, Vol. 14, pp. 370-378, 1946.
7. C. W. HEWLETT, "High-sensitivity photoconductive cell," *General Elec. Rev.*, Vol. 50, pp. 22-25, April, 1947.
8. J. G. BOSE, U. S. Patent 755,840 (1901).
9. R. J. CASHMAN, "Development of sensitive lead sulfide photoconductive cells for detection of intermediate infra-red radiation," *O.S.R.D. Report* 5998, Oct. 31, 1945.
10. G. K. TEAL, J. R. FISHER, and A. W. TREPTOW, "New bridge photocell employing a photoconductive effect in silicon. Some properties of high-purity silicon," *J. Applied Phys.*, Vol. 17, pp. 879-886, 1946.
11. R. FRERICHs, "The photo-conductivity of 'incomplete phosphors,'" *Phys. Rev.*, Vol. 72, pp. 594-601, 1947.



## Chapter 11

# PHOTOVOLTAIC CELLS

The effect of light on a photoconductive cell can be made evident on a current meter only if a voltage supply is inserted in the cell circuit. The efficient utilization of the photoemissive effect, also, demands the provision of an external electromotive force. Photovoltaic cells, on the other hand, are self-contained current and voltage generators, setting up a potential difference between their terminals when exposed to light. They may conveniently be divided into wet and dry cells. Wet photovoltaic cells consist of two electrodes immersed in an electrolyte, dry photovoltaic cells of a semiconducting layer between two metal electrodes. Because in recent years the dry "photoelements" have almost completely displaced the less convenient and less stable wet cells, the wet cells will be touched on only briefly.

**Wet Photovoltaic Cells.** The fact that an electromotive force is generated when light falls on one of a pair of electrodes immersed in an electrolyte was discovered by E. Becquerel<sup>1</sup> over a hundred years ago. With pure metal electrodes the effect is very small. If, however, the illuminated electrode is coated with a semiconductor, such as copper oxide or a silver halide, the electromotive force generated (for open circuit) may be of the order of 0.1 volt, and the current sensitivity (for short circuit), 150 microamperes per lumen.<sup>2</sup> In both cases the passage of photocurrent is frequently accompanied by chemical changes at the electrode surface which give rise to fatigue effects and complicate the observed phenomena. It is thus not surprising that two conflicting points of view have arisen on the origin of the Becquerel effect. One group has taken the stand that the primary process is the photoelectric emission of electrons from the electrode into the electrolyte; the other group maintains that the light initiates a photochemical reaction which changes the surface character of the illuminated electrode in such a manner that the potential difference of the two cell electrodes is altered. Although the first interpretation is in better harmony with the observed

<sup>1</sup> See reference 1.

<sup>2</sup> See Fink and Alpern, reference 2.

behavior of the most effective of the wet photovoltaic cells, neither picture explains all observations on all cells.

Cells consisting of metal electrodes immersed in a fluorescent electrolyte also exhibit relatively large photovoltaic effects with linear current response. Open-circuit voltages of the order of 0.25 volt are observed, the illuminated electrode becoming negative with respect to the unilluminated electrode. Here the electromotive force generated by the light is ascribed not to photoemission from the illuminated electrode, but, instead, to the photoionization of the fluorescent molecules in the adjoining portions of the electrolyte.<sup>3</sup>

**The Cuprous Oxide Barrier-Layer Cell.** If a disk of copper is heated in air or oxygen at a temperature of 1000° to 1040° C, a layer of red cu-

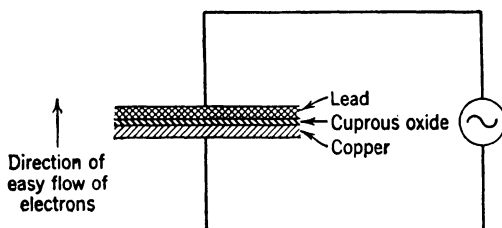


FIG. 11.1. The Cuprous Oxide Rectifier.

prous oxide ( $\text{Cu}_2\text{O}$ ) is formed on its surface, coated by a film of black cupric oxide ( $\text{CuO}$ ). Baking for 5 minutes at 1000° C forms a cuprous oxide layer approximately 0.1 millimeter thick. If, after cooling, the black cupric oxide is removed by grinding or dissolved with a sodium cyanide solution, and a lead electrode is pressed on the exposed cuprous oxide, an effective current rectifier is obtained. If the copper electrode is made a few volts negative with respect to the lead electrode, a current of an ampere may flow through a cell with a surface area of the order of a square inch; if the polarity is reversed, the current is reduced to a fraction of a milliamper (Fig. 11.1).

L. O. Grondahl,<sup>4</sup> who discovered this rectifying action in 1920, observed, with P. H. Geiger, a few years later that if the opaque lead electrode was replaced by a loose spiral of lead wire, illumination of the cuprous oxide through the interstices caused a current to flow in an external circuit without an auxiliary source of electromotive force. This photovoltaic effect was rediscovered, separately, by B. Lange<sup>5</sup> and

<sup>3</sup> See Lowry, reference 3.

<sup>4</sup> See reference 4.

<sup>5</sup> See references 5 and 6.

W. Schottky,<sup>6</sup> who with their collaborators made a careful analysis of its properties and developed the cells to a point of practical usefulness.

Lange's immediate contribution was the employment of a transparent contact electrode, usually of gold or silver, sputtered on the cuprous oxide surface. The more intimate contact between top electrode and oxide layer and the reduced obstruction of the incident light attained in this manner greatly increased the current sensitivity of the cell. Schottky, on the other hand, established that both the photoelectrons originated and the rectifying action took place in a thin insulating layer at the junction of the cuprous oxide and the mother copper.<sup>6</sup> He named

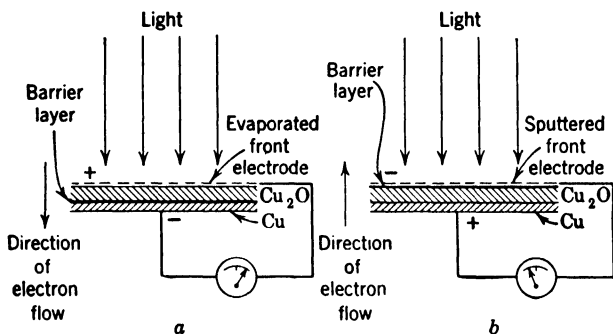


FIG. 11.2. Cuprous Oxide Back-Wall (a) and Front-Wall (b) Cells.

this layer the *barrier layer* (*Sperrschicht*) and identified it as pure cuprous oxide, free from excess oxygen which makes the remainder of the cuprous oxide a (defect) semiconductor. Subsequent measurements showed that the thickness of the barrier layer was of the order of 1 micron ( $10^{-6}$  meter). Under illumination the photoelectrons travel from the cuprous oxide to the copper, that is, in the high-resistance direction.

Since, in the cells described so far, the barrier layer lies at the boundary between the cuprous oxide layer and the mother copper, remote from the point of incidence of the light, Schottky named these cells *back-wall cells* (Fig. 11.2a). Lange and Duhme and Schottky<sup>7</sup> showed that it is also possible to produce *front-wall cells* (Fig. 11.2b), in which the photoelectric and rectifying action takes place primarily at the boundary between the top electrode and the cuprous oxide. The direction of the current flow is here, of course, opposite to that for the back-wall cells. The front-wall cells possess the advantage that the light is not absorbed by the ineffective cuprous oxide layer before giving rise to the barrier-

<sup>6</sup> See reference 7. It will be seen below that, contrary to earlier views, the "barrier layer" need not differ chemically from the remainder of the semiconductor.

<sup>7</sup> See reference 8.

layer photocurrent. Consequently its current sensitivity is much greater than that of the back-wall cell. Furthermore, the spectral response, which for the back-wall cell extends from the long-wave threshold of 14,000 Angstrom units to the yellow (5700 A.U.) with a maximum near 6300 Angstrom units, is shifted largely toward shorter wave lengths, the short-wave cut-off being determined by the absorption of the top electrode (Fig. 11.3).

Front-wall cells may be produced by chemically or electrolytically reducing the surface layer of the cuprous oxide to form the (copper) top

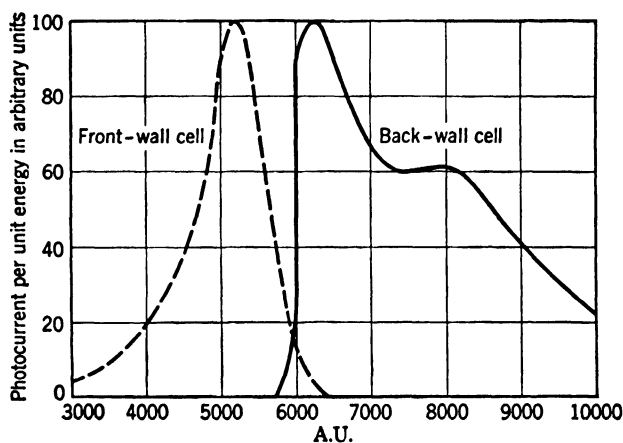


FIG. 11.3. Spectral Response of Cuprous Oxide Back-Wall and Front-Wall Cells. (Lange, reference 6.) (Courtesy of Reinhold Publishing Corporation.)

electrode or by sputtering the top electrode material (gold, silver, platinum, or nickel) onto the cleaned cuprous oxide surface in a reducing atmosphere. An effective method consists in quenching the disks oxidized at a temperature near 1000° C in a bath of mineral oil or formaldehyde. The essential feature of these methods is that cupric oxide and excess oxygen are completely removed from the surface. Depositing the top electrode by evaporation in vacuum or spraying it on in the form of a grid by the Shoup process does not accomplish this result and, generally, leads to back-wall cells.

**Origin of Photocurrent.** The mechanism of the copper-cuprous oxide barrier-layer cell has been the subject of extensive theoretical investigation. The following picture, based on the work of Mott<sup>8</sup> and, particularly, Schottky,<sup>9</sup> is in agreement with the known experimental findings.

<sup>8</sup> See reference 9.

<sup>9</sup> See reference 10.

Cuprous oxide containing excess oxygen is a defect conductor, that is, conducts current by virtue of holes present in its uppermost filled energy band. These holes are formed when electrons are thermally excited from this band, filling impurity levels provided by the excess oxygen atoms. The transfer of an electron from the filled band to such an impurity level requires at least 0.3 electron volt. A considerably higher energy—0.7 electron volt, approximating the threshold for the photovoltaic effect (14,000 A.U. or 0.9 electron volt)—is needed to raise electrons from the filled band to the empty conduction band.

Imagine now that the cuprous oxide is brought into contact with the mother metal. Since the work function of the cuprous oxide is considerably higher than that of the copper, electrons from the metal will fill the nearest impurity levels, building up a negative space charge, which in turn will induce an equal positive space charge at the surface of the metal. Hence a field is established across the insulating layer, produced where the impurity levels are filled by electrons, as shown by the potential diagram in Fig. 11.4.<sup>10</sup> The field—and the thickness of the barrier layer—will take on such a value that the top of the electron distribution in the metal coincides with a level midway between the top of the filled band and the empty impurity levels in the interior of the semiconductor; at the metal-semiconductor interface the relative positions of the levels are fixed by the difference in the values of the two work functions. Under these conditions there is equilibrium between the drift of charges in the two directions.

If, now, electrons are raised by photoexcitation from the filled band to the empty conduction band in the semiconductor, they will drop quickly into one of the many empty impurity levels and not contribute to conduction. On the other hand, if the excitation takes place in the barrier layer, their lifetime will be relatively long, since there are no empty levels to drop into. The field across the barrier layer will accelerate the electrons toward the metal, so that they give rise to a photocurrent in the observed direction. According to the theory given, the open-circuit potential should approach, for strong illumination, the difference in the work functions of metal and semiconductor or—on the

<sup>10</sup> It may be noted that the filling of the impurity levels near the surface, that is, the creation of the barrier layer, may take place even in the absence of the metal, by the transfer of electrons from localized surface states on the semiconductor surface to the acceptor levels until the top of the electron distribution of the surface states coincides with the Fermi limit in the interior (Bardeen, reference 11). The picture presented in Fig. 11.4 applies also in this case. For a sufficient concentration of surface states the rectification properties of a contact cease to depend on the work function of the contact metal. Schottky has shown that this condition is not generally realized; in particular, it does not apply for selenium.

surface-level picture—half the difference of the excitation potential from the filled band to the conduction band and that from the filled band to the impurity levels. The observed maximum open-circuit potential of about 0.2 volt is of the right order of magnitude. For this voltage difference the field across the surface layer of the semiconductor, and hence the barrier layer itself, vanish, and photoelectrons are no

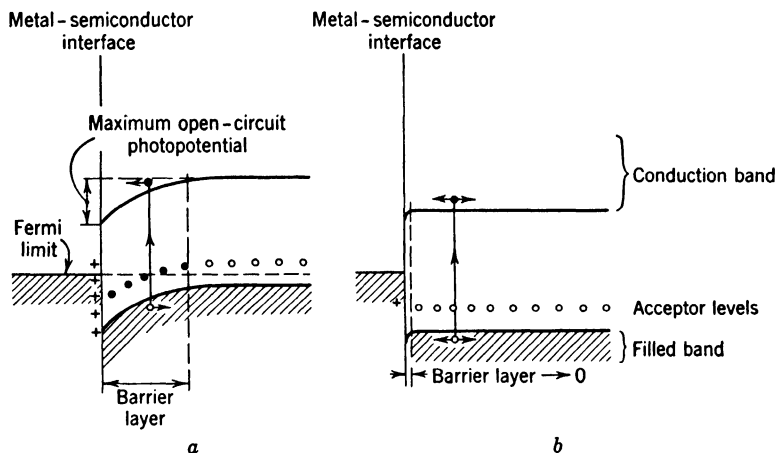


FIG. 11.4. Origin of Photovoltaic Effect in Copper-Cuprous Oxide Cell. (a) Equilibrium condition for low illumination or short-circuited electrodes: Electrons fill acceptor levels to such depth that field across resulting barrier layer causes top of occupied band in metal to coincide with average between top of filled band and acceptor levels in interior of semiconductor. (b) Equilibrium condition for high illumination and open circuit: Photoelectrons charge metal, and electrons in acceptor levels occupy vacancies created by photoexcitation in filled band so that barrier layer shrinks and field accelerating photoelectrons toward metal vanishes.

longer accelerated toward the metal. For low light intensities the open-circuit photopotential is equal to the product of the primary photocurrent and the resistance of the barrier layer in the low-impedance or flow direction. Typical voltage sensitivities are  $25 \cdot 10^{-6}$  volt per lux for a front-wall cell and  $15 \cdot 10^{-6}$  volt per lux for a back-wall cell. The quantum yields of copper oxide front-wall cells of favorable construction are of the order of 25 per cent.

**The Selenium Barrier-Layer Cell.** The cuprous oxide cell is neither the only dry photovoltaic cell nor the first to be discovered. Photovoltaic effects had been observed before with natural silver sulfide, zinc sulfide, molybdenum sulfide, lead sulfide, and a number of other materials. The effect in selenium was discovered by Adams and Day<sup>11</sup> as early as

<sup>11</sup> See reference 12.

1876, shortly after the finding of the photoconductive properties of selenium. Fritts,<sup>12</sup> in New York, prepared, in 1884, sensitive selenium barrier-layer cells which, in many particulars, resembled modern types and received the favorable attention of Werner Siemens. Nevertheless, the practical application of selenium photoelements—as they are at times called to distinguish them from selenium photoconductive cells—was delayed until their rediscovery by Lange<sup>13</sup> and Bergmann<sup>14</sup> in 1930 and 1931, respectively.

The methods of preparing selenium barrier-layer cells are described mainly in the patent literature. The basic process consists of melting the selenium on an iron base, cleaned and roughened by sandblasting,

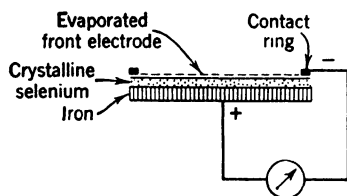


FIG. 11.5. The Selenium Barrier-Layer Photocell.

at a temperature of about 175° C, and subsequently annealing the layer at 80° C to return the selenium to its crystalline modification. The addition of small amounts (about 2 per cent) of thorium, zirconium, or cerium to the selenium is found to increase both the rectifying action and the photocurrents obtained from the resulting cell.<sup>15</sup> The top electrode may be applied by evaporation, sputtering, or spraying; the effect of the material of the top electrode on the cell characteristic is found to be negligible. Selenium barrier-layer cells are invariably front-wall cells (Fig. 11.5). Like cuprous oxide, selenium is a defect semiconductor; the mechanism of the photovoltaic effect in the two cells is probably closely analogous.<sup>16</sup>

As compared with the cuprous oxide cells, the selenium cells are less sensitive to temperature differences and more stable in their response over long periods of time. For this reason practically all barrier-layer cells on the market at the present time are selenium cells. Their spectral response has a maximum close to the point of maximum sensitivity of the human eye and differs but little from cell to cell. Relative response curves for various cells of American manufacture are plotted in Fig. 11.6. Several firms supply visual correction filters for their cells. Thus Weston Photronic cells provided with Viscor filters match the response of the average human eye almost perfectly, while retaining 40 per cent of their sensitivity without filter (Fig. 11.7).

<sup>12</sup> See reference 13.

<sup>13</sup> See Lange and Eitel, reference 14.

<sup>14</sup> See reference 15.

<sup>15</sup> See Fleischer and Teichmann, reference 16.

<sup>16</sup> See Schottky, reference 10.

Electrically a barrier-layer cell can conveniently be represented, as shown in Fig. 11.8, as a current generator, shunted by the capacity  $C$  and the inner resistance  $R_i$ , in series with a small resistance  $R_s$ . If the

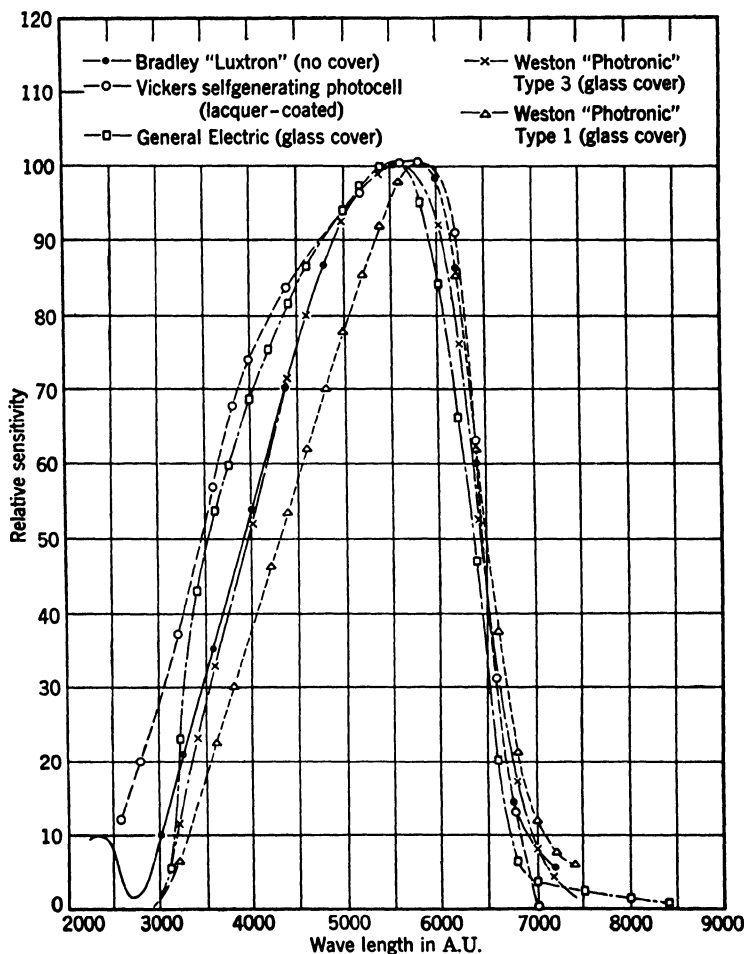


FIG. 11.6. Spectral Response of Various Selenium Barrier-Layer Cells of American Manufacture. (Data supplied by manufacturers.)

primary photoelectric current is  $i_p$  and the load resistance is  $R$ , the current through the latter becomes simply

$$i = \frac{i_p R_i}{R_i + R_s + R} \quad (11.1)$$



For the sake of orientation it may be noted that the series resistance,  $R_s$ , which is almost entirely due to the top electrode, is, in the case of the Weston Photronic cells, about 50 ohms. The capacity of the cell,

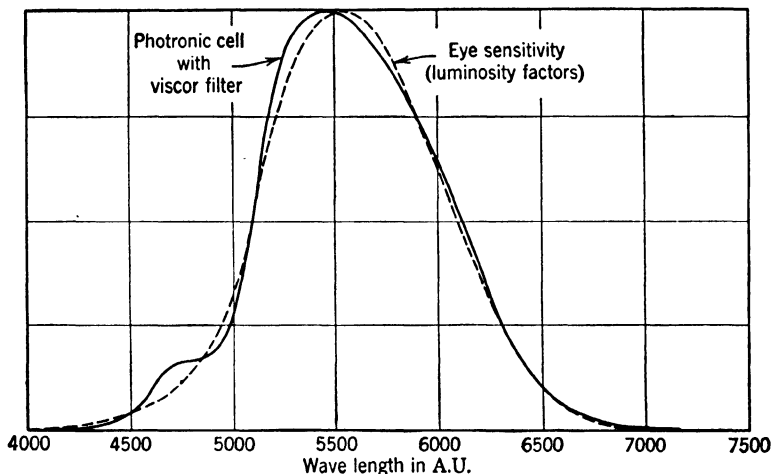


FIG. 11.7. Comparison of Response of Weston Type 3 Photronic Cell with "Viscor" Filter with Visual Sensitivity Curve of Human Eye. (Courtesy of Weston Electrical Instrument Corporation.)

corresponding to the capacity across the very thin barrier layer, is quite large. For a cell of normal size (1 to 2 square inches) it generally is a few tenths of a microfarad. The approximate capacity value for Weston Photronic cells (cell area: 1.7 square inches) is 0.5 microfarad.

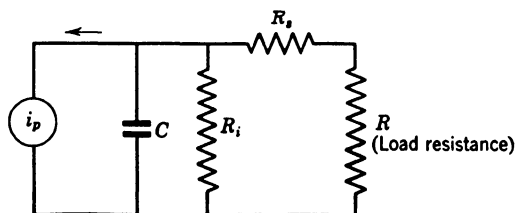


FIG. 11.8. Equivalent Circuit of a Barrier-Layer Cell.

The usefulness of formula 11.1 is reduced by the fact that the internal resistance  $R_i$  is a function of the potential across the cell and, hence, both of the intensity of illumination and the magnitude of the load resistance. Its variation for a Weston cell is shown in Fig. 11.9. The

illumination in foot-candles (1 foot-candle = 10.8 lux) is plotted as abscissa. The two other cell parameters of interest are the open-circuit potential (Fig. 11.10) and the current sensitivity. The open-circuit potential of a selenium cell is highly nonlinear and rises to values of the

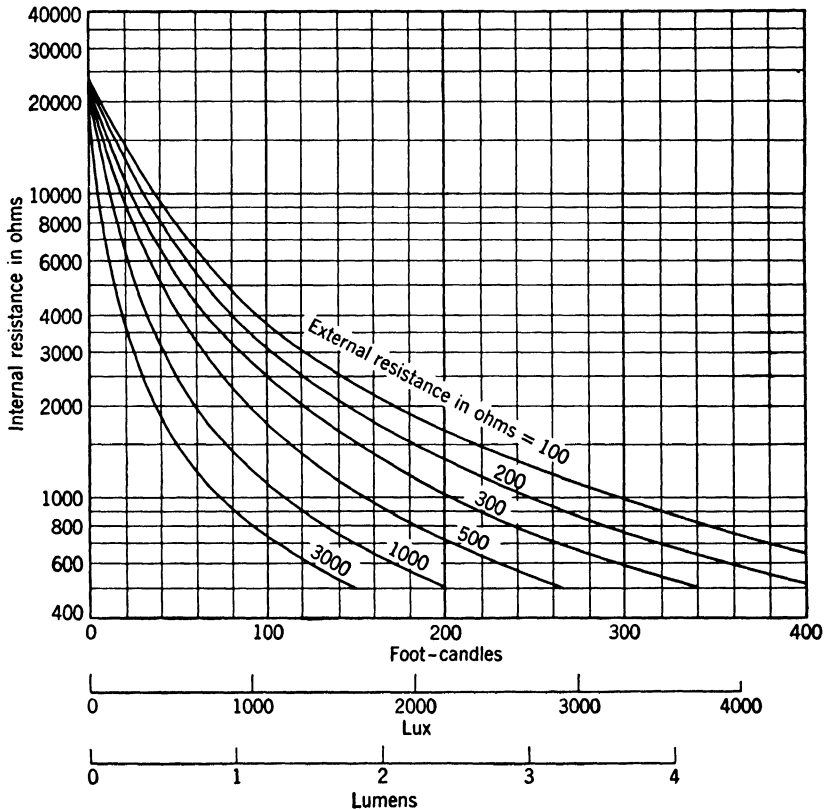


FIG. 11.9. Variation of Internal Resistance of Selenium Cell with Illumination and Load Resistance. Weston Photronic Cell, Type 3. (Courtesy of Weston Electrical Instrument Corporation.)

order of 0.6 volt at very high illuminations. It should be noted that, while the short-circuit current is a practically linear function of the total light flux incident on the cell surface, the open-circuit potential depends on the illumination, or flux per unit area.

It follows from Eq. 11.1 that, for finite values of the load resistance  $R$ , the variation of current becomes increasingly nonlinear as the internal cell resistance  $R_i$  decreases. At the same time, there is a negative cor-

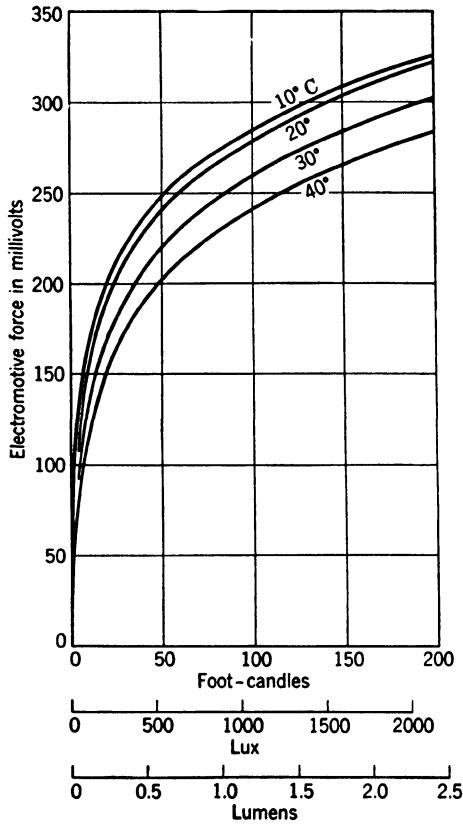


FIG. 11.10. Open-Circuit Potential of a Selenium Cell as Function of Illumination and Temperature. Weston Photronic Cell, Type 3GB. (Courtesy of Weston Electrical Instrument Corporation.)

relation between the current sensitivity of the cell and its internal resistance. It follows that the characteristics for the more sensitive cells are less linear (in particular for large values of the load resistance  $R$ ) than those for less sensitive cells. Figure 11.11, showing the current varia-

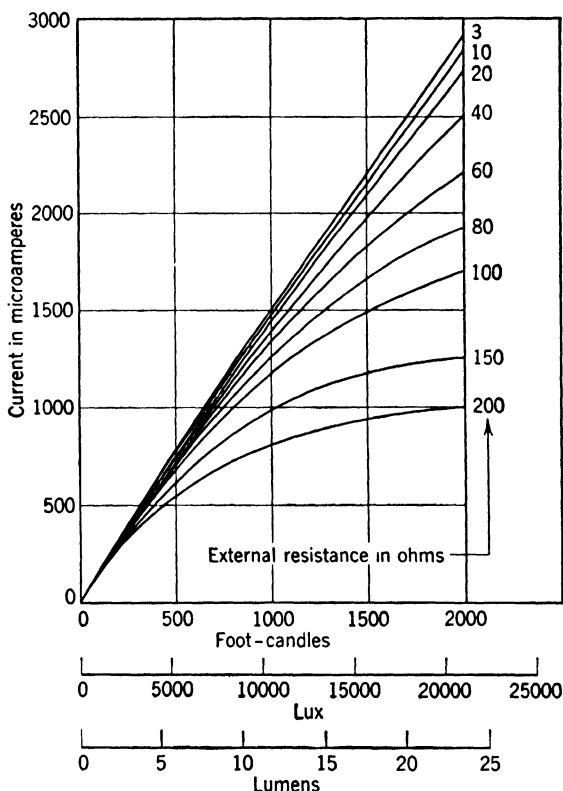


FIG. 11.11A. Photocurrent Characteristics of Selenium Barrier-Layer Cells. Weston Photronic Cell for High-Illumination Measurements. (Courtesy of Weston Electrical Instrument Corporation.)

tion for different values of the external resistance for two Weston Photronic and a Bradley Luxtron cell, in increasing order of sensitivity, illustrates this relationship. The characteristics of General Electric and Vickers cells are comparable with those of the two more sensitive cells shown here. It should be stressed that current sensitivity and other properties of cells of a given type vary considerably from cell to cell; the curves shown are merely representative.

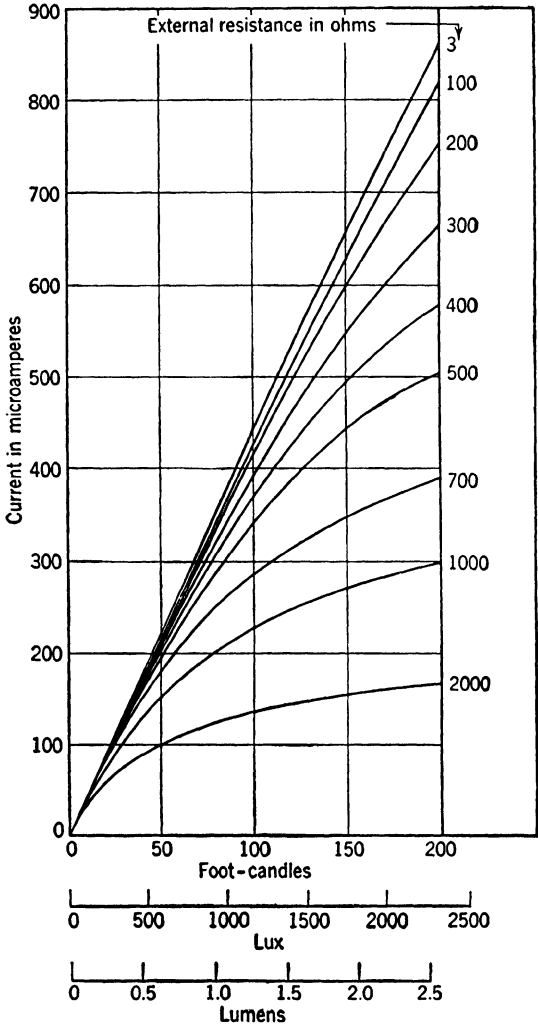


FIG. 11.11B. Photocurrent Characteristics of Selenium Barrier-Layer Cells. Standard Weston Photronic Cell Type 3RR. (Courtesy of Weston Electrical Instrument Corporation.)

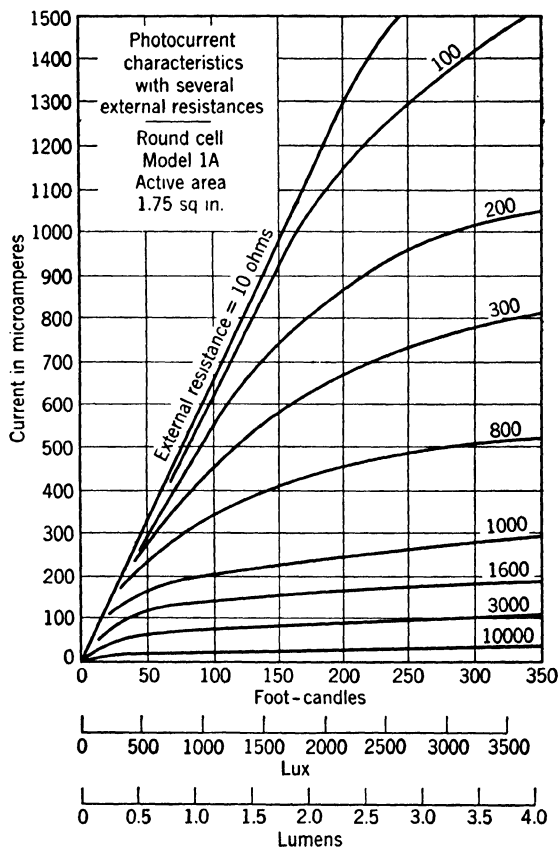


FIG. 11.11C. Photocurrent Characteristics of Selenium Barrier-Layer Cells. Bradley Luxtron Cell. (Courtesy of Bradley Laboratories, Inc.)

**Power Conversion by Barrier-Layer Cells.** The power output of a barrier-layer cell is obtained by multiplying the square of the output current  $i$ , as given by Eq. 11.1, by the load resistance  $R$ . If the internal resistance  $R_i$  were constant and  $R_s$  negligible, the power output would be a maximum, for a given primary current  $i_p$ , if the load resistance  $R$  were made equal to the internal resistance. The dependence of the internal resistance on the load resistance has the effect of making the optimum load resistance more nearly equal to two-thirds the internal resistance.<sup>17</sup> Figure 11.12 indicates both the variation of the optimum load resistance and the corresponding power output of a type 3 Photronic cell as function of the illumination. It is seen that the efficiency

<sup>17</sup> See Wood, reference 17.

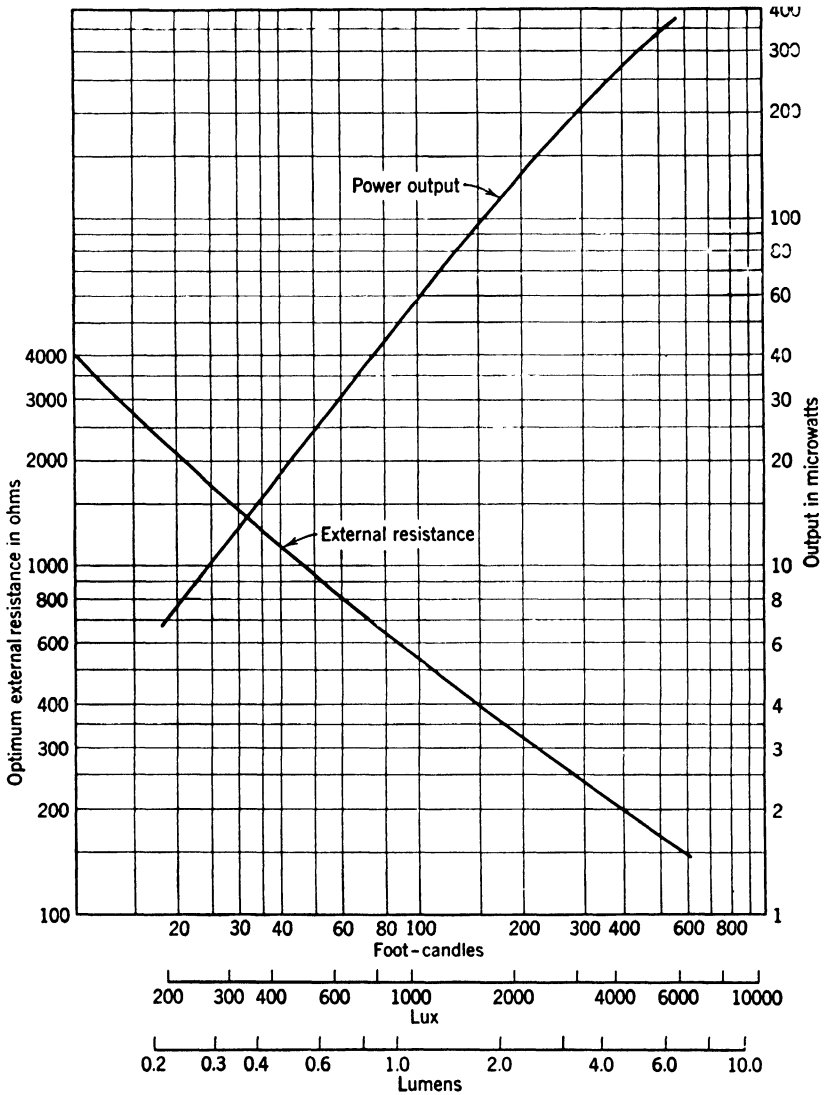


FIG. 11.12. Variation of Optimum Load Resistance and Corresponding Power Output with Illumination for Weston Photronic Cell, Type 3RR. (Data supplied by Weston Electrical Instrument Corporation.)

increases slightly, within the range covered, with the illumination. Taking the cell area to be 1.7 square inches, the efficiency at 500 foot-candles illumination with  $2700^{\circ}\text{K}$  light is 58 microwatts per lumen. If all the light is concentrated at the point of greatest sensitivity of both the cell and the eye (5550 A.U.) the efficiency of a highly sensitive selenium cell becomes, according to Weston, 38 microwatts per lumen or 2.6 per cent. The barrier layer cell thus constitutes a rather inefficient means of converting light into electrical energy.

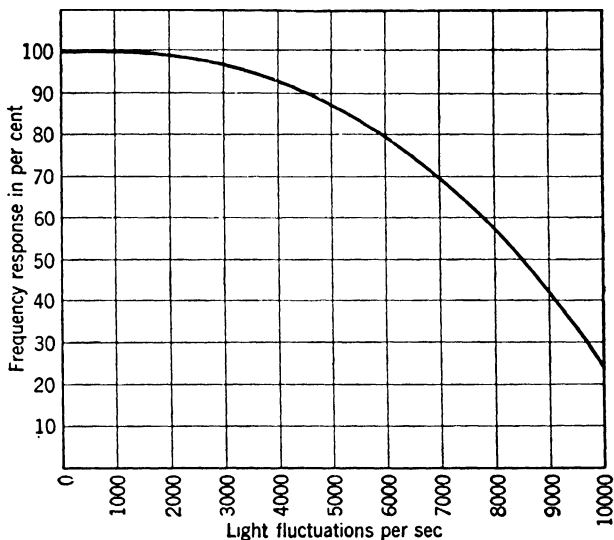


FIG. 11.13. Dynamic Response of an R10 Vickers Selenium Cell. (Courtesy of Vickers Electric Division, Vickers, Inc.)

**Dynamic Response; Fatigue and Temperature Effects.** The response of the selenium and cuprous oxide barrier-layer cells is practically instantaneous. The magnitude of the output current, however, drops off fairly rapidly for light signals interrupted at a frequency of a few thousand cycles per second. This effect is shown, for a Vickers selenium cell, in Fig. 11.13. The decline in output with increasing frequency arises from the high capacity of the cells and can hence be compensated by suitable external circuit elements. The measurement on which Fig. 11.13 is based was made with an external resistance of 50 ohms and can be interpreted as the result of a cell capacity of approximately 0.5 microfarad and a series resistance  $R_s$  of the order of 50 ohms. Cuprous oxide cells show a better dynamic response since their capacity is appreciably smaller.



Selenium barrier-layer cells exhibit temporary fatigue on exposure to light as illustrated by Fig. 11.14. The magnitude of this fatigue increases in general fairly rapidly with the intensity of illumination. Temporary fatigue varies greatly from cell to cell and with the magnitude of the external resistance, eventually even reversing sign. For moderate illumination equilibrium is attained in a few minutes. After the illumination is cut off the cell gradually recovers its initial sensitivity. The long-

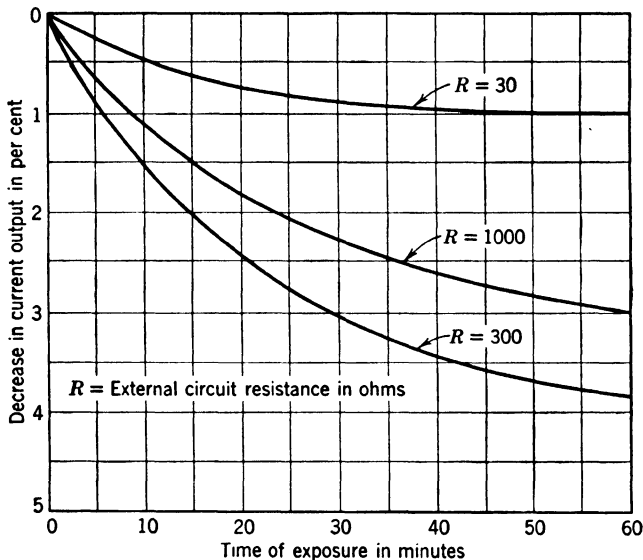


FIG. 11.14. Temporary Fatigue of Selenium Barrier-Layer Cell at 120-foot-candle (1290 lux) Illumination. (Courtesy of General Electric Company.)

time stability of these cells is very great. Lange reports that a selenium cell exposed to diffuse daylight, attaining illumination values of 10,000 lux or 1000 foot-candles, for half a year lost only 8 per cent of its sensitivity; a similar cell exposed to direct sunlight lost twice as much. For an illumination meter in daily use in a laboratory the deviations experienced in the course of a year were less than 1 per cent.<sup>18</sup>

The effect of temperature on the output of a selenium cell is shown in Fig. 11.15. The temperature affects the output because of the strong dependence of the internal resistance on the temperature. Accordingly, the change in photocurrent with temperature is very small for low load resistances and proportional to the change in internal resistance for very

<sup>18</sup> See Lange, reference 6.

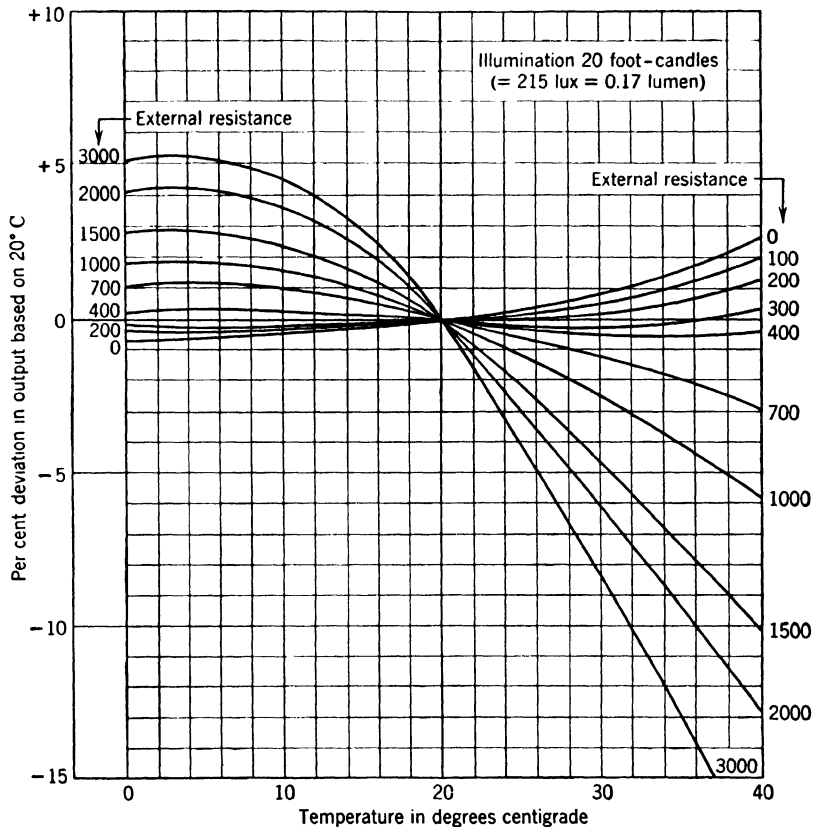


FIG. 11.15. Variation of Current Output with Temperature at 20-foot-candle Illumination. Weston Photronic Cell Type 3. (Courtesy of Weston Electrical Instrument Corporation.)

high load resistances. Raising the temperature of the cell above  $60^{\circ}\text{C}$  may alter its characteristics permanently.

**Commercial Selenium Barrier-Layer Cells.** Selenium barrier-layer cells are used principally in light meters and for the operation of relays. Their great long-time stability and the superfluity of a power source suit them well for these purposes. They are commonly housed in a bakelite case (Fig. 11.16), with the sensitive surface protected by glass, lacquer, or a filter. Short-circuit current sensitivities range from about

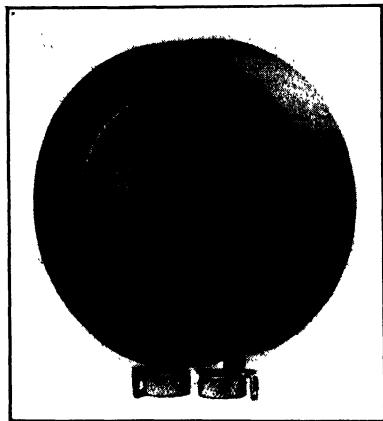


FIG. 11.16. Weston Photronic Cell Model 594 in Bakelite Housing. (Courtesy of Weston Electrical Instrument Corporation.)

140 to nearly 600 microamperes per lumen, the less sensitive cells being designed for use at high illumination levels. Power conversion ratios from 40 to 60 microwatts per lumen may be achieved at an illumination of 100 foot-candles.

### REFERENCES

1. E. BECQUEREL, "On electric effects under the influence of solar radiation," *Compt. rend.*, Vol. 9, p. 561, 1839.
2. C. G. FINK and D. K. ALPERN, "Development of photovoltaic cells," *Trans. Am. Electrochem. Soc.*, Vol. 58, pp. 275-295, 1930.
3. W. N. LOWRY, "The location of the electromotive force in the photovoltaic cell," *Phys. Rev.*, Vol. 35, pp. 1270-1283, 1930.
4. L. O. GRONDAHL, "The copper-cuprous oxide rectifier and photoelectric cell," *Revs. Mod. Phys.*, Vol. 5, pp. 141-168, 1933.
5. B. LANGE, "New kind of photoelectric cell," *Physik. Z.*, Vol. 31, pp. 139-140 and 964-969, 1930.
6. B. LANGE, *Photoelements*, Reinhold Publishing Corporation, New York, 1938.
7. W. SCHOTTKY, "Origin of photoelectrons in copper-oxide photoelectric cells," *Physik. Z.*, Vol. 31, pp. 913-925, 1930.

8. E. DUHME and W. SCHOTTKY, "Rectifying and photoelectric effects at contacts between cuprous oxide and sputtered electrodes," *Naturwissenschaften*, Vol. 18, pp. 735-736, 1930.
9. N. F. MOTT, "Note on copper cuprous-oxide photocells," *Proc. Roy. Soc. (London)*, Vol. A 171, pp. 283-285, 1939.
10. W. SCHOTTKY, "Simplified and extended theory of the barrier layer rectifiers," *Z. Physik*, Vol. 118, pp. 539-592, 1941.
11. J. BARDEEN, "Surface states and rectification at a metal semi-conductor contact," *Phys. Rev.*, Vol. 71, pp. 717-727, 1947.
12. W. G. ADAMS and R. E. DAY, "The action of light on selenium," *Proc. Roy. Soc. (London)*, Vol. A 25, pp. 113-117, 1877.
13. C. E. FRITTS, "On a new form of the selenium cell and some electrical discoveries made with it," *Am. J. Sci.*, Vol. 26, pp. 465-472, 1883.
14. B. LANGE and W. EITEL, "On a method of studying the absorption of mineralogical microspecimens with the aid of barrier layer photocells," *Mineralog. u. petrog. Mitt.*, Vol. 41, pp. 435-452, 1931.
15. L. BERGMANN, "On a new selenium barrier layer photocell," *Physik. Z.*, Vol. 32, pp. 286-288, 1931.
16. R. FLEISCHER and H. TEICHMANN, *Die Lichtelektrische Zelle*, Steinkopf, Dresden and Leipzig, 1932.
17. L. A. WOOD, "Current-voltage relations in blocking-layer photocells," *Rev. Sci. Instruments*, Vol. 6, pp. 196-201, 1935.

## Chapter 12

# PHOTOCELL CIRCUITS AND AMPLIFICATION

Photocells serve, basically, two purposes: the measurement of light intensities and the actuation of machinery in response to changes in illumination.<sup>1</sup> The first requires, in general, the operation of an indicator whose deflection is a continuous function of the light flux falling on the cell;<sup>2</sup> the second requires the closing or opening of a relay as the light flux exceeds or falls below prescribed values.

**Basic Circuits for Light Measurements.** Figure 12.1 shows the basic circuits for the measurement of light intensities with the phototube, the

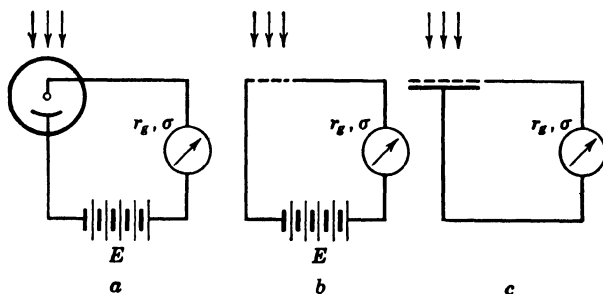


FIG. 12.1. Elementary Circuits for the Measurement of the Photocurrent of (a) a Phototube, (b) a Photoconductive Cell, and (c) a Photovoltaic Cell.

photoconductive cell, and the photovoltaic cell. In the first two cases the circuit is completed by a source of electromotive force  $E$  and a current-measuring instrument of internal resistance  $r_g$  and current sensitivity (measured in scale divisions per ampere)  $\sigma$ ; for the photovoltaic

<sup>1</sup> A third use, namely the conversion of radiant energy into electrical energy, which is a possible function of the photovoltaic cell, has been referred to on p. 211.

<sup>2</sup> In more complex applications, such as motion-picture sound and television, the trace on the film, the sound output, and the picture element brightness on the viewing tube screen take the place of the meter indication in a light-intensity measurement.

cell the current-measuring instrument alone is sufficient. The multiplier phototube, which requires a somewhat more complex voltage supply, will be considered in the next chapter as will the use of laboratory instruments of very great sensitivity for the measurement of minute photocurrents. For the present it will suffice to compare the performance of the three types of cells used in conjunction with a rugged, inexpensive current-measuring instrument.

The most common meter movement consists of a coil mounted on a pivot, rotating in a radial magnetic field. The return torque is supplied by a spiral spring, and a pointer, rigidly joined to the coil, yields the readings on a scale. When current passes through the coil, a torque is exerted on it which is proportional to the current, the radial magnetic field intensity, and the product of the cross-section area of the coil and the number of turns. The coil and pointer come to rest at the position where this torque is just balanced by the return torque exerted by the spring; the return torque is simply proportional to the angular displacement from the equilibrium position. It follows that the current sensitivity, that is, the ratio of the deflection in scale divisions to the current through the coil in amperes, is also proportional to the magnetic field, the cross-section area of the coil, and the number of turns, and inversely proportional to the stiffness of the spring. Suppose that, for a given meter design, the stiffness of the spring and the moment of inertia of the coil about its axis—the two factors governing the speed with which the pointer reaches its equilibrium position—as well as the gross geometry of the coil and the magnetic field are fixed and that the mass of the coil is made up almost entirely by the current-carrying conductor. Then both the current sensitivity and the coil resistance may be increased by reducing the thickness of the conductor and increasing, correspondingly, the number of turns, the current sensitivity increasing in proportion to the square root of the coil resistance. Thus the deflection is determined simply by the square root of the energy dissipation in the meter coil. Although the conditions laid down may be fulfilled only over a rather narrow range of the coil resistance, the fact of a positive correlation between resistance and sensitivity is evident from any listing of meter characteristics.

Assume that the meter to be employed is an ordinary small panel microammeter, such as the Weston Model 301 meter recommended for use with a Photronic cell (200 microamperes full scale, 40 divisions,  $r_g = 260$  ohms). As shown in Fig. 11.11*B*, the current response of a 3RR Photronic cell with a series resistance of 260 ohms is practically linear for a light flux up to 0.6 lumen, corresponding to an illumination of about 2200 lux. In this range the response decreases from an initial

value of about 400 microamperes per lumen to approximately 330 microamperes per lumen. The sensitivity of circuit 12.1c, employing the microammeter recommended, is hence, at low illumination levels,  $400 \cdot 40 / 200 = 80$  scale divisions per lumen or 0.088 scale division per lux.

Consider next a vacuum phototube, such as the type 929, with a current sensitivity of 45 microamperes per lumen, operated with a 100-volt source in series.<sup>3</sup> Since the response of the tube is practically independent of the applied voltage down to 10 volts or less, the measuring instrument may, in principle, have a resistance of several megohms even when the maximum rated photocurrent of 20 microamperes is attained. On the other hand, if the choice is to be restricted to simple, sturdy meters of the type described, a Weston Model 301 meter with a 20-microampere scale of forty divisions with an internal resistance of 1520 ohms becomes a reasonable selection. The sensitivity of circuit *a* in Fig. 12.1 then becomes  $45 \cdot 40 / 20 = 90$  scale divisions per lumen, corresponding, in view of the effective cathode area of 0.5 square inch, to 0.029 scale division per lux. With gas phototubes sensitivities may be attained three to seven times those given here.

Finally, a sensitive thallous sulfide cell, made with the materials used in the commercial process, may be taken as an example of the photoconductive cells. The dark resistance of this cell is 4.5 megohms, and its response, for an illumination of 54 lux, 930 microamperes for an applied voltage of 45 volts. It will be recalled that the response of these cells is a distinctly nonlinear function of illumination. If, again, the 20-microampere full-scale meter with an internal resistance of 1520 ohms is employed, the illumination sensitivity becomes (more precisely at an illumination level of 10 lux)  $(930/54)(40/20) = 34$  scale divisions per lux. Since the area of the cell is approximately 1 square inch, the sensitivity per unit light flux is 93,000 scale divisions per lumen.

Summarizing, the photoconductive cell yields, with the simple circuits considered, by far the highest sensitivity. Of the two other cells, the photovoltaic cell possesses the considerable advantage of requiring no auxiliary voltage source. In addition, it has a greater range than the photoemissive cells and, because barrier-layer cells of large sensitive surface are readily prepared, is well suited for routine illumination measurements. On the other hand, the photovoltaic cell is inferior to the phototube in being more sensitive to temperature changes and in exhibiting temporary fatigue. It is thus not so well adapted for preci-

<sup>3</sup> The tube in question may be operated at voltages up to 250 volts; applications requiring extreme constancy over long periods of time, however, may make a lowering of the voltage to 20 volts or less desirable.

sion measurements as a phototube operated at relatively low voltage. Lag in response, great sensitivity to temperature changes, and nonlinearity are, furthermore, drawbacks of the more sensitive photoconductive cells which may militate against their use in numerous applications. These drawbacks are less pronounced in the lead sulfide and silicon cells than in the thallous sulfide cells. The great sensitivity in the infrared of all these photoconductive cells reserves a special sphere of usefulness for them.

**The Operation of Relays by Photocells.** A relay is essentially a switch controlling a relatively large current and operated by much smaller changes of current. When the current through the relay coil exceeds a certain amount, an iron armature is drawn toward it so as to establish a firm contact connecting the load to the power source. As the current through the coil is reduced, the contact will not be broken by a spring attached to the armature until it has reached a value well below that required to close the contact, since the magnetic attraction of the armature, for equal coil current, is much greater in the "closed" than in the "open" position. The factors which describe the sensitivity of the relay are the minimum current required to close the contact and the difference in the "make" and "break" currents through the coil. Both, particularly the second, may be varied to some extent by changing the position of the stop at which the armature comes to rest in the open position. Apart from the stop position the sensitivity of the relay, like that of the moving-coil current meter, is determined, for given geometry and stiffness of the armature spring, by the number of turns in the coil and the coil cross section.

Simple electromagnetic relays are, in general, too insensitive for direct operation by photocurrents, requiring at least 100 microamperes for closing the contact.<sup>4</sup> Much greater sensitivity is attained by letting the needle of a moving-coil instrument establish the contact closing the circuit to be controlled. This arrangement has the drawback, on the other hand, of permitting the control of only very small currents. The load capacity can be increased, as in the Weston Sensitrol relay, by providing the needle with an iron armature and using a magnetic contact, which must then be opened manually. The relative position of the three types of photocells, used with such relay instruments, is of course the same as in light measurements. Highly ingenious multiple relays with automatic release mechanisms have been devised for controlling large currents with the output of barrier-layer cells.<sup>5</sup> They will

<sup>4</sup> They are, however, readily operated by the output current of a multiplier phototube.

<sup>5</sup> See Lange, reference 1.



not be discussed further, however, since, particularly with phototubes and photoconductive cells, the control of large currents can be carried out more simply with gas relay tubes (thyratrons), which will be considered in a later section.

**The Need for Amplification.** It is seen that the least light flux which can be measured directly, with reasonable accuracy, by a phototube or barrier-layer cell and a sturdy, inexpensive meter is of the order of 0.1 lumen; the least illumination is of the order of 100 lux. The operation of a light relay demands at least as large values. To overcome this limitation it is necessary to amplify the photocurrent, that is, provide a device which will, in effect, multiply the photocurrent by a constant factor of adequate magnitude. The same need of amplification arises in the more complex applications of photocells and photoemissive devices as in the operation of loudspeakers by photocurrents in the reproduction of sound-on-film, or the modulation, in a television transmitter, of high-frequency alternating currents by the photocurrent of a pickup system. The devices which meet this need are known as vacuum-tube amplifiers.

**Thermionic Vacuum Tubes and Their Operation.** When a metallic electrode (*cathode*) is heated it emits electrons<sup>6</sup> which may be collected by a second, more positive, electrode (*anode*) if the two are enclosed in an evacuated envelope. This emission increases very rapidly with the temperature and decreases with increasing work function of the emitting surface. Thus high thermionic emission may be attained either by heating metals with very high melting points, such as tungsten or tantalum, to very high temperatures (of the order of 3000° K) or providing the metal surface with a coating (thorium on tungsten or strontium and barium oxides on nickel) which reduces the work function sufficiently that the cathode will yield large thermionic currents even at moderate temperatures. The oxide-coated cathodes, providing currents of the order of 10<sup>4</sup> amperes per square meter at operating temperatures of the order of 1000° K, are most commonly em-

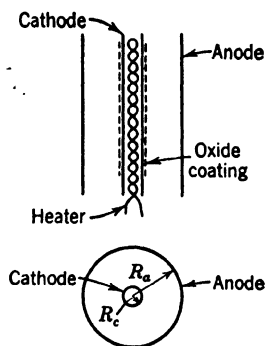


FIG. 12.2. Arrangement of Electrodes in Cylindrical Diode.

<sup>6</sup> The dependence, on the temperature  $T$  of the cathode, of the electron current leaving unit area is given by

$$j = AT^2 e^{-w/kT} \quad (12.1)$$

where  $w$  is the work function of the surface,  $T$  the absolute temperature, and  $k$ , Boltzmann's constant.  $A$  is a constant which, for many metals, has the value  $1.2 \cdot 10^6$  amperes/(meter · degree)<sup>2</sup>. If  $w$  is expressed in electron volts,  $w/(kT) = 11,607w/T$ .

ployed in thermionic amplifier tubes. The heating of the cathode is frequently indirect. For this purpose a coiled heater filament, coated with an insulating refractory material, is inserted into the tubular cathode. Thus the essential components of a two-element thermionic tube, or *diode*, with cylindrical symmetry may be arranged as shown in Fig. 12.2.

Figure 12.3 shows the expected variation of the current through an external circuit, connecting the cathode and the anode, with the magni-

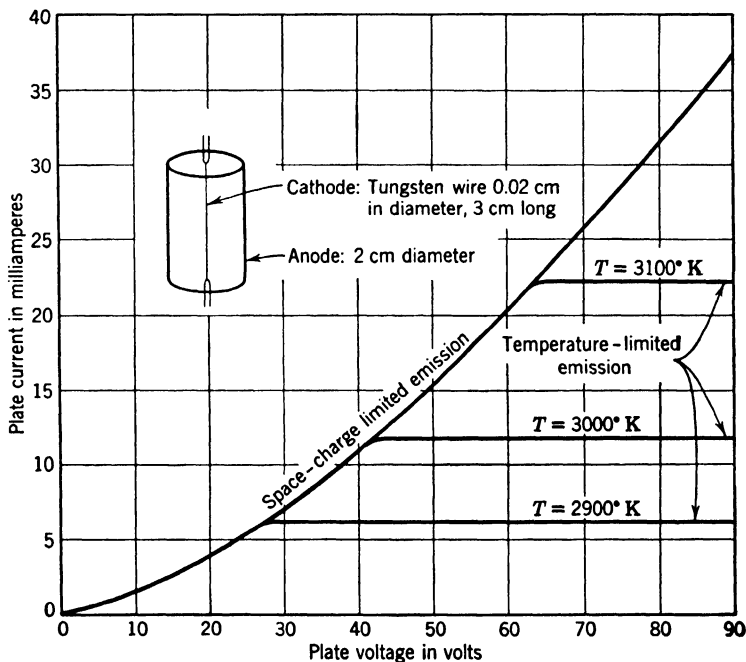


FIG. 12.3. Variation of Diode Current with Applied Voltage for Different Cathode Temperatures.

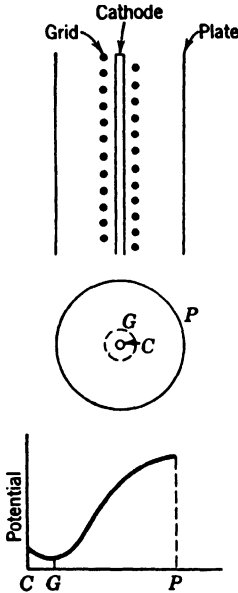
tude of the applied voltage<sup>7</sup> for different cathode temperatures. At very low temperatures a constant, saturation, current is reached for accelerating voltages of the order of a volt or less, corresponding to the small emission velocities of the thermionic electrons.<sup>8</sup> On the other hand, for higher temperatures and correspondingly higher saturation currents, the ascent of the current with increasing applied voltage is

<sup>7</sup> See Langmuir, reference 2.

<sup>8</sup> The average energy of emission associated with the velocity component normal to the surface is  $T/11,600$  electron volt, or about 0.1 electron volt for an oxide cathode.

quite gradual. This effect becomes more pronounced as the spacing of cathode and anode is increased. It arises from the fact that, for low accelerating voltages, the electrons emitted with small forward velocities are driven back into the cathode by the opposing field of the electron cloud surrounding the cathode.

A diode, such as is shown in Fig. 12.2, may be used as a rectifier for alternating currents. It will transmit current whenever the anode is positive with respect to the cathode and stop current flow whenever it is negative. Consider now a tube with three electrodes, or *triode*, in which the anode of the diode is replaced by a *grid*  $G$ , consisting, for instance, of a closely spaced wire helix, and a *plate*  $P$ , at some distance from the grid and cathode (Fig. 12.4). The plate is generally made sufficiently positive with respect to the cathode that the space charge between the grid and the plate will not turn back toward the cathode any electrons which have passed through the grid. Hence the amount of current collected by the plate is determined simply by that which reaches the plane of the grid or, in other words, by the effective potential in the plane of the grid. It is given simply by



$$V = V_g + \frac{V_p}{\mu} \quad (12.2)$$

FIG. 12.4. Structure and Field Distribution in Triode (Schematic).

Here  $V_g$  is the grid potential,  $V_p$  is the plate potential, and  $\mu$  is the voltage amplification factor of the tube.<sup>9</sup> The effect of changes in  $V$  on the plate current is, again, represented by the curves in Fig. 12.3. If the grid is made appreciably negative with respect to the cathode and the plate positive, none of the current from the cathode is collected by the grid wires. Thus relatively large plate currents can be controlled by the grid voltage without appreciable energy dissipation by the grid voltage source. The temperature of the cathode is normally chosen high enough so that the operating range of the tube falls entirely on the initial, more

<sup>9</sup> It is seen that, for a change in the grid voltage  $\Delta V_g$ , the plate voltage must be increased by  $-\mu\Delta V_g$  if the plate current is to remain unchanged. Furthermore, if the cathode and the plate are connected by a voltage source in series with a very high resistance, a change  $\Delta V_g$  in the grid voltage will result in a change  $-\mu\Delta V_g$  in the plate voltage.

steeply ascending, portion of the characteristics in Fig. 12.3. Under this "space-charge limited" condition small temperature changes of the cathode do not affect the plate current.

The application of a triode for the amplification and measurement of small photocurrents is exemplified by the circuit in Fig. 12.5. The properties of the 6J5 triode employed here are given by its "plate characteristics," that is, the variation of the plate current with the plate voltage for fixed values of the grid voltage (Fig. 12.6).<sup>10</sup> Let a straight

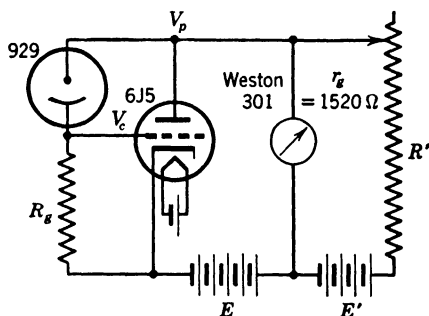


FIG. 12.5. Simple Triode Amplifier for Measurement of Small Photocurrents.

$$E = 90 \text{ volts}$$

$$E' = 45 \text{ volts}$$

$$R_g = 1 \text{ megohm}$$

$$R' = 4800 \text{ ohms}$$

$$g_m = 3 \cdot 10^{-3} \text{ ohm}^{-1}$$

$$r_p = 6700 \text{ ohms}$$

$$\frac{dV_p}{dV_c} = g_m \frac{r_p r_g R'}{r_p r_g + r_g R' + R' r_p} = 3$$

line be drawn through the point of the axis of abscissas corresponding to the plate voltage for zero plate current (about 101 volts) and with a negative slope numerically equal to the reciprocal of the load resistance (1150 ohms for the 20-microampere full-scale Weston 301 meter considered on page 218 in parallel with the resistance  $R' = 4800$  ohms). The intersections of this line—the *load line*—with the plate characteristics indicate the values of the plate current and plate voltage for the grid voltages of the characteristics. In the example shown the grid bias is made zero, so that the plate current is about 9.4 milliamperes when no light falls on the phototube. The auxiliary voltage  $E'$  and the resistance  $R'$  are provided to make the current through the meter zero for zero photocurrent. The movable contact on the resistance  $R'$  forms a sensitive zero adjustment. The voltage gain of this circuit, given by

<sup>10</sup> This representation is to be preferred to plotting the plate current as function of the grid voltage for fixed plate voltages since it simplifies taking account of the voltage drop across the plate load.

the transconductance <sup>11</sup> multiplied by the plate resistance in parallel with the load resistance, is about 3, corresponding to a gain in current sensitivity  $3R_g/r_g = 2000$ . For a tube response of 45 microamperes per lumen the overall circuit sensitivity becomes 180,000 scale divisions per lumen or 58 scale divisions per lux. A drawback of this circuit is

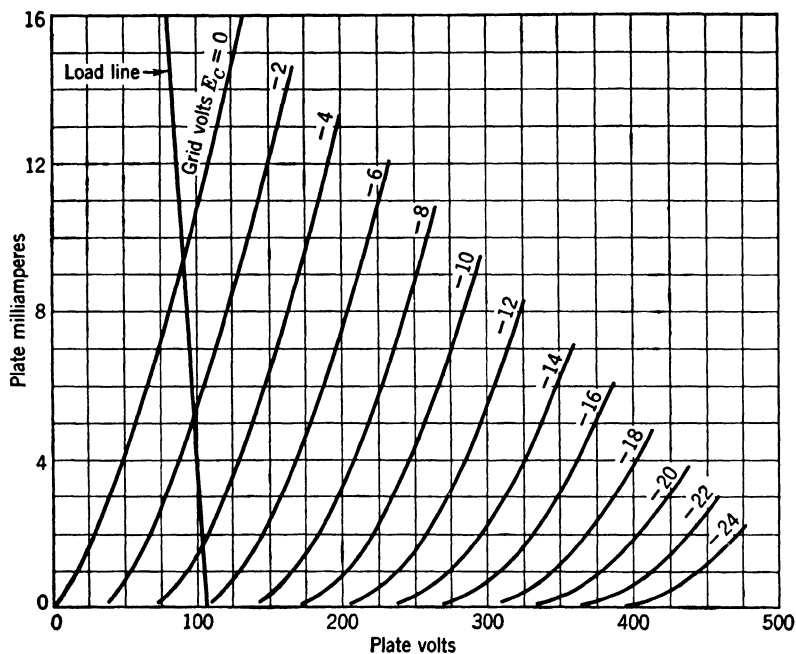


FIG. 12.6. Plate Characteristics of a Triode (6J5). (*RCA Tube Handbook*.)

that it is relatively sensitive to small changes in the supply voltages and tube characteristics.

It is seen that, in the triode, changes in the plate potential, arising from the voltage drop across the plate load, affect the plate current by altering the potential in the plane of the grid. This alteration reduces the effect of grid voltage changes on the plate current. In addition, changes in the plate voltage affect the grid voltage itself as a result of the mutual capacity of grid and plate. In high-frequency applications this reaction of the plate voltage on the grid voltage may give rise to spontaneous electrical oscillations which render the tube useless as an amplifier. These undesirable effects may be minimized by providing an

<sup>11</sup> The transconductance of the tube is defined as the rate of change of the plate current with the grid voltage, the plate voltage being held constant.

additional grid—a *screen grid*—at a fixed positive potential between the plate and the control grid. The screen grid isolates the plate from the grid electrostatically and yet collects only a fraction of the electrons that have passed through the control grid. It is normally maintained at a high positive potential so that large electron currents can be drawn from the cathode. When, in such a four-element tube or *tetrode*, the

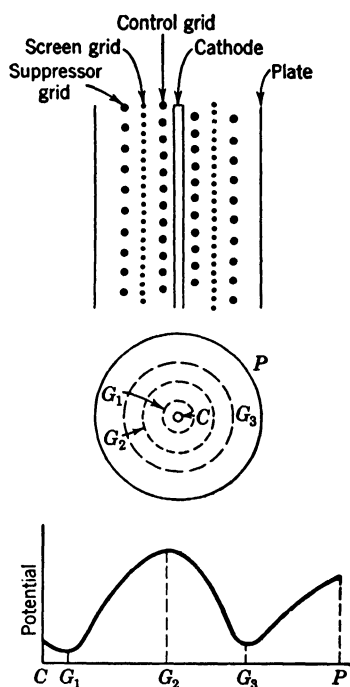


FIG. 12.7. Arrangement of Grids and Potential Distribution in a Pentode (Schematic).

plate voltage falls below the screen-grid voltage, secondary electrons ejected from the plate will be collected by the screen grid and will reduce the plate current correspondingly—eventually even reversing its direction. To prevent this, it is common practice to insert, in screen-grid amplifier tubes, a third grid, or *suppressor grid*, at cathode potential between the plate and the screen grid. The arrangement of the grids and the potential distribution in the resulting pentode are shown schematically in Fig. 12.7.

The suppression of the secondary emission from the plate may also be achieved by creating a region of low potential between the screen

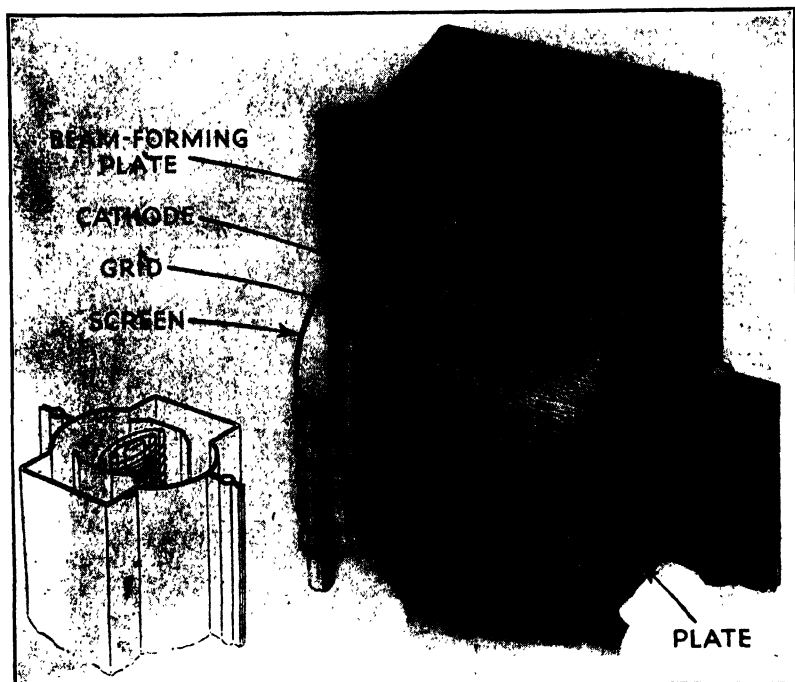


FIG. 12.8. Electrode Structure and Beam Formation in 6L6 Power Tube. (Courtesy of *Proc. Inst. Radio Engrs.*, Vol. 26, pp. 137-181, 1938.)

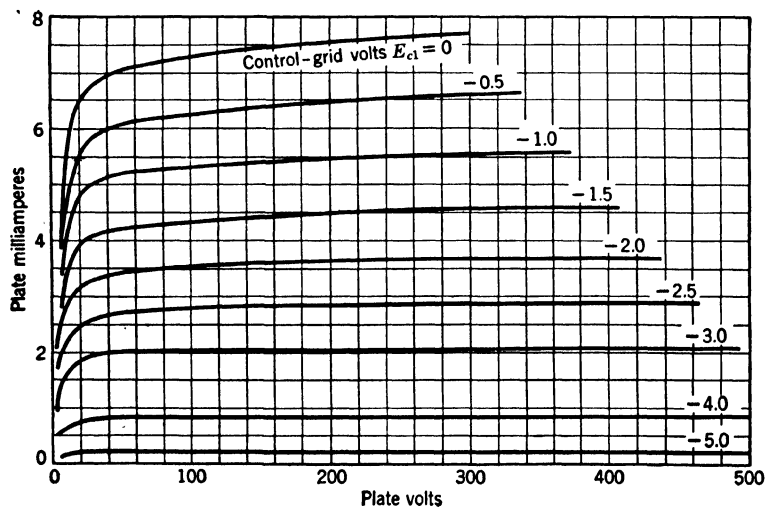


FIG. 12.9. Plate Characteristics of a Pentode (6J7). (*RCA Tube Handbook.*)

grid and the plate through the cooperation of the electronic space charge and suitably disposed electrodes at cathode potential ("beam-forming plates"). The structure of a *beam tube* employing this principle, in which the electrons are bundled into a series of flat pencils by the combined action of the aligned control and screen grids, is shown in Fig. 12.8. Such beam tubes are particularly well suited for handling relatively large amounts of power. Their characteristics are similar to those of a pentode.

The plate characteristics of a typical pentode, the 6J7, show the expected slight dependence of the plate current on the plate voltage which results from the screening of the grid from the plate (Fig. 12.9).

### Direct-Current Amplifying Circuits for Phototubes; Inverse Feedback.

If a single-stage amplifier, such as that shown in Fig. 12.5, does not increase the output of the phototube by a sufficiently large factor, sev-

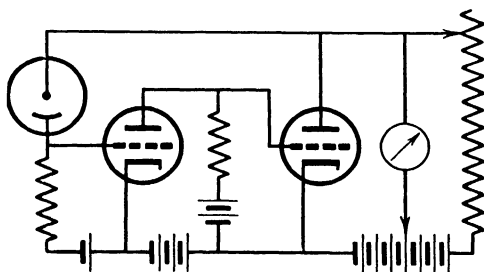


FIG. 12.10. Direct-Coupled Amplifier for Photocurrents.

eral such stages may be connected in cascade, as in Fig. 12.10. The output meter may be connected to such a point of the voltage supply that it indicates zero when no light is falling on the phototube. Again, however, the arrangement shown has the drawback that the amplifier gain is sensitive to small changes in the operating conditions of the tubes, particularly if the number of stages is large and the overall gain is high. This sensitivity may result in an objectionable meter drift and non-permanence of a calibration of the system as a light meter.

These effects may be minimized, at the cost of reducing the gain per stage, by inverse feedback, whose principle is shown in Fig. 12.11. A fraction  $-\beta E_2$  of the output voltage  $E_2$ , with a polarity opposite to that of  $E_1$ , the voltage to be amplified, is added to  $E_1$ . It follows that, if the gain of the amplifier without feedback is  $G_o$ ,

$$E_2 = G_o(E_1 - \beta E_2) \quad (12.3)$$

so that the gain of the feedback amplifier becomes

$$\frac{E_2}{E_1} = \frac{G_o}{1 + \beta G_o} \cong \frac{1}{\beta} \quad \text{for } \beta G_o \gg 1 \quad (12.4)$$



For large amplification factors  $G_o$ , the gain is thus determined entirely by the perfectly stable passive circuit constants of the feedback network.

An application of this principle to form a rugged, sensitive dry-cell-operated vacuum-tube microammeter, suitable for the measurement of small photocurrents, is shown in Fig. 12.12.<sup>12</sup> It consists of a three-

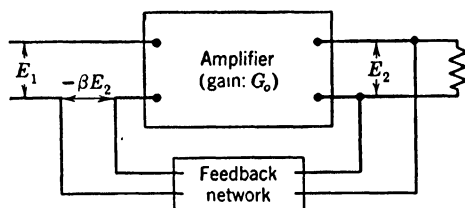


FIG. 12.11. Principle of Inverse Feedback.

stage amplifier employing low-drain vacuum tubes with an overall voltage amplification of about 500, whose full output voltage is applied, in series with the potential drop across the input resistor, between the grid and the cathode of the first tube. Since the number of stages is odd, the output voltage is of opposite polarity to the input voltage. The feedback constant  $\beta$  being unity in the present case, Eq. 12.4 indicates

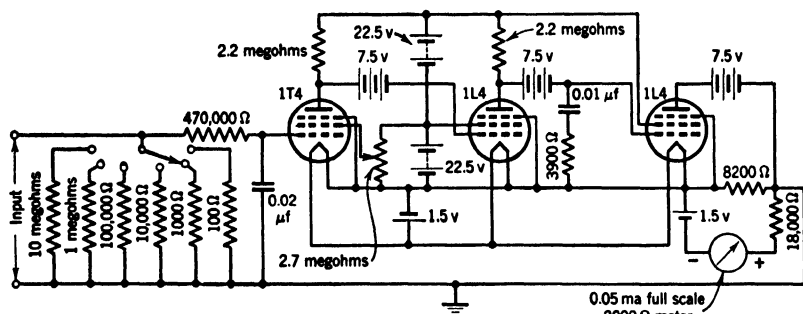


FIG. 12.12. Sensitive Microammeter Circuit Employing Feedback. (Vance, reference 3.)

that the input and output voltages must be the same to within about 0.2 per cent. The output load is essentially a low-resistance voltmeter with a full-scale reading of 1 volt (or a current meter with a 0.05-milliampere scale and a series resistance of 20,000 ohms). The scale-factor switch selects, as input resistor, any one of six resistances ranging from 100 ohms to 10 megohms, corresponding to a full-scale deflection for

<sup>12</sup> See Vance, reference 3.

10 milliamperes to 0.1 microampere, respectively. The shunt and series resistances of the meter are adjusted so that, for zero input current, the voltage drop produced by the plate current of the final tube is just compensated by that produced by a 1.5-volt dry cell. A zero fine adjustment is provided by variation of the screen voltage on the input tube. It may be mentioned that the condenser-resistance shunt on the grid of the third tube serves to prevent the initiation of high-frequency oscillations, to which such feedback circuits are liable unless precautions are taken. In addition, the half-megohm resistance and shunt capacitance at the input function as a "low-pass filter," shunting out high-frequency currents which might enter the amplifier from the circuit to which the meter is connected. One of the great advantages of this meter, apart from its freedom from drift and variation in sensitivity, is the fact that the meter proper cannot be damaged by overloads; the current which passes through it is limited by the saturation current of the last tube.

Numerous other negative feedback amplifier circuits, eventually employing the alternating current line in place of batteries as source of power, have been developed for the amplification of phototube currents. Figure 12.13 shows a circuit combining high current amplification with rapid response to light changes.<sup>13</sup> The alternating current is rectified by the double-diode rectifier tube 25Z6 which is connected so as to yield a 300-volt direct-current output smoothed by the two large electrolytic capacitances  $C_1$  and  $C_2$ . The voltage drop produced by the photocurrent across the very large resistance  $R_4$  is applied to the grid of the first, *cathode-follower*, stage, whose output, taken from the cathode resistance  $R_5$ , is applied to the grid of the power amplifier tube 25L6. The function of this first stage is simply to reduce the effective value of the resistance across which the voltage generated by the photocurrent appears to a value sufficiently low to drive the power tube.<sup>14</sup> The circuit is adjusted by first moving the contacts on the  $R_3$  and  $R_6$  resistors to the positive end of their ranges and adjusting the contact on the  $R_7$  resistor (that is, the screen voltage of the 25L6) until the power tube delivers the maximum plate current desired—which may be as great as 25 to 50 milliamperes. Then the contact on  $R_6$  is displaced toward

<sup>13</sup> From RCA Manufacturing Co., Inc., *Phototubes*, 1940.

<sup>14</sup> If  $g_m$  is the transconductance (rate of change of plate current with grid voltage for constant plate voltage) of the 38 pentode, and  $V_i$  is the input voltage, the voltage across  $R_5$  becomes  $g_m R_5 V_i / (1 + g_m R_5) \cong V_i$  since  $g_m = 10^{-3} \text{ ohm}^{-1}$  and  $R_5 = 5 \cdot 10^5 \text{ ohms}$ . It is seen that the output voltage of the cathode-follower stage is independent, within wide limits, of both the tube gain and variations in the effective value of the load resistance.

the negative end until the 25L6 plate current just begins to decrease, indicating that the grid of this tube is slightly negative with respect to the cathode. Finally, with the maximum illumination to be measured

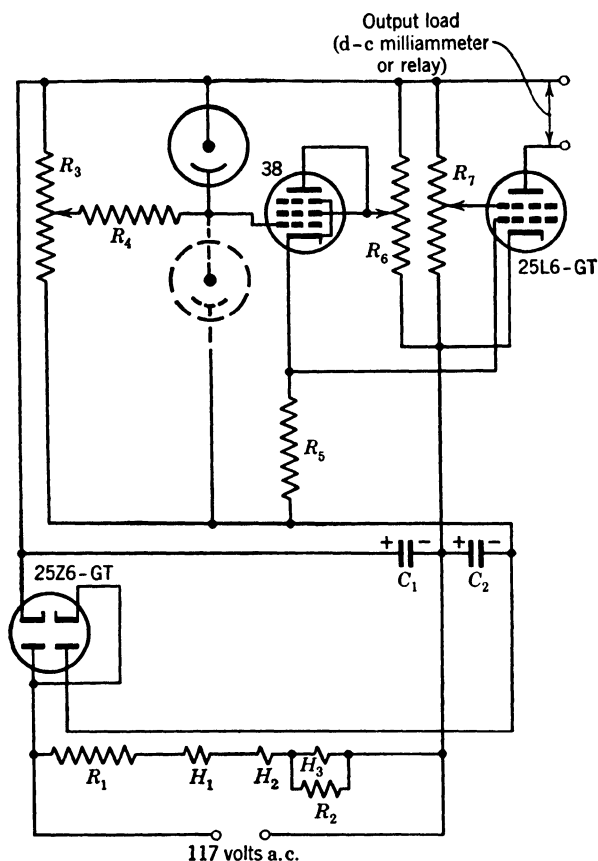


FIG. 12.13. Fast-Acting, Alternating-Current-Operated Amplifying Circuit for Light Measurement and Relay Operation.

$C_1 = C_2 = 8 \mu\text{f}$  (250 volts)

$H_1 = 25Z6\text{-GT}$  heater

$H_2 = 25L6\text{-GT}$  heater

$H_3 = 38$  heater

$R_1 = 200$  ohms (20 watts)

$R_2 = 50$  ohms (1 watt)

$R_3 = 1$  megohm

$R_4 = 100$  megohms

$R_5 = 0.5$  megohm

$R_6 = R_7 = 0.1$  megohm

falling on the photocathode, the contact on  $R_3$  is displaced toward the negative end until the 25L6 plate current is affected. Then the circuit is ready for operation. If the illuminations to be measured are fairly large, the last adjustment may be possible only if the resistance  $R_4$  is

reduced in magnitude. It may be noted that, to minimize grid current, the heater of the 38 pentode is operated at only about two-thirds its normal voltage rating.

### Vacuum-Tube Circuits for Photovoltaic and Photoconductive Cells.<sup>15</sup>

Photovoltaic and photoconductive cells differ from phototubes in a much greater dependence of the photocurrent on the applied voltage. Thus, if a large resistance, such as the input resistance of a conventional amplifier, is connected in series with them, the current output becomes a nonlinear function of illumination. For the photovoltaic (barrier-layer) cells this is demonstrated by the curves in Fig. 11.11. Since, as has been seen, the voltage difference between grid and cathode remains practically constant, independent of the magnitude of the input signal, in an inverse-feedback amplifier such as a cathode-follower circuit, connecting the photovoltaic or photoconductive cell between these two points should assure a constant potential across the cell and, hence, linearity of response to illumination. The circuit shown in Fig. 12.14 ac-

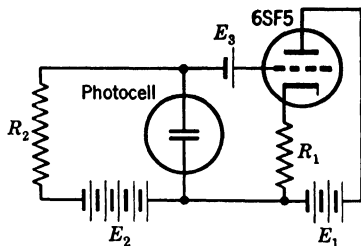


FIG. 12.14. Vacuum-Tube Circuit Correcting Nonlinearity of Response of Photovoltaic and Photoconductive Cells. (Rittner, reference 4.)

complishes just that.  $E_1$  is the plate voltage supply,  $E_3$  is the grid bias, and  $E_2$ , which is not required for a photovoltaic cell, is the voltage source for the photocell. The signal voltage is simply  $i_p R_2$ , where  $i_p$  is the photocurrent generated by the cell. The voltage across the photocell is readily calculated to be  $E_2 - i_p(R_1 + R_2)/(1 + g_m R_1)$ , so that the effective external resistance has been reduced by the factor  $1/(1 + g_m R_1)$ . For a 6SF5 tube ( $g_m = 1.8 \cdot 10^{-3} \text{ ohm}^{-1}$ ) and  $R_1 = 100,000$  ohms, this factor becomes  $1/80$ . Figure 12.15 shows the voltage across the resistor  $R_2$  as function of illumination for a Weston RR Photronic cell, indicating the gain in linearity with the vacuum-tube circuit.

A second, two-stage, circuit employing a single 6F8-G double triode, which combines a reduction in the effective resistance in series with the photocell with considerable amplification of the photocurrent, is shown in Fig. 12.16. Here the measured current is  $-g_m' R_1 i_p (1 + g_m' R_4)$ , assuming that  $E_4$  has been adjusted to yield zero current reading for zero illumination;  $g_m'$  represents the transconductance of each stage, taking account of the presence of the cathode resistor, and amounts to

<sup>15</sup> See Rittner, reference 4.

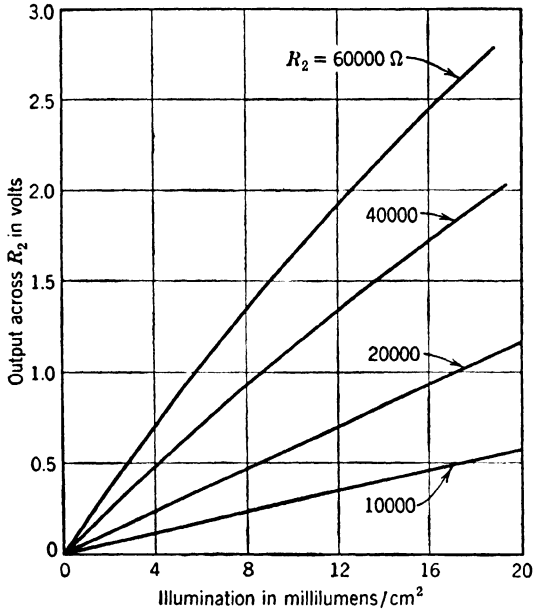


FIG. 12.15. Variation of Voltage across Load Resistor  $R_2$  with Illumination of Weston RR Photronic Cell, Employing Circuit Shown in Fig. 12.14. (Rittner, reference 4.) (Courtesy of Rev. Sci. Instruments.)

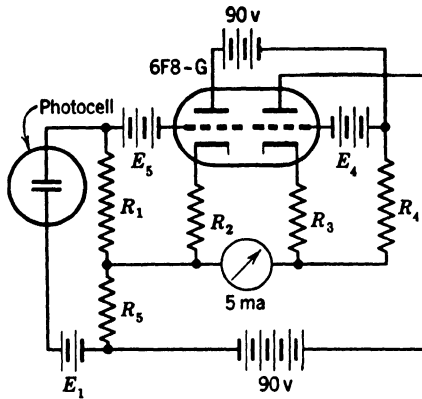


FIG. 12.16. Vacuum-Tube Circuit for Photovoltaic and Photoconductive Cells Combining Amplification and Nonlinearity Correction. (Rittner, reference 4.) (Courtesy of Rev. Sci. Instruments.)

- |   |                                |
|---|--------------------------------|
| $E_1$ = Voltage applied to photocell      | $R_1 = 25,000$ ohms            |
| $E_4$ = No-signal balancing voltage       | $R_2 \cong R_3 \cong 500$ ohms |
| $E_5$ = Dark-current compensating voltage | $R_4 \cong R_5 \cong 800$ ohms |

about  $1.3 \cdot 10^{-3} \text{ ohm}^{-1}$  in the present example. The voltage across the photocell can readily be shown to be  $E_1 = i_p(R_1 + R_5 - g_m'^2 R_1 R_4 R_5)$ , which becomes independent of the photocurrent  $i_p$  if the values of the resistances are chosen appropriately. With a Weston RR Photronic cell and the circuit constants indicated, this circuit has been found to yield a perfectly linear response of 20 milliamperes per lumen for a light flux up to a fifth of a lumen.

**Relay Circuits; the Thyatron.** Practically all the vacuum-tube circuits described so far are suitable for the operation of relays. In particular, the circuit shown in Fig. 12.13 will act as relay-closing circuit

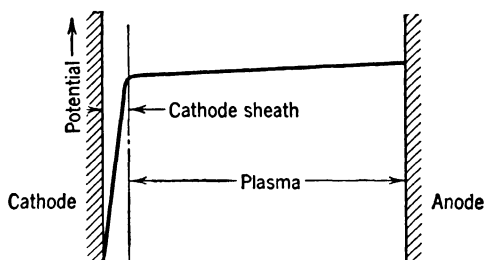


FIG. 12.17. Potential Distribution in a Gas Diode When Conducting Current.

with an extraordinarily rapid response to light fluctuations. If the phototube is connected as indicated by the full lines, the circuit will close the relay as the illumination rises above a certain level; if it is in the dotted position, it will close it as the illumination sinks below a set level. However, if, as in most applications, it is sufficient for the relay to respond to light changes lasting more than  $1/60$  second, the use of gas tubes in alternating-current-operated circuits offers a simpler solution.

If an inert gas, in particular a noble gas or mercury vapor, at a pressure of several millimeters of mercury is introduced into a vacuum tube, the characteristics of the tube are greatly changed. Considering, first, a diode, the electrons accelerated toward the plate ionize the gas, and the newly formed ions and electrons enhance the current through the tube. The tube may ultimately be destroyed unless the current is limited by a series resistance which maintains the voltage drop across the tube at a value of the same order as, and generally slightly below, the ionization potential of the gas. This operating voltage is considerably lower than that required to initiate "breakdown" or "firing" of the tube. In the conducting condition practically the entire potential drop is concentrated in a narrow sheath immediately in front of the cathode (Fig. 12.17). The electrons leaving the cathode acquire their

high velocity in this sheath and lose it by repeated collisions, resulting in part in ionization, in the succeeding nearly equipotential region or *plasma*. Here electrons and ions, in approximately equal concentration, along with the neutral gas atoms, execute random thermal motions, on which a slow drift velocity, caused by the residual electrical field, is superposed. Near the cathode the positive ions are drawn out

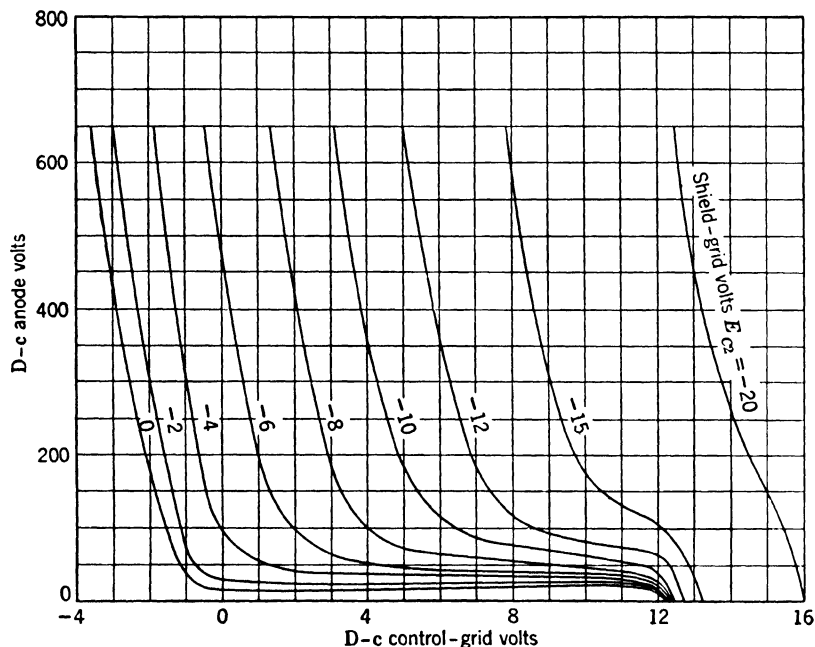


FIG. 12.18. Control Characteristics of Type 2050 Screen-Grid Thyatron. (*RCA Tube Handbook.*)

of the plasma, forming a positive space charge barrier which screens the plasma from the negative field of the cathode.

Consider, next, a gas triode. Such a tube will fire when the potential in the plane of the grid approaches the breakdown potential for a diode. However, when the plasma has once been established, in the manner described, a decrease in the grid potential will not affect the operation of the tube. As the grid potential is reduced, a positive-ion sheath forms around the grid wires, neutralizing the effect of the grid on the discharge. Only when the plate voltage, also, drops below the value required to maintain the discharge will the discharge be extinguished. Gas triodes of this type are generally designated as *thyatrons*, if they employ a heated cathode. Cold-cathode gas triodes, which operate in similar

manner, but have much lower current-carrying capacity, are known as *grid-glow tubes*. As in the case of vacuum amplifier tubes, the grid-plate capacity and the reaction of plate voltage changes on the operation of the tube may be minimized, in thyratrons, by the insertion of a

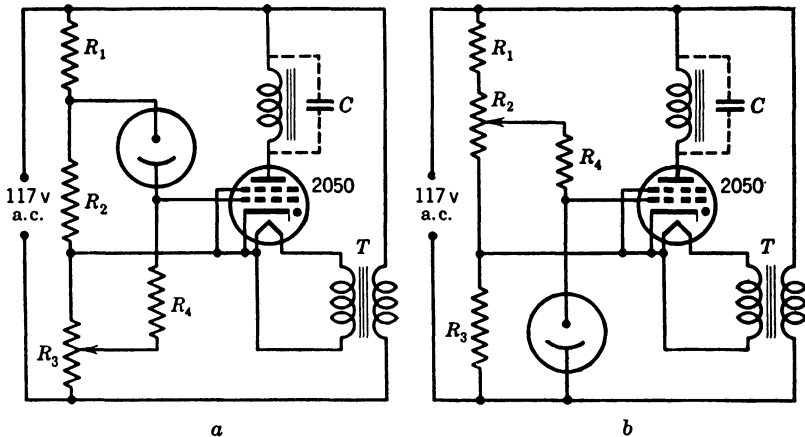


FIG. 12.19. Light-Controlled Relay Circuits Employing Thyratrons: (a) Relay Closed as Illumination Is Increased; (b) Relay Closed as Illumination Is Decreased.

$C = 2-8 \mu\text{f}$  (250 volts)       $T = \text{Heater transformer (6.3 volts, 0.6 ampere)}$   
 $R_4 = 1-10 \text{ megohms}$

- a*
- |   |                        |
|---|------------------------|
| $R_3 = 1000 \text{ ohms (1 watt)}$                      |                        |
| $R_1 = 0$   | } for vacuum phototube |
| $R_2 = 20,000 \text{ ohms (1 watt)}$                    |                        |
| $R_1 = 10,000 \text{ ohms } (\frac{1}{2} \text{ watt})$ | } for gas phototube    |
| $R_2 = 9,000 \text{ ohms } (\frac{1}{2} \text{ watt})$  |                        |
- b*
- |                                     |                        |
|-------------------------------------|------------------------|
| $R_3 = 100 \text{ ohms (1 watt)}$   |                        |
| $R_1 = 0$                           | } for vacuum phototube |
| $R_2 = 5000 \text{ ohms (4 watts)}$ |                        |
| $R_1 = 3000 \text{ ohms (2 watts)}$ | } for gas phototube    |
| $R_2 = 2000 \text{ ohms (1 watt)}$  |                        |

screen grid between the control grid and the plate. The control characteristics of a particular gas tetrode or screen-grid thyatron, the 2050, are shown in Fig. 12.18. These curves indicate the relation between the control-grid potential and the plate voltage values (for fixed screen-grid potential) for which firing takes place. The voltage drop across this tube when in the conducting state is only about 8 volts; it is capable of furnishing continuous plate currents up to 200 milliamperes.



If a thyatron, with a suitable ballast resistance in series, is connected across an alternating-current line, it will pass a sizable current in every positive half cycle in which the control grid attains a voltage high enough to initiate the discharge, as indicated by the characteristics. On the negative half cycles, on the other hand, the discharge is extinguished and the plasma dissipated, so that the tube will respond once more to grid control in the succeeding half cycle. This operation suggests the simple light-controlled relay circuits shown in Fig. 12.19, *a* and *b*.<sup>16</sup> The first circuit closes the relay as the light intensity exceeds an amount determined by the tube sensitivity and the magnitude of  $R_4$ , the second closes it as the light drops below a value set by adjusting the contact on  $R_2$ . The resistance  $R_1$  is required only if gas phototubes are employed and is then chosen approximately equal to  $R_2$ ; it serves to keep the peak voltage across the tube within the maximum rating. The relay and  $R_3$  together provide the ballast resistance for the thyatron, which may have to be supplemented by an additional resistance in series with the relay;  $R_3$  by itself furnishes the negative grid bias. The capacitance  $C$  shunting the relay prevents relay chatter during the negative half cycles of current-conducting periods. Relays which close for an exciting current of 25 milliamperes or less operate satisfactorily in these circuits.

**Alternating Currents.** When a varying voltage is impressed on a network consisting entirely of resistances, the variation of both current and voltage at any point of the network is strictly proportional to the impressed voltage. In particular, the ratio of the voltage across the terminals of a network to the current passing through it is expressed by a simple constant, the resistance. On the other hand, when other passive circuit elements, such as capacitances and inductances, are added to the network, the relationship between current and voltage becomes, for arbitrarily varying voltage, exceedingly complex. Only if the voltage can be expressed in the general form

$$V = A \sin (2\pi\nu t + \phi) \quad (12.5)$$

where  $A$ ,  $\nu$ , and  $\phi$  are three constants—the amplitude, frequency, and phase of the voltage oscillation—and  $t$  is the time, will the current and voltage at any point of the circuit have the same form, with different amplitude and phase constants  $A$  and  $\phi$ . Furthermore, the magnitude of these constants can be determined as for the purely resistive network, if an *impedance*, or complex resistance,  $1/(2\pi\nu jC)$ , is assigned to every capacitance  $C$  and an impedance  $2\pi\nu jL$  is assigned to every inductance  $L$  in the network. The factor  $j$  is treated mathematically as

<sup>16</sup> From RCA Manufacturing Company, Inc., *Phototubes*, 1940.

$\sqrt{-1}$ . Its appearance as a factor in the amplitude of a current or voltage signifies that the current or voltage in question is advanced in phase by a quarter cycle ( $\pi/2$ ) with respect to a current or voltage with a real amplitude factor.<sup>17</sup>

Since capacitances and inductances serve many useful purposes in electrical circuits, it is a decided advantage that an arbitrary variation of current or voltage may be regarded as the resultant of many sinusoidally alternating components differing in amplitude and phase. Two conditions, illustrated in Fig. 12.20, *a* and *b*, may be distinguished. The first is that the variation has a definite periodicity with a fundamental frequency  $\nu_0$ . In this case all the components are *harmonics* of the fundamental component or have frequencies which are integer multiples of  $\nu_0$ .<sup>18</sup> On the other hand, an aperiodic variation may be represented by a superposition of components of all frequencies with varying ampli-

<sup>17</sup> As illustration, suppose that an alternating voltage of amplitude  $A$  and frequency  $\nu$  is applied to a capacity  $C$  in series with a resistance  $R$ . The amplitude of the current through this "impedance" is then given by

$$\frac{A}{R + \frac{1}{2\pi\nu jC}} = \frac{2\pi\nu jCA}{1 + 2\pi\nu jCR} = \frac{-4\pi^2\nu^2 C^2 RA + 2\pi\nu jCA}{1 + 4\pi^2\nu^2 C^2 R^2}$$

The real component of the amplitude represents a current in phase with the voltage, and the imaginary component (that is, that multiplied by  $j$ ), represents one advanced in phase by  $\pi/2$  with respect to it. The addition of these two components yields a current whose amplitude  $A'$  is equal to the square root of the sum of the squares of the component amplitudes:

$$A' = 2\pi\nu CA \frac{1}{(1 + 4\pi^2\nu^2 C^2 R^2)^{1/2}}$$

and whose phase angle  $\phi'$  has a tangent equal to the ratio of the imaginary to the real component:

$$\phi' = \arctan \frac{-1}{2\pi\nu CR}$$

<sup>18</sup> If the function  $f(t)$  has a period  $1/\nu_0$ ,

$$f(t) = \sum_{n=0}^{\infty} (a_n \cos(2\pi n\nu_0 t) + b_n \sin(2\pi n\nu_0 t)) \quad (12.6)$$

with

$$a_n = 2\nu_0 \int_0^{1/\nu_0} f(t) \cos(2\pi n\nu_0 t) dt \quad n \neq 0$$

$$a_0 = \nu_0 \int_0^{1/\nu_0} f(t) dt$$

$$b_n = 2\nu_0 \int_0^{1/\nu_0} f(t) \sin(2\pi n\nu_0 t) dt$$

tude.<sup>19</sup> As indicated in Fig. 12.20, the *frequency spectrum* of the periodic variation is discrete, that of the aperiodic variation, continuous.

Alternating currents are employed in electric power systems because of the ease of converting, with the aid of transformers, low-voltage alternating currents into high-voltage alternating currents and vice versa. In the United States the frequency of the line alternations is,

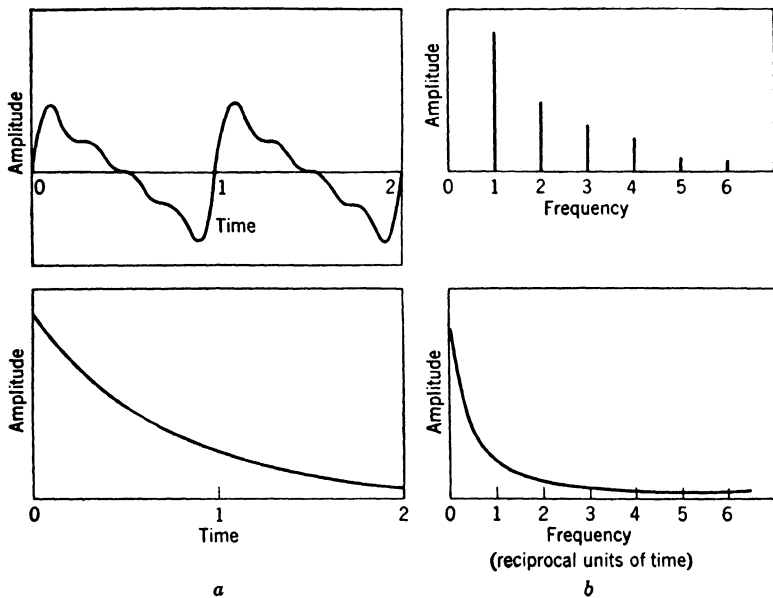


FIG. 12.20. (a) Periodic and (b) Aperiodic Function of Time and Corresponding Frequency Spectrum.

generally, 60 cycles per second. When an external circuit is attached to a microphone, alternating currents are generated in the circuit by sound waves impinging on the microphone. Similar currents are caused to flow in a phototube circuit when the phototube is exposed to a light beam that has passed through motion-picture sound track. The range of frequencies involved in these cases is, approximately, 30 to 10,000

<sup>19</sup> In this case

$$f(t) = \int_0^{\infty} \{A(\nu) \cos(2\pi\nu t) + B(\nu) \sin(2\pi\nu t)\} d\nu \quad (12.7)$$

with

$$A(\nu) = 2 \int_{-\infty}^{\infty} f(t) \cos(2\pi\nu t) dt$$

$$B(\nu) = 2 \int_{-\infty}^{\infty} f(t) \sin(2\pi\nu t) dt$$

cycles. Finally, television pickup tubes generate a *video signal*, reflecting the brightness variations in the image to be broadcast, which contains components with frequencies varying all the way from 30 cycles to 4 or 5 million cycles. In all these cases the signal of interest has, itself, the character of an alternating current or voltage or of a superposition of such currents or voltages. Under other circumstances it may be advantageous to convert a slowly varying, direct-current signal into alternating current in order to benefit by the greater ease of distinguishing the alternating current from background interference and by the intrinsic advantages of alternating-current amplification as compared with direct-current amplification. The last case requires, in general, the transmission of a relatively narrow band of frequency components, since the rate of variation of the signal or the *modulation frequency* is small compared to that of the alternating current being modulated or the *carrier*. The frequencies represented in the modulated carrier are simply the sums and differences of the carrier frequency and the modulation frequencies.<sup>20</sup> Their upper and lower limits are  $\nu_o + f_{\max}$  and  $\nu_o - f_{\max}$ , where  $\nu_o$  is the carrier frequency and  $f_{\max}$  indicates the most rapid variations of the original signal which are to be measured. For example, if the variations correspond to a change occurring within a second and the carrier frequency is 100 cycles per second, the frequency range of the modulated carrier is 99 to 101 cycles per second. This principle of modulation of a carrier is, of course, also employed in radio broadcasting, where a radio-frequency carrier of some 1,000,000 cycles per second is modulated by a sound or audio-frequency wave with  $f_{\max} = 5000$  cycles per second. This is seen to demand a broadcast frequency band 10,000 cycles per second wide, corresponding to only 1 per cent of the carrier frequency.

**Wide-Band Alternating-Current Amplifiers.** Alternating-current amplifiers which have to amplify signals covering a large range of fre-

<sup>20</sup> The modulated current may be represented by

$$i = A \sin (2\pi\nu_o t) \quad (12.8)$$

with

$$A = 1 + \sum_f a_f \cos (2\pi f t) + \sum_f b_f \sin (2\pi f t)$$

$\nu_o$  is the carrier frequency,  $a_f$  and  $b_f$  are modulation constants, and  $f$  represents the modulation frequencies. By the laws governing the combination of trigonometric functions the expression for the current  $i$  may be converted into a sum of sinusoidal components:

$$i = \sin (2\pi\nu_o t) + \sum_f \frac{1}{2} \{ a_f [\sin (2\pi(\nu_o + f)t) + \sin (2\pi(\nu_o - f)t)] \\ - b_f [\cos (2\pi(\nu_o + f)t) - \cos (2\pi(\nu_o - f)t)] \}$$

quencies show the greatest resemblance to direct-current amplifiers and, at the same time, present the most difficult design problems. The audio amplifiers of sound equipment, with a frequency range of 30 to 10,000 cycles per second, and the video amplifiers of television, having a pass band of 30 cycles to 4 megacycles per second or more, are typical representatives of this class of amplifiers. For their detailed consideration, the reader is referred to textbooks specializing in the subject.<sup>21</sup> Here it will suffice to discuss briefly the properties of the resistance-capacitance coupled amplifier, shown schematically in Fig. 12.21. The

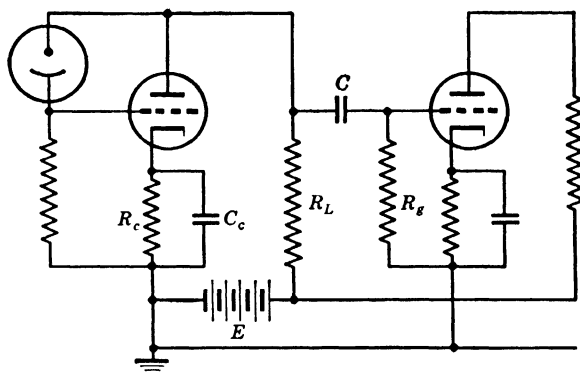


FIG. 12.21. Resistance-Capacitance-Coupled Amplifier.

principal difference between this amplifier and the direct-coupled amplifier shown in Fig. 12.10 is the presence of the *blocking condenser*  $C$  and the consequent possibility of employing a single voltage source for an amplifier of many stages. The grid bias is provided by the voltage drop produced by the direct-current component of the plate current in the cathode resistance  $R_c$ . The large parallel capacitance  $C_c$  of an electrolytic condenser provides a low-impedance path for the alternating-current component which, hence, does not effect the potential difference between cathode and ground. The primary advantage of this alternating-current amplifier over the direct-coupled amplifier is that it is easily adjusted and insensitive to small changes in the voltage supplies and the operating point of the tubes. The blocking condenser  $C$  must be chosen so that it has negligible leakage conductance; a change in the direct-current plate potential of one stage will then have no effect on the operation of the next.

The complete equivalent circuit of the coupling between two stages may be represented in the manner shown in Fig. 12.22. The amplifier

<sup>21</sup> See E.E. Staff of M.I.T., reference 5, Chapters 8–10, and Zworykin and Morton, reference 6, Chapter 14.

tube may be regarded as a current generator shunted by the internal tube resistance  $r_p$ , given by the slope of the plate characteristics of the tube. The current generated is given simply by the product of the signal voltage on the grid,  $V_g$ , and the transconductance  $g_m$ . Two additional shunt impedances, which are implicit in the diagram of Fig. 12.21, are the plate capacitance  $C_p$  and the grid capacitance  $C_g$ . The coupling circuit shown will give uniform response in the range of frequencies for which, on the one hand, the impedance of the grid resistance  $R_g$  in series with the parallel combination of the plate resistance  $r_p$  and the load resistance  $R_L$  is very large compared to the impedance of the blocking

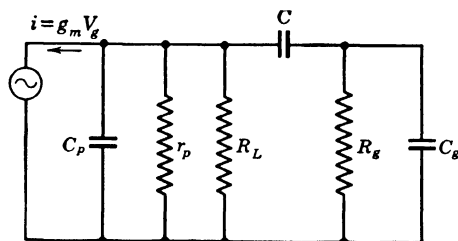


FIG. 12.22. Equivalent Circuit of a Resistance-Capacitance-Coupled Amplifier Stage.

capacitance  $C$  and, on the other, the shunt capacitances have a much smaller admittance (reciprocal impedance) than the three resistances in parallel.<sup>22</sup> For a given blocking capacitance the response at low frequencies is thus limited by the maximum permissible grid resistance; at high frequencies a flat response requires a small load resistance, cutting down the gain per stage. To give a numerical example, with a blocking capacitance of 0.1 microfarad and a grid resistance of 0.5 megohm, the low-frequency point at which the response is reduced to half its value at intermediate frequencies is about 30 cycles per second; at the high-frequency end, for a load resistance of 2000 ohms and a shunt capacitance of 20 micromicrofarads, the frequency at which the response is correspondingly reduced is approximately 4 megacycles per second.

In the simple resistance-capacitance coupled amplifier shown in Fig. 12.21 the variation of response with frequency at the two ends of

<sup>22</sup> The frequency  $f_1$  at which the response of a single stage is reduced to one half its value for  $C = \infty$  and that,  $f_2$ , at which it has dropped to one half the value for  $C_p = C_g = 0$  are given (see reference 5, p. 478) by

$$f_1 = \frac{1}{2\pi C R_1} \quad R_1 = \frac{r_p R_L}{r_p + R_L} + R_g = \frac{r_p R_L + r_p R_g + R_g R_L}{r_p + R_L} \quad (12.9)$$

$$f_2 = \frac{1}{2\pi(C_p + C_g)R_2} \quad R_2 = \frac{r_p R_L R_g}{r_p R_L + r_p R_g + R_L R_g} \quad (12.10)$$

the useful range is rather gradual. Various artifices have been employed to maintain the response at a nearly constant level up to a certain frequency, letting it drop rather sharply beyond this point. Thus the high-frequency response may be corrected to some extent by adding an inductance  $L = 0.44(C_p + C_g)R_L^2$  in series with the load resistance,<sup>23</sup>

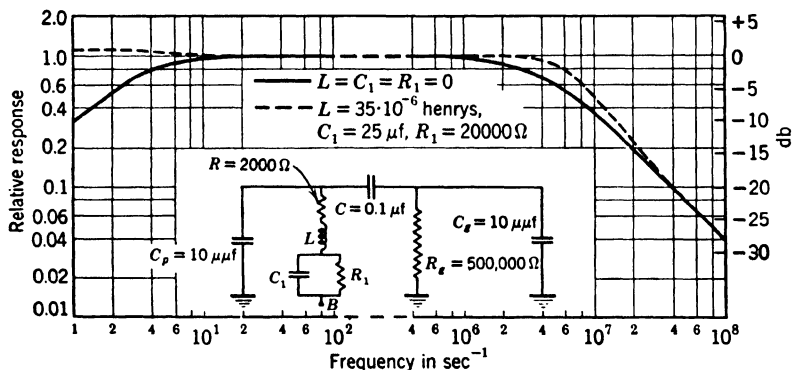


FIG. 12.23. Variation of Response with Frequency for a Resistance-Capacitance-Coupled Amplifier Stage and Effect of Adding Response-Correcting Network to Load Resistance.

and the low-frequency response, by adding a resistance  $R_1$  and capacitance  $C_1$ , of suitable dimensions, in parallel. The effect of such measures on the response is shown in Fig. 12.23.

**Periodically Interrupted Signals; Narrow-Band Alternating-Current Amplification.** The periodic interruption of a light beam offers the possibility of simultaneously converting a slowly varying signal into a

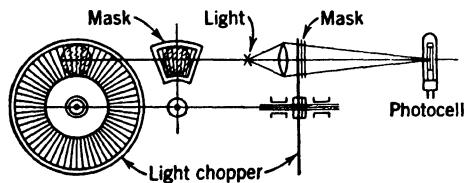


FIG. 12.24. Periodic Interruption of Light Beam to Be Measured by a Mechanical Light Chopper.

narrow-band high-frequency signal, with the attendant ease of amplification, and of discriminating between the light signal of interest and photocell dark currents as well as the effects of background lighting of the photosensitive surface. A simple way of accomplishing the interruption is shown in Fig. 12.24. The light beam is incident on a disk with

<sup>23</sup> See Zworykin and Morton, reference 6, p. 407.

a series of regularly arranged slots, driven by a synchronous motor or by clockwork. The stationary mask, into which is cut a series of slots identical with those on the disk, makes it possible to employ beams of considerable diameter. For constant illumination the photocurrent consists of a sequence of pulses with a fundamental frequency given by the product of the angular speed of rotation of the disk and the number of slots. This succession of pulses is equivalent to the sum of a direct-current component, given by the average of the photocurrent, a fundamental oscillation with a frequency equal to the repetition rate of the

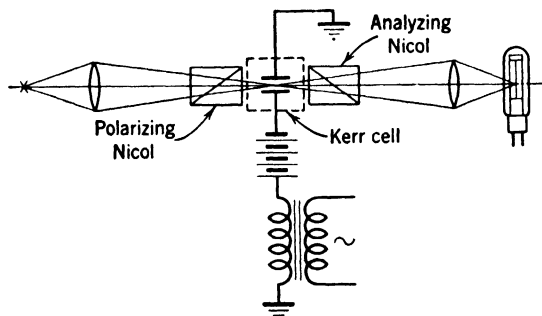


FIG. 12.25. Interruption of Light Beam by Kerr Cell Excited with Alternating Current.

pulses, and the harmonics of this fundamental frequency. Both the direct-current component and the several harmonics are readily eliminated by suitable electrical filter circuits, so that only the fundamental oscillation is left; for a slowly varying light intensity this oscillation is accompanied by "side bands," covering a range of frequencies which is a small fraction of the fundamental frequency or carrier.

The Kerr cell, used with a pair of polarizing filters, offers a nonmechanical method of interrupting the light beam (Fig. 12.25).<sup>24</sup> It consists of a glass vessel containing a suitable liquid (such as nitrobenzene) which is subjected to a strong electric field by a pair of condenser plates immersed in it. Polarizing filters, oriented at 45 degrees with respect to the electric field direction, and at right angles to each other, are placed on either side of the cell, so that, in the absence of the electric field, no light is transmitted through the cell. The electric field renders the liquid birefringent, so that an amount of light depending on the field strength passes through the combination of cell and polarizing filters. In the figure Nicol prisms are shown as polarizing filters; the direct-current bias on the cell serves to double the maximum field that may

<sup>24</sup> See Zworykin, Lynn, and Hanna, reference 7.



be applied to the cell. With this arrangement the interruption frequency becomes just equal to the frequency of the alternating field applied to the cell.

For the amplification of the interrupted photocurrent an amplifier employing tuned transformer coupling, as shown in Fig. 12.26, is suitable. This will filter out the direct-current component and the harmonics and, at the same time, give high gain for the fundamental frequency or carrier and its narrow side bands. For a pentode, with high plate resistance, the gain per stage of such an amplifier becomes, at the resonant

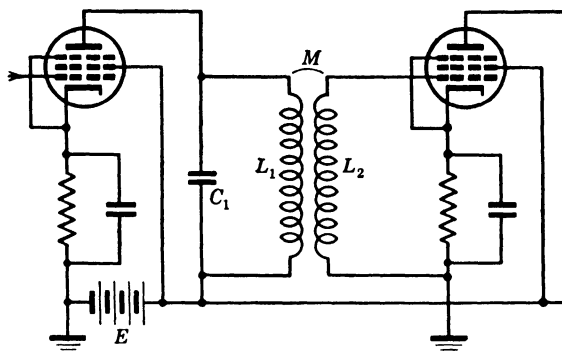


FIG. 12.26. Narrow Frequency Band Amplifier Stage Employing Tuned Transformer Coupling.

frequency  $\nu_o$  of the plate circuit  $L_1 C_1$ ,  $2\pi\nu_o g_m M Q$ ; here  $M$  is the mutual inductance of the transformer and  $Q$  is the ratio of the impedance of the inductance  $L_1$ ,  $2\pi\nu_o L_1$ , to the resistance  $R_1$  in the resonant circuit. The response is reduced to approximately one half its value at the resonant frequency ( $\nu_o \cong 1/[2\pi(L_1 C_1)^{1/2}]$ ) at frequencies which differ from  $\nu_o$  by  $\nu_o/Q$ . To give a numerical example,  $g_m = 10^{-3}$  ohm $^{-1}$ ,  $\nu_o = 1000$  cycles per second,  $L_1 = 0.1$  henry,  $L_2 = 1$  henry, and  $Q = 20$ , lead, for close transformer coupling ( $M = (L_1 L_2)^{1/2}$ ), to a voltage gain per stage equal to 40.

Obtaining interstage transformers with sufficiently high inductance and  $Q$  presents the major difficulty in circuits of this type. In the circuit shown in Fig. 12.27 this difficulty is circumvented by the use of positive or regenerative feedback at the carrier frequency. In this two-stage resistance-capacitance coupled amplifier the input impedance is a low- $Q$  resonant circuit. A fraction of the output is fed back to the input by means of the resistance  $R_1$ , and another portion, to the cathode resistance of the first stage by means of the resistance  $R_2$ . The first fraction adds, for the resonant frequency, but not for other frequen-

cies,<sup>25</sup> a voltage in phase with the original input, so as to enhance the amplification; the second acts as inverse feedback at all frequencies, stabilizing the gain of the amplifier. In practice, the resistances  $R_1$  and

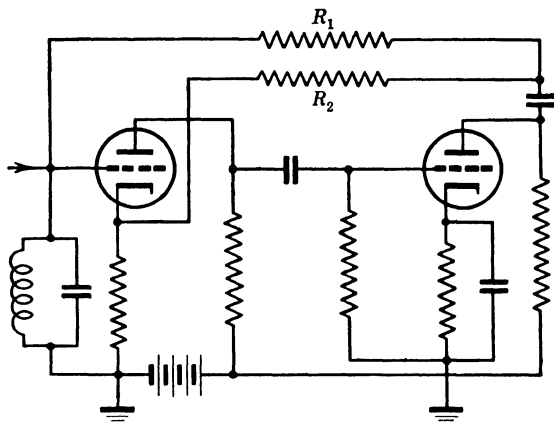


FIG. 12.27. Narrow-Band Amplifier Employing Regeneration at Carrier Frequency.

$R_2$  are adjusted until the gain and selectivity of the circuit are those desired.

The strength of the original signal may be measured by placing an alternating-current voltmeter or oscilloscope across the output of the amplifier. Alternatively, a direct-current instrument may be employed in conjunction with a diode circuit, as shown in Fig. 12.28. The product of the capacitance  $C$  and the resistance  $R$  is made of the same order as the least time interval (in seconds) for which signal changes are to be measured. During every positive half cycle of the carrier frequency, current passes through the diode and charges the condenser  $C$ , which has no opportunity to discharge appreciably in the course of the succeeding negative half cycle, maintaining a voltage difference corresponding to the amplitude of the carrier.

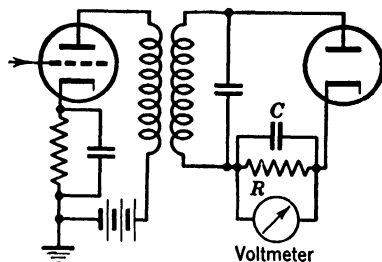


FIG. 12.28. Circuit Employing Diode and Direct-Current Meter for Measuring Amplitude of Amplifier Output.

<sup>25</sup> This follows from the fact that the impedance of the resonant circuit is a pure resistance for the resonant frequency, but deviates therefrom to an increasing extent with increasing deviation from resonance.

**Voltage and Current Regulation.** The satisfactory operation of amplifier circuits frequently requires voltage and current supplies of high constancy. Several methods have been developed for increasing the stability of power supplies.

The simplest means for obtaining constant currents, in the range of 30 milliamperes to 10 amperes, either alternating or direct current, is the *ballast tube*.<sup>26</sup> It consists of a thin iron filament in a helium or

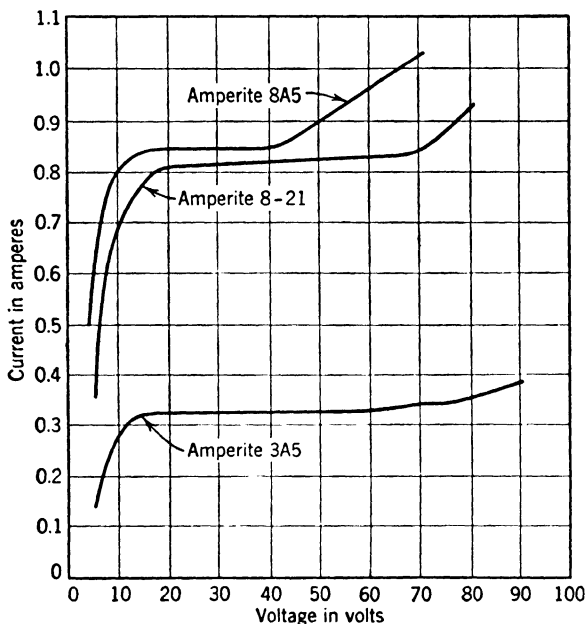


FIG. 12.29. Current-Voltage Characteristics of Some "Amperite" Ballast Tubes. (Taylor, reference 8.) (Courtesy of *Electronics*.)

hydrogen atmosphere enclosed in a glass bulb. As current flows through the wire and heats it, its resistance increases rapidly, so that, over a certain range, the filament current varies by less than 10 per cent for a change in voltage by a factor of 3. Typical ballast tube characteristics are shown in Fig. 12.29. The ballast tube, which is simply placed in series with the load (as, for example, a number of vacuum-tube filaments), has the drawback of a relatively slow reaction to voltage changes, reaching equilibrium in a period ranging from seconds to minutes.

The *magnetic regulator* (or constant-voltage transformer) serves primarily to smooth out voltage variations in an alternating-current

<sup>26</sup> See Taylor, reference 8.

line. It is faster than the ballast tube, correcting fluctuations within 1 or 2 cycles. The basic element of the magnetic regulator is a reactor or transformer which saturates in the range of operation of the regulator. The voltage output of this nonlinear circuit element is balanced against the output of linear circuit elements in such fashion that a constant output is obtained for a variable input. Figure 12.30 shows, as example, a three-legged transformer whose central leg saturates and outbalances the flux produced in the first leg, whose winding is in series with that of the central leg. As the primary current is increased, the flux produced in the third leg remains constant over a considerable range, the flux produced by each primary coil being increased by the same absolute amount.<sup>27</sup> Such magnetic regulators, manufactured by the General Electric Company and the Sola Electric Company in Chicago for a large range of power ratings, provide output voltages constant within about 1 per cent for variations in the input voltage between 95 and 130 volts. Their

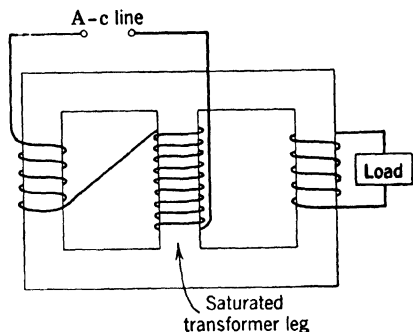


FIG. 12.30. Simple Magnetic Alternating-Current Regulator.

performance may be improved by the incorporation of capacitors.<sup>28</sup> Furthermore, if it is of importance to obtain an output which closely approximates a sinusoidal voltage variation, the output should be shunted by a number of inductance-capacity circuits which are series resonant for the harmonics of the fundamental frequency. This is necessary since harmonics accounting for approximately 25 per cent of the power output are normally generated by the nonlinear reactor.

The direct-current voltage across a load may conveniently be held constant by shunting it with a *gas-discharge regulator tube*, as shown in Fig. 12.31. In the rated range of operation of the tubes—generally from 5 to 30 or 40 milliamperes—the voltage drop across them varies by no more than 1 to 5 volts. The magnitude of the voltage drop may be 75 volts (type OA3), 90 volts (type 874), 105 volts (type OC3), or 150 volts (types OD3 and OA2). It is necessary to place a protective resistance in series with these tubes to prevent the current through them from exceeding the rated maximum value. A number of regulator tubes placed in series form a convenient potential divider whenever the cur-

<sup>27</sup> See Way, reference 9.

<sup>28</sup> See Uttal, reference 10.

rent demands of the load and the power output of the voltage supply meet their ratings.

High precision and high speed in voltage and current regulation are most readily attained with the aid of *vacuum-tube regulating circuits*.

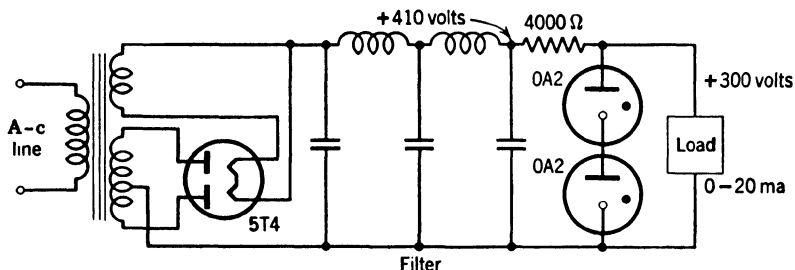


FIG. 12.31. Employment of Gas-Discharge Regulator Tubes for Stabilizing Output of Direct-Current Voltage Supply.

A comprehensive review of this field has been given by Hunt and Hickman.<sup>29</sup> Two feedback circuits, suitable for voltage and for current regulation, respectively, are represented in Fig. 12.32. In both cases a sample voltage, in the form of a fixed fraction of the voltage across the load or the potential drop produced by the load current across a fixed

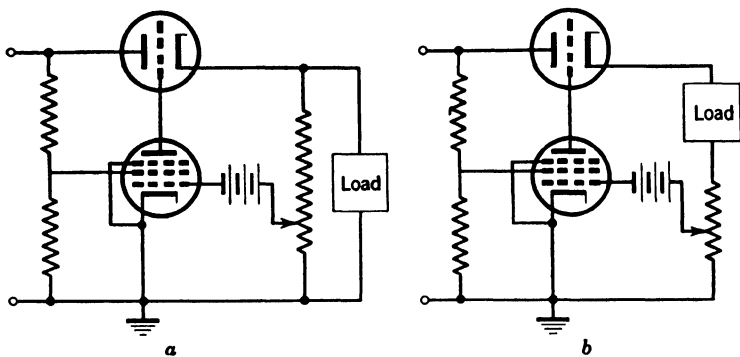


FIG. 12.32. Feedback Circuits for Stabilizing (a) Voltage across Load and (b) Current through Load.

resistance, is balanced against a standard battery and applied to the grid of a voltage amplifier tube, such as the 6SJ7. The amplified difference signal, in turn, is applied to the grid of a power triode in a cathode-follower connection. In high-voltage circuits the amplified

<sup>29</sup> See reference 11.

sample voltage may, instead, control the primary current of the high-voltage transformer or the amplitude of an exciting oscillator.<sup>30</sup>

## REFERENCES

1. B. LANGE, *Photoelements*, Reinhold Publishing Corporation, New York, 1937.
2. I. LANGMUIR, "The effect of space charge and residual gases on thermionic currents in high vacuum," *Phys. Rev.*, Vol. 2, pp. 450-486, 1913.
3. A. W. VANCE, "An improved vacuum tube microammeter," *Rev. Sci. Instruments*, Vol. 7, pp. 489-493, 1936.
4. E. S. RITTNER, "Improvement of the characteristics of photo-voltaic and photo-conductive cells by feedback circuits," *Rev. Sci. Instruments*, Vol. 18, pp. 36-38, 1947.
5. Electrical Engineering Staff of Massachusetts Institute of Technology, *Applied Electronics*, John Wiley and Sons, New York, 1943.
6. V. K. ZWORYKIN and G. A. MORTON, *Television—the Electronics of Image Transmission*, John Wiley and Sons, New York, 1940.
7. V. K. ZWORYKIN, L. B. LYNN, and C. R. HANNA, "Kerr cell method of recording sound," *Trans. Soc. Motion Picture Engrs.*, Vol. 12, pp. 748-759, 1928.
8. S. G. TAYLOR, "Ballast tubes as automatic voltage regulators," *Electronics*, Vol. 15, pp. 26-30, January, 1942.
9. K. J. WAY, "Voltage regulation using magnetic regulators," *Electronics*, Vol. 10, pp. 14-16, July, 1937.
10. J. A. UTTAL, "Voltage stabilizers," *Electronic Industries*, Vol. 4, pp. 90-94, 150, 154, August, 1945.
11. F. V. HUNT and R. W. HICKMAN, "On electronic voltage stabilizers," *Rev. Sci. Instruments*, Vol. 10, pp. 6-21, 1939.
12. V. K. ZWORYKIN, G. A. MORTON, E. G. RAMBERG, J. HILLIER, and A. W. VANCE, *Electron Optics and the Electron Microscope*, John Wiley and Sons, New York, 1945.

<sup>30</sup> See Zworykin, Morton, Ramberg, Hillier, and Vance, reference 12, Chapter 7.

## Chapter 13

# THE MEASUREMENT OF SMALL PHOTOCURRENTS

Suppose that a photocell, illuminated by a weak light beam interrupted at an audio frequency, is connected to a high-gain amplifier whose output, in turn, is fed to a loudspeaker. A tone corresponding to the frequency of interruption will be found to issue from the loudspeaker. As the light intensity is reduced, the loudness of the tone may be brought back to its original level by increasing the amplifier gain. However, this is possible only up to a certain point. Beyond this point the tone will be found to be submerged, first partly, then wholly, by a hiss which is a function of the properties of the amplifier only and is unaffected by further reduction of the light signal. This hiss or *noise* determines the smallest light signal which can successfully be detected and measured with the equipment under consideration.

**Shot Noise.** There are two principal sources of noise. The first, which results from the randomness with which electrons are emitted from a cathode, is known as *shot noise*, because, both in origin and in its frequency spectrum, this noise is closely analogous to that produced when metal shot is poured onto a plate. Suppose that the average number of electrons emitted by a cathode in a time interval  $T$  is  $n_o$ . The number  $n$  emitted by a cathode in any one particular time interval of this duration will then be, in general, slightly larger or slightly smaller than  $n_o$ . Statistics teaches that if the individual emissions of electrons are independent of each other, the average of the square of the difference of  $n$  and  $n_o$ , the *mean square deviation*, determined for many different intervals of equal duration  $T$ , is simply  $n_o$ :

$$\overline{(n - n_o)^2} = n_o \quad (13.1)$$

It applies both to thermionic emission and to the photoelectrons ejected

from a surface by illumination.<sup>1</sup> Finally, if  $n_o$  thermionic electrons fall, on the average, in the time interval  $T$  on a secondary-emissive surface with secondary-emission gain  $G$ , the mean square deviation in the number  $N$  of secondary electrons may be expected to be equal to the sum of the mean square deviation of the incident electrons multiplied by  $G^2$  and a term,  $Gn_o$ , which results from the random fluctuation in the gain factor for each individual primary electron:<sup>2</sup>

$$\overline{(N - Gn_o)^2} = G^2 n_o + Gn_o \quad (13.2)$$

In any external circuit connected to a thermionic tube, phototube, or secondary-emission multiplier, these random variations in electron emission give rise to fluctuations in electric current. Every individual current pulse corresponding to a single emission may be regarded as a superposition of sinusoidal current components of different frequency and phase. If all these are added up, squared, and averaged over a long time interval, the mean square value of the noise current contained within any frequency band  $f_2 - f_1$  may be calculated.<sup>3</sup> The result, valid for thermionic or photoemission, is

$$\overline{i_n^2} = 2ei_o(f_2 - f_1) = 32 \cdot 10^{-20} i_o(f_2 - f_1) \quad (13.3)$$

Here  $i_o$  is the average emission current. It is seen that the noise is uniformly distributed over the frequency spectrum.<sup>4</sup> Furthermore, as expected, it is proportional to the magnitude of the electronic charge, which specifies the "coarseness" of the "shot." For the secondary emission from a target of gain  $G$ , bombarded by a primary current  $i_o$ , the noise current becomes

$$\overline{i_n^2} = 2(G^2 + G)ei_o(f_2 - f_1) = 2(G + 1)ei_1(f_2 - f_1) \quad (13.4)$$

Here  $i_1$  is the secondary current. For moderately high gain  $G$ , the noise introduced by the secondary-emission multiplication is negligible

<sup>1</sup> Formula 13.1 is strictly applicable to photoemission only for low values of the quantum efficiency, where the randomness in the arrival of the photons at the surface plays a negligible role compared with the randomness in the emitted photoelectrons. More generally, Eq. 13.2, with  $G$  signifying the quantum efficiency (number of photoelectrons emitted, on the average, per incident light quantum) and  $n_o$  the number of incident light quanta, should be used.

<sup>2</sup> See Zworykin and Morton, reference 1, p. 36.

<sup>3</sup> See Zworykin and Morton, reference 1, p. 12.

<sup>4</sup> This applies for all frequencies small compared to the reciprocal transit time of the electrons in the tube. For higher frequencies the noise decreases.



compared with the multiplied noise present in the incident primary beam.<sup>5</sup>

**Thermal Noise.**<sup>6</sup> The second principal source of noise is to be sought in the random thermal motion of the charges within an electrical resistance. The average magnitude of the resulting voltage fluctuations across the terminals of the resistance is given by

$$\overline{V_n^2} = 4kTR(f_2 - f_1) = 1.6 \cdot 10^{-20} R(f_2 - f_1) \quad (13.6)$$

Here  $k$  is Boltzmann's constant,  $T$  is the absolute temperature,  $R$  is the resistance measured in ohms, and  $f_2$  and  $f_1$  are the upper and lower limits of the frequency band considered. The numerical coefficient has been calculated for room temperature ( $T = 293^\circ \text{K}$ ). Equation 13.6 gives the noise voltage for an arbitrary impedance,  $R$  denoting its resistive component.

**Noise Sources in Thermionic Amplifiers.** The primary sources of noise in a thermionic amplifier are (1) the resistive component of the input impedance and (2) the shot noise of the electron current in the first tube of the amplifier. Noise generated in later stages may usually be disregarded since it receives less subsequent amplification. Even though the tube noise is not given exactly by Eq. 13.3—it is reduced, on the one hand, by the action of space charge and increased, on the other, by the distribution of the electrons over different collector electrodes<sup>7</sup>—it is evenly spread over the frequency spectrum like true shot noise and thermal noise. For this reason it has become customary to describe the tube noise by indicating the value of an input resistance giving rise to equal voltage and current fluctuation in the output. Table 13.1<sup>7</sup> shows the equivalent noise resistance of a series of common amplifier tubes under typical conditions of operation.

In addition to this noise, amplifier tubes employing oxide-coated cathodes exhibit a type of noise known as *flicker*, which is limited to frequencies below 500 cycles per second. Flicker arises from random

<sup>5</sup> If Eq. 13.4 is applied to the case of photoemission ( $G$  = quantum efficiency,  $i_1$  = photocurrent), the ratio of the signal current  $i_s$  to the noise current  $(\bar{i_n^2})^{1/2}$  is seen to become independent of the quantum efficiency  $G$ , provided that the quantum efficiency is very large compared with unity and that the photocurrent is the chief source of noise:

$$\frac{i_s}{(\bar{i_n^2})^{1/2}} = k \cdot \frac{i_s}{(Gi_1)^{1/2}} = k \cdot \frac{L_s}{L_1^{1/2}} \quad (13.5)$$

Here  $L_s$  and  $L_1$  are the light signal, and the total amount of light falling on the photocathode, and  $k$  is the constant  $[2e(f_2 - f_1)]^{-1/2}$ .

<sup>6</sup> See Johnson, reference 2, and Nyquist, reference 3.

<sup>7</sup> See Thompson, North, and Harris, reference 4.

variations in the surface condition of the thermionic cathode. Unlike shot noise and thermal resistor noise, it is not an inherent property of amplifying systems and may be minimized or eliminated by proper choice and preparation of the cathode. *Microphonic noise*, resulting from instabilities in the amplifying tubes and circuit components, may

TABLE 13.1. EQUIVALENT NOISE RESISTANCE OF AMPLIFIER TUBES

<i>Type</i>	<i>Equivalent Noise Resistance in Ohms</i>
6SJ7 (as pentode)	5800
6AC7 (as pentode)	700
6AC7 (as triode)	200
6J5 (triode)	960
955 (triode)	1250

similarly be avoided by proper care in the design, construction, and installation of the amplifying apparatus.

**Electrometers and Electrometer Tubes.** The electrometer constitutes a straightforward instrument for the measurement of very small currents or voltages. In it a delicately suspended mobile member, maintained at a constant potential, is subjected to the electrostatic field between a pair of fixed quadrants, which are electrically connected to

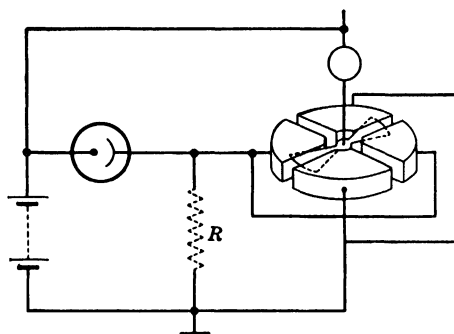


FIG. 13.1. Measurement of Photocurrents with the Quadrant Electrometer.

the point whose potential is to be measured, and a second pair of quadrants which are grounded. The deflection of the mobile member indicates the difference in potential between the two pairs of quadrants. Photocurrents may be measured with the electrometer in either of two ways (Fig. 13.1). If the photocurrent is made to flow to ground through the high resistance  $R$ , the potential drop across this resistance may be measured. As an alternative, the resistance may be removed, and the

rate measured at which the photocurrent charges up the electrometer capacity. In either case, the measurement of very low light levels requires excellent insulation of both the phototube electrodes (anode) and the electrometer electrodes. The principal drawback of this system is that high sensitivity demands extraordinarily delicate construction and adjustment of the electrometer.

This inconvenience is avoided if the electrometer is replaced by a vacuum tube. In principle, an amplifier tube with negative grid be-

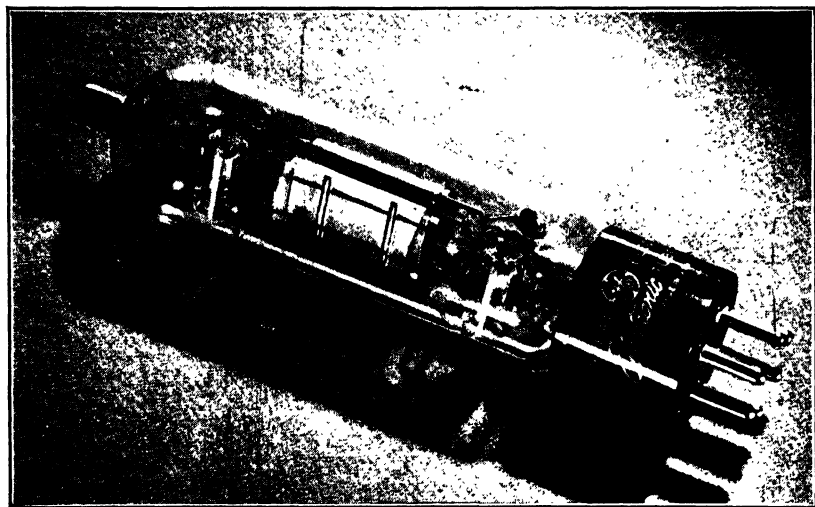


FIG. 13.2. The GI-5674 ("Split FP-54") Electrometer Tube. (Courtesy of General Electric Company, Schenectady, N. Y.)

haves very much like an electrometer. Ideally, the electrostatic potential of the grid controls the plate current (and hence the voltage indication) without any loss of charge. Unfortunately, this ideal condition is far from being realized in practice. Most amplifier tubes, under normal conditions of operation, draw sufficient grid current to make the employment of grid resistance in excess of a megohm inadvisable. Metcalf and Thompson <sup>8</sup> list six sources of this grid current:

1. Leakage over glass or insulation.
2. Ions formed by gas present in the tube.
3. Thermionic grid emission due to heating by the cathode heating power.
4. Ions emitted by the cathode.

<sup>8</sup> See reference 5.

5. Photoelectrons emitted by the control grid under action of light from the cathode.
6. Photoelectrons emitted from the control grid by soft x-rays produced by the normal anode current.

Fig. 13.2 shows a new version of the FP-54 electrometer tube<sup>9</sup> developed to eliminate these sources by proper construction and operation. Leakage is here minimized by bringing the grid lead out at the top of the tube and by careful internal insulation (1); ionization of the residual gas (2) and the production of soft x-rays (6) are prevented by the employment of a plate voltage of only 6 volts; thermal grid emission (3) and the emission of photoelectrons (5) are prevented by operating the filamentary cathode at a very low temperature; finally, the collection by the control grid of positive ions emitted by the filament (4) is prevented by the interposition of a positive *space-charge grid* between the cathode and the control grid. Normal conditions of operation of the FP-54 correspond to these parameters:

Filament voltage	2.5 volts
Plate voltage	6.0 volts
Control-grid bias	-4.0 volts
Space-charge grid voltage	4.0 volts
Filament current	100 ma
Plate current	40 $\mu$ a
Transconductance	$25 \cdot 10^{-6}$ ohm <sup>-1</sup>
Amplification factor	1.0
Plate resistance	40,000 ohms

In this manner a grid current less than  $10^{-15}$  ampere may be obtained and currents as small as  $10^{-17}$  ampere (60 electrons per second) can be detected if a high-sensitivity galvanometer is placed in the plate circuit.

Nielsen has since shown that quite comparable results may be obtained with standard radio tubes of the Acorn<sup>10</sup> type (Fig. 13.3).<sup>11</sup> The excellent insulation of all electrodes in these tubes makes it practical to use the third grid (normally the suppressor grid) as control grid and the screen grid as the space charge grid. As a typical example, a 959 Acorn tube, operated with plate and space-charge grid at 6 volts, first grid at 0.5 volt, a filament voltage of 0.5 volt, and a grid bias of -3.5 volts,

<sup>9</sup> Manufactured by the General Electric Company. Other electrometer tubes, the D-96475 and VW-41, are manufactured by the Western Electric Company and the Victoreen Instrument Company, respectively.

<sup>10</sup> The several electrodes of these tubes are brought out widely separated through the glass envelope.

<sup>11</sup> See Nielsen, reference 6.

yielded a plate current of 21 microamperes, a transconductance of  $20 \cdot 10^{-6} \text{ ohm}^{-1}$ , a grid current of  $1.7 \cdot 10^{-15}$  ampere, and an effective (negative) grid resistance of  $10^{16}$  ohms.

For normal phototube applications it is pointless to reduce the grid current to this extent, since the leakage current of the phototube itself is much larger; for the cartridge-type phototube 922 it is of the order of  $10^{-10}$  ampere. Hence a screen-grid tube with the control grid brought

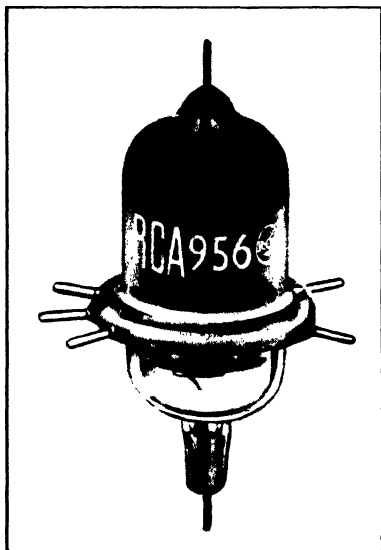


FIG. 13.3. An "Acorn" Tube.

out to a grid cap, such as the type 38, is quite satisfactory provided that the operating voltages and heater currents are kept small. For a screen voltage of 12 volts, a plate voltage of 8 volts, a heater voltage of 6 volts, and a grid bias of  $-2.25$  volts, Nielsen obtained, with the type 38 tube, a plate current of 200 microamperes, a transconductance of  $225 \cdot 10^{-6} \text{ ohm}^{-1}$ , a grid current of  $4 \cdot 10^{-12}$  ampere, and a grid impedance of  $0.8 \cdot 10^{12}$  ohms. A circuit for the measurement of small photocurrents employing the type 38 tube under somewhat similar operating conditions has already been shown in Fig. 12.13.

It should be noted that the employment of electrometer tubes for the measurement of extremely

small currents demands special methods of neutralizing the effects of battery drift and variations in the thermionic emission of the tube filament. Figure 13.4 shows a circuit by DuBridge and Brown<sup>12</sup> which realizes both requirements. All tube voltages are obtained from a single battery. The galvanometer reading is made independent of emission fluctuations by adjusting  $R_o$  so that  $R_b/R_o = I_p/I_s$ , since it may be assumed that the space-charge grid current  $I_s$  and the plate current  $I_p$  are equally affected by emission fluctuations. In addition, the variation of the galvanometer reading with the filament current  $I_f$  (that is, with the battery voltage) is made zero by adjusting either the grid bias ( $R_1$ ) or the resistance  $R_2$  until  $dI_p/dI_f = (R_b/R_o)(dI_s/dI_f)$ .

<sup>12</sup> See reference 7.

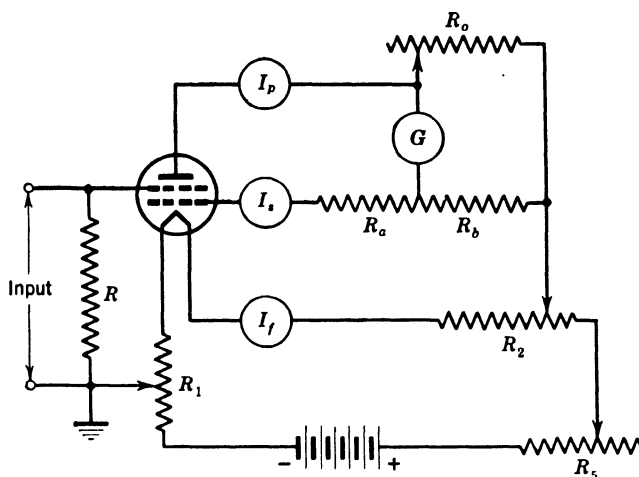


FIG. 13.4. Stabilized Electrometer Tube Circuit. (DuBridge and Brown, reference 7.) (Courtesy of Rev. Sci. Instruments.)

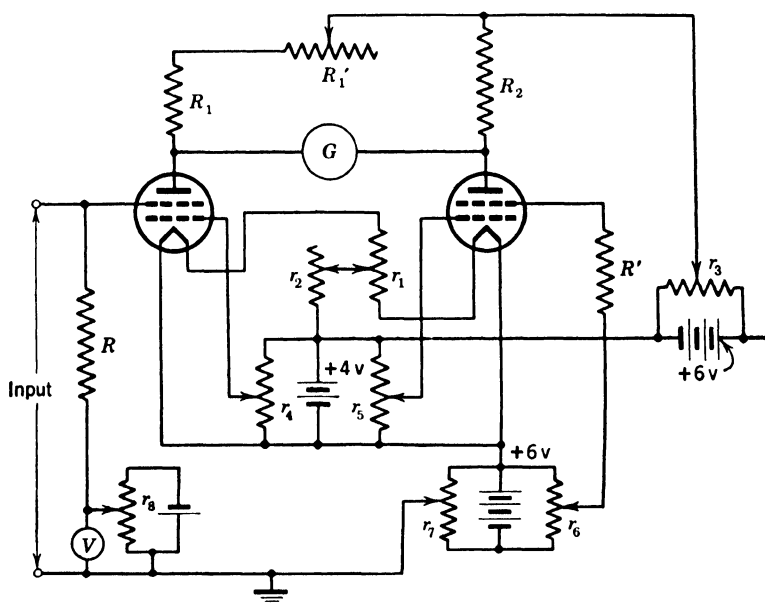


FIG. 13.5. Push-Pull Electrometer Tube Circuit. (DuBridge, reference 8.) (Courtesy of Phys. Rev.)

Still greater sensitivity and stability may be obtained with the bridge circuit employing two matched low-grid-current tubes shown in Fig. 13.5.<sup>13</sup> Here  $R_1'$  is varied until small changes in plate voltage, brought about by changing  $r_3$ , do not affect the galvanometer deflection. Furthermore, the contact on  $r_1$  is adjusted until small changes in  $r_2$ , controlling the filament current, leave the deflection unchanged. The galvanometer zero is restored after every adjustment by readjusting the grid potentials.

**Noise Reduction by Secondary-Emission Amplification.** Whenever the voltage drop produced by a photocurrent in an input resistor  $R$  is applied to the grid of the input tube of an amplifier, thermal resistance noise is added to the shot noise in the photocurrent. More precisely, whenever the voltage drop in the resistor produced by the total photocurrent  $i$  is less than 0.05 volt, the thermal resistance noise exceeds the shot noise.<sup>14</sup> Since the input resistance cannot be increased without limit<sup>15</sup> this condition is commonly met in practice. It then becomes very desirable to preamplify the photocurrent to a relatively high value by some method which does not introduce thermal noise. Such a method is secondary-emission amplification as applied in the multiplier phototube. A more detailed analysis<sup>16</sup> shows that the mean square noise current in the output of the multiplier exceeds only slightly the mean square noise current in the emission of the photocathode multiplied by the square of the gain of the multiplier tube. This excess decreases as the gain per stage of the multiplier is increased; for a gain per stage equal to 5, it is about 25 per cent. Secondary-emission amplification in the multiplier phototube raises the level of the signal current to a point

<sup>13</sup> See DuBridge, reference 8. For a simpler circuit using a single split FP-54 (GI-5674) tube see J. M. Lafferty and K. H. Kingdon, *J. Applied Phys.*, Vol. 17, pp. 894-900, 1946.

<sup>14</sup> The total noise voltage at the input is given by

$$\overline{V_n^2} = (2eiR^2 + 4kTR)(f_2 - f_1) = 1.6 \cdot 10^{-20} R(20iR + 1)(f_2 - f_1) \quad (13.7)$$

<sup>15</sup> This is especially true in high-frequency applications where the tube capacitances present a large shunt admittance.

<sup>16</sup> The considerations which led to Eq. 13.4, applied to the problem of deriving the noise output of an  $n$ -stage multiplier with a gain  $G$  per stage, result in this formula:

$$\overline{i_n^2} = 2ei_o(f_2 - f_1) \frac{G^{2n+1} - G^n}{G - 1} = 2ei_o(f_2 - f_1) \left( 1 + \frac{1}{G} + \cdots \right) G^{2n} \quad (13.8)$$

Here  $i_o$  is the emission current from the photocathode, comprising both photoemission and thermionic emission (dark current). Since the output signal current is  $i_s G^n$ ,  $i_s$  being the photocurrent generated by the light signal, the ratio of signal to noise currents becomes

$$\frac{i_s G^n}{(\overline{i_n^2})^{1/2}} = \frac{i_s}{\left[ 2ei_o(f_2 - f_1) \left( 1 + \frac{1}{G} + \cdots \right) \right]^{1/2}} \quad (13.9)$$

at which the amplified shot noise in the original photocurrent overrides the thermal noise generated in the input resistance of a succeeding conventional amplifier—as well as the tube noise of the amplifier—*without* reducing the signal-to-noise ratio to a value appreciably below that of the original photocurrent.

**Multiplier Phototube Circuits.** Insofar as the multiplier phototube requires operating voltages of the order of 1000 volts or more, it necessitates power supplies which differ from those for ordinary phototubes. A number of these are shown in Fig. 13.6, *a-d*.<sup>17</sup> The first (*a*) represents a multiplier operated directly by a high-voltage transformer connected to the alternating-current line. When illuminated, the multiplier passes appreciable current only near the peak of the positive half cycles, since the multiplier gain increases very rapidly with increasing voltage. The arrangement shown is particularly convenient for relay applications. In (*b*) the multiplier is fed by direct current, obtained by rectifying the output of a high-voltage transformer and smoothing the remaining pulsations with the aid of an electric filter, here represented simply by a shunt capacitance. The resistance bleeder from which the voltages for the individual electrodes are obtained must be dimensioned so that the current through it is at least ten times as large as the maximum current drawn by any of the electrodes; otherwise the tube gain will be appreciably affected by changes in illumination. A circuit of this type, with good filtering, will be found suitable for the measurement of very small light fluxes. In portable equipment similar operating characteristics may be obtained (*c*) by generating the high voltage with the aid of a battery-operated automobile vibrator.<sup>18</sup> At the instant at which the current is interrupted a relatively high voltage peak appears across the primary of the transformer, which is tuned by a shunt capacitance to the resonant frequency of the secondary. The output of the secondary is rectified, filtered, and applied to the bleeder for the multiplier electrodes. This voltage supply, developed for infrared detection equipment, will deliver 0.15 watt output at up to 4000 volts for an input of 1 watt and weighs only about 2½ pounds.

A last circuit is shown in (*d*). Here a high radio-frequency voltage is developed across the coil of a series resonant circuit fed by an oscillator; the multiplier electrodes are connected directly to taps on the coil. As in (*a*), the multiplier passes current only near the peak of each cycle. This circuit can measure any light variations extending over a time which is appreciably longer than the period of the radio frequency. The apparent sensitivity is approximately the same with direct- and alter-

<sup>17</sup> See Rajchman and Snyder, reference 9.

<sup>18</sup> See Morton and Flory, reference 10.



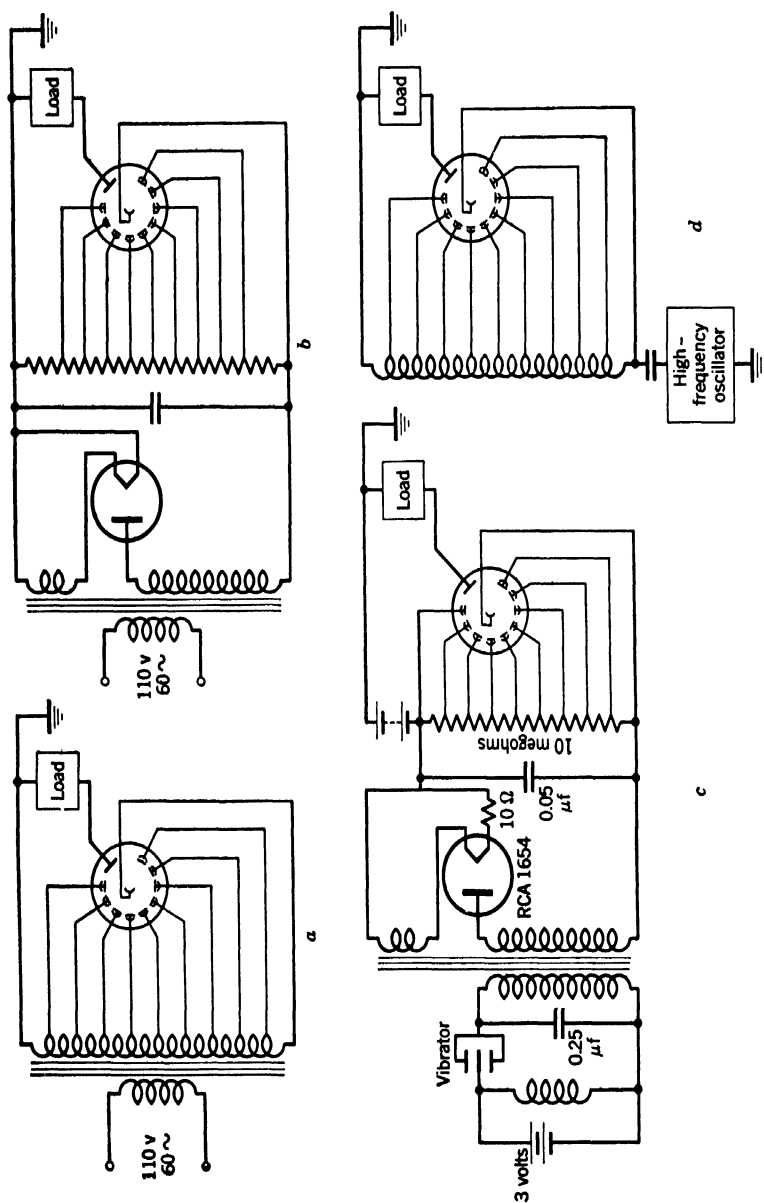


FIG. 13.6. Multiplier Phototube Circuits: (a) Alternating-Current Operation; (b) Direct-Current Supply, Derived from A-C Line; (c) Direct-Current Supply, Derived from Battery-Operated Vibrator; (d) High-Frequency Operation.

nating-current operation, for equal root-mean-square operating voltages. However, the signal-to-noise ratio is smaller with alternating-current operation by a factor of  $\frac{1}{4}$ , primarily because of the small fraction of each cycle during which the multiplier operates.

### Measurement of Very Low Light Levels with a Multiplier Phototube.

The employment of multiplier phototubes for the measurement of low

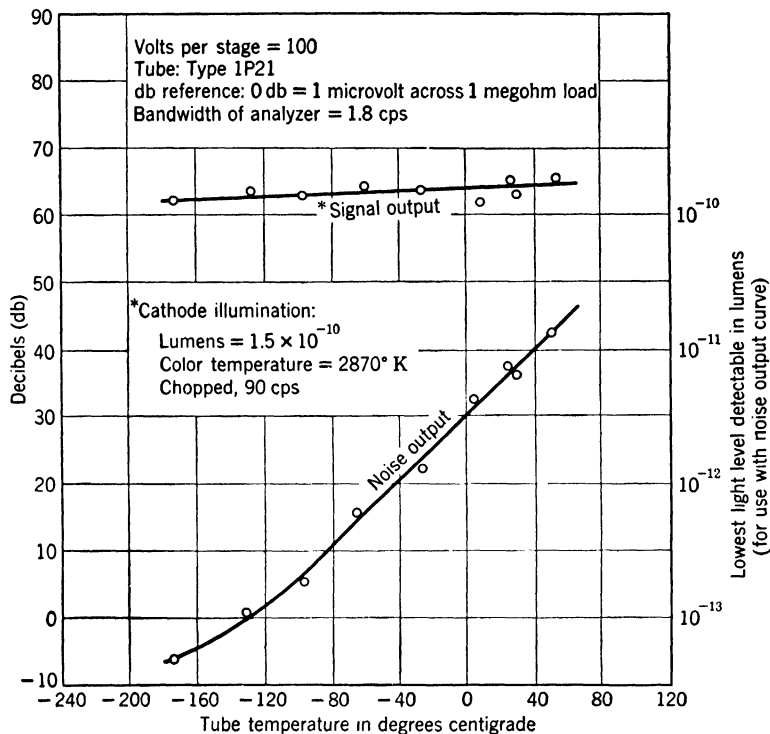


FIG. 13.7. Signal Output and Noise Output of 1P21 Multiplier Phototube as Function of Temperature. (Engstrom, reference 11.) (Courtesy of *J. Optical Soc. Am.*)

light levels has been studied in some detail by R. W. Engstrom.<sup>19</sup> Figure 13.7 shows results obtained with a 1P21 multiplier phototube illuminated by light interrupted at a frequency of 90 cycles per second. The output was measured after amplification by an amplifier with a 1.8 cycle-per-second pass band. It is seen that, as the tube is cooled, the noise output decreases rapidly—in consequence of the decreasing thermionic emission—although the signal output is scarcely affected. At liquid-air temperature ( $-180^\circ \text{C}$ ) the signal-to-noise ratio is approx-

<sup>19</sup> See reference 11.

imately 68 decibels<sup>20</sup> or 2500 for a light flux of  $1.5 \cdot 10^{-10}$  lumen. Accordingly, light fluxes down to about  $6 \cdot 10^{-14}$  lumen can be detected

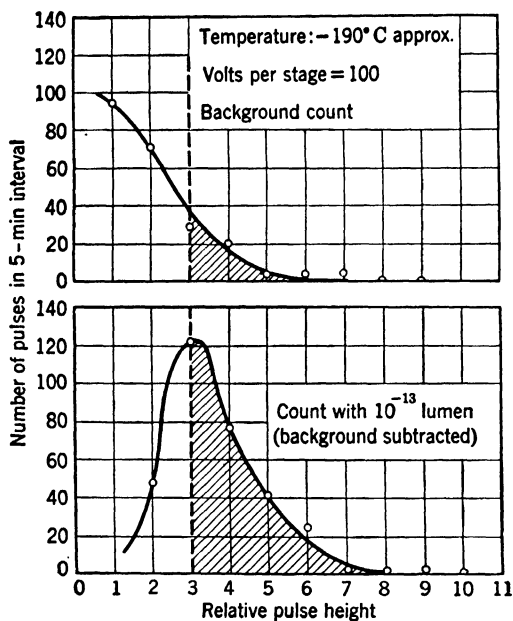


FIG. 13.8. Pulse Height Distribution in Output of 1P21 Multiplier Phototube: (a) Without Illumination; (b) With Light Flux of  $10^{-13}$  Lumen on Photocathode, the Dark Current Having Been Subtracted Out. Shaded areas show the number of counts remaining in each case if only those exceeding a certain amplitude are recorded. (Engstrom, reference 11.) (Courtesy of *J. Optical Soc. Am.*)

with this arrangement. An equal flux of green light corresponds to about 260 quanta per second.

<sup>20</sup> The decibel (abbreviated db) is a logarithmic measure of power. The power  $P$ , in decibels, referred to the reference level  $P_0$ , is defined as

$$P(db) = 10 \log_{10} \frac{P}{P_0} \quad (13.10)$$

Since the voltage (or current) required to generate a given power in a fixed impedance is proportional to the square root of that power, voltage and current may similarly be measured in decibels in accord with the equations

$$V(db) = 20 \log_{10} \frac{V}{V_0} \quad i(db) = 20 \log_{10} \frac{i}{i_0} \quad (13.11)$$

$V_0$  and  $i_0$  here correspond to the reference level  $P_0$ . It is seen, for example, that 60 decibels correspond to a voltage ratio of 1000 or a power ratio of 1,000,000.

The greatest sensitivity can be obtained by counting individual current bursts at the anode, resulting from photoelectrons and thermionic electrons emitted by the photocathode. For this purpose the output of the multiplier phototube is fed through a broad-band amplifier to a cathode-ray oscillograph. The current peaks appearing on the screen of the oscillograph are counted over a prolonged period, both with the cathode in the dark and with it exposed to the light to be measured. The difference of the two counts yields the number of photoelectrons emitted in the period in question. A plot of the distribution of the number of counts with respect to their amplitude is shown in Fig. 13.8. It is seen that a much larger proportion of the dark-current pulses than of those arising from the illumination is of small amplitude. The small-amplitude pulses result primarily from thermionic electrons given off by the intermediate multiplier stages, which are multiplied by a smaller factor. The width of the pulse distribution for the photoelectrons results simply from the statistical fluctuation in the secondary-emission multiplication process. By counting only pulses higher than some arbitrary value, slightly below the most frequent pulse height for the photoelectron pulses, the background count can be greatly reduced. This reduction will also be reflected in a reduction in the error resulting from the fluctuation of the background count between the two counts, or in the noise which limits the least light signal that can be detected. Light fluxes of the order of  $2 \cdot 10^{-16}$  lumen, giving rise to about a count per minute, can still be detected in this manner. This illumination corresponds to approximately 1 quantum of light per second falling on the cathode. The counting method described yields very high signal-to-noise ratios, since here the effective frequency band is simply equal to the reciprocal of the counting time.

**Gas-Discharge Counters.** Another device which makes it possible to count individual photoelectrons and which may therefore be used to measure extremely low light levels is the gas-discharge counter, commonly designated as the Geiger-Mueller counter. For details of this exceedingly valuable tool in the field of nuclear physics the reader is referred to Korff's monograph.<sup>21</sup> The most common form of the Geiger-Mueller counter is a cylindrical cathode with a thin wire anode stretched along its axis, all enclosed in a glass envelope, as shown in Fig. 13.9. The filling of the counter is a suitable gas at such a pressure that the mean free path of an electron in it is much smaller than the separation of cathode and anode. Physically, it is thus very similar to a gas-filled phototube. However, it differs from it materially in its mode of opera-

<sup>21</sup> See reference 12. Regarding the application of the multiplier phototube in the nuclear field, see Chapter 14, p. 316.

tion. In the gas-filled phototube every photoelectron causes a limited number of ionizations, amplifying the photocurrent, but the tube current remains proportional to the number of photoelectrons emitted. In the counter, on the other hand, a sufficiently high voltage is applied between the electrodes so that the emission of a photoelectron simply initiates a self-sustained gas discharge whose amplitude and duration

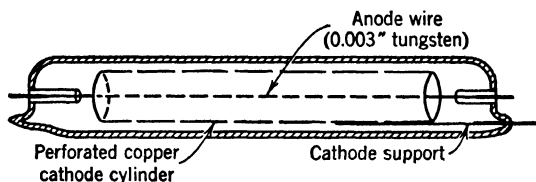


FIG. 13.9. Geiger-Mueller Counter Suitable for Ultraviolet Radiation Measurements.

are determined by the external circuit. As shown in Fig. 13.10, the discharge continues until the discharge current has charged the capacitance  $C$  sufficiently negative that the potential difference between cathode and anode no longer suffices to maintain the discharge. Electrons, between collisions, do not acquire enough energy from the applied field to ionize. The resistance  $R$  is chosen high enough so that the voltage

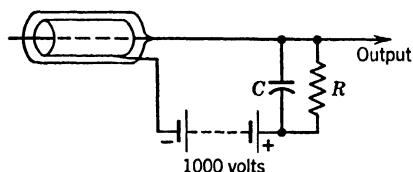


FIG. 13.10. Counter Circuit for Quenching Gas Discharge.

does not have time to build up again before the free charges have returned to the electrodes.

In the measurement of very small light fluxes the gas discharge counter is inferior to the multiplier phototube insofar as the rapidity with which counts can be made is limited by the recovery time, during which the

counter is insensitive. This is of the order of  $10^{-4}$  second. The counting speed of the multiplier phototube, on the other hand, is limited only by the speed of the counting system. There are applications, however, for which the gas-discharge counter is especially suitable. The fire and flame detector of Weisz<sup>22</sup> is an example. Ordinary enclosed light sources, as well as daylight, supply practically no ultraviolet radiation in the range beyond 2700 Angstrom units. Open fires,

<sup>22</sup> See reference 13. For more general discussions of photoelectric counters and their uses, the reader is referred to Locher, reference 14, and Duffendack and Morris, reference 15.

flames, and sparks, on the other hand, give off such radiations in appreciable amounts. The radiant power emitted by a burning match, considered as a black body at  $1700^{\circ}\text{C}$ , in the range of 2550 to 2650 Angstrom units, is approximately  $10^{-5}$  watt per square meter—about a millionth as much at 2600 Angstrom units as in the yellow, at 6000 Angstrom units. Even at a distance of 30 feet from the burning match, approximately 300 quanta in the range of 2550 to 2650 Angstrom units arrive at 1 square centimeter area from 1 square centimeter of the flame in every second.

**Noise in Photoconductive Cells.**<sup>23</sup> Two types of noise are observed in photoconductive cells: thermal resistance noise, which is independent of the applied voltage, and voltage-sensitive noise, which may be ascribed to fluctuations in the thermal excitation of the semiconductor. The total noise voltage is thus given by

$$\overline{V_n^2} = k_1 \frac{w}{l} + k_2 \frac{E^2}{lw} \quad (13.12)$$

Here  $k_1$  and  $k_2$  are (temperature-sensitive) constants,  $w$  is the width of the semiconductor strip (separation of electrodes),  $l$  is its length, and  $E$  is the applied voltage. The second, voltage-dependent, term predominates in thallous sulfide photoconductive cells and in lead sulfide cells of very small surface area (or cells operated at high voltages). Since the effect of illumination is, ideally, to produce a proportional change in the conductivity of the semiconducting layer, the signal voltage is given by

$$V_s = k_3 \frac{L_s E}{lw} \quad (13.13)$$

$L_s$  denotes the light flux incident on the cell. It follows from Eqs. 13.12 and 13.13 that the signal-to-noise ratio is inversely proportional to the square root of the cell area for constant flux, directly proportional to the square root of the cell area for constant illumination—provided that the voltage-sensitive part of the noise predominates. This circumstance leads to the practical conclusion that the greatest sensitivity can be obtained by reducing the flux to be measured to the smallest cross-section area possible and adapting the cell dimensions to this cross-section area.

The voltage-sensitive part of the noise, like the signal, shows appreciable dependence on the frequency. This dependence is exhibited by

<sup>23</sup> See Cashman, reference 16.

the curves in Fig. 13.11, showing signal and noise for a particular cell at room temperature and dry-ice temperature ( $-80^{\circ}\text{C}$ ) as a function of frequency. It is seen that the signal is affected to a much greater extent by the cell temperature than the noise. The cell resistance at room temperature was 0.5 megohm, its area was 0.5 millimeter squared.

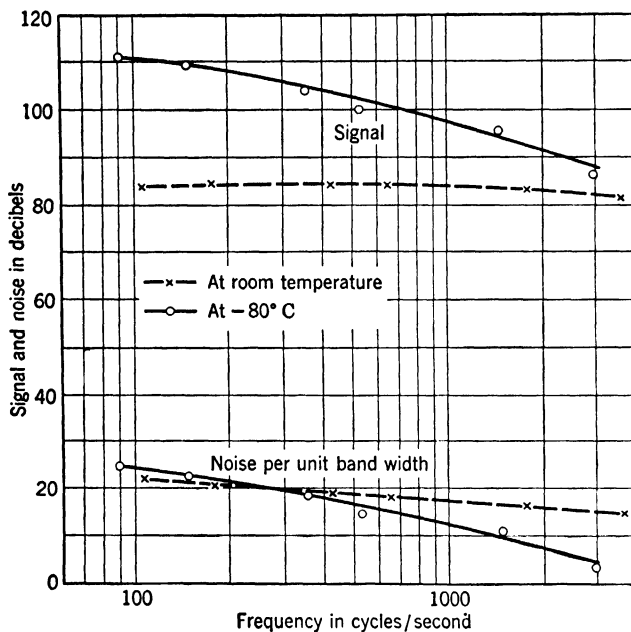


FIG. 13.11. Signal and Noise for a Lead Sulfide Photoconductive Cell at Room Temperature and at Dry Ice Temperature ( $-80^{\circ}\text{C}$ ) as Function of Frequency. Light flux:  $10^{-6}$  hololumen from  $2848^{\circ}\text{K}$  source. Operating voltage: 45 volts. Cell area: 0.5 mm<sup>2</sup>. Dark resistance at room temperature: 0.5 megohm. Reference level (0 db): 1 microvolt. (Cashman, reference 16.)

Another quantity of interest is the amount of radiant energy from a body at a temperature above ambient temperature required to produce a signal in the photocells just equal to the noise. This least detectable radiant flux is plotted as function of the temperature of the source in Fig. 13.12. The cell is the same as that yielding the values plotted in Fig. 13.11.

It is unfortunately not practical to make a direct comparison of the sensitivity of photoconductive cells and multiplier phototubes on the basis of available data. Some indication of this is given, however, by the following statement: The signal-to-noise ratio at low frequencies and per unit band width is, for a light flux of 1 microhololumen, for a lead

sulfide cell cooled to  $-80^{\circ}\text{C}$ , 87 decibels;<sup>24</sup> for a 1P21 multiplier phototube it is, under similar circumstances, 130 decibels.<sup>25</sup> By this test the multiplier phototube is thus more than one hundred times as sensitive as the particular lead sulfide cell considered. This suggests that, in the

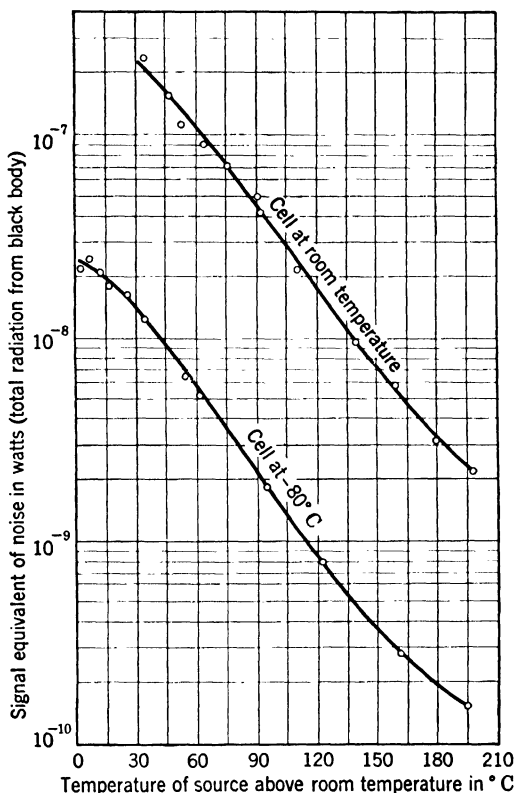


FIG. 13.12. Signal Equivalent of Noise as Function of the Temperature of the Source for the Same Lead Sulfide Photoconductive Cell as Fig. 13.11. Frequency: 270 cycles per second; Band width: 5 cycles per second. (Cashman, reference 16.)

detection of very small amounts of radiation, the multiplier phototube is superior except where, as in the infrared, it is relatively insensitive. In this region the photoconductive cells are supreme.

As compared with ordinary phototubes, both the thallous sulfide and the lead sulfide cells have an advantage in sensitivity in the range of low signal frequencies. A comparison of the lead sulfide cell with a gas-

<sup>24</sup> See Cashman, reference 16.

<sup>25</sup> See Engstrom, reference 11.



filled phototube is particularly valid, since both have a linear response to illumination and comparable dynamic characteristics in the audio range. Figure 13.12 shows that a particular lead sulfide cell at room temperature, irradiated with 1 microhololumen, yields a signal-to-noise ratio, for unit frequency band width, of about 64 decibels. A gas-filled phototube with a sensitivity of 125 microamperes per lumen, employed with a coupling resistance of 500,000 ohms—equal to the dark resistance of the lead sulfide cell—yields, for the same illumination, a signal-to-noise ratio of  $20 \log_{10} [V_s/(\bar{V}_n^2)^{1/2}] = 20 \log_{10} [iR/(1.6 \cdot 10^{-20} R)^{1/2}] = 57$  decibels.

### REFERENCES

1. V. K. ZWORYKIN and G. A. MORTON, *Television*, John Wiley & Sons, New York, 1940.
2. J. B. JOHNSON, "Thermal agitation of electricity in conductors," *Phys. Rev.*, Vol. 32, pp. 97-109, 1928.
3. H. NYQUIST, "Thermal agitation of electric charge in conductors," *Phys. Rev.*, Vol. 32, pp. 110-113, 1928.
4. B. J. THOMPSON, D. O. NORTH, and W. A. HARRIS, "Fluctuations in space-charge-limited currents at moderately high frequencies," *RCA Rev.*, Vol. 4, pp. 269-285, 441-472, 1940; Vol. 5, pp. 244-260, 371-388, 505-528, 1940-1941; and Vol. 6, pp. 114-124, 1941.
5. G. F. METCALF and B. J. THOMPSON, "A low grid-current vacuum tube," *Phys. Rev.*, Vol. 36, pp. 1489-1494, 1930.
6. C. E. NIELSEN, "Measurement of small currents; characteristics of types 38, 954, and 959 as reduced grid current tubes," *Rev. Sci. Instruments*, Vol. 18, pp. 18-31, 1947.
7. L. A. DuBRIDGE and H. BROWN, "An improved d.c. amplifying circuit," *Rev. Sci. Instruments*, Vol. 4, pp. 532-536, 1933.
8. L. A. DuBRIDGE, "The amplification of small direct currents," *Phys. Rev.*, Vol. 37, pp. 392-400, 1931.
9. J. A. RAJCHMAN and R. L. SNYDER, "An electrically focused multiplier phototube," *Electronics*, Vol. 13, pp. 20-23, December, 1940.
10. G. A. MORTON and L. E. FLORY, "An infra-red image tube and its military applications," *RCA Rev.*, Vol. 7, pp. 385-413, 1946.
11. R. W. Engstrom, "Multiplier phototube characteristics: application to low light levels," *J. Optical Soc. Am.*, Vol. 37, pp. 420-431, 1947.
12. S. A. KORFF, *Electron and Nuclear Counters*, D. Van Nostrand Company, New York, 1946.
13. P. B. WEISZ, "Electronic fire and flame detector," *Electronics*, Vol. 19, pp. 106-109, July, 1946.
14. G. L. LOCHER, "Photoelectric quantum counters for visible and ultra-violet light," *Phys. Rev.*, Vol. 42, pp. 525-546, 1932.
15. O. S. DUFFENDACK and W. E. MORRIS, "An investigation of the properties and applications of the Geiger-Müller photoelectron counter," *J. Optical Soc. Am.*, Vol. 32, pp. 8-24, 1942.
16. R. J. CASHMAN, "Development of sensitive lead sulfide photoconductive cells for detection of intermediate infra-red radiation," *O.S.R.D. Report 5998*, Oct. 31, 1945.

## Chapter 14

# PHOTOELECTRIC MEASURING DEVICES

The most obvious use of the photocell is for the measurement of radiant flux. In this capacity it can effectively substitute for a human observer. In certain respects it can even go considerably beyond the human observer. First of all, it may be used to measure infrared and ultraviolet radiations, to which the eye is not sensitive. Second, it does not require continuous comparison of the measured light with the output of a standard light source, though this procedure may enhance the accuracy of the results.

**Phototube and Barrier-Layer Cell in Photometry.** The condition that the response remain constant over long periods of time is fulfilled only approximately by most photosensitive devices. This limitation was recognized, for the phototubes of their time, by Ives and Kingsbury<sup>1</sup> and other early workers. Measurements of the highest precision, therefore, require comparison methods similar to those used in visual photometry. It has been found that photoelectric methods of detection lend themselves well to such procedures of measurement.

It should be emphasized, however, that continuous comparison is necessary only in very high precision work. With reasonable precautions vacuum phototubes will be found to give reliable results if they are recalibrated periodically. As long as the output current and the operating voltage<sup>2</sup> are kept well below their maximum rating, the voltage supply is well regulated, and the ambient temperature is maintained reasonably constant, the response is linear and free from short-period fatigue effects. Gas phototubes are not well suited for measurement purposes.

<sup>1</sup> See reference 1.

<sup>2</sup> Linearity of response requires also that the operating voltage be high enough for the emission to be substantially saturated. Great long-time stability in vacuum phototubes, on the other hand, may be attained by keeping the operating voltage below 20 volts.

The barrier-layer photocell is less well adapted for precision measurements than the vacuum phototube for two reasons: (1) It exhibits a certain amount of fatigue at all light levels—approximately 3 minutes may elapse before the equilibrium current for a given illumination is attained—and (2) its response is nonlinear, often even at low light levels.<sup>3</sup> It has been seen that the second factor may be nullified by vacuum tube circuits which keep the voltage across the cell constant.<sup>4</sup> Furthermore, the measurement of very small light fluxes is made difficult by the very large cell capacity and its low voltage sensitivity. Finally, in some special applications, lack of choice in the spectral response of the barrier-layer cells may militate against their use.

Against these drawbacks may be set a series of decided advantages, such as the superfluity of a voltage supply, very great current sensitivity, and mechanical ruggedness. Furthermore, the selenium barrier-layer cells are characterized by a very large operating range and good long-time stability. Their spectral response comes closer to that of the eye than that of any commercial phototube and may be corrected, by the addition of a low-absorption filter, so as to follow the mean visibility curve very closely.<sup>5</sup>

These considerations mark out the proper spheres of application of phototubes and barrier-layer cells. Phototubes are used to advantage primarily where the precision required is high and where the light flux to be measured is small. Examples are precision lamp photometry and spectrophotometry—a field in which the extraordinary sensitivity of multiplier phototubes is particularly valuable. In addition, phototubes are required whenever measurements are extended into the ultraviolet region. Barrier-layer photocells, on the other hand, are applied predominantly for the measurement of illumination and photographic exposure by portable instruments. Here the light flux to be measured is generally relatively large, and the required precision is only moderate. At the same time the compactness and the simplicity of the barrier-layer cell measuring equipment are decided advantages.

**Measurement of Light Sources and Illumination.** One of the principal objectives of photometry is the measurement of the total light output, the color temperature, and the angular distribution of light flux from light sources. The methods to be used depend to some extent on the nature of the light source. They have been developed most completely for the incandescent lamp.

<sup>3</sup> See Björnstahl, reference 2.

<sup>4</sup> See Chapter 12, p. 231.

<sup>5</sup> See Fig. 11.7, p. 204.

The total light output of a lamp is generally determined by placing the lamp into a large *integrating sphere* with diffusely reflecting inner walls (Fig. 14.1). A photocell receives the light flux leaving the sphere through a small window. The system is calibrated by measuring the photocurrent obtained when a standard light source of known emission characteristics is placed in the sphere. If the response of the photocell is linear, the ratio of the two photocurrents so measured is equal to the ratio of the luminous flux emitted by the source to be measured and

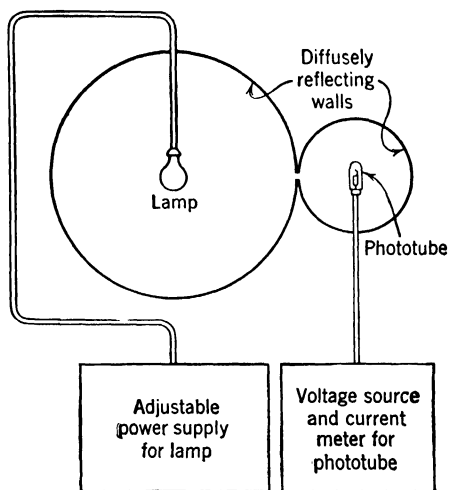


FIG. 14.1. The Measurement of the Total Light Output of a Lamp.

that emitted by the standard lamp, provided that *either* of these conditions is fulfilled:

1. The two sources have the same spectral distribution. For thermal sources with a distribution approximated by Planck's radiation law <sup>6</sup> this is equivalent to saying that they have the same color temperature.
2. The spectral response of the photocell, eventually modified by suitable filters, corresponds to the mean visibility curve of the human eye.<sup>7</sup>

In practice, filters increase the similarity between the effective photocell spectral response and the visibility curve. Forsythe <sup>8</sup> found that,

<sup>6</sup> See Chapter 2, pp. 16 and 17.

<sup>7</sup> See Fig. 2.7, p. 23.

<sup>8</sup> See reference 3.

if the sources are restricted to filament lamps with color temperatures ranging from 2270° to 2970° K (corresponding to a 500-watt gas-filled tungsten lamp), an accuracy of 1 per cent could be obtained with a (red-sensitive) silver-cesium phototube and a green filter. If two

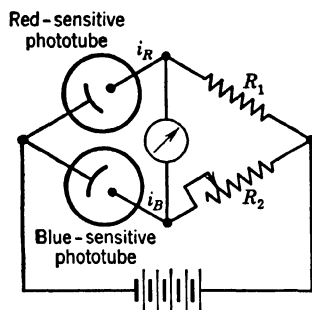


FIG. 14.2. Bridge Circuit for Determining Color Temperature of a Lamp.

two windows are provided in the integrating sphere and the light flux through them is received by a red-sensitive and a blue-sensitive phototube, respectively, the ratio of their photocurrents may, furthermore, be employed to determine the color temperature of the source.<sup>9</sup> The ratio of the photocurrents is most conveniently measured by a null method, using a Wheatstone bridge with the two cells in two of the arms (Fig. 14.2). If one of the resistances in the other arms is adjusted to give zero current through the galvanometer, the ratio of the two

photocurrents  $i_R$  and  $i_B$  is seen to be given by  $i_R/i_B = R_2/R_1$ .

Phototubes with suitable amplification have been found particularly valuable in determining the characteristics of low-level light sources,

<sup>9</sup> The ratio of the photocurrents is given, for a thermal source, by

$$K = \frac{\int \mu_1 \epsilon J d\lambda}{\int \mu_2 \epsilon J d\lambda}$$

Here  $\epsilon(\lambda)$  is the emissivity of the sources,  $J(\lambda) = (8\pi hc/\lambda^5) \cdot \exp[-hc/(k\lambda T)]$ , the spectral emission of a black body at temperature  $T$  (approximated by Wien's law), and  $\mu_1(\lambda)$  and  $\mu_2(\lambda)$  are the spectral responses of the two phototubes. In the particularly simple case when the phototubes respond only to radiation of wave lengths  $\lambda_1$  and  $\lambda_2$ , respectively,

$$K = \frac{\mu_1 \epsilon_1}{\mu_2 \epsilon_2} \left( \frac{\lambda_2}{\lambda_1} \right)^5 e^{-\frac{hc}{k} \left( \frac{1}{\lambda_1} - \frac{1}{\lambda_2} \right) \frac{1}{T}}$$

For a true black body,  $\epsilon_1 = \epsilon_2 = 1$ ; hence the effective color temperature of the source becomes

$$T_c = \frac{\frac{hc}{k} \left( \frac{1}{\lambda_1} - \frac{1}{\lambda_2} \right)}{\log_e \left[ \left( \frac{\lambda_2}{\lambda_1} \right)^5 \frac{\mu_1}{\mu_2 K} \right]}$$

All the constants in this expression are either known or can be measured. In practice the apparatus is calibrated with a number of thermal sources of known color temperature.

such as black-out luminaires.<sup>10</sup> The illuminations to be measured here range from 0.002 to 0.2 lux; hence the sensitivity of the barrier-layer cells (about 0.3 microampere per lux) is too low for the purpose. A phototube, supplemented by a single stage of amplification with a reduced grid-current tube,<sup>11</sup> on the other hand, yields 40 microamperes

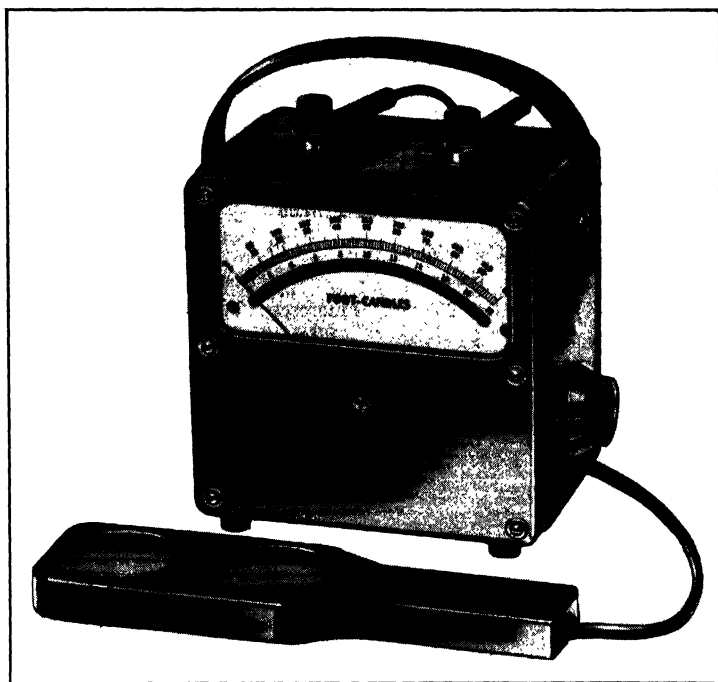


FIG. 14.3. Weston Barrier-Layer Cell Illuminometer, Model 756. (Courtesy of Weston Electrical Instrument Company.)

per lux, which is adequate. A 931-A multiplier phototube, provided with a Wratten 11 (X-1) filter to match its spectral response to the response of the eye, was also found to be highly satisfactory. The multiplier phototube may be operated directly by an alternating-current transformer, whose primary current has been stabilized with the aid of a saturated-core constant-voltage transformer.<sup>12</sup>

Many other photometric problems which neither deal with very low light levels nor require unusual precision can be solved satisfactorily with barrier-layer cells. The Weston instrument shown in Fig. 14.3

<sup>10</sup> See Committee on Instruments and Measurements, reference 4.

<sup>11</sup> See Chapter 13, p. 254.

<sup>12</sup> See Chapter 12, p. 246.

is a typical illuminometer employing a pair of selenium barrier-layer cells whose output is measured by a portable microammeter. The cells are simply brought into the plane in which the illumination is to be measured. The meter is calibrated directly in foot-candles,<sup>13</sup> a full-scale deflection corresponding to 20, 100, and 500 foot-candles, respectively.

The closeness with which the spectral response of the barrier-layer cells approaches the response of the eye—especially with filter correction—makes them highly suitable for intensity measurements on gaseous discharge lamps and other distinctly nonthermal sources. If the illu-

TABLE 14.1. CORRECTION FACTORS FOR GENERAL ELECTRIC LIGHT-SENSITIVE CELL WITHOUT FILTER

<i>Source</i>	<i>Correction Factor</i>	<i>Source</i>	<i>Correction Factor</i>
Tungsten (2700° K)	1.00	Fluorescent lamps:	
Neon tubing	0.85	White daylight (6500° K)	0.84
Mercury (high pressure) H-6	0.70	White (3500° K)	1.04
Mercury (low pressure) DH-1	0.84	Green	1.45
Sodium	1.36	Blue	0.46
Carbon arc (white flame)	0.48	Pink	0.93
		Gold	1.27
		Red	0.68

minometer is used to measure the light output or the illumination provided by such sources, the reading, generally calibrated for a tungsten lamp with a color temperature of 2700° K, must be multiplied by a correction factor. The values of the correction factors for a General Electric light-sensitive cell without filter are listed in Table 14.1.<sup>14</sup>

In earlier work, with similar correction factors and no filters, an accuracy of 5 to 10 per cent was obtained in illumination measurements. With a filter the accuracy was  $\pm 5$  per cent. To obtain the best results, it is often advisable to select cells for low fatigue which, for a given type of cell, is frequently an accompaniment of high sensitivity. Errors from slow drifts in the sensitivity of the barrier-layer cell may be avoided by periodic recalibration with a test box.<sup>15</sup> The illumination in the test box is provided by a 25-watt coiled-filament lamp (color temperature: 2700° K), the current being controlled by a rheostat and voltmeter. The cell is fitted into a frame opposite the lamp and  $9\frac{1}{2}$  inches from it.

<sup>13</sup> 1 foot-candle = 10.76 lux.

<sup>14</sup> See Buck, reference 5.

<sup>15</sup> See Committee on Photoelectric Portable Photometers, reference 6.

The interior of the box is, of course, made optically black to suppress reflections. Errors in illuminometer readings arising from changes in temperature are of the order of 0.2 per cent per degree centigrade.

Portable barrier-layer cell light meters have been modified in various ways to serve special purposes. With the cells mounted on extensible fishpoles, the meter remaining at hand level, they may be used to explore inaccessible places.<sup>16</sup> If a hole is bored through the center of the cell, to transmit the incident light, the cell may be used to measure light reflected in a forward direction by the reflecting buttons in "cat's eye" highway signs (Fig. 14.4).<sup>17</sup> The light incident from a particular direction may be measured by a cell provided with a conical hood with spiral baffles to suppress reflections.<sup>18</sup> On the other hand, the illumination

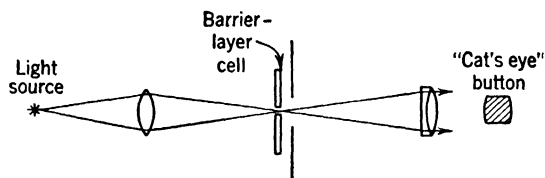


FIG. 14.4. Arrangement for Measuring Forward Reflection of "Cat's Eye" Buttons. (Kingslake, reference 8.) (Courtesy of *J. Optical Soc. Am.*)

arising from light incident at a large angle on a surface can be determined accurately, independent of the effect of window reflections and partial shadowing by the frame of the cell, by a simple calibration procedure (Fig. 14.5).<sup>19</sup> Let the meter reading obtained for a distant light source, with the illumination incident on the cell at an angle  $\alpha$  to the normal, be  $R_\alpha$ , and that obtained when the cell is turned so that the light is incident normally, be  $R_n$ . Construct a chart of concentric circles of radius  $h \tan \alpha$  and label each circle with the corresponding value of  $(R_n \cos \alpha)/R_\alpha$ . If now a pointer of height  $h$  and normal to the chart is placed at the origin and the chart is brought into the plane of the photo-cell, the shadow of the point will indicate the value of the factor  $(R_n \cos \alpha)/R_\alpha$ , by which the reading must be multiplied to yield the true illumination.

A rather special application of photoelectricity to the measurement of light sources is the determination of the total biologically active ultra-

<sup>16</sup> See Staley, reference 7.

<sup>17</sup> See Kingslake, reference 8.

<sup>18</sup> See Hurd, reference 9.

<sup>19</sup> See Goodbar, reference 10. Errors from these causes have been minimized by laminating suitable lenses to cell surface—see Buck, reference 5.



violet radiation incident, at a particular location, from the sun and sky.<sup>20</sup> The spectral band in question extends approximately from 2900 to 3200

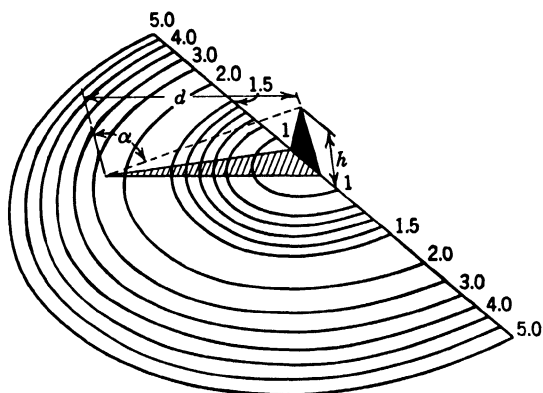


FIG. 14.5. Chart for Compensating Barrier-Layer Cell Reading Errors for Oblique Illumination. (Goodbar, reference 10.) (Courtesy of *Illum. Eng.*)

Angstrom units. The response of a pure zirconium phototube developed for measuring this radiation covers approximately the same range.<sup>21</sup> The cathode is a flat disk, 35 millimeters in diameter; the anode is a

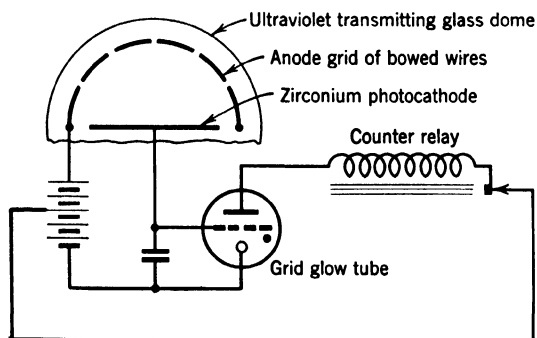


FIG. 14.6. Principle of Ultraviolet Recording Photometer for Solar and Sky Radiation.

grid of fine arched wires supported by a heavy ring surrounding the cathode (Fig. 14.6). A condenser and a grid glow tube,<sup>22</sup> which dis-

<sup>20</sup> The total radiant energy reaching the earth is generally measured by non-selective pyrheliometers which determine the energy absorbed by an exposed black body from its temperature rise.

<sup>21</sup> See Coblenz, reference 11, and Coblenz and Stair, reference 12.

<sup>22</sup> See Chapter 12, p. 235; also Rentschler, reference 13.

charges the condenser when the photocurrent has raised the potential of its grid to a certain definite value, are sealed in the same high-silica glass envelope with the remainder of the tube. Only the 8-centimeter diameter hemisphere forming the portion of the envelope above the level of the cathode projects out of the metal housing containing the remaining equipment. Whenever the grid glow tube discharges the condenser, the plate current actuates a counter relay, which in turn interrupts the plate circuit and thus stops the discharge in the grid glow tube. Every count measures a fixed amount of ultraviolet radiation that has fallen on the photocathode, determined by the sensitivity of the phototube and the capacitance of the condenser. A printer records the counts and the time on a tape at periodic intervals, furnishing an automatic record of the incidence of biologically active ultraviolet radiation at the station in which the phototube is installed. On an average clear day in Washington, at noon, this ultraviolet radiation constitutes approximately one-thousandth of the total radiant energy received; the radiant flux is of the order of 1 gram-calorie per minute per square centimeter or 700 watts per square meter. An hour before sunset, at which time the total radiant flux has been reduced to only one half its peak value, the ultraviolet component has become quite negligible.

**Reflectometers, Fluorometers, and Refractometers.** Photocells find manifold applications in the measurement of the reflection, transmission, and emission from materials which do not qualify as light sources in the narrow sense. The reflection properties of such materials may be measured by a *reflectometer* or *goniophotometer*. The multipurpose reflectometer of the National Bureau of Standards<sup>23</sup> serves primarily to measure specular reflection (specular gloss), diffuse reflection, and their ratio (contrast gloss) for a fixed angle of incidence (45 degrees) and of reflection (45 and 0 degrees, respectively). (See Fig. 14.7.) The illuminating beam is split, and part of it is reflected by a small mirror to the vertical sample surface for the measurement of specular reflection; the remainder falls on the horizontal sample surface and is diffusely reflected toward the "reflection" barrier-layer cell. The specularly reflected light from the vertical sample, on the other hand, ultimately reaches the "gloss" barrier-layer cell. The two cells are connected so that their photocurrents are in opposite directions. A measurement of the vertical displacement of the reflection cell required to bring the galvanometer deflection to zero indicates the ratio between the specular and diffuse reflection (contrast gloss). To measure specular gloss the horizontal sample surface is replaced by a perfect diffusing surface; to measure diffuse reflectance, the vertical sample is replaced by a mirror. Various

<sup>23</sup> See Hunter, reference 14.

attachments are provided permitting the determination, in addition, of the color characteristics, transmission, and sheen (specular reflection at large angle of incidence) of samples.

The M.I.T. goniophotometer<sup>24</sup> is designed as a precision instrument for the measurement of specular and diffuse reflectance at all angles.

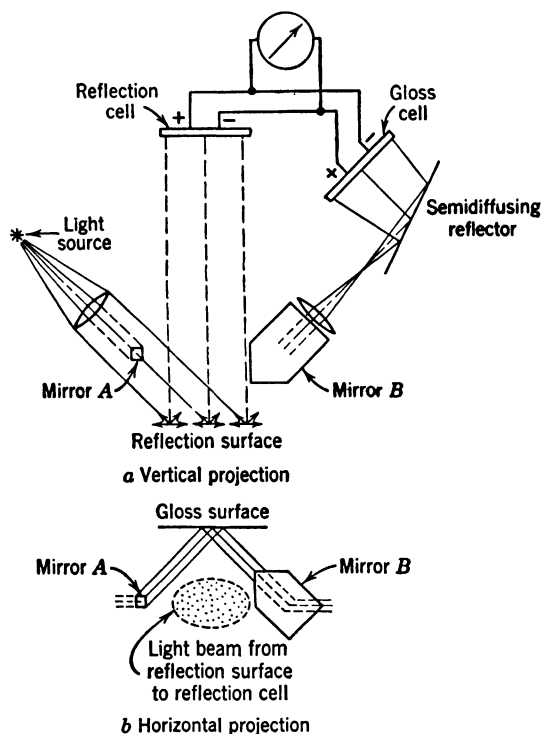


FIG. 14.7. Multipurpose Reflectometer: (a) Vertical and (b) Horizontal Projection. (Hunter, reference 14.) (Courtesy of *J. Optical Soc. Am.*)

The specimen is mounted vertically on a rotating table, the receptor (a barrier-layer photocell) on a moving arm. For the measurement of specular reflection (Fig. 14.8a) stops are employed so that every part of the specular image of the source illuminates every point of the cell. For the measurement of diffuse reflectance (Fig. 14.8b) the stops are such that every exposed point of the cell receives light only from fully illuminated portions of the sample. The specular reflectance of the sample for a particular angle of incidence is obtained as the ratio of two light flux measurements: the first, with both the incident beam and the

<sup>24</sup> See Moon and Laurence, reference 15.

cell arm forming this angle with the normal to the surface of the sample, the second, with the sample removed and light source and cell on the

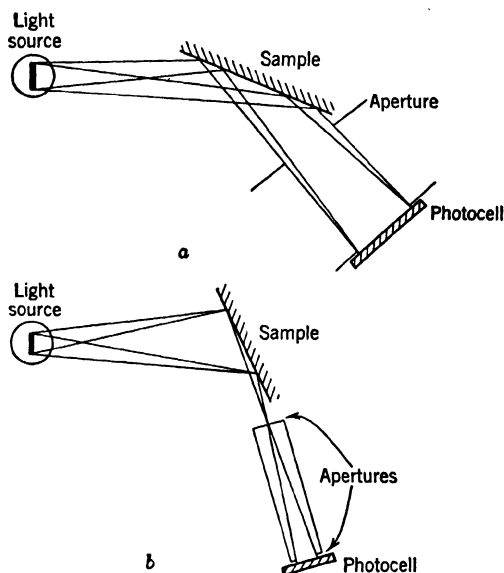


FIG. 14.8. Measurement of (a) Specular and (b) Diffuse Reflectance with Goniophotometer. (Moon and Laurence, reference 15.) (Courtesy of *J. Optical Soc. Am.*)

same diameter. The diffuse reflectance of the sample, for a particular angle of incidence and observation, is obtained as the ratio of the flux measurement with the sample in the appropriate position and with it replaced by a perfectly diffusing surface, such as a magnesium oxide block.

The relative magnitude of the light flux is determined in every case by the resistance  $R_1$ , in the circuit shown in Fig. 14.9, required to make the galvanometer reading zero; the galvanometer sensitivity is  $10^{-9}$  ampere per division. The value of the resistance  $R_2$  is chosen to be very large compared to  $R_1$ . With this method of measurement, in which the barrier-layer cell is maintained in a short-circuit condition, fatigue errors could be reduced to  $\pm 1$  per cent.

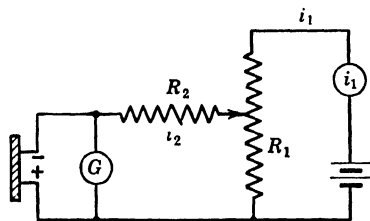


FIG. 14.9. Compensating Circuit for Reflectance Measurements. (Moon and Laurence, reference 15.) (Courtesy of *J. Optical Soc. Am.*)

*Fluorimetry* has been defined as the photometry of a luminous volume. Figure 14.10 shows a simple fluorometer for the determination of vitamin concentrations in liquids.<sup>25</sup> The light source—a high-pressure mercury arc—emits two beams, one passing through a specimen in a nonfluorescing glass cell, the other through a standard fluorescent substance, such as a plate of uranium glass or flourspar. Before impinging on the specimen or standard, the light beam passes through a Wratten 18A filter to remove the visible radiation, leaving an ultraviolet beam consisting primarily of 3650 Angstrom units radiation. After passage

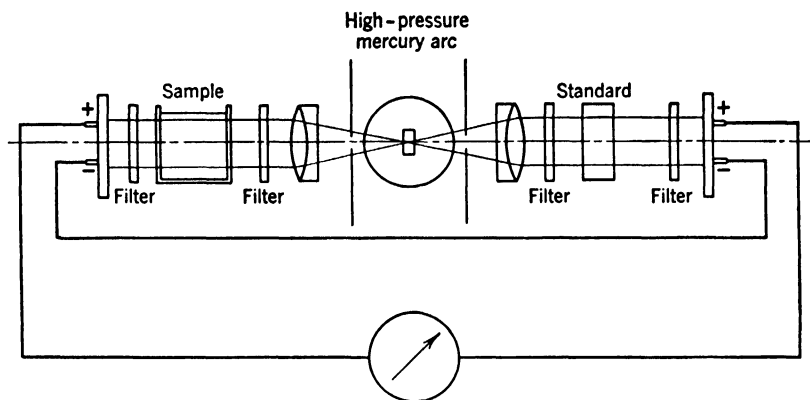


FIG. 14.10. Barrier-Layer Cell Fluorometer. (Ellinger and Holden, reference 16.)  
(Courtesy of *J. Soc. Chem. Ind.*)

through the fluorescing substance the ultraviolet is filtered out by 2 millimeters of Chance OY13 glass and a Wratten 2A filter, so that only visible fluorescent radiation falls on the two barrier-layer cells, which are connected in opposition. An iris diaphragm in the comparison path is used to adjust galvanometer readings to zero; the setting of the iris indicates the concentration of fluorescent material in the solution.

For weakly fluorescing substances, such as those encountered in the quantitative analysis of beryllium ores, the barrier-layer cell methods are too insensitive. For them a blue-sensitive phototube and amplifier serve as detector, the exciting ultraviolet beam and the measured fluorescent emission being at right angles to each other.<sup>26</sup> Still greater sensitivity is attained with a multiplier phototube.

Closely related to the measurement of fluorescence is the measurement of bacterial luminescence.<sup>27</sup> The bioluminescence of a culture of bacteria

<sup>25</sup> See Ellinger and Holden, reference 16.

<sup>26</sup> See Fletcher, White, and Sheftel, reference 17.

<sup>27</sup> See Griner, Tytell, and Kersten, reference 18.

such as *Achromobacter fischeri* may be determined quantitatively by placing a phototube and preamplifier under a flat-bottomed cell containing the bacterial suspension; violent oscillation of a table on which the assembly is mounted serves to supply the culture with the necessary aeration. A flexible cable connects the preamplifier with a stationary amplifier and measuring instrument.

The measurement of turbidity, also, presents the problem of measuring light emitted from an extended volume of material. The turbidity comparator shown schematically in Fig. 14.11<sup>28</sup> has two clear-bulb incandescent lamps to illuminate the test tube containing the sample liquid through narrow slits. A slit system at right angles to the path of illumination guides scattered light to the phototube, whose amplified response is a measure of the turbidity of the sample. The system is calibrated with a standard suspension. A fundamentally similar system has found application in measuring the effectiveness of air filters.<sup>29</sup> Light scattered by the unfiltered air is guided by a series of mirrors to the cathode of a 931-A multiplier phototube and is compared with light scattered by the same air after filtering, the latter light reaching the phototube by a different path.

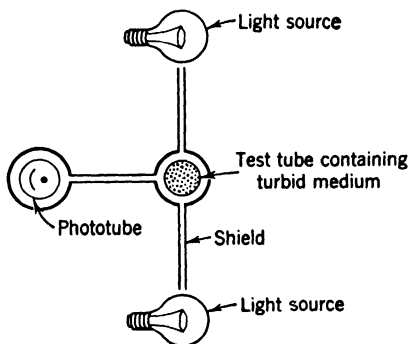


FIG. 14.11. Turbidity Comparator (Schematic). (Krebs, Perkins, Tytell, and Kersten, reference 19.)

Another useful application for the phototube is the objective measurement of films precipitated, for example, in the form of insoluble soaps, on surfaces immersed in washing solutions.<sup>30</sup> Glass plates which have been washed in the solution under study and subsequently dried are stacked to form a small angle (for example, 18 degrees) with a light beam which falls through them on a type 919 phototube forming part of a Roberts photometer (Fig. 14.12). The photometer<sup>31</sup> indicates, by the frequency of a succession of clicks heard in a set of headphones, the light flux which falls on the photocathode. The light absorption and scattering of the films are indicated by the reduction in the number of clicks per unit time resulting from the immersion of the plates in the

<sup>28</sup> See Krebs, Perkins, Tytell, and Kersten, reference 19.

<sup>29</sup> See Barnett and Free, reference 20.

<sup>30</sup> See Wilson and Mendenhall, reference 21.

<sup>31</sup> See p. 294.

solution. The stacking of several plates and their inclination to the light beam increase the absorption and scattering and reduce random variations.

Photoelectric measurements of light scattering have also been used for the determination of the molecular weight of the solute in solutions

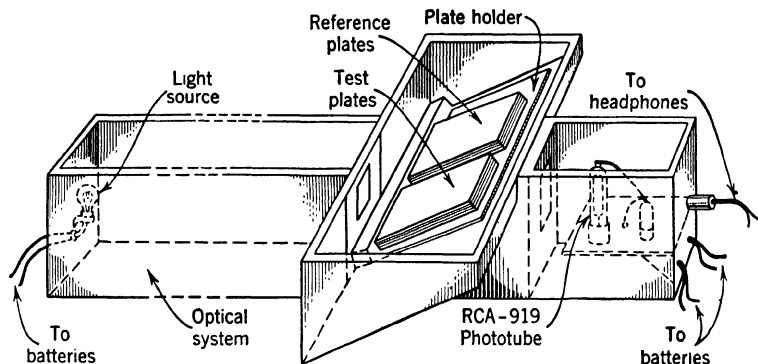


FIG. 14.12. Measurement of Film Deposits on Glass. (Wilson and Mendenhall, reference 21.) (Courtesy of *Ind. Eng. Chem., Anal. Ed.*)

of polymers (plastics and rubbers).<sup>32</sup> Such determinations demand the measurement of the scattering of monochromatic light as a function of the angle of scattering.<sup>33</sup> The measuring apparatus (Fig. 14.13) has a high-pressure mercury discharge tube, whose radiation is passed through a monochromatic filter and is collimated before entering the

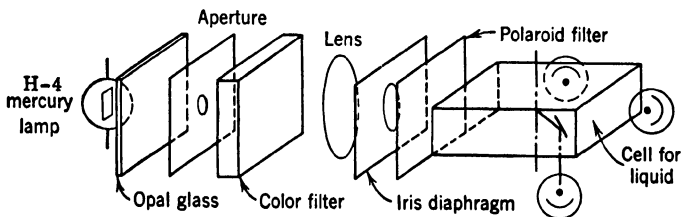


FIG. 14.13. Determination of Light Scattering by Solutions of Polymers (Schematic). (Debye, reference 22.) (Courtesy of *J. Applied Phys.*)

solution cell. A 45-degree mirror, which rotates about a vertical axis, dips into the solution and directs light scattered at an angle corresponding to its azimuthal setting into a 929 phototube directly below it, out-

<sup>32</sup> See Debye, reference 22.

<sup>33</sup> See Debye, reference 23.

side the cell containing the liquid. Three additional 929 phototubes measure the intensity of the primary beam and of the transmitted light, and the light scattered at right angles to the primary beam.

Photoelectric methods are also suitable for measuring small differences in the refractive index of liquids. Figure 14.14 shows a refractometer whose operation is uninfluenced by the absorption of light by the specimen since the test beam does not enter it.<sup>34</sup> The liquid is contained in a cell whose lower face is formed by a glass prism. A light

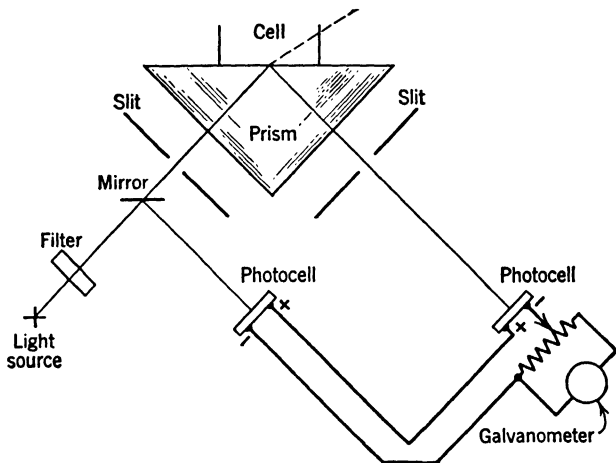


FIG. 14.14. Photoelectric Refractometer. (Karrer and Orr, reference 24.) (Courtesy of *J. Optical Soc. Am.*)

beam incident on the glass-liquid interface at an angle close to the critical angle for total reflection is partially reflected toward a barrier-layer phototube whose output is balanced, for a standard liquid, against that of a second cell receiving a fraction of the incident beam. The difference in the amount of reflected light resulting from the difference in refractive index between the standard and the sample liquid results in a galvanometer deflection. This deflection (for water as a standard) is linear in a range of  $n = 1.330$  to  $1.345$  with a dependable accuracy of measurement of  $0.00005$ .

**Colorimetry and Pyrometry.** It is found empirically that the stimulus received by the eye from any light source may be matched perfectly by the superposed stimuli, in proper proportion, of three primary light sources of different spectral composition. There is an infinite number of primary source combinations which satisfy this condition. Furthermore, there is a certain statistical variation among people in the amount

<sup>34</sup> See Karrer and Orr, reference 24.



of light from each primary source required to reproduce the stimulus in question. Hence, to obtain a standard specification of color, the International Commission of Illumination (ICI) has set up a "standard observer" with properties corresponding to an average of many observers with normal vision. The response of the standard observer to monochromatic radiation in terms of three primary stimuli is specified by the curves of Fig. 14.15.<sup>35</sup> The ordinates represent the "color co-

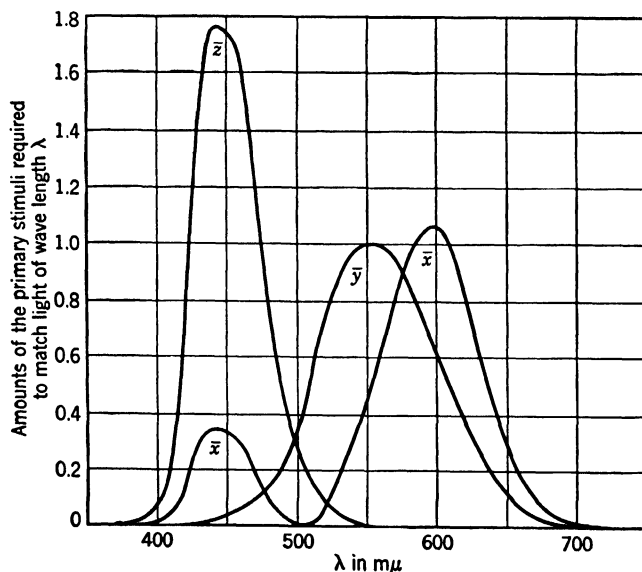


FIG. 14.15. The Color Coordinates of Monochromatic Radiation. (Judd, reference 25.) (Courtesy of *J. Optical Soc. Am.*)

ordinates"  $\bar{x}$ ,  $\bar{y}$ , and  $\bar{z}$  of the monochromatic radiation, or the amount of each primary stimulus required to produce the same sensation as the monochromatic radiation in question. The function  $\bar{y}$  is simply the visibility function so that the value of  $\bar{y}$  immediately specifies the luminous intensity of the light received by the eye.

The application of the curves in Fig. 14.15 to objective colorimetry, the determination of the color coordinates of a given light flux, is obvious. If three photocells are provided with filters so that the spectral responses of the cell-filter combinations are given by  $\bar{x}$ ,  $\bar{y}$ , and  $\bar{z}$ , respectively, the response of the cells, exposed to the light flux in turn, will yield directly the color coordinates of the light flux.

<sup>35</sup> See Judd, reference 25.

A colorimeter based on this principle was constructed, primarily for the photometry of fluorescent lamps, by B. T. Barnes<sup>36</sup> of General Electric's Lamp Development Laboratory. Four cell-filter units (one of which consists of two General Electric barrier-layer cells) are employed rather than three, since the  $x$ -response is more readily realized by two separate units (one for each peak of the curve) than by a single one. The filter specifications are given in Table 14.2.<sup>36</sup> Cells  $B$ ,  $C$ , and  $D$  will generally require some masking by an adjustable aperture; this adjustment is carried out with the aid of a light source of known color

TABLE 14.2. FILTER SPECIFICATIONS FOR GENERAL ELECTRIC COLORIMETER  
(From B. T. Barnes, "A direct-reading colorimeter," *Rev. Sci. Instruments*, Vol. 16, p. 339, 1945)

Filter	Response	Corning Glass, No.	Thick- ness, mm	Filter at	Transmission, per cent
A	$x$ ( $>5050$ A.U.)	3304	3.2	5350 A.U.	2.8
		3962	3.6	6600	17.5
B	$y$	3304	1.7	4850	5.4
		4308	3.0	6350	10.0
C	$z$	3389	2.5	4200	38.0
		5543	4.0	5000	8.0
D	$x$ ( $<5050$ A.U.)	3385	2.2	4200	26.0
		5543	7.5	4800	0.72

coordinates. To obtain the proper characteristics, the cells to be used with filters  $A$  and  $B$  should be selected to have a response at 6350 Angstrom units, which is  $61 \pm 3$  per cent of the response at 5650 Angstrom units.

The arrangement for measuring the color coordinates of a light source is shown schematically in Fig. 14.16. The resistance  $r_1 + r_2$  represents a 100-ohm decade box;  $R$  is a high resistance which may be made either 0.1 or 0.4 megohm. To begin with, all the switches are closed and  $r_3$  and  $R$  are adjusted to obtain zero galvanometer deflection. Then the switches for  $A + D$  ( $x$ ),  $B$  ( $y$ ), and  $C$  ( $z$ ) are closed in turn, and the value of  $r_2$  is adjusted every time to give balance. The three values of the resistance  $r_2$ , so obtained, are numerically equal to the color coordinates of the light source to which the cells have been exposed. The cells must, of course, be arranged relative to the light source in such fashion that their illumination is the same throughout. It was found that if a single standard source was used to calibrate the colorimeter, the errors in the color coordinates were of the order of 1 per cent. Much greater accuracy

<sup>36</sup> See Barnes, references 26 and 27.

was obtained when the lamp to be measured and the standard lamp were of the same type.

In some applications color characteristics are specified without reference to the standardized ICI color coordinates. An example is the densitometry of color film as carried out by the color densitometer developed by M. H. Sweet of the Ansco Research Laboratories.<sup>37</sup> The absorption

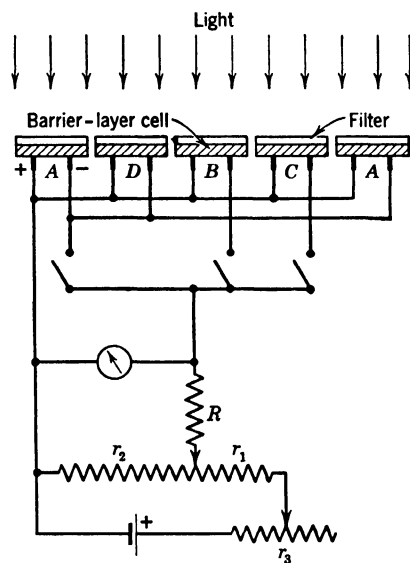


FIG. 14.16. Arrangement of General Electric Barrier-Layer Cell Colorimeter. (Barnes, references 26 and 27.) (Courtesy of *J. Optical Soc. Am.* and *Rev. Sci. Instruments*.)

of the three dyes (yellow, magenta, and cyan) forming the image is shown in Fig. 14.17. It is seen that the relative representation of the dyes can be inferred from the absorption of the film at 4400, 5400, and 6800 Angstrom units. Corresponding narrow spectral bands may be isolated from white light with the aid of filters having the density<sup>38</sup> characteristics shown in Fig. 14.18.<sup>39</sup> A 2 per cent copper chloride solution filter serves to cut off the transmission of the red filter above 7000 Angstrom units, as indicated by the dotted line.

Since the density of reversible color film is very high, a very sensitive detector was necessary. A multiplier phototube, selected for high red response and low dark current ( $= 0.002$  microampere), was the logical choice.

Furthermore, it was desired that the output meter should read densities, given by the logarithm of the photocurrent, directly. This can be attained if the cathode<sup>40</sup> of the phototube is connected to the insulated amplifier-tube control grid. In this case the grid voltage must adjust itself so that the photocurrent becomes just equal to the cathode current collected by the grid. In view

<sup>37</sup> See Sweet, reference 28.

<sup>38</sup> Density  $= \log_{10} (I_o/I)$ , where  $I_o$  is the incident and  $I$  is the transmitted light.

<sup>39</sup> The blue filter pack consists of Wratten 36, 2A, and 38 filters; the green filter pack of Wratten 62 and 16 filters; and the red filter pack of Wratten 70 and 16 filters plus 1 centimeter of 2 per cent copper chloride solution.

<sup>40</sup> For a multiplier phototube, the last dynode.

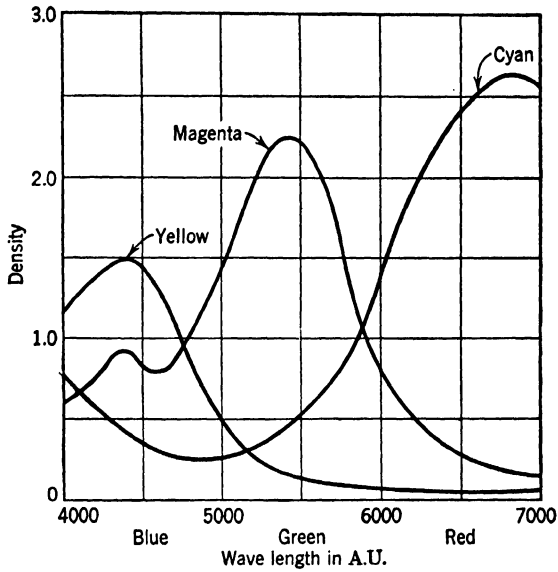


FIG. 14.17. Absorption of Dyes in Reversible Color Film. (Sweet, reference 28.)  
(Courtesy of *Electronics*.)

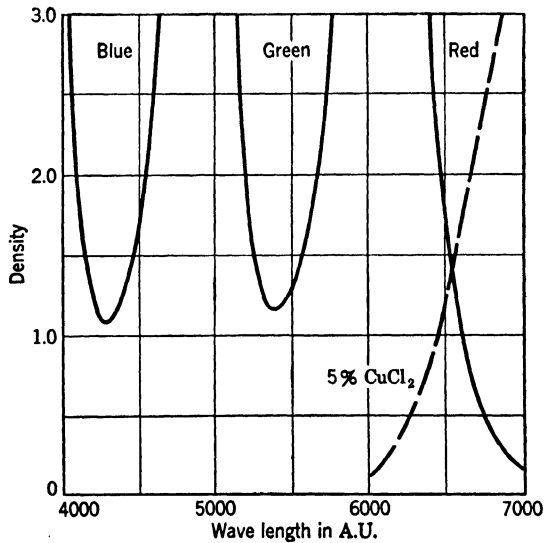


FIG. 14.18. Narrow Spectral Band Filters for Ansco Color Densitometer. (Sweet, reference 28.) (Courtesy of *Electronics*.)

of the exponential energy distribution of the thermionic electrons the grid-cathode current is, for negative grid voltages, an exponential function of the grid-cathode voltage; vice versa, the grid-cathode voltage, and hence the plate current of the amplifier tube, must be proportional to the logarithm of the photocurrent.

The system described demands a highly insulated battery power supply for the multiplier phototube. It was later replaced by the feedback system shown schematically in Fig. 14.19*b*, which permits the use of a line-operated power source.<sup>41</sup> The multiplier output current, passing through the resistance  $R_G$ , determines the grid voltage on the control tube, which regulates the current through the voltage bleeder of the multiplier. Since the resistance  $R_G$  is made large and the gain of the control tube is high, the multiplier voltages are automatically adjusted to make the output current constant, irrespective of the illumination of the photocathode. Under these circumstances the voltage becomes a nearly linear function of the logarithm of the illumination over a considerable range—more precisely so with the introduction of suitable meter shunt circuits—so that densities may be read directly on the voltmeter.

The light source is a 15-candlepower auto lamp fed by a stabilized current supply. As each filter, in turn, is switched into the light beam, the lamp current is modified so as to equalize the photocurrents generated in the absence of the film. The meter readings cover a range of densities from 0 to 3 (1:1000).

A very ingenious method for the rapid determination of the spectral distribution of light sources has been devised by G. C. Sziklai and A. C. Schroeder of the RCA Laboratories.<sup>42</sup> It rests on the fact that, for exciting frequencies not too far removed from the threshold frequency, the higher derivatives of the retarding potential curves for phototubes are large only in the immediate neighborhood of  $V = (h/e)(\nu - \nu_0)$ , where  $\nu$  is the frequency of the exciting light and  $\nu_0$  is the threshold frequency of the photocathode, and on the fact that the magnitude of these derivatives at the point in question does not vary greatly with frequency.<sup>43</sup> Hence, if the second or third derivative, with respect to the retarding potential  $V$ , of the photocurrent excited by a heterochromatic light source is plotted against the retarding potential, the curve becomes very nearly identical with the spectral distribution curve

<sup>41</sup> See Sweet, reference 29.

<sup>42</sup> See reference 30.

<sup>43</sup> For a spherically symmetrical phototube the second derivative, and for one with plane parallel electrodes, the third derivative of the current with respect to the retarding potential may be used. For the usual phototubes, with quasi-cylindrical

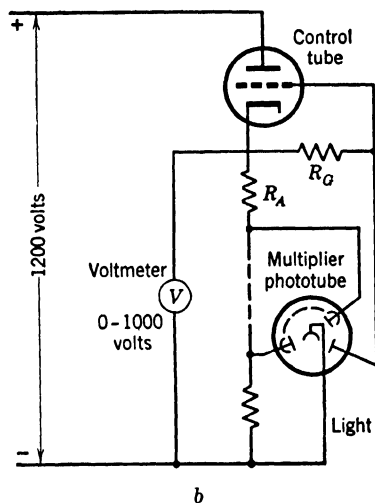
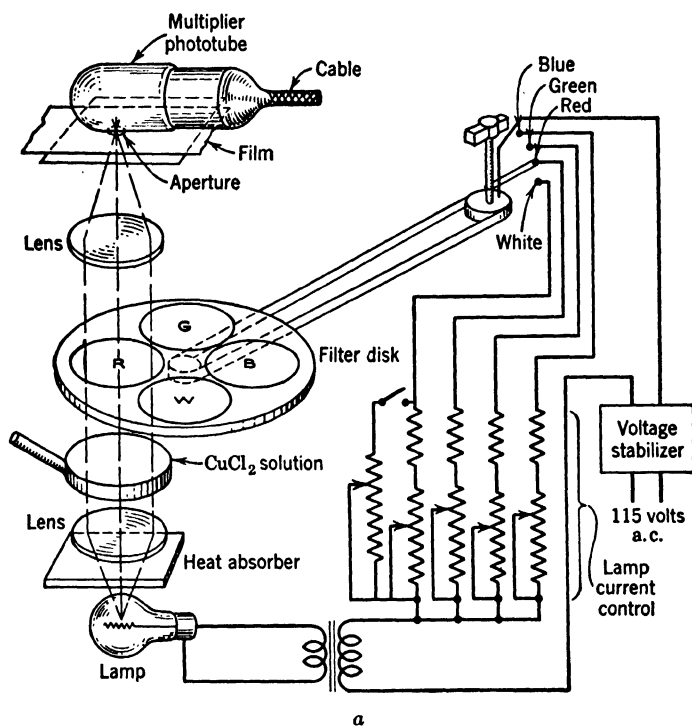


FIG. 14.19. Ansco Color Densitometer: (a) Optical Arrangement. (b) Measuring Circuit (Schematic). (Sweet, references 28 and 29.) (Courtesy of *Electronics*.)

of the source, plotted with respect to the frequency  $\nu = \nu_o + eV/h$ . In practice, both the differentiation and the recording of the curve are carried out electronically. A sawtooth retarding voltage is applied to the phototube and to the horizontal plates of a cathode-ray oscillograph. The current output of the tube is passed through several capacity-resistance differentiating networks separated by amplifiers and applied to the vertical plates of the oscillograph, on whose screen the spectral distribution curve is observed directly (Fig. 14.20). With an

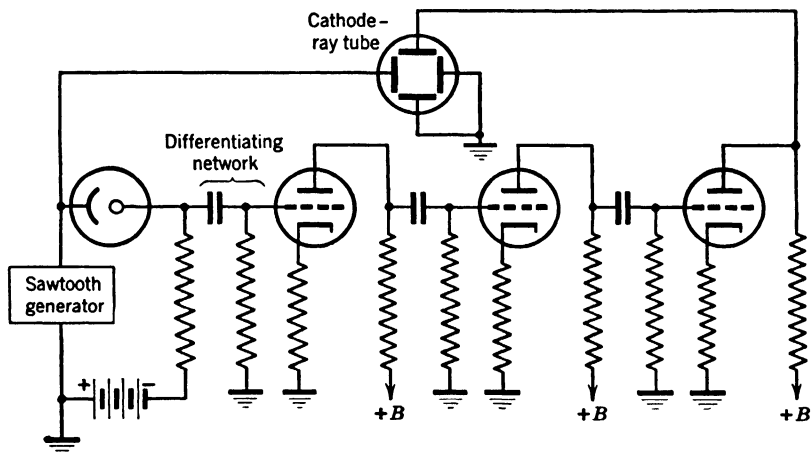


FIG. 14.20. Schematic Arrangement of Electronic Spectrometer. (Sziklai and Schroeder, reference 30.)

ideal phototube the system, which has been refined in several ways, functions as a recording spectrograph with a resolution which, at room temperature and 5000 Angstrom units, is somewhat better than 200 Angstrom units.<sup>44</sup> Ordinary phototubes introduce difficulties, not

symmetry, the second derivative may be employed, but the spectral distributions obtained are poor approximations of the true spectral distribution. For a phototube with plane electrodes exposed to radiation with the spectral distribution  $F(\nu)$ , the simple theory of the surface photoeffect leads, neglecting the variation of excitation probability with frequency, to the relation

$$\frac{d^2 i}{dV^2} = -\text{const} \int F(\nu) \frac{\exp [(eV + h\nu_o - h\nu)/(kT)]}{\{1 + \exp [(eV + h\nu_o - h\nu)/(kT)]\}^2} d\nu$$

$$\cong -\text{const}' F(\nu_o + eV/h)$$

<sup>44</sup> The resolution is determined by the range of frequencies which contribute materially to the value of the derivative for a particular retarding potential  $V$ . For the plane phototube, this is seen to be of the order of  $4kT/h$ , since the coefficient of  $F(\nu)$  in the integral is reduced to slightly less than half its peak value for  $\Delta\nu = \pm 2kT/h$ . The corresponding spread in wave length is  $4kT\lambda^2/hc$ . The resolution may be improved by cooling the phototube.

readily overcome by circuit modifications, which limit the practical application of the system.

There are two basic methods in photoelectric *pyrometry*—the determination of the temperature of incandescent bodies, such as the interiors of furnaces, by means of their radiation. Either the total emission of the body, which increases very rapidly with the temperature, may be measured, or the emission in two different spectral bands may be compared by two photocells with different spectral response or the same cell with different filters. The “two-color” pyrometers have the advantage

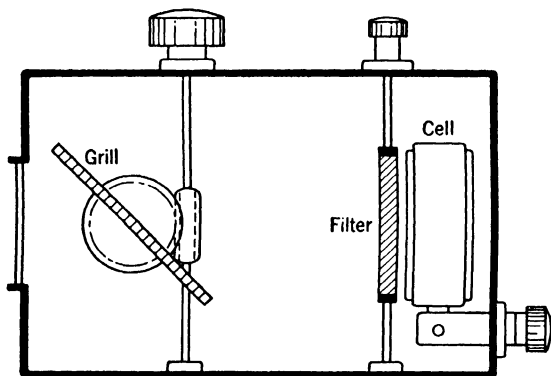


FIG. 14.21. Barrier-Layer Cell Two-Color Pyrometer. (Hubing, reference 32.)  
(Courtesy of *J. Optical Soc. Am.*)

that their reading is uninfluenced by the absolute value of the emissivity of the hot body and by the presence of neutral absorbers in the light path. Furthermore, when barrier-layer cells are employed, a comparison method avoids errors arising from sensitivity drift of the cells.<sup>46</sup>

A simple barrier-layer cell pyrometer is shown in Fig. 14.21.<sup>46</sup> Its principal components are the photocell, a filter, which may be moved out of the light path, and a rotatable grill serving to attenuate the light falling on the cell. The cell current is measured by a null method. The first step is to adjust the grill, with the filter out of the way, until a null reading is obtained with a fixed potentiometer setting. Then the filter is inserted and the potentiometer adjusted to yield once more zero deflection. The potentiometer scale reads directly in degrees Kelvin. Adjusting the photocurrent without filter to a constant value has the advantage of preventing errors arising from the nonlinearity of the cell. The operating range of this pyrometer is from about 1600° to 2900° K. The errors are of the order of 1 per cent at 2000° K.

<sup>46</sup> See Hall, reference 31.

<sup>46</sup> See Hubing, reference 32.



High-precision two-color pyrometers may be constructed by using two phototubes with suitable filters.<sup>47</sup> An instrument of this type is shown in Fig. 14.22. The light from the source is split by a semitransparent evaporated gold filter. The reflected part falls on a cesium-silver phototube after passing through a red filter; the transmitted part falls on a similar phototube after passing through a green filter. The tubes form part of a Wheatstone bridge which is balanced by adjusting the re-

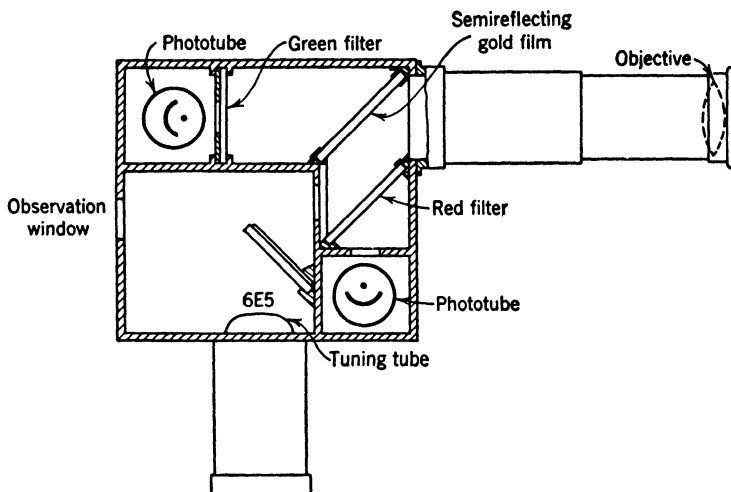


FIG. 14.22. Two-Color Pyrometer Employing Phototubes. (Russell, Lucks, and Turnbull, reference 33.) (Courtesy of *J. Optical Soc. Am.*)

sistance in one of the two remaining arms. Balance is indicated by a 6E5 tuning tube, to which the amplified potential difference between the poles of the Wheatstone bridge is applied. The pyrometer may be sighted on the source by viewing its reflection in the red filter; the tuning tube is observed through the same opening in the pyrometer box. This instrument has also been modified for continuous recording. The reading errors are of the order of  $10^\circ \text{C}$ .

**The Measurement of Photographic Exposure.** The photoelectric device most familiar to the layman is, unquestionably, the photographic exposure meter. These meters, of which an example is shown in Fig. 14.23, consist normally of a barrier-layer cell, a microammeter, and a set of dials which facilitate determination of the proper shutter speed corresponding to a given lens opening and meter reading. In the example shown, furthermore, a cover is provided which reduces the light

<sup>47</sup> See Russell, Lucks, and Turnbull, reference 33, and Sweet, reference 34.

falling on the cell to  $1/10$ . In addition, the whole upper half of the instrument constitutes a hood whose removal leaves the flat cell surface exposed. In this condition the meter reads the illumination in the plane of the cell directly in foot-candles; with the hood in place it measures, instead, the brightness or *luminance* of the scene toward which it is

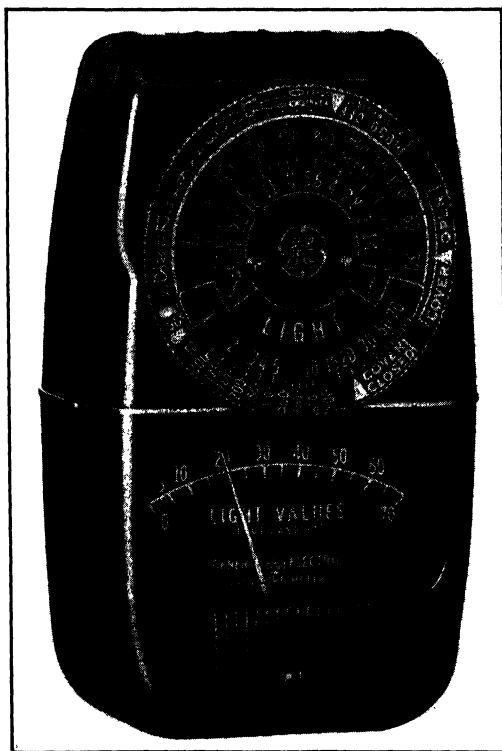


FIG. 14.23. General Electric Exposure Meter. (Courtesy General Electric Company.)

pointed, in arbitrary units. This is the usual method of determining exposure. The procedure with the exposure meter is this. The index at the left is set at the ASA (American Standards Association) rating of the film or plate used in the camera. Then the outer rim of the dials is rotated until the proper index (for instance, that designated by "cover open" if the hood is in place and the cover is opened) coincides with the meter reading on the "light" dial when the exposure meter is pointed at the scene. Coincident points on the shutter-speed and  $f$ -value dials then indicate the exposure time for any given lens opening.



The operation of the circuit is the following. Suppose that, to begin with, the triode section ( $T_1$ ) grid of the 1D8GT tube is negative, below cut-off. Without photocurrent the system would establish itself at an equilibrium point at which the plate voltage of the pentode section ( $T_2$ ) is slightly positive with respect to the cathode. The photocurrent charges the condenser  $C$  and makes the grid potential on  $T_1$  less negative until the resulting plate current through  $T_1$  increases the potential drop across  $R_c$  to the point where the plate current through  $T_2$  is suppressed. The process is accelerated by the reduction in plate current through  $T_2$ , which raises the potential of the grid of  $T_1$  through  $C$ . Eventually the grid of  $T_1$  becomes positive and the condenser  $C$  is discharged by grid current. As the current through  $T_1$  declines, the drop across  $R_c$  decreases, and current through  $T_2$  begins to flow. Since, by the coupling through the condenser  $C$ , the voltage drop across the plate load decreases the grid potential of  $T_1$  and the voltage drop across  $R_c$  arising from the plate current through  $T_1$ , the current through  $T_2$  increases very rapidly, eventually leveling off to its initial value. The double reversal of current in the headphones, taking place in rapid succession, gives rise to an audible click. Successive clicks are thus separated by longer periods during which the photocurrent charges the capacitance  $C$ . The length of these periods is evidently proportional to the magnitude of the capacitance  $C$  and inversely proportional to the photocurrent. Clicks resulting from surface leakage currents are minimized by coating the tube envelopes with ceresin.

A very elaborate method of exposure control is used in commercial color printing by Pavele Color, Inc., in New York.<sup>51</sup> The installation, which processes some 20,000 color prints a day, employs phototubes at four distinct steps. Careful control is essential since the latitude of the color printing material (Ansco Color Printon) is small and there is no choice of contrast grade. The printing material, 5 inches wide, is fed in 250-foot rolls through the enlarger and processing baths. As a first step, every transparency is checked for the ratio between the transmission of the significant part of the negative and its average overall transmission and is given a corresponding code signal (Fig. 14.25). This is accomplished with the aid of two phototubes, one of which, in a fixed position, receives a fraction of the total light transmitted by the negative, the other, mobile, being exposed to a certain portion of the image. A meter indicates the ratio of the two photocurrents.

The coded transparencies are inserted in the enlarger (Fig. 14.26). Here the coding is employed to set the initial voltage of a condenser which is discharged by the photocurrent of a phototube receiving light

<sup>51</sup> See Robins and Varden, reference 38.

that has passed through the transparency being enlarged. The discharging is initiated by the opening of the shutter. The shutter is closed again, and the printing material is moved forward when the condenser voltage has dropped to a certain fixed value, tripping a thyatron relay circuit.<sup>62</sup> Furthermore, the color temperature of the light source

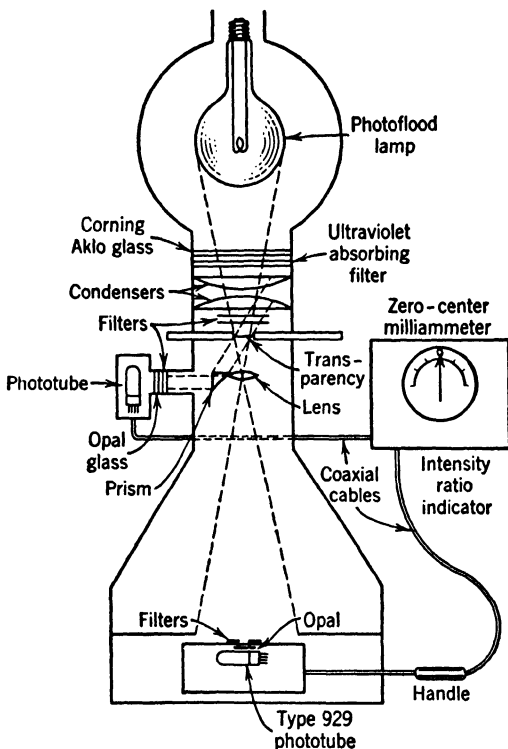


FIG. 14.25. Color Transparency Coder for Pavelle Color Printing Process. (Robins and Varden, reference 38.) (Courtesy of *Electronics*.)

is controlled by a red-sensitive and a blue-sensitive phototube. When the photocurrent in the red-sensitive phototube decreases by a small amount, it causes a thyatron relay circuit to actuate a motor which decreases the resistance in the lamp circuit. Conversely, if the photocurrent in the blue-sensitive phototube increases, a similar circuit causes the motor to run in the opposite direction, increasing the series resistance.

A final use of the phototube in this installation is to assure adequate second exposure (for reversal) of the printing material, after the initial

<sup>62</sup> See Fig. 12.19, p. 235.

processing. This is normally accomplished by a bank of four mercury vapor lamps. If these lamps fail, a monitoring 929 phototube causes a relay circuit to turn on a supplementary bank of tungsten lamps, which can take the place of the mercury lamps for a period up to 20 to 30 minutes without excessive overheating.

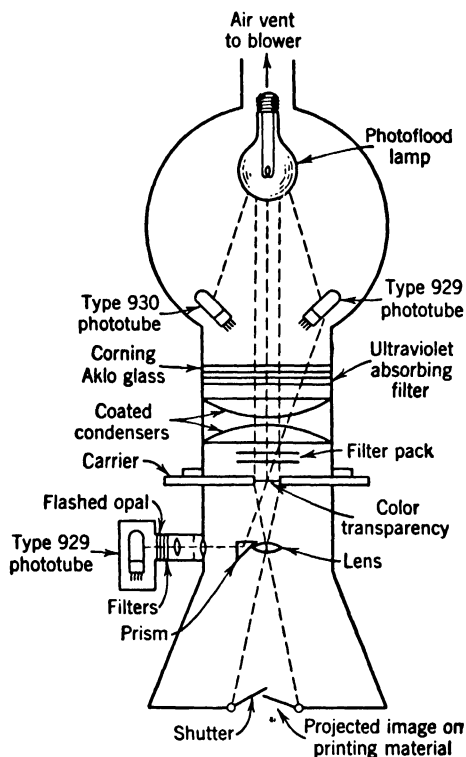


FIG. 14.26. Enlarger for Color Transparencies. (Robins and Varden, reference 38.) (Courtesy of *Electronics*.)

**Photoelectric Spectrophotometry.** Phototubes—especially multiplier phototubes—have achieved great importance in the study of spectra. Even where conventional photographic methods are employed to record the spectrum, phototubes may be used to advantage to control the exposure and to evaluate the recorded spectrum. Exposure may be controlled by having a portion of the primary beam from the arc or spark light source reflected by a rotating sector into a phototube. The photocurrent charges a condenser up to a certain voltage, at which a relay circuit is tripped and interrupts the current for the light source.<sup>53</sup> Since

<sup>53</sup> See Cosby, reference 39.

the usual arc and spark sources tend to be quite unsteady, this method of exposure control is valuable in insuring spectrograms of proper density.

The analysis of photographically recorded spectra is commonly carried out by a microphotometer, whose optical system is shown schematically in Fig. 14.27. A carefully adjusted, straight tungsten lamp filament is imaged by a microscope objective on the spectrum plate mounted on a mobile stage. A second, similar, microscope objective images the filament image transmitted by the spectrum plate on a slit in front of the cathode of a phototube. In a precision recording micro-

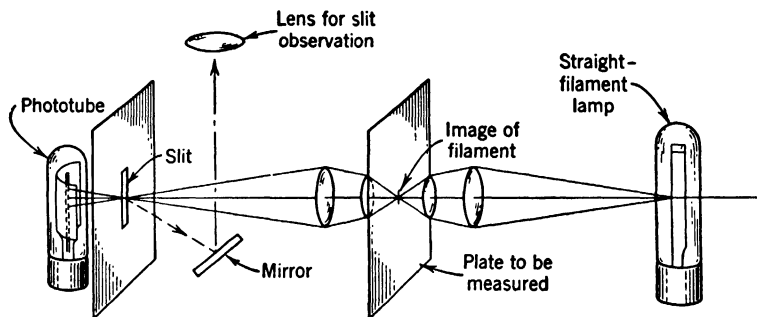


FIG. 14.27. Optical Arrangement of a Photoelectric Microphotometer (Schematic).

photometer, such as the Leeds and Northrup apparatus shown in Fig. 14.28, the photocurrent controls the deflection of a recording pen which indicates directly the density of the spectrum plate. The density variation of the spectrum is recorded on a roll of paper whose velocity of translation is a definite multiple of the velocity of translation of the microphotometer stage.

Of more immediate interest, however, are the various spectrophotometers in which the detection itself is carried out by phototubes. It has been found that resolution and sensitivity of quite the same order can be obtained with multiplier phototube detection as with photographic recording.<sup>54</sup> Furthermore, the photoelectric method has the advantage of a great saving in time and freedom from difficulties arising from variations in spectral response and the development schedule of the photographic plates. Figure 14.29 shows a part of the iron spectrum photographed and analyzed with a microphotometer compared with a direct record obtained by photoelectric detection. These results were obtained by Dieke and Crosswhite<sup>54</sup> with a 21-foot grating. The multiplier phototube was mounted behind a slit on a carriage in such fashion that

<sup>54</sup> See Dieke and Crosswhite, reference 40.

the slit could be moved on rails along the focal curve of the spectrometer, the carriage being pressed against the rails by a motor-driven steel tape. The voltage supply for the multiplier phototube was obtained from a constant-voltage transformer and employed nine voltage-stabilizing tubes. The output of the phototube was either applied di-

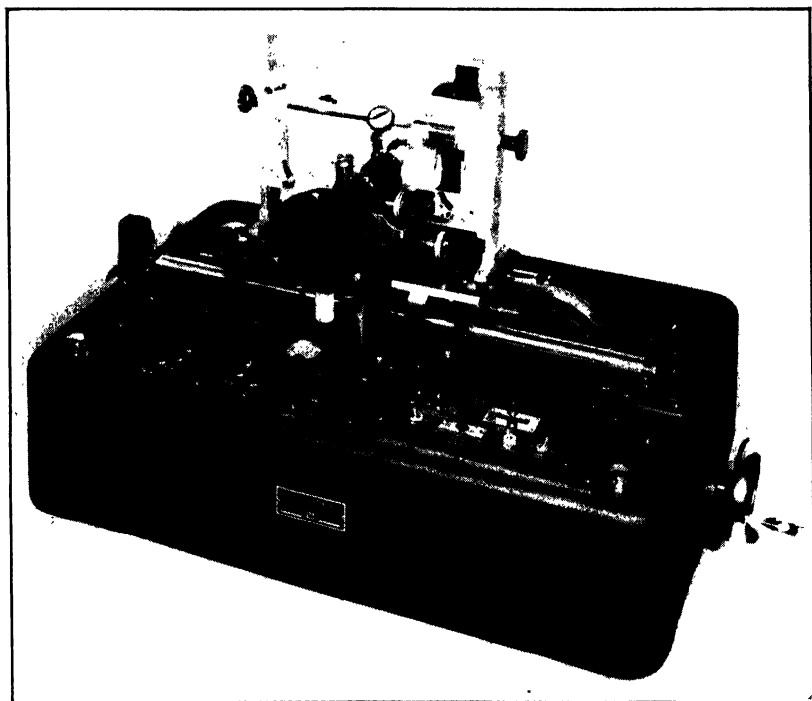


FIG. 14.28. Leeds & Northrup Recording Microphotometer (without "Speedo-max" Recorder). (Courtesy of Leeds and Northrup Company.)

rectly to a Leeds and Northrup recording microammeter, with a full-scale deflection for 5 microamperes or, for the measurement of very low intensity lines, first amplified by a direct-current amplifier with a gain of 400. A 931-A multiplier phototube was found satisfactory from about 6000 to 3000 Angstrom units, a 1P28 tube, for wave lengths of 3000 to 2000 Angstrom units. According to Rank, Pfister, and Coleman<sup>55</sup> any line which can be photographed in 2 hours may be measured directly with a multiplier phototube.

A high-speed recording spectrophotometer for absorption measure-

<sup>55</sup> See reference 41.



ments is described by Harrison and Bentley.<sup>56</sup> This instrument, employing a 10-foot grating and a multiplier phototube as detector, covers the range from 9800 to 3400 Angstrom units in 70 seconds. The spectral

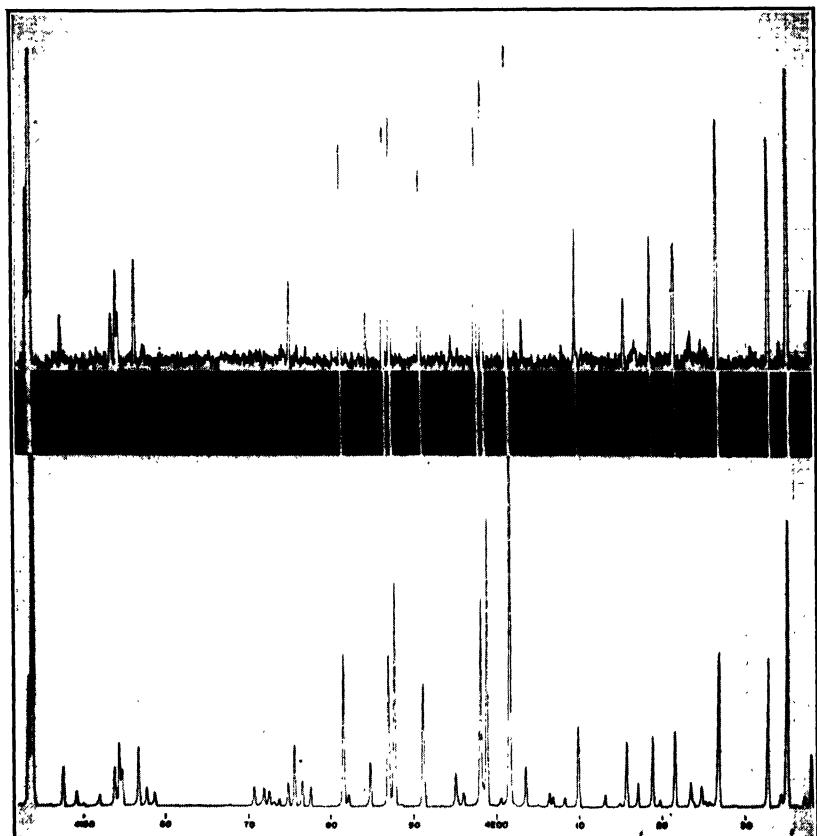


FIG. 14.29. Portion of Iron Spectrum: (a) Photographically Recorded and Measured with Microphotometer and (b) Photoelectrically Recorded. (Dieke and Crosswhite, reference 40.) (Courtesy of Professor G. H. Dieke.)

band selected by the slit is 0.5 to 10 Angstrom units wide. The lamp and entrance slit, as well as the exit slit and detector, are here stationary. The grating table is rotated and displaced in such a manner by a cam mechanism that the spectral region selected by the exit slit is always in sharp focus (Fig. 14.30). The absorption of the sample is measured by a comparison method. An oscillating biprism causes the light from the

<sup>56</sup> See reference 42.

exit slit to fall in turn on the sample cell and a comparison cell. While the biprism is in the first position the photocurrent charges a condenser. As the biprism shifts to direct the light to the comparison cell, the primary beam is momentarily cut off by a photometric rotating sector at

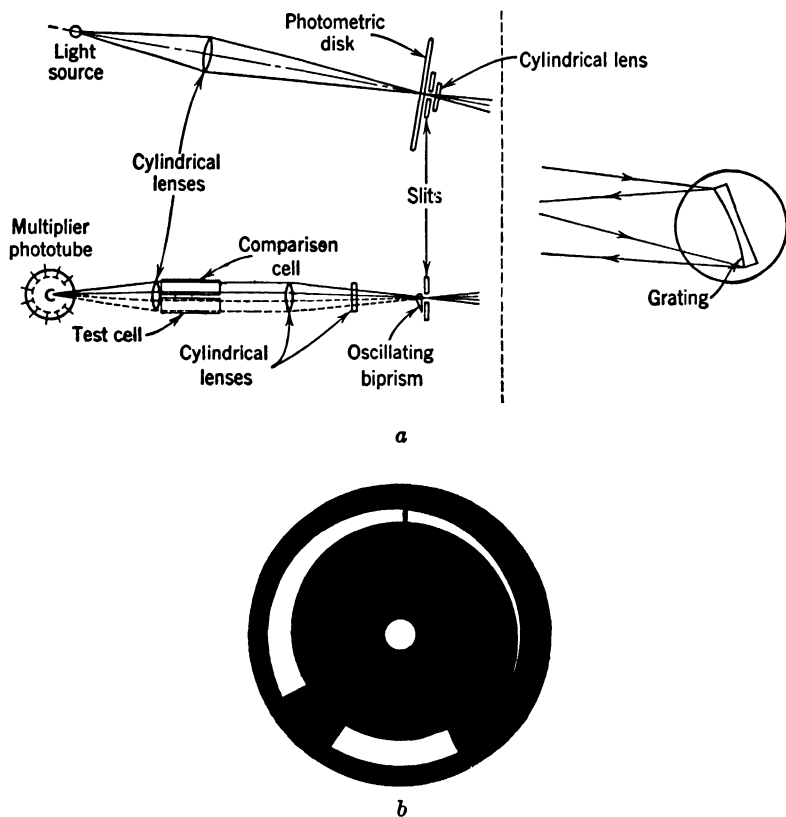


FIG. 14.30. Absorption Spectrophotometer of Harrison and Bentley: (a) Optical Arrangement. (b) Photometric Disk. (Reference 42.) (Courtesy of *J. Optical Soc. Am.*)

the entrance slit. The sector subsequently transmits an increasing amount of light, and the phototube connections are switched so that the photocurrent discharges the condenser. When the discharge is complete, a spark coil is actuated which punches a hole in the recording paper at an ordinate corresponding to the total discharge time. The displacement of the recording paper in the abscissal direction is, of course, coupled with the grating displacement mechanism so as to

establish the wave-length scale. The photometric disk is calculated to yield a linear transmission or density scale.

A more compact, prism, spectrophotometer has been designed by Hardy<sup>57</sup> and produced commercially by the General Electric Company.<sup>58</sup> The plan of this instrument is shown in Fig. 14.31. The spectrometer proper is a double monochromator with two 60-degree prisms. The wave length is selected by the linear displacement of the intermedi-

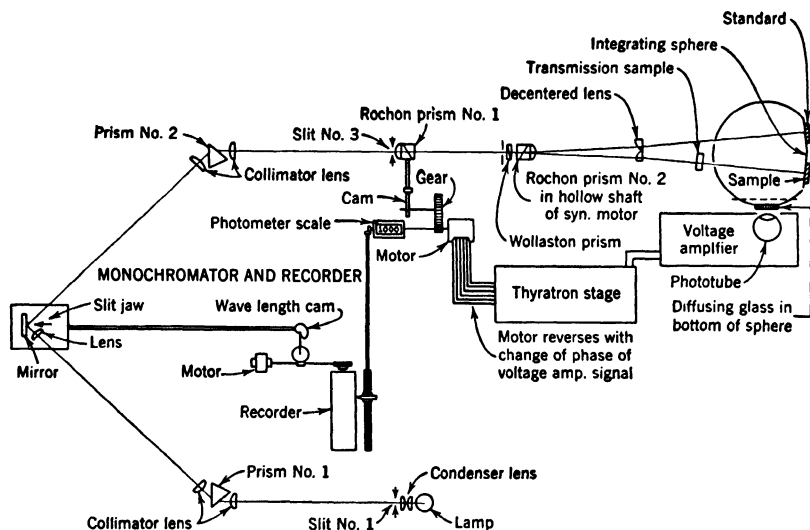


FIG. 14.31. General Electric Spectrophotometer. (Michaelson and Liebhaufsky, reference 44.) (Courtesy of *Gen. Elec. Rev.*)

ate slit, formed by a mirror and a single slit jaw. The light leaving the exit slit (slit 3) is plane polarized by Rochon prism 1 and split into two beams, polarized at right angles to each other, by a Wollaston prism.<sup>59</sup> The relative intensity of the two beams is determined by the angular position of the Rochon prism 1 relative to the stationary Wollaston prism. After passing through the Wollaston prism, both light beams pass through Rochon prism 2; the latter prism is rotated by a synchronous motor so that the two beams are alternately suppressed at a frequency of 60 cycles per second. The beams, further separated by a split lens, eventually enter the integrating sphere. If the spectral distribution of the reflection of a sample is to be determined by the color analyzer, one of the beams falls on the sample, the other on a standard

<sup>57</sup> See reference 43.

<sup>58</sup> See Michaelson and Liebhaufsky, reference 44.

<sup>59</sup> See Houstoun, reference 45, p. 197.

diffusing surface. If the transmission of a sample is to be measured, the sample is placed in one of the beams, and both are incident on similar diffusing surfaces in the integrating sphere. The phototube (actually placed symmetrically with respect to the two beams) is placed behind an opal-glass window in the sphere. Unless the light falling on the opal window from the two beams is equal in intensity, an alternating component will exist in the photocurrent. This component, after ampli-

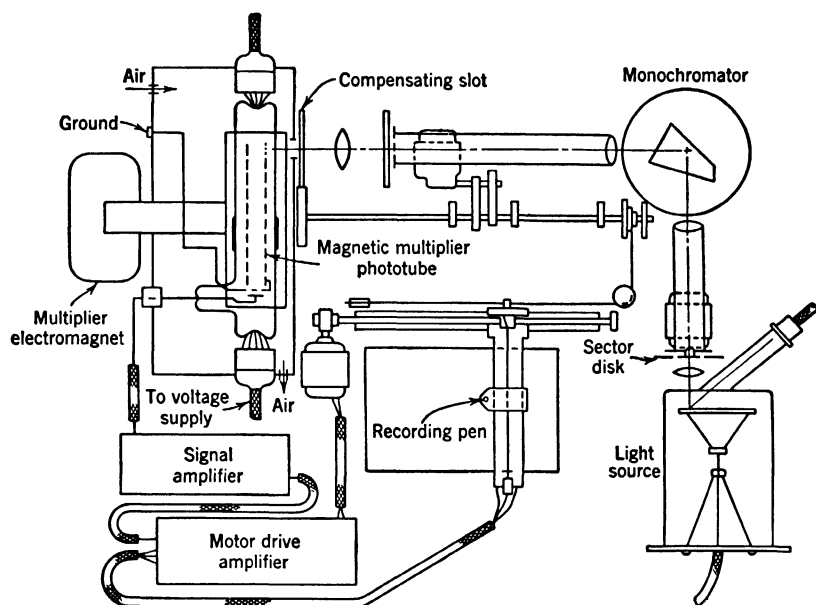


FIG. 14.32. Recording Spectrophotometer for Cathodoluminescent Materials. (Zworykin, reference 46.) (Courtesy of *J. Optical Soc. Am.*)

fication, actuates a motor which displaces the Rochon 1 prism, and the recorder scribe coupled to it, until balance is obtained. The direction of rotation of the motor is governed by the phase of the alternating component of the photocurrent. The primary application of the instrument is in the field of colorimetry and chemical analysis by absorption spectrometry. The immediate comparison feature makes the readings quite independent of variations in the sensitivity and of fatigue phenomena in the phototube.

Another automatic recording prism spectrophotometer, which has been found very useful in the study of the spectral distribution of the emission of cathodoluminescent materials, is shown in outline in Fig. 14.32.<sup>80</sup> Because of the low luminosity of the light sources to be meas-

<sup>80</sup> See Zworykin, reference 46.

ured, high light-gathering power of the spectrometer and high sensitivity of the detector were essential. A Gaertner monochromator, used in conjunction with a multiplier phototube, was chosen. The samples are mounted on a rotatable glass disk in a demountable tube and are bombarded by an oblique beam of 6000-volt electrons. The light beam falling on the entrance slit is interrupted by a rotating sector with a frequency of 150 cycles per second. In front of the exit slit of the monochromator a compensating slot, geared to the prism table, adjusts the effective slit height so that, throughout the spectrum, equal radiant energy per unit wave length range gives rise to the same photocurrent. The alternating component of the photocurrent, amplified and rectified, drives the pen motor on the recorder. The displacement of the wave length scale is, of course, coupled with the prism table of the monochromator. The calibration of the apparatus is carried out with a standard tungsten ribbon lamp. It was found that a light emission (luminance) of the sample as small as  $10^{-3}$  lumen per square centimeter still yields a useful record.

An apparatus serving similar purposes and based on similar principles has been installed by Austin Hardy at the RCA tube plant in Lancaster, Pennsylvania, for the routine checking of phosphors used in television tubes (Fig. 14.33). The spectral distribution curve appears directly on the face of a 12-inch cathode-ray tube. The same equipment measures a series of other important properties of phosphors.

Plymale<sup>61</sup> has studied the spectral distribution of the luminescence of materials such as cloth samples with ultraviolet excitation from a high-pressure mercury arc (General Electric EH 4 with Corning 5860 filter). He employed a Gaertner monochromator with a 1P22 (red-green-blue sensitive) multiplier phototube as detector. The samples were hinged at a suitable angle in front of the monochromator entrance slit.

The photoelectric detection method has the special advantage of making possible the study of the intensity variations of spectral lines in extremely short intervals. Dieke and his coworkers<sup>62</sup> have used their 21-foot grating spectrograph with a 1P28 multiplier phototube at the exit slit for investigating line intensity variations in arcs and sparks. The output of the phototube was applied directly to a cathode-ray oscillograph. The arrangement permitted the resolution of intensity variations lasting a fraction of a microsecond. Such high time resolution is needed in the study of intensity surges such as occur, for example, in the low-pressure mercury arc.

<sup>61</sup> See reference 47.

<sup>62</sup> See Dieke, Loh, and Crosswhite, reference 48.

A number of photoelectric spectrophotometers have been constructed specifically for the ultraviolet region. Examples are Drabkin's absorption spectrophotometer,<sup>63</sup> with a gas-filled cesium phototube as

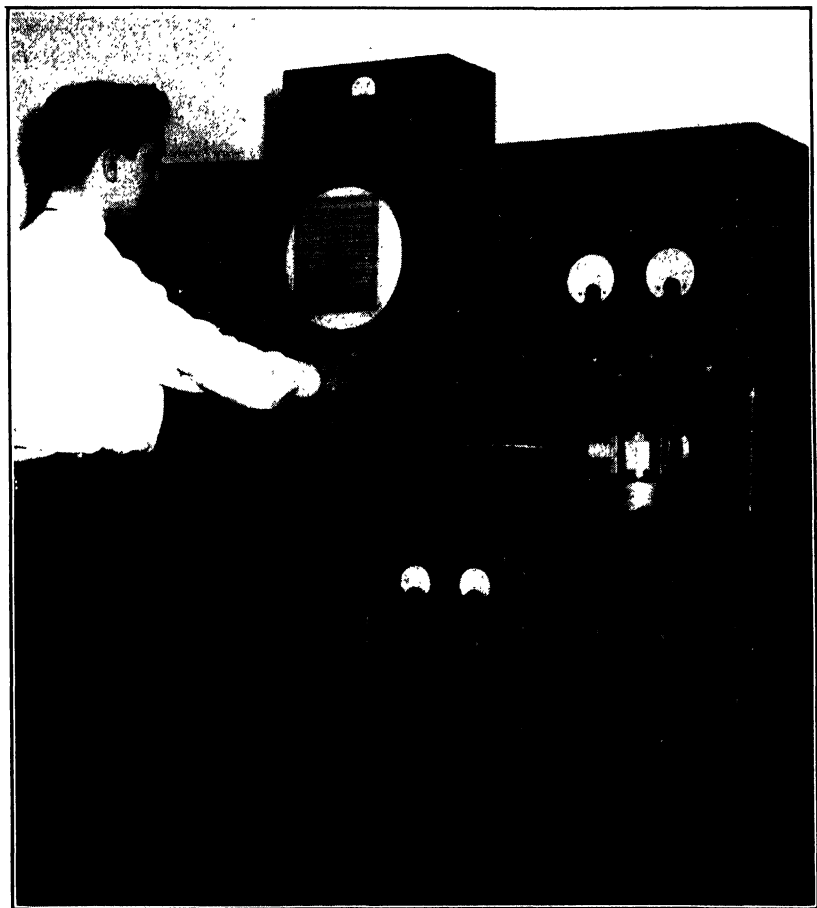


Fig. 14.33. Spectroradiometer for Routine Control of Phosphors. (RCA Tube Department, Lancaster, Pa.)

detector and a low grid-current amplifier and galvanometer, and Little's spectrophotometer for the Schumann region (1230 to 2200 A.U.).<sup>64</sup> Little employed a phototube whose platinum photocathode had been cleaned for 15 hours by discharge in hydrogen. A fluorite

<sup>63</sup> See Drabkin, reference 49.

<sup>64</sup> See Little, reference 50.

window transmitted the very short wave length radiation to the photocathode.

**Spectrochemical Analysis.** Any of the spectrophotometers described may be used for spectrochemical analysis. Here the photoelectric methods of detection are particularly advantageous since the time ele-

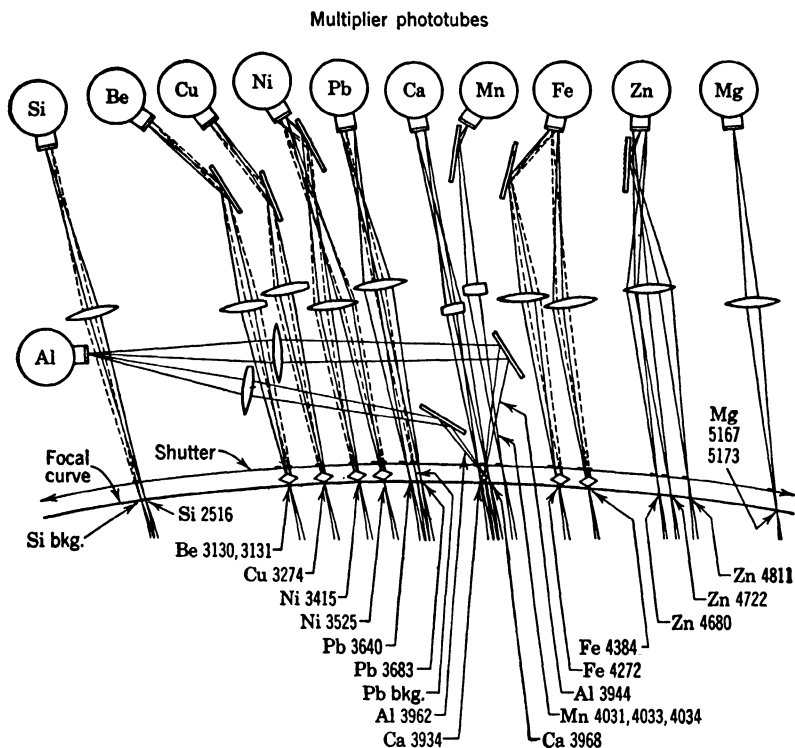


FIG. 14.34. Optical Arrangement of Spectrochemical Analyzer of Dow Chemical Company. (Saunderson, Caldecourt, and Peterson, reference 52.) (Courtesy of *J. Optical Soc. Am.*)

ment is frequently of crucial importance. In alloy metallurgy the decision of whether to pour or not to pour a melt often must await the findings of the analyst. In the surveillance of industrial processes an immediate indication of the composition of working materials may assure continuous efficient operation. Hasler and Dietert<sup>65</sup> have estimated that, in emission spectrum analysis, the time required to analyze samples may be reduced to one fourth in passing from photographic to photoelectric methods.

<sup>65</sup> See reference 51.

Perhaps the most highly automatic and precise system for direct spectrochemical analysis is represented by the installation for alloy analysis at the alloy plant of the Dow Chemical Company,<sup>66</sup> which handles about 4000 samples a month. The 2-meter grating spectrograph employs 11 multiplier phototubes, each arranged to receive the light from one or several lines of a particular element which may be

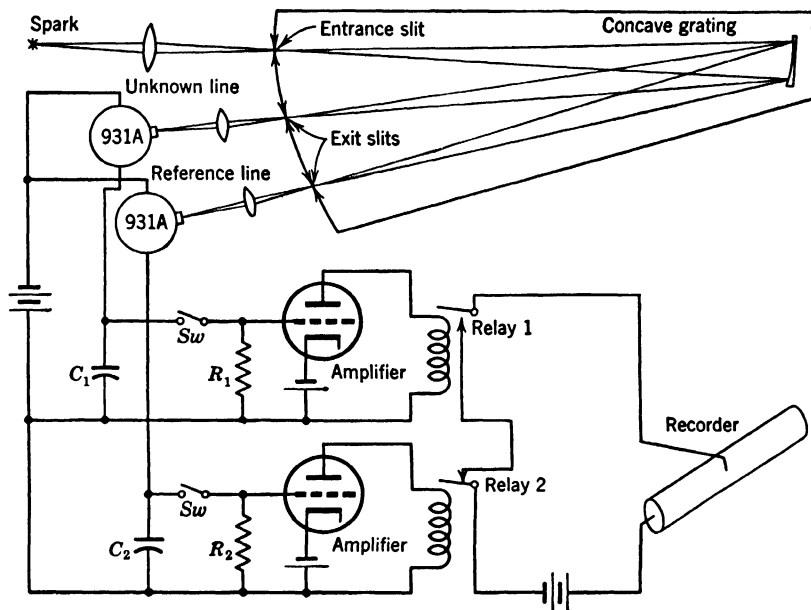


FIG. 14.35. Measurement Circuit of the Dow Analyzer (Schematic). (Saunderson, Caldecourt, and Peterson, reference 52.) (Courtesy of *J. Optical Soc. Am.*)

present in an alloy (Fig. 14.34). The intensities are compared with the intensity of a magnesium line, which serves as an internal standard. The several slits defining the positions of the lines are imaged on ground glass or ground quartz windows in front of the phototube cathodes, mirrors separating the close lines. Without such diffusing screens the phototube response depends critically on the tube position, since the effective photosensitivity of the multiplier photocathode varies considerably from point to point. The arrangement of biprisms and shutters at a number of the slits permits correction for background light.

The process of measurement is indicated schematically in Fig. 14.35. The spark between the sample electrodes operates for 20 seconds, during which time each multiplier phototube charges a condenser  $C$  to a voltage

<sup>66</sup> See Saunderson, Caldecourt, and Peterson, reference 52.



determined by the integrated photocurrent and the capacitance of  $C$ . Subsequently the switches  $Sw$  are closed and the condensers  $C$  discharge through the resistances  $R$ . The products  $RC$  are identical for all the circuits, though the values of  $C$  may be varied to yield charging voltages of the same order for the maximum concentration of the element encountered. When the voltage on any one condenser has dropped to a fixed value, for instance, 1 volt, a relay is tripped and depresses the corresponding pen on the moving recording tape. Thus, starting at different instants, depending on the intensity of the line in question, a series of parallel lines corresponding to different elements is traced on the record. Finally, when the condenser for the reference line has discharged to the same voltage, all the pens are raised and the record is complete. The length of each line is a measure of the time  $\Delta t$  which has elapsed between the instants at which the condenser for a particular element and that for the reference element have reached the same voltage. Since this time interval is proportional to the logarithm of the ratio of the initial voltages of the two condensers,<sup>67</sup> or of their accumulated photoelectric charge, the lengths of the recorded lines give directly a logarithmic measure of the concentration of the several components in the alloy. In practice, scales relating concentration and line length are established empirically with the aid of standard alloys of known composition. With these scales the concentration of seven elements can be read off from the record. An eighth line which is traced during the entire discharge period for the reference element indicates the least concentration that can be determined for any one element. If the line intensity for any one element is too small to charge the corresponding condenser up to relay-tripping potential, the recorded line is equal in length to the reference line and only indicates an upper limit to the concentration of the element.

Values of the concentrations measured with this apparatus have been found accurate to within 2 per cent of the concentration. The logarithmic scale is advantageous in making the reading error independent of the magnitude of the concentration. The relatively long period of integration (20 seconds) was found essential to keep the mean deviation low.

Less complex equipment serving similar purposes has been used by Boettner and Brewington<sup>68</sup> of the Wyandotte Chemical Company and

<sup>67</sup> If  $E_1$  is the initial voltage of the first condenser and  $E_o$  is that of the second, corresponding to the reference element, the magnitude of  $\Delta t$  is given by the condition

$$E_1 e^{-t/(RC)} = E_o e^{-(t+\Delta t)/(RC)} \quad \text{or} \quad \Delta t = RC \log_e \frac{E_o}{E_1}$$

<sup>68</sup> See reference 53.

Nahstoll and Bryan<sup>69</sup> of the Ford Motor Company. The former used a grating spectrograph, the latter a Bausch & Lomb quartz prism spectrograph. In both spectrographs a number of slits were arranged at locations corresponding to principal lines of the components of the sample. In the Ford equipment a mirror behind the slit for a reference line reflects its light into a 1P28 multiplier phototube within the spectrometer housing; the other 1P28 phototube may be placed behind any

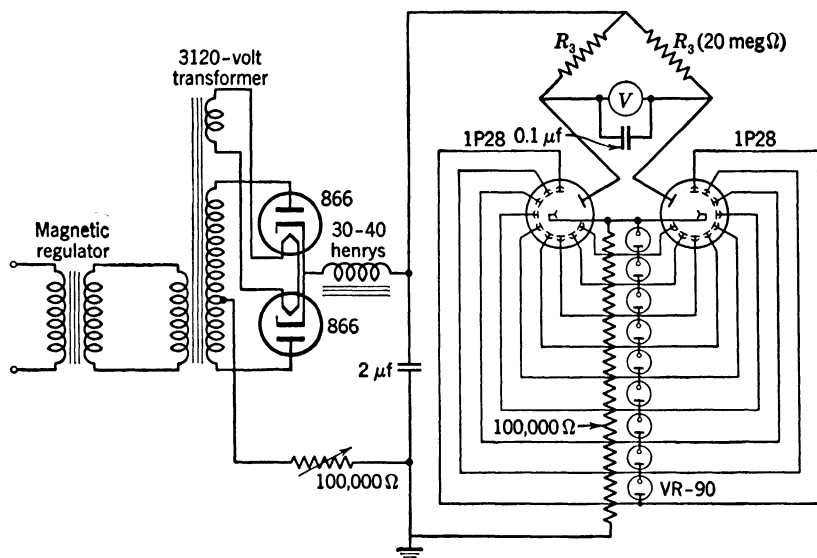


FIG. 14.36. Measurement Circuit Employing a Bridge and Vacuum-Tube Voltmeter. (Nahstoll and Bryan, reference 54.) (Courtesy of *J. Optical Soc. Am.*)

one of seven slits corresponding to different elements. In both systems a simple bridge (Fig. 14.36) was used to measure the ratio of the intensities of the two lines. Nahstoll and Bryan used a vacuum-tube voltmeter to measure the potential drop of the photocurrents across 20-megohm resistances ( $R_3$ ). If the variable resistance is adjusted so that the reference line yields a fixed deflection, the meter, connected in the bridge, may be calibrated to read the concentrations of the several elements in the alloy directly. A 0.1-microfarad capacitance is connected across the voltmeter in order to average the ratio of intensities over several seconds. Boettner and Brewington found that the concentration could be determined accurately from the increase in the operating voltage of the multiplier phototube for the sample line, required to attain balance.

<sup>69</sup> See reference 54.

An ingenious direct-reading analyzer has been devised by Dieke and Crosswhite.<sup>70</sup> The outputs of phototubes exposed to spectral lines of different elements are connected to a set of resistance-capacity circuits with identical value of  $RC$  (Fig. 14.37). The phototube for the reference element (here iron) is connected directly to the horizontal plates of an oscillograph, whereas the outputs of the other photo tubes are connected in turn (for instance, for  $\frac{1}{20}$  second at a time) to the vertical

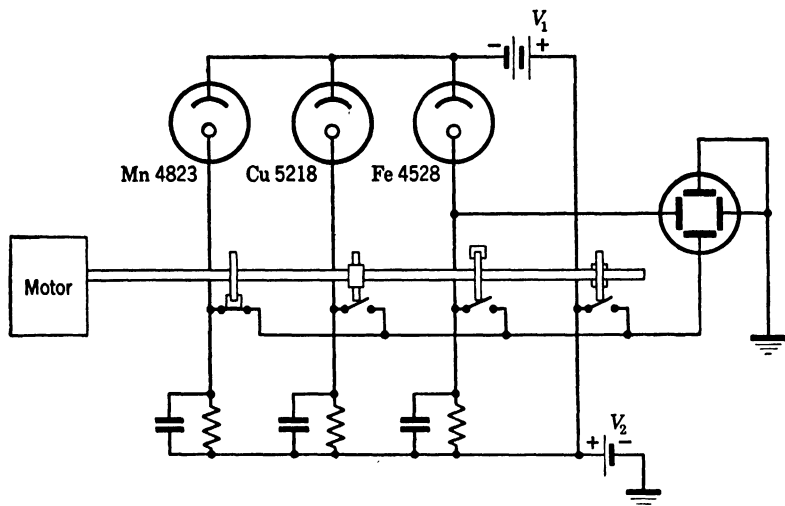


FIG. 14.37. Spectrochemical Analyzer Employing Oscillograph as Indicator. (Dieke and Crosswhite, reference 55.) (Courtesy of *J. Optical Soc. Am.*)

plates. Figure 14.38 shows the type of record obtained if the oscillograph screen is photographed, the lens shutter being left open after the spark source has been extinguished. Each component element gives rise to a dashed line with a different slope, which is proportional to its concentration. The position of the dashes, corresponding to intervals in which the commutator connects a particular phototube to the vertical plates, permits identification of the element which gives rise to the sloping line. The time constant of the  $RC$  circuits is, of course, chosen large compared with the frequency of revolution of the commutator, so that the effects of light source fluctuations is minimized.

Numerous other photoelectric devices serve to give a quantitative indication of the presence of specific substances in a given volume of air or liquid. An interesting example is the device shown schematically in Fig. 14.39. It is used by the U. S. Weather Bureau for the deter-

<sup>70</sup> See reference 55.

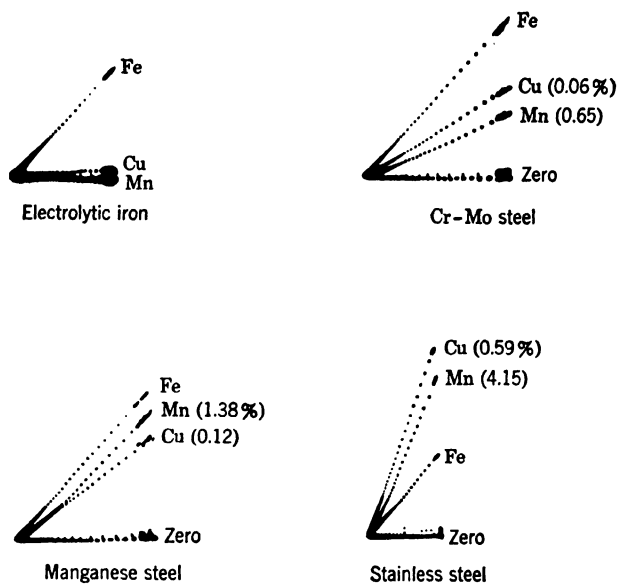


FIG. 14.38. Oscillograph Indications from Dieke and Crosswhite's Analyzer. (Dieke and Crosswhite, reference 55.)

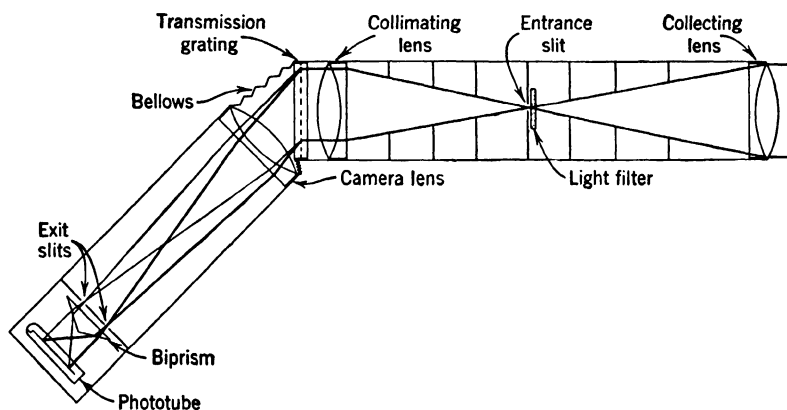


FIG. 14.39. Determination of Water Vapor Content in Atmosphere. (Foster and Foskett, reference 56.)

mination of the water-vapor content of the atmosphere.<sup>71</sup> Water vapor absorbs strongly in the infrared at a wave length of 9340 Angstrom units but is quite transparent to radiation at 10,130 Angstrom units. Hence, to measure the water-vapor content of the atmosphere, sunlight is dispersed by a 14,400 line-per-inch transmission grating, and narrow spectral bands centered on the above lines, separated by slits, are made to fall alternately on the same photocathode area of a type 919 infrared-

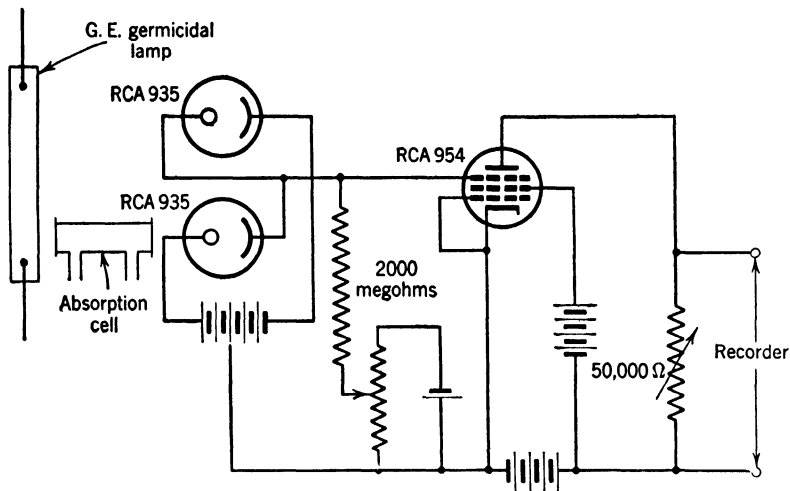


FIG. 14.40. Determination of Poisonous Gases in Air by Their Ultraviolet Absorption. (Klotz and Dole, reference 57.) (Courtesy of *Ind. Eng. Chem., Anal. Ed.*)

sensitive phototube. The phototube output is amplified by a negative-feedback direct-current amplifier.<sup>72</sup> The ratio of the photocurrents when one or the other slit is obscured by a shutter measures the absorption of the water vapor and hence its total amount in a column of the atmosphere extending from the observer to the sun. A heliostat keeps the instrument aimed at the sun.

Other instruments detect poisonous gases by their strong absorption for certain lines in the ultraviolet. One such arrangement is shown in Fig. 14.40.<sup>73</sup> Two ultraviolet-sensitive, type 935, phototubes are exposed to the radiation of a General Electric germicidal lamp, which emits about 95 per cent 2537 Angstrom units radiation. An absorption cell through which the contaminated air is drawn is placed between the

<sup>71</sup> See Foster and Foscett, reference 56.

<sup>72</sup> See Chapter 12, p. 227.

<sup>73</sup> See Klotz and Dole, reference 57.

light source and one of the cells. The difference in the photocurrent in the two cells creates a potential drop over a 2000-megohm input resistance which is amplified by a low grid-current tube and applied to a recorder. Dupont has a similar system to detect harmful concentrations of carbon disulfide gas in working areas.<sup>74</sup>

As an example of photoelectric methods in the surveillance of working liquids, a TVA ammonia plant applies Weston barrier-layer cells to check the concentration of bivalent copper ions in solutions used to remove harmful impurities ( $\text{CO}$ ,  $\text{CO}_2$ ,  $\text{O}_2$ ) from the synthesized gases.<sup>75</sup> The strongly absorbing liquids are passed through thin cylindrical Pyrex cells within which are placed 6-candlepower lamps, operated at low current for long life. The barrier-layer cells receive the light that has passed through a layer of liquid of definite thickness; their photocurrent is continually registered on a recording microammeter. Fatigue effects are slight, since the illumination of the cells is continuous.

**The Measurement of Corpuscular Radiations and X-Rays by Photocells.** It has already been pointed out, in the discussion of multiplier phototubes, that such structures can be employed effectively for the direct measurement of corpuscular and x-radiations.<sup>76</sup> Similarly, von Ardenne<sup>77</sup> has found the barrier-layer cell bombarded directly by the high-velocity image-forming electrons useful for gaging exposures in electron microscopy. In many other applications the corpuscular or x-radiation is first converted into light by an efficient fluorescent screen and then measured with a conventional phototube.

Thus Blau and Dreyfus<sup>78</sup> have found it convenient to measure the strength of alpha-particle emitting sources, such as polonium, by a simple arrangement. The specimen, mounted on a carriage, excites fluorescence in a screen in front of a multiplier phototube, whose output is measured by a microammeter. The sensitivity of the phototube is checked by a lamp on a second carriage. The apparatus is calibrated by a standard radium source. Since radium emits gamma and beta rays as well as alpha rays, it is necessary to measure the photocurrent with and without a filter for alpha rays interposed, and to take the difference for the calibration.

The combination of a fluorescent screen and a multiplier phototube is also utilized in the scanning electron microscope.<sup>79</sup> In this instrument

<sup>74</sup> See reference 58.

<sup>75</sup> See Brown and Cline, reference 59.

<sup>76</sup> See Chapter 8, p. 150.

<sup>77</sup> See von Ardenne, reference 60.

<sup>78</sup> See reference 61.

<sup>79</sup> See Zworykin, Hillier, and Snyder, reference 62.

a fine electron probe is deflected across a minute section of the surface of an opaque specimen. The secondary electrons ejected from the surface by the probe strike a fluorescent screen whose light emission is directed by a lens onto the cathode of a multiplier phototube (Fig. 14.41). The signal generated by the photocurrent, which is determined by the secondary-emission ratio of the surface element scanned at any instant, controls the recording density of a facsimile printer,<sup>80</sup>

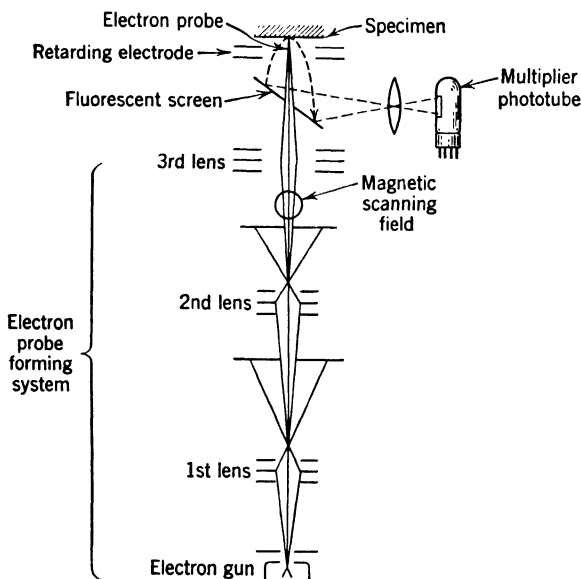


FIG. 14.41. Employment of Multiplier Phototube in Scanning Electron Microscope. (Zworykin, Hillier, and Snyder, reference 62.)

whose recording speed is coupled to the beam deflection across the specimen surface. In this manner the printer traces out an image of the specimen with a magnification equal to the ratio of the printer speed to the beam deflection speed. A small aperture is drilled in the inclined fluorescent screen to admit the narrow scanning beam. The electrode configuration in front of the specimen is made so that the secondary electrons are spread over an area of the fluorescent screen which is large compared to the aperture.

In x-ray intensity measurements it is convenient to apply the phosphor directly to the envelope of the multiplier phototube.<sup>81</sup> The phosphor is either silver-activated zinc sulfide or calcium tungstate, both of which

<sup>80</sup> See Chapter 16, p. 359.

<sup>81</sup> See Smith, reference 63.

have blue emissions matching the sensitivity peak of the 931-A multiplier phototube and relatively short persistence. Such a unit, operated with a stable voltage supply, may be calibrated, for any one x-ray wavelength, directly in terms of roentgens ( $r$ ) <sup>82</sup> per second—the physiological unit of x-ray dosage. Connected so as to charge a condenser, the multiplier phototube with the fluorescent coating may be used to measure integrated dosage.

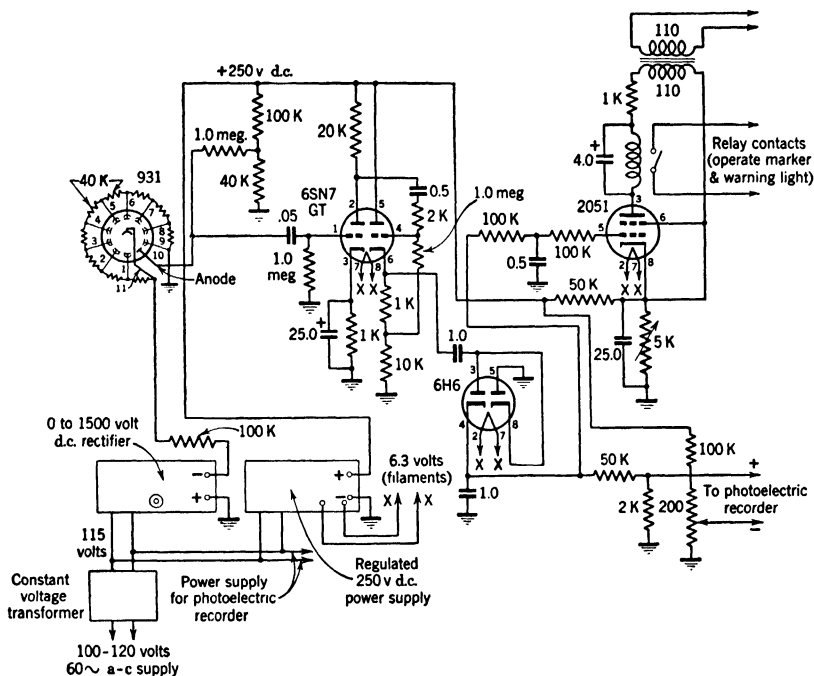


FIG. 14.42. Circuit Employed for X-ray Inspection of Sealed Units. (Smith, reference 63.) (Courtesy of *Gen. Elec. Rev.*)

The same combination lends itself well to automatic x-ray inspection methods. In this connection it is important that both the x-ray tube voltage and the multiplier voltage are carefully stabilized, since the output may vary as a high power of either. Since the x-ray emission is usually pulsed at 60 cycles, the output of the multiplier may be amplified by alternating-current amplifiers. Figure 14.42 shows a circuit which has been employed for the inspection of sealed units, causing rejection of those which are slack-filled and hence give rise to increased

<sup>82</sup> A roentgen or *r*-unit is the x-ray dosage which, passing through 1 cubic centimeter of air under standard conditions, liberates  $3.3 \cdot 10^{-10}$  coulomb of charge.



photocurrent. The output of the multiplier is reversed in sign by the first section of the 6SN7 tube, impressed across a reduced impedance by the second section, acting as a cathode-follower stage, rectified, and applied to the grid of the rejection-relay controlling thyatron. If thicknesses of materials are checked by x-ray inspection—for instance, the thickness of hot and cold strip in steel mills—it is convenient to employ two phototube detectors, with identical voltage supply and x-ray source, and to measure the output difference for a

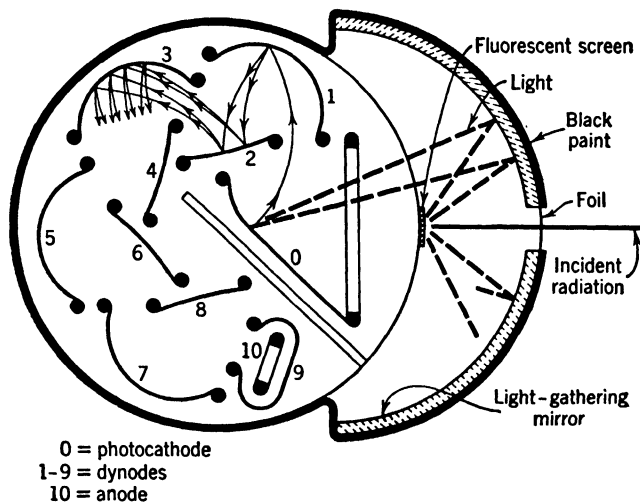


FIG. 14.43. Photomultiplier Radiation Detector. (Coltman and Marshall, reference 64.) (Courtesy of *Nucleonics*.)

transradiated standard sample and the material tested. Such x-ray methods of inspection are particularly valuable for the detection of excess admixtures of materials of high atomic weight, which are exceedingly effective x-ray absorbers.

Figure 14.43 shows an arrangement of the multiplier phototube, a zinc sulfide phosphor with blue luminescence, and a mirror cap to concentrate the light from the phosphor on the photocathode, which constitutes a detector of extraordinary sensitivity for x-ray, gamma ray, and corpuscular radiation.<sup>83</sup> Neutron detection is accomplished by mixing boron with the phosphor, the boron reacting with slow neutrons to emit alpha particles. Since the radiation passes through an extremely thin, evaporated aluminum window and the exterior of the mirror and tube envelope are painted black, no ambient light reaches

<sup>83</sup> See Coltman and Marshall, reference 64.

the interior of the tube. The pentode input circuit and the pentode output circuit are arranged to have the same time constant, equal to the phosphor decay constant (17 microseconds—Fig. 14.44). This integrates the pulses for the several light quanta arising from a single incident particle or gamma-ray photon, so that the average pulse resulting from this source greatly exceeds the average dark-current pulse in amplitude. A cathode follower stage matches the output to a cable connecting the system with an amplifier or counter; for a radium gamma-

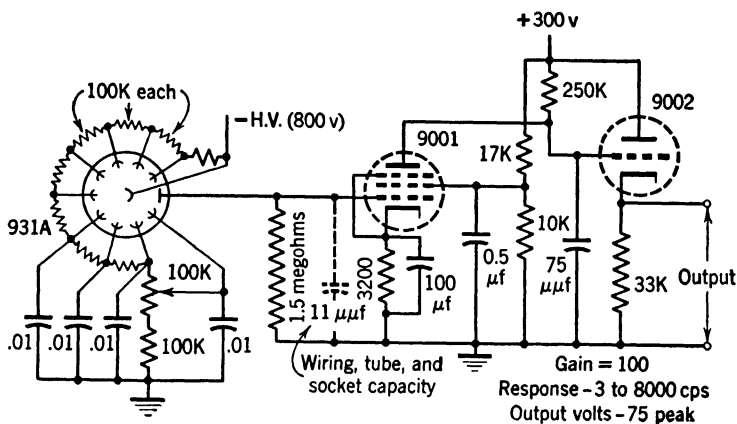


FIG. 14.44. Amplifying Circuit for Radiation Detector. (Courtesy of J. Coltman, Westinghouse Research Laboratories.)

ray photon the output signal amplitude is about 20 volts. As a counter this device has been found to be about twice as sensitive as a Geiger counter for gamma rays, beta rays, and 8-kilovolt x-rays; in addition, it is considerably faster. Very high efficiencies in the detection of gamma rays and electrons have also been obtained by the employment of relatively thick naphthalene, anthracene, and other organic crystals as fluorescent screens in conjunction with multiplier phototubes.<sup>84</sup>

Perhaps the simplest use of a phototube in x-ray technique is as an exposure timer, as in the Westinghouse Phototimer (Fig. 14.45).<sup>85</sup> A phototube, laterally displaced from the lens of the camera, receives light from the fluorescent screen on which the x-ray shadowgraph of the object is formed. The resulting photocurrent charges a condenser until the grid of a thyratron is raised to a potential at which it breaks down and interrupts, by a relay, the primary of the x-ray transformer. The desired exposure is set by adjusting the capacitance of the condenser.

<sup>84</sup> See Kallmann, reference 65, and Marshall, Coltman, and Bennett, reference 66.

<sup>85</sup> See reference 67.

Phototubes also find application in precision x-ray absorption photometers. One instrument<sup>86</sup> employs two beams leaving the x-ray tube target in opposite directions; one passes through the sample, the other through a standard. Just beyond the specimen and standard are fluorescent screens whose light is guided by silvered glass tubes, transmitting 90 to 60 per cent of the entering light, to a shutter disk in a lightproof housing. The disk, rotating at 1800 revolutions per minute, transmits, in turn,

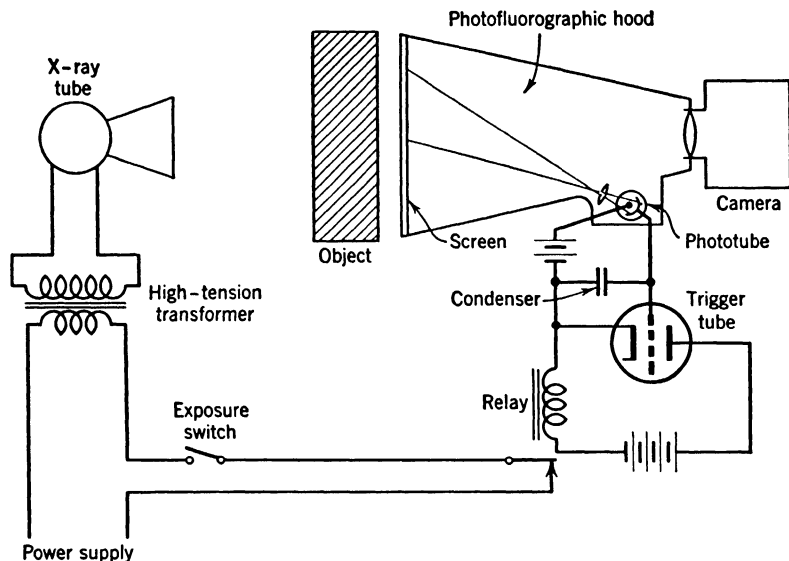


FIG. 14.45. Westinghouse Phototimer for Timing X-ray Exposures. (Reference 67.)  
(Courtesy of *Rev. Sci. Instruments*.)

light from the sample and from the standard to the multiplier-phototube cathode. The signal amplitude corresponding to the difference in the two intensities is amplified, rectified, and applied to a recording microammeter if, for instance, the equipment is to be used for the continuous surveillance of strip materials. This system will measure 1 per cent out-of-balance absorption.

A second x-ray photometer represents a commercial General Electric Company instrument.<sup>87</sup> Here the x-ray beam itself is interrupted by a shutter disk in such manner that it passes in turn through the sample and through the standard. The light excited by the x-ray beam on a fluorescent screen falls on the cathode of a phototube, whose photo-

<sup>86</sup> See Moriarty, reference 68.

<sup>87</sup> See Michel and Rich, reference 69.

current controls the position of a calibrated attenuator wedge as well as the recorder pen. The wedge is displaced in the x-ray beam in such a manner as to make the 60-cycle component of the photocurrent vanish.

## REFERENCES

1. H. E. IVES and E. F. KINGSBURY, "The applicability of photoelectric cells to colorimetry," *J. Optical Soc. Am.*, Vol. 21, pp. 541-563, 1931.
2. Y. BJÖRNSTAHL, "Is the barrier-layer photoelement suitable for precision photometric measurements?," *Z. Instrumentenk.*, Vol. 62, pp. 181-186, 1942.
3. W. E. FORSYTHE, "The present status of photometry," *Illum. Eng.*, Vol. 31, pp. 193 ff., 1936.
4. Committee on Instruments and Measurements, "Equipment and procedures for photometric measurements of blackout and dimout luminaires," *Illum. Eng.*, Vol. 38, pp. 509-517, 1943.
5. G. B. BUCK II, "Optically corrected cells," *Gen. Elec. Rev.*, Vol. 51, pp. 38-42, October, 1948.
6. Committee on Photoelectric Portable Photometers, "Report," *Illum. Eng.*, Vol. 32, pp. 379-420, 1937.
7. K. A. STALEY, "New meters simplify brightness studies," *Elec. World*, Vol. 124, p. 126, Oct. 13, 1945.
8. R. KINGSLAKE, "An apparatus for testing highway sign reflector units," *J. Optical Soc. Am.*, Vol. 28, pp. 323-326, 1938.
9. Y. G. HURD, "Measurement of helios with a barrier layer photocell," *Illum. Eng.*, Vol. 41, pp. 306-311, 1946.
10. I. GOODBAR, "New procedure to measure accurately illumination at large angles of incidence with a barrier layer cell," *Illum. Eng.*, Vol. 40, pp. 830-835, 1945.
11. W. W. COBLENTZ, "The measurement of ultra-violet radiation useful in heliotherapy," *J. Optical Soc. Am.*, Vol. 36, pp. 72-76, 1946.
12. W. W. COBLENTZ and R. STAIR, "A daily record of ultra-violet solar and sky radiation in Washington, 1941-1943," *J. Res. Natl. Bur. Standards*, Vol. 33, pp. 21-44, 1944.
13. H. C. RENTSCHLER, "An ultra-violet light meter," *Trans. A.I.E.E.*, Vol. 49, pp. 576-578, 1930.
14. R. S. HUNTER, "A multipurpose photoelectric reflectometer," *J. Optical Soc. Am.*, Vol. 30, pp. 536-559, 1940.
15. P. MOON and J. LAURENCE, "Construction and test of a goniophotometer," *J. Optical Soc. Am.*, Vol. 31, pp. 130-139, 1941.
16. P. ELLINGER and M. HOLDEN, "Fluorimetry: the estimation of the concentration of fluorescent pigments from their fluorescent intensity," *J. Soc. Chem. Ind.*, Vol. 63, pp. 115-121, 1944.
17. M. H. FLETCHER, C. E. WHITE, and M. S. SHEFTEL, "Fluorometric attachment for the Beckman spectrophotometer," *Ind. Eng. Chem., Anal. Ed.*, Vol. 18, pp. 204-205, November, 1946.
18. A. M. GRINER, A. A. TYTELL, and H. KERSTEN, "A luminometer for measuring bacterial luminescence," *Rev. Sci. Instruments*, Vol. 16, pp. 10-14, 1945.
19. R. P. KREBS, P. PERKINS, A. A. TYTELL, and H. KERSTEN, "A turbidity comparator," *Rev. Sci. Instruments*, Vol. 13, pp. 229-232, 1942.

20. G. F. BARNETT and A. L. FREE, "Photoelectric dust meter," *Electronics*, Vol. 19, pp. 116-119, December, 1946.
21. J. L. WILSON and E. E. MENDENHALL, "Measurement of detergency," *Ind. Eng. Chem., Anal. Ed.*, Vol. 16, pp. 251-253, 1944.
22. P. P. DEBYE, "A photoelectric instrument for light scattering measurements and a differential refractometer," *J. Applied Phys.*, Vol. 17, pp. 392-398, 1946.
23. P. DEBYE, "Light scattering in solutions," *J. Applied Phys.*, Vol. 15, pp. 338-342, 1944.
24. E. KARRER and R. S. ORR, "A photoelectric refractometer," *J. Opt. Soc. Am.*, Vol. 36, pp. 42-46, 1946.
25. D. B. JUDD, "The 1931 standard observer and coordinate system for colorimetry," *J. Optical Soc. Am.*, Vol. 23, pp. 359-374, 1933.
26. B. T. BARNES, "A four-filter photoelectric colorimeter," *J. Optical Soc. Am.*, Vol. 29, pp. 448-452, 1939.
27. B. T. BARNES, "A direct-reading photoelectric colorimeter," *Rev. Sci. Instruments*, Vol. 16, pp. 337-339, 1945.
28. M. H. SWEET, "Direct-reading color densitometer," *Electronics*, Vol. 18, pp. 102-106, March, 1945.
29. M. H. SWEET, "Logarithmic photometer," *Electronics*, Vol. 19, pp. 105-109, November, 1946.
30. G. C. SZIKLAI and A. C. SCHROEDER, "Electronic spectroscopy," *J. Applied Phys.*, Vol. 17, pp. 763-767, 1946.
31. J. A. HALL, "Drift of selenium photoelectric cells in relation to their use in temperature measurement," *J. Iron Steel Inst.*, London, Vol. 149, pp. 547-557, 1944.
32. G. F. HUBING, "A portable blocking-layer photocell pyrometer," *J. Optical Soc. Am.*, Vol. 26, pp. 260-261, 1936.
33. H. W. RUSSELL, C. F. LUCKS, and I. G. TURNBULL, "A new two-color optical pyrometer," *J. Optical Soc. Am.*, Vol. 30, pp. 248-250, 1940.
34. M. H. SWEET, "Photoelectric color temperature meter for incandescent lamps," *J. Optical Soc. Am.*, Vol. 30, pp. 568-571, 1940.
35. A. J. BRUNNER, "A photoelectric exposure meter for metallurgy," *Materials and Methods*, Vol. 22, pp. 416-417, 1945.
36. P. A. HAYTHORNE and R. W. POWELL, "An inexpensive photometer for metallography," *Iron Age*, Vol. 153, pp. 66-69, May 11, 1944.
37. W. VAN B. ROBERTS, "A simplified high-sensitivity photometer or exposure meter for enlarging," *Rev. Sci. Instruments*, Vol. 11, pp. 159-160, 1940.
38. J. ROBINS and L. E. VARDEN, "Photocell control for color printing," *Electronics*, Vol. 19, pp. 110-115, June, 1946.
39. J. R. COSBY, "Spectrograph exposure control," *Electronics*, Vol. 19, pp. 123-125, April, 1946.
40. G. H. DIEKE and H. M. CROSSWHITE, "Direct intensity measurements of spectrum lines," *J. Optical Soc. Am.*, Vol. 35, pp. 471-480, 1945.
41. D. H. RANK, R. J. PFISTER, and P. D. COLEMAN, "Photoelectric detection and intensity measurement in Raman spectra," *J. Optical Soc. Am.*, Vol. 32, pp. 390-396, 1942.
42. G. R. HARRISON and E. P. BENTLEY, "An improved high-speed recording spectrophotometer," *J. Optical Soc. Am.*, Vol. 30, pp. 290-294, 1940.
43. A. C. HARDY, "A new recording spectrophotometer," *J. Optical Soc. Am.*, Vol. 25, pp. 305-311, 1935.

44. J. L. MICHAELSON and H. A. LIEBHAFSKY, "A new spectrophotometer and some of its applications," *Gen. Elec. Rev.*, Vol. 39, pp. 445-450, 1936.
45. R. A. HOUSTOUN, *A Treatise on Light*, Longmans, Green and Company, London, 1924.
46. V. K. ZWORYKIN, "An automatic recording spectroradiometer for cathodoluminescent materials," *J. Optical Soc. Am.*, Vol. 29, pp. 84-91, 1939.
47. W. S. PLYMALE, JR., "A sensitive photoelectric method for determining the chromaticity of phosphorescent and fluorescent materials," *J. Optical Soc. Am.*, Vol. 37, pp. 399-402, 1947.
48. G. H. DIEKE, H. Y. LOH, and H. M. CROSSWHITE, "Spectral intensity measurements with phototube and the oscillograph," *J. Optical Soc. Am.*, Vol. 36, pp. 185-191, 1946.
49. D. L. DRABKIN, "A new form of photoelectric ultra-violet spectrophotometer," *J. Optical Soc. Am.*, Vol. 35, pp. 163-169, 1945.
50. E. P. LITTLE, "Photoelectric spectrophotometry for the Schumann region," *J. Optical Soc. Am.*, Vol. 36, pp. 168-171, 1946.
51. M. F. HASLER and H. W. DIETERT, "Direct-reading instrument for spectrochemical analyses," *J. Optical Soc. Am.*, Vol. 34, pp. 751-758, 1944.
52. J. L. SAUNDERSON, V. J. CALDECOURT, and E. W. PETERSON, "A photoelectric instrument for direct spectrochemical analysis," *J. Optical Soc. Am.*, Vol. 35, pp. 681-697, 1945.
53. A. BOETTNER and G. P. BREWINGTON, "Application of multiplier phototube to quantitative spectrochemical analysis," *J. Optical Soc. Am.*, Vol. 34, pp. 6-11, 1944.
54. G. A. NAHSTOLL and F. R. BRYAN, "An application of multiplier phototubes to the spectrochemical analysis of magnesium alloys," *J. Optical Soc. Am.*, Vol. 35, pp. 646-650, 1945.
55. G. H. DIEKE and H. M. CROSSWHITE, "Spectrochemical analysis with the oscillograph," *J. Optical Soc. Am.*, Vol. 36, pp. 192-195, 1946.
56. N. B. FOSTER and L. W. FOSKETT, "A spectrophotometer for the determination of the water vapor in a vertical column of the atmosphere," *J. Optical Soc. Am.*, Vol. 35, pp. 601-610, 1945.
57. I. M. KLOTZ and M. DOLE, "Automatic-recording ultra-violet photometer for laboratory and field use," *Ind. Eng. Chem., Anal. Ed.*, Vol. 18, pp. 741-745, 1946.
58. "Rapid gas analysis for vapor control," *Electronics*, Vol. 17, pp. 148-150, September, 1944.
59. E. M. BROWN and J. E. CLINE, "Continuous photometric determination of bivalent copper in ammoniacal solution," *Ind. Eng. Chem., Anal. Ed.*, Vol. 17, pp. 284-285, 1945.
60. M. v. ARDENNE, "On a new universal electron microscope with high power magnetic objective and reduced thermal object loading," *Kolloid-Z.*, Vol. 108, pp. 195-208, 1944.
61. M. BLAU and B. DREYFUS, "The multiplier phototube in radioactive measurements," *Rev. Sci. Instruments*, Vol. 16, pp. 245-248, 1945.
62. V. K. ZWORYKIN, J. HILLIER, and R. L. SNYDER, "A scanning electron microscope," *ASTM Bulletin* 117, pp. 15-23, August, 1942.
63. H. M. SMITH, "X-ray inspection with phosphors and photoelectric tubes," *Gen. Elec. Rev.*, Vol. 48, pp. 13-17, March, 1945.

64. J. W. COLTMAN and F.-H. MARSHALL, "Photomultiplier radiation detector," *Nucleonics*, Vol. 1, pp. 58-64, November, 1947.
65. H. KALLMANN, *Natur u. Tech.*, July, 1947.
66. F.-H. MARSHALL, J. W. COLTMAN, and A. I. BENNETT, "The photomultiplier radiation detector," *Rev. Sci. Instruments*, Vol. 19, 744-770, 1948.
67. "Electronic x-ray timer," *Rev. Sci. Instruments*, Vol. 16, p. 46, 1945.
68. C. D. MORIARTY, "X-ray flicker photometer," *Gen. Elec. Rev.*, Vol. 50, pp. 39-42, February, 1947.
69. T. C. MICHEL and T. A. RICH, "X-ray photometer," *Gen. Elec. Rev.*, Vol. 50, pp. 45-48, February, 1947.

## Chapter 15

# PHOTOTUBES IN SOUND REPRODUCTION

The sound accompaniment is, today, felt to be an essential feature of any motion-picture presentation. Few would now be satisfied with the pantomime of the silent films. Even in the field of home movies 16-millimeter sound projectors are finding wide acceptance. In the early days of sound movies the sound was often supplied by a disk record synchronized with the motion picture film, but this record has now been almost wholly replaced by a sound track printed directly on the projected film. In this manner synchronization difficulties are completely avoided. The translation of the sound track into sound requires a light beam and a photocell. There are well over 25,000 motion-picture houses in the United States alone; it is thus obvious that sound films represent an important application of photosensitive devices.

**The Recording of Sound on Film.**<sup>1</sup> The first successful efforts to record sound on film go back to the beginning of the twentieth century. E. Ruhmer, in 1901, employed the "speaking carbon arc" for this purpose; E. Gehricke, three years later, used a modulated gas-discharge tube. However, the recording systems were not developed to a point of perfection which permitted commercial exploitation until the late twenties. In America there are three current methods of recording the sound track: the modulated glow lamp,<sup>2</sup> the mechanical light valve,<sup>3</sup> and the vibrating mirror or shutter.<sup>4</sup> A fourth light-beam modulator, the Kerr cell, has an excellent frequency response, but does not find commercial application because of its excessive modulating voltage re-

<sup>1</sup> See Kellogg, reference 1.

<sup>2</sup> In particular, the "Aeolight," a hot-cathode tube containing a mixture of gases, of the Case Laboratories (Auburn, N. Y.), which is a part of Fox Movietone equipment.

<sup>3</sup> Developed by Western Electric Company. See, for example, MacKenzie, reference 2.

<sup>4</sup> Employed in RCA Phototone equipment. See Dimmick, reference 3.



quirements.<sup>5</sup> All these devices may be used for producing a variable-density track (Fig. 15.1*a*). However, the vibrating mirror is more commonly employed to form a variable-area track (Fig. 15.1*b*), and suitable forms of the mechanical light valve may serve the same purpose.<sup>6</sup> In the variable-density track the changes in sound pressure at the microphone are reflected in changes in density or opacity of a strip of constant width; in the variable-area track they are reflected in variations in width of the exposed area.

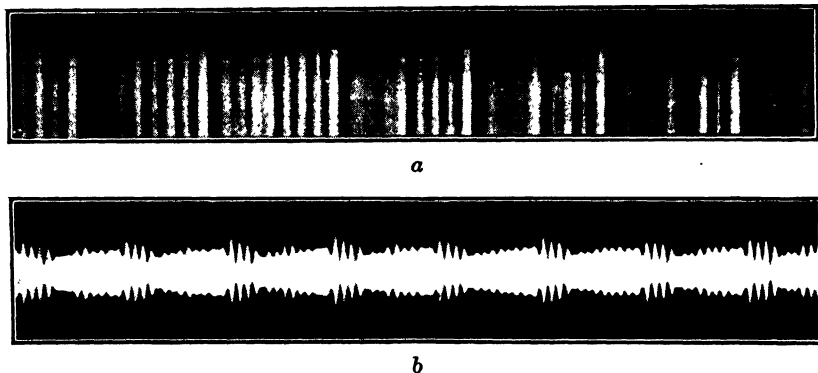


FIG. 15.1. (a) Variable-Density Track and (b) Variable-Area Track. (Kellogg, reference 1.)

Figure 15.2 shows the recording of a variable-density track with a light valve. Light from an intense source is focused on the slit between two closely spaced metal ribbons placed in a strong magnetic field. As the amplified microphone currents pass through the ribbons in opposite directions, they are displaced laterally so as to increase or decrease the slit width and, hence, the amount of light falling on the film. The ribbons are slightly displaced axially to prevent their striking each other.

A system for variable-area recording with a mirror galvanometer is shown in Fig. 15.3. A triangular aperture in a mask uniformly illuminated by the light source is imaged, after reflection by a galvanometer mirror, on a slit which, in turn, is imaged on the film. The amplified microphone currents passing through the galvanometer rotate the mirror about a horizontal axis and cause the slit to coincide with a wider or narrower portion of the triangle, resulting in a corresponding change in the width of the exposed portion of the film. In practice a bias current

<sup>5</sup> See Zworykin, Lynn, and Hanna, reference 4, and Fig. 12.25 on p. 243.

<sup>6</sup> The three-ribbon light valve described by Frayne, Cunningham, and Pagliarullo, reference 5, with the valve ribbons normal to the slit, may be so employed.

approximately equal to the instantaneous amplitude of the audio-frequency current is applied to the galvanometer. Thus the track is very nearly 100 per cent modulated at all amplitudes. In this manner

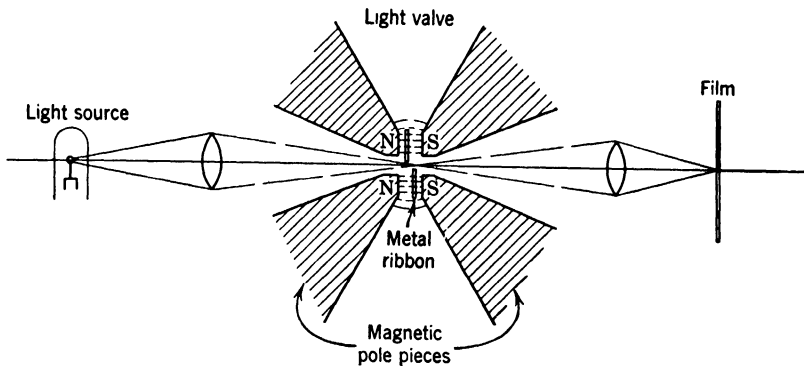


FIG. 15.2. Variable-Density Recording with a Light Valve (Schematic).

the clear area in the positive, employed for reproducing the sound, is minimized, and ground noise arising from dust and scratches is reduced. Figure 15.4 shows different types of variable-area track which may be produced with this system, employing different aperture shapes and

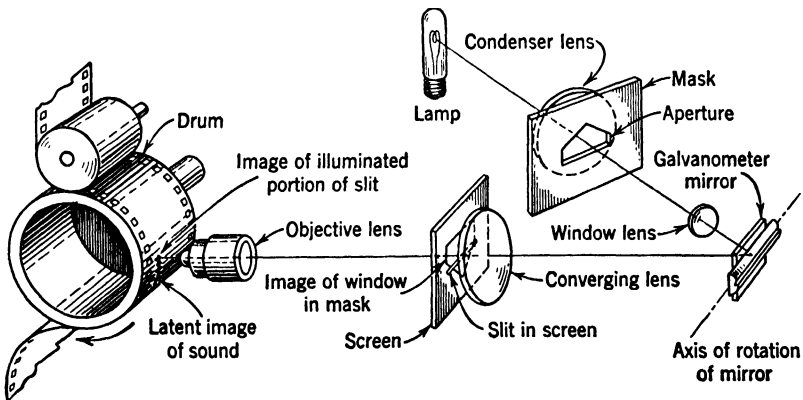


FIG. 15.3. Variable-Area Recording with the Mirror Galvanometer. (Kellogg, reference 1.) (Courtesy of *J. Soc. Motion Picture Engrs.*)

motions relative to the slit imaged on the film. The push-pull Class B track, in particular, combines an improvement in fidelity with ground-noise reduction.<sup>7</sup>

<sup>7</sup> See Dimmick and Belar, reference 6.

The variable-area recording equipment may also be used for variable-density recording. For this purpose the aperture is displaced so that its constant-width section is imaged on the slit. A screen with a horizontal edge is interposed between the lamp and the aperture in such a manner that the section of the aperture image on the slit is in the penumbra of the edge.<sup>8</sup> As the aperture image is displaced across the slit by the gal-

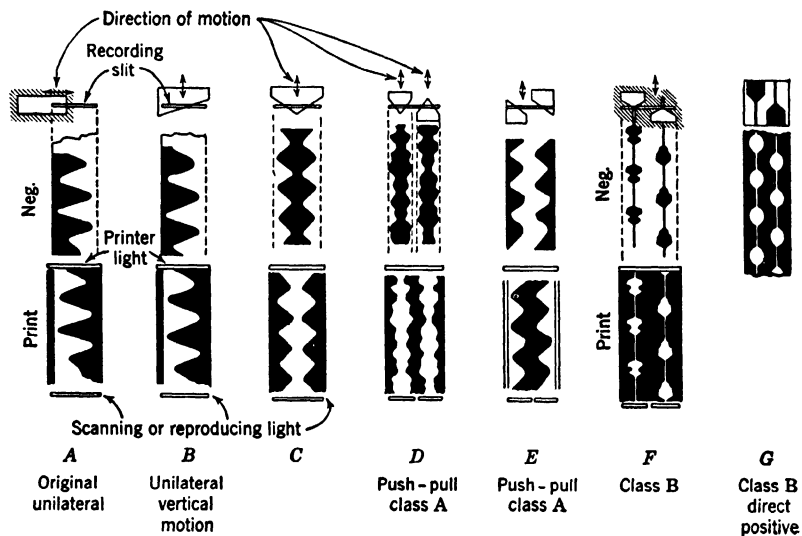


FIG. 15.4. Different Types of Variable-Area Sound Track. (Kellogg, reference 1.)  
(Courtesy of *J. Motion Picture Engrs.*)

vanometer oscillations, a variable amount of light passes through the slit to form the record.

A considerable improvement in the high-frequency response and improved latitude in film-processing control can be attained by ultra-violet recording (and printing), selecting out a narrow spectral band, 3400 to 3940 Angstrom units, from the total emission of the recording light source with the aid of a filter.<sup>9</sup> It arises from the reduced spreading of the radiation in the film emulsion and the restriction of the record to a thin top layer.

Although in America photographic recording is universally employed, the Philips-Miller system, developed in Holland, uses an electromagnetically driven cutter to trace a variable-area track on a film with a thin opaque layer deposited on a gelatin base.<sup>10</sup>

<sup>8</sup> See Dimmick, reference 7.

<sup>9</sup> See Dimmick, reference 8.

<sup>10</sup> See Vermeulen, reference 9.

**Phototube Monitoring of Sound Recorders.** Faithful reproduction of recorded sound is possible only if the amplitudes of the recording currents are kept within the linear range of the recording system. More specifically, in variable-area recording the effective slit length must vary linearly with the deflection of the aperture image throughout and must not extend beyond the allocated width of track. To assure this, a glass plate may be inserted in the light paths between the slit and film so as to deflect a portion of the light through a suitable auxiliary optical system onto a monitoring card. Here the slit image is reproduced to enlarged scale between two markings which indicate the maximum permissible deflection amplitude. The recordist simply controls the microphone current amplifier so that the slit image at no time exceeds the limits indicated by the markings on the monitoring card.

In variable-density recording the light intensity on the film must be held within such limits that the transmission of the ultimate sound track print bears an approximately linear relation to the microphone currents and, hence, the film illumination. Since visual methods are ineffective for this purpose,<sup>11</sup> phototubes are used quite generally for measuring both the amplitude of the light-intensity variations and the light level for zero signal, which is determined by the bias current applied to the recording galvanometer or light valve. For example, Fig. 15.5 shows the optics of a Western Electric light-valve recorder installed at the Twentieth Century-Fox Film Corporation Studios, designed for recording push-pull variable-density sound track.<sup>12</sup> An image of the double slit of the light valve is formed on the split collimating lens, which directs the light from each portion of the slit on the cathode of a separate type 929 phototube. The output of the phototubes is amplified by a push-pull amplifier and rectified so as to operate a meter which indicates the amplitude of the light variations. To measure the light level for zero signal, a lever is operated which raises a tone wheel into position so as alternately to interrupt the light paths to the two phototubes. Blue-sensitive phototubes are here employed since they match most closely the spectral sensitivity of the film. On the other hand, it is possible to reduce greatly the light loss arising from the use of a monitoring system by employing, in place of the deflector glass plate, a thin glass wedge coated with dichroic films which selectively reflect infrared radiation to the (red-sensitive) monitoring phototubes and freely transmit the actinic component of the light. The wedge is dimensioned so that no reflected light reaches the film (Fig. 15.6).<sup>13</sup>

<sup>11</sup> Except in the penumbra method.

<sup>12</sup> See Grignon and Corcoran, reference 10.

<sup>13</sup> See Dimmick, reference 11.

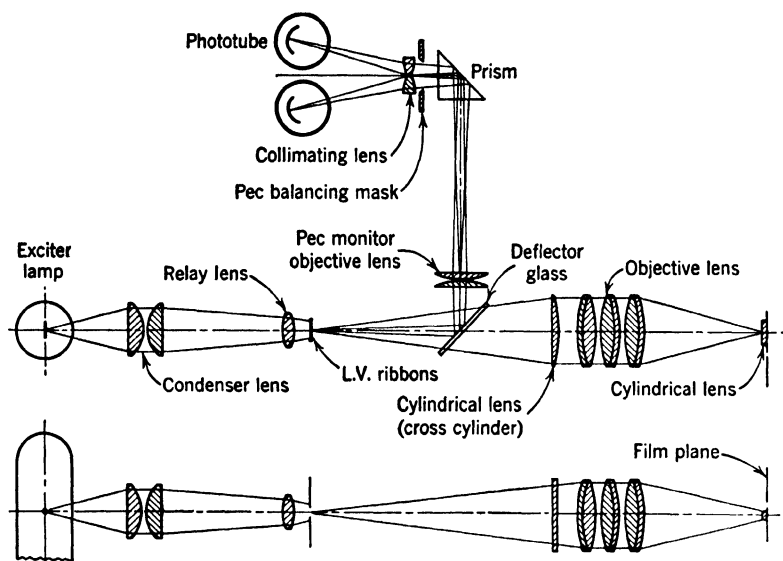


FIG. 15.5. Optics of Light-Valve Recorder at Twentieth Century Fox Studios, with Phototube Monitoring System. (Grignon and Corcoran, reference 10.) (Courtesy of *J. Soc. Motion Picture Engrs.*)

Numerous variations in the method of phototube monitoring have found application. In the penumbra method of variable-density recording monitoring of a push-pull track with a twin phototube may be

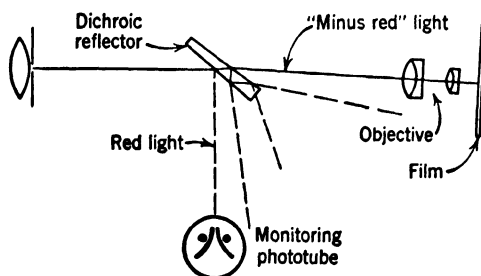


FIG. 15.6. Dichroic Reflector for Monitoring System. (Dimmick, reference 11.) (Courtesy of *J. Motion Picture Engrs.*)

combined with visual monitoring (Fig. 15.7).<sup>14</sup> In other variable-density systems a separate phototube commonly takes over the function of measuring the light incident on the film for zero signal, the required

<sup>14</sup> See Faulkner and Batsel, reference 12.

reflector being inserted in the light path automatically whenever the microphone amplifier is turned off.<sup>15</sup>

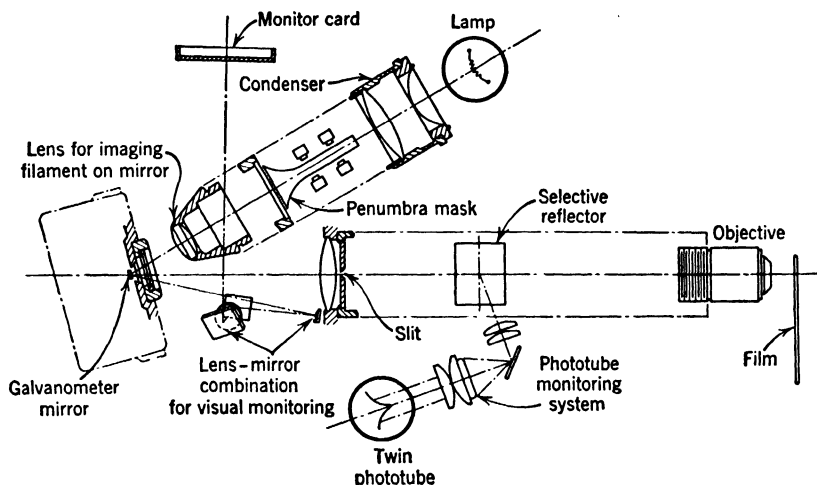


FIG. 15.7. Monitoring System in Penumbra Variable-Density Recording. (Faulkner and Batsel, reference 12.) (Courtesy of *J. Motion Picture Engrs.*)

**Rerecording.** After the original sound recording, made on a separate film synchronized with the camera, has been prepared, it is cut, edited, spliced, and rerecorded on a master negative. Duplicates made of this negative and of the corresponding picture negative are used to prepare the final release print.

The rerecording system consists of a film phonograph (Fig. 15.8) and a recorder. Optically and mechanically, the film phonograph differs little from the sound head of the ultimate projector, which will be discussed in greater detail. The image of a narrow illuminated slit is formed on the sound track traveling at uniform speed. The transmitted light falls on the cathode of a phototube, whose amplified output controls the recorder. Figure 15.9 shows the optical arrangement required for reproducing push-pull sound track.<sup>16</sup> A split lens serves to direct the light from the two halves of the track onto the two sections of a twin phototube; a step-down transformer matches the impedance of the phototube circuit to the cable connecting it to the amplifier. This system permits rerecording from push-pull track spliced with standard track without any readjustment of the apparatus, provided that the standard track is aligned with half the (double-width) push-

<sup>15</sup> See, for example, Frayne, Cunningham, and Pagliarullo, reference 5.

<sup>16</sup> See Cook, reference 13.

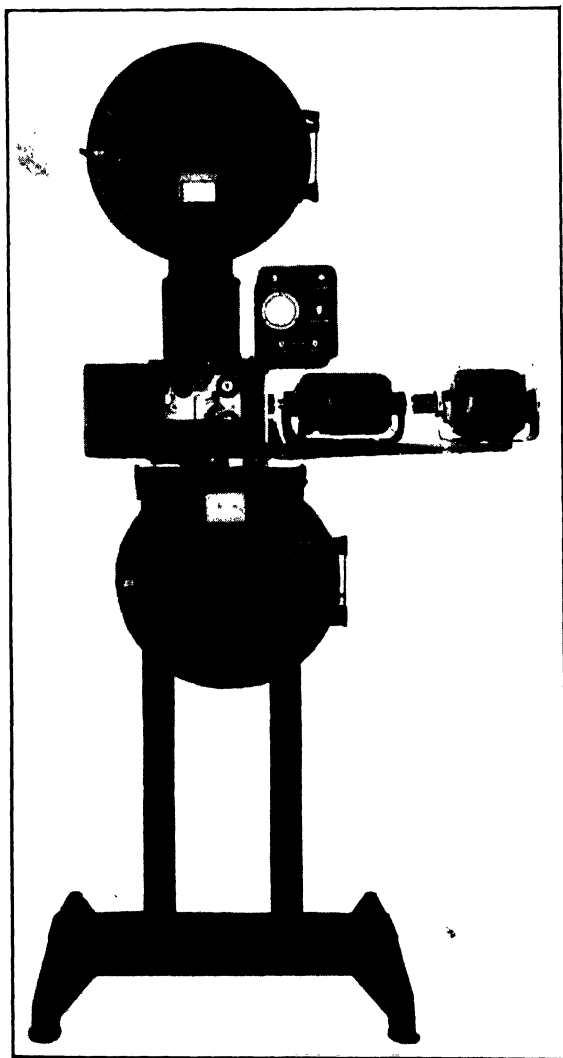


FIG. 15.8. Rerecording Film Phonograph. (Cook, reference 13.)

pull track; one section of the twin phototube simply becomes inactive during the recording of the standard track.

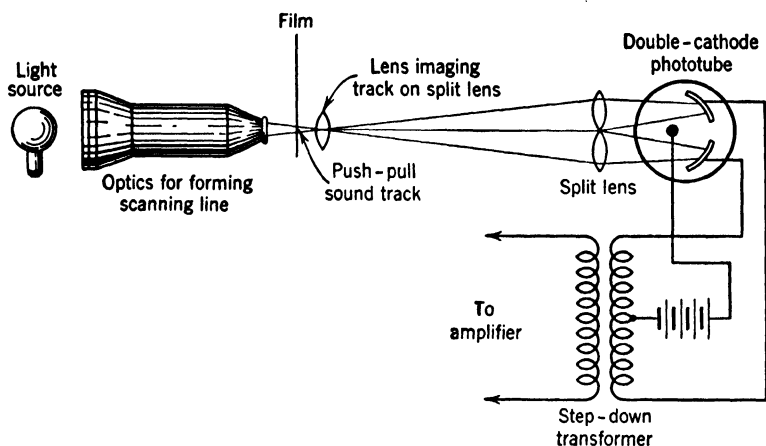


FIG. 15.9. Sound Reproduction from a Push-Pull Track. (Cook, reference 13.)  
(Courtesy of *J. Motion Picture Engrs.*)

**The Sound Track on the Projected Film.** The dimensions and position of the sound track on the release prints are of necessity closely standardized. Figure 15.10 shows the space allotted to the sound track on 35-millimeter and 16-millimeter film. In the 35-millimeter film the sound track occupies a strip between the picture and one row of sprocket holes; the maximum width of this strip is 0.076 inch for the variable-area track, 0.100 inch for the variable-density track. In 16-millimeter sound film only one set of sprocket holes is provided, the sound track being placed on the opposite side. It has a maximum width of 0.060 and 0.080 inch for variable-area and variable-density track, respectively. The film speed for 35-millimeter film, required to project 24 pictures per second, is 18 inches per second; that for 16-millimeter film is 7.2 inches per second. The 16-millimeter positive film with sound track is commonly prepared from 35-millimeter film and track. This is accomplished either by photographic reduction (projection printing) with an "anamorphic" lens system giving a reduction of 2.5 parallel to the track and a reduction of only 1.265 perpendicular thereto, or by rerecording. The rerecording method, which is preferable for obtaining high-quality results, has the added advantage of permitting compression of the volume range of the 35-millimeter film to accommodate it to the smaller range of most 16-millimeter projection equipment.



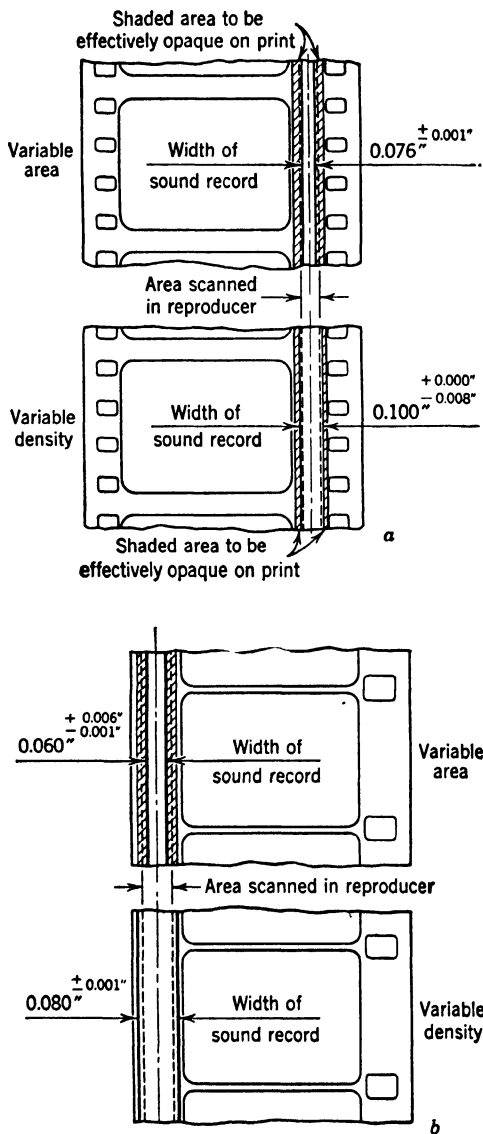


FIG. 15.10. Position of Sound Track on (a) 35-mm Film and (b) 16-mm Film (Courtesy of American Standards Association.)

Special sound effects may be obtained with more complex arrangements of the sound recordings. An extreme example is "Fantasound,"<sup>17</sup> developed for the presentation of Walt Disney's "Fantasia." Four standard tracks were enlarged to double width on 35-millimeter film, three to operate loudspeaking equipment at various points in the theatre, and the fourth to control the levels of the several reproducing units. In a more moderate modification, permitting the projection of the film with standard equipment, a control track is recorded between the sprocket holes in addition to the regular sound track.<sup>18</sup>

**Sound-Reproduction Equipment; Requirements.** The basic optics for sound reproduction are the same for variable-area and variable-density track. A horizontal line of light is projected on the film sound track traveling at uniform speed, and the transmitted light is directed onto the cathode of a phototube. The width of the line is determined by the highest frequency which is to be reproduced. Present-day commercial equipment requires a practically flat response in the range of 30 to 7500 cycles per second. The speed of a 35-millimeter film being 18 inches per second, the shortest wave length to be recorded on the film without loss in response becomes 0.0024 inch. In practice the line width is made equal to 0.00125 inch, or half a wave length. For 16-millimeter film the line width should be less than half as great, in view of the lower speed of the film, to attain an equal frequency range. In practice the frequency response requirements are less stringent here, so that the line width is not much smaller than for 35-millimeter equipment.

Much engineering effort has gone into fulfilling the requirement of constant speed of the film as it is scanned by the light probe.<sup>19</sup> In the reproducing equipment this problem is accentuated by the fact that the film is moved intermittently through the projection window, coming to complete rest for the projection of the picture. The intermittent motion of the film at the projection window and its uniform motion at the sound head are made possible by providing a slack length of film between these two points—the sound precedes the picture by 20 frames in 35-millimeter film, by 26 frames in 16-millimeter film. The residual nonuniformities of motion introduced by the sprocket drive are generally removed by passing the film over a smooth drum attached to a flywheel and scanning the sound track where it projects over the edge of this drum. The motion of the flywheel itself may be smoothed, as in the RCA rotary stabilizer,<sup>20</sup> by viscous friction. The stabilizing element

<sup>17</sup> See Garrity and Hawkins, reference 14.

<sup>18</sup> See Reiskind, reference 15.

<sup>19</sup> See Kellogg, reference 16.

<sup>20</sup> See Loomis and Reynolds, reference 17.

consists of a heavy flywheel, floating freely on a ball bearing coupled to the outer casing of the flywheel by a filling of light oil.

**The Optical System of the Reproducer.** The usual optical arrangement of the reproducer sound head is shown in Fig. 15.11. It consists of a lamp, usually operated at 10 volts, 5 amperes, a condenser lens imaging the filament into the objective, a slit, and a microscope objective imaging the slit on the film as it passes over the flywheel drum. The transmitted light either falls directly on the cathode of a phototube or, more commonly, is directed by a system of mirrors, prisms, and/or lenses on the photocathode. The second arrangement makes it possible to make the cathode area covered independent of the point of origin of the light at

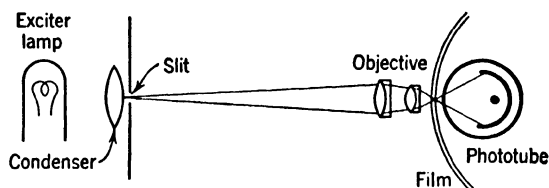


FIG. 15.11. Basic Optics of Reproducing System.

the film, so that variations in sensitivity over the surface of the cathode do not affect the signal obtained with variable-area sound track. A relatively complex optical system, designed for quick change-over from push-pull track to standard track, is shown in Fig. 15.12.<sup>21</sup> While this system, necessarily, uses a twin phototube, a simple gas-filled, red-sensitive silver cesium-oxide cesium phototube, such as the type 868, is most common in commercial reproducing equipment. A step-down transformer or a single amplifier tube in cathode-follower connection mounted close to the phototube generally serve to match the impedance of the phototube circuit to that of the cable connecting the phototube unit to the amplifier (Fig. 15.13.)

There are several modifications of the arrangement described. One of them consists of the direct imaging of a coiled filament on the sound track in one plane and the imaging of a slit in front of the filament in the plane at right angles thereto. Such a system, using cylindrical lenses, is incorporated in the RCA 16-millimeter sound projector<sup>22</sup> and, more recently, in a 35-millimeter sound system designed by Eastman.<sup>23</sup> The alternative procedure of projecting a relatively wide spot on the film and forming a precision image of the sound track on a defining slit in

<sup>21</sup> See Miller, reference 18.

<sup>22</sup> See Holden, reference 19.

<sup>23</sup> See McLeod and Altman, reference 20.

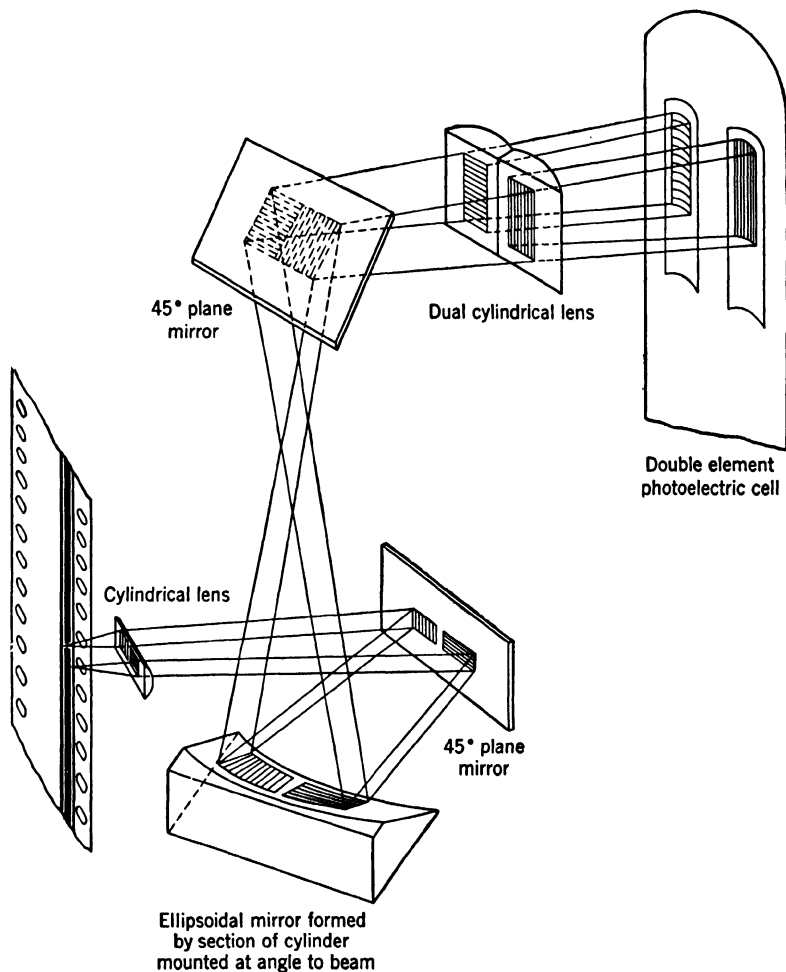


FIG. 15.12. Optics of Reproducer for Push-Pull Track at M.G.M. Studios. (Miller, reference 18.) (Courtesy of *J. Motion Picture Engrs.*)

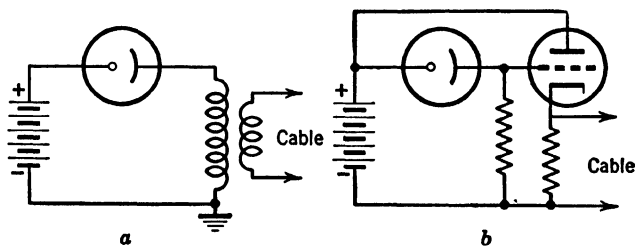


FIG. 15.13. Impedance Matching of Phototube Output to Cable by (a) Stepdown Transformer and (b) Cathode-Follower Stage of Amplification.

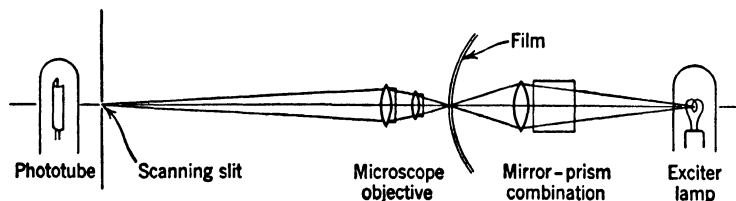


FIG. 15.14. Projection System for Scanning Sound Track. (Davidson reference 21.)

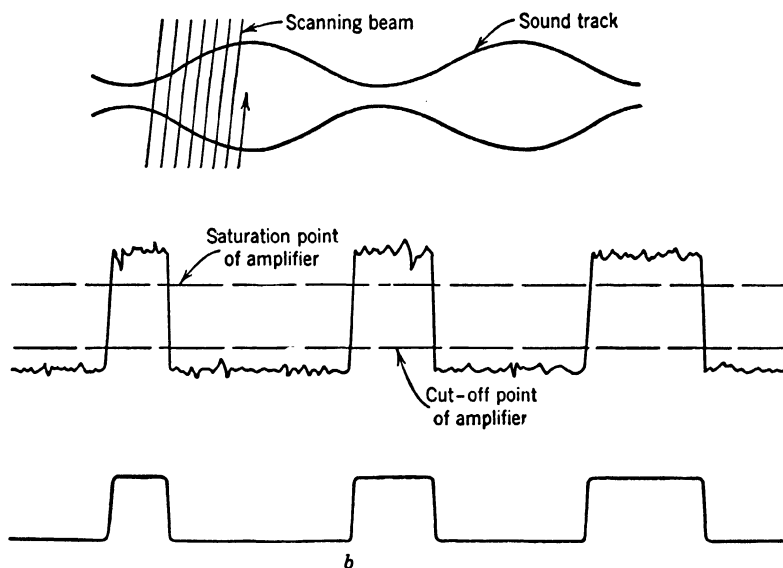


FIG. 15.15. Wave Shape Obtained with Transverse Scanning of Sound Track (a) before and (b) after Passage through Limiter. (Westmijze, reference 22.) (Courtesy of *J. Motion Picture Engrs.*)

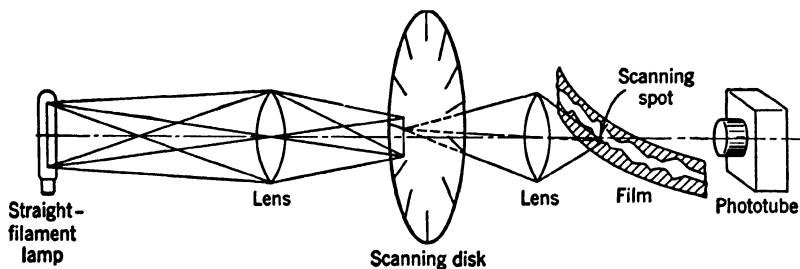


FIG. 15.16. System for Effecting Transverse Scanning of Sound Track. (Westmijze, reference 22.) (Courtesy of *J. Motion Picture Engrs.*)

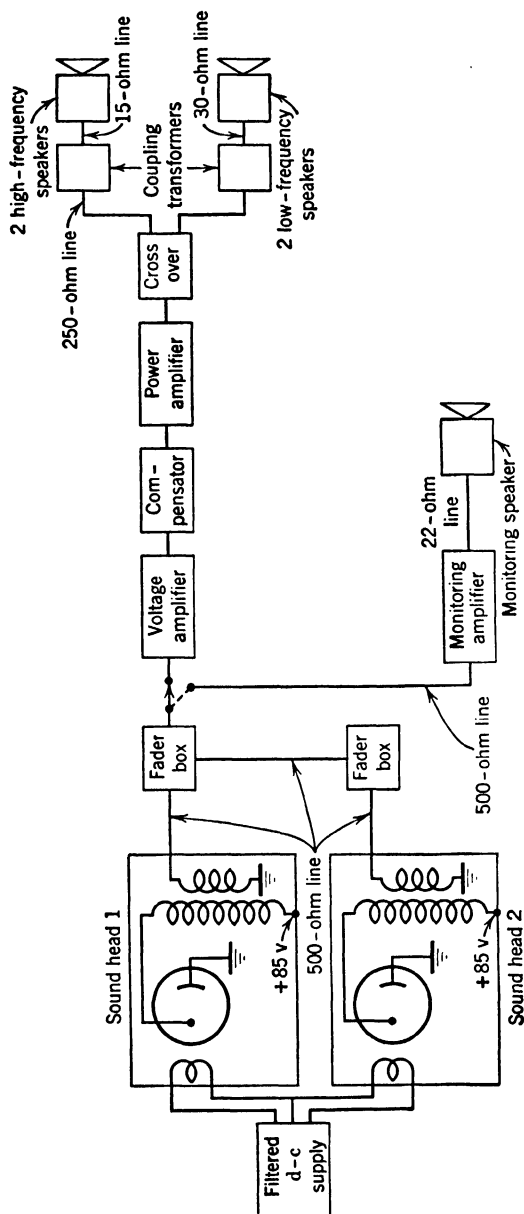


Fig. 15.17. Block Diagram of 35-mm Theatre Projection System.

front of the phototube (Fig. 15.14) is utilized in a Western Electric reproducer.<sup>24</sup> This arrangement facilitates the adjustment of the slit relative to the sound track.

A novel and ingenious method of minimizing noise originating from scratches and dirt in the clear portions of variable-area sound track is used in a sound reproduction method developed by W. K. Westmijze of Philips in Holland.<sup>25</sup> It consists of scanning the sound track transversely with a light spot at a frequency (50 kilocycles per second) high compared to the highest audio frequency recorded. The output of the phototube

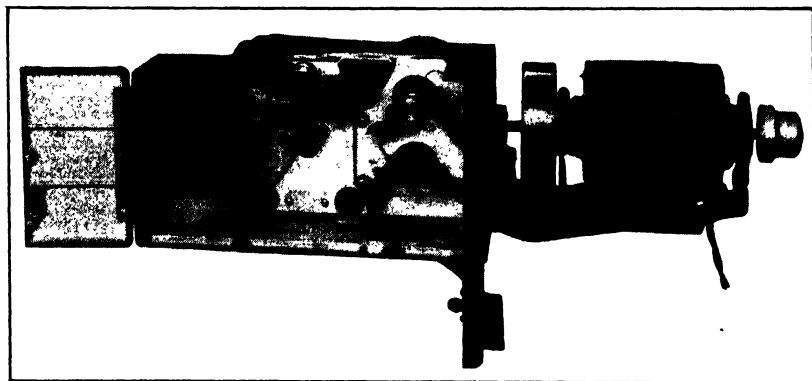


FIG. 15.18a. The RCA MI 9030 Sound Head (Cover Partly Removed).

is passed through a high-gain limiting amplifier (Fig. 15.15) so that only a square-topped wave, whose vertical sides mark the traversals of the sound track boundaries, remains. If this wave is passed through a low-pass filter with a cut-off above the top audio frequency recorded, the audio signal is obtained, unaffected by any disturbances except such as overlap the edge of the sound track pattern.

Figure 15.16 shows the manner in which the scanning is realized. A disk with a series of radial slots rotates with an edge speed of 1300 feet per second across an image of the high-power linear light source. It causes a spot 0.0008 by 0.004 inch to scan the sound track transversely. The system has been found to yield considerable improvement for films which had been used repeatedly, so that dirt and scratches had accumulated on the sound track.

**Complete Sound-Reproducer Systems.** Figure 15.17 shows a block diagram of a complete 35-millimeter theatre sound-projection system. Two projector units feed through a *fading box*, providing smooth change-

<sup>24</sup> See Davidson, reference 21.

<sup>25</sup> See Westmijze, reference 22.

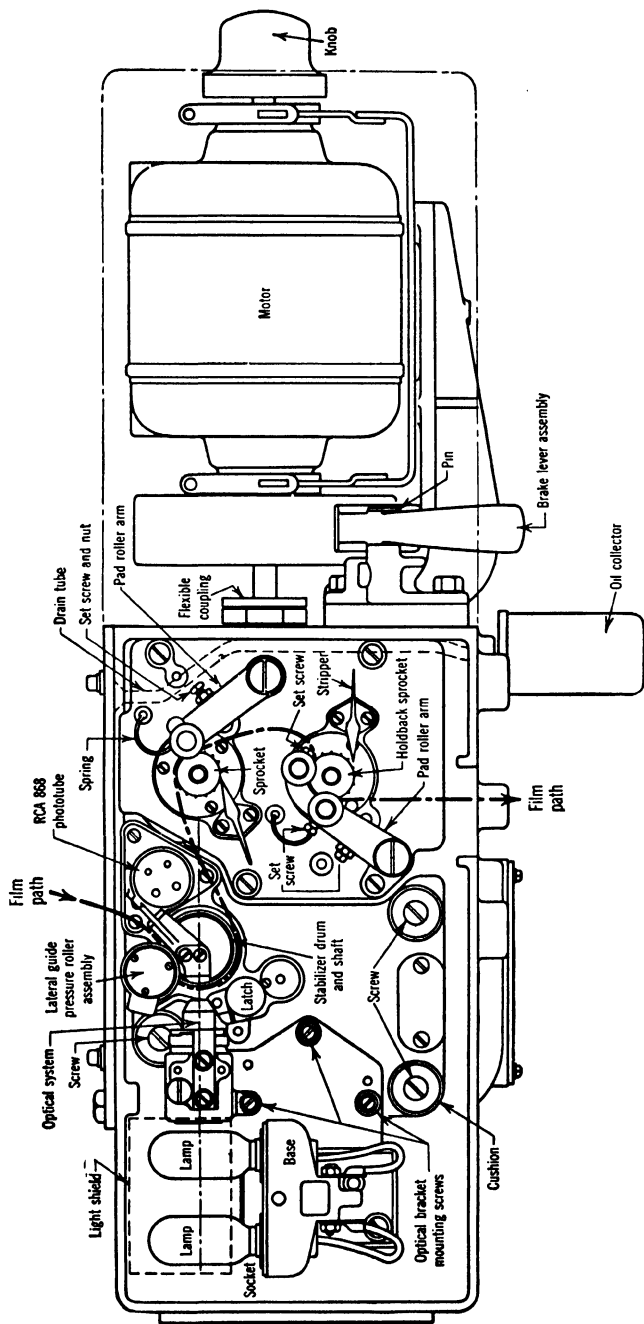


Fig. 15.18b. Plan of RCA MI 9030 Sound Head, Showing Film Path.



over, without alteration of volume, from one reel to the next, into the amplifier. This increases the audio signal level several million times, permitting operation of the loudspeakers. The loudspeakers have, in

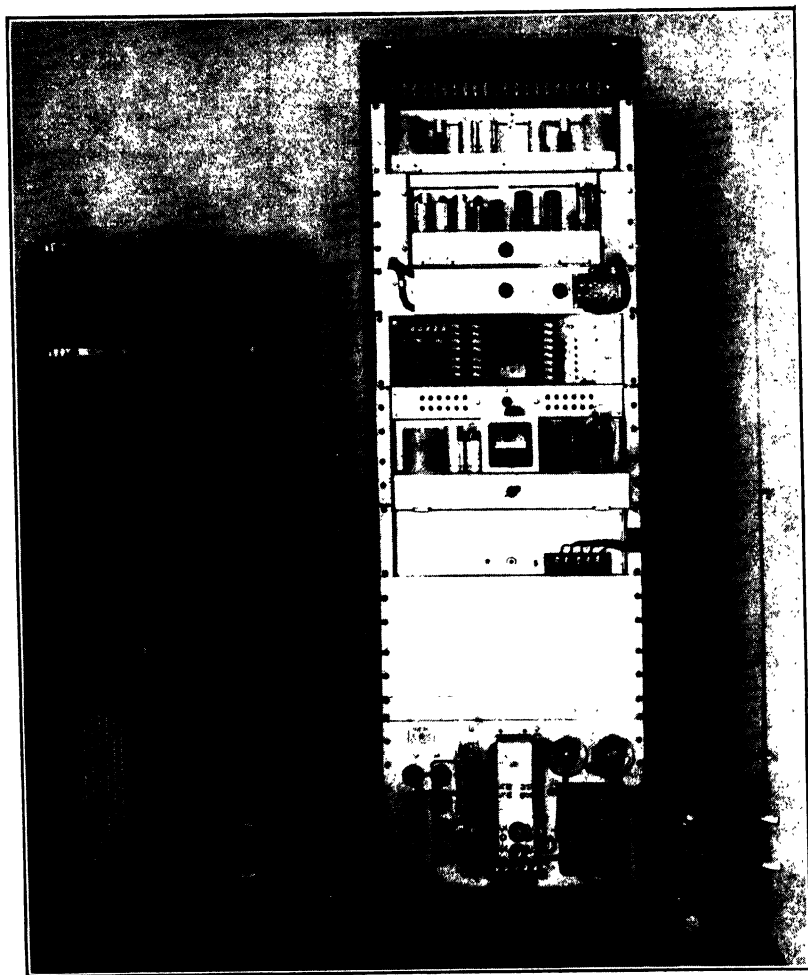


FIG. 15.19. Amplifier Panel and Fader Boxes for RCA 35-mm Sound System.

general, multiple exponential horns for both high-frequency and low-frequency response. The appearance of the RCA MI 9030 sound head is shown, with part of the cover removed, in Fig. 15.18a; the film path through this mechanism has been traced on the corresponding line drawing, Fig. 15.18b. Two exciter lamps are provided on a reversible mount-

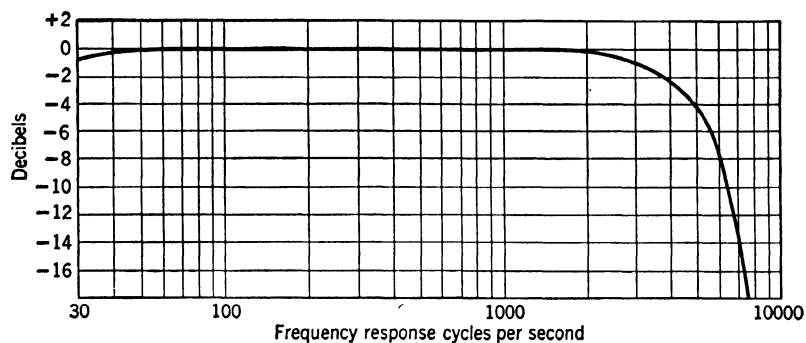


FIG. 15.20. Frequency Response of 35-mm Sound System, for Test Film Corresponding to Average Recording.

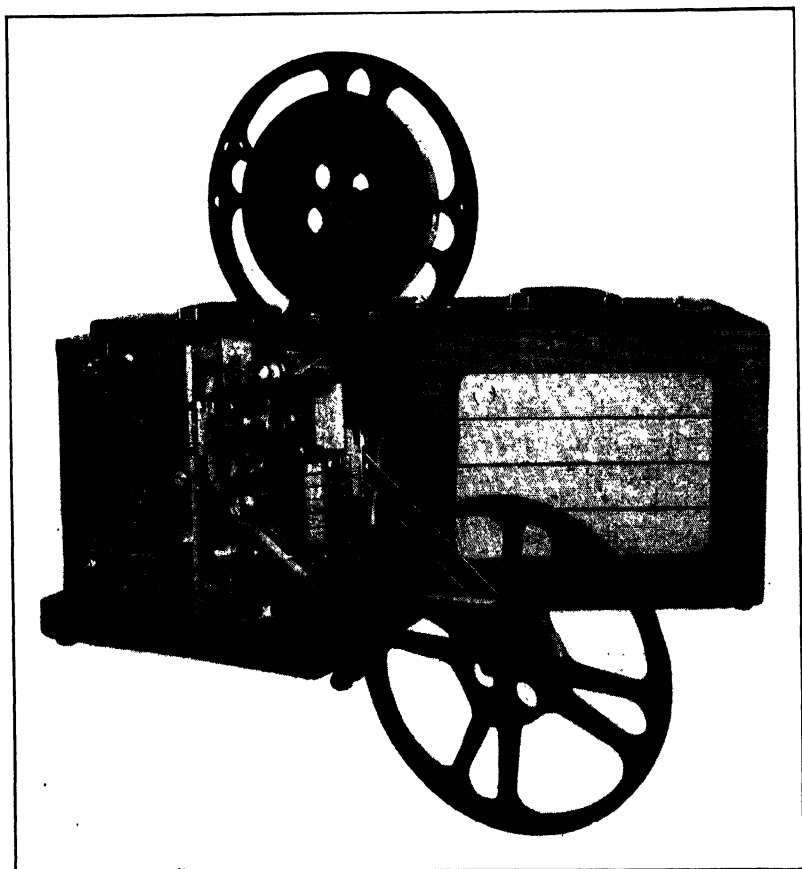


Fig. 15.21. Portable 16-mm Sound Projector.

ing for instant interchange in case one of them fails. The appearance of the amplifier rack, together with the fader boxes, for the sound system is shown in Fig. 15.19. Figure 15.20 indicates the frequency response of the system, measured at the input of the loudspeakers, for a test film representative of an average recording. It has been found empirically that this characteristic is, on the average, the most desirable.

The 16-millimeter projection equipment does not have to meet quite as exacting standards of quality of reproduction as 35-millimeter theatre equipment. On the other hand, it must be much more compact and simpler in construction. A portable 16-millimeter projector is shown in Fig. 15.21. The amplifier system is in the base of the projector, the speaker in a separate case connected to the projector by cable.

**Sound Reproduction from Dye Tracks.** With the increasing use of dye-image color film, such as Kodachrome, Ansco Color Film, and Kodacolor, it became a matter of convenience and economy for sound track to be recorded in the same medium.<sup>26</sup> It was soon found, however, that dye tracks, reproduced with the usual red- and infrared-sensitive phototubes, gave very unsatisfactory results. The modulation was found to be low, the noise level high. Görisch and Görlich,<sup>27</sup> who investigated the matter, found that this condition was caused by the high transparency of the dye emulsions—and, in fact, of all dye-gelatin filters—for the infrared; noise introduced by dust and scratches is high since they modulate the output strongly at any part of the sound track. The solution was found to lie in replacing the red-sensitive phototube by a predominantly blue-sensitive phototube.<sup>28</sup> A phototube of this type, with approximately the same sensitivity to tungsten light as the type 868, is the gas-filled antimony-cesium type 1P37.<sup>29</sup>

The spectral response of the 1P37 (S-4) surface to illumination from a tungsten filament lamp at a color temperature of 2870° K is compared with that of the 868 (S-1) surface in Fig. 15.22. The response of the first tube is concentrated in the visible part of the spectrum and is negligible in the infrared. In view of the greater sensitivity of the S-4 surface a relatively small gas-amplification factor—of the order of 3—is sufficient to match the sensitivity of the 1P37 to that of the 868. This is fortunate, since difficulties are experienced in obtaining a long life

<sup>26</sup> In the more complicated Technicolor process a silver sound track is employed.

<sup>27</sup> See reference 23.

<sup>28</sup> The need of a blue-sensitive phototube for the recording of dye track was pointed out by A. M. Glover (RCA) even before World War II.

<sup>29</sup> See Glover and Moore, reference 24.

with gas-filled antimony-caesium tubes operated with a high gas amplification factor. In addition, the low gas amplification factor causes the frequency response of the 1P37 (Fig. 15.23) to be flatter than that of the 868. In fact, the 1P37 is inferior to the 868 only in being more sensitive

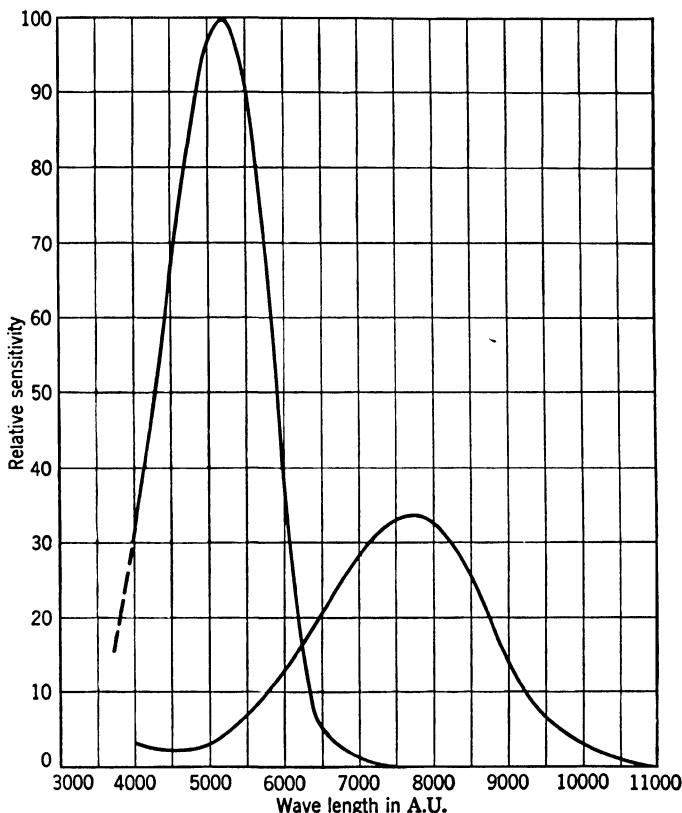


FIG. 15.22. Spectral Response of S-1 and S-4 Surface to Light for 2870° K Tungsten Light Source. (Glover and Moore, reference 24.) (Courtesy of *J. Motion Picture Engrs.*)

to temperature changes of the exciter lamp filament. As a result, if the lamp is alternating-current-operated, the hum level obtained with the 1P37 is 4 decibels higher than that obtained with the 868, the signal level being assumed the same.<sup>30</sup>

The arrangement of layers in a typical tripack color film (Ansco Color Duplicating Film) is shown in Fig. 15.24. The three sensitive layers contain transparent dye-formers yielding, during color development,

<sup>30</sup> See Phyfe, reference 25.

colors complementary to their effective spectral sensitivity.<sup>31</sup> The silver halide grains rendered developable in the first exposure are reduced, by a normal developer, to silver. A second, uniform exposure

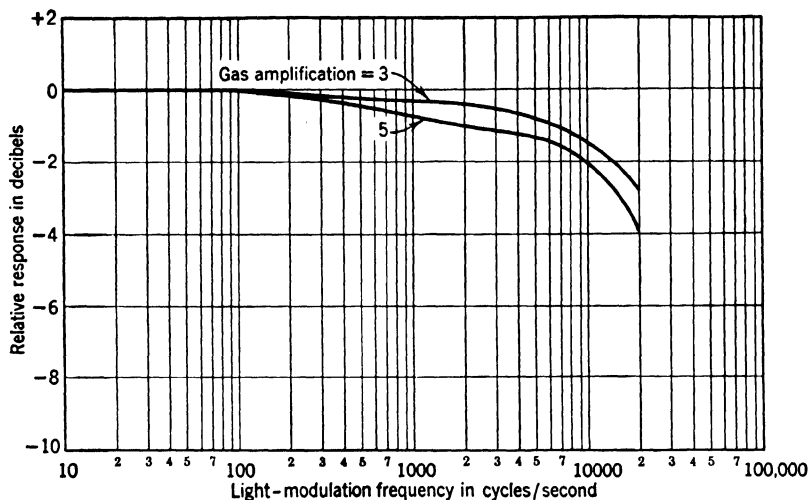


FIG. 15.23. Dynamic Response of Type 1P37 for Gas Amplification Factors of 3 and 5. (Glover and Moore, reference 24.)

renders all the remaining grains developable. The reaction products liberated by their reduction in the second, color, development react with the dye-formers and the color developer to form the several dyes

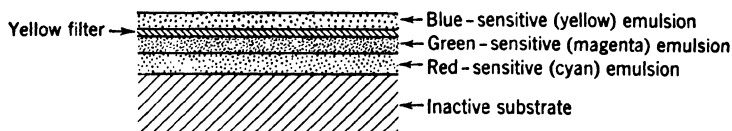


FIG. 15.24. Layer Structure of a Tripack Color Film, such as Ansco Color Duplicating Film.

in proportion to the concentration of originally unexposed grains at any point. A final bleaching process removes the reduced silver and produces the positive color transparency.<sup>32</sup>

<sup>31</sup> A layer of yellow dye placed below the top, blue-sensitive, layer renders the two deeper layers *effectively* insensitive to the blue.

<sup>32</sup> See Forrest, reference 26.

The transmission of the individual layers of dye as well as that of the unexposed, developed film is shown in Fig. 15.25,<sup>33</sup> bringing out clearly the fact that the film is practically transparent at the point of maximum spectral response of the S-1 surface. It is thus not surprising that the range of densities of the color film, as measured with the red-sensitive phototube, is extremely limited, as compared with the density range

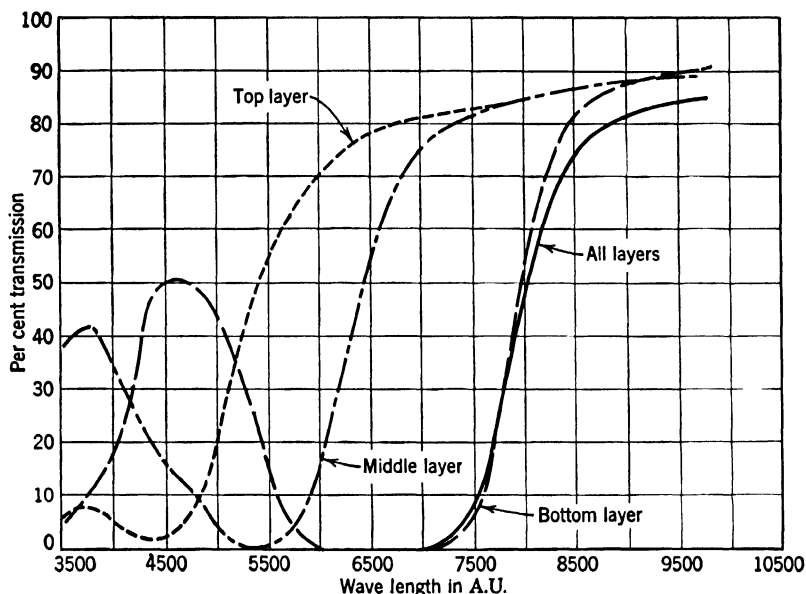


FIG. 15.25. Spectral Transmission of Individual Dye Layers and Complete Unexposed, Developed Color Film. (Drew and Johnson, reference 27.) (Courtesy of *J. Motion Picture Engrs.*)

measured, for the same illumination, with the blue-sensitive phototube (Fig. 15.26). Figure 15.27 indicates the rapid increase in the noise level obtained with the red-sensitive tube resulting from the accumulation of scratches and dust over the entire track area. With the blue-sensitive cell a certain improvement in frequency response can be obtained by flashing the sound track with red light before or after printing (from a positive silver sound track) since this light prevents the formation of dye in the deepest (cyan) layer and thus reduces the spreading of the image arising from light diffusion. The gain is like that obtained by printing silver sound track with ultraviolet radiation so that the photographic action is limited to the top layer of the emulsion.

<sup>33</sup> See Drew and Johnson, reference 27.

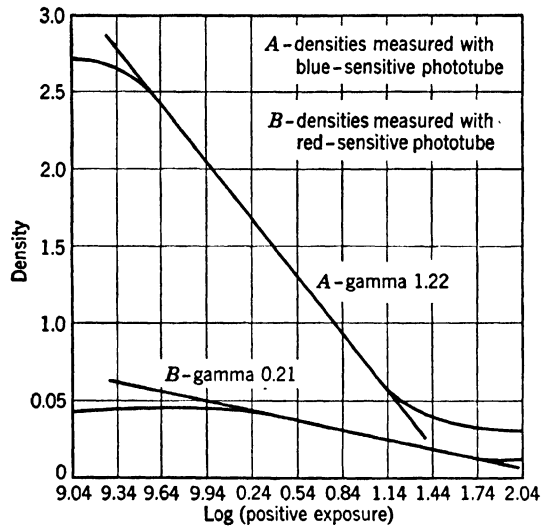


FIG. 15.26. Density as Function of Exposure for Anso Reversible Color Film Measured with 2870° K Tungsten Light and the Type 868 or Type 1P37 Phototube. (Drew and Johnson, reference 27.) (Courtesy of *J. Motion Picture Engrs.*)

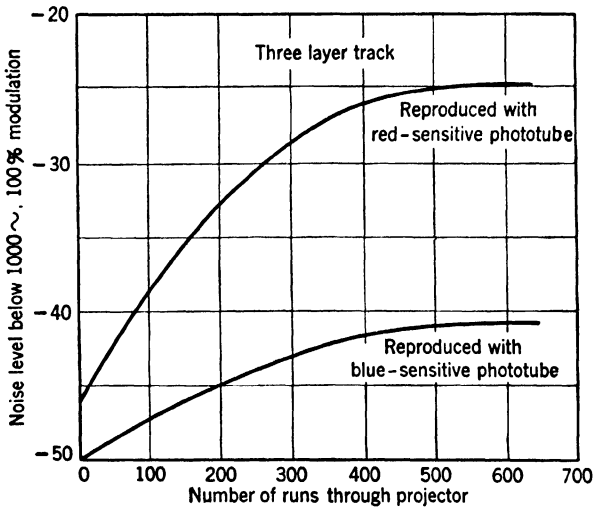


FIG. 15.27. Increase in Noise Level of Dye Sound Track Reproduced with Type 868 and with Type 1P37 Phototube with the Number of Runs of the Film through the Projector. (Drew and Johnson, reference 27.) (Courtesy of *J. Motion Picture Engrs.*)

**Photoconductive Cells in Sound Reproduction.** It has been brought out, at the end of Chapter 13,<sup>34</sup> that lead sulfide photoconductive cells have considerably greater sensitivity than the conventional gas-filled phototubes. Apart from this their response varies linearly with illumination and exhibits, within the audio range, a variation with frequency of the same order as that of the gas-filled phototubes. Preliminary experiments with lead sulfide photocells in sound heads have given promising results.<sup>35</sup> Their sensitivity to infrared radiation up to about 3.5 microns permits the employment of indirectly heated sources of radiation (at about 1800° K) of sufficient thermal inertia for the heating to be carried out with alternating current without danger of introducing excessive hum in the photocell output. It is obvious that these advantages of the lead sulfide cell apply only to reproduction from silver sound track.

## REFERENCES

1. E. W. KELLOGG, "The ABC of photographic sound recording," *J. Soc. Motion Picture Engrs.*, Vol. 44, pp. 151-194, 1945.
2. D. MACKENZIE, "Sound recording with the light valve," *Trans. Soc. Motion Picture Engrs.*, Vol. 12, pp. 730-747, 1928.
3. G. L. DIMMICK, "The RCA recording system and its adaptation to various types of sound track," *J. Soc. Motion Picture Engrs.*, Vol. 29, pp. 258-273, 1937.
4. V. K. ZWORYKIN, L. B. LYNN, and C. R. HANNA, "Kerr cell method of recording sound," *Trans. Soc. Motion Picture Engrs.*, Vol. 12, pp. 748-759, 1928.
5. J. G. FRAYNE, T. B. CUNNINGHAM, and V. PAGLIARULLO, "An improved 200-mil push-pull density modulator," *J. Soc. Motion Picture Engrs.*, Vol. 47, pp. 494-518, 1946.
6. G. L. DIMMICK and H. BELAR, "An improved system for noiseless recording," *J. Soc. Motion Picture Engrs.*, Vol. 23, pp. 48-54, 1934.
7. G. L. DIMMICK, "Optical control of wave shape and amplitude characteristic in variable-density recording," *J. Soc. Motion Picture Engrs.*, Vol. 33, pp. 650-663, 1939.
8. G. L. DIMMICK, "Improved resolution in sound recording and printing by the use of ultra-violet light," *J. Soc. Motion Picture Engrs.*, Vol. 27, pp. 168-178, 1936.
9. R. VERMEULEN, "The Philips-Miller method of recording sound," *J. Soc. Motion Picture Engrs.*, Vol. 30, pp. 680-693, 1938.
10. L. D. GRIGNON and J. P. CORCORAN, "A 200-mil push-pull film recording system," *J. Soc. Motion Picture Engrs.*, Vol. 42, pp. 127-144, 1944.
11. G. L. DIMMICK, "A new dichroic reflector and its application to photocell monitoring systems," *J. Soc. Motion Picture Engrs.*, Vol. 38, pp. 36-55, 1942.
12. C. W. FAULKNER and C. N. BATSEL, "Operation of the variable-intensity recording system," *J. Soc. Motion Picture Engrs.*, Vol. 36, pp. 125-136, 1941.
13. E. D. COOK, "Methods of rerecording," *J. Soc. Motion Picture Engrs.*, Vol. 25, pp. 522-539, 1935.

<sup>34</sup> See p. 267.

<sup>35</sup> See Cashman, reference 28.



14. W. E. GARRITY and J. N. A. HAWKINS, "Fantasound," *J. Soc. Motion Picture Engrs.*, Vol. 37, pp. 127-146, 1941.
15. H. I. REISKIND, "Multiple-speaker reproducing systems for motion pictures," *J. Soc. Motion Picture Engrs.*, Vol. 37, pp. 154-163, 1941.
16. E. W. KELLOGG, "A review of the quest of constant speed," *J. Soc. Motion Picture Engrs.*, Vol. 28, pp. 337-376, 1937.
17. F. J. LOOMIS and E. W. REYNOLDS, "A new high-fidelity sound head," *J. Soc. Motion Picture Engrs.*, Vol. 25, pp. 449-460, 1935.
18. W. C. MILLER, "The M.G.M. record and reproducer equipment units," *J. Soc. Motion Picture Engrs.*, Vol. 40, pp. 301-326, 1943.
19. H. C. HOLDEN, "A 16-mm sound-on-film projector," *J. Soc. Motion Picture Engrs.*, Vol. 19, pp. 228-236, 1932.
20. J. H. McLEOD and F. E. ALTMAN, "An optical system for the reproduction of sound from 35-mm film," *J. Soc. Motion Picture Engrs.*, Vol. 31, pp. 36-45, 1938.
21. J. C. DAVIDSON, "A new high-quality film reproducer," *J. Soc. Motion Picture Engrs.*, Vol. 28, pp. 202-206, 1937.
22. W. K. WESTMIJZE, "A new method of counteracting noise in sound-film reproduction," *J. Soc. Motion Picture Engrs.*, Vol. 47, pp. 426-440, 1946.
23. R. GÖRISCH and P. GÖRLICH, "Reproduction of color film sound records," *J. Soc. Motion Picture Engrs.*, Vol. 43, pp. 206-213, 1944.
24. A. M. GLOVER and A. R. MOORE, "A phototube for dye image sound track," *J. Soc. Motion Picture Engrs.*, Vol. 46, pp. 379-386, 1946.
25. J. D. PHYFE, "Behavior of a new blue-sensitive phototube in theatre sound equipment," *J. Soc. Motion Picture Engrs.*, Vol. 46, pp. 405-408, 1946.
26. J. L. FORREST, "Machine processing of 16-mm Ansco Color Film," *J. Soc. Motion Picture Engrs.*, Vol. 45, pp. 313-324, 1945.
27. R. O. DREW and S. W. JOHNSON, "Preliminary sound recording tests with variable-area dye tracks," *J. Soc. Motion Picture Engrs.*, Vol. 46, pp. 387-404, 1946.
28. R. J. CASHMAN, "Lead-sulfide photoconductive cells for sound reproduction," *J. Soc. Motion Picture Engrs.*, Vol. 49, pp. 342-346, 1947.

## Chapter 16

# PHOTOTUBES IN PICTURE TRANSMISSION

It is customary to distinguish between two types of electrical picture transmission: the practically instantaneous transmission of live scenes, known as *television* or "vision at a distance," and the reproduction of pictures and printed records at distant points, known as *facsimile*. In both, photosensitive devices perform the essential role of converting light values into electrical signals which may be transmitted by radio waves or by wire; in fact, the practical realization of television and facsimile rests on the same basic technical principles. Many of the differences follow from differences in the time which may be utilized for the transmission of a single picture with comparable detail. In television, as in motion pictures, a complete picture must be transmitted within an interval of the order of a thirtieth of a second to give the impression of continuity of motion to the observer. In facsimile, on the other hand, it is generally quite adequate for the reproduction of the picture to consume a number of minutes. This difference in the transmission period has resulted in the development of quite distinct transmission and reproducing equipment in the two fields. However, as the rate of transmission of facsimile is raised to the level of that of television pictures, facsimile equipment becomes, in fact, a specialized version of television equipment for film transmissions. Even here, the basic distinction remains that television presents a transitory image to the eye of the viewer, whereas facsimile creates a permanent record of the transmitted material.

**The Scanning Principle.** All successful methods of electrical picture transmission utilize the principle of subdividing the picture or scene to be transmitted into an array of minute *picture elements*. Every picture element gives rise to an electrical signal determined by the brightness of the picture element. In printing practice the picture elements are represented by the familiar halftone dots; picture reproductions in news-

papers generally utilize 60 to 120 dots per inch, high-quality work in magazines, up to 250 dots per inch. Lighter portions of the picture are represented by smaller dots.

In principle, it is possible to transmit all the signals from the different picture elements either simultaneously or in succession. The first

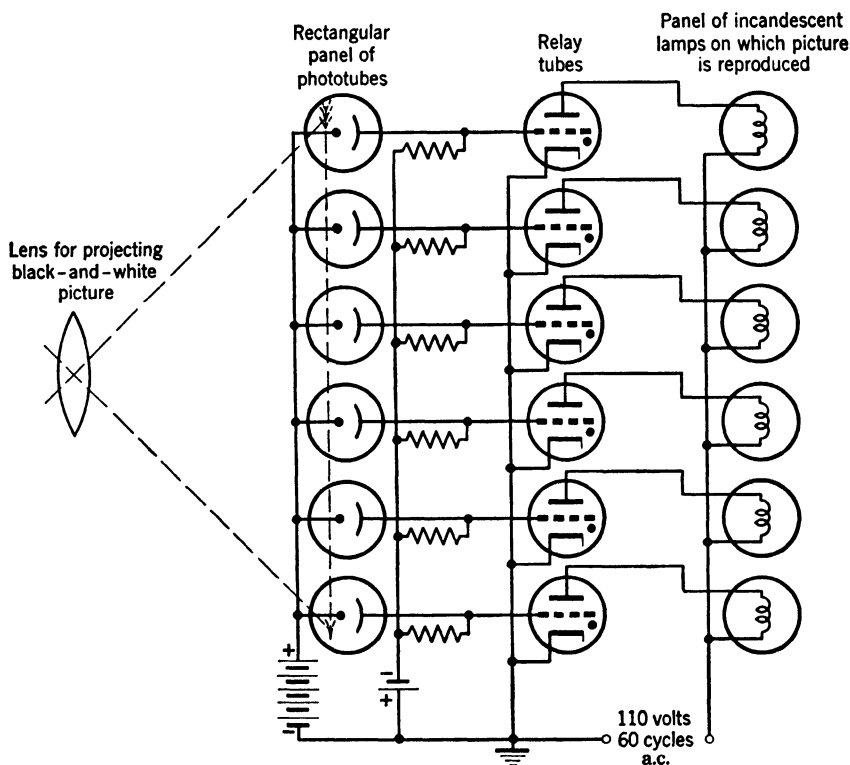


FIG. 16.1. Picture Transmission with Simultaneous Transmission of Picture Element Signals.

method, originally proposed by Carey in 1875 as a method of television, now finds application only in animated advertising signs.<sup>1</sup> In the modern version a silhouette cartoon is projected on a rectangular array of phototubes which individually control, by relay, the lighting of a similar array of light bulbs, constituting the sign (Fig. 16.1). Such a system becomes unreasonably complex and ponderous if the total number of picture elements (nearly a half million in modern television) be-

<sup>1</sup> See reference 1.

comes large. Hence the successive transmission of the electrical signals from individual picture elements is universally employed both in television and in facsimile. The process of selecting the light from successive picture elements in a set order to produce the electrical signal is known as *scanning*.

The most usual form of scanning, in both facsimile and television, orders the picture elements in parallel lines whose width is equal to the width of the picture element. If the separations of centers of successive

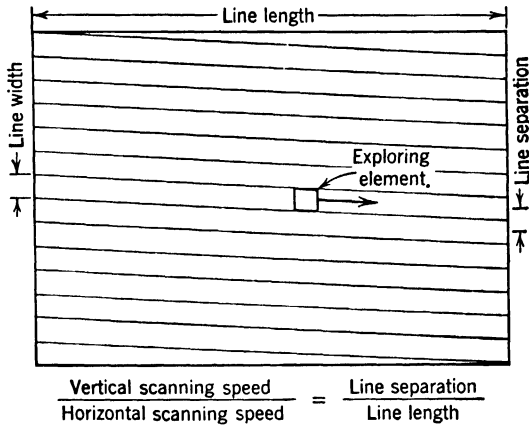


Fig. 16.2. Sequential Line Scanning.

lines are also made equal to the element width (sequential scanning), all the picture elements are accounted for as the exploring element sweeps along the lines from the top to the bottom of the picture (Fig. 16.2). For a square picture the speed of the exploring element in a downward direction is seen to be just equal to its speed along a scanning line divided by the number of lines.

In any picture transmission system the electrical signal generated as a result of the scanning process controls, after traversing a suitable communication channel, the brightness at a corresponding point of a scanning pattern at the receiver, synchronized with the scanning pattern at the transmitter. The quality of the received picture depends thus on four factors: (1) the scanner in the transmitter or the *pickup*; (2) the transmission system; (3) the reproducer or recorder in the receiver; and (4) the synchronization of the scanning patterns in the transmitter and the receiver. These factors will be taken up in turn for facsimile and for television.

**Facsimile Scanners.**<sup>2</sup> The most elementary and most widely used facsimile scanning system is represented graphically in Fig. 16.3. A small aperture illuminated by a lamp is imaged by a well-corrected optical system (microscope objective) so as to form a spot of light somewhat smaller than a picture element on the material to be transmitted. The diffusely reflected light<sup>3</sup> collected by a condenser lens is directed on the photocathode of the phototube generating the picture signal; in modern high-speed systems this is a multiplier phototube. The copy to be trans-

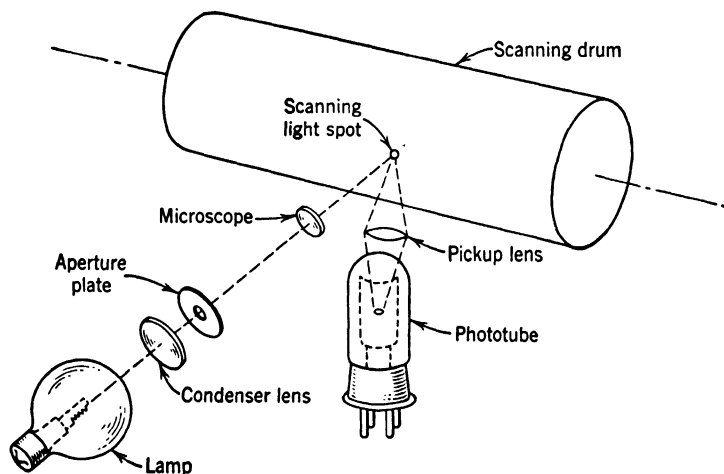


FIG. 16.3. Facsimile Drum Scanner. (H. Pender and K. McIlwain, *Electrical Engineers Handbook*, 3rd Ed., John Wiley, New York, 1936.)

mitted, which may be in the form of photographs or printed or type-written messages, is mounted on a drum rotating at constant speed, whereas the scanning head is displaced lengthwise at a much smaller velocity. This arrangement permits the scanning of successive parallel lines without interruption.

The normal lateral dimension of a picture element in facsimile work, as given by the separation of the scanning lines, is 0.01 inch. The ratio of the line length—9 inches for the transmission of letter-size material—to the line separation is known as the *index of cooperation* of the transmitting equipment. Identity of the index of cooperation of the transmitting and reproducing equipment is necessary if the reproduced picture

<sup>2</sup> For a detailed discussion of facsimile equipment and its operation the reader is referred to the article by M. Artzt, "Facsimile transmission and reception," in Pender and McIlwain, reference 2.

<sup>3</sup> It is essential that the illuminating beam and the phototube be so disposed relative to the material that no specularly reflected light reaches the phototube.

is to be geometrically similar to the original. The other characteristic which must be identical in transmitting and reproducing equipment is the number of lines or *strokes* transmitted per minute. It is common practice to describe a transmission by the index of cooperation and the number of strokes (per minute). For a scanner with 9-inch lines and a line advance of 100 lines per inch operating at 40 strokes per minute the designation would be 40-900. It will be noted that the transmission speed of the system described is 3.6 square inches per minute.

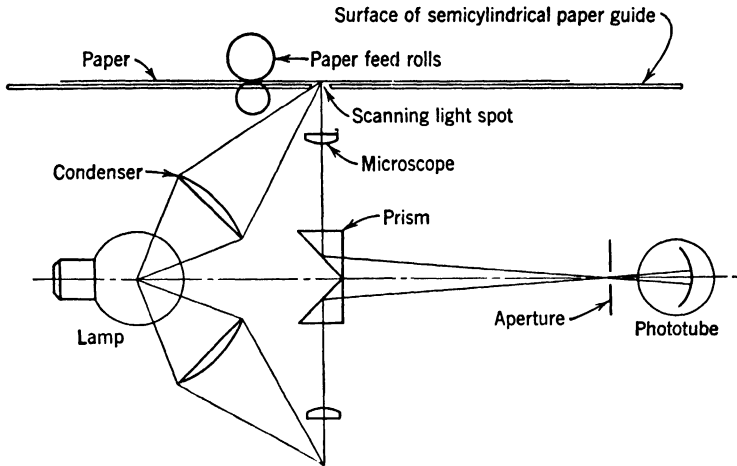


FIG. 16.4. Facsimile Drum Scanner with Double-Ended, Rotating Optics. (H. Pender and K. McIlwain, *Electrical Engineers Handbook*, 3rd Ed., John Wiley, New York, 1936.)

However, it has been found possible to operate regular facsimile equipment at speeds up to 80 square inches per minute.

All the various scanner designs currently employed may be regarded as modifications of the system shown in Fig. 16.3. Thus, in the scanner head, a simple lens may be used to image the source on the copy, and the microscope objective and spot defining aperture may be placed ahead of the phototube. Similarly, the line advance motion may be imparted to the otherwise stationary drum and the optical system may be rotated. An arrangement which is particularly valuable for high-speed transmissions is shown schematically in Fig. 16.4. The copy is placed face down on a transparent semicylindrical drum. This drum rests on guides and is displaced longitudinally by a lead screw which it engages by a half nut. The scanning head is "double-ended"; identical optical systems, 180 degrees apart, are rotated about the cylinder axis inside the cylinder. The light reflected by the copy is picked up by

either of the two identical microscope objectives, which image the scanned material on the same selecting aperture in front of the phototube. Two lines are scanned for every full rotation of the optical system. This arrangement has the advantage of great ease of loading without interruption of the line-scan motion and the synchronization.

**The Transmission System.** The signal current leaving the phototube of the scanner may adequately be regarded as a superposition of sinusoidal current components with frequencies ranging from zero to one half the number of picture elements transmitted per second. The upper

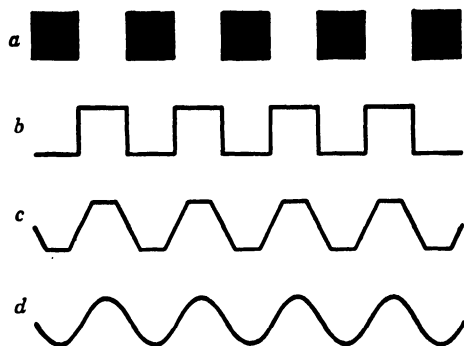


FIG. 16.5. Simulation of Alternating Black and White Dot Signals by Sine Wave. (a) Dots on Original. (b) Signal for Infinitely Narrow Aperture. (c) Signal for Aperture of Half Dot Width. (d) Sine Wave.

limit of this range is established as follows. The finest detail to be transmitted by the system considered would consist of alternate black and white dots, each just one picture element in size (Fig. 16.5a). For an infinitely narrow scanning aperture, the corresponding signal would be the square wave shown in Fig. 16.5b. Actually, however, the aperture is not infinitely narrow. If its width is just half that of a picture element, the output of the phototube is as shown in Fig. 16.5c. It is seen that the difference between this and a pure sinusoidal variation with a wave length equal to two picture element widths (Fig. 16.5d) is less than the difference between the variations produced by the infinitely narrow and the finite aperture. In other words, the *aperture distortion* is more significant than the distortion resulting from the omission of components with frequencies above one half the number of picture elements transmitted per second.

To take a concrete example, the frequency band which must be amplified and transmitted is, for a line length of 9 inches (900 elements) and a transmission speed of 100 lines per minute ( $\frac{5}{3}$  line per second),

0 to 750 cycles per second. As compared with the frequency ranges encountered in telephone and audio amplification, this range is quite moderate. On the other hand, the fact that the range extends down to zero presents a serious inconvenience, since amplification of the signal demands a direct-current amplifier, which cannot be economically constructed to have both high gain and freedom from drift.<sup>4</sup> This difficulty is generally avoided by using the phototube signal to modulate an audio frequency two to three times as great as the highest frequency represented in the phototube signal. The resulting wave may be amplified and either transmitted over a wire line to the receiver or employed to modulate a radio-frequency carrier wave, which is radiated by a transmitter antenna.

Either amplitude or frequency modulation of the audio frequency (subcarrier) may be employed. In the first case<sup>5</sup> the resulting wave consists of an audio-frequency wave whose amplitude varies as the phototube signal; in the second, of a wave of constant amplitude, whose frequency varies with the signal strength (Fig. 16.6, *b* and *c*). A simple amplitude modulator, in which the carrier is applied to the screen grids of two tubes in push-pull connection, is shown in Fig. 16.6*d*. The control grid of the second tube is generally so biased that zero signal is obtained for maximum photocurrent (white), and maximum signal, for zero photocurrent (black). Frequency-modulation circuits generally operate on the principle of inserting a photocurrent-controlled vacuum tube, representing a variable impedance, in the frequency-determining circuit of an oscillator.

For long-range radio transmission the carrier is either frequency-modulated directly by the direct-current signal from the phototube or amplitude-modulated by a frequency-modulated subcarrier. Here the employment of frequency modulation at one point is found to be essential to minimize the effects of interference and fading on the signal controlling the reproducer. With frequency modulation the effects of peaks and amplitude variations thus introduced may be minimized by passing the received signal through a limiting amplifier, whose plate current is saturated for a low-signal amplitude;<sup>6</sup> succeeding low-pass filters eliminate the harmonics introduced by the limiting amplifier. Finally, frequency modulation is converted into amplitude modulation by passing

<sup>4</sup> See Chapter 12, p. 227.

<sup>5</sup> An amplitude-modulated phototube output may be obtained directly by chopping the light beam or modulating the source; vacuum-tube modulation is generally more efficient and convenient, however.

<sup>6</sup> For a more precise description of the suppression of interference with frequency modulation, see, for example, E.E. Staff of M.I.T., reference 3, pp. 709-715.



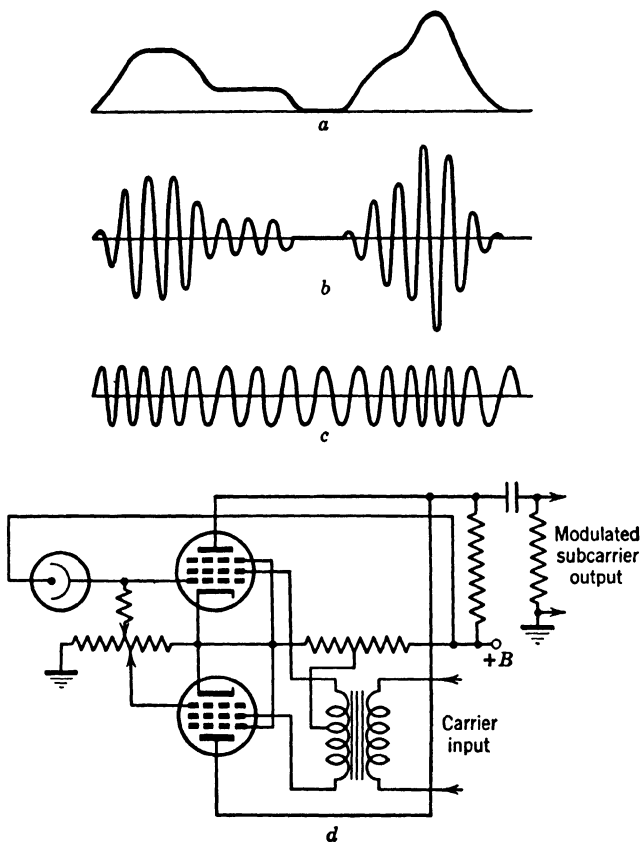


FIG. 16.6. Audio-Frequency Subcarrier Modulated by Picture Signal. (a) Picture Signal. (b) Amplitude-Modulated Subcarrier. (c) Frequency-Modulated Subcarrier. (d) Circuit for Obtaining Amplitude-Modulated Subcarrier.

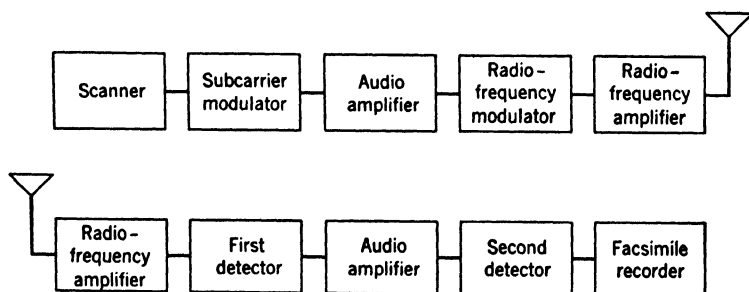


FIG. 16.7. Block Diagram of Radio Facsimile System.

the constant-amplitude frequency-modulated signal through a discriminator which, in essence, is a filter with a uniformly sloping response in the range of frequencies represented in the frequency-modulated wave. As a last stage, the amplitude-modulated subcarrier is detected by a diode circuit and, after a stage of power amplification, provides the control current for the reproducing mechanism.

Figure 16.7 presents, in a general block diagram, the principal components of a facsimile system with radio transmission; a wire system would omit the carrier modulator, as well as the radio-frequency amplifier and first detector in the receiver.

**Facsimile Recorders.** There are four current methods of recording: the photographic, wet electrolytic, dry electrolytic, and carbon-paper processes.

In the photographic method, which gives the most perfect reproductions and is therefore employed when the received copy is to be further

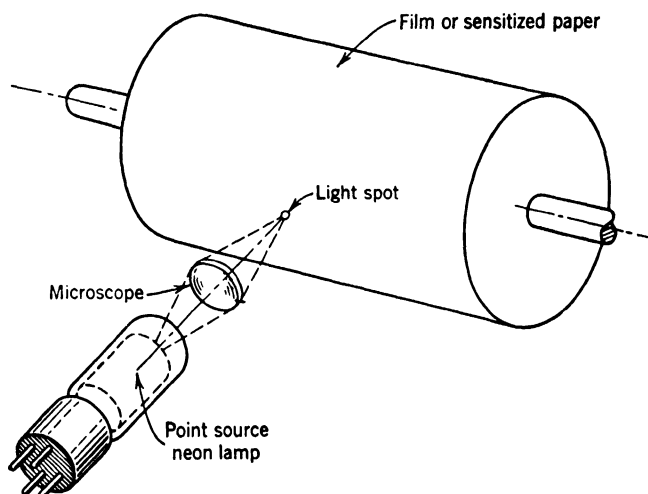


FIG. 16.8. Photographic Recorder. (H. Pender and K. McIlwain, *Electrical Engineers Handbook*, 3rd Ed., John Wiley, New York, 1936.)

reproduced, the sensitive paper is mounted on a drum (Fig. 16.8). The recording head consists of a light source whose output can be controlled electrically and an optical system which forms a light spot of the exact width of a scanning line on the sensitive paper. The relative motion of the drum and the recording head may be effected in any of the ways employed in the scanner. The light source whose output is controlled by the signal current is, most commonly in American practice, a gas-

discharge tube with an internal diaphragm. However, the other methods of light control found useful in sound-on-film recording<sup>7</sup>—the oscillograph mirror, ribbon light valve, and Kerr cell—also find application here. The main disadvantage of the photographic method is that the received picture is not visible until it has been processed, so that it cannot be used to check the operation of the system currently.

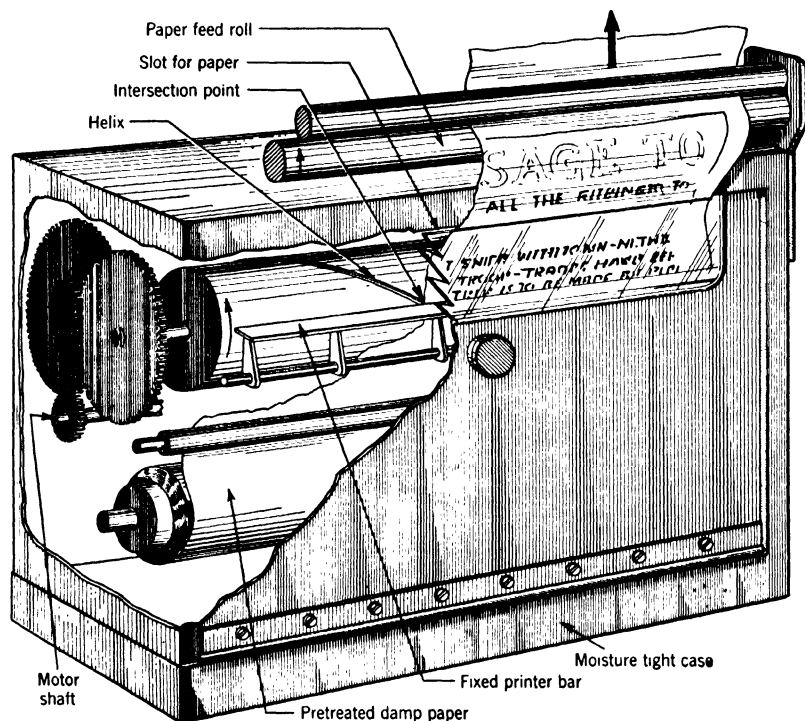


FIG. 16.9. Recorder for Wet Electrolytic Process. (H. Pender and K. McIlwain, *Electrical Engineers Handbook*, 4th Ed., John Wiley, New York. In press.)

In the dry electrolytic recording process, which is free of these objections, the mechanical arrangement is similar to that of the photographic process, the optical recording head being replaced by a stylus dragging over the surface of the prepared paper. As current is passed between the stylus and the paper backing, a dark mark is traced on the surface. One particular recording paper, Teledeltos,<sup>8</sup> consists of a black conducting matrix with a thin, light-gray surface layer which is burned away by the

<sup>7</sup> See Chapter 15, p. 323.

<sup>8</sup> Registered Trade Mark.

signal current. Although the dry electrolytic process is not so fast as the photographic and wet electrolytic processes, nor reproduces half-tones quite so faithfully, it has the distinct advantage of providing an immediately visible, permanent copy without further processing. It is, therefore, not surprising that it finds very extensive commercial application.

In the wet electrolytic process, as well as in the carbon-paper process, the scanning point is generally established by the point of coincidence of a helical ridge on a rotating drum and the edge of a printer bar paral-

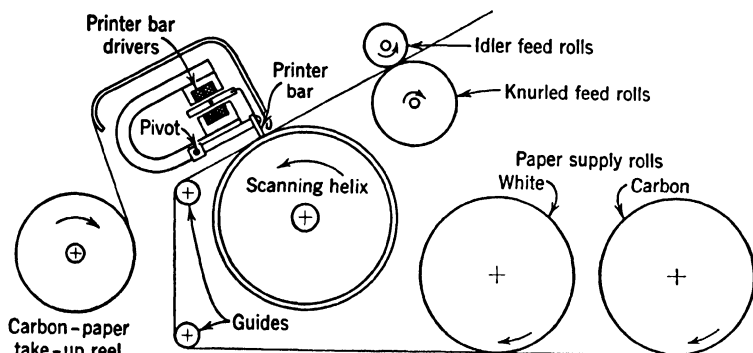


FIG. 16.10. Carbon Paper Facsimile Recorder. (H. Pender and K. McIlwain, *Electrical Engineers Handbook*, 3rd Ed., John Wiley, New York, 1936.)

lel to the axis of the cylinder. In the wet electrolytic process (Fig. 16.9) the printer bar simply drags on the moist paper, which is advanced one line width for every rotation of the drum. As current passes through the paper between the printer bar and the helical ridge of the drum, a chemical reaction forms a color at the point of contact between the printer bar and the paper. In some processes the printer bar itself is gradually decomposed and worn down in the reaction, in others the dye is formed entirely by components of the electrolyte. The paper, generally in the form of large rolls, is either obtained premoistened with the electrolyte or passed through a solution just before the recording; in some processes the record may be fixed simply by passing over hot ironing rolls. The recording speeds by this method are high—up to 90 square inches (a full letter-size sheet) per minute—and the quality of halftone reproduction is excellent.

In the carbon-paper recording process (Fig. 16.10) carbon paper is fed continuously, at reduced speed, over the white recording paper. The printer bar is normally slightly retracted and pressed against the drum helix only when signal current passes through one or more electro-

magnetic drivers. The record left by the carbon paper is darker in proportion as the pressure between printer bar and helix is greater. The carbon paper is retracted in such fashion that the record becomes

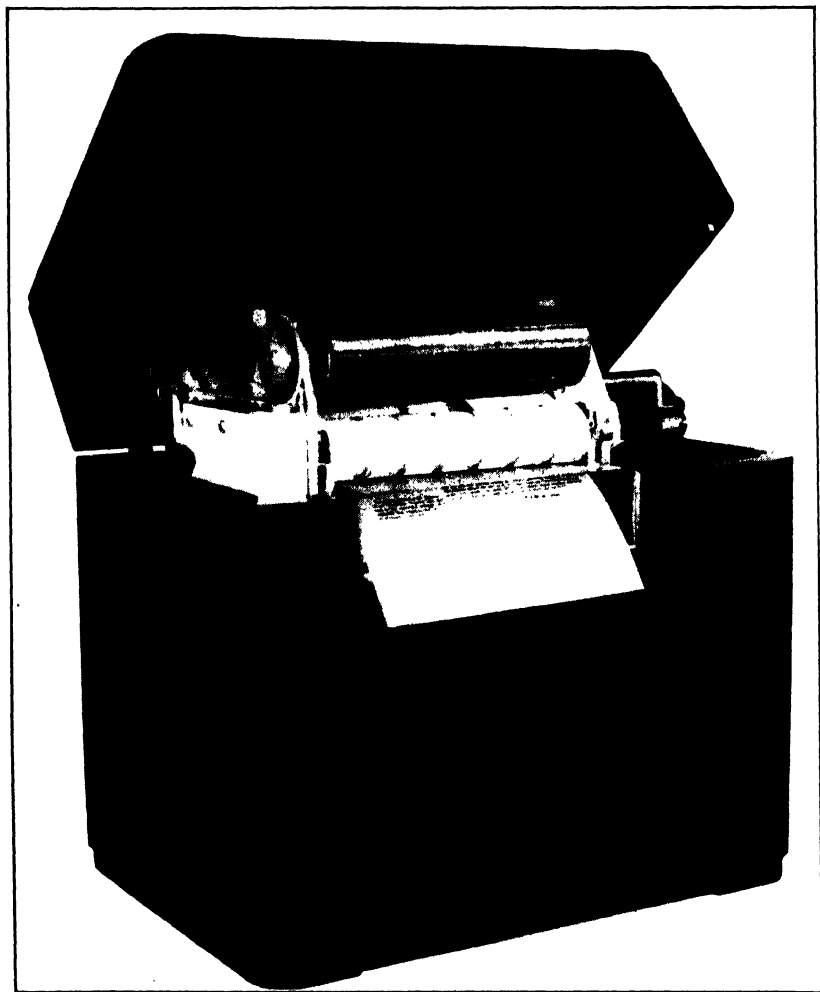


FIG. 16.11. External Appearance of a Carbon-Paper Facsimile Recorder.

immediately visible after printing. The speed of the recorder is limited by the mass of the lightest usable printer bar; high speeds demand excessive driving power. In practice, the maximum speed has been found to be about 10 square inches per minute. It should also be noted

that the halftone reproduction of the carbon-paper recorder is not so perfect as that obtained by photographic and electrolytic recording. On the other hand, the recording material is inexpensive, requires no processing, and immediately provides a permanent record. This makes the carbon-paper recorder particularly suitable for such purposes as the printing of home newspapers in the early hours of the morning, when broadcast channels may be freed for facsimile transmissions. Another advantage of the carbon-paper process is that it permits the rapid preparation of copies of the transmitted material, by using either a multiple layer of paper and carbons or hectographing carbons. Figure 16.11 shows the external appearance of a carbon-paper recorder.

**Facsimile Synchronization.** Two conditions must be fulfilled for the copy obtained to be an undistorted replica of the original. (1) The



FIG. 16.12. Effect of Speed Difference (b) and Difference in Starting Point of Scanner and Recorder (c) on Appearance of Reproduced Picture (a).

speed of scanning must be identical at scanner and reproducer, and (2) scanning must be begun in the same phase, so that, for instance, the left edge of the reproduced picture corresponds to the left edge of the original. Failure to fulfill the first condition results in a skewing of the transmitted copy; failure to fulfill the second, in a splitting up of the material into two parts (Fig. 16.12).

For short-range facsimile transmissions, which are limited to regions with interconnected alternating-current lines, the requirement of constant speed is adequately satisfied by the employment of synchronous motors to operate the scanners and reproducers. For long-range facsimile, tuning forks mounted in a thermostated oven are used as frequency standards. The oscillations produced by them in a magnetic pickup may be amplified to a power level sufficiently high to operate a synchronous motor which runs the scanner or reproducer. Alternatively, an induction motor may be kept in phase with the tuning-fork oscillations by providing a magnetic brake on the motor shaft whose braking power increases whenever the motor tends to run ahead of the tuning-fork oscillations.

For recorders which stop between transmissions, the proper starting phase can be assured if the drum always comes to rest in the same position and is started by a starting signal releasing a magnetic clutch. In

continuously running recorders, the motor may be thrown temporarily out of synchronism and may be brought back under control when a neon tube, fed by line-starting pulses passed through a commutator, indicates proper phasing. These pulses may also be used for an automatic adjustment of phasing: for this purpose they are passed through a commutator which is open only at the start of the line in the recorder. With the commutator closed, the pulses actuate a relay which temporarily opens the circuit of the synchronous motor, causing the drum to be retarded slightly. Only as the starting pulses reach the commutator at its open position is the recorder maintained steadily at its proper running speed.

**Tape Facsimile.** A specialized form of facsimile, used for the transmission of messages, is tape facsimile. The message is written, printed, or typewritten on a tape and run through a scanner whose stroke corresponds to the width of the tape (Fig. 16.13). The deflection of the spot, focused on the tape by three cylindrical lenses, is effected by refraction in a rotating hexagonal prism. The number of lines scanned per minute is equal to three times the number of revolutions of the prism per minute. The diffusely reflected light is directed to the photocathode by a pair of curved mirrors. In the reproducer a small helix drum,

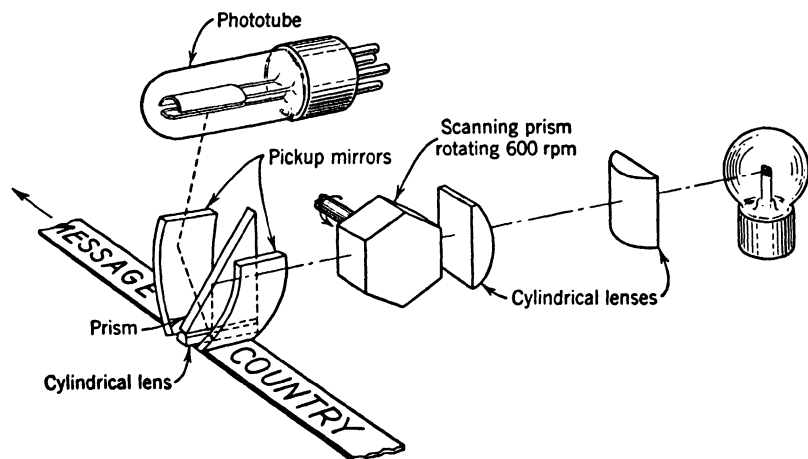


FIG. 16.13. Scanner for Tape Facsimile. (H. Pender and K. McIlwain, *Electrical Engineers Handbook*, 4th Ed., John Wiley, New York. In press.)

inked by a felt roller, leaves a record on the tape whenever the printer bar raises the tape against the helix (Fig. 16.14). The advantage that this facsimile method has over teletype transmission is that interference which, in teletype transmission, may lead to the printing of the wrong

character will, in facsimile, at most render the character unreadable. Figure 16.15 shows a typewriter equipped with a tape facsimile scanner. The method of transmission described is used most widely for hand-written and printed copy.

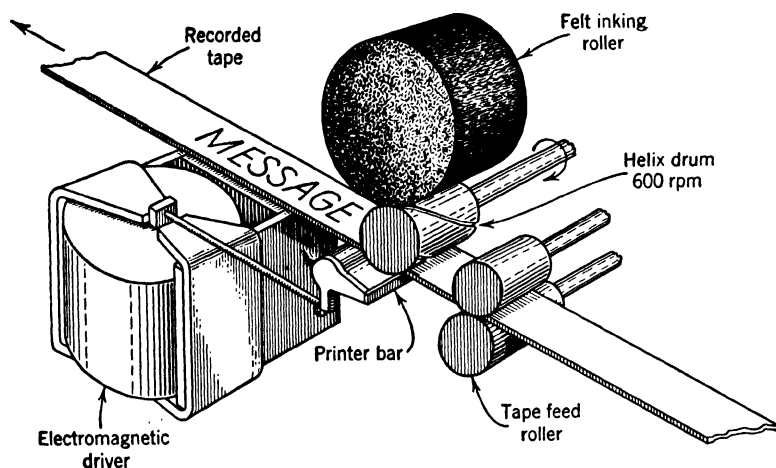


FIG. 16.14. Recorder for Tape Facsimile. (H. Pender and K. McIlwain, *Electrical Engineers Handbook*, 4th Ed., John Wiley, New York. In press.)

**Copying by Facsimile.** If the rotating mechanism of the scanner and recorder are mounted on a common shaft, a high-speed duplicator for any type of printed and illustrated material is obtained; with a wet electrolytic process the time required for copying a letter page becomes only about a minute. Furthermore, if the stylus vibrates at high frequency in the recorder, the system may be utilized for the cutting of high-quality stencils without danger of tearing the stencil paper. The time for preparing a stencil in this manner is 10 to 15 minutes.

**Facsimile of Color Pictures.** A number of different methods have been devised for the transmission of color pictures by facsimile. In one of these<sup>9</sup> the color print is mounted on the scanner drum and scanned by a head with a rotating three-color filter disk in front of the phototube. For every rotation of the drum, the filter disk rotates by a third of a revolution, changing the color of the light incident on the phototube. The recorder drum has three times the circumference and one third the angular velocity of the scanner drum. Three films of the same size as the transmitted print are mounted side by side on the recorder drum. Photographic recording, using the signals obtained through the three

<sup>9</sup> See reference 4.





FIG. 16.15. Typewriter Equipped with Tape Facsimile Scanner. (RCA Communications.)

different color filters, yields the separation negatives required for building up a color print by conventional techniques.

A more recent system—the Colorfax system invented by L. R. Philpott and W. G. H. Finch<sup>10</sup>—reproduces the color picture directly, without any further processing. In the transmitter, which is similar to that just described, each line is scanned in succession with a red filter, a green filter, a blue filter, and without filter. In the recorder, cyan, magenta, yellow, and black pencils, controlled by the complement of the phototube signal, trace out the successive parallel lines which form the color image on a moving strip of white paper. The pencils are mounted at four peripheral points of a rotating disk which is pressed against the curved paper strip by the signal currents.

**The Requirements of Television.** It has already been noted that a major difference between facsimile and television is the much greater speed of transmission required in television. Apart from this, the subject matter in television is not—except for film transmissions—confined to a flat surface, and the reproduced picture *must* be so arranged that it can be viewed directly.

The impression of continuous observation of the transmitted scene is created in television, as in motion pictures, by the presentation to the eye of images of the scene in such rapid succession that the brain fuses them into a single image. The motion-picture industry has adopted, for this purpose, a standard picture repetition rate or *frame frequency* of 24 pictures per second. American television practice demands 30 frames per second, which is a simple submultiple of the power frequency and hence results in less objectionable interference from the power lines.

The frame frequency, together with the detail demanded in the reproduced image, fixes the required speed of scanning. The image detail is given by the number of lines forming the image and the *aspect ratio*, which is the ratio of the length of a (horizontal) scanning line and the height of the picture. The number of lines used at present in television broadcasting is, in America, 525; the aspect ratio is  $\frac{4}{3}$ . If the picture is to have equal horizontal and vertical resolution, it means that the total number of picture elements is  $\frac{4}{3} \cdot (525)^2 = 367,500$ . The amount of detail in such a picture corresponds, roughly, to a facsimile picture, or high-quality halftone, 5 by 7 inches in dimension.

It is seen that the television picture signal must be capable of reproducing the intensities of some 11 million picture elements per second, so that, by the criterion previously established, frequencies ranging

<sup>10</sup> See reference 5.

from 30 cycles<sup>11</sup> to 5.5 megacycles per second should be represented in the picture signal. A more detailed consideration of the effects of the finite intensity distribution in the scanning element<sup>12</sup> indicates that the upper limit may be reduced to approximately 4.25 megacycles per second if equal resolution in a horizontal and vertical direction is the objective sought.

Several consequences may be drawn from these figures. The first, obvious one is that the amplifiers for a television picture signal must be constructed to transmit extraordinarily large bandwidths without distortion and that radio carriers employed for television broadcasting must lie in the ultrahigh-frequency range (above 40 megacycles per second). Next, in view of the high scanning speed—15,750 lines per second—mechanical scanning methods such as are employed in facsimile are likely to be impracticable. Finally, in view of the extremely brief scanning period of a picture element, the simple phototube pickups of facsimile may be used only under very favorable conditions of illumination of the subject.

As an example, assume that the scene to be transmitted is an outdoor scene on a bright day, with a subject brightness of 500 lumens per square foot. Let this scene be imaged by an  $f/2$  lens (with an optical efficiency of 5 per cent) on an area 4 by 3 inches in dimension, and let an aperture of picture element size scan this area. Finally, let the light transmitted by the aperture fall on a phototube with a sensitivity of 20 microamperes per lumen, which generates the picture signal. The total light falling on the image area will then be  $500 \cdot 0.05/12 \cong 2$  lumens, the average photocurrent,  $2 \cdot 2 \cdot 10^{-5}/367,500 \cong 10^{-10}$  ampere, and the charge liberated in the scanning of one picture element,  $10^{-10}/11 \cdot 10^6 \cong 10^{-17}$  coulomb or some 60 electrons. Even in this extremely favorable case the signal level is seen to be low enough for statistical fluctuations in the emission of the photoelectrons to make themselves felt in the form of "noise."<sup>13</sup>

**Mechanical Television Systems.** In the earliest television systems—which, of course, did not aspire to a picture quality of present standards—scanning was mechanical throughout. The prototype of the many ingenious mechanical scanners is the scanning disk invented by Paul Nipkow as early as 1884. An elementary system, which employs the scanning disk both in the sender and in the receiver, is shown in Fig.

<sup>11</sup> Since the picture signal, except for the presence of moving objects in the scene, is repeated periodically with frame frequency, it consists primarily of harmonics of 30 cycles per second.

<sup>12</sup> See Zworykin and Morton, reference 6, Chapter 6.

<sup>13</sup> See Chapter 13, p. 250.

16.16. The disk itself has a spiral of apertures bored in its periphery. Each aperture is the size of a picture element and is displaced radially relative to its predecessor by one line separation. The angular displacement between apertures is  $2\pi/n$  radian, where  $n$  is the number of lines in the scanning pattern. Let a lens project an image of the scene to be transmitted on the periphery of the rotating disk, with a horizontal dimension equal to the separation between two successive apertures and a vertical dimension equal to the radial separation of the outermost and innermost apertures of the spiral. Each aperture in turn will then

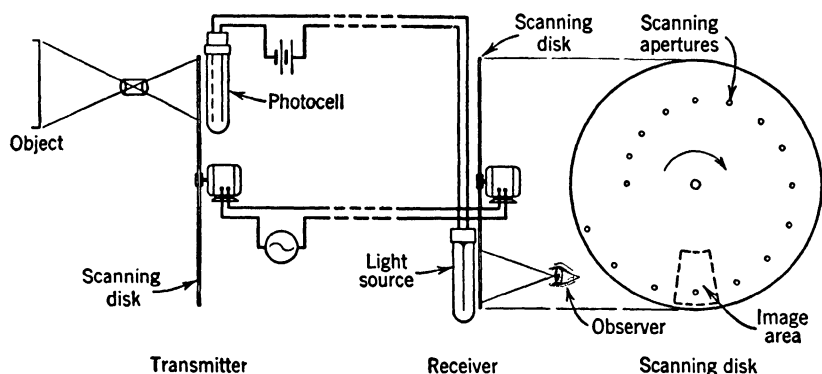


FIG. 16.16. Mechanical Television System Employing Nipkow Disk in Pickup and Receiver.

trace out a scanning line across the image until, after a full revolution of the disk, the whole image has been scanned by the apertures. A phototube placed behind the disk, with a photocathode large enough to intercept the entire light beam forming the image, will then generate a picture signal whose amplitude corresponds to the brightness of successive picture elements. This picture signal, after amplification, may be used to control the brightness of a gas discharge or glow tube which is placed behind a Nipkow disk rotated in synchronism with the first disk. If the gas discharge covers the entire image area and the two disks are rotated sufficiently rapidly, an observer will see the original scene reproduced in the plane of the viewing disk.

The process described may be used for the transmission of scenes by television under exceptionally favorable circumstances. On the other hand, the modification of the pickup system shown in Fig. 16.17 yields considerably stronger signals and was, in fact, utilized in the first successful demonstration of television transmitted by radio.<sup>14</sup> Here a

<sup>14</sup> See Jenkins, reference 7.

powerful source of light, such as an electric arc, illuminates a mask marking out an area, equal to the full scanning pattern, on the scanning disk. The same area of the scanning disk is imaged by an objective on the scene or subject to be transmitted. A condenser lens, imaging the source into the objective, prevents the loss of any light that passes through the mask. As the disk is rotated, this optical system causes a spot of light—namely, the image of a brightly illuminated aperture of the scanning disk—to sweep out a scanning pattern across the subject.

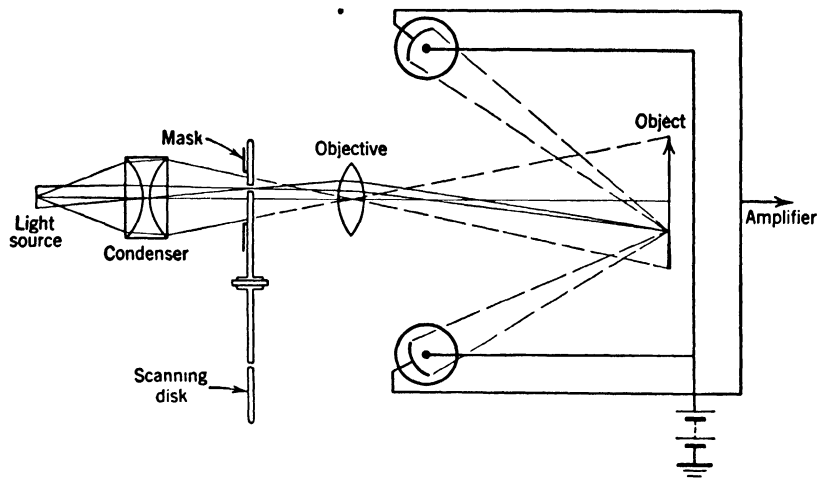


FIG. 16.17. Flying Spot Scanner Employing Nipkow Disk.

Light which is reflected by the portion of the subject intercepting the light spot is collected in part by the oversize cathodes of special phototubes or directed by reflectors toward the cathodes of phototubes of normal size. The sum of the photocurrents of these tubes represents the picture signal current.

This "inverted" system of scanning, first proposed by A. Ekström in 1910 and more commonly designated as *flying-spot scanning*, has two advantages over the direct system. The effective picture elements of the subject can be illuminated more brilliantly than is possible with the direct system, and the photocathodes (or phototube reflectors) intercept a larger fraction of the reflected light than the objective lens in the direct system. Flying spot scanning also has two drawbacks. It cannot be carried out in normal illumination and it distorts brightness values. Objects with the same reflection coefficient appear darker if they are at a greater distance from the light-gathering phototubes.

**Electronic Flying-Spot Scanning.** The resolution attainable with the flying-spot scanning system just described is limited by the maximum size of the scanning disk which can be rotated at a frame frequency of 1800 revolutions per minute. This limit is probably reached, if not exceeded, with present television standards. In any case, the design of the mechanical equipment for high resolutions becomes complex, its execution difficult, and the equipment itself cumbersome. In fact, it is

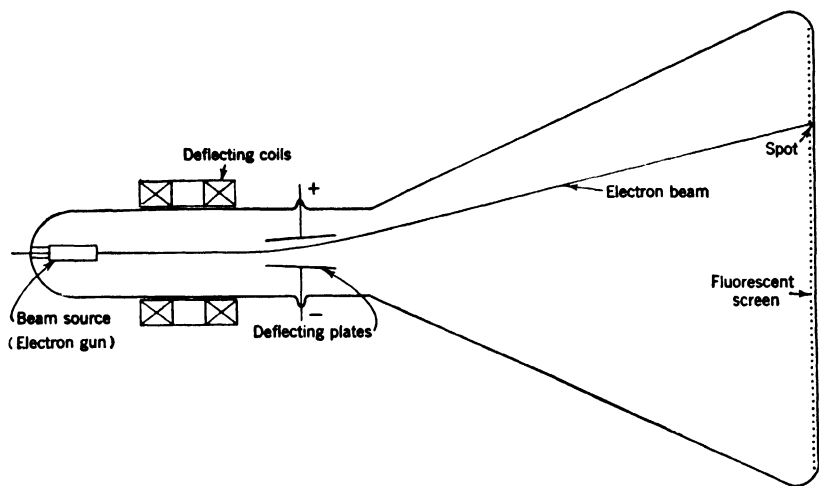


FIG. 16.18. The Cathode Ray Tube. (From Zworykin, Morton, Ramberg, Hillier, and Vance, *Electron Optics and the Electron Microscope*, John Wiley, New York, 1945.)

unlikely that television would have attained great popularity if a scanning method had not been found which obviated the necessity of setting great masses into motion. This method utilizes the practically instantaneous deflection of high-velocity electron beams by electric and magnetic fields which, in the cathode-ray tube, is used to measure the voltages and currents, respectively, which produce these fields.

The essential elements of the cathode-ray tube (Fig. 16.18) are an electron gun which forms an electron beam converging to a narrow spot, transverse electric and/or magnetic fields which deflect the beam,<sup>15</sup> and

<sup>15</sup> The deflection by a uniform electric field is in the direction of the field. If  $d$  is the separation of the deflection plates,  $l$  is their length,  $V_d$  is their difference of potential, and  $V$  is the accelerating voltage of the beam, the angle of deflection (for small fields) is  $lV_d/(2dV)$ . The deflection by a magnetic field, formed by current flowing through a pair of deflection coils outside the tube neck, is at right angles to the direction of the field. Here small angles of deflection are given by  $2.97 \cdot 10^4 Hl/V^{1/2}$ , where  $H$  is the magnetic field in webers per square meter,  $l$  is the length of the deflecting field in meters, and  $V$  is the accelerating potential in volts.

a fluorescent screen which converts a portion of the kinetic energy of the beam into light. The construction of a typical electron gun is shown in Fig. 16.19. It consists of a cathode which emits the electrons,

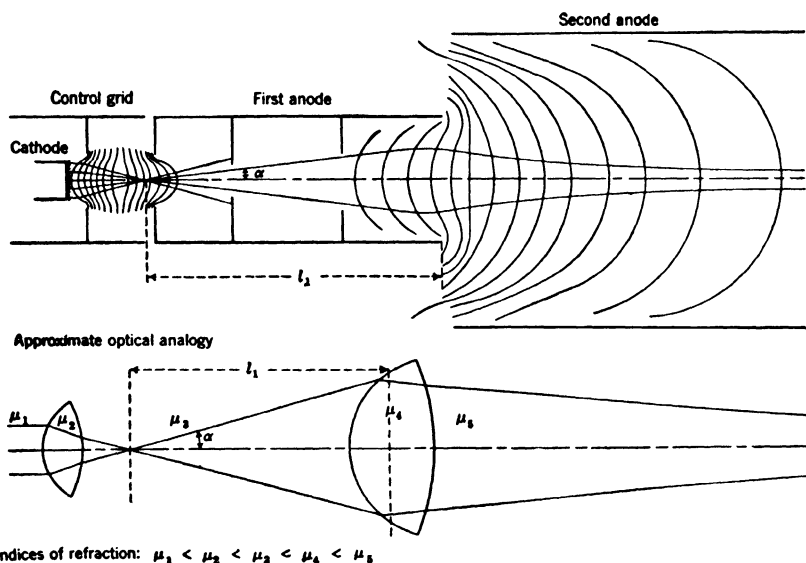


FIG. 16.19. Cross Section of an Electron Gun and Its Light-Optical Analogue. (From Zworykin, Morton, Ramberg, Hillier, and Vance, *Electron Optics and the Electron Microscope*, John Wiley, New York, 1945.)

a negative control grid which limits the number of electrons passing through its aperture to form part of the beam, and two positive electrodes, the first and second anode. The cathode itself is a round oxide-

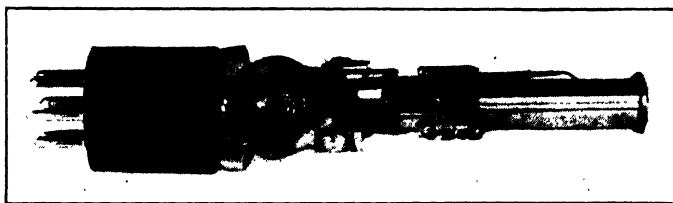


FIG. 16.20. A Typical Kinescope Gun. (From Zworykin and Morton, *Television*, John Wiley, New York, 1940.)

coated disk at the end of an indirectly heated cylinder; the remaining electrodes form a system of axially symmetric electric fields, which act on the electrons like a pair of converging lenses;<sup>16</sup> the curved lines repre-

<sup>16</sup> See Chapter 9, p. 157.

senting equipotential surfaces play a similar role as lens surfaces in light optics. The potential difference between the first anode cylinder and the second anode cylinder is adjusted so that the electron lens formed between them images the point at which the beam has its narrowest cross section (the *crossover*) on the fluorescent screen. A typical electron gun—without the second anode, which is commonly a conducting coating on the envelope of the tube—is shown in Fig. 16.20.

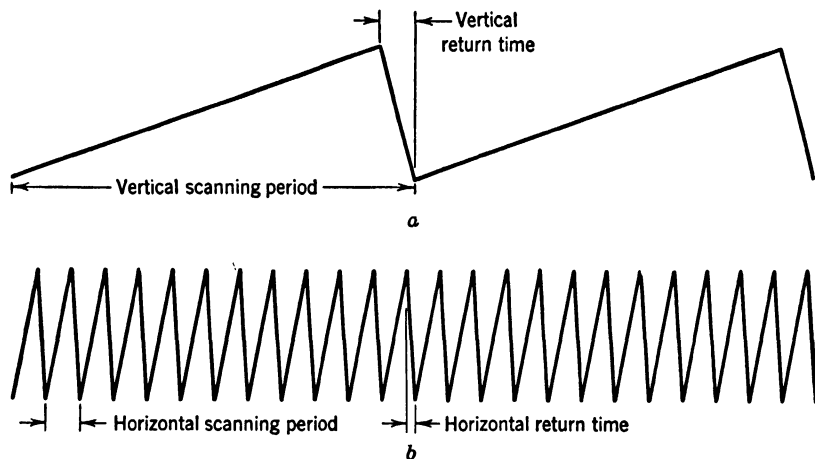


FIG. 16.21. Wave Shapes of Deflection Currents for (a) Vertical and (b) Horizontal Deflection (Schematic).

The deflection of the beam in two perpendicular directions may be effected either by two mutually perpendicular pairs of deflecting plates mounted inside the tube or by a deflection yoke consisting of two pairs of deflecting coils slipped over the neck of the tube—or, finally, by a pair of plates and a pair of coils, as indicated in Fig. 16.18. In television applications purely magnetic deflection is most common.

Suppose now that two sawtooth-shaped alternating currents, as shown in Fig. 16.21, are passed through the two deflecting coils, the one passing through the horizontal deflection coil having line frequency (15,750 cycles per second), and the one passing through the vertical deflection coil having field frequency (60 cycles per second).<sup>17</sup> Such a sawtooth

<sup>17</sup> With a field frequency equal to twice the frame or picture frequency and an odd number of scanning lines, the scanning lines in the second vertical traversal of the beam fall just between those in the first traversal. This method of scanning the field twice over for every picture, known as *interlaced scanning*, reduces flicker effects. A similar effect is sought in motion-picture practice by interrupting the illumination of the screen in the middle of every frame.



wave may be generated by the circuit shown in Fig. 16.22. The condenser  $C$  is charged through the resistance  $R$ , giving rise to a linear increase in potential of the grid of the pentode, until a sharp positive synchronizing pulse on the grid of the triode renders the triode conduct-

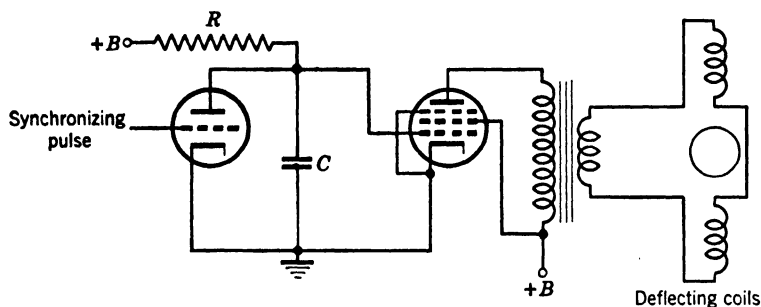


FIG. 16.22. Circuit Capable of Generating Sawtooth-Shaped Deflecting Currents.

ing, discharging the condenser. After completion of the discharging process, the linear charging cycle is repeated. The pentode serves to convert the sawtooth voltage variation on its grid into a similar current variation in the stepdown transformer providing the deflection current.

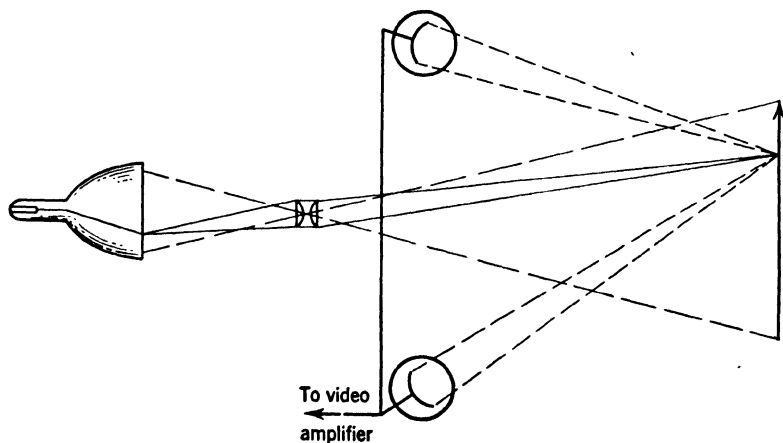


FIG. 16.23. Electronic Flying Spot System.

The effect of applying these two sawtooth currents to the two deflection coils is to have the spot on the fluorescent screen of the cathode-ray tube describe a series of parallel horizontal lines making up a standard scanning pattern. The synchronizing pulses, inverted in sign and ap-



FIG. 16.24. Two Experimental Multiplier Phototubes with Large Cathodes and "Pinwheel" Multipliers Compared with Standard 931-A Multiplier Phototube.

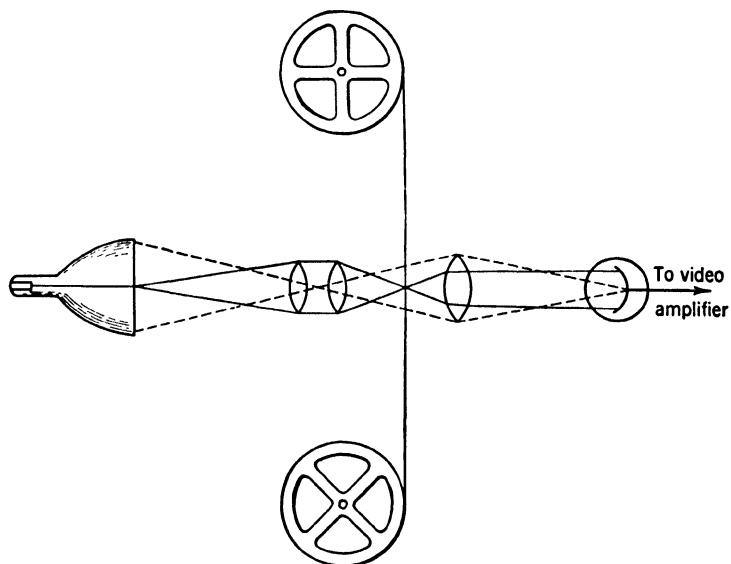


FIG. 16.25. Flying Spot Pickup for Film Transmission.

plied to the control grid of the cathode-ray tube, suppress the beam during the short return periods. Such a cathode-ray tube, provided with a fluorescent screen whose light emission lasts only a fraction of the time required for scanning a picture element after bombardment, constitutes a *flying-spot tube*. The screen is simply imaged on the sub-

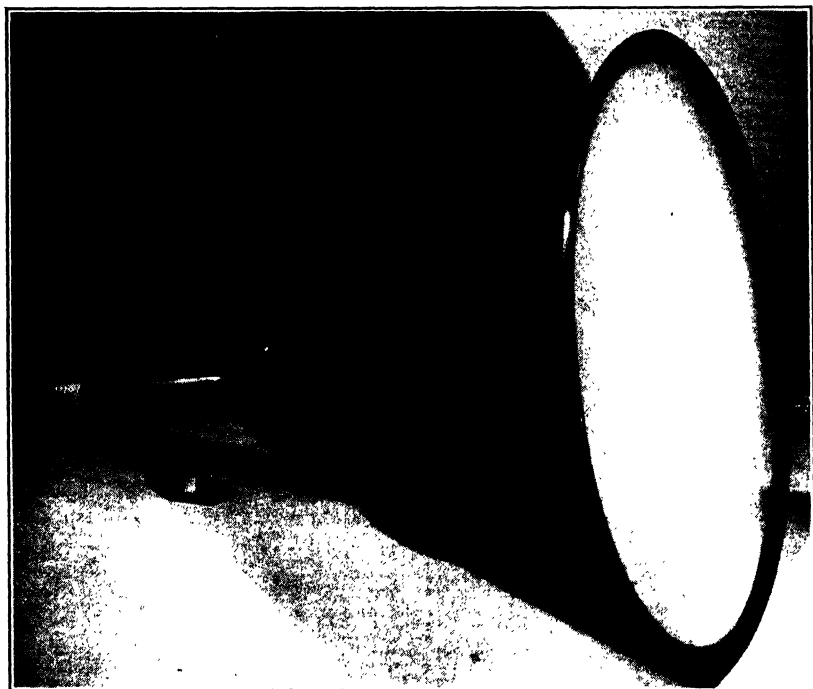


FIG. 16.26. 16-Inch Kinescope for Direct Viewing.

ject to be transmitted, and the reflected light is collected by phototubes (Fig. 16.23).

The basic idea of this simple electronic television pickup system is relatively old.<sup>18</sup> Its realization as a high-definition system has depended, however, on the development of high-efficiency low-persistence screens on the one hand and of suitable multiplier phototubes on the other. Flying-spot tubes with zinc oxide screens, operated at 12 kilovolts, have given satisfactory results. A number of multiplier phototubes, ranging from the standard commercial type to models with extraordinarily large photocathodes, are shown in Fig. 16.24. The field distribution in the larger tubes, which have only been constructed experimentally, is such

<sup>18</sup> See Zworykin, reference 8.

as to draw the photoelectrons into the multiplier structure, which consists of a series of "pinwheels" at increasing potentials. An electron incident on a vane of one of the pinwheels ejects there secondary electrons, which are accelerated toward the next pinwheel. A high-transmission tungsten wire screen shields the vanes from the field of the preceding stage, which would otherwise suppress the secondary emission.

The application of the flying-spot system to direct pickup requires tubes which are still in the course of development and is handicapped by certain inherent drawbacks, already noted. It does not have these disadvantages in its use for motion-picture transmission (Fig. 16.25). Here only the horizontal deflection coils of the flying-spot tube are actuated, the vertical scanning being provided by the uniform displacement of the motion-picture film. Since the light transmitted by the film is concentrated directly on the photocathode of the multiplier tube, it is here unnecessary to employ special large-area phototubes.

**Electronic Viewing Tubes or Kinescopes.** The employment of electronic methods of reproducing the television image preceded their adoption in television pickup systems. The basic viewing tube, or *kinescope*,<sup>19</sup> differs from the flying-spot tube in two respects. (1) The control grid of the gun is not maintained at a fixed voltage, but varied in potential by the picture signal, causing a corresponding variation in the brightness of the spot on the fluorescent screen; and (2) phosphors with a longer persistence (usually activated zinc sulfide, zinc-cadmium sulfide, or zinc orthosilicate—willemite—or mixtures thereof), approaching a frame period, are used for the fluorescent screen. The employment of these phosphors serves both to increase the efficiency of conversion of electron energy into light and to reduce flicker effects.

<sup>19</sup> See Zworykin, reference 9.

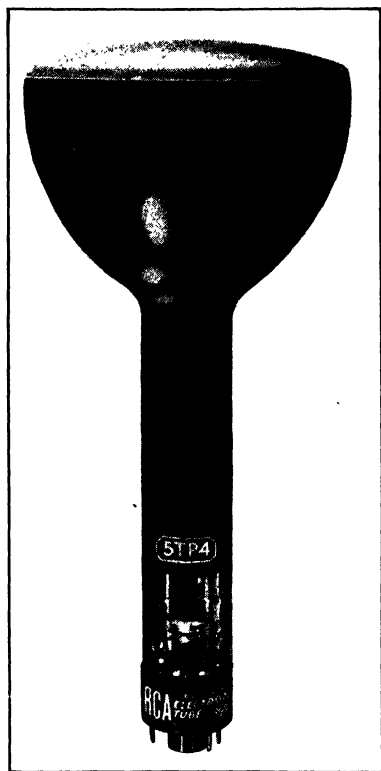


FIG. 16.27. Projection Kinescope.

The image formed on the fluorescent screen may be either viewed directly or optically projected on a larger viewing screen. Figure 16.26 shows a typical kinescope for direct viewing, Fig. 16.27 shows one for projection. The direct-viewing tubes are relatively large, having screens



FIG. 16.28. Table-Type Television Receiver.

up to 20 inches in diameter, and are operated at lower voltages (4 to 12 kilovolts). A table-type receiver with a direct-viewing tube is shown in Fig. 16.28. The smaller projection kinescopes are operated at about 30 kilovolts in home receivers, at up to 100 kilovolts in theatre television projectors. Efficient operation at these high voltages is made possible, in part, by the deposition of thin reflecting films of aluminum over the inside surface of the fluorescent screen.<sup>20</sup> The metal film both prevents charging up of the screen under bombardment and increases the amount

<sup>20</sup> See Epstein and Pensak, reference 10.

of light emitted in a forward direction. The largest possible fraction of the emitted light is utilized for the image formed on the projection screen by employing a reflective projection system whose spherical aberration is corrected by an aspheric correction plate.<sup>21</sup> The optical system for a projection receiver for the home is shown in Fig. 16.29. The image from the kinescope face is projected upward and deflected through 90 degrees by a mirror toward the vertical viewing screen. The optical efficiency of the system shown is six or seven times that of an  $f/2$  lens.

#### Color Transmission System for Slides and Film.

The flying-spot system lends itself readily to the television transmission of pictures in natural color. A schematic diagram of the system is shown in Fig. 16.30.<sup>22</sup> The light from the scanning pattern on the screen of a flying-spot tube with a white fluorescent screen is directed, through a beam-splitting system, onto the photocathodes of three multiplier phototubes. The beam splitting is carried out by two dichroic plates;<sup>23</sup> they, together with auxiliary filters, cause the red content of the light transmitted by the film image to fall on one photocathode, the green content on the second, and the blue content on the third. The three picture signals thus generated are transmitted on separate radio or cable channels to the receiver, in which they modulate the scanning beams of three separate kinescopes. The screens of these kinescopes, eventually provided with compensating filters, are chosen so that the three images are red, green, and blue, respectively. These three images are optically superposed on a viewing screen, where they form a natural color image of the original film picture.

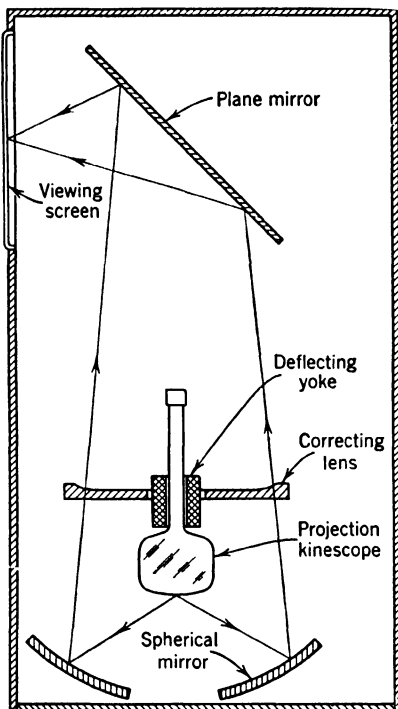


FIG. 16.29. Optical System of Projection Receiver for the Home. (Epstein and Maloff, reference 11.)

<sup>21</sup> See Epstein and Maloff, reference 11.

<sup>22</sup> See Kell, Sziklai, Ballard, Schroeder, Wendt, and Fredendall, reference 12.

<sup>23</sup> These plates reflect one primary color, transmit its complement.

A flying-spot color pickup for slides is shown in Fig. 16.31, and a console receiver with three separate projection kinescopes and  $f/2$  lenses, in Fig. 16.32. The use of reflective projection systems in an experimental theatre projector for color television is represented in Fig. 16.33.

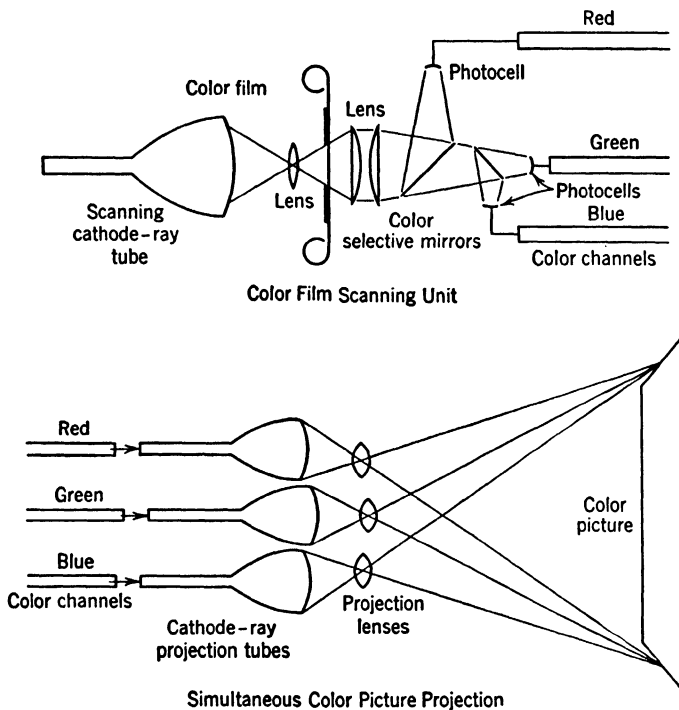


FIG. 16.30. System for the Transmission of Film Pictures in Natural Color. (Reference 12.)

**Ultrafax.** The flying-spot scanning of moving film also lends itself well to providing a facsimile or message transmission service of extraordinary speed. The messages would be transferred photographically on standard film, which would be run at the standard television speed of 30 frames per second through a scanner. The resulting picture signal would modulate a horizontally deflected beam in another flying-spot tube in the receiver, whose screen would be photographed on a second continuously moving film, reproducing the original message thereon. Since the range of the ultrahigh-frequency radio waves, which would act as carriers for the picture signals, is limited to line of sight, a network of relay stations would have to be provided to guide the signals from their point of origin to their final destination; automatic routing signals would precede each

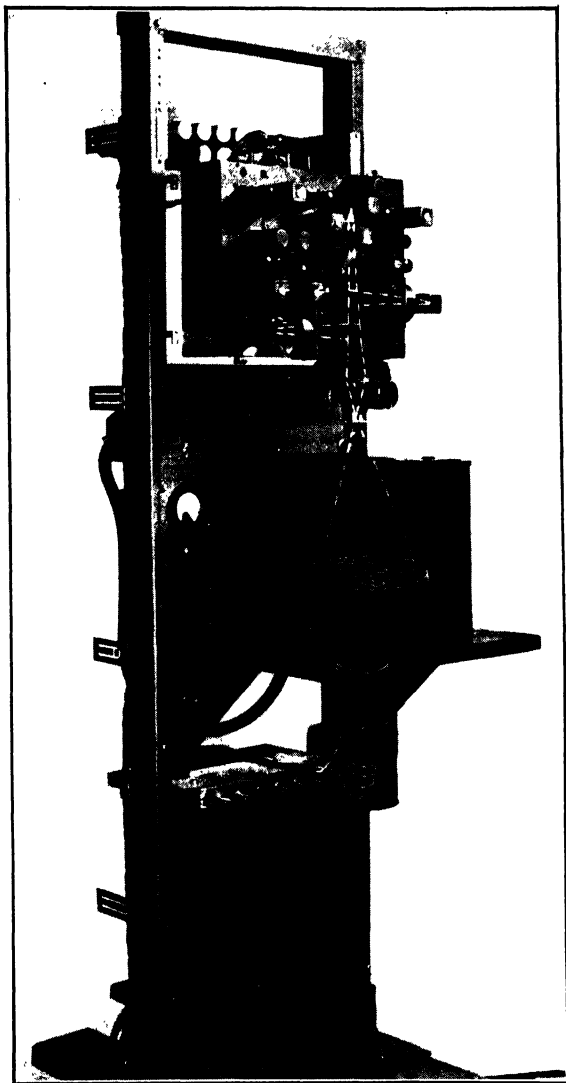


FIG. 16.31. Flying-Spot Color Pickup for Still Pictures. (Reference 12.)



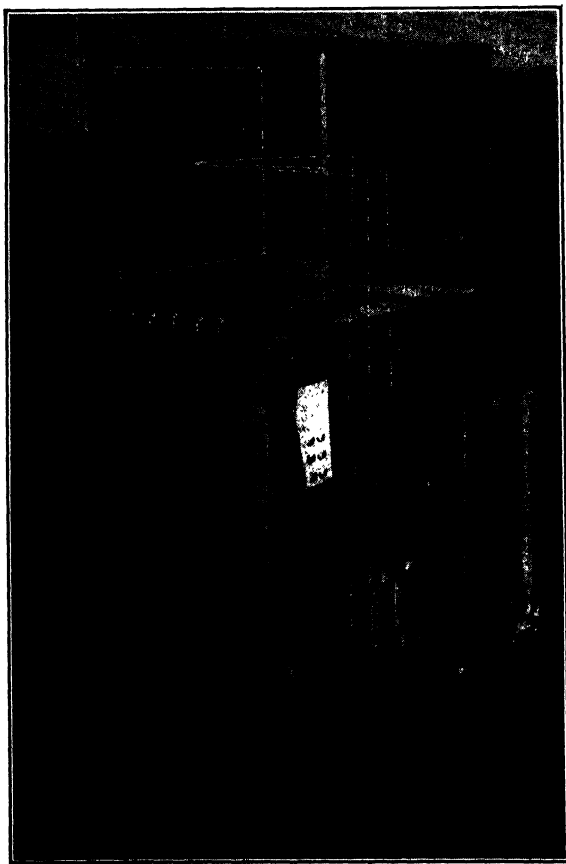


FIG. 16.32. Experimental Console Color Television Receiver. (Reference 12.)

message. The general arrangement of an *ultrafax* message transmission service is indicated in Fig. 16.34. An ultrafax scanner designed for testing the operation of the system is shown in Fig. 16.35.

If the average number of words on a page is 300, the ultrafax system will transmit over half a million words a minute. In heavy message-traffic areas this speed of transmission, far exceeding that of any earlier

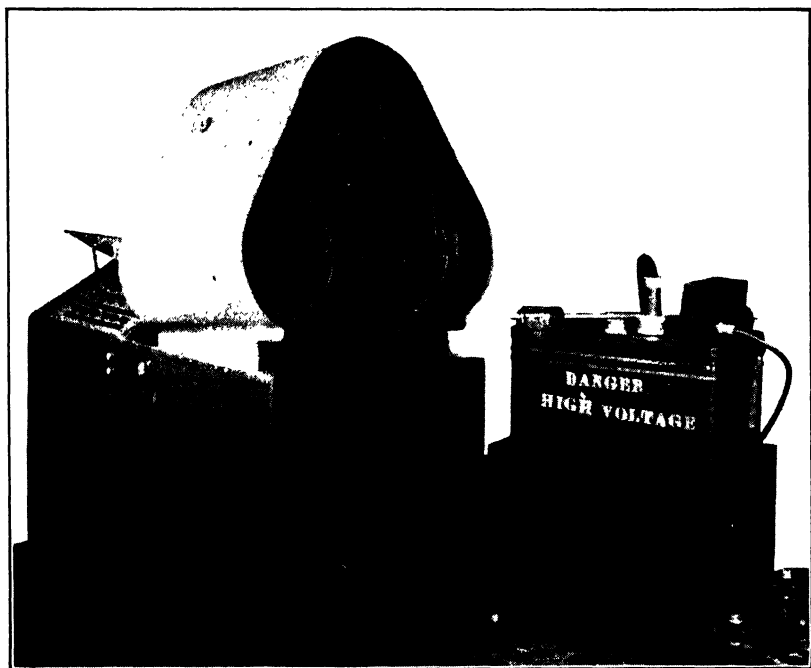


FIG. 16.33. Experimental Theatre Television Projector for Color Pictures.

system of message sending, should yield considerable economies. Furthermore, the service time of the relay system could be so divided up that it would double as a network for television broadcasts.

**Flying-Spot Microscope.** If the scanning pattern from a flying spot tube is imaged on a microspecimen by a high-power microscope objective and the transmitted light is collected by a multiplier phototube, the photocurrents generated in the phototube may be employed to reproduce a highly magnified image of the specimen on a television receiver screen. For very high magnifications, given by the ratio of the size of the scanning pattern on the receiver screen to the size of that on the specimen, the flying-spot tube would simply be placed in the position of the plate

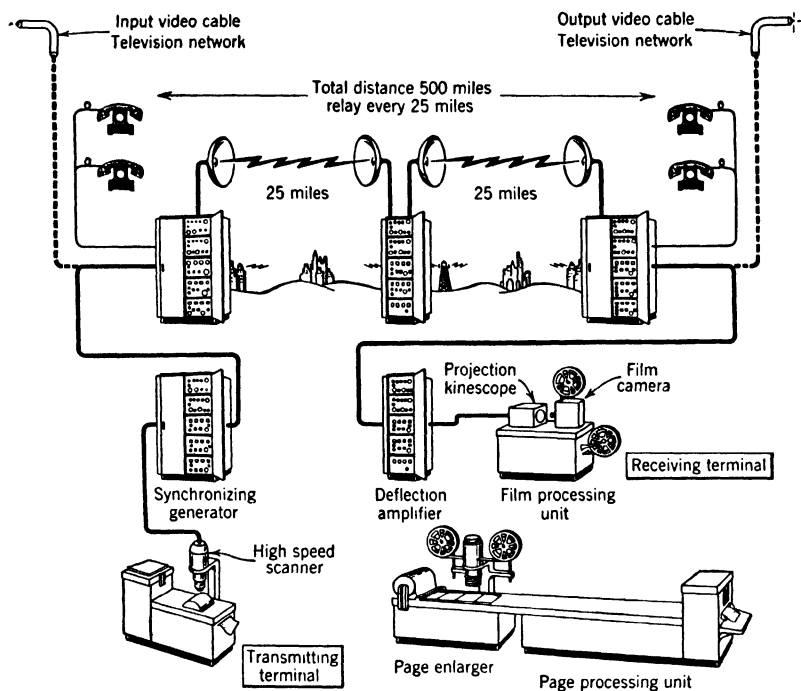


FIG. 16.34. Schematic Diagram of RCA Ultrafax Message Transmission System.

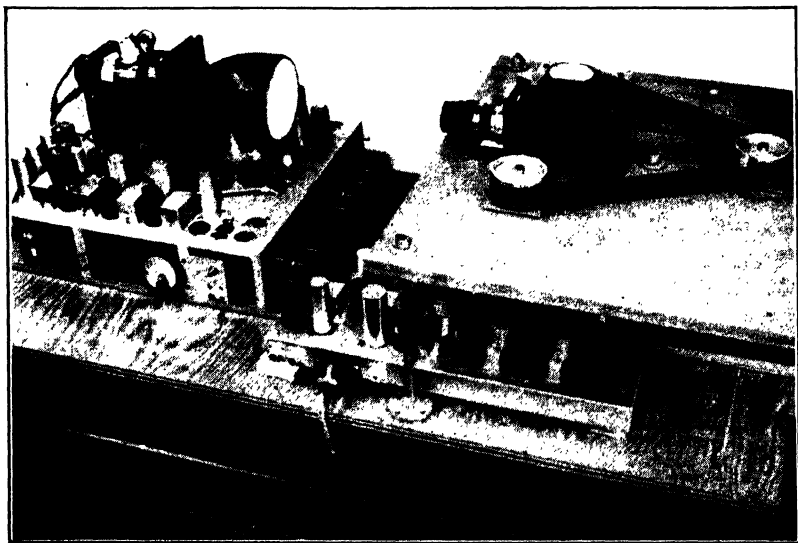


FIG. 16.35. An Ultrafax Scanner for Testing Purposes.

holder of a photomicrographic camera; the multiplier phototube, in the position of the condenser (Fig. 16.36). The advantage of such a micro-

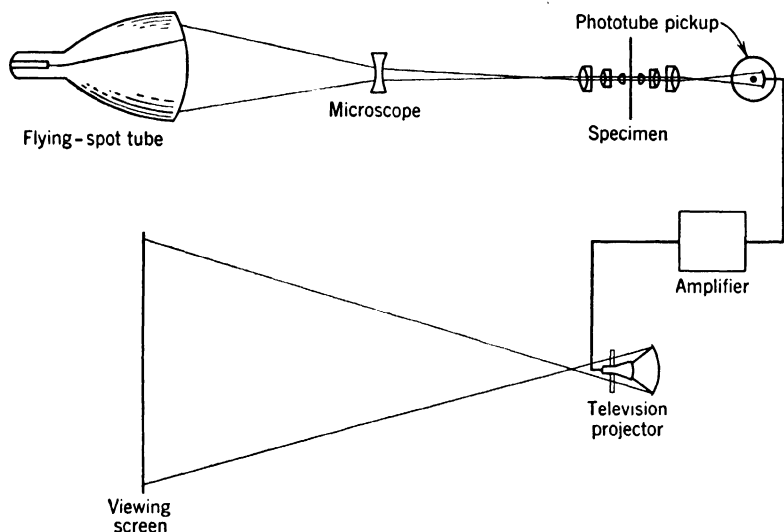


FIG. 16.36. Flying-Spot Microscope. (R. C. Webb.)

scope, which possesses the same ultimate limits of resolution as an ordinary light microscope, is that it permits large groups to view the image, eventually even projected on a large theatre screen, at high light levels.

## REFERENCES

1. "Electronics on Broadway," *Electronics*, Vol. 10, p. 21, September, 1937.
2. H. PENDER and K. McILWAIN, *Electrical Engineers Handbook: Electrical Communications and Electronics*, 4th Edition, John Wiley and Sons, New York. In press.
3. Electrical Engineering Staff of M.I.T., *Applied Electronics*, John Wiley and Sons, New York, 1943.
4. "Transmission of color pictures by facsimile," *Electronics*, Vol. 18, pp. 236-244, April, 1945.
5. L. R. PHILPOTT and W. G. H. FINCH, "Color facsimile," *Electronics*, Vol. 20, pp. 104-105, October, 1947.
6. V. K. ZWORYKIN and G. A. MORTON, *Television—the Electronics of Image Transmission*, John Wiley and Sons, New York, 1940.
7. C. F. JENKINS, *Vision by Radio, Radio Photographs, Radio Photograms*, Nation Capital Press, Washington, 1925.
8. V. K. ZWORYKIN, "Television System," U. S. Patent 2,141,059, filed December 29, 1923.
9. V. K. ZWORYKIN, "Description of an experimental television system and the kinescope," *Proc. Inst. Radio Engrs.*, Vol. 21, pp. 1655-1673, 1933.

10. D. W. EPSTEIN and L. PENSAC, "Improved cathode ray tubes with metal-backed luminescent screens," *RCA Rev.*, Vol. 7, pp. 5-10, 1946.
11. D. W. EPSTEIN and I. G. MALOFF, "Projection television," *J. Soc. Motion Picture Engrs.*, Vol. 44, pp. 443-455, 1945.
12. "An experimental simultaneous color television system," *Proc. Inst. Radio Engrs.*, Vol. 35, pp. 861-875, 1947: R. D. KELL, "I. Introduction," G. C. SZIKLAI, R. C. BALLARD, and A. C. SCHROEDER, "II. Pickup equipment," K. R. WENDT, G. L. FREDENDALL, and A. C. SCHROEDER, "III. Radio-frequency and reproducing equipment."

## Chapter 17

# PHOTOSENSITIVE CAMERA TUBES IN TELEVISION

Although the phototube had an important part in the early stages of television and continues to be a valuable tool in specialized applications, it has largely been displaced by camera tubes which combine the process of scanning and signal generation in one envelope. As compared with the one phototube pickup system, which is free of the drawbacks of mechanical scanning—the flying-spot system—the camera tube systems have these advantages: (1) They operate under normal illumination conditions; (2) picture detail is not dependent on the distance of the corresponding objects from the pickup; and (3) the utilization of the storage principle, introduced with the iconoscope, makes possible enormously enhanced sensitivity. It is to be noted that the first two factors play no role in film transmissions, where, in fact, the flying-spot system has retained its greatest utility.

**The Image Dissector.** The Farnsworth image dissector <sup>1</sup> (Fig. 17.1) represents the most direct translation of the Nipkow disk pickup into a system employing electronic scanning. In essence, it consists of an image tube <sup>2</sup> with the fluorescent screen replaced by a fine aperture equal in size to a single picture element. Any electrons which pass through the aperture are multiplied by a secondary-emission multiplier which acts as a low-noise preamplifier for the signal current.

In more detail, a lens projects an image of the scene to be transmitted on a photocathode. The photoelectrons which leave the illuminated portions of the cathode are accelerated by the electric field between the cathode and the anode wall coating and focused by a uniform magnetic field into the plane of the aperture in front of the multiplier. Two pairs of deflection coils produce transverse magnetic deflecting fields which sweep the electron image horizontally across the aperture at line fre-

<sup>1</sup> See Farnsworth, reference 1.

<sup>2</sup> See Chapter 9.

quency and vertically at field frequency. In this manner the aperture selects the photoemission for successive picture elements of the scene to be transmitted, just as the apertures in a Nipkow disk select the light of successive picture elements, and permit it to generate photocurrent in a phototube.

It is evident therefore that the sensitivity of the image dissector is the same as that of a scanning-disk system using a multiplier phototube as signal generator. The great advantage of the image dissector over the mechanical system is the practically inertia-free deflection of the elec-

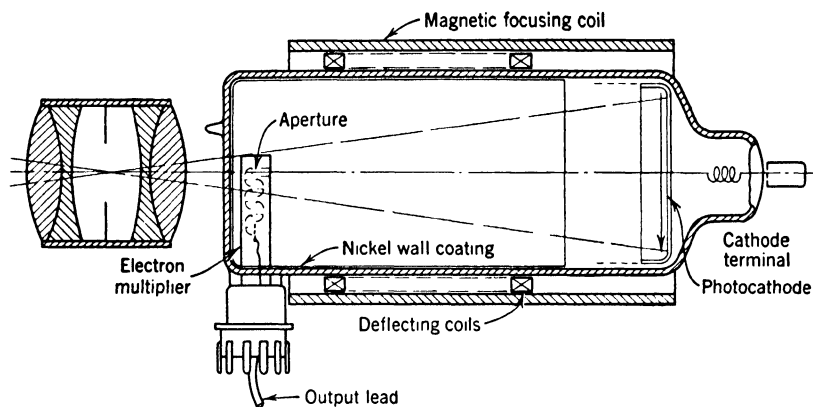


FIG. 17.1. The Image Dissector (Schematic Diagram).

trons by magnetic fields, which permits not only a deflection rate of the order of 16,000 lines per second—demanded by present-day television standards—but even considerably greater speeds whenever they may be required. Although the image dissector is capable of transmitting pictures of excellent quality when sufficient illumination is available, its relatively low sensitivity—compared with the other camera tubes to be described—severely limits its range of application.

**The Iconoscope.** The iconoscope (Fig. 17.2), which is somewhat earlier in conception than the image dissector,<sup>3</sup> represents a more radical departure from previous television pickup technique. Again, a lens projects an image of the scene to be transmitted on a photosensitive surface. However, this surface is not a continuous conducting photocathode, but a *mosaic* of photosensitive elements deposited on a sheet of mica. The individual photosensitive elements, commonly silver globules sensitized with cesium, are small compared with a picture element. It is permissible, therefore, to regard the mosaic surface of the mica

<sup>3</sup> See Zworykin, reference 2.

sheet simply as a continuous photosensitive insulating surface. The other side of the sheet is painted with a conducting coating of platinum, which constitutes the *signal plate* of the iconoscope.

Under the influence of illumination, photoelectrons leave the mosaic, with the result that the more brightly illuminated portions are charged more positively than the remainder of the mosaic. Periodically a sharply focused 1000-volt electron beam, describing a standard scanning pattern

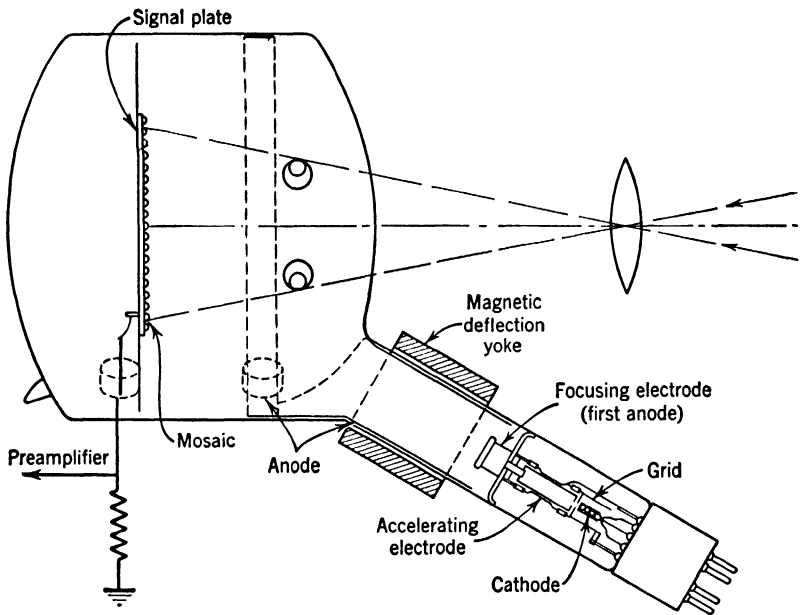


FIG. 17.2. The Iconoscope (Schematic Diagram).

on the mosaic, sweeps across each picture element in turn and returns its potential to an equilibrium value. The resulting dissipation of the charge stored by photoemission in the picture element of the mosaic since the preceding scan causes a corresponding charge of opposite sign to be released from the signal plate. This released charge, passing through the amplifier input resistor  $R$ , generates the picture signal voltage. If each picture element of the mosaic is regarded as a small separate photocell backed by its capacitance with respect to the signal plate, the beam acts as a commutator which grounds the several photocathodes in regular succession (Fig. 17.3).

It is readily seen that the signal currents obtained with a storage system, such as the iconoscope, must be very large compared to those derived from a nonstorage pickup, like the image dissector or Nipkow



disk. For the storage system the charge released from a picture element is equal to its photoemission during an entire picture period; for the nonstorage pickup, equal to that during the actual time of scanning. The ratio of these two times is equal to the total number of picture elements—367,500 for a 525-line picture. This large factor represents the ratio in the signal currents generated by an ideal storage system and an ideal nonstorage system, and, hence, their relative sensitivity.<sup>4</sup>

The actual gain in sensitivity realized with the iconoscope was found to be only about a thousand times. The rather large discrepancy be-

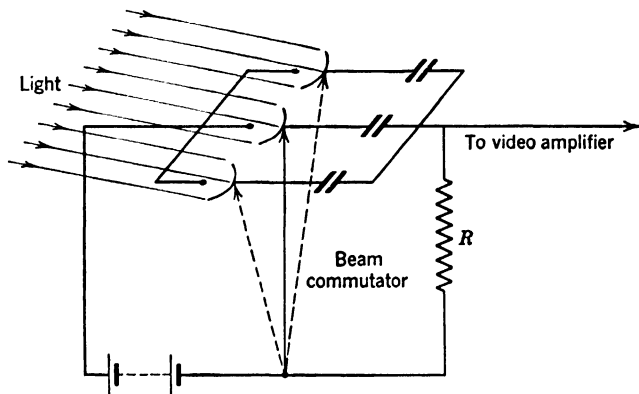


FIG. 17.3. Elementary Concept of the Operation of the Iconoscope.

tween this and the gain for an ideal storage system can be ascribed to two causes. The first is that the level of the output signal of the iconoscope is sufficiently low that random voltage fluctuations introduced by the input resistance and first thermionic amplifier tube limit the effective sensitivity.<sup>5</sup> The second is that the field conditions in front of the mosaic are unfavorable for the collection of electrons ejected from it by the incident light and the electron beam.

A detailed examination of the operation of the iconoscope<sup>6</sup> indicates that the potential of an illuminated and unilluminated picture element of the mosaic varies with time, as shown in Fig. 17.4. Since the secondary-emission ratio of the mosaic surface for 1000-volt electrons is greater than 1—it is commonly of the order of 5—the scanning beam charges the surface positive up to a potential at which all but one secondary electron

<sup>4</sup> Relative sensitivity may be defined as the reciprocal of the ratio of the least object brightness for which a satisfactory image (with prescribed signal-to-noise ratio) can be obtained.

<sup>5</sup> See Chapter 13, p. 258.

<sup>6</sup> See Zworykin, Morton, and Flory, reference 3.

per incident primary electron is returned, by the retarding field in front of the scanned element, to this element. This takes place when the element is approximately 3 volts positive with respect to the anode surfaces, which function as collector. It should be noted, however, that not all the secondary electrons which succeed in leaving the element reach the anode. Approximately three-fourths of them return to other portions of the mosaic, particularly to the region which has just been scanned and is hence more positive than the rest. These redistributed electrons reduce the strength of the picture signal. After scanning, the

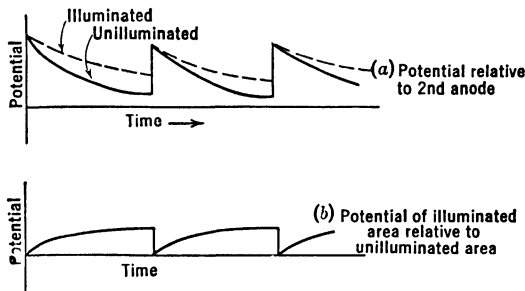


FIG. 17.4. Time Variation of the Potential of an Illuminated and an Unilluminated Picture Element on the Mosaic of the Iconoscope. (From Zworykin and Morton, *Television*, John Wiley, New York, 1940.)

potential of an unilluminated element decreases, as the result of redistribution, eventually reaching an equilibrium potential which lies between 0 and  $-1\frac{1}{2}$  volts, measured relative to the anode. If the element is illuminated, the decrease in potential is reduced, the receipt of redistributed electrons being partially compensated by the emission of photoelectrons. Here also a large fraction of the photoelectrons is returned to the emitting element, reducing the storage efficiency to about a fifth, and other photoelectrons are redistributed to the remainder of the mosaic. The unfavorable field conditions in front of the mosaic thus reduce the picture signal to about a twentieth of that obtained with an ideal system. In addition, redistribution gives rise to spurious shading effects in the image which must be compensated by the addition of special "shading signals" to the picture signal.

In spite of these defects the iconoscope (Fig. 17.5) has been found to be an extremely effective camera tube, particularly for studio and motion-picture film transmissions, yielding high-quality reproduced images. Its potential resolving power is well in excess of what can be utilized by the allocated transmission channels.

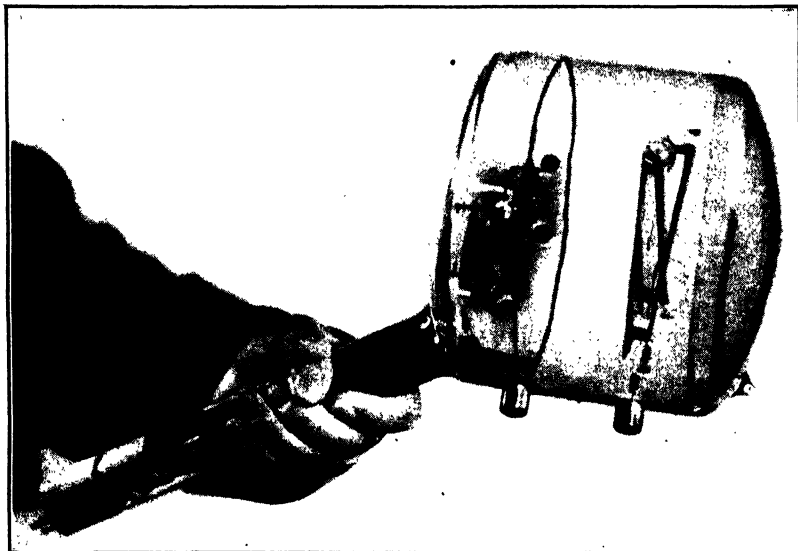


FIG. 17.5. The Iconoscope.

**The Image Iconoscope.** One successful method of obtaining a stronger picture signal and, hence, greater sensitivity consists in placing an image tube section<sup>7</sup> ahead of the mosaic. This was realized in the image

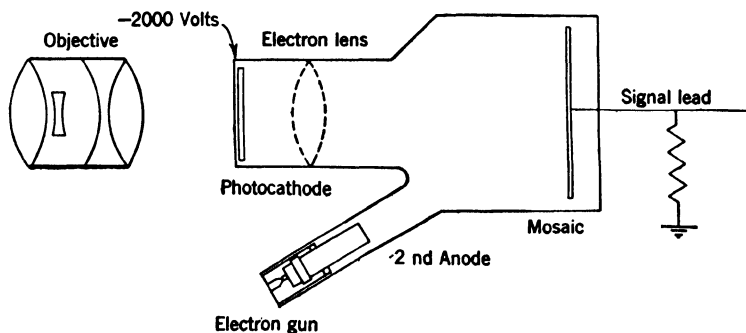


FIG. 17.6. The Image Iconoscope (Schematic Diagram). (Iams, Morton, and Zworykin, reference 4.) (Courtesy of *Proc. Inst. Radio Engrs.*)

iconoscope<sup>8</sup> and its counterpart, the Superemitron, developed in England.<sup>9</sup> In the image iconoscope (Fig. 17.6) the image of the scene is

<sup>7</sup> See Chapter 9.

<sup>8</sup> See Iams, Morton, and Zworykin, reference 4.

<sup>9</sup> See reference 5.

projected on a transparent photocathode instead of on the mosaic. The photoelectrons emitted by the photocathode are accelerated and focused by an electric or magnetic lens on the mosaic, charging the mosaic positive by the emission of secondary electrons. The gain in sensitivity resulting from the higher photoelectric response of the continuous photocathode, as compared with that of the mosaic, and the gain resulting from the high secondary-emission ratio of the mosaic, add up to a total gain in sensitivity by a factor of 6 to 10. The external appearance of an electrostatic image iconoscope is shown in Fig. 17.7.

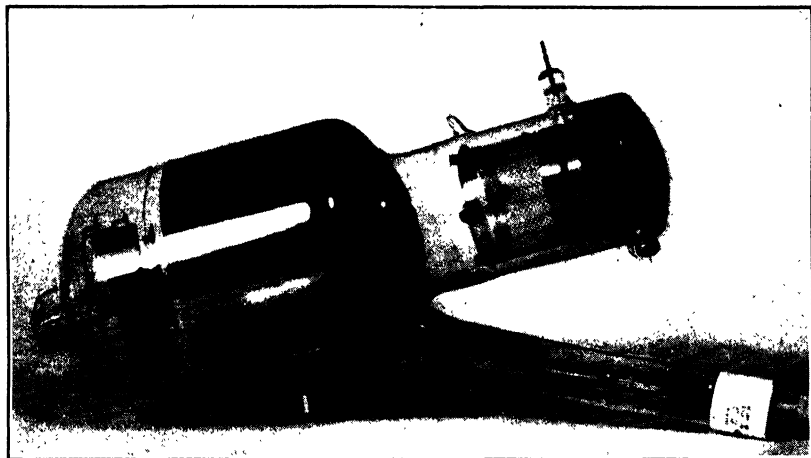


Fig. 17.7. An Electrostatic Image Iconoscope.

**The Orthicon.** A more radical attack on the weak points of the iconoscope led to the orthicon—short for “orth-iconoscope” or “true iconoscope.”<sup>10</sup> The theory of the orthicon rests on the realization that if an electron is incident on the mosaic with sufficiently low kinetic energy—for instance, less than 10 electron volts—it will give rise, on the average, to less than one secondary electron. Thus, under low-velocity bombardment, the mosaic surface will become increasingly negative until it is slightly below the potential of the electron source, so that no additional electrons can reach it. This is the equilibrium condition in which an element of the mosaic is left after scanning by a low-velocity beam. If, in the period elapsing up to the next scan, no light reaches the element in question, the potential of the element remains unchanged. Consequently the scanning beam, on its next traversal, merely grazes the element, but deposits no charge on it, so that the corresponding signal cur-

<sup>10</sup> See Rose and Iams, reference 6.

rent is zero. On the other hand, an element exposed to light will emit photoelectrons, all of which are collected by the positive anode. Thus a positive charge will be stored up, during the period between scans, on the element of the mosaic. This charge, which is released by the deposition of electrons during the next scan, is exactly proportional to the intensity of illumination. Figure 17.8 shows, schematically, the voltage variation of an unilluminated and an illuminated element in a low-velocity iconoscope or orthicon.

The orthicon thus yields a signal which is entirely free of spurious shading and exactly proportional to the intensity distribution in the

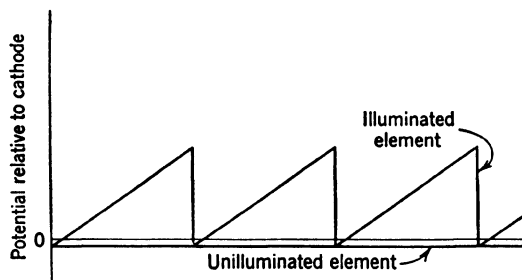


FIG. 17.8. Time Variation of the Potential of an Illuminated and an Unilluminated Picture Element on the Target of an Orthicon.

scene. On the other hand, its range of operation has an upper limit, which is reached when the mosaic is charged sufficiently positive between successive scans so that the scanning beam no longer can fully discharge it. Under these circumstances the potential of the strongly illuminated portion of the mosaic rises approximately to anode potential, and the picture signal may be actually reversed, corresponding to "blacker than black." This happens when an orthicon camera is pointed directly at the sun or at an exploding flashbulb. After removal of the brilliant light source from the field, leakage gradually reestablishes normal operating conditions.

Although the theory of operation of the orthicon is relatively simple, the problem of designing a tube with a low-velocity scanning beam providing a spot of the required resolution is decidedly complex. Figure 17.9 shows, schematically, the method of focusing and beam deflection in an early orthicon. The tube is immersed in a longitudinal magnetic focusing field with a magnetic flux density of the order of 0.01 weber per square meter (100 gauss). A superposed electric field deflects the beam of 100-volt electrons issuing from the narrow anode aperture in a horizontal direction (line scanning),<sup>11</sup> and a succeeding

<sup>11</sup> See Chapter 6, p. 107.

transverse magnetic field deflects it vertically. In this manner the beam, which is retarded approximately to cathode potential as it approaches the mosaic, strikes the mosaic perpendicularly for all deflections. A transparent signal plate permits the image to be projected from the right. Orthicons constructed in this manner have been found

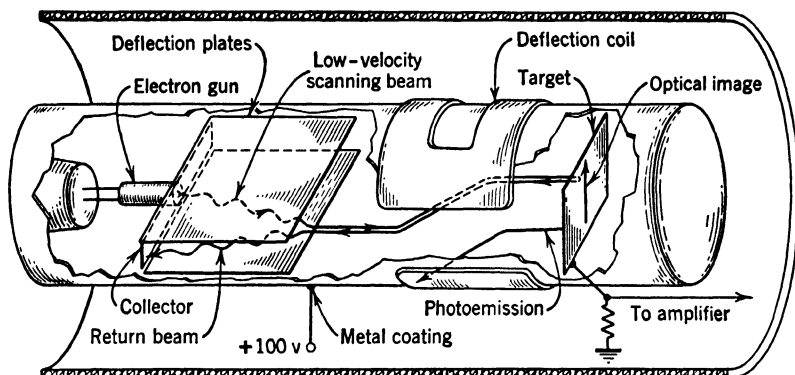


FIG. 17.9. Schematic Diagram of an Orthicon with Electrostatic Horizontal Deflection. (Rose and Iams, reference 6.)

to have the expected gain in sensitivity over the iconoscope and to be free of shading.

**The Image Orthicon.** The conversion of the orthicon into an ideal storage camera tube demanded the fulfilment of two conditions. On the one hand, the level of the output signal had to be raised by two or three orders of magnitude, so that it might override amplifier noise; on the other, it had to be rendered stable at all light levels. An intensive research program, undertaken to attain these objectives, resulted in the image orthicon,<sup>12</sup> shown schematically in Fig. 17.10. The focusing coil envelops both the image section and the scanning section; the deflecting yoke, the scanning section alone. Magnetic fields are used for both vertical and horizontal deflection. Since the electrons tend to spiral about the magnetic-field lines, the return beam, consisting of electrons which have grazed the target or mosaic without being collected by it as well as of reflected and secondary electrons, follows very nearly the same path as the scanning beam. The increase in signal strength is brought about by the introduction of an electron multiplier for amplifying the signal current by secondary emission as well as by the provision of an image tube stage ahead of the target. Stability at high light levels is obtained by use of a collecting screen, at a potential very slightly higher

<sup>12</sup> See Rose, Weimer, and Law, reference 7.

than the equilibrium potential of the target, for collecting the secondary electrons emitted by the target.

In more detail, a lens projects an image of the scene on a transparent photocathode, maintained about 300 volts negative with respect to the target screen. The photoelectrons emitted as a result are accelerated toward the target screen and at the same time focused into a sharp electron image at the target. The target screen, having 50 per cent transparency and 500 to 1000 meshes per inch, permits half the electrons to pass through and does not greatly interfere with the sharpness of the

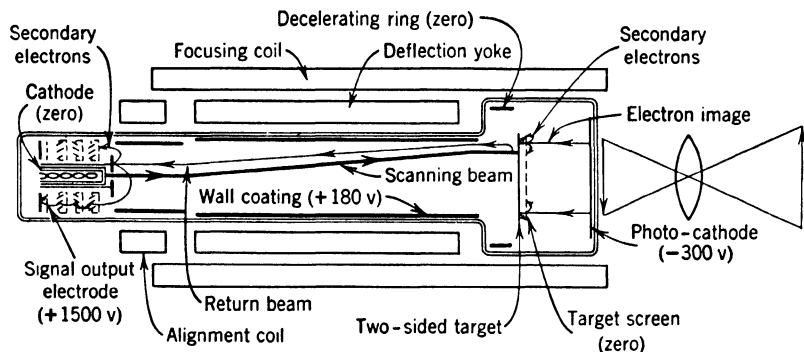


FIG. 17.10. Schematic Diagram of an Image Orthicon. (Rose, Weimer, and Law, reference 7.)

image formed on the target. As the electrons fall on the target, just beyond the target screen, they emit secondary electrons in excess of the number of incident primary photoelectrons. Thus a positive-charge image is built up on the target; the secondary electrons are collected by the target screen.

The target itself consists of a thin film of glass—sufficiently thin so that differences in potential between the two sides are substantially nullified by conduction in the course of a frame time, although the leakage of charge between adjoining picture elements is negligible.

The other side of the target is scanned by a low-velocity beam, similar to the scanning beam in the orthicon. If the potential of a certain picture element of the target has been raised by secondary emission from the other side, the scanning beam deposits just enough electrons to bring it back down to equilibrium potential, which may be a volt or so negative with respect to the cathode of the electron gun. The remainder of the beam—that is, the constant-current beam from which the electrons constituting the picture signal have been subtracted—returns, following, approximately, the same magnetic field lines as the incident

beam, to a dynode disk, which has the beam-defining aperture at its center. Only a very small fraction of the returning electrons actually falls on the aperture; the remainder, striking the dynode disk with a kinetic energy of 100 to 200 electron volts, eject secondary electrons therefrom. The electrostatic field conditions surrounding the dynode disk are such that these secondary electrons are drawn into a pinwheel multiplier of the type shown in Fig. 16.24, page 373. The output current of the multiplier, which surrounds the gun structure, is applied

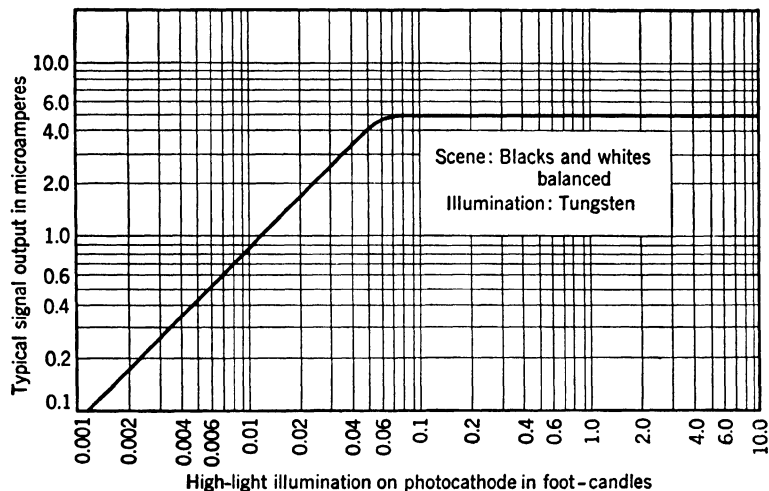


FIG. 17.11. Variation of Signal Output with Illumination of Photocathode of Image Orthicon 2P23. (*RCA Tube Handbook*.)

to a suitable thermionic amplifier. This current consists of a constant current, the multiplied scanning-beam current, and a variable component, which constitutes the picture signal. The total gain of the five-stage electron multiplier, which is operated at 1500 volts, is 300 to 1000.

The performance of the image orthicon is in accord with expectations. At low light levels its sensitivity is several hundred times that of an iconoscope—effectively that to be expected from an ideal storage system. Here the picture signal is strictly a linear function of the brightness of the picture element. For high light levels this is no longer the case. Since the average potential which the target can assume is limited by the potential of the target screen, the response flattens out as shown in Fig. 17.11. However, even in the region of flat response good pictures may be transmitted with the image orthicon. Target elements corresponding to more brightly illuminated portions of the image emit a larger number of secondary electrons, of which the major portion is



redistributed over the remainder of the target, reducing its potential. These elements, therefore, become more positive than the rest. Even though the average potential of the mosaic is not increased by increas-

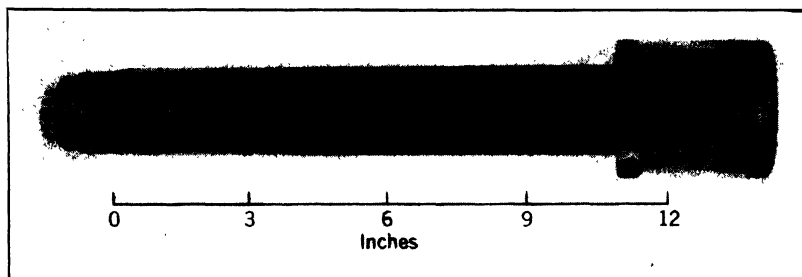


FIG. 17.12. The Image Orthicon.

ing the illumination, brightness differences in the image are reflected in variations in the charge stored on the target surface. Thus contrasts are properly reproduced in the transmitted picture.

The external appearance of an image orthicon is shown in Fig. 17.12. The gun structure with the pinwheel multiplier is visible at the left, the

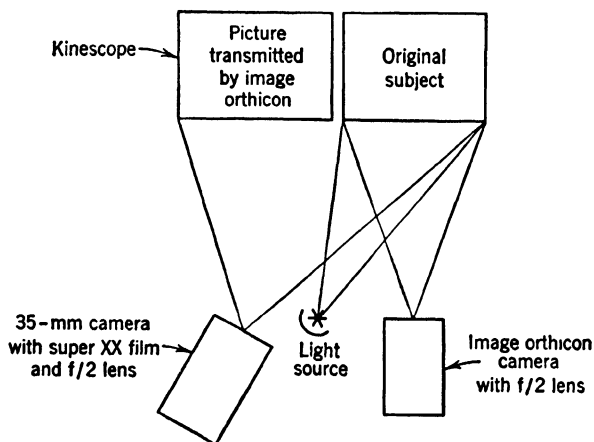


FIG. 17.13a. Sensitivity Comparison of Image Orthicon and 35-mm Super XX Film. Disposition of Apparatus. (Rose, Weimer, and Law, reference 7.) (Courtesy of *Proc. Inst. Radio Engrs.*)

photocathode at the extreme right. In this tube the effective area of the photocathode is 1.6 inches in diameter. Smaller, more compact, image orthicons have been constructed for special purposes.<sup>13</sup>

<sup>13</sup> See, for example, Weimer, Law, and Forgue, reference 8.

The sensitivity of the image orthicon approaches that of the human eye and is considerably greater than that of high-sensitivity motion-picture film. This is brought out strikingly by Fig. 17.13. A motion-

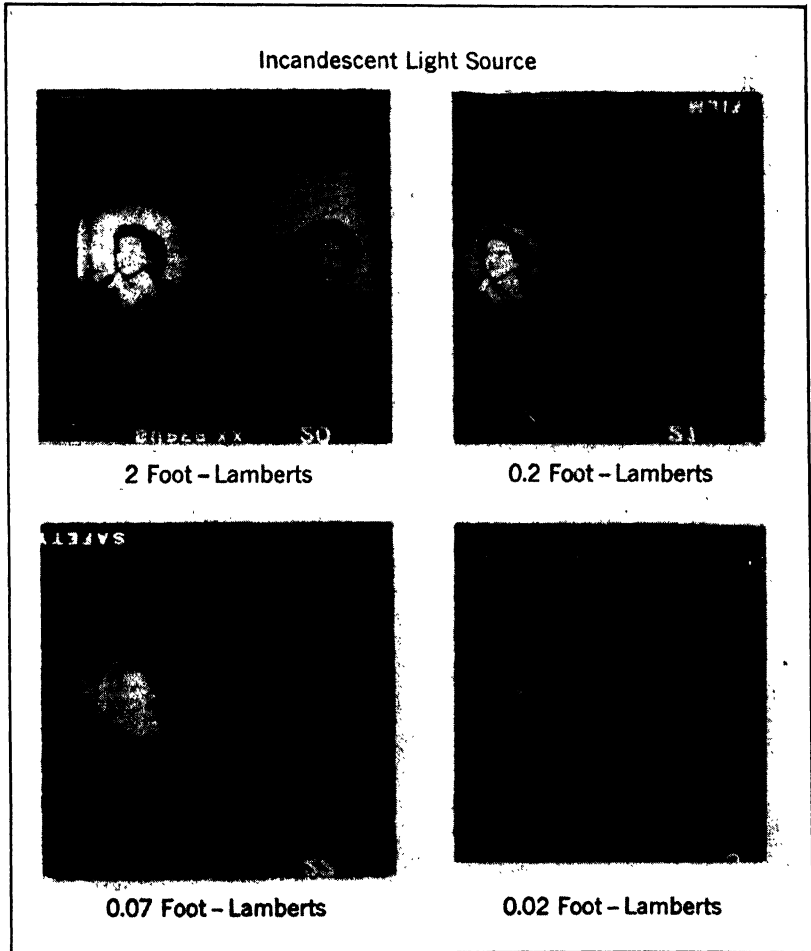


FIG. 17.13b. Sensitivity Comparison of Image Orthicon and 35-mm Super XX Film. Photographs of Receiver Screen and Subject. (Rose, Weimer, and Law, reference 7.) (Courtesy of *Proc. Inst. Radio Engrs.*)

picture camera with an  $f/2$  lens, using 35-millimeter Super XX film, was trained on a subject and an adjoining television receiver. This receiver was connected by cable with an image orthicon camera, also using an  $f/2$  lens, which was aimed at the same subject. The illumination of the

subject was provided by a 40-watt incandescent bulb, whose output could be attenuated by neutral filters. Figure 17.13*b* shows the result of decreasing, in steps, the subject brightness from 20 lumens per square meter to 0.2 lumen per square meter. It is seen that the motion-picture camera fails to record a picture of the subject after the first reduction of the illumination, whereas the television system continues to provide a recognizable image even at a surface brightness of 0.2 lumen per square meter, the approximate brightness of a white surface in full moonlight.

**Television Pickup Cameras.** The essential elements of a television camera are the camera tube and the lens which projects the image on the mosaic or photocathode of the camera tube. Other, auxiliary, equip-

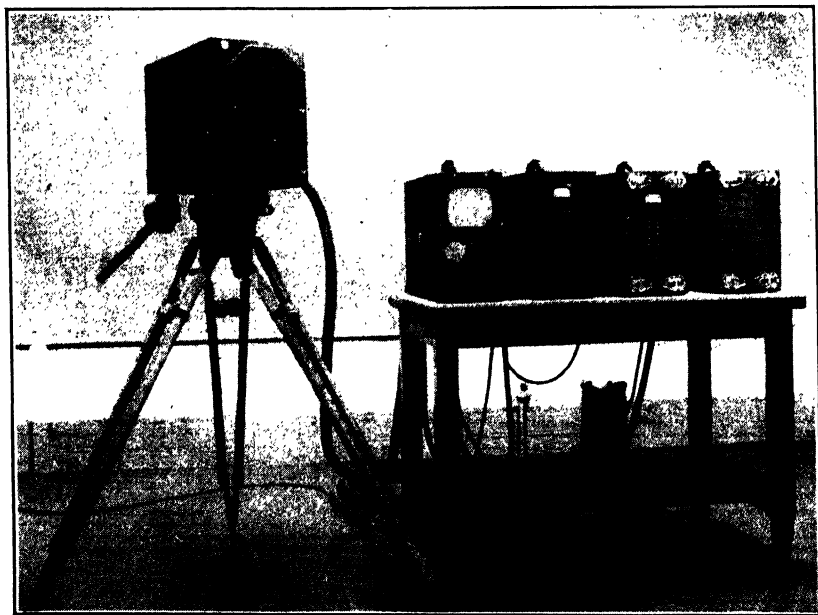


FIG. 17.14. Image Orthicon Camera for Spot Pickup and Auxiliary Equipment. (Courtesy National Broadcasting Company.)

ment which is necessary for the smooth and efficient operation of the camera includes the finder—commonly in the form of a monitoring kinescope—focusing adjustments, interchangeable lenses for shifting from long shots to close-ups, signal and blanking amplifiers, and means for rotating and displacing the camera. The latter equipment will differ considerably for spot pickup and studio pickup. A typical image

orthicon camera for spot pickup, together with auxiliary equipment, is shown in Fig. 17.14.

The arrangement is, of course, quite different for the television transmission of motion-picture film. With nonstorage systems, such as the image dissector, the film is moved continuously, and the scanning is carried out in a horizontal direction only, just as in the flying-spot method. Since the standard television field frequency (twice the picture frequency with interlaced scanning) is 60 per second, whereas the

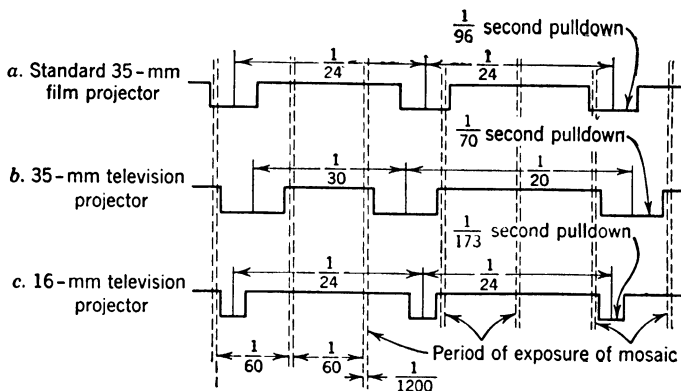


FIG. 17.15. Time Division for (a) Standard Film Projector, (b) 35-mm Television Film Projector, and (c) 16-mm Television Film Projector. (Little, reference 9.)  
(Courtesy of *J. Motion Picture Engrs.*)

normal motion-picture frame frequency is only 24 per second, only specially prepared film can be used in this system. With storage tubes, such as the iconoscope, this difficulty may be avoided. The picture from a modified intermittent projector is simply flashed on the mosaic or photocathode of the camera tube during the vertical return time of the scanning beam, which comprises approximately 8 per cent of a vertical scanning period. During this time (just as during the horizontal return time) the scanning beam is biased off and the signal amplifier blanked. The time relation between the film progress and the exposures of the pickup tube is indicated in Fig. 17.15.<sup>14</sup> Successive frames are projected alternately twice and three times. The time division is somewhat different with 35-millimeter and 16-millimeter film, since the latter can tolerate the higher accelerations corresponding to a shorter pulldown time. With 35-millimeter film alternate frame times in the special television projector are  $\frac{1}{20}$  and  $\frac{1}{30}$  second, so that the pulldown time, lasting approximately  $\frac{1}{70}$  second, does not interfere with the projection

<sup>14</sup> See Little, reference 9.

of the picture during the vertical return time of the scanning beam. With 16-millimeter film the same thing is accomplished by reducing the pulldown time to  $\frac{1}{173}$  second (from  $\frac{1}{96}$  second in standard projectors) without changing the frame time ( $\frac{1}{24}$  second).

There are two methods by which the intervals may be selected during which the film image is projected on the pickup tube mosaic or photocathode. In the first method an ordinary projection lamp is used, and a shutter disk, rotating at 3600 revolutions per minute, is inserted between the condenser lens and the film window. The shutter opening is so dimensioned that it transmits light for approximately 5 per cent of a period of revolution. This is the arrangement in the RCA 16-millimeter television film projector, illumination being provided by a 1000-watt airblast-cooled projection lamp. The other method of timing the projection of the film pictures has a pulsed discharge lamp as light source, obviating the large, high-speed shutter disk. The source in the RCA 35-millimeter television projector is a General Electric Synrolite high-pressure mercury arc, pulsed to produce light flashes with the approximate duration of a millisecond.

**The Complete Electronic Television System.** In addition to the camera tube at the transmitter and the viewing tube at the receiver the operation of a modern television system requires extensive auxiliary equipment, as indicated in the block diagrams of the transmitter and the receiver shown in Fig. 17.16 and Fig. 17.17. Two separate channels are provided for the picture (or video) signal and the accompanying sound. The sound channel differs only in the high frequency of the radio carrier from an ordinary broadcast channel and requires no further discussion.<sup>15</sup>

With regard to the picture channel, it has already been seen that the horizontal and vertical deflection of the scanning beam in the camera tube is accomplished by sawtooth currents flowing through the coils of the deflection yoke. The timing of these deflection currents is controlled by pulses from a synchronizing generator which is normally tied in with the 60-cycle alternations of the local power system. The same synchronizing generator controls the blanking pulses which are applied to the grid of the electron gun so as to cut off the electron beam during the horizontal and vertical return time of the electron beam.

The picture signal from the camera tube is first amplified by the pre-amplifier within the camera to a level sufficiently high that it can be transmitted by cable to the fixed video voltage amplifier. Here, if the

<sup>15</sup> While sound is normally transmitted on its own frequency-modulated carrier, it may also be transmitted during the line-blanking intervals of the picture signal. See Fredendall, Schlesinger, and Schroeder, reference 10.

camera tube is an iconoscope, shading signals, derived from the deflection circuits, are added so as to compensate the spurious effects arising from redistribution on the mosaic. The effect of the addition may be observed by the monitoring engineer on a monitor kinescope. In a succeeding amplifier synchronizing pulses are added to the signal, in the

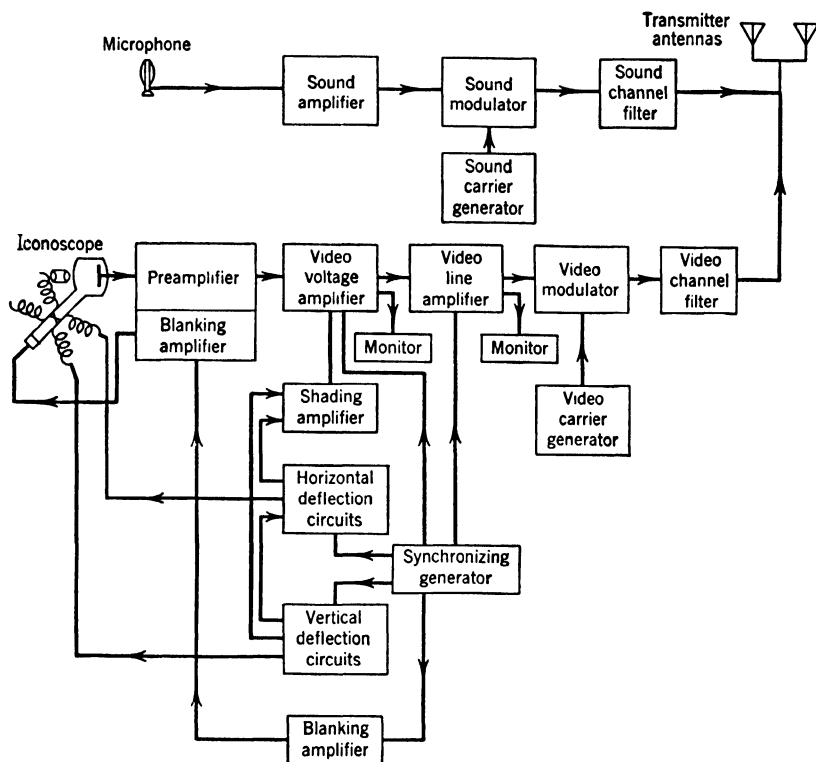


FIG. 17.16. Block Diagram of Television Transmitter.

intervals corresponding to the return times of the scanning beam, by the synchronizing generator. These pulses, selected out by appropriate circuits, serve to lock the deflection currents of the receiver in step with those in the transmitter. The amplified video signal modulates the video carrier wave, generated by a crystal-controlled oscillator and a series of frequency multiplying circuits. The carrier frequency lies, depending on the frequency allocation of the broadcasting station, anywhere between forty and several hundred megacycles per second. The modulated carrier extends over a frequency band of some 8.5 megacycles, whose limits are determined by the sum and difference of the carrier

frequency and the maximum modulating video frequency (4.25 megacycles per second). A video channel filter removes the major portion of one of the two side bands, so that the allocated 6-megacycle channel can accommodate both the modulated video carrier and the accompanying 10-kilocycle sound channel. The two carriers are radiated by separate antennas.

At the receiver the signals first pass through a selective stage of radio-frequency amplification, which prevents radiation of the local oscillator

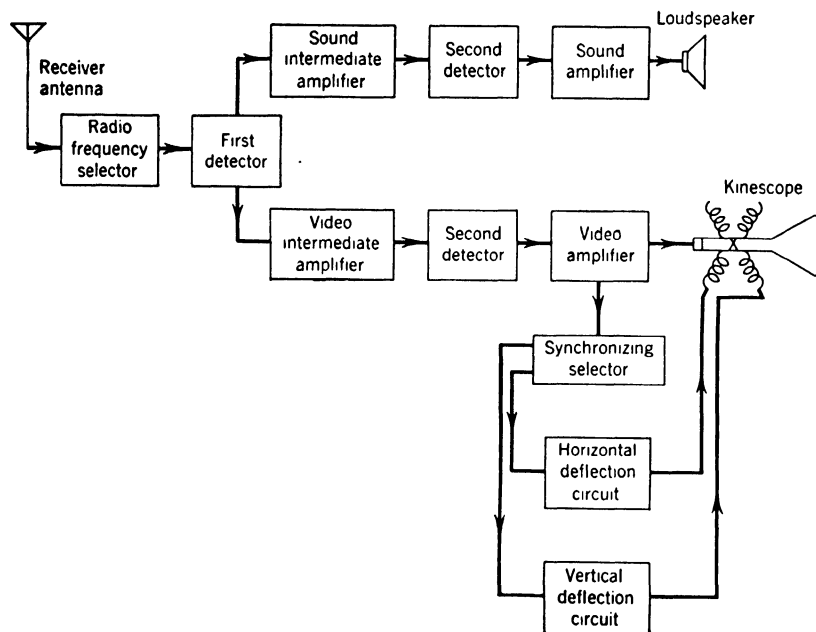


FIG. 17.17. Block Diagram of Television Receiver.

frequencies from the receiver antenna. Beyond this point the sound and the video signals are amplified and detected in separate superheterodyne circuits. The video signal is ultimately applied to the grid of the viewing tube, whose deflection is controlled by synchronizing pulses selected out from the signal.

It should perhaps be noted that most actual television systems will differ from the one described in a number of details. For these the reader is referred to the extensive technical literature dealing with television.<sup>16</sup>

<sup>16</sup> See, for example, Zworykin and Morton, reference 11; Fink, reference 12; and more recent papers in the *Proceedings of the Institute of Radio Engineers*.

**Special Applications of Television Equipment.** Broadcast television is only one of the useful applications of television equipment, though a very important one. This was fully realized during the war, when its development for use in guided missiles<sup>17</sup> and as a medium of observation was furthered. Compact pickup cameras with extraordinarily great sensitivity, as in Fig. 17.18,<sup>18</sup> played a special role in this connection. An even broader field appears reserved for it in the peacetime needs of

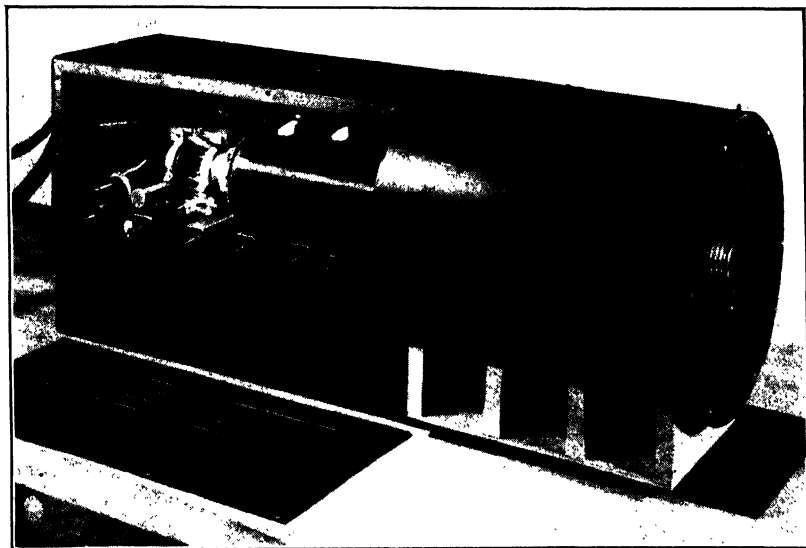


FIG. 17.18. Image Orthicon Camera Employing Reflective Projection Optics. (Kell and Sziklai, reference 14.)

industry and commerce. Examples are the surveillance of dangerous and inaccessible industrial processes, the supervision of automatic substations from a central station, and the display of goods and processes to an extended audience. Figure 17.19 illustrates the use of television pickup equipment in the medical field. The television camera, mounted directly over the working area at a rare operation, affords an intimate view, unattainable otherwise, to visiting physicians gathered around receivers in an adjoining room. In many of these applications the value of this equipment can be accentuated if it will provide images in natural color. A particularly sensitive color camera, which may be used in conjunction with the color receivers discussed on page 377, is shown

<sup>17</sup> See Kell and Sziklai, reference 13.

<sup>18</sup> See Kell and Sziklai, reference 14.



schematically in Fig. 17.20. The light from the scene to be transmitted is broken up, by two dichroic plates at a 45-degree angle to the incident

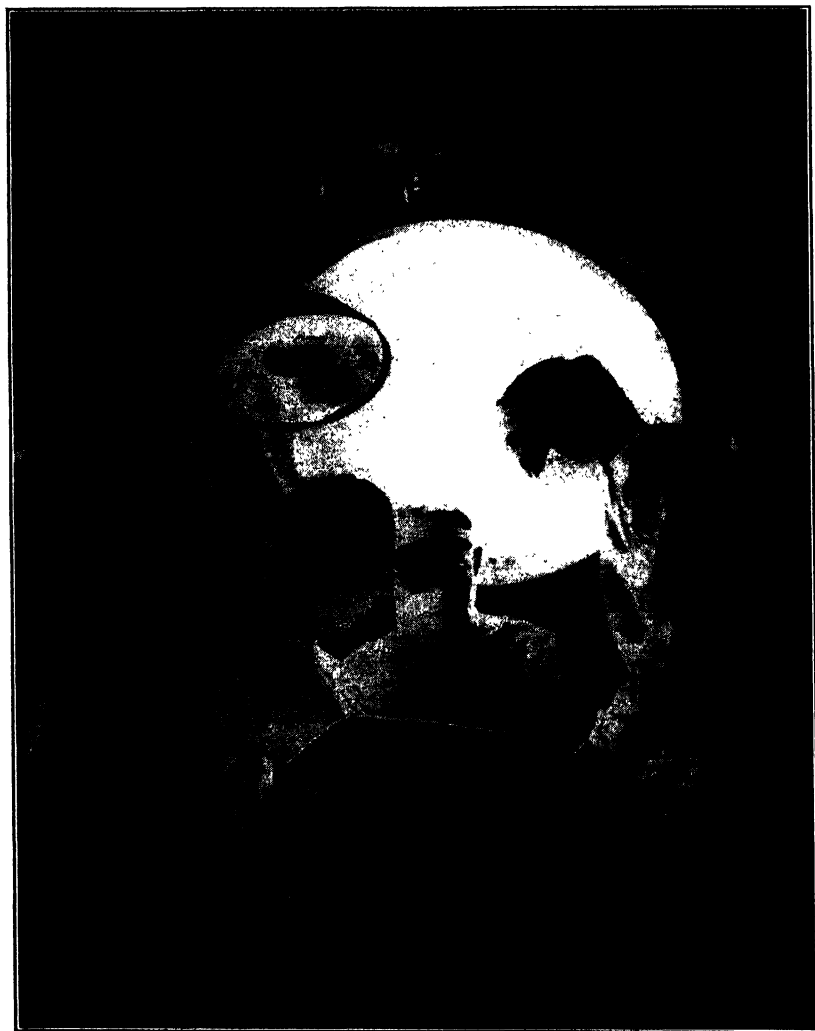


FIG. 17.19. Television Camera in Operating Room at Johns Hopkins University Hospital.

beam, into three beams of different color—red, green, and blue. Each beam is focused by an objective lens into an image on one of the three image orthicon tubes which generate the signals for the three primary color channels.

A much earlier application of television camera tubes, pointing in a different direction, is the utilization of the ultraviolet and infrared sensitivity of the iconoscope for rendering visible ultraviolet or infrared microscope images.<sup>19</sup> Here the image of a specimen illuminated by such invisible radiations, formed by a light microscope, is projected on the mosaic of an iconoscope. The visible image, whose brightness may be

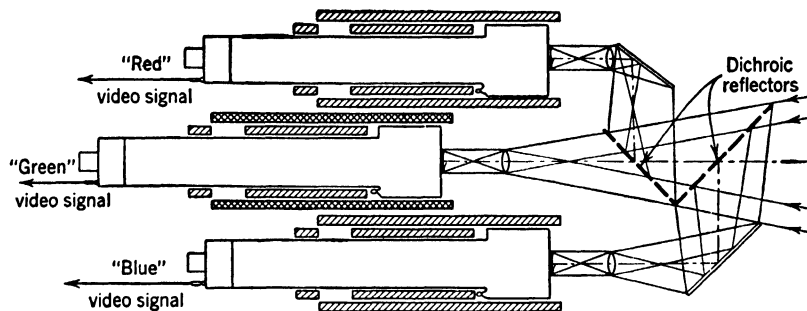


FIG. 17.20. Color Television Camera Employing Three Image Orthicons (Optical Arrangement).

controlled independently of the intensity of illumination, appears on the screen of a kinescope controlled by the picture signal of the iconoscope.

## REFERENCES

1. P. T. FARNSWORTH, "Television by electron image scanning," *J. Franklin Inst.*, Vol. 218, pp. 411-444, 1934.
2. V. K. ZWORYKIN, "The Iconoscope," *Proc. Inst. Radio Engrs.*, Vol. 22, pp. 16-32, 1934.
3. V. K. ZWORYKIN, G. A. MORTON, and L. E. FLORY, "Theory and performance of the iconoscope," *Proc. Inst. Radio Engrs.*, Vol. 25, pp. 1071-1092, 1937.
4. H. IAMS, G. A. MORTON, and V. K. ZWORYKIN, "The image iconoscope," *Proc. Inst. Radio Engrs.*, Vol. 27, pp. 541-547, 1939.
5. "Super-Emitron Camera," *Wireless World*, Vol. 41, pp. 497-498, 1937.
6. A. ROSE and H. IAMS, "The orthicon, a television pickup tube," *RCA Rev.*, Vol. 4, pp. 186-199, 1939.
7. A. ROSE, P. K. WEIMER, and H. B. LAW, "The image orthicon—a sensitive television pickup tube," *Proc. Inst. Radio Engrs.*, Vol. 34, pp. 424-432, 1946.
8. P. K. WEIMER, H. B. LAW, and S. V. FORGUE, "MIMO—miniature image orthicon," *RCA Rev.*, Vol. 7, pp. 358-366, 1946.
9. R. V. LITTLE, JR., "Film projectors for television," *J. Soc. Motion Picture Engrs.*, Vol. 48, pp. 93-110, 1947.
10. G. L. FREDENDALL, K. SCHLESINGER, and A. C. SCHROEDER, "Transmission of television sound on the picture carrier," *Proc. Inst. Radio Engrs.*, Vol. 34, pp. 49-61, 1946.

<sup>19</sup> See Zworykin, reference 15.

11. V. K. ZWORYKIN and G. A. MORTON, *Television—the Electronics of Image Transmission*, John Wiley and Sons, New York, 1940.
12. D. G. FINK, *Principles of Television Engineering*, McGraw-Hill Book Company, New York, 1940.
13. R. D. KELL and G. C. SZIKLAI, "Miniature airborne television equipment," *RCA Rev.*, Vol. 7, pp. 338–357, 1946.
14. R. D. KELL and G. C. SZIKLAI, "Image orthicon camera," *RCA Rev.*, Vol. 7, pp. 67–76, 1946.
15. V. K. ZWORYKIN, "Electric microscope," I° Congresso Internazionale di Electroradiobiologia, Atti I, September, 1934, pp. 672–686.

## Chapter 18

# LIGHT BEAM SIGNALING AND INFRARED DETECTION

Since prehistoric times light has been a means of transmitting information over distances beyond the reach of the human voice; smoke signals, wig-wag signals, blinker signals have played their parts in war and peace. Even in the present day, communication by light beams—more precisely, infrared beams—has certain advantages over radio communication which have made a special place for it. These advantages are freedom from interference by natural or artificial electromagnetic disturbances (“static” and “jamming”), absence of “ghosts” and “fading” arising from the passage of the signals along different paths, and greater difficulty of detection by unauthorized persons. In numerous applications these considerations outweigh drawbacks, such as the obscuring of the signal by smoke, fog, or clouds, which constitute no obstacle to radio beams.

**Infrared Transmission of the Atmosphere.** The absorption of infrared radiation by the water vapor in the atmosphere restricts the usable

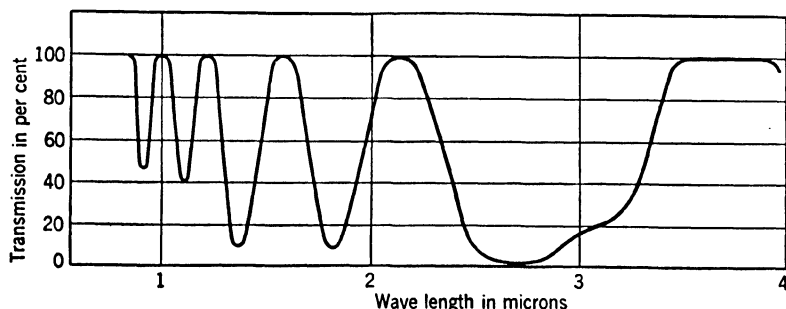


FIG. 18.1. Transmission of the Atmosphere in the Infrared (2.7 cm precipitated water vapor in path). (Cashman, reference 1.)

radiation to certain wave-length ranges. These are indicated in the plot of the spectral transmission of the atmosphere shown in Fig. 18.1, based

on measurements by J. R. Platt.<sup>1</sup> Beyond about 5 microns the absorption is so great that this constitutes an effective upper wave-length limit for infrared signaling. If the detectors are either photoemissive (Ag-Cs<sub>2</sub>O-Cs) or thallous sulfide photoconductive cells, only the region of 0.8 to 1.2 microns is of importance.<sup>2</sup> Utilization of the longer-wave-length transmission bands 1.5 to 1.7 microns, 2.0 to 2.3 microns, and 3.4 to 4.5 microns requires the use of lead sulfide,<sup>3</sup> lead selenide, or lead telluride cells.

**Infrared Light Sources.** The most common source of infrared radiation is the incandescent tungsten filament lamp. Its spectral energy

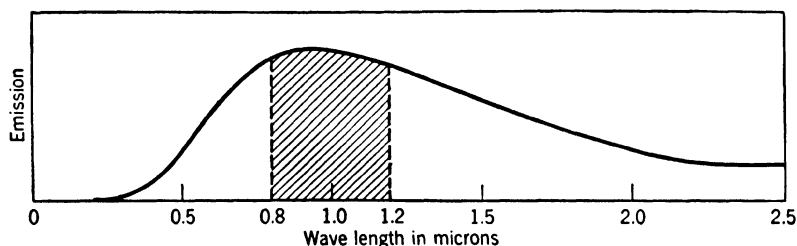


FIG. 18.2. Spectral Distribution of Emission from Tungsten Filament Source with a Color Temperature of 3000° K. (Fluke and Porter, reference 2.) (Courtesy of *Proc. Inst. Radio Engrs.*)

distribution is shown in Fig. 18.2,<sup>4</sup> which indicates that the energy contained in the range of primary interest—0.8 to 1.2 microns—is a relatively small fraction of the total.<sup>5</sup> The ordinary incandescent lamp has the added drawback that the response of its radiant emission to “keying,” that is, the opening and closing of the lamp circuit, is slow, as shown in Fig. 18.3; the “build-up” time is of the order of 0.2 second. As a result, the top speed with which messages in Morse code can be transmitted by keying an ordinary tungsten lamp is about 8 words per minute. Keying the signals with mechanical shutters has not proved satisfactory because of the inadequate ruggedness of low-inertia shutters. An appreciable gain in speed has been attained, however, by the use of lamps with very thin filaments, having low thermal inertia. Such lamps are the S-6 6-watt 220-volt pilot lamps. With them a transmission speed of 12 words per minute, which is the upper limit for most receivers, is readily achieved.

<sup>1</sup> See Cashman, reference 1.

<sup>2</sup> See the curve for S-1, Fig. 6.10, on p. 115, and Fig. 10.11 on p. 187.

<sup>3</sup> See Fig. 10.13 on p. 189.

<sup>4</sup> See Fluke and Porter, reference 2.

<sup>5</sup> For a black body at a temperature of 3000° K this fraction may be calculated to be 26 per cent.

It is obvious that incandescent lamps as infrared sources for secret signaling require filters to absorb the visible radiation. For most ex-

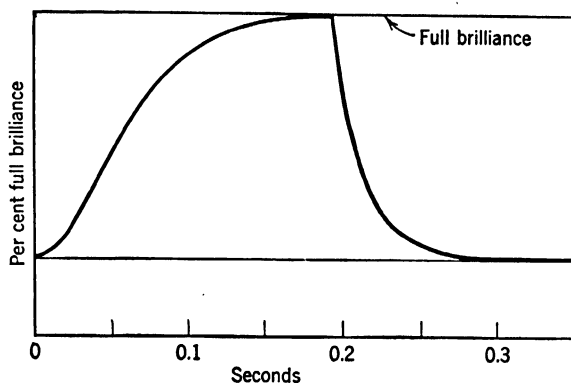


FIG. 18.3. Build-up and Decay of Light Emission from Tungsten Lamp. (Fluke and Porter, reference 2.) (Courtesy of *Proc. Inst. Radio Engrs.*)

perimental purposes the Wratten filter 87 (Fig. 18.4) performs this function very satisfactorily. In applications demanding complete removal of visible radiations as well as great permanence and insensitivity

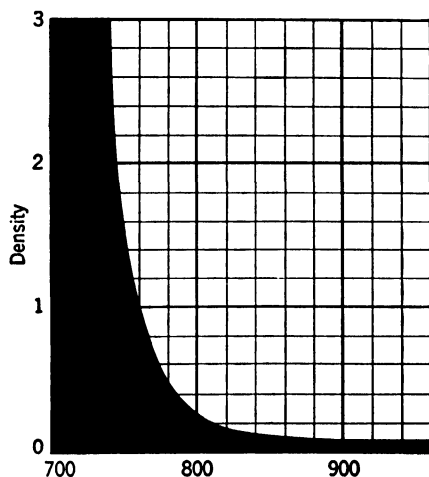


FIG. 18.4. Spectral Density Distribution of Wratten Filter No. 87. (From "Wratten Light Filters," Eastman Kodak Company, Rochester, New York, 1944.)

to shock, exposure, and high temperatures, plastic (Polaroid XRX series) or glass (Corning 2540) filters, with the transmission characteristics shown in Fig. 18.5, may have to be substituted.

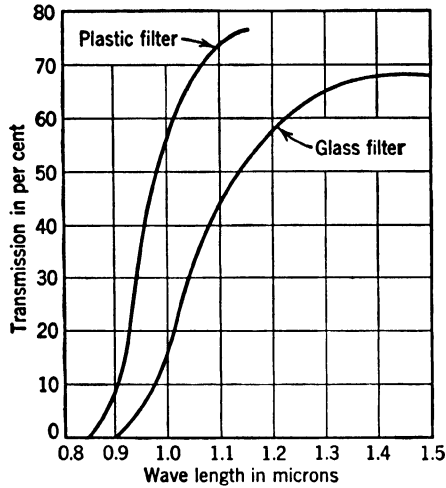


FIG. 18.5. Plastic and Glass Infrared Transmitting Filters: Transmission Characteristics. (Fluke and Porter, reference 2.) (Courtesy of *Proc. Inst. Radio Engrs.*)

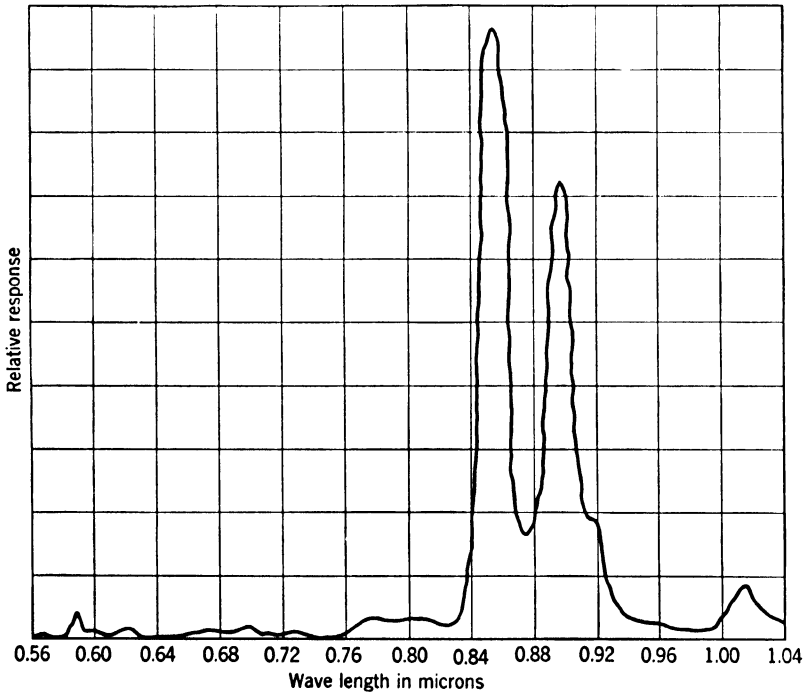


FIG. 18.6. Spectral Distribution of Emission of Cesium Vapor Lamps. (Fluke and Porter, reference 2.) (Courtesy of *Proc. Inst. Radio Engrs.*)

It is generally desirable to modulate the emission of signaling sources so that the signal is readily separated from background illumination and may be amplified with a narrow-band alternating-current amplifier.<sup>6</sup> This modulation may be carried out, in an incandescent source, with a rotating sector disk. Direct electrical modulation may be used, in-

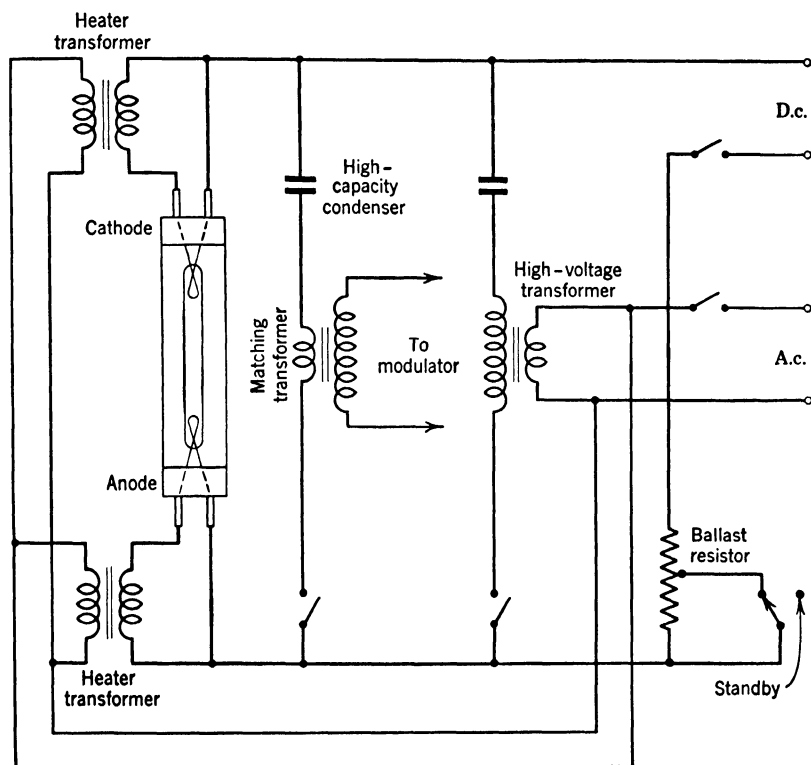


FIG. 18.7. Circuit for Modulating Light Emission from Cesium Vapor Lamp. (Fluke and Porter, reference 2.) (Courtesy of *Proc. Inst. Radio Engrs.*)

stead, with the cesium vapor lamps developed by the Westinghouse Lamp Division.<sup>7</sup> These lamps emit almost entirely cesium resonance radiation, with wave lengths of 8521 and 8943 Angstrom units (Fig. 18.6). Therefore, as near-infrared emitters, they are about five times as efficient as an incandescent lamp, adequate filtering being provided in both cases. The lamps, which resemble sodium vapor lamps<sup>8</sup> in con-

<sup>6</sup> See Chapter 12, p. 242.

<sup>7</sup> See Beese, reference 3.

<sup>8</sup> See Chapter 2, p. 22.



struction and operation, use a double envelope for thermal insulation. The arc is started between heated electrodes in an argon atmosphere by an alternating voltage and is subsequently maintained by a relatively low direct-current voltage. A modulating circuit is shown in Fig. 18.7. In practice care is taken that the modulation amplitude is sufficiently low so that the arc is not extinguished during negative portions of the modulation cycle. The modulation of the light output follows the modulation of the tube current very closely up to high voice frequencies (Fig. 18.8).

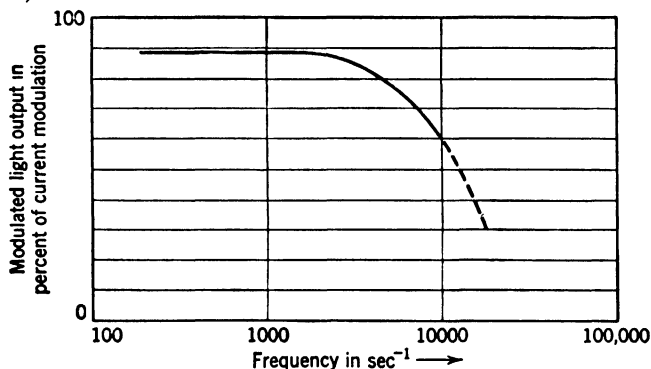


FIG. 18.8. Relative Modulation of Radiation and Current of Cesium Vapor Lamp as Function of Frequency (Current Modulation: 50 per cent). (Fluke and Porter, reference 2.) (Courtesy of *Proc. Inst. Radio Engrs.*)

**Detection of Code and Voice Signals Transmitted on an Infrared Beam.** The detection of signals transmitted on an infrared beam may be carried out by means of a thallous sulfide cell or any other photoconductive cell, or by a multiplier phototube or an image tube. The highly sensitive thallous sulfide cell is particularly advantageous for night reception. In the daytime the strong background illumination translates the operating point of the cell to a region of relatively low sensitivity.<sup>9</sup> Lead sulfide cells and silicon cells as well as vacuum phototubes are here preferable because of the linearity of their response. The lead sulfide cells, which may advantageously be made as small as 0.027 square millimeter in area,<sup>10</sup> are usually placed at the focus of a parabolic reflector collecting the radiation from the distant source (Fig. 18.9). In this manner a radiant flux of the order of  $10^{-10}$  watt falling on the sensitive surface may still be detected.<sup>10</sup> A tenfold gain in sensitivity may be achieved by using a detecting cell cooled with dry ice.<sup>11</sup>

<sup>9</sup> See Fig. 10.9, p. 186.

<sup>10</sup> See Krizek and Vand, reference 4.

<sup>11</sup> See Chapter 13, p. 267.

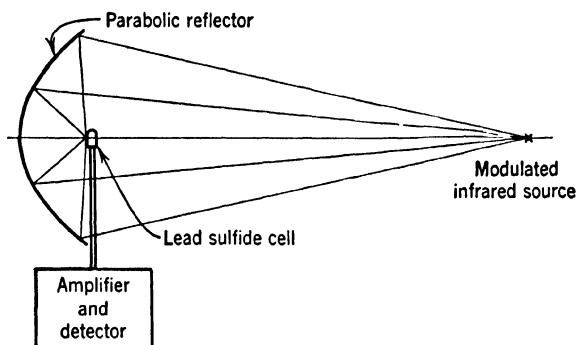


FIG. 18.9. Infrared Signaling with Lead Sulfide Cell Detection.

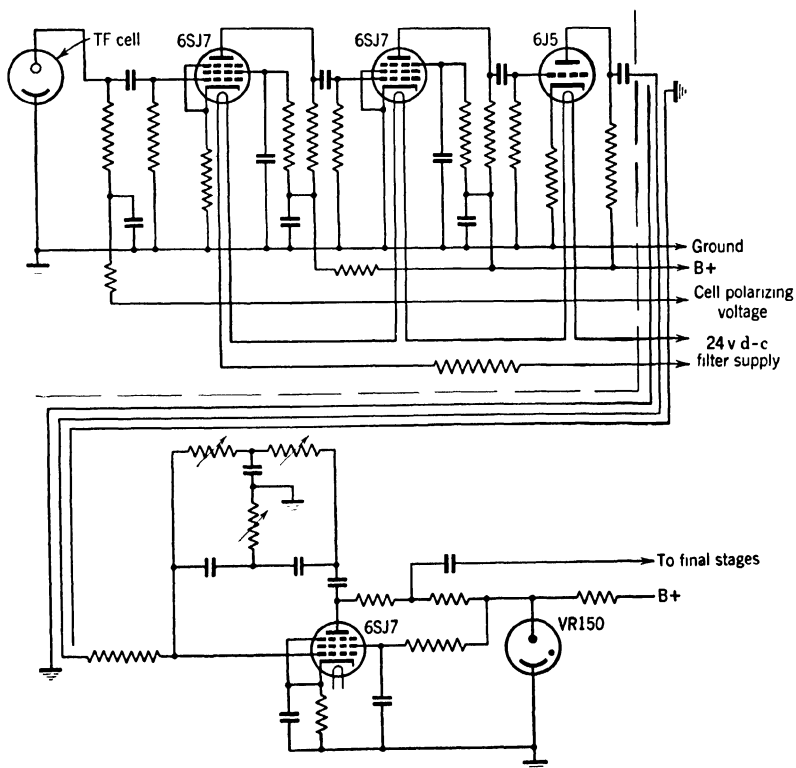


FIG. 18.10. Thallous Sulfide Cell Detecting Circuit for Morse Code Signals. (Fluke and Porter, reference 2.) (Courtesy of *Proc. Inst. Radio Engrs.*)

A circuit designed to translate modulated Morse code signals received by a thallous sulfide cell into audible dot-dash sounds is shown in Fig. 18.10.<sup>12</sup> The voltage is applied to the cell through a 5-megohm resistor. The first three stages constitute a preamplifier. Negative feedback in the succeeding stage makes the amplifier highly selective for the modulation frequency, since the resistance-capacity feedback network constitutes a band elimination filter for this frequency.<sup>13</sup> This stage saturates for a signal amplitude approximately twice as large as the least detected signal, so that the succeeding amplifier stages are not overloaded at high signal strengths.

It should be noted that the utilization of quite another photoelectric phenomenon<sup>10</sup> has been found to yield sensitivities comparable with those attained with the lead sulfide cell at room temperature. Phosphors of the ZnS, CdS, CdSe, and CdTe type, duly activated, change their dielectric constant when illuminated with infrared radiation. Such materials may be inserted between comb-shaped condenser electrodes forming part of the tuning circuit of a high-frequency oscillator. If the output of this oscillator is mixed with that of another high-frequency oscillator, the beat note obtained indicates the illumination falling on the phosphor dielectric.

**The Detection of Hot Bodies.** Quite apart from signaling, the detection of infrared radiations assumed importance during the war, since practically all military targets—ships, tanks, planes, factories, and even persons—either are warmer than their surroundings or emit hot exhaust gases and may therefore be distinguished by enhanced infrared radiations. Since these radiations are predominantly at relatively long wave lengths, photoconductive cells of the lead sulfide type represent the most efficient detectors. The sensitivity of one of these cells, both at room temperature and when cooled with dry ice to  $-80^{\circ}\text{C}$ , is shown in Fig. 13.12 on page 267. A brief calculation indicates the significance of these curves. By Stefan's law<sup>14</sup> the net emission of a black body at absolute temperature  $T$  in surroundings at a temperature  $T_0$  is given by  $5.672 \cdot 10^{-8}(T^4 - T_0^4)$  watts per meter<sup>2</sup>. If the body in question is a square meter in projected area and at a temperature  $30^{\circ}$  above ambient temperature ( $293^{\circ}\text{K}$ ), its total radiation is approximately 200 watts. For a distance  $r$  between emitter and detector and a receiving area  $A$  (area of the parabolic reflector concentrating the radiation on the cell), a fraction  $A/(\pi r^2)$  of the radiant flux reaches the cell. According to the

<sup>12</sup> See Fluke and Porter, reference 2.

<sup>13</sup> This network has a very high impedance, and hence does not cause appreciable degeneration, for the frequency  $f$  given by  $2\pi fRC = 1$ .

<sup>14</sup> See p. 14.

curves in Fig. 13.12, a flux of  $2.7 \cdot 10^{-7}$  watt can still be detected. For a reflector diameter of 10 centimeter (0.1 meter) this is the amount of energy falling on the cell if the warm body is placed a distance of 1360 meters—nearly a mile—from the detector. If the detector is cooled with dry ice, the maximum distance for detection is approximately four times as great.

**Infrared-sensitive Image Tube.** In many cases the detection of an infrared-emitting object is not sufficient. It is also necessary to view its outlines to make identification possible. The essential element of an infrared viewing device or “infrared telescope” is an image tube which converts an infrared image into a visible image.<sup>15</sup> Since the image tubes available at the present time respond only to the infrared radiation in the neighborhood of 1 micron, they are not effective in detecting, by their thermal radiation, bodies only slightly different in temperature from their surroundings. Hence, additional infrared illumination must be supplied. The way it is supplied depends on the use to which the infrared viewing device is to be put. If it is used to permit a ship, plane, or vehicle to keep its place in a convoy, infrared sources may simply be mounted on the leading units. In signaling, where the image tube has the advantage of detecting a source and indicating its direction without close aiming, the radiation is supplied by the signaling source itself. On the other hand, if it is desirable to view the surrounding terrain in darkness, without betraying the presence of the observer, an infrared searchlight must be provided.

The basic arrangement of the observing system, the “infrared telescope,” is the same in all cases. Two optical systems are shown in Fig. 18.11. The second utilizes the great optical efficiency attainable with a Schmidt reflective telescope objective. Since this is coupled with small depth of field, it is best suited for signal detection. The 1P25 image tube itself, operating normally at 4000 volts, uses a Ag-Cs<sub>2</sub>O-Cs photocathode with a sensitivity of 30 to 50 microamperes per lumen and a synthetic willemite phosphor screen with a conversion efficiency of 1 to 3 candlepowers per watt. It follows that for 1 lumen of radiation (from a 2870° K source) incident on the photocathode 0.5 to 1 lumen is emitted by the luminescent screen. These tubes and their auxiliary equipment were designed for mass production and operation under very exacting conditions. With tubes of higher voltage—for instance, 20,000 volts—a tenfold multiplication of the light incident on the photocathode has been obtained.<sup>16</sup> It has already been indicated that the light gain can be greatly increased by using a multiple-stage image tube, the suc-

<sup>15</sup> See Chapter 9.

<sup>16</sup> See Krizek and Vand, reference 4.

ceeding stages being separated by a thin "sandwich" of a fluorescent screen and a photocathode with matched responses.<sup>17</sup>

The requirement of extreme portability which had to be met in most image-tube applications called for special power-supply designs.<sup>18</sup> One of them has already been discussed as a portable supply for the multiplier phototube.<sup>19</sup> It is suitable for the operation of the 1P25 image tube with an anode potential of 4000 volts.

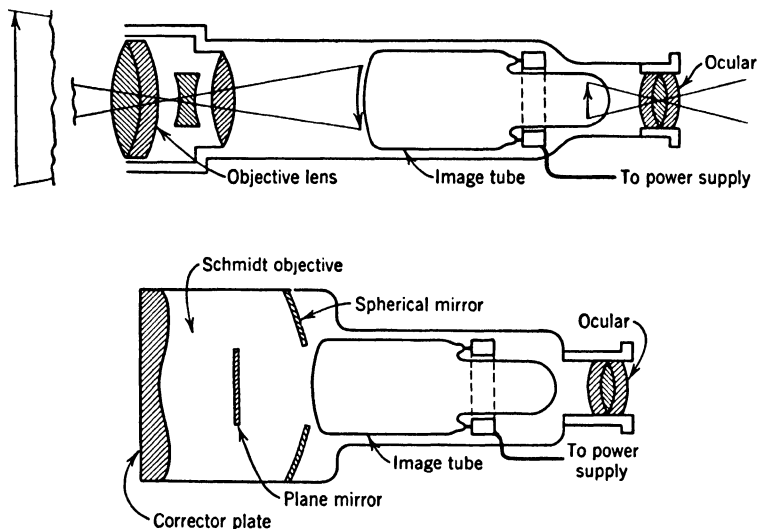


FIG. 18.11. Optical Systems of Infrared Telescopes. (Morton and Flory, reference 5.)

Another extremely lightweight and low-current drain voltage supply has been developed<sup>18</sup> for use with an image tube having only an anode and a cathode connection. Here the primary circuit of the transformer is closed for a brief interval every  $\frac{1}{4}$  second by an electrically driven balance wheel. During this interval a condenser is charged through a gas rectifier to the peak operating voltage. In the succeeding  $\frac{1}{4}$ -second period the photocurrent through the image tube partly discharges the condenser. Such a circuit will operate for 50 hours on a single size-D flashlight cell.

Extreme current economy is dictated only for observation instruments which depend on external sources of illumination (signals or pilot

<sup>17</sup> See Chapter 9, p. 172.

<sup>18</sup> See Morton and Flory, reference 5.

<sup>19</sup> See Fig. 13.6c, p. 260.

lights), such as the helmet binocular shown in Fig. 18.12. If an infrared searchlight must be supplied, the power consumption of the searchlight dwarfs that of the telescope. A "snooperscope," in which the searchlight is joined directly to the observation telescope, is shown in Fig. 18.13. The infrared beam is provided by a General Electric sealed



FIG. 18.12. Type Z Helmet Binocular. (Morton and Flory, reference 5.)

beam lamp with a 12- or 15-degree spread and a maximum beam candle-power of 80,000, provided with Corning 2540 or Polaroid XRX filters. The "sniperscope" has a somewhat similar arrangement; the infrared observation instrument is mounted on a rifle as sighting telescope.

The emphasis in the development of infrared equipment has, in the past, been on military applications. The image tube and the infrared telescope, however, have also a number of valuable peacetime uses, which may be expected to multiply. Examples are the detection of forgeries, infrared microscopy,<sup>20</sup> and the observations of processes, common in photography, from which visible light must be excluded.

<sup>20</sup> See Zworykin and Morton, reference 6.

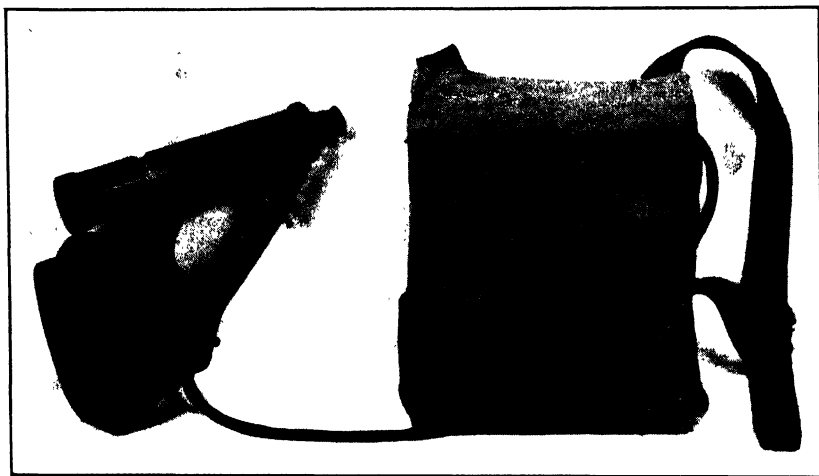


FIG. 18.13. Laboratory Prototype Snooperscope. (Morton and Flory, reference 5.)

**Attempts at Extending the Wave-Length Range of Infrared Viewing Devices.** The "infrared iconoscope" and the electron mirror image tube, of which certain forms were developed in Germany, are attempts at realizing image-forming devices whose infrared sensitivity extends considerably farther than that of the image tube, namely, to about 2.5 microns.<sup>21</sup> The infrared iconoscope is similar to the ordinary iconoscope<sup>22</sup> in construction, a layer of a photoconductive semiconductor replacing the mica sheet coated with a mosaic of photoemissive elements. The signal plate is maintained at a voltage slightly negative with respect to the voltage of the anode coating, which determines the potential assumed by the semiconductor surface under bombardment. Illuminated elements will, in the course of the frame time succeeding scanning, become more negative by conduction than unilluminated elements and therefore will give rise to a larger picture signal at the next beam scanning.

The operation of the mirror image tube is shown schematically in Fig. 18.14. A broad electron beam is incident on a highly resistive photoconductive layer on a metal backing. Under the bombardment the exposed surface tends to assume an equilibrium potential at which no more electrons can reach the surface, so that the beam electrons are reflected. This equilibrium potential is reached more slowly, for a positively biased metal backing, for elements which are illuminated,

<sup>21</sup> See Krizek and Vand, reference 4.

<sup>22</sup> See Chapter 17, p. 386. A pickup tube with photoconductive target is described by Krawinkel, Kronjäger, and Salow, reference 7.

so that a portion of the beam electrons are drawn through the layer to the metal backing. In practice the velocity of the electron beam is modulated, for instance, between 5 and 6 kilovolts, and the reflected electrons are observed on a fluorescent screen; infrared-emitting portions of the scene appear darker than the rest. Both lead sulfide mixed with lead oxide, formed by simultaneous deposition of lead oxide and

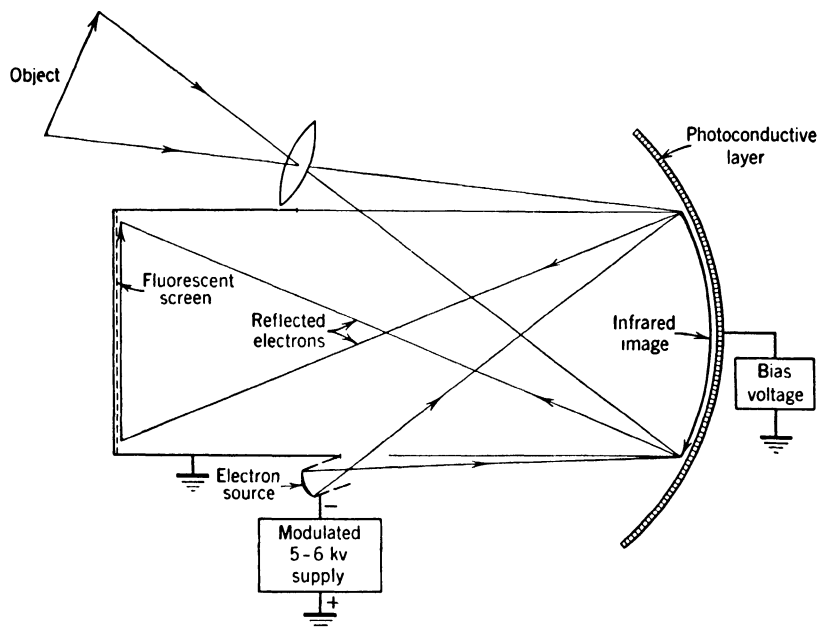


FIG. 18.14. Principle of the Electron Mirror Image Tube.

sulfur at 150° C and subsequent ripening in air at 300 to 320° C, and zinc oxide on a manganese mirror have yielded satisfactory semiconducting layers.

**Photovision.** An interesting application of light-beam signaling is the transmission of television programs over a beam of light.<sup>23</sup> The picture signals, derived from the pickup system and duly amplified, are applied to the control grid of a cathode-ray tube mounted on a transmitting tower. The stationary beam is not focused sharply but spread over a large area of the very short persistence fluorescent screen. The receiving system consists simply of a multiplier phototube together with an optical system aimed at the transmitter, which concentrates the light from the screen of the transmitting tube on the photocathode. The re-

<sup>23</sup> See DuMont Laboratories, reference 8.



ceived signals—which include the synchronizing signal in the usual manner—are amplified and used to control the beam intensity and beam deflection of a kinescope just as in an ordinary television receiver. In fact, the receiver differs from the usual receiver only in having the precisely aimed optical system and phototube replace the antenna, radio-frequency stage, and intermediate-frequency stages. Sound is transmitted over a separate light beam, concentrated on a second phototube. For the transmission of color pictures with sound, altogether four light beams are employed, the arrangement being basically the same as for a simultaneous all-electronic color television system.<sup>24</sup>

The advantages of *photovision* over radio-transmitted television are noninterference between stations and complete absence of reflection and “static” effects. An obvious shortcoming is that the communication channel may be blocked by rain, clouds, fog, and smoke. Furthermore, it is limited strictly to line-of-sight. A determination of the sphere of utility of this interesting development must be left to the future.

#### REFERENCES

1. R. J. CASHMAN, “Development of sensitive lead sulfide photoconductive cells for detection of intermediate infra-red radiation,” *O.S.R.D. Report* 5998, Oct. 31, 1945.
2. J. M. FLUKE and N. E. PORTER, “Some developments in infra-red communication components,” *Proc. Inst. Radio Engrs.*, Vol. 34, pp. 876–883, 1946.
3. N. C. BEESE, “Cesium vapor lamps,” *J. Optical Soc. Am.*, Vol. 36, pp. 555–560, 1946.
4. V. KRIZEK and V. VAND, “The development of infra-red technique in Germany,” *Electronic Eng.*, Vol. 18, pp. 316–317, 322, 1946.
5. G. A. MORTON and L. E. FLORY, “An infra-red image tube and its military applications,” *RCA Rev.*, Vol. 7, pp. 385–413, 1946.
6. V. K. ZWORYKIN and G. A. MORTON, “Applied electron optics,” *J. Optical Soc. Am.*, Vol. 26, pp. 181–189, 1936.
7. G. KRAWINKEL, W. KRONJÄGER, and H. SALOW, “On a storing picture pick-up with semiconducting dielectric,” *Z. tech. Physik*, Vol. 19, pp. 63–73, 1938.
8. Allen B. DuMont Laboratories, Inc., “Television via light beams,” *Rev. Sci. Instruments*, Vol. 18, pp. 253–255, 1947.

<sup>24</sup> See Chapter 17, p. 377.

## Chapter 19

# MISCELLANEOUS APPLICATIONS OF PHOTOELECTRICITY

The varied applications of photocells are, today, far too numerous to permit a comprehensive treatment of them in a book of moderate size. This chapter will limit itself to examples from several fields of usefulness which have not as yet been covered. It will be found that there are few areas of human activity in which photoelectricity does not play some role.

**Illumination Control.** An obvious function of photoelectric cells is the automatic control of artificial lighting to supplement or replace daylight. Photoelectric lighting-control units find application in schools, stores, offices, airports, and street-lighting systems. An interesting example of such a control unit, designed specifically for controlling a single or a limited number of street luminaires, is the compact Sunswitch shown in Fig. 19.1.<sup>1</sup> The unit is mounted on a lighting pole with the window facing north so as to be protected from direct sunlight. The circuit, represented schematically in Fig. 19.2, is arranged so that the lighting relay closes as the illumination drops to approximately 1 foot-candle (10.8 lux)—normally about 25 minutes after sunset—and opens as it rises to a somewhat higher value. A 20-second time delay is provided by the insertion of two *RC* delay networks (for closing and opening the relay, corresponding to current flowing through the first and second section of the double triode, respectively), so that the relay does not react to lightning flashes and the shadows of objects flying past. It will be noted that the unit is entirely alternating-current-operated.

Other types of illumination controls serve to illuminate swiftly moving objects with an intense momentary flash of light, making possible their photography. An example is the General Electric High-Speed Photolight.<sup>2</sup> Here a large capacitance is charged through a resistance to a

<sup>1</sup> See Marshall, reference 1.

<sup>2</sup> See Bellinger, reference 2.

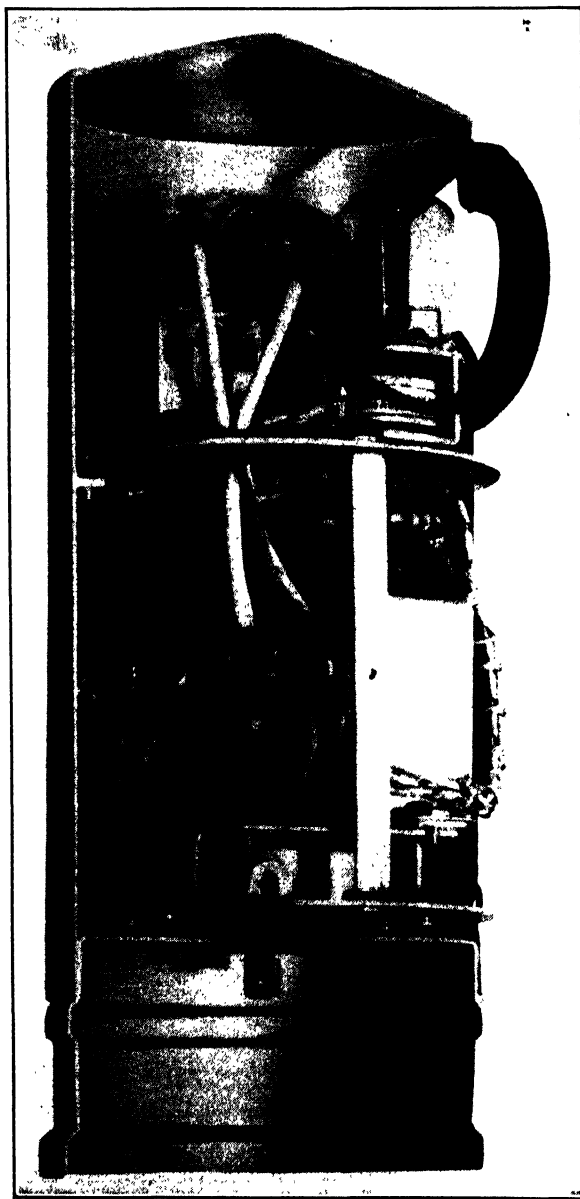


FIG. 19.1. "Sunswitch" Lighting Control Unit. (Courtesy of Ripley Company, Middletown, Conn.)



indicated in Fig. 19.3. Million-watt flashes lasting 3 microseconds are obtained in this manner. The light flash, or light-beam interruption, which triggers the discharge is appropriately coupled to the moving object to be photographed.

In aerial night photography a phototube controls the camera shutter rather than the light source, which is here a flash bomb. The phototube relay circuit is triggered by the first rise of illumination produced by the flash bomb. The time delay of the shutter system is such that the shutter is fully open at the peak of illumination provided by the bomb.

**Light Relays.** The photolight control represents one of many applications in which a light beam performs the function of a relay arm whose actuation demands no dissipation of power. Another very simple example is the conversion of a current meter into a relay by boring a small hole in the scale card of the meter and placing a flashlight bulb below it and a phototube above it.<sup>3</sup> If the phototube is connected into a thyatron circuit similar to that shown in Fig. 12.19*b*, the obscuring of the light beam by the pointer of the meter may close a power relay.

Light beams and phototubes have also been variously used for increasing the accuracy of galvanometer readings. Figure 19.4 shows, schematically, a high-sensitivity recording galvanometer for measuring the potential drop across a thermocouple in infrared spectrometry.<sup>4</sup> The vertical coiled filament of a lamp is imaged, after reflection from a galvanometer mirror, on the cathodes of a twin phototube; the potential drops across the phototube load resistances are applied in push-pull to a double-triode cathode-follower stage which controls directly a recording meter. The galvanometer is damped by a feedback resistor  $R_3$ , which compensates 90 per cent of the thermocouple voltage. With a galvanometer giving a 1-millimeter deflection at 1 meter for 0.32 microvolt, such a system yields a full-scale deflection for 1 microvolt with an accuracy of the order of 1 per cent.

Hourly time signals in the form of light flashes are utilized by the station WQXR in New York to actuate a studio chime as well as to reset a master clock at a distant transmitter.<sup>5</sup> A phototube-controlled thyatron relay circuit keys both the chime and a 15-kilocycle oscillator whose output is sent from the studio to the transmitter over a high-fidelity line to actuate the clock-resetting mechanism.

Light beams and phototubes are also employed to advantage for the starting and stopping of standard stop watches, eliminating errors resulting from variations in the speed of human reaction.<sup>6</sup>

<sup>3</sup> See Laing, reference 3.

<sup>4</sup> See Assett, reference 4.

<sup>5</sup> See Valentine, reference 5.

<sup>6</sup> See Wey and Jupe, reference 6.

An interesting application of light-operated relays in the communication field is the use of typewriters with standard keyboard for the sending of teletype messages.<sup>7</sup> In the apparatus shown in Fig. 19.5, the in-

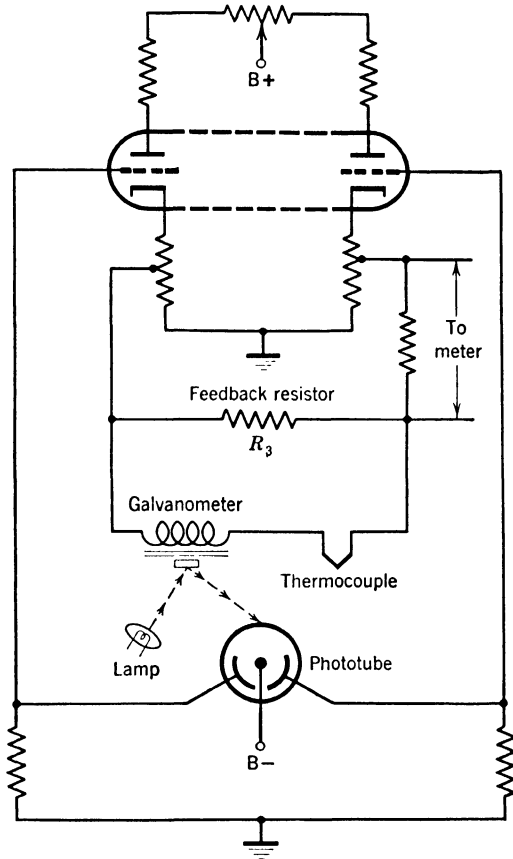


FIG. 19.4. Photoelectric Galvanometer Amplifier. (Assett, reference 4.) (Courtesy of *Electronics*.)

dividual typewriter keys are provided with sets of shutters which, on depression, interrupt one or several light channels. Associated with each light channel is a phototube and thyatron circuit, which causes a relay to punch a hole in a paper tape. In this manner the message is translated into teletype code, which may be transmitted in conventional manner. The system has the advantage that, in this way, any typist, rather than only a trained teletypist, can operate the message transmitter.

<sup>7</sup> See Bush, reference 7.

Another, relatively complex, light-relay system is used in an "odograph" or map tracer.<sup>8</sup> It serves to register the path of a vehicle, such as a jeep, on a blank map mounted on it. The speed of the vehicle is communicated to the plotting pen by the engine transmission; its direction is communicated by a compass mounted in the vehicle. The

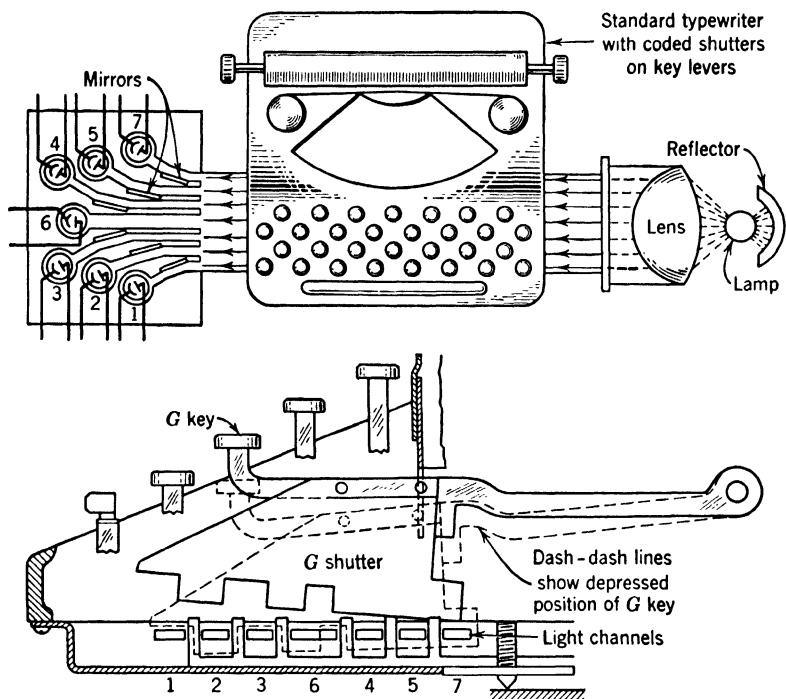


FIG. 19.5. System for Sending Teletype Messages with Standard Typewriter Keyboard. (Bush, reference 7.) (Courtesy of *Electronics*.)

arrangement of the compass is shown in Fig. 19.6. A mirror mounted on the compass card reflects light from a lamp placed, along with two phototubes and two thyratrons, on a mobile table. If the light beam does not fall symmetrically on the dihedral mirror, the excess photocurrent generated by the one or the other phototube causes the corresponding thyatron to fire, actuating a motor which rotates the mobile table back toward the symmetrical position. In practice, the table overshoots slightly before it is brought back by the action of the second thyatron, reversing the direction of motion, so that it hunts about the equilibrium position through  $\pm 5$  degrees. The mobile table is coupled

<sup>8</sup> See Faustman, reference 8.

to the plotting unit, so that the direction of motion of the pen depends at all times on the azimuth of the table relative to the vehicle chassis.

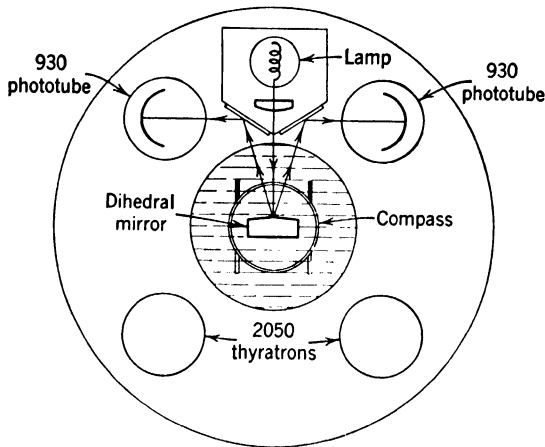


FIG. 19.6. Compass Mounting for Map Tracer. (Faustman, reference 8.) (Courtesy of *Electronics*.)

**Traffic Control.** Perhaps the most familiar use of the phototube in traffic control is as automatic door opener.<sup>9</sup> The common swinging doors in railroad stations, public buildings, and restaurants normally utilize a thyratron relay circuit to open and close a compressed air valve which actuates a piston. A typical arrangement of the doors and light beams is shown in Fig. 19.7. Separate doors are employed for entry and exit. The light projectors as well as the phototubes and auxiliary equipment are mounted in hollow metal posts. The interruption of the first light beam causes the door to open as a person approaches it. The second light beam, passing diagonally through the doorway, prevents the door from closing while the person walks through. This second door-opening circuit is switched off by the door itself as it approaches the halfway-closed position, so that it does not keep the door open permanently. Photoelectric door-opening mechanisms, generally controlling a motor rather than a compressed-air system, are also widely used to open garage doors, truck entrances, and so forth. If the approaches to an entrance are multiple, the interruption of the light beam may, in addition, control a red signal light, preventing vehicles approaching by another route from entering.

Often a somewhat similar system controls signal lights at a crossing of a major highway and a less-traveled secondary road. A pair of light

<sup>9</sup> See Bendz, reference 9.



beams and phototubes, spaced somewhat less than a car length apart, is placed on the secondary road. When an approaching car interrupts both beams, the signal lights, normally showing green for the highway and red for the secondary road, are reversed. After the car has passed, the normal condition of the traffic lights is restored by a time switch. There are two beams to prevent the tripping of the signal by a pedestrian.

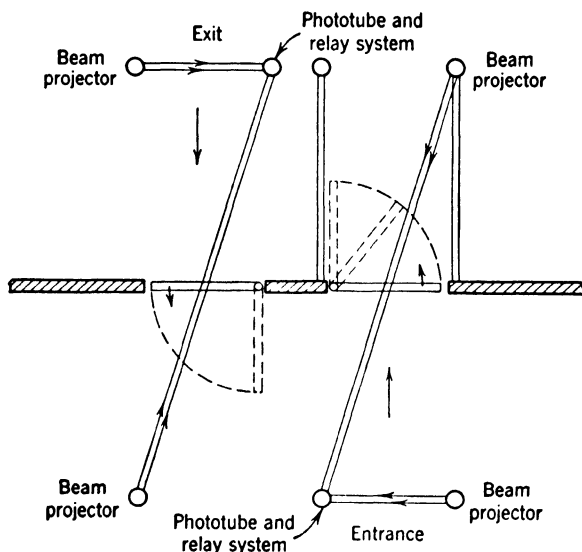


FIG. 19.7. Arrangement of Light Beams in Photoelectric Door-Opening System. (Bendz, reference 9.) (Courtesy of *Electronics*.)

Similar systems have also found application in single-track railroads.<sup>10</sup> The track is divided into a series of "blocks," at whose ends passing turnouts are placed. Two pairs of light beams cross the track near the two ends of every block. The interruption of the outer pairs turns on the green signal lights; that of the inner pairs, the red signal lights. Thus red signal lights indicate that there is a train within the block in question; green signal lights, that the block is clear.

A novel photoelectric control system has been employed by the German State Railways.<sup>11</sup> A light projector and a barrier-layer photocell are mounted side-by-side on the train engine. A mirror, whose inclination is controlled by the signal setting, is mounted on the signal posts and serves to reflect the light beam back toward the photocell which, through a relay system, sets the brakeshoes in motion or issues a

<sup>10</sup> See reference 10.

<sup>11</sup> See Lange, reference 11, pp. 274-277.

warning signal. The light beam is chopped by a compressed-air-driven disk, so that alternating-current amplification may be used and daylight does not interfere with the reception of the signal. The mirror, furthermore, is a triply reflecting triangular pyramid prism with the property of simply reversing the direction of incident light for a considerable range of angle of incidence.

There are many other examples of the use of phototubes in traffic control. An interesting one is the determination of the proper locking position of the 1600-ton moving span of a road bridge over the Forth in Scotland.<sup>12</sup> The registry of light beams on the fixed abutment and of phototubes on the moving span indicates to the operator the instant for shooting bolts and wedges into place to hold the bridge in its normal position.

Photoelectric mechanisms lend themselves well to the counting of highway traffic.<sup>13</sup> For this purpose two infrared beams 3 feet apart are directed diagonally across a highway onto a pair of phototubes (Fig. 19.8). A counter relay is actuated by a thyratron circuit whenever both beams are interrupted. An electric clock mechanism may be employed to record the count, along with the time, on a paper tape at hourly intervals.

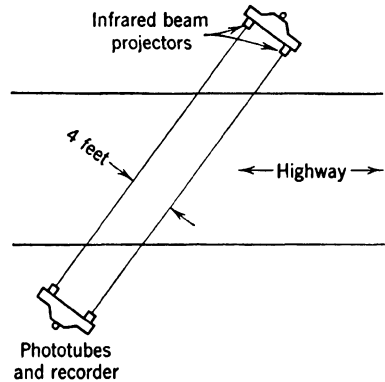


FIG. 19.8. Arrangement of Infrared Beams for Counting Highway Traffic. (Reference 13.) (Courtesy of *Electronics*.)

**Photoelectric Safety Devices.** Every traffic-control device is, in a sense, also a safety device. There are, in addition, many other photoelectric devices whose unique function is the protection of persons and property.

One of the important hazards against which photocells stand guard is fire. Photoelectric fire detectors depend either on the direct action of an open flame or spark to elicit the alarm-triggering photocurrent or, more commonly, on the interruption of light beams by smoke. A device of the first kind is the Weisz fire and flame detector,<sup>14</sup> which has already been mentioned in Chapter 13.<sup>15</sup> It is a gas-discharge counter with a

<sup>12</sup> See Jupe, reference 12.

<sup>13</sup> See reference 13.

<sup>14</sup> See Weisz, reference 14.

<sup>15</sup> See p. 264.

perforated, pure copper cathode, and a thin wire anode. As indicated in Fig. 19.9, the response of such a counter, enclosed in Corning 9741 ultraviolet-transmissive glass, is negligible above 2800 Angstrom units so that it responds neither to sunlight, which has been filtered by the ozone layers of the outer atmosphere, nor to any ordinary glass-enclosed light sources. It is sensitive, however, to the slight ultraviolet content of the light from open flames and sparks. Thus a burning match at a distance of 30 feet from a flame detector with an effective cathode area of 30 square centimeters gives rise to 100 counts, or photoelectron-initiated gas discharges, per second, whereas cosmic rays and natural radioactivity account for less than one count per second.

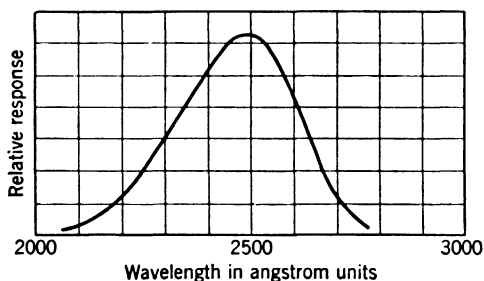


FIG. 19.9. Spectral Response of Weisz Fire and Flame Detector. (Weisz, reference 14.) (Courtesy of *Electronics*.)

The alarm-triggering circuit used with the flame detector is shown in Fig. 19.10. The negative pulses from the counter tube are applied to one section of a 6N7 double triode, which converts them into positive pulses, applied to the grid of the second section. These positive pulses build up the potential across the  $RC$  circuit in the cathode lead of this section to a value corresponding to the total charge delivered by the pulses in a period corresponding to the time constant  $RC$  of the circuit. If this potential exceeds the firing voltage of the 2051 thyatron, a relay in the thyatron plate circuit closes the alarm circuit. Accordingly, a certain threshold number of pulses per second sets off the alarm.

Often the evolution of smoke precedes the appearance of an open fire. In such cases a smoke detector will give earlier warning than a fire detector. Ships—particularly naval vessels—have elaborate smoke-detection devices.<sup>16</sup> In one example air is drawn, in rotation, with the aid of a rotating selector, from the several protected ship spaces and is passed through a tube containing a light beam and a barrier-layer photocell. When smoke in the tube reduces the photocurrent below a

<sup>16</sup> See reference 15.

set level, a sensitive relay stops the selector so as to indicate the source of the smoke and rings a smoke gong so that the crew may take appropriate action.

Another specific example where smoke detection is important is in the operation of air-conditioned theatres. Smoke accidentally drawn

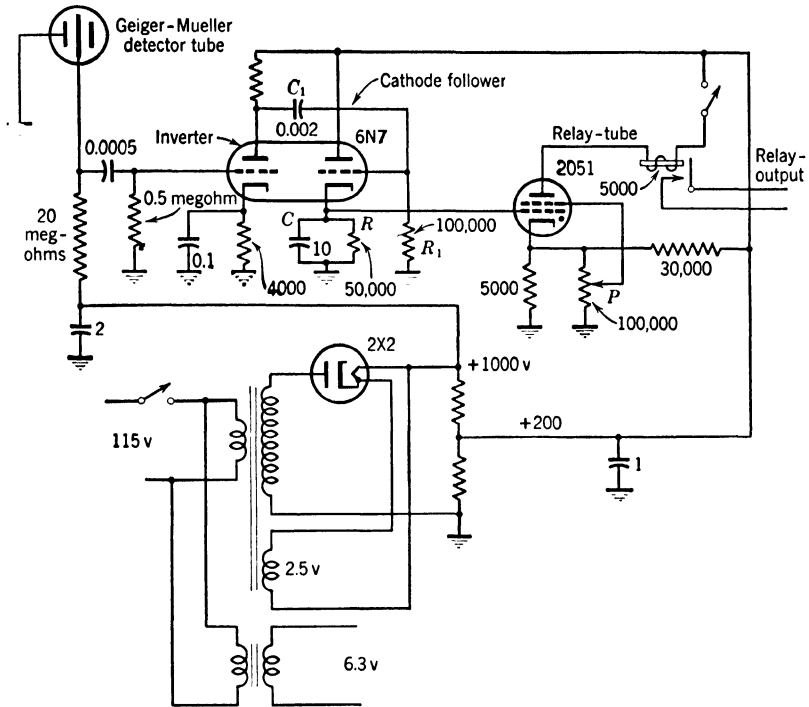


FIG. 19.10. Alarm-Triggering Circuit Employed with Fire and Flame Detector. (Weisz, reference 14.) (Courtesy of *Electronics*.)

into the air-conditioning system may cause a panic even in the absence of a fire. Here a transverse light beam is passed through the air-conditioning duct;<sup>17</sup> the presence of smoke triggers a thyatron circuit which shuts off the blower, closes a damper, and lights a warning lamp.

Light beams and phototubes may similarly detect human intruders.<sup>18</sup> Infrared beams, obtained by filtering out the visible radiation of incandescent lamps, are universally employed. For internal use the beam projector generally consists of an automobile headlight lamp, filter, and simple lens in a light-tight housing. The detector consists of a photo-

<sup>17</sup> See Morin, reference 16.

<sup>18</sup> See MacDonald, reference 17.

tube with an auxiliary relay circuit and a lens to focus the beam on the photocathode. Mirrors may direct the beam in a crisscross pattern

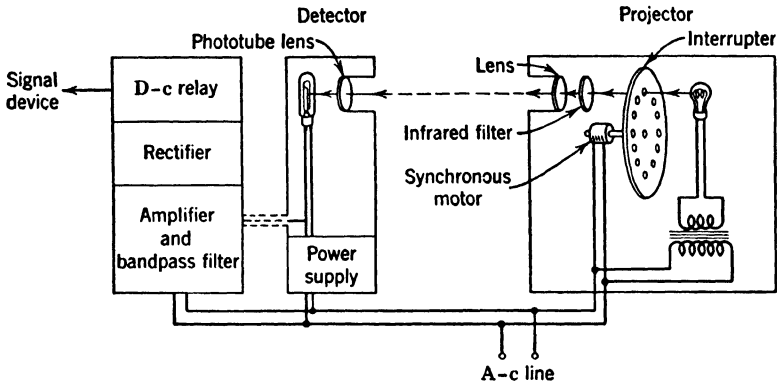


FIG. 19.11. Modulated Infrared Beam Projector and Detector for Intrusion Detection (Schematic Diagram). (MacDonald, reference 17.)

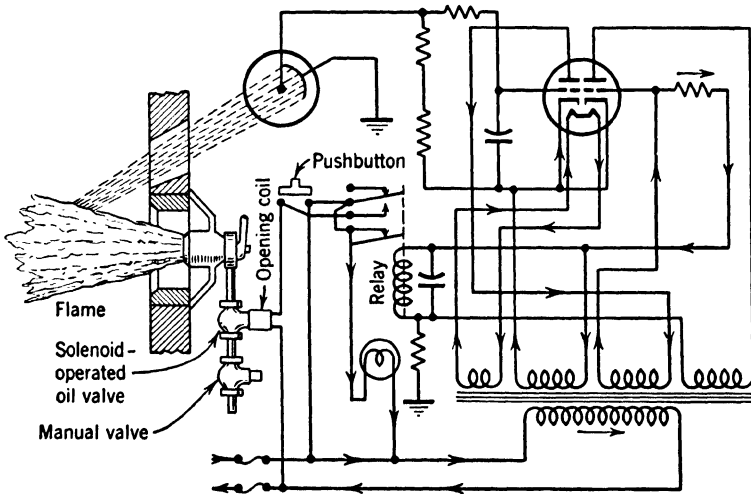


FIG. 19.12. Circuit of Flame-Failure Detector. (Reference 18.) (Courtesy of *Electronics*.)

through the protected area, the total length of the light beam being up to 150 feet.

Outdoor protection is more complex. Mirrors should generally be avoided since they are easily obscured by dust and condensation. Both the projector and the detector should be recessed to prevent deposition

of obscuring materials; heating may have to be applied to prevent condensation of moisture; and vertical louvers in front of the detector have been found useful to prevent the nesting of small birds. To increase the sensitivity of detection and reduce the interference of daylight the projected beam is generally modulated by a chopper disk. Figure 19.11 shows the essential elements of such intrusion detection equipment. One particular installation by the American District Telegraph Company

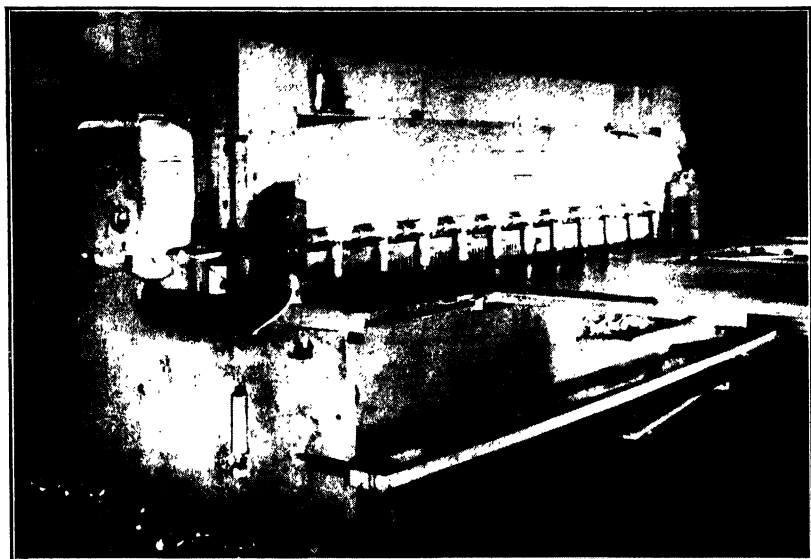


FIG. 19.13. Large Press with Light-Curtain Protection. (Courtesy of Ripley Company, Middletown, Conn.)

guarded 3000 feet of sea approach with a single beam. Both projector and detector were floated in a vertical bronze channel so as to maintain the beam level at 3 feet above the level of the water. A broad 18-inch beam was employed so that seagulls would not trigger the detection circuit.

Photoelectric safety devices have also many uses in industry. A flame-failure detector for oil furnaces is an example.<sup>19</sup> Its alternating-current-operated circuit (Fig. 19.12) has, as principal element, a double triode, whose first section is blocked when the flame is on and photocurrent flows. The second section conducts current, closing the relay which opens the solenoidal oil valve. In case of flame failure, the first

<sup>19</sup> See reference 18.

section conducts, the second is blocked, and the solenoidal oil valve is closed, with the simultaneous lighting of a warning lamp.

Even more common are "light curtains" to protect operators of heavy machines. The light curtain about the area of danger is formed by a series of beam projectors and mirrors, the beams falling ultimately on a set of phototubes. The machinery is stopped instantly when one of the beams is interrupted by the operator, reaching into the protected area. An example is shown in Fig. 19.13, and a suitable triggering circuit, in

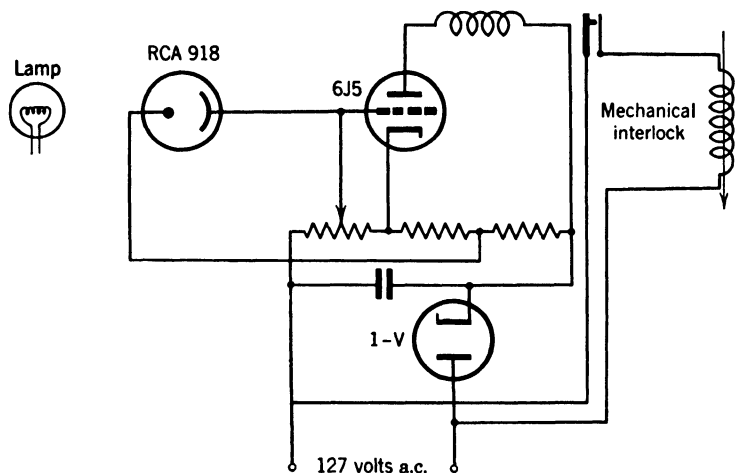


FIG. 19.14. Phototube Circuit for Shutting Off Machines in Response to Penetration of Light Curtain. (Reference 19.) (Courtesy of *Product Engineering*.)

Fig. 19.14.<sup>20</sup> Equipment of this type has been applied widely to large-scale hydraulic and electrical presses.<sup>21</sup> The Hewitt Rubber Company has a light beam 50 feet long to enable an operator to stop a large mandrel used in making rubber hose at any point along its length.<sup>22</sup> The light curtain, as a protective device, finds an important application also in preventing the motion of an elevator as long as there is an obstruction in the doorway.

**Photoelectric Controls for Industrial Processes.** Quite apart from reducing accident risks, phototubes can greatly increase the economy of industrial operations. Thus, equipment similar to that used in smoke-alarm systems may be installed in stacks to measure smoke densities.<sup>23</sup>

<sup>20</sup> See reference 19.

<sup>21</sup> See Powers, reference 20.

<sup>22</sup> See reference 21.

<sup>23</sup> See reference 22.

The resulting information is useful as a guide to economical firing and facilitates compliance with smoke-abatement ordinances (Fig. 19.15).

In chemical plants a uniform flow of liquid through a supply pipe may be maintained with the aid of phototubes independently of the

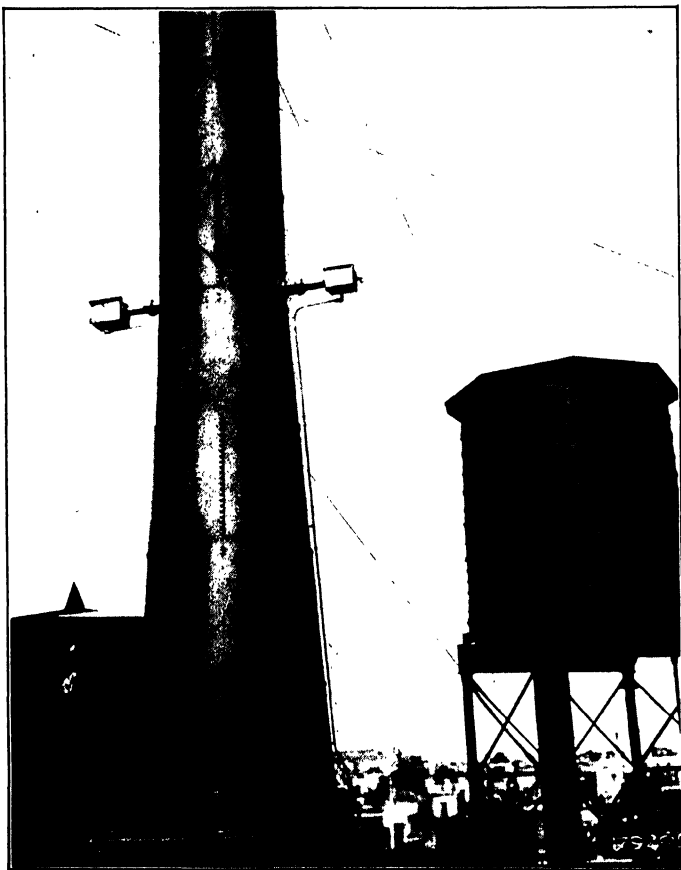


FIG. 19.15. Photoelectric Smoke-Recording Installation. (Courtesy of Westinghouse Electric Corporation.)

pressure of the supply.<sup>24</sup> For this purpose a "rotameter" is used, a tapered vertical tube in which the height of a float indicates the rate of flow of the liquid. Two light beams are arranged to graze the top portion and the bottom portion of the float. They fall on separate phototubes, whose difference in output controls a motor which opens or closes

<sup>24</sup> See McNickle, reference 23.



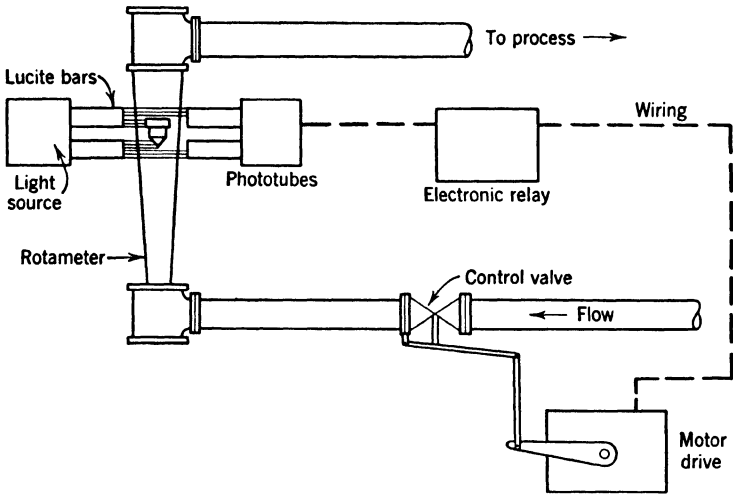


FIG. 19.16. Photoelectric Control of the Flow of Liquid. (McNickle, reference 23.) (Courtesy of *Electronics*.)

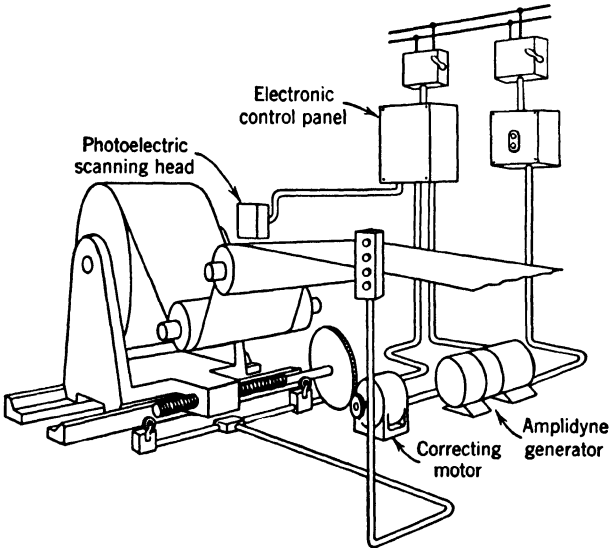


FIG. 19.17. Photoelectric Side-Register Control. (Cockrell, reference 24.) (Courtesy of *Electrical Engineering*.)

the intake valve. In this manner an upward displacement of the float reduces the intake, a downward displacement increases it (Fig. 19.16).

In the paper industry photoelectric side register controls (Fig. 19.17) are used to produce smooth-ended rolls. In one control system, developed by the General Electric Company,<sup>25</sup> a lens disk rotated by a synchronous motor projects 90-degree arcs of light on the edge of the paper, passing over a dark roll. A phototube receives the diffusely reflected light. The output of the phototube is converted, with the aid

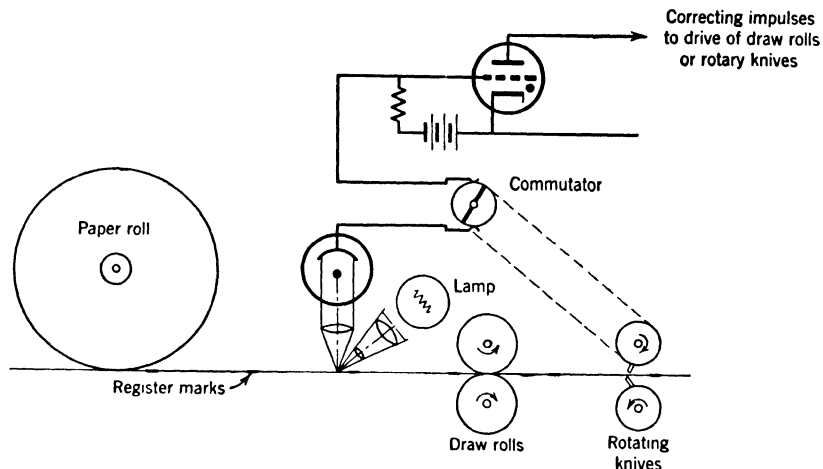


FIG. 19.18. Principle of Phototube Control for the Cutting of Printed Wrappers. (Cockrell, reference 26.)

of suitable circuits, into a succession of sharp pulses corresponding to the sudden increase in the photocurrent as the light spot crosses the edge of the paper. Applied to the grids of a pair of triodes whose plate voltage is supplied by the alternating-current line operating the lens disk motor, these pulses provide an output whose sign depends on whether the pulse precedes or follows the transit of the voltage wave through zero. This output controls an "amplidyne" motor generator, which provides the power for a motor shifting the rollers sidewise so as to restore proper registry. A somewhat different system, with electronic amplification throughout, has been developed by Westinghouse.<sup>26</sup>

Phototubes also have a vital role in the packaging industry. The problem is to cut wrappers, printed on continuous rolls, at the right point with reference to the printing.<sup>27</sup> For this purpose a dark marking

<sup>25</sup> See Cockrell, reference 24.

<sup>26</sup> See reference 25.

<sup>27</sup> See Cockrell, reference 26.

line,  $\frac{1}{16}$  inch wide and  $\frac{1}{2}$  inch long, normal to the direction of motion of the paper, is printed at a convenient point on each wrapper. A scanning head projects a line of light on the paper, whose reflection is picked up by a phototube, which operates a thyatron circuit (Fig. 19.18). A mechanical commutator connects this circuit only at the time when the dark line should be under the scanner; consequently the thyatron fires

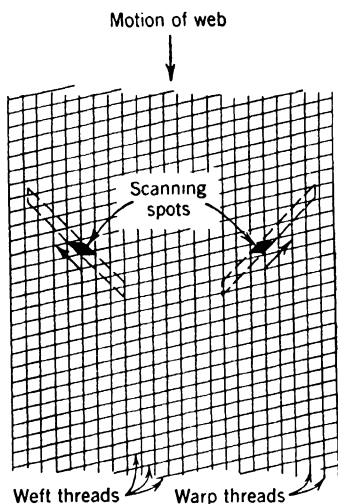


FIG. 19.19. Motion of Scanning Spots across Web with Skew Weft Threads. Scanning spot at left is interrupted more frequently by weft threads, giving rise to higher-frequency signal current, than scanning spot at right.

only if the wrapper is slightly off register. In an intermittent machine, where the wrappers are cut at rest, this pulse is employed to move the paper ahead<sup>28</sup> so as to bring it closer to registry. In a continuous-feed machine, with rotating knives, the magnitude of the pulses may be used to control the speed with which the differential gear housing for the main drive is rotated by an auxiliary motor. Many modifications of these arrangements have been utilized. Photoelectrically controlled machines turning out 400 to 500 feet of wrappers per minute are found to maintain an accuracy of cutting of  $\pm \frac{1}{64}$  inch.

transmitted light is directed onto a phototube, one unit being provided at each side of the web. If the web is skew, the frequency of interruption of the light by the weft threads will be greater for one side than for the other. The output of the two phototubes is applied to a frequency-selective circuit, whose output is proportional to the difference in the frequency of interruption of the two light beams. This signal readjusts pins holding the weft threads. An installation using this method of weft-straightening is shown in Fig. 19.20.

In the textile industry phototubes straighten the weft threads of cloth.<sup>29</sup> Flat light beams 0.004 by  $2\frac{1}{8}$  inches are projected on the continuously moving web from below. Rotating disks select a narrow spot which moves outward; relative to the web its motion is in a diagonal direction (Fig. 19.19). The

<sup>28</sup> It is assumed that the machine has been set to run more slowly than the correct speed.

<sup>29</sup> See reference 27.

Phototubes also find numerous applications in the metals industry.<sup>30</sup> At the mine the opening of dump pockets is controlled by the interruption of light beams by the ore trucks; photoelectric relays serve to level the giant power shovels used in open-pit mines. In the steel mill furnace temperatures are checked with photoelectric pyrometers. In the Bessemer process a photoelectric registration of the variation in the light emission of the converter flame gives valuable information regarding

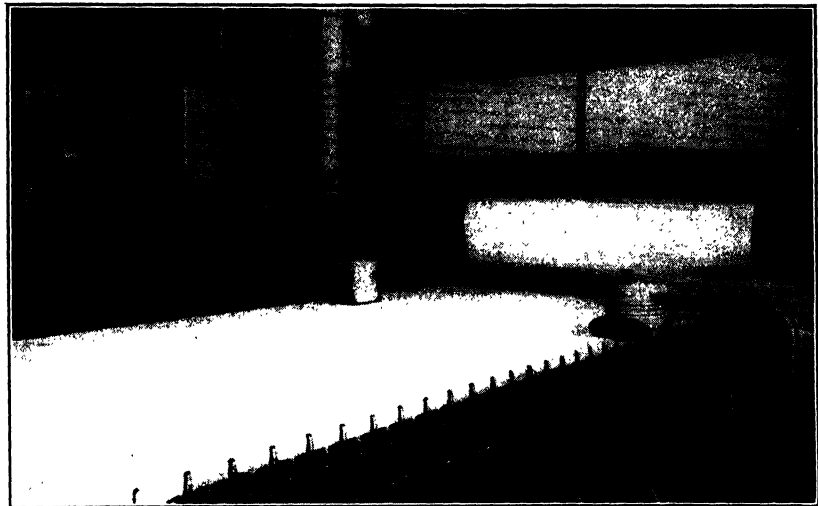


FIG. 19.20. General Electric Weft-Straightening Control Equipment Installed at Danvers Bleachery and Dye Works in Peabody, Mass. (Courtesy of General Electric Company.)

the nitrogen content and other properties of the steel so prepared.<sup>31</sup> Photoelectric relays make it possible to control pouring operations from a distance, dropping the pouring ladle back as soon as the light emission from the mold indicates that it is filled<sup>32</sup> (Fig. 19.21). Time-delay photorelays cut off the cold front portion of hot strip with a flying shear before approaching the finishing stands. Pinholes in sheet metal are detected by phototubes, preventing loss by spoilage in the canning industry. Photoelectric counters control the stacking of the cut sheets and stop conveyors when a prescribed number has been reached. In preparing rolls of sheet metal, side register controls are used as in the paper industry.

<sup>30</sup> See Zeluff, reference 28.

<sup>31</sup> See reference 29.

<sup>32</sup> See reference 30.

Several ingenious photoelectric methods have been developed for speeding up the cutting of metal sheet with blow torches from prescribed patterns. One of these, engineered by the General Electric Company and the Air Reduction Sales Company,<sup>33</sup> employs a pantograph linkage

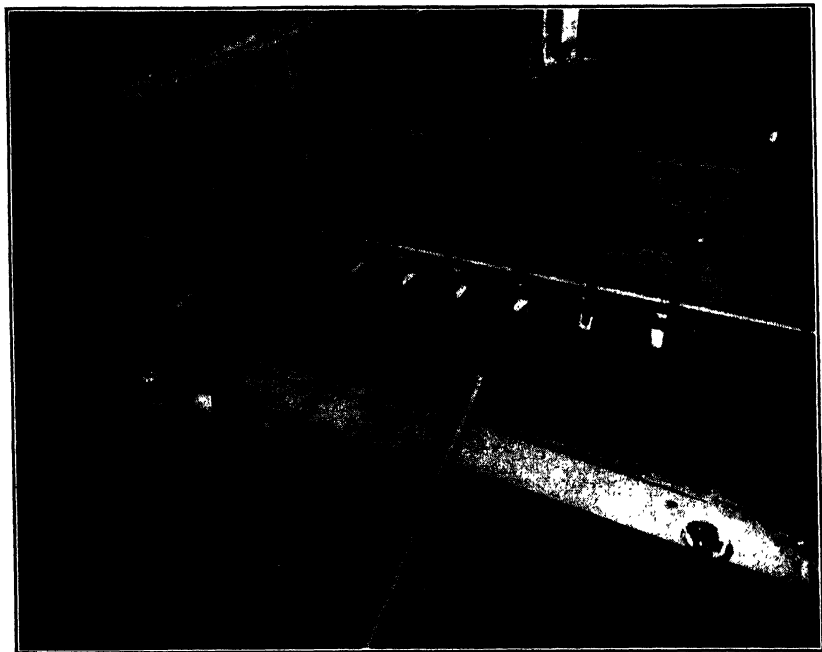


FIG. 19.21. Photoswitch Control of Automatic Pouring at American Brake Shoe Company Plant. (Reference 30.) (Courtesy of Photoswitch, Inc., New York.)

between a scanning head, traveling over a black-and-white pattern drawing, and the cutting torch. In this manner the motion of the scanning head on the pattern and that of the torch on the metal are at all times identical. The scanner projects a  $\frac{3}{32}$ -inch spot, offset with respect to the optic axis, on the edge of a pattern line so that half falls on white, half on black. If, as the scanner carriage moves over the pattern, driven by a motor, the spot shifts relative to the pattern line so that either more or less light enters the phototube, the phototube actuates a steering motor rotating the steering wheel and thus restores the equilibrium condition.

In the system developed by the Industrial Scientific Company<sup>34</sup> the controlling information is registered in the form of white dots on the

<sup>33</sup> See Helmkamp, reference 31.

<sup>34</sup> See Walker, reference 32.

circumferences of four black bakelite drums scanned by phototubes. One of these drums controls the longitudinal motion of the cutting torch, a second its transverse motion, and the other two determine whether these motions are in a forward or reversed direction. When a white dot on the drum controlling the longitudinal motion is scanned, the phototube causes a thyatron to fire, which stops the longitudinal motor and starts the transverse motor. Thus an inclined line is described by a zig-zag motion, the motors making as many as one hundred starts and stops per minute. A considerable number of units can be cut simultaneously. The longitudinal motion is performed by a carriage moving on tracks; the transverse motion, by moving the torches along arms projecting from the carriage. All four drums are inscribed simultaneously with jeweled styli as a scribing machine traces the finished product.

**Automatic Inspection.** An important use for phototubes in industry is the automatic inspection of products. An example is the sorting out



FIG. 19.22. Sorting Machines at the Plant of the Michigan Bean Company. (Reference 33.) (Courtesy of Michigan Bean Company.)

of off-color beans, peas, coffee beans, and so forth by machinery of the type used on a large scale at the plant of the Michigan Bean Company (Fig. 19.22).<sup>35</sup> The system is shown in Fig. 19.23. The beans are picked

<sup>35</sup> See reference 33.

up one at a time from a chute by a sorter, which exposes them to a light beam. The reflected light is directed by a half-silvered mirror to a red-

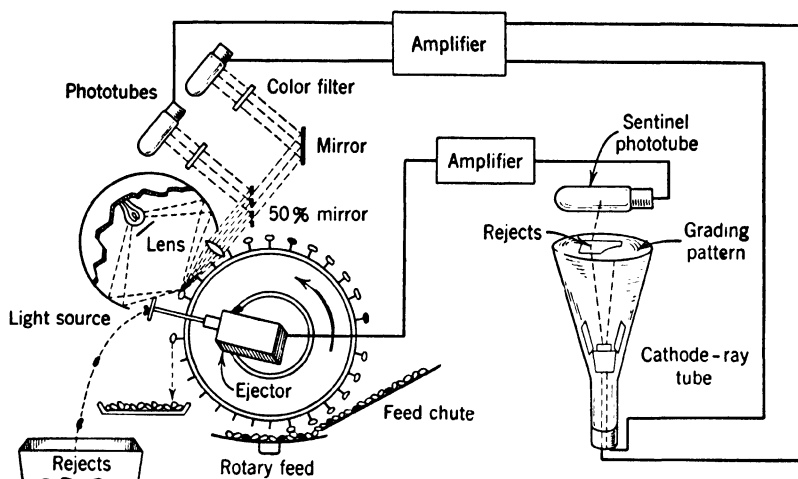


FIG. 19.23. Diagram of Bean-Sorting Machine. (Reference 33.) (Courtesy of *Electronics*.)

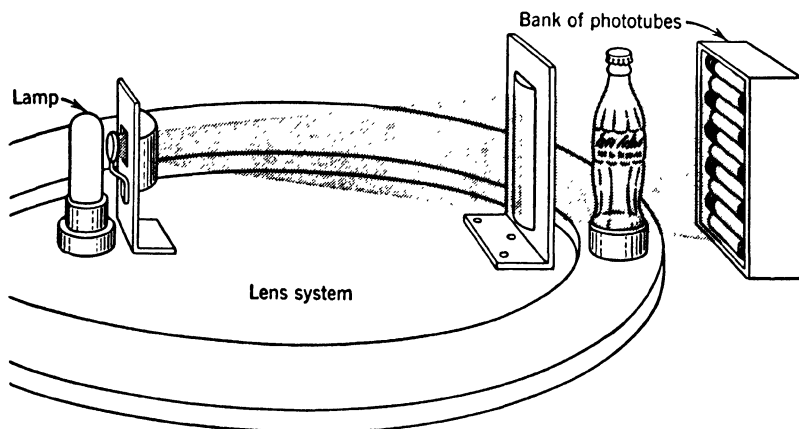


FIG. 19.24. Machine for Inspecting Bottled Beverages for Foreign Particles. (Reference 34.) (Courtesy of *Machine Design*.)

sensitive phototube (type 918) with a red filter and then, by a second mirror, to a blue-sensitive phototube (type 1P29) with a green filter. The outputs of the two phototubes are applied to the vertical and horizontal deflection of a cathode-ray tube. The color and brightness

of the bean are thus indicated by the position of the beam spot on the screen of the cathode-ray tube. A mask is made to cover the area of of the screen which corresponds to acceptable reflection characteristics of the bean. A third phototube, placed in front of the cathode-ray tube, thus receives light only when the bean is off-color: it then actuates a relay which projects the bean into the rejection bin.

Another food-inspection machine, developed by RCA for the Coca Cola Company, checks bottled beverages for foreign particles (Fig. 19.24).<sup>36</sup> A flat light beam passes through the bottle onto a bank of phototubes. The bottle is whirled, then stopped. Foreign particles in the liquid will continue to rotate and cause an alternating component in the photocurrent. This is detected, and the bottle is rejected. The same principle of whirling a glass jar or bottle and utilizing an alternating component in the transmitted light as a basis for rejection is used in an inspection system for detecting flaws in the container, developed by the General Electric Company and the Hartford Empire Company.<sup>37</sup>

**Photoelectric Gages.** Phototubes find manifold application in the routine measurement of thickness, time, distance, and even electric power. Figure 19.25 shows the principle of an electronic micrometer for wire, razor blades, tube stock, and so forth, developed by the Wilmotte Manufacturing Company.<sup>38</sup> A parallel light beam projects a shadow of the material to be measured on the central one of three rectangular apertures in a mask. The top aperture is made equal in area to the central aperture minus the minimum permissible area of the shadow of the material; the bottom aperture is made equal to the central aperture minus the maximum permissible area of the shadow of the material. The light passing through the three apertures falls on a phototube whose output is connected to the vertical deflection plates of a cathode-ray oscillograph. The horizontal deflection is made proportional to the time. It is controlled by a commutator on a chopping disk, which lets the light fall in turn on each of the three apertures, so that a complete horizontal deflection corresponds to the time during which one aperture is exposed. In this manner the top and bottom apertures form two lines of constant height, while the line corresponding to the central aperture fluctuates between them as the thickness of the specimen varies. If the thickness of the specimen exceeds the permissible limits in either direction, the line corresponding to the central aperture falls outside the region between the fixed lines. The persistence of the screen

<sup>36</sup> See reference 34.

<sup>37</sup> See reference 35. For the employment of phototubes in x-ray inspection methods, see Chapter 14, p. 315.

<sup>38</sup> See reference 36.



makes the three lines visible simultaneously. This system will check materials ranging from 0.005 inch to 0.6 inch in thickness to within  $\pm 0.0002$  inch.

The problem of controlling photoelectrically the width of a web or sheet has been solved by the General Electric Company in the manner shown schematically in Fig. 19.26.<sup>39</sup> A light beam reflected from the

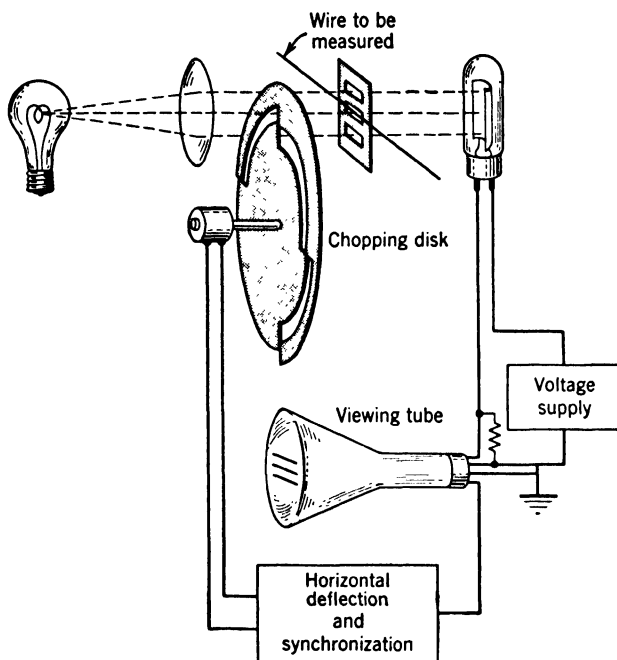


FIG. 19.25. Principle of Object Micrometer for Thin Materials. (Reference 36.)

mirror of a moving-coil galvanometer falls on each edge of the web, the uninterrupted part being collected by a phototube. The output of the phototube is amplified and applied to the moving-coil instrument in a direction to make the web cut off just half the beam. Thus, at any instant, the difference in photocurrent, and the mirror deflection, measure the deviation of the web edge from its normal position. The two differences for the two sides of the web are combined in the width-indicating instrument to yield a direct indication of the deviation in width of the web from the value corresponding to the equilibrium position of the galvanometer mirrors.

<sup>39</sup> See Alexander, reference 37.

Photoelectric gages are also useful in determining the elastic properties of wire and strip materials.<sup>40</sup> For this purpose a mask of alternating opaque and transparent horizontal strips is suspended from the sample and brought into registry with a similar fixed mask so that opaque strips just cover transparent strips and vice versa. No part of a light beam incident on one side of the masks will now fall on a photo-

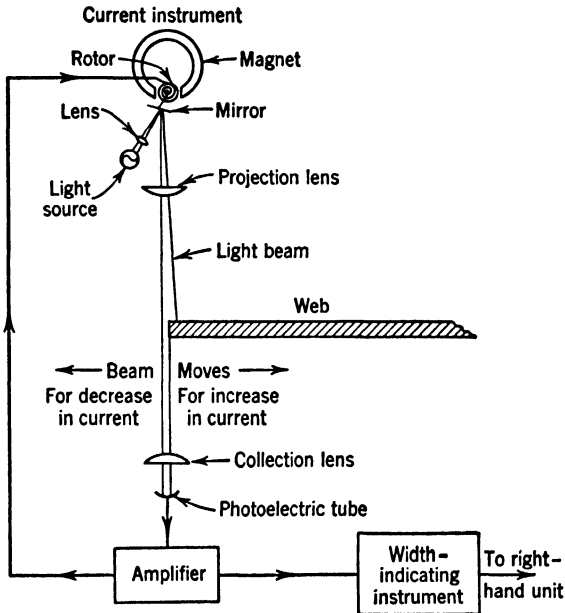


FIG. 19.26. System for Measuring Width of Web or Strip. (Alexander, reference 37.) (Courtesy of *Gen. Elec. Rev.*)

tube situated on the opposite side. On the other hand, as the sample is stretched by a known weight, the amount of light falling on the phototube is proportional to the extension of the sample.

Light beams and phototubes are also used by the Sheffield Corporation in a device for checking piston rings.<sup>41</sup> The ring is inserted in a master ring and rotated. One light beam directed at a phototube scans the separation of the sample ring and the master and causes the lighting of a rejection lamp if this exceeds the permitted tolerance; a mechanical shutter cuts off this beam as the gap is scanned. A second beam, scanning the gap, causes the lighting of other lamps if the gap is either

<sup>40</sup> See Zeluff, reference 28.

<sup>41</sup> See reference 38.

too large or too small. The whole inspection cycle takes less than 5 seconds.

A circuit for measuring the delay in the lighting of fluorescent lamps, suggested by Trevor Temple of the Sylvania Electric Products Company, is shown in Fig. 19.27.<sup>42</sup> As long as the lamp is not lighted and there is, therefore, no photocurrent, the cathode-follower stage draws a maxi-

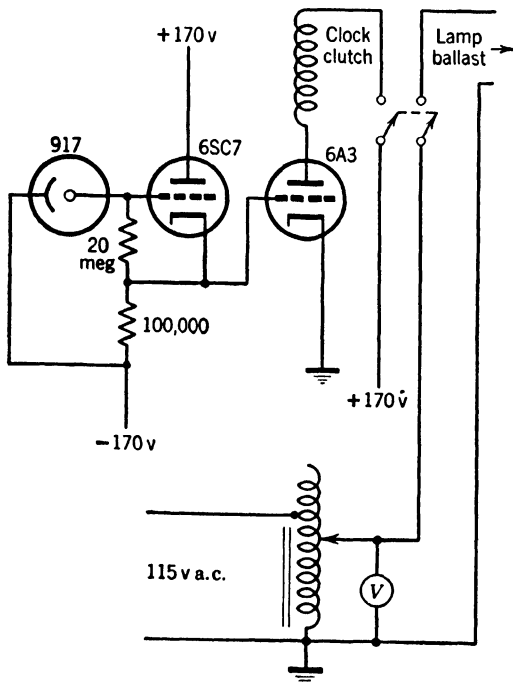


FIG. 19.27. Circuit for Measuring Time Delay of the Lighting of Fluorescent Lamps. (Reference 39.) (Courtesy of *Electronics*.)

mum current and causes the grid of the type 6A3 tube to be positive so that, on closing the lamp circuit, the clock clutch (requiring 40 to 50 milliamperes) is operated. As the tube lights, the photocurrent renders the grids of the type 6SC7 and type 6A3 tubes negative. This causes the clock clutch to drop, so that the clock indicates the delay between the closing of the switch and the lighting of the lamp.

Apparatus for the rapid testing of iris and focal-plane camera shutters has been developed by the Fairchild Camera and Instrument Company.<sup>43</sup> Figure 19.28 shows the principle of operation of the system for

<sup>42</sup> See reference 39.

<sup>43</sup> See Redemske, reference 40.

testing iris shutters. A parallel beam of light is incident on the shutter. The transmitted light falls on a diffusing plate whose emission is collected, in part, by a phototube. The amplified photocurrent, passing through a potential divider, actuates a set of ten styli. They are brought into contact with Teledeltos recording paper<sup>44</sup> on a rotating drum and trace out parallel lines as the input voltage on the individual thyatron circuits comes to exceed approximately 1 volt. The potential divider is

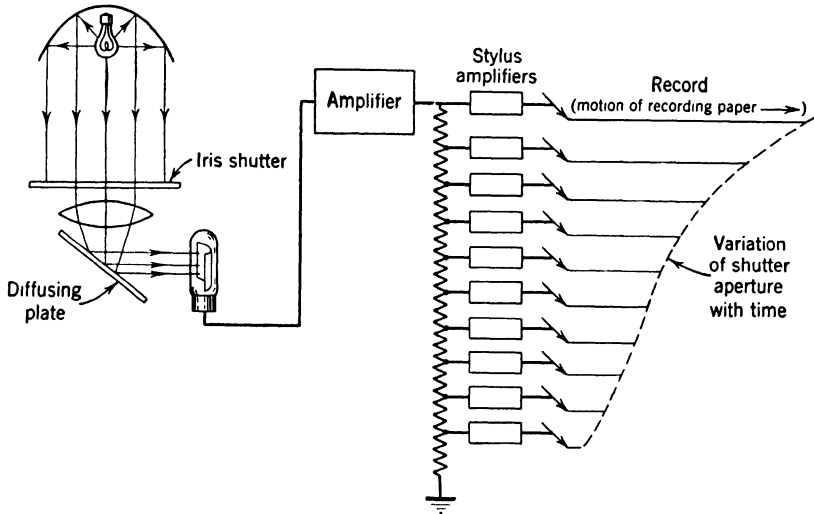


FIG. 19.28. System for Measuring Characteristics of Iris Shutters. (Redemske, reference 40.) (Courtesy of *Electronics*.)

arranged so that this occurs, successively, when the total drop across the divider exceeds 1, 11, 21, . . . 91 volts. The set of equally spaced parallel lines obtained in this manner fills out the area below the curve indicating the variation of light transmission with time.

Barrier-layer cells have been found useful in testing the output, in the range of 20 to 40 watts, of very-high-frequency (100 megacycle per second) transmitters.<sup>45</sup> For this purpose a lamp matching the antenna in impedance—for instance, a 60-watt, 110-volt lamp for a 70-ohm line—replaces the antenna. The cell, at the end of a bakelite tube, is placed sufficiently far from the lamp so that there is no danger of excessive heating. The photocurrent reading may then be taken as a measure of the power dissipation of the lamp.

<sup>44</sup> See Chapter 16, p. 358.

<sup>45</sup> See Maron, reference 41.

An application of the phototube which is of great importance to aviation is the system of measuring cloud heights developed by scientists of the General Electric Company and the U. S. Weather Bureau.<sup>46</sup> The principle of the system is illustrated in Fig. 19.29. A modulated light beam is projected vertically upward. It is scanned by a photoelectric "ceilometer" stationed at a distance of some 1000 feet. The cloud height is then given by the product of the base line and the tangent

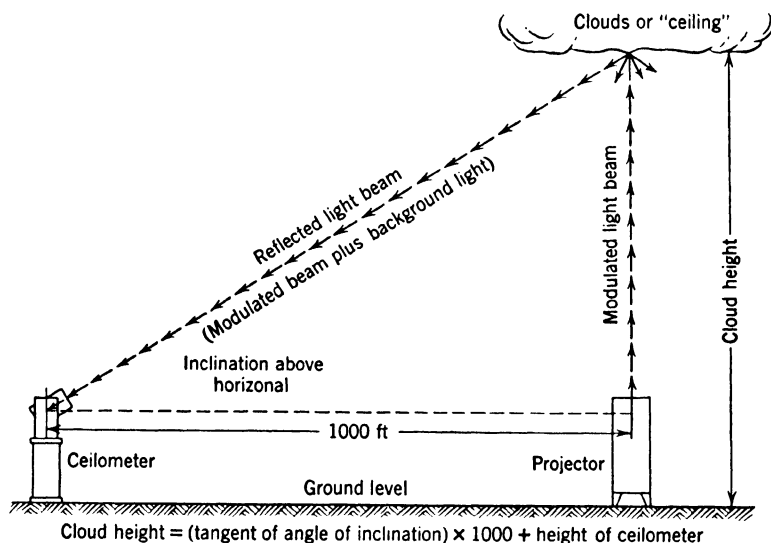


FIG. 19.29. Photoelectric Method of Determining Cloud Heights. (Houser, reference 42.) (Courtesy of *Gen. Elec. Rev.*)

of the angle of elevation of the ceilometer for which a strong signal is recorded. The external appearance of the ceilometer is shown in Fig. 19.30.

The most difficult feature of the design is overcoming the "noise"<sup>47</sup> arising from the strong daylight illumination which, even in the final design, is commonly a million times as great as that of the scattered signal beam. Hence a powerful, concentrated beam is essential. It is provided by a 900-watt airblast-cooled mercury arc lamp with a 24-inch reflector; its light emission is modulated 96 per cent at 120 cycles per second. Furthermore, the photocurrent generated by the light incident on the phototube in the ceilometer must be filtered so that the indicating instruments are controlled by a very narrow frequency band

<sup>46</sup> See Houser, reference 42.

<sup>47</sup> See Chapter 13, p. 250.

about 120 cycles per second. This is made possible by making the angular scanning speed of the ceilometer very small (1 cycle in 12 minutes) and electrically chopping the output so that current is transmitted only during the positive half cycles of the modulating current. Background noise, which may be either positive or negative in these intervals, aver-



FIG. 19.30. The Ceilometer. (Courtesy of General Electric Company.)

ages to zero, while the signal adds up to an amount proportional to the period of the recording instrument. In practice two records are obtained. The first shows the variation of the signal strengths with time and thus indicates the densities of the clouds; the second recorder is biased to leave an indication only when the signal exceeds an amount corresponding to reflection at a cloud and thus yields simply the variation in ceiling with time. The pen deflection is given here by the angle of elevation of the ceilometer. Cloud heights exceeding 20,000 feet are readily measured in full daylight by this method. Balloon-borne photoelectric devices for measuring the depth of clouds at various altitudes had

before then been developed by F. W. Dunmore of the Bureau of Standards.<sup>48</sup>

**Phototubes in Astronomy.** Phototube attachments for the objective measurement of star intensities were employed by Guthnick<sup>49</sup> on the 50-inch reflector at the Babelsberg Observatory near Berlin as early as 1924. Not long afterward E. and B. Strömgren<sup>50</sup> used the transit of star images across a set of apertures in front of a phototube to leave a

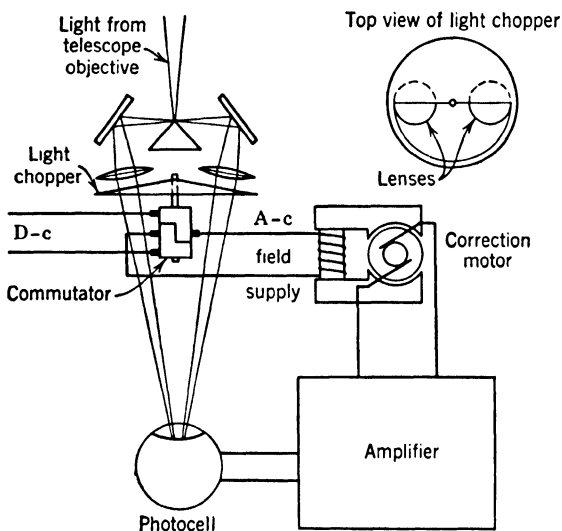


FIG. 19.31. Principle of Photoelectrically Controlled Telescope Drive. (Whitford and Kron, reference 46.) (Courtesy of *Rev. Sci. Instruments*.)

time record of the passage of the star across the meridian, obtaining, in this manner, accurate measurements of fixed-star positions. More recently one of the important uses of the phototube in astronomy has been the accurate guidance of telescopes, so that star images are maintained in stationary position during a prolonged exposure. The clock-work drive of the telescope alone is not adequate for this purpose. Figure 19.31 shows the principle of a photoelectrically controlled drive constructed by Whitford and Kron<sup>51</sup> at the Washburn Observatory of the University of Wisconsin in 1937. The image of the guiding star is focused on the edge of a roof prism which splits the incident light into two beams guided separately, with the aid of mirrors and lenses, to the

<sup>48</sup> See Winters, reference 43.

<sup>49</sup> See Guthnick, reference 44.

<sup>50</sup> See Simon and Suhrmann, reference 45.

<sup>51</sup> See reference 46.

cathode of the same multiplier phototube. A light-chopping disk, half transparent and half opaque, interrupts the two beams alternately. Hence the photocurrent contains an alternating component if the star image deviates from the prism edge, with a phase determined by the direction of the deviation. This alternating component corrects the clock drive. The system is sufficiently sensitive so that a star of magnitude 8.6 may be guiding star for a 60-inch reflector. The arrangement shown corrects the motion in one direction only. For correction along two rectangular coordinates the system would have to be duplicated, either using two knife-edge prisms at right angles to each other and two guiding stars, or a four-sided pyramid with a single guiding star.

One of the authors<sup>52</sup> has proposed a somewhat similar system, employing inertia-free electronic methods of correction, to eliminate the disturbing effects of atmospheric currents on sidereal images. The image of the star field produced by the telescope is projected on the photocathode of an image iconoscope,<sup>53</sup> whose mosaic is provided with a small central aperture. The observer views a picture of the field on a television receiver controlled by the picture signals delivered by the image iconoscope. Below an aperture in the mosaic there is a four-sided pyramid whose sides form the first target electrodes of four electron multipliers. The output of these electron multipliers is fed to a magnetic deflecting yoke about the image section of the image iconoscope in such a manner that the guiding star is always centered on the apex of the pyramid, regardless of fluctuations of the star images on the photocathode. Since the electron image on the mosaic remains, thus, perfectly stationary, the image on the television receiver screen also remains sharp and stationary throughout.

A photoelectric sight for a coronagraphic telescope at the Harvard College Observatory in Colorado is described by W. O. Roberts.<sup>54</sup> The problem here is to keep the sun's image accurately centered on a reflecting disk in the focal plane of the telescope, so as to permit the corona to be photographed without interference of scattered light from the sun, which is some 600,000 times as bright as the detail of interest in the corona. The problem was solved by mounting rigidly on the barrel of the telescope a sighting telescope of smaller aperture but equal focal length (Fig. 19.32). At the focus of the sighting telescope a disk slightly smaller than the sun's image is mounted. Light from the North, South, East, and West points on the edge of the disk is guided by lucite rods to four phototubes. The difference in output of the North and

<sup>52</sup> See Zworykin, reference 47.

<sup>53</sup> See Chapter 17, p. 386.

<sup>54</sup> See reference 48.





FIG. 19.32. Photoelectric Sight for Coronagraphic Telescope of Harvard Observatory. (Roberts, reference 48.) (Courtesy of Dr. W. O. Roberts.)

South phototubes is used to correct the declination of the telescope; that of the East and West phototubes, to correct the hour angle drive. In the control amplifier <sup>55</sup> (Fig. 19.33) the pair of phototubes acts as a potential divider for the input of a low grid current (type 38) amplifier

<sup>55</sup> Designed by Mr. J. R. Balsley.

tube. If the solar disk is decentered, the relays controlling an antihunt unit are either both closed or both opened, depending on the direction of the decentering. In either case a time-delay switching motor is started which, eventually, connects the main correcting motor with the control amplifier and thus rectifies the orientation of the telescope. This switching arrangement is designed to prevent the operation of the correction system in response to the random vibration of the solar image

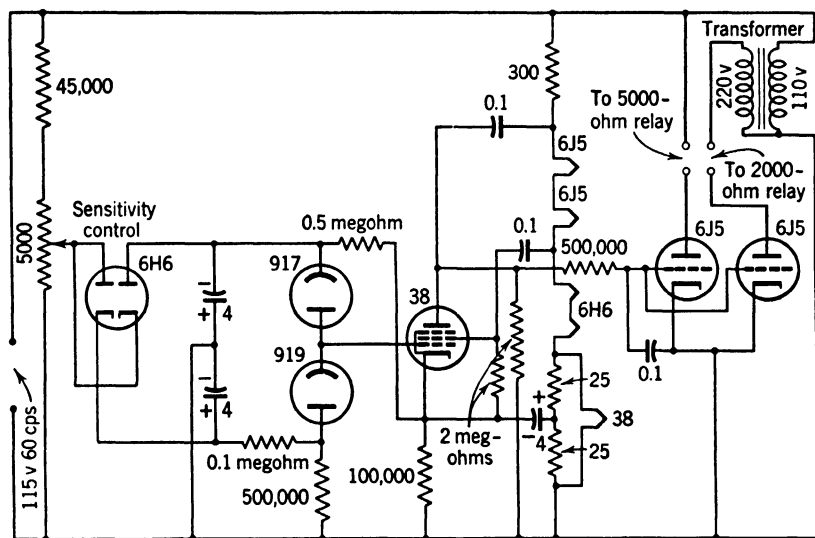


FIG. 19.33. Control Amplifier for Photoelectric Sight. (Roberts, reference 48.)  
(Courtesy of *Electronics*.)

arising from atmospheric currents. It is interesting to note that the system has been in operation for two years, with temperatures ranging from  $-29^{\circ}\text{C}$  to  $+18^{\circ}\text{C}$ , without even requiring inspection of the electronic equipment.

An important problem in the study of galaxies is the determination of the number and magnitudes of the stars in a given field. Since this number may be as large as 50,000, any mechanical simplification of the counting process is a decided advantage. Figure 19.34 shows a photoelectric system for counting stars and classifying them according to magnitude developed by McCuskey and Scott<sup>56</sup> at the Case School Observatory in East Cleveland. The several star images are brought in turn into coincidence with the reduced image of a light source. The transmitted light falls on a type 918 phototube, whose output is am-

<sup>56</sup> See reference 49.

plified and applied to a sequence of thyratron counters, which are adjusted to fire whenever the star magnitude is greater than a set series of prescribed values.

A very ingenious use of the phototube by A. E. Whitford of Washburn Observatory is the determination of star sizes from the diffraction

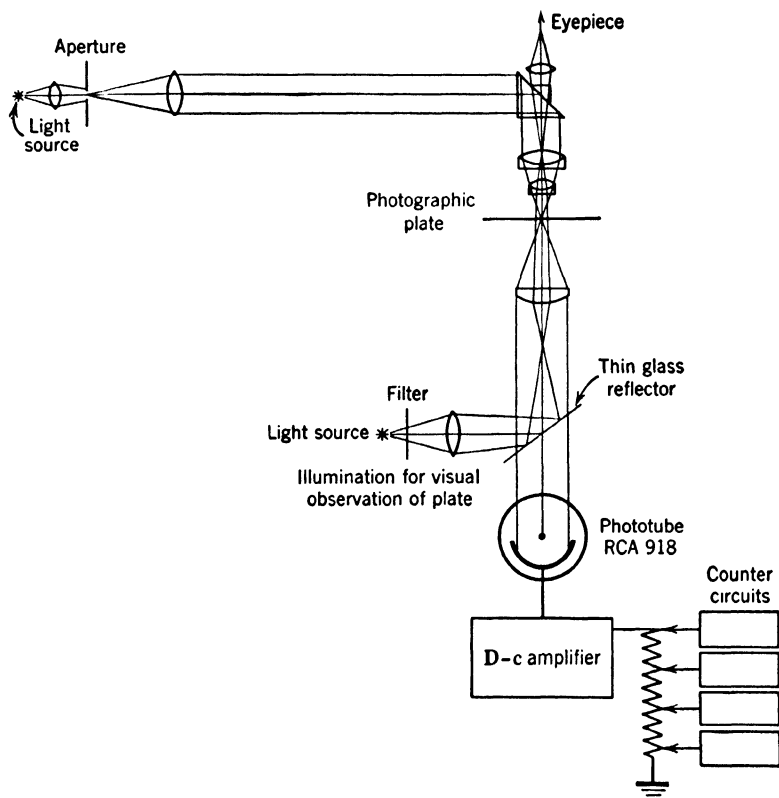


FIG. 19.34. System for Counting and Classifying Stars. (McCuskey and Scott, reference 49.) (Courtesy of *Rev. Sci. Instruments*.)

of the star light as the star passes behind the lunar disk.<sup>57</sup> With the moon at a distance of 238,000 miles from the earth, the diffraction fringes are approximately 30 feet apart and travel over the earth's surface at a speed of over 1000 miles per hour. The finite size of the star reduces the amplitude of the intensity variations in the fringes. Thus the pattern produced, by the output of a phototube exposed to the diffracted light, on an oscillograph with a horizontal sweep period of the order of  $\frac{1}{50}$  second indicates the size of the star producing the fringes.

<sup>57</sup> See reference 50.

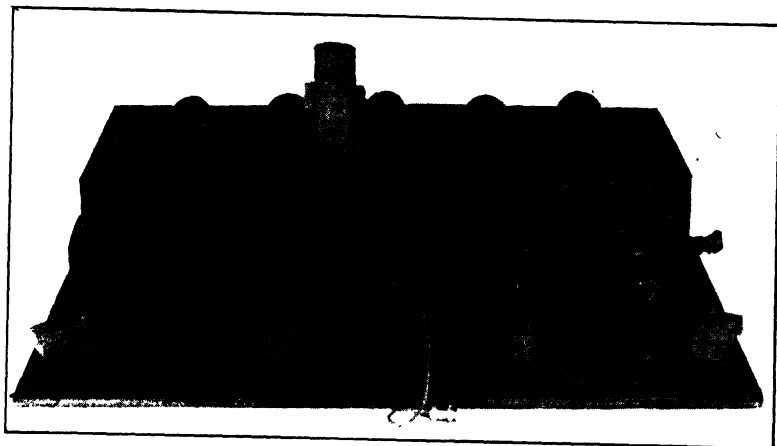
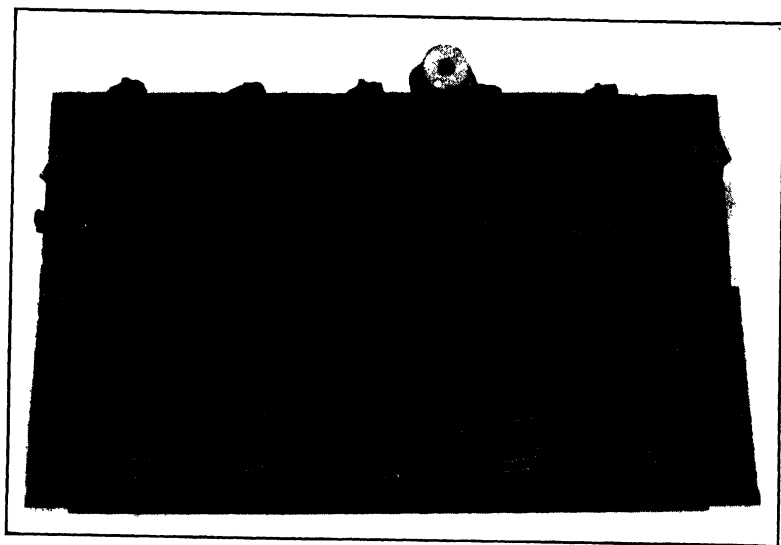
*a**b*

FIG. 19.35. Mechanism of Electronic Organ; (a) Rear View, (b) Top View. (Campbell and Greenlee, reference 51.) (Courtesy of Mr. L. E. Greenlee.)

**Photoelectric Organ.** R. E. Campbell and L. E. Greenlee<sup>58</sup> have built a simple photoelectric organ whose mechanism is represented in Fig. 19.35. It consists of five basic units, corresponding to five octaves. The system for a single octave is shown in Fig. 19.36. The light from a

<sup>58</sup> See reference 51.

direct-current-operated lamp passes through a tone wheel having twelve circular sound tracks corresponding to the twelve notes in an octave. A shutter operated by a key on the organ keyboard prevents the transmission of light to a mirror unless the key is depressed. The light which strikes the mirror is reflected, through a graded diffusing plate operated by a volume-control pedal, onto the cathode of a phototube. The output of the phototube is amplified and applied to a loudspeaker. Green-

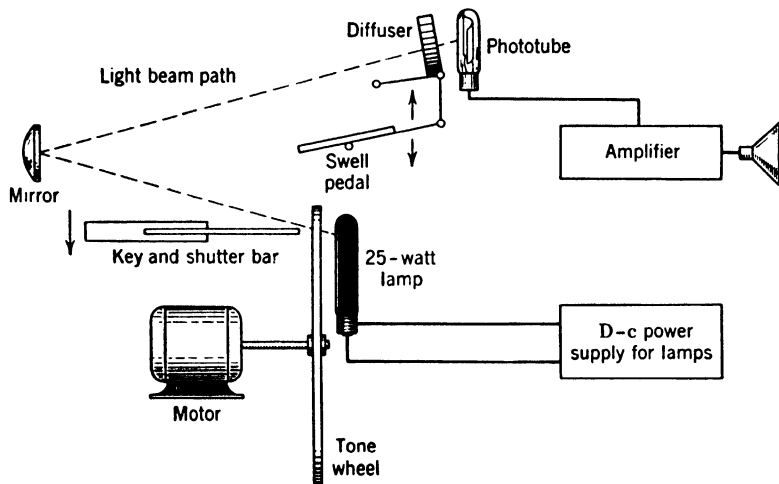


FIG. 19.36. Tone-Generating System for One Octave of Photoelectric Organ. (Campbell and Greenlee, reference 51.) (Courtesy of *Radio News*.)

lee<sup>59</sup> found it also possible to dispense with the shutter and mirrors by providing a set of minute flashlight lamps registered with the individual sound tracks, placing the phototube on the other side of the tone wheel, and keying the lamps individually.

**Photoelectric Aids for the Blind.** It stands to reason that the photoelectric cell, popularly known as the “electric eye,” should find use in supplementing the senses of the sightless. Efforts to realize this have taken primarily two directions: the development of reading machines and guiding devices for the blind.

The first of the reading machines—the Optophone of Fournier d’Albe<sup>60</sup>—has a siren disk with five or more rings of apertures so spaced as to interrupt the light from a linear filament source at frequencies

<sup>59</sup> See reference 52.

<sup>60</sup> See reference 53.

corresponding to the musical notes  $g$ ,  $c'$ ,  $d'$ ,  $e'$ , and  $g'$  (Fig. 19.37). The disk is imaged through a slit in a selenium photoconductive cell on a line of type on a printed page resting on a glass plate, the five modulated light spots falling on a line of the same height as the type, perpendicular to the printed line. The reflected light falls on the selenium cell, which controls an earphone or loudspeaker. The nature of the sound emitted by the loudspeaker thus depends on the amount of black and white in

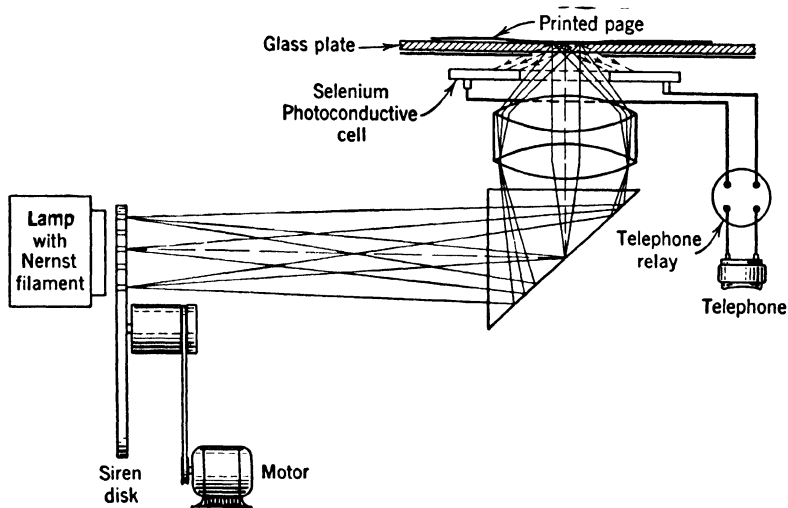


FIG. 19.37. Fournier D'Albe's Optophone (Schematic).

the vertical section of a letter scanned by the light spots at any instant. As the page is slowly moved parallel to the printed lines a series of characteristic sounds are emitted which the blind person can learn to identify as corresponding to different letters.

Other instruments, such as the Visagraph,<sup>61</sup> have attempted to translate printed matter into raised type so that the tactile sense of the reader might be substituted for sight, as in Braille. As in the Optophone, the line of type is scanned by a series of light spots modulated at different frequencies. The output of the single phototube is fed to frequency-discriminating circuits which actuate magnetic plungers to produce raised letters on thin aluminum sheet. This sheet is translated across the line of plungers by the same drive that moves the original across the scanning beam.

Although this second system may have valuable applications in facilitating the perception of drawings and diagrams, the auditory method

<sup>61</sup> See Walker and Lance, reference 54, pp. 325-328.

appears more promising for rapid reading. It has, accordingly, received most attention in recent years. In the approach to the problem it came to be realized that any reading machine, to be satisfactory, should permit the hand scanning of the reading matter with an easily manipulated stylus or probe, should be relatively insensitive to the alignment of the



FIG. 19.38. A Photoelectric Reading Machine. (Zworykin and Flory, reference 55.)

pickup with the type, should be usable with different sizes of type, should respond to black rather than white signals, and should give distinctive signals for different letters or words.

An instrument constructed in an attempt to meet these conditions is shown, in use, in Fig. 19.38.<sup>62</sup> It is seen to consist of a hand-held stylus, a small case containing batteries and electric circuit components, and an earphone. The print is scanned by a light spot vibrating at 30 cycles per second across the line of type. The reflected light is collected by a phototube. The output of the phototube controls the amplitude of a tone generator whose frequency is varied in synchronism with the spot

<sup>62</sup> See Zworykin and Flory, reference 55.

scanning the line of type. At the top of the line the frequency is high; at the bottom, low.

The interior of the stylus is shown in Fig. 19.39. Light from a small aircraft indicator lamp in a light-tight housing is reflected by a 45-degree mirror, mounted on a magnetized armature and vibrated by current passing through a coil, and focused into a small spot on the page. The diffusely reflected light is guided by a lucite rod to the photocathode

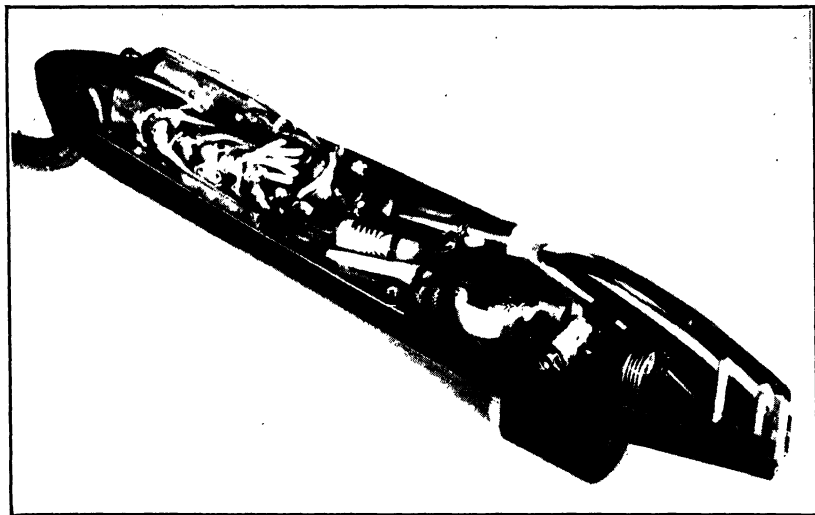


FIG. 19.39. Construction of Stylus of Reading Machine. (Zworykin and Flory, reference 55.)

of a type 1P42 miniature phototube. The output of the phototube is amplified by a two-stage hearing-aid tube amplifier in the stylus and then guided by cable to the main amplifier in the case.

The tone in the earphone is produced by beating together the outputs of two oscillators with resonant frequencies near 50,000 cycles per second. One of them has a fixed frequency; the frequency of the other is varied by vibrating the core of the tuning inductance in phase with the vibration of the scanning spot. The amplitude of the beat note is controlled by the photocurrent and drops to zero when the photocurrent corresponds to reflection from the white background of the page.

It has been found that the tones corresponding to the several letters can be learned fairly rapidly. Although the maximum reading speeds obtained so far—of the order of 15 words per minute—are by no means adequate, the results are sufficiently promising to justify further work



in this direction. It is reasonable to expect the attainment of much higher reading speeds with a machine, now under development, which identifies the individual letters and pronounces either the letters or their characteristic sounds, providing a phonetic rendering of the printed words.

A photoelectric guidance device for the blind, which is as yet in an experimental stage, has been developed by the Signal Corps Engineering Laboratories.<sup>63</sup> This device projects a narrow beam of modulated light

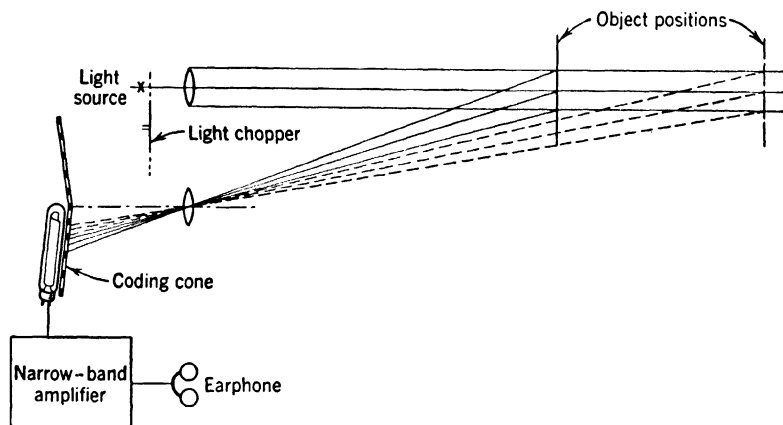


FIG. 19.40. Principle of Operation of Guidance Device. (Cranberg, reference 56.)

in the direction in which it is pointed (Fig. 19.40). In addition to the projector it has a detector for the light reflected by any object in the path of the beam. Depending on the distance of the object, the reflected light falls on a different section of a "coding cone" which imposes either a low-frequency modulation varying with distance or easily differentiated dot-dash signals. The transmitted light falls on a phototube whose output is passed through a stage of amplification tuned to the modulating frequency (500 cycles per second) and then through a regular hearing-aid amplifier. The apertures in the coding disk are shaped to minimize the introduction of high-frequency harmonics which might arise from intense ambient light.

Figure 19.41 shows the complete device, with the projector, showing both the  $f/1.5$  lens and modulating disk, at the top, the detector, with a second  $f/1.5$  lens and the coding disk, in the center, and the amplifier case, swung to the side, at the bottom. The light source is a 3-watt flashlight lamp. Different pure signals are obtained when the reflecting

<sup>63</sup> See Cranberg, reference 56

object is at a distance of 3.5, 5, 7, 10, and 20 feet. In effect, the guidance unit constitutes a nonmaterial cane with which the user can probe his environment over a range of 3 to 20 feet without danger of damage or offense. This sets definite limits to its sphere of usefulness as sensory aid. A broadening of its functions, as well as an improvement in the ease

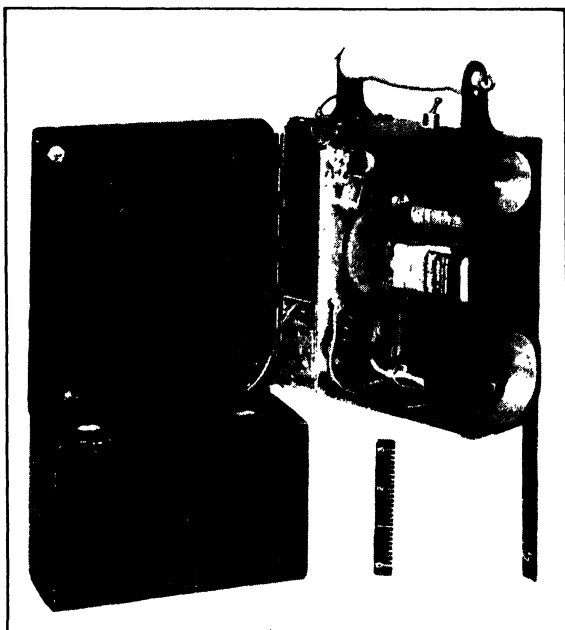


FIG. 19.41. The Guidance Device, Showing Internal Construction. (Courtesy of Signal Corps Engineering Laboratories.)

of interpretation of its indications, must await further research and experiment.

#### REFERENCES

1. C. E. MARSHALL, "Photoelectric street lighting control," *Electronics*, Vol. 19, pp. 134-136, September, 1946.
2. S. L. BELLINGER, "High-speed photolight," *Gen. Elec. Rev.*, Vol. 47, pp. 31-33, March, 1944.
3. K. M. LAING, "Sensitive photoelectric control," *Electronics*, Vol. 19, pp. 174, 178, 182, October, 1946.
4. G. ASSETT, "A photoelectric galvanometer amplifier," *Electronics*, Vol. 18, pp. 126-129, February, 1945.
5. R. D. VALENTINE, "Dual time signal at WQXR," *Electronics*, Vol. 17, pp. 108-109, November, 1944.

6. R. J. WEY and J. H. JUPE, "Electronic operation of a standard stopwatch," *Electronics*, Vol. 17, pp. 202, 206, 210, October, 1944.
7. G. L. BUSH, "Photoelectric transmitting typewriter," *Electronics*, Vol. 20, pp. 96-99, April, 1947.
8. D. J. FAUSTMAN, "Automatic map tracer for land navigation," *Electronics*, Vol. 17, pp. 94-99, November, 1944.
9. W. I. BENDZ, "Applying electronic door openers," *Electronics*, Vol. 11, pp. 14-17, February, 1938.
10. "Photoelectric system controls traffic in Continental Divide Tunnel," *Elec. Eng.*, Vol. 61, p. 457, 1942.
11. B. LANGE, *Photoelements*, Reinhold Publishing Corporation, New York, 1938.
12. J. H. JUPE, "Phototube controls swing bridge," *Electronics*, Vol. 10, p. 36, March, 1937.
13. "Traffic count printed hourly by photoelectric recorder," *Electronics*, Vol. 16, pp. 130, 132, May, 1943.
14. P. B. WEISZ, "Electronic fire and flame detector," *Electronics*, Vol. 19, pp. 106-109, July, 1946.
15. "Detecting fire at sea," *Electronics*, Vol. 17, p. 125, July, 1944.
16. E. R. MORIN, "Air-conditioning safety device for theatres," *J. Soc. Motion Picture Engrs.*, Vol. 37, pp. 307-312, 1941.
17. W. W. MACDONALD, "Electronic intrusion detection systems," *Electronics*, Vol. 15, pp. 38-43, February, 1942.
18. "Flame failure control for industrial furnaces," *Electronics*, Vol. 17, pp. 152, 154, 156, September, 1944.
19. "Photoelectric eye guards against mishaps," *Product Eng.*, Vol. 14, p. 482, 1943.
20. R. A. POWERS, "Phototube controls punch press," *Electronics*, Vol. 10, pp. 21-23, July, 1937.
21. "Photoelectric switch gives remote control for huge machine," *Sci. Am.*, Vol. 175, p. 23, 1946.
22. "Smoke density indicator and recorder for industrial plants," *Electronics*, Vol. 18, p. 148, February, 1945.
23. R. C. McNICKLE, "Phototube control of fluid flow," *Electronics*, Vol. 17, pp. 110-113, September, 1944.
24. W. D. COCKRELL, "Radar techniques in an industrial control," *Elec. Eng.*, Vol. 66, pp. 365-368, 1947.
25. "Side shift of paper corrected in roll-winding machine," *Electronics*, Vol. 16, pp. 144, 146, 148, April, 1943.
26. W. D. COCKRELL, "Phototube control of packaging machinery," *Electronics*, Vol. 16, pp. 94-99, 180, 182, October, 1943.
27. "Phototube weft straightening in textile industry," *Electronics*, Vol. 18, pp. 316, 321, 324, November, 1945.
28. V. ZELUFF, "Metals by electronics," *Sci. Am.*, Vol. 172, pp. 210-212, 1945.
29. "Phototube control for Bessemer steelmaking," *Electronics*, Vol. 14, pp. 124-126, June, 1941.
30. "Automatic metal pouring in foundries," *Electronics*, Vol. 18, p. 152, June, 1945.
31. R. F. HELMKAMP, "Electronics actuates tracer control," *Machine Design*, Vol. 18, pp. 137-142, April, 1946.
32. D. S. WALKER, "Phototube-controlled flame cutter," *Electronics*, Vol. 18, pp. 100-103, July, 1945.
33. "Phototubes control food-sorting system," *Electronics*, Vol. 19, p. 152, July, 1946.

34. "Automatic inspection of bottled beverages," *Machine Design*, Vol. 18, pp. 107-108, July, 1946.
35. "Bottle watcher automatically rejects those with flaws," *Sci. Am.*, Vol. 173, p. 51, 1945.
36. "Electronic micrometer for thin materials," *Electronics*, Vol. 19, p. 190, October, 1946.
37. E. H. ALEXANDER, "Measuring width of moving webs and strips by light beam and photoelectric devices," *Gen. Elec. Rev.*, Vol. 44, pp. 615-617, November, 1941.
38. "Photoelectric gauging of piston rings," *Electronics*, Vol. 18, p. 148, May, 1945.
39. "Fluorescent lamp delay timer," *Electronics*, Vol. 20, pp. 184-188, March, 1947.
40. R. F. REDEMSKE, "Electronic shutter testing," *Electronics*, Vol. 19, pp. 128-134, February, 1946.
41. W. MARON, "Power measurement at very high frequencies," *Electronics*, Vol. 18, p. 216, October, 1945.
42. P. H. HOUSER, "Cloud heights and densities," *Gen. Elec. Rev.*, Vol. 48, pp. 7-12, April, 1945.
43. S. R. WINTERS, "Determining cloud depths," *Radio News*, Vol. 29, pp. 44-45, 106, October, 1943.
44. P. GUTHNICK, "A new photoelectric star photometer," *Z. Instrumentenk.*, Vol. 44, pp. 303-310, July, 1924.
45. H. SIMON and R. SUHRMANN, *Lichtelektrische Zellen und ihre Anwendung*, J. Springer, Berlin, 1932.
46. A. E. WHITFORD and G. E. KRON, "Photoelectric guiding of astronomical telescopes," *Rev. Sci. Instruments*, Vol. 8, pp. 78-82, 1937.
47. V. K. ZWORYKIN, "Telectroscope," U. S. Patent 2,304,755, filed October 11, 1940.
48. W. O. ROBERTS, "Photoelectric sight for solar telescope," *Electronics*, Vol. 19, pp. 100-103, June, 1946.
49. S. W. McCUSKEY and R. M. SCOTT, "A photoelectric counter," *Rev. Sci. Instruments*, Vol. 12, pp. 597-601, 1941.
50. "Moon has no atmosphere," *Science News Letter*, Vol. 50, p. 181, September 21, 1946.
51. R. E. CAMPBELL and L. E. GREENLEE, "Photo-electronic organ," *Radio News*, Vol. 35, pp. 25-27, June, 1946.
52. L. E. GREENLEE, "Photoelectric tone generator," *Electronics*, Vol. 19, pp. 93-95, September, 1946.
53. E. E. FOURNIER D'ALBE, "On a type-reading optophone," *Proc. Roy. Soc. (London)*, Vol. A 90, pp. 373-375, 1914.
54. R. C. WALKER and T. M. C. LANCE, *Photoelectric Cell Applications*, Pitman Publishing Corporation, New York, 1938.
55. V. K. ZWORYKIN and L. E. FLORY, "Reading aid for the blind," *Electronics*, Vol. 19, pp. 84-87, August, 1946.
56. L. CRANBERG, "Sensory aid for the blind," *Electronics*, Vol. 19, pp. 116-119, March, 1946.

## Chapter 20

# PHOTOCELLS IN THE FUTURE

It may confidently be expected that development in the field of photocells will follow the same pattern in the future as it has in the past. As new discoveries are made in photoelectricity, new applications will be found; and these applications, in turn, will direct research into channels which will lead to new discoveries.

**Retrospect.** After Elster and Geitel and Hallwachs had realized, in the zinc amalgam and the copper oxide cells, photocells of reproducible and permanent characteristics, the potential usefulness of the photoelectric effect for objective photometry became obvious. This stimulated a search for photosensitive materials which would respond to the visible as well as to the ultraviolet. The evacuated alkali phototubes, sensitive to the visible and, eventually, to the near infrared, resulted. With the creation of stable cells sensitive to visible light the applications multiplied rapidly and, with them, the demand for ever greater sensitivity. In particular, the needs of the new art of television led to the development of entirely new types of phototubes, such as the multiplier phototube and the image tube. Numerous applications of the great sensitivity of the multiplier phototube for the measurement of extraordinarily small quantities of light and the counting of high-speed particles and x-ray quanta have already been noted. The infrared-sensitive image tube, on the other hand, has realized the prediction made by one of the authors many years ago:

The present indications are, however, that attention will be focused upon the infra-red region of the spectrum. The cells that will ultimately be developed will respond most readily to heat radiations that are totally invisible to the human eye. The natural application will be *nocturnal vision*. It is not at all fantastic to expect a simplified form of television apparatus which will pick up heat radiations from invisible physical objects and transform them into visible outlines on a suitable screen.<sup>1</sup>

The cesium-cathode image tube has not, however, represented an endpoint in the development of infrared-sensitive devices. On the con-

<sup>1</sup> Zworykin and Wilson, reference 1, p. 321.

trary, it has stimulated the development of photocells which would respond to infrared radiation beyond the range of the known photoemissive surfaces, since they would permit the employment of such radiations for signaling purposes without the danger of detection by other means. The lead sulfide, lead selenide, and other photoconductive cells met this need.

**Scope for Future Advances.** Further advances in this direction are to be expected. They will take the form of an extension of the response to longer wave lengths and an increase in the photosensitivity or "quantum efficiency" of the photoemissive devices. It should be noted, however, that a shift in the sensitivity to longer and longer wave lengths is not necessarily advantageous. Thus, in signaling applications, the signal intensity must be increased with increasing wave length to override the effects of the random thermal radiation of the surroundings. In an enclosure at room temperature, the number of quanta incident per second on a square centimeter of area is, on the average, within a range of 1 per cent of the wave length, given, according to Planck's law,<sup>2</sup>

at 1 micron:	by 1	at 5 microns:	by $10^{15}$
at 2 microns:	by $10^{10}$	at 10 microns:	by $10^{16}$

Simultaneously, it becomes increasingly difficult to obtain signaling sources with very high specific emission with increasing wave length.

The useful upper limit of the quantum efficiency of a photosensitive device is, at any one wave length, unity. Higher quantum efficiencies lead to no appreciable reduction in the least light signal that can be measured or reproduced. In the range of quantum efficiencies above unity this least light signal is determined by the random fluctuations in the number of light quanta incident on the photosensitive device.<sup>3</sup>

<sup>2</sup> See Chapter 2, p. 16.

<sup>3</sup> This applies primarily to photoemissive devices in which the shot noise of the photoelectrons leaving the cathode is the only important noise source; this condition is realized most perfectly in multiplier phototubes, particularly if the tube is cooled to minimize thermionic emission. The quantum efficiency is then simply the ratio of the number of electrons leaving the cathode to the number of light quanta falling on it. In photoconductive and photovoltaic cells other noise sources, in particular thermal or resistance noise, are present; in addition, the measurable output current is not equal to the primary photocurrent. Such cells should hence be compared with photoemissive cells on the basis of the signal-to-noise ratio in their output, under identical conditions of illumination and for the same frequency band. Some such comparisons have been given in Chapter 13. The effective quantum efficiency of a photoconductive or photovoltaic cell might then be defined as the product of the quantum efficiency of the photoemissive cell with which it is compared and the square of the ratio of the signal-to-noise ratio of the cell in question and that of the comparison cell.

The quantum efficiencies of several commercially available types of phototubes, at a number of different wave lengths, are given in Table 20.1. It is seen that they range from 13 per cent at the blue end of the visible spectrum (S-4 surface) to about 0.3 per cent at the red end (S-1 surface). At the mercury resonance line in the ultraviolet (2537 A.U.) the quantum efficiency of the S-5 surface is 10 per cent, whereas in the near infrared the optimum value attained, with the S-1 surface, is only 0.3 per cent. Higher values for the quantum efficiencies are, of course, obtained in various experimental and special-purpose tubes. They range from about 25 per cent at the blue end of the visible spectrum to about 2 per cent at the red end and in the near infrared (8000 A.U.).

TABLE 20.1. AVERAGE QUANTUM EFFICIENCIES OF PHOTOTUBES AT VARIOUS WAVE LENGTHS

Type	Wave Length, A.U.								
	2537	3400	4000	5000	6000	7000	8000	9000	10,000
922 S-1				0.0010	0.0019	0.0029	0.0031	0.0022	0.0008
926 S-3			0.0049	0.0035	0.0019	0.0010	0.0004		
929 S-4		0.13	0.13	0.073	0.009				
935 S-5	0.10	0.10	0.074	0.037	0.006				

It appears, therefore, that there is relatively little room for improvement at the shorter wave lengths, but a great deal at the longer wave lengths, in particular the red and infrared. This is true even in view of the excellent results achieved with modern photoconductive cells.

The relatively low efficiency of available phototubes at the longer wave lengths of the visible spectrum is brought out graphically by Fig. 20.1, which represents the photosensitivity of the surfaces listed in Table 20.1 as function of wave length. It is seen that the sensitivity of available photocathodes has a minimum near 6500 Angstrom units.<sup>4</sup> The fact that barrier-layer cells show high sensitivity in this region does not remove the need for phototubes with a similar response, since the barrier-layer cells are suitable neither for the measurement of very low light levels nor for high-frequency applications.

**Ultimate Limits in the Enhancement of Vision.** The question naturally presents itself as to what extent the photoelectric effect may be used to enhance human vision—not only at the very short (ultraviolet) and very long (infrared) wave lengths, to which the eye is insensitive, but also at the peak of sensitivity of the eye. It should be noted to begin with that the eye is a remarkably sensitive organ. At the peak of

<sup>4</sup> The characteristic of the S-8 surface is intermediate between those of the S-4 and S-3 surfaces.

sensitivity for monochrome vision<sup>5</sup> it is estimated that approximately 70 light quanta are sufficient, on the average, to elicit a sensation of light.<sup>6</sup> Of these, only 1 to 4 quanta are absorbed by quantum processes

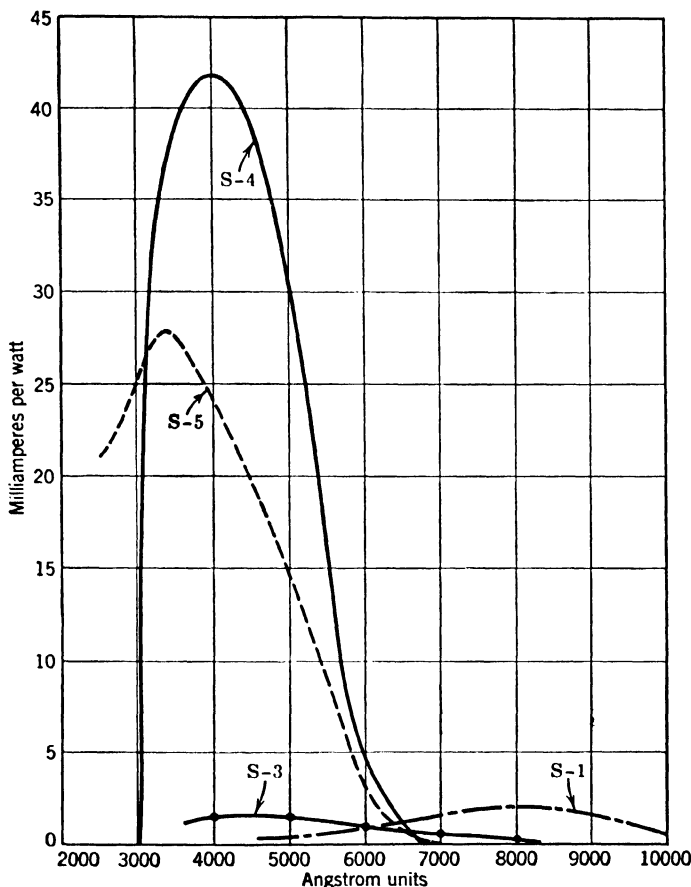


FIG. 20.1. Spectral Sensitivities of Standard Photocathodes.

which contribute to vision.<sup>7</sup> It is an interesting feature of the eye that the number of quanta required for detection of a light source does not

<sup>5</sup> Monochrome, or rod, vision, in the peripheral portions of the retina, has a maximum of sensitivity at 5100 Angstrom units. Cone vision at the center of fixation of the eye, which is responsible for the discrimination of color, demands approximately 4200 quanta for the perception of a source.

<sup>6</sup> See De Vries, reference 2. Seventy quanta correspond to about  $3 \cdot 10^{-17}$  joule and a light flux of about  $7.5 \cdot 10^{-17}$  watt, the stimulus being effectively integrated over about 0.4 second.

<sup>7</sup> See De Vries, reference 2, and Hecht, reference 3.



increase materially if the source is spread over a visual angle as large as 30 minutes, although at high light levels sources separated by angles as small as 1 minute are resolved. As the brightness is increased, the resolving power of the eye increases by a large factor.

A photoelectric system for enhancing the perception of the eye is represented schematically in Fig. 20.2. Such a system has already been discussed, briefly, in Chapter 9, page 172. The object  $O$  is focused by a large-aperture lens  $L$  on the photocathode of the multiple image tube

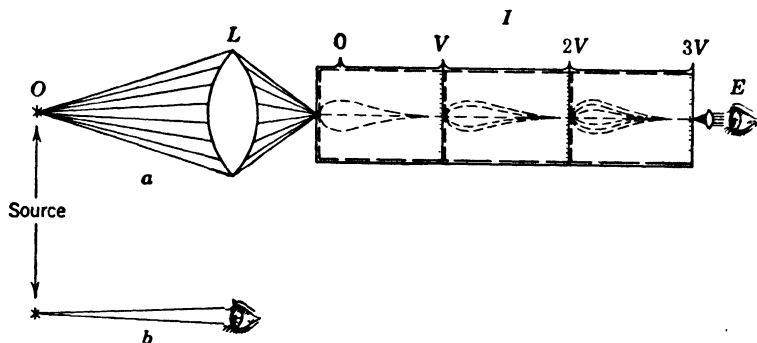


FIG. 20.2. Perception of a Faint Light Source (a) with a Multiplier Image Tube and (b) with the Unaided Eye. Gain in signal-to-noise ratio:

$$\cong 6 \left( \frac{\text{Number of electrons emitted by 1st photocathode}}{\text{Number of light quanta reaching unaided eye}} \right)^{1/2}$$

Gain in apparent brightness: Ratio of total number of light quanta reaching pupil of eye.

*I.* The image tube is assumed to increase the brightness of the image by a large factor before it is presented to the eye  $E$ . Since a very large number of light quanta are emitted by the final screen for every photoelectron leaving the photocathode, the signal-to-noise ratio in the image ultimately formed on the retina of the eye is limited only by the solid angle of the cone of light accepted by the lens and the quantum efficiency  $k$  of the photocathode. Assume that approximately 1 quantum in 40 of those incident on the retina gives rise to a quantum absorption contributing to the visual process. Then, if the diameter of the lens is  $D$ , and that of the pupil is  $d$ , the gain in the signal-to-noise ratio over that of the unaided eye becomes  $6k^{1/2}D/d$ . In the observation of a very faintly illuminated scene, this gain will take the form of showing an increased amount of detail to the eye, which, as just noted, has the remarkable faculty of adjusting, within limits, its perception of detail to the available light intensity. In some respects the action of the system described is reminiscent of that of the ordinary telescope or micro-

scope. However, in these cases the apparent brightness of the image observed by the eye is never increased above that of the object. More detail may become visible than with the unaided eye; but this detail will be spread over a larger solid angle, so that the image will not appear sharper than the object. Only the combination of the large-aperture lens and image-intensifying tube makes possible an increase in resolution and brilliance without increase in apparent size. Thus the photoelectric effect offers the possibility of seeing what is now invisible, not because it is too small or too distant, but because it emits too little light for the unaided eye to perceive it.

**Compact Photocells of High Output.** Apart from the trend toward the detection of ever lower light levels, which is approaching its theoretical limit in modern multiplier phototubes, a trend may be expected in the direction of photocells of increasing compactness and simplicity of operation, yielding very high output currents. The cadmium sulfide photoconductive crystals described in Chapter 10, page 193, exemplify this tendency. In these crystals, as in thallous sulfide photoconductive cells, the number of charges transferred by the photocurrent far exceeds the number of primary photoelectric excitations. Such large secondary currents may, in principle, arise in two different ways. Either photoexcitation modifies the charge distribution within the crystal in a manner favorable to the passage of current between cathode and anode, or the primary photoelectrons receive sufficient accelerations between collisions to excite other electrons, resulting in an avalanche of electrons for each primary excitation. The first mechanism has been postulated to explain the secondary currents in thallous sulfide. Since its effectiveness depends on a long lifetime of the photoexcited states which create the modified space-charge distribution, a large current gain is directly connected with a large time lag. In addition, the light response of photoconductors of this type may be expected to be nonlinear. The second type of current multiplication should be observed only in very thin insulating layers to which electric fields close to the break-down field for the material in question are applied. Even so, photoconductors of either or both types may find important uses in view of their extraordinary compactness and the simplicity of the auxiliary equipment required.

**Conversion of Solar Energy into Electric Power.** It is a tantalizing fact that enormous quantities of solar energy, falling on deserts and lakes, go to waste. It has already been pointed out <sup>8</sup> that, at the latitude of Washington, D. C., at noontime on an average clear day, energy is received from the sun at the rate of approximately 700 watts per square meter. Averaged around the clock, this quantity may be reduced by a

<sup>8</sup> See Chapter 14, p. 277.

factor of the order of 5,<sup>9</sup> leaving 140 watts per square meter. It is not surprising that many attempts have been made to harness this energy for useful purposes. Perhaps the simplest of these attempts is the direct conversion of sunlight into electrical energy with the aid of photovoltaic cells. By utilizing the figure of 58 microwatts per lumen for the maximum power conversion efficiency of a selenium cell<sup>10</sup> and Luckiesh's estimate of 100 lumens per watt for the light content of solar radiation reaching the earth's surface,<sup>11</sup> the conversion efficiency of a selenium cell for solar radiation becomes approximately 0.6 per cent. Thus, of the 140 watts per square meter provided by the sun, the selenium cell could make available not quite 1 watt of electrical power per square meter of cell surface. Even this amounts to over 2000 kilowatts per square mile. A cell area 200 miles in diameter would match, in power output, the total electric power plant capacity of the United States (estimated at 70 million kilowatts). Up to the present this photovoltaic method of utilizing solar energy has not been able to compete economically with water power, wind power, and solar energy stored in plants during past ages. Low conversion efficiency, large initial cost, and the production of a relatively inconvenient form of electrical power (direct current) combine to lead to this result. It must be left to the future whether the discovery of materially more efficient cells will reopen this possibility of the conversion of solar energy.

**New Materials for Phototubes.** The hope of utilizing the heaviest of the alkali metals, element 87, for which the name francium has been proposed, to form photocathodes superior in their red and infrared sensitivity to cesium-activated surfaces, appears more remote than ever. The only known isotope of this element is radioactive and has a half life of only 21 minutes.<sup>12</sup> On the other hand, there is every reason to believe that the future will familiarize us with new types of compound photocathodes, whose characteristics represent improvements, in specific directions, over those of any now known. It need be remembered only that the remarkable properties of the group of photocathodes of which the antimony-cesium surface is the principal exponent were quite unforeseen. The next important advance may be attained, as in the past, largely by accident, in pursuit of some other goal; or, again, it may be reached through a better understanding of the electrical properties of

<sup>9</sup> This accounts for night and day, variation in the angle of incidence of the solar radiation, and change in atmospheric absorption with time of day. See Fowle, reference 4, p. 418.

<sup>10</sup> See Chapter 11, p. 211. The light responses to sunlight and 2700° K tungsten light are very nearly equal.

<sup>11</sup> See Luckiesh, reference 5, page 92.

<sup>12</sup> See Mattauach and Flügge, reference 6, p. 158.

solid matter. In any case, it may be taken for granted that careful search and patient study in this field will continue to be rewarded by furthering the progress of science and contributing to the amenities of daily life.

#### REFERENCES

1. V. K. ZWORYKIN and E. D. WILSON, *Photoelectric Cells and Their Application*, 2nd Edition, John Wiley and Sons, New York, 1934.
2. H. DE VRIES, "The quantum character of light and its bearing on threshold of vision, differential sensitivity, and visual acuity of the eye," *Physica*, Vol. 10, pp. 553-564, 1943.
3. S. HECHT, "Quantum relations of vision," *J. Optical Soc. Am.*, Vol. 32, pp. 42-49, 1942.
4. F. F. FOWLE, *Smithsonian Physical Tables*, Smithsonian Institution, Washington, D. C., 7th Edition, 1929.
5. M. LUCKIESH, "Light and Work," D. Van Nostrand Company, New York, 1924.
6. J. MATTAUCH, *Nuclear Physics Tables*, and S. FLÜGGE, *An Introduction to Nuclear Physics*, Interscience Publishers, Inc., New York, 1946.



# APPENDIX

TABLE A1. THE CHEMICAL ELEMENTS BY ATOMIC NUMBER

(The asterisk denotes elements which have been prepared only artificially. Atomic weight figures here denote the atomic weight of the stablest isotope which has been prepared. For element 61 the name promethium, Pm, has also been suggested.)

<i>Atomic Number</i>	<i>Element</i>	<i>Sym- bol</i>	<i>Atomic Weight</i>	<i>Atomic Number</i>	<i>Element</i>	<i>Sym- bol</i>	<i>Atomic Weight</i>
1	Hydrogen	H	1.0078	49	Indium	In	114.8
2	Helium	He	4.002	50	Tin	Sn	118.70
3	Lithium	Li	6.940	51	Antimony	Sb	121.76
4	Beryllium	Be	9.013	52	Tellurium	Te	127.5
5	Boron	B	10.82	53	Iodine	I	126.932
6	Carbon	C	12.00	54	Xenon	Xe	130.2
7	Nitrogen	N	14.008	55	Cesium	Cs	132.81
8	Oxygen	O	16.000	56	Barium	Ba	137.36
9	Fluorine	F	19.00	57	Lanthanum	La	138.90
10	Neon	Ne	20.183	58	Cerium	Ce	140.13
11	Sodium	Na	22.997	59	Praseodymium	Pr	140.92
12	Magnesium	Mg	24.32	60	Neodymium	Nd	144.27
13	Aluminum	Al	26.97	61 *	Cyclonium	Cy	
14	Silicon	Si	28.06	62	Samarium	Sm	150.43
15	Phosphorus	P	31.02	63	Europium	Eu	152.0
16	Sulfur	S	32.06	64	Gadolinium	Gd	157.3
17	Chlorine	Cl	35.457	65	Terbium	Tb	159.2
18	Argon	A	39.944	66	Dysprosium	Dy	162.46
19	Potassium	K	39.10	67	Holmium	Ho	163.5
20	Calcium	Ca	40.08	68	Erbium	Er	167.64
21	Scandium	Sc	45.10	69	Thulium	Tm	169.4
22	Titanium	Ti	47.90	70	Ytterbium	Yb	173.5
23	Vanadium	V	50.95	71	Cassiopeium	Cp	175.0
24	Chromium	Cr	52.01	72	Hafnium	Hf	178.6
25	Manganese	Mn	54.93	73	Tantalum	Ta	181.4
26	Iron	Fe	55.84	74	Tungsten	W	184.0
27	Cobalt	Co	58.94	75	Rhenium	Rh	186.31
28	Nickel	Ni	58.69	76	Osmium	Os	190.8
29	Copper	Cu	63.57	77	Iridium	Ir	193.1
30	Zinc	Zn	65.38	78	Platinum	Pt	195.23
31	Gallium	Ga	69.72	79	Gold	Au	197.2
32	Germanium	Ge	72.60	80	Mercury	Hg	200.61
33	Arsenic	As	74.93	81	Thallium	Tl	204.39
34	Selenium	Se	78.961	82	Lead	Pb	207.22
35	Bromine	Br	79.916	83	Bismuth	Bi	209.00
36	Krypton	Kr	82.9	84	Polonium	Po	210
37	Rubidium	Rb	85.44	85 *	Astatine	At	211
38	Strontium	Sr	87.63	86	Radon	Rn	222
39	Yttrium	Y	88.92	87 *	Francium	Fr	
40	Zirconium	Zr	91.22	88	Radium	Ra	225.97
41	Columbium	Cb	93.3	89	Actinium	Ac	227
42	Molybdenum	Mo	96.0	90	Thorium	Th	232.12
43 *	Technetium	Tc		91	Protactinium	Pa	231
44	Ruthenium	Ru	101.7	92	Uranium	U	238.14
45	Rhodium	Rh	102.94	93 *	Neptunium	Np	237
46	Palladium	Pd	106.7	94 *	Plutonium	Pu	239
47	Silver	Ag	107.880	95 *	Americium	Am	
48	Cadmium	Cd	112.41	96 *	Curium	Cu	

TABLE A2. PERIODIC TABLE OF THE ELEMENTS

	Group I	Group II	Group III	Group IV	Group V	Group VI	Group VII	Group VIII
Period I							1 H	2 He
II	3 Li	4 Be	5 B	6 C	7 N	8 O	9 F	10 Ne
III	11 Na	12 Mg	13 Al	14 Si	15 P	16 S	17 Cl	18 Ar
IV	19 K	20 Ca	21 Sc	22 Ti	23 V	24 Cr	25 Mn	26 27 28 Fe Co Ni
	29 Cu	30 Zn	31 Ga	32 Ge	33 As	34 Se	35 Br	36 Kr
V	37 Rb	38 Sr	39 Yt	40 Zr	41 Nb	42 Mo	43 Tc	44 45 46 Ru Rh Pd
	47 Ag	48 Cd	49 In	50 Sn	51 Sb	52 Te	53 I	54 Xe
VI	55 Cs	56 Ba	57-71 Rare earths	72 Hf	73 Ta	74 W	75 Re	76 77 78 Os Ir Pt
	79 Au	80 Hg	81 Tl	82 Pb	83 Bi	84 Po	85 At	86 Rn
VII	87 Fr	88 Ra	89-96 Actinides					

Rare earths: 57 58 59 60 61 62 63 64 65 66 67 68 69 70 71  
La Ce Pr Nd Sm Eu Gd Tb Dy Ho Er Tm Yb Lu

Actinides: 89 90 91 92 93 94 95 96  
Ac Th Pa U Np Pu Am Cm

TABLE A3. UNITS AND CONVERSION FACTORS

The MKS (Meter-Kilogram-Second) system of units possesses the advantage that it permits the employment of the familiar practical units (volt, ampere, watt, ohm, farad, henry) in the fundamental relations of electromagnetism without the addition of numerical coefficients. The relations of MKS units and other commonly employed units are given below.

## MECHANICAL UNITS

(Usual  
symbols)

*Length*

$$\begin{aligned}
 1 \text{ meter} &= 100 \text{ centimeters} = 1000 \text{ millimeters} = 10^6 \text{ microns} \\
 \text{m} &\qquad \qquad \text{cm} \qquad \qquad \qquad \text{mm} \qquad \qquad \qquad \mu \\
 &= 10^9 \text{ millimicrons} = 10^{10} \text{ Angstrom units} = 10^{13} \text{ X-units} \\
 &\qquad \qquad \text{m}\mu \qquad \qquad \qquad \text{A.U.} \qquad \qquad \qquad \text{X.U.} \\
 &= 3.2808 \text{ feet} = 39.3700 \text{ inches} \\
 &\qquad \qquad \text{ft} \qquad \qquad \qquad \text{in.}
 \end{aligned}$$

TABLE A3. UNITS AND CONVERSION FACTORS (*Continued*)(Usual  
symbols) $(m, M)$ *Mass*

$$1 \text{ kilogram} = 1000 \text{ gram} = 2.2046 \text{ pounds (av.)} = 35.2740 \text{ ounces (av.)}$$

$$\begin{array}{cccc} \text{kg} & \text{g} & \text{lb} & \text{oz} \\ & = 1.5432 \cdot 10^4 \text{ grains} & & \end{array}$$

$$\text{gr}$$

 $(t, \tau, T)$  *Time*

$$1 \text{ second} = 1.6667 \cdot 10^{-2} \text{ minute} = 2.7778 \cdot 10^{-4} \text{ hour}$$

$$\begin{array}{ccc} \text{sec} & \text{min} & \text{h} \\ & = 1.1574 \cdot 10^{-5} \text{ day} = 3.1682 \cdot 10^{-8} \text{ year} & \\ & \text{d} & \text{yr} \end{array}$$

 $(f, F)$ *Force*

$$1 \text{ newton} = 10^5 \text{ dynes} = 101.97 \text{ gram weight} = 7.2330 \text{ poundal}$$

$$= 0.2248 \text{ pound weight}$$

 $(p, P)$ *Pressure*

$$1 \text{ newton/meter}^2 = 10 \text{ dynes/centimeter}^2 = 10^{-5} \text{ bar}$$

$$\begin{array}{c} \text{barye} \\ = 0.9869 \cdot 10^{-5} \text{ atmosphere} \\ \text{atm} \\ = 7.5006 \cdot 10^{-3} \text{ millimeters of mercury} \\ \text{mm Hg, tor} \\ = 1.4504 \cdot 10^{-4} \text{ pounds/inch}^2 \\ \text{lb/in.}^2 \end{array}$$

 $(W, w)$ *Energy*

$$1 \text{ joule} = 10^7 \text{ ergs} = 2.778 \cdot 10^{-7} \text{ kilowatt-hour} = 0.23889 \text{ gram-calorie}$$

$$= 2.3889 \cdot 10^{-4} \text{ kilogram-calories} = 9.480 \cdot 10^{-4} \text{ British thermal unit}$$

 $(P, E)$ *Power*

$$1 \text{ watt} = 10^7 \text{ ergs/second} = 10^{-3} \text{ kilowatt} = 1.3412 \cdot 10^{-3} \text{ horsepower}$$

$$= 650 \text{ lumens (at } \lambda = 5550 \text{ A.U.)}$$

## ELECTRICAL UNITS

In the conversion factors given here the velocity of light is approximated by  $3 \cdot 10^8$  meters/second; cgs electrostatic units are indicated by esu, cgs electromagnetic units, by emu

(Usual  
symbols) $(R, r)$ *Resistance*

$$1 \text{ ohm} = 10^{-6} \text{ megohm} = (9 \cdot 10^{11})^{-1} \text{ esu} = 10^9 \text{ emu}$$

$$\Omega$$

 $(i, I)$ *Current*

$$1 \text{ ampere} = 10^3 \text{ milliamperes} = 10^6 \text{ microamperes} = 3 \cdot 10^9 \text{ esu}$$

$$\begin{array}{ccc} \text{amp} & \text{ma, mA} & \mu\text{a, } \mu\text{A} \\ & = 10^{-1} \text{ emu} & \end{array}$$

 $(e, V, \mathcal{E}, \Phi)$  *Electromotive Force or Electric Potential*

$$1 \text{ volt} = (300)^{-1} \text{ esu} = 10^8 \text{ emu}$$



TABLE A3. UNITS AND CONVERSION FACTORS (*Continued*)(Usual  
symbols)

(q)

*Charge*

$$1 \text{ coulomb} = 3 \cdot 10^9 \text{ esu} = 10^{-1} \text{ emu}$$

(C)

*Capacitance*

$$1 \text{ farad} = 10^6 \text{ microfarads} = 10^{12} \text{ micromicrofarads} = 9 \cdot 10^{11} \text{ esu}$$

$$\text{fd} \qquad \qquad \mu\text{f} \qquad \qquad \mu\mu\text{f}$$

$$= 10^{-9} \text{ emu}$$

(L)

*Inductance*

$$1 \text{ henry} = 10^3 \text{ millihenrys} = 10^6 \text{ microhenrys} = (9 \cdot 10^{11})^{-1} \text{ esu}$$

$$\text{mh} \qquad \qquad \mu\text{h}$$

$$= 10^9 \text{ emu}$$

(E)

*Electric field strength*

$$1 \text{ volt/meter} = (3 \cdot 10^4)^{-1} \text{ esu} = 10^6 \text{ emu}$$

(D)

*Dielectric flux density*

$$1 \text{ coulomb/meter}^2 = 3 \cdot 10^5 \text{ esu} = 10^{-5} \text{ emu}$$

(N, Φ)

*Magnetic flux*

$$1 \text{ weber} = (300)^{-1} \text{ esu} = 10^8 \text{ maxwells (emu)}$$

(B)

*Magnetic flux density*

$$1 \text{ weber/meter}^2 = (3 \cdot 10^6)^{-1} \text{ esu} = 10^4 \text{ gauss (emu)}$$

(H)

*Magnetic field strength*

$$1 \text{ MKS oersted} = 3 \cdot 10^7 \text{ esu} = 10^{-3} \text{ oersted (emu)}$$

(ε, k)

*Dielectric constant of vacuum*

$$(9 \cdot 10^9)^{-1} \text{ second/(ohm} \cdot \text{meter)}$$

(μ)

*Permeability of vacuum*

$$10^{-7} \text{ ohm} \cdot \text{second/meter}$$

## PHOTOMETRIC UNITS \*

(Recom-  
mended  
symbols)

(F)

*Luminous flux*

$$1 \text{ lumen} = \text{average light emission, as visually determined, of 1 candle into unit solid angle (steradian).}$$

\* Based in part on the Report of the Committee on Nomenclature and Standards of the Illuminating Engineering Society (*Illuminating Engineering*, Vol. 36, pp. 813-848, 1941). See also Committee on Colorimetry, "The psychophysics of color," *J. Optical Soc. Am.*, Vol. 34, pp. 245-266, 1944.

TABLE A3. UNITS AND CONVERSION FACTORS (*Continued*)

(Recommended symbols)

(U) *Radiant flux*

1 watt = 660 lumens of radiation at peak of visual sensitivity (5550 A.U.)

1 hololumen = radiant flux from a tungsten filament lamp having a color temperature of 2848° K, comprising a luminous flux of 1 lumen.

(I) *Luminous intensity* (luminous flux per unit solid angle in a given direction)  
1 candlepower(B) *Brightness* (luminance—luminous intensity of a surface in a given direction per unit projected area of the surface as viewed from that direction)  
1 candle/meter<sup>2</sup> = 10<sup>-4</sup> stilb = 3.142 · 10<sup>-4</sup> Lambert  
= 6.45 · 10<sup>-4</sup> candles/inch<sup>2</sup> = 0.292 foot-Lambert(E) *Illumination* (illuminance—density of luminous flux on a surface)  
1 lux = 0.0929 foot-candle = 10<sup>-4</sup> phot

TABLE A4. PHYSICAL CONSTANTS IN MKS UNITS

(Based on R. T. Birge, "A New Table of Values of the General Physical Constants as of August 1941," *Reviews of Modern Physics*, Vol. 13, pp. 233-239, October, 1941.)

velocity of light, $c$	$2.9978 \cdot 10^8$ meter · sec <sup>-1</sup>
charge of the electron, $-e$	$-1.6020 \cdot 10^{-19}$ coulomb
mass of the electron, $m$	$9.107 \cdot 10^{-31}$ kg
specific charge of the electron, $-e/m$	$-1.759 \cdot 10^{11}$ coulomb/kg
mass of the proton, $M_p$	$1.6725 \cdot 10^{-27}$ kg
mass of unit atomic weight	$1.6604 \cdot 10^{-27}$ kg
atomic weight of proton (on chemical scale)	1.0073
Planck's constant, $h$	$6.624 \cdot 10^{-34}$ joule · sec
Boltzmann's constant, $k$	$1.3805 \cdot 10^{-23}$ joule · deg <sup>-1</sup>
Avogadro's number, $N_o$	$6.023 \cdot 10^{26}$ (kg-mole) <sup>-1</sup>
Loschmidt number, $n_o$	$2.687 \cdot 10^{25}$ meter <sup>-3</sup>
Ice point on absolute scale	273.16° K
Stefan-Boltzmann constant, $\sigma$	$5.672 \cdot 10^{-8}$ watt · meter <sup>-2</sup> · deg <sup>-4</sup>
Wien's displacement law constant, $A$	$2.897 \cdot 10^{-2}$ meter · deg
threshold wave length corresponding to work function of 1 electron volt	$1.2395 \cdot 10^{-6}$ meter (1.2395 $\mu$ )
mechanical equivalent of heat	$4.185 \cdot 10^{-3}$ joule (kg-calorie) <sup>-1</sup>
least mechanical equivalent of light	$0.00154$ watt · lumen <sup>-1</sup>
velocity of a 1-volt electron	$5.932 \cdot 10^6$ meter · sec <sup>-1</sup>
radius of curvature of path of 1-volt electron in a magnetic field with an induction of 1 weber/meter <sup>2</sup> normal to it	$3.3715 \cdot 10^{-6}$ meter
frequency of rotation of electron in a magnetic field with a flux density of 1 weber/meter <sup>2</sup>	$2.8003 \cdot 10^{10}$ sec <sup>-1</sup>
de Broglie wave length of a 1-volt electron	$12.262 \cdot 10^{-10}$ meter

TABLE A5. RELATIVE LUMINOSITY FACTORS

(From Report of the Committee on Nomenclature and Standards of the Illuminating Engineering Society, *Illuminating Engineering*, Vol. 36, pp. 813-848, 1941.)

<i>Wave Length, A.U.</i>	<i>Relative Luminosity</i>	<i>Wave Length, A.U.</i>	<i>Relative Luminosity</i>	<i>Wave Length, A.U.</i>	<i>Relative Luminosity</i>
3800	0.00004	5100	0.503	6400	0.175
3900	0.00012	5200	0.710	6500	0.107
4000	0.0004	5300	0.862	6600	0.061
4100	0.0012	5400	0.954	6700	0.032
4200	0.0040	5500	0.995	6800	0.017
4300	0.0116	5600	0.995	6900	0.0082
4400	0.023	5700	0.952	7000	0.0041
4500	0.038	5800	0.870	7100	0.0021
4600	0.060	5900	0.757	7200	0.00105
4700	0.091	6000	0.631	7300	0.00052
4800	0.139	6100	0.503	7400	0.00025
4900	0.208	6200	0.381	7500	0.00012
5000	0.323	6300	0.265	7600	0.00006

## AUTHOR INDEX

- Abbott, T. A., 71  
 Adams, W. G., 201  
 Alberti, E., 7  
 Alexander, E. H., 444  
 Allen, J. S., 150  
 Alpern, D. K., 196  
 Altman, F. E., 334  
 Anderson, C. D., 12  
 von Ardenne, M., 313  
 Arfvedson, J. A., 82  
 Arkadiewa, A. Glagolewa, 13  
 Artzt, M., 352  
 Asao, S., 49, 50, 51, 52  
 Assett, G., 424
- Bacher, R. F., 122  
 Back, E., 12  
 Ballard, R. C., 377  
 Balsley, J. R., 452  
 Bardeen, J., 200  
 Barnes, B. T., 285  
 Barnes, R. B., 25  
 Barnett, G. F., 281  
 Batsel, C. N., 328  
 Bay, Z., 150  
 von Bayer, O., 13  
 Beams, J. W., 113  
 Becker, J. A., 37  
 Becquerel, E., 1, 2, 196  
 Beese, N. C., 19, 411  
 Belar, H., 325  
 Bellinger, S. L., 421  
 Bendz, W. I., 427  
 Bennett, A. I., 317  
 Bentley, E. P., 300  
 Bergmann, L., 202  
 Berzelius, J. J., 175  
 Bethe, H. A., 12  
 Birge, R. T., 16, 17, 477  
 Björnstahl, Y., 270  
 Blau, M., 313
- de Boer, J. H., 41, 45, 46, 47, 52, 53, 137, 139, 155  
 Boettner, A., 308  
 Bohr, N., 30  
 Boltzmann, L., 14  
 Bose, J. G., 189  
 Bowen, I. S., 10  
 Brady, J. J., 39, 41, 105  
 Brewington, G. P., 308  
 Bricker, W. K., 73  
 Briggs, H. B., 39, 42  
 de Broglie, L., 161  
 Brown, E. M., 313  
 Brown, H., 256  
 Bruining, H., 137, 139  
 Brunner, A. J., 294  
 Bryan, F. R., 309  
 Buck, G. B., II, 274  
 Buckingham, W. D., 19, 20  
 Bunsen, R., 82  
 Burt, R. C., 89  
 Burton, J. A., 58  
 Busch, H., 157  
 Bush, G. L., 425
- Calbick, C. J., 162  
 Caldecourt, V. J., 307  
 Campbell, N. R., 78, 93, 126  
 Campbell, R. E., 455, 456  
 Carey, G. R., 350  
 Case, T. W., 52, 91, 184  
 Cashman, R. J., 30, 188, 189, 265, 267, 347, 407, 408  
 Chaney, N. K., 19  
 Charlton, E. E., 12  
 Chesley, F. G., 184, 186, 187  
 Cline, J. E., 313  
 Coblenz, W. W., 276  
 Cockrell, W. D., 437  
 Coleman, P. D., 299  
 Coltman, J. W., 316, 317

- Cook, E. D., 329  
Corcoran, J. P., 327  
Cosby, J. R., 297  
Cranberg, L., 460  
Crosswhite, H. M., 298, 300, 304, 310  
Cunningham, T. B., 324, 329  
Czerny, M., 25
- Davidson, J. C., 338  
Davisson, C. J., 162  
Davy, H., 82  
Day, R. E., 201  
Debye, P., 282  
Debye, P. P., 282  
Deibert, C. R., 19, 20  
Denmark, H. S., 184, 186, 187  
Dessauer, F., 12  
Dieke, G. H., 298, 300, 304, 310  
Dietert, H. W., 306  
Dimmick, G. L., 323, 325, 326, 327  
Disney, W., 333  
Dole, M., 312  
Downing, J. R., 78  
Drabkin, D. L., 305  
Drew, R. O., 345, 346  
Dreyfus, B., 313  
Drude, P., 25  
Duane, W., 12  
DuBridge, L. A., 256, 258  
Duffendack, O. S., 264  
Duhme, E., 198  
Dunmore, F. W., 450  
Dushman, S., 68, 77
- Ebert, H., 4  
Einstein, A., 26  
Eitel, W., 202  
Ekström, A., 368  
Elenbaas, W., 19  
Ellinger, P., 280  
Elster, J., 5, 6, 8, 9, 44, 92, 464  
Engstrom, R. W., 127, 147, 148, 150, 153, 261, 267  
Epstein, D. W., 172, 376, 377  
Essig, S., 72
- Fan, H. Y., 33  
Farnsworth, P. T., 150, 385 •  
Faulkner, C. W., 328  
Faustman, D. J., 426
- Finch, W. G. H., 365  
Fink, C. G., 196  
Fink, D. G., 402  
Fisher, J. R., 191  
Fleischer, R., 52, 202  
Fleischmann, R., 41  
Fletcher, M. H., 280  
Flory, L. E., 169, 259, 388, 416, 417, 418, 458  
Flügge, S., 470  
Fluke, J. M., 408, 409, 410, 411, 412, 413  
Fonda, G. R., 19, 22  
Foote, P. D., 122  
Forgue, S. V., 396  
Forrest, J. L., 344  
Forro, M., 90  
Forsythe, W. E., 18, 19, 271  
Foskett, L. W., 312  
Foster, N. B., 312  
Found, C. G., 77  
Fournier d'Albe, E. E., 456  
Fowle, F. E., 470  
Fowler, R. H., 28  
Frayne, J. G., 324, 329  
Fredendall, G. L., 377, 400  
Free, A. L., 281  
Frerichs, R., 193  
Fritts, C. E., 202
- Gaede, W., 67  
Garner, L. P., 73  
Garritty, W. E., 333  
Gehricke, E., 323  
Geiger, P. H., 197  
Geitel, H., 5, 6, 8, 9, 37, 44, 92, 464  
Glass, S. W., 19  
Glover, A. M., 342, 344  
Görisch, R., 342  
Goerlich, P., 52, 55, 56, 57, 58, 342  
Goodbar, I., 275  
Goodman, D., 12  
Goudsmit, S., 122  
Greenlee, L. E., 455, 456  
Grignon, L. D., 327  
Griner, A. M., 280  
Grondahl, L. O., 197  
Guthnick, P., 450
- Hale, C. F., 78  
Hall, J. A., 291

- Hallwachs, W., 4, 6, 8, 464  
Hamilton, W. R., 156  
Hamister, V. C., 19  
Hanna, C. R., 243, 324  
Hardy, A., 304  
Hardy, A. C., 302  
Harris, W. A., 252  
Harrison, G. R., 300  
Hasler, M. F., 306  
Hawkins, J. N. A., 333  
Haythorne, P. A., 294  
Hecht, S., 467  
Hegbar, H. R., 64, 73  
Helmkamp, R. F., 440  
Henry, D. E., 44, 99, 100, 101  
Hertz, H., 3, 4  
Hertzberg, G., 122  
Hewlett, C. W., 188  
Hickman, K. C. D., 70, 71  
Hickman, R. W., 248  
Hillier, J., 97, 108, 142, 146, 157, 158, 166,  
173, 249, 313, 369, 370  
von Hippel, A., 184, 186, 187  
Holden, H. C., 334  
Holden, M., 280  
Holst, G., 155  
Holweck, F., 67  
Hopkins, B. S., 83  
Hopshtein, N. M., 58  
Houser, P. H., 448  
Houskeeper, W. G., 63  
Houstoun, R. A., 302  
Hubing, G. F., 291  
Hunt, F. L., 12  
Hunt, F. V., 248  
Hunter, R. S., 277  
Hurd, Y. G., 275  
Hustrulid, A., 71  
Huxford, W. S., 30, 52, 126, 127  
  
Iams, H. E., 144, 166, 390, 391  
Ives, H. E., 25, 39, 42, 89, 103, 269  
  
Jamison, N. C., 30  
Jenkins, C. F., 367  
Johnson, J. B., 252  
Johnson, S. W., 345, 346  
Johnsrud, A. L., 103  
Judd, D. B., 284  
Jupe, J. H., 424, 429  
  
Kallmann, H., 317  
Karrer, E., 283  
Kell, R. D., 377, 403  
Kellogg, E. W., 323, 324, 325, 326, 333  
Kelly, M. J., 93  
Kennard, E. H., 14, 121  
Kersten, H., 280, 281  
Khlebnikov, N. S., 58  
Khorosh, D. M., 58  
Kingdon, K. H., 43  
Kingsbury, E. F., 269  
Kingslake, R., 275  
Kirchhoff, G., 82  
Klotz, I. M., 312  
Kluge, W., 48, 55, 167  
Knowles, D. D., 19  
Knowlton, A. E., 19  
Kollath, R., 105, 136  
Koller, L. R., 44, 47, 48, 93, 126  
Korff, S. A., 263  
Krawinkel, G., 418  
Krebs, R. P., 281  
Krizek, V., 172, 412, 414, 415, 418  
Kron, G. E., 450  
Kronjäger, W., 418  
Kruithof, A. A., 124, 128, 130  
Kunz, J., 88  
  
Laing, K. M., 424  
Lance, T. M. C., 457  
Lange, B., 197, 198, 202, 212, 219, 428  
Langmuir, I., 37, 68, 221  
Larson, C. C., 148  
Laurence, J., 278  
Lauster, F., 65  
Law, H. B., 393, 394, 396, 397  
Lawrence, E. O., 110, 113  
Lenard, P., 6, 8  
Liebhafsky, H. A., 302  
Linford, L. B., 110  
Little, E. P., 305  
Little, R. V., Jr., 399  
Livingston, M. S., 12  
Locher, G. L., 264  
Lockyer, N., 80  
Loh, H. Y., 304  
Loomis, F. J., 333  
Lowry, W. N., 197  
Luckiesh, M., 470  
Lucks, C. F., 292

- Lukirsky, P. I., 45  
 Lummer, O., 14, 16  
 Lynn, L. B., 243, 324  
  
 MacDonald, W. W., 431  
 MacKenzie, D., 323  
 Maloff, I. G., 377  
 Malter, L., 142  
 Marden, J. W., 19  
 Maron, W., 447  
 Marshall, C. E., 421  
 Marshall, F. H., 316, 317  
 Marx, E., 25  
 Mattauch, J., 470  
 McCuskey, S. W., 453  
 McIlwain, K., 352, 353, 357, 358, 359, 362, 363  
 McLeod, J. H., 334  
 McNickle, R. C., 435  
 Meister, G., 19  
 Mellen, G., 78  
 Mendenhall, E. E., 281  
 Merritt, E., 7  
 Metcalf, G. F., 254  
 Michaelson, J. L., 302  
 Michel, T. C., 318  
 Miller, W. C., 334  
 Millikan, R. A., 10, 28  
 Mitchell, K., 32, 105  
 Mohler, F. L., 122  
 Moon, P., 278  
 Moore, A. R., 342, 344  
 Moriarty, C. D., 318  
 Morin, E. R., 431  
 Morris, W. E., 264  
 Morton, G. A., 70, 108, 142, 146, 157, 158, 166, 168, 169, 170, 173, 240, 242, 249, 251, 259, 366, 369, 370, 388, 389, 390, 402, 416, 417, 418  
 Mott, N. F., 199  
 Mueller, G. E., 13  
 Musson-Genon, R., 158  
  
 Nahstoll, G. A., 309  
 Neddermeyer, S. H., 12  
 Nelson, R. B., 77  
 Nichols, E. F., 13  
 Nielsen, C. E., 255  
 Nier, A. O., 71  
 Nipkow, P., 366  
  
 Noel, E. B., 66  
 North, D. O., 252  
 Nyquist, H., 252  
  
 Olpin, A. R., 55, 89, 103  
 Orr, R. S., 283  
 Osgood, T. H., 12  
  
 Pagliarullo, V., 324, 329  
 Patai, E., 90  
 Pender, H., 352, 353, 357, 358, 359, 362, 363  
 Penning, F. M., 77  
 Pensak, L., 172, 376  
 Perkins, P., 281  
 Peterson, E. W., 307  
 Pfister, R. J., 299  
 Philpott, L. R., 365  
 Phyfe, J. D., 343  
 Pike, E. W., 140  
 Pirani, M. V., 78  
 Planck, M., 16  
 Platt, J. R., 408  
 Plymale, W. S., Jr., 304  
 Pohl, R., 32, 46  
 Porter, N. E., 408, 409, 410, 411, 412, 413  
 Powell, R. W., 294  
 Powers, R. A., 434  
 Prescott, C. H., Jr., 93  
 Pringsheim, E., 14, 16  
 Pringsheim, P., 32, 46  
  
 Rajchman, J. A., 145, 259  
 Ramadanoff, D., 54  
 Ramberg, E. G., 108, 142, 146, 157, 158, 166, 168, 170, 173, 249, 369, 370  
 Ramsay, W., 80  
 Rank, D. H., 299  
 Rayleigh, Lord, 16, 80  
 Rechou, G., 12  
 Redemske, R. F., 446  
 Reimann, A. L., 27, 30, 149  
 Reimert, L. J., 54  
 Reiskind, H. I., 333  
 Rentschler, H. C., 44, 99, 100, 101, 276  
 Reynolds, E. W., 333  
 Rich, T. A., 318  
 Richtmyer, F. K., 14  
 Righi, A., 4

- Rijanoff, S., 44, 45  
Ritchie, D., 126  
Rittner, E. S., 184, 186, 187, 231  
Roberts, W. O., 451, 452, 453  
Roberts, W. von B., 294  
Robins, J., 295, 296, 297  
Rogowski, W., 19  
Rose, A., 172, 391, 393, 394, 396, 397  
Rubens, H., 13  
Ruedy, J. E., 97, 140  
Rühlemann, E., 19  
Ruhmer, E., 323  
Russell, H. W., 292  
Rutherford, E., 30  
  
Salinger, H., 148  
Salow, H., 418  
Salzberg, B., 144  
Saunderson, J. L., 307  
Schaffernicht, W., 167  
Schlesinger, K., 400  
Schottky, W., 198, 199, 200  
Schroeder, A. C., 288, 377, 400  
Schubin, S., 32  
Scott, R. M., 453  
Seiler, E. F., 34, 88  
Sheftel, M. S., 280  
Siemens, W., 202  
Simon, H., 450  
Slater, J. C., 178  
Smith, H. M., 314  
Smith, K. O., 99, 101  
Smith, P. T., 64, 73  
Smith, W., 2, 175  
Snyder, R. L., 259, 313  
Sommer, A., 58  
Stair, R., 276  
Staley, K. A., 275  
Stefan, J., 14  
Stevens, C. M., 71  
Stewart, O. M., 7  
Stoletow, A., 5  
Strömgren, B., 450  
Strömgren, E., 450  
Suhrmann, R., 39, 44, 450  
Suzuki, M., 49  
Sweet, M. H., 286, 288, 289, 292  
Sziklai, G. C., 288, 377, 403  
  
Taylor, J. B., 37  
Taylor, S. G., 246  
Teal, G. K., 191  
Tear, J. D., 13  
Teichmann, H., 202  
Temple, T., 446  
Teves, M. C., 45, 46, 47, 53, 155  
Theissing, H., 39, 44  
Thompson, B. J., 252, 254  
Thomson, J. J., 6, 30  
Travers, M. W., 80  
Treptow, A. W., 191  
Tumlirz, O., 25  
Turnbull, L. G., 292  
Tytell, A. A., 280, 281  
  
Ulin, P. B., 184, 186, 187  
Uttal, J. A., 247  
Uyterhoeven, W., 19, 21, 22  
  
Valentine, R. D., 424  
Vance, A., 108, 142, 146, 157, 158, 166,  
173, 228, 249, 369, 370  
Vand, V., 172, 412, 414, 415, 418  
Varden, L. E., 295, 296, 297  
Veenemans, C. F., 155  
Vermeulen, R., 326  
De Vries, H., 467  
  
Walker, D. S., 440  
Walker, R. C., 457  
Way, K. J., 247  
Webb, R. C., 383  
Weimer, P. K., 393, 394, 396, 397  
Weiss, G., 144  
Weisz, P. B., 264, 429  
Wendt, K. R., 377  
Westendorp, W. F., 12  
Westmijze, W. K., 338  
Wey, R. J., 424  
Wheatcroft, E. L., 130  
White, C. E., 280  
Whitford, A. E., 450, 454  
Wiedemann, E., 4  
Wien, W., 16  
Wilson, E. D., 90, 464  
Wilson, J. L., 281  
Wing, A. K., 77  
Winters, S. R., 450  
Wood, L. A., 209



Worthing, A. G., 18

Young, A. H., 19, 22

Zeluff, V., 439, 445

Zworykin, V. K., 70, 90, 96, 108, 140, 142,  
145, 146, 157, 158, 166, 168, 169, 170,  
173, 240, 242, 243, 249, 251, 303, 313,  
324, 366, 369, 370, 374, 375, 386, 388,  
389, 390, 402, 405, 417, 451, 458, 464

## SUBJECT INDEX

- Absolute temperature, 14
- Accelerating-field tube, 155
- Acceptor level, 179
- Acorn tube, 255
- Adsorption, 38
- Aeolight, 323
- Alkali metals, 32, 82
  - absorption of light, 42
  - by chemical reaction, 92
  - introduction, 88
  - layer thickness, 40
  - on metal base, 37
  - on platinum-iridium, 42
  - on quartz, 41
- Alkaline earth metals, 32
- Alloy analysis, 307
- Alloy surfaces, 55
- Alpha particles, measurement, 313
- Alphatron, 78
- Alternating currents, 236
- Amperite tube, 246
- Amplifier, direct-coupled, 227
  - feedback, 227
  - narrow-band, 242
  - wide-band, 239
- Analysis, gas, 312
  - liquids, 313
  - spectrochemical, 306
- Angstrom unit, 10
- Angular distribution, photoelectrons, 103
- Antimony alloys, 98
- Antimony-cesium, 55, 114
  - preparation, 96
  - secondary emission, 137
- Aperture, focal length, 162
- Aperture distortion, 354
- Argon, 80
- Aspect ratio, 365
- Astronomy, 450
- Atomic structure, 30
- Back-wall cell, 198
- Baking, 71
- Ballast tube, 246
- Barium, work function, 30
- Barium phototube, 91
- Barium-strontium oxide, 52
- Barrier-layer cell, 197
  - electron bombardment, 313
  - theory, 199
- Battery, photoelectric, 5
- Bauer valve, 81
- Beam tube, 227
- Bean sorter, 441
- Becquerel effect, 196
- Betatron, 12
- Beverage inspection, 442
- Bioluminescence, 280
- Bismuth-cesium, 55
- Black-body radiation, 14
- Blind aids, 456
- Blocking condenser, 240
- Boltzmann's constant, 16, 120, 477
- Box-type multiplier, 146
- Bridge, selenium, 176
- Brightness, light sources, 19
- Brightness amplification, 172, 468
- Brightness temperature, 17
- Bumping, 69
- Cadmium sulfide cell, 193
- Calcium, work function, 30
- Cameras, television, 398
- Candle, 19, 24
- Candlepower, 24
- Capacity, phototubes, 116, 118, 152
- Carbon arc, 17, 19
- Carrier, 239
- Cat's eye button, 275
- Cathode follower, 229
- Cathode-ray tube, 369
- Ceilometer, 448
- Cesium, 82
  - on calcium fluoride, 45

- Cesium, on cesium oxide, 46  
  on tungsten, 37  
  trinatriide, 91  
  vapor lamp, 20, 411  
  work function, 30
- Cesium-antimony, 55, 114
- Cesium-bismuth, 55, 114
- Cesium-magnesium phototube, 90, 114
- Chopper, light, 242
- Circuits, photocell, 216
- Circular multiplier, 146, 152
- Clock control, 424
- Cloud heights, 448
- Color analyzer, 302
- Color coordinates, 284
- Color densitometer, 286
- Color facsimile, 363
- Color film, 343
- Color sensitivity, *see* Spectral response
- Color television, 377, 403
- Color temperature, 17, 272
- Colorimetry, 283
- Concentrated-arc lamp, 19, 20
- Condensation pump, 68
- Conduction, mechanism, 177
- Contact potential, 30
- Conversion factors, 474
- Copper oxide phototube, 8
- Copying, facsimile, 363
- Corex, 63, 65, 100
- Corning 9741, 63, 100
- Corona photography, 451
- Corpuscular radiation, measurement, 313
- Cosine distribution, 103
- Cosmic rays, 12
- Counter, electron multiplier, 263, 316  
  gas-discharge, 263
- Crossed fields, motion in, 107
- Crossover, 371
- Cuprous oxide cell, preparation, 199  
  sensitivity, 201  
  spectral response, 199  
  theory, 199
- Current-light flux relation, gas photo-  
  tube, 126  
  lead sulfide cell, 189  
  selenium barrier-layer cell, 207-209  
  selenium cell, 184  
  thallous sulfide cell, 186  
  vacuum phototube, 112
- Current range, phototubes, 116, 132
- Current regulation, 246
- Current-voltage relation, effect of geom-  
  etry, 111  
  gas phototubes, 125, 132  
  vacuum phototubes, 108
- Cycloidal paths, 107
- Dark current, multiplier phototube, 148
- Deflection, 369
- Detection, fire, 429  
  flaws, 443  
  hot bodies, 414  
  infrared signals, 412  
  intrusion, 431  
  smoke, 430
- Detergency measurement, 281
- Dichroic films, 327, 377, 404
- Dielectric constant, effect of light, 414
- Diode, 221
- Diode detection, 245
- Discriminator, 357
- Disk of confusion, 156
- Donor level, 179
- Door opener, 427
- Dumet, 63, 65
- Dye tracks, 342
- Dynamic multiplier, 150
- Dynamic response, barrier-layer cell, 211  
  gas phototube, 127, 133, 344  
  selenium photoconductive cell, 183  
  silicon cell, 192  
  thallous sulfide cell, 186  
  vacuum phototube, 113
- Dynode, 142
- Efficiency, light sources, 19  
  power conversion, 209, 469  
  quantum, 465
- Einstein's equation, 25
- Electric double layer, 39
- Electric fields, motion in, 105
- Electrical units, 475
- Electrolysis through glass, 89
- Electrometer, 253
- Electrometer tube, 254
- Electrometer tube circuits, 256
- Electron, 6
- Electron gun, 370
- Electron index of refraction, 156, 157

- Electron lenses, 157, 162
- Electron optics, 156
- Electron path, 158
- Electron wave length, 161
- Electrostatic lenses, 157
- Electrostatic multiplier, 144
- Elements, 473
- Emissive power, 14
- Emissivity, spectral, 17
- Energy bands, 177
- Energy distribution, photoelectrons, 103
  - secondary electrons, 136
- Equipotential surfaces, 157
- Evaporation of metals on photocathodes, 49
- Exposure control, 295, 297
  - x-rays, 317
- Exposure meter, 292
  - for enlargements, 294
  - metallographic, 294
- Extensometer, 445
- Eye, sensitivity, 25, 466
- Facsimile, 349
  - color, 363
  - copying, 363
  - frequency band, 354
  - recorders, 357
  - scanners, 352
  - synchronization, 361
  - tape, 362
  - transmission, 354
- Fading box, 338
- Fantasound, 333
- Fatigue, barrier-layer cell, 212
  - photoelectric, 53
  - secondary emission, 141
- Feedback, inverse, 227
  - regenerative, 244
- Fernico, 64, 65
- Film transmission, 399
- Fire detector, 429
- Flame-cutter control, 440
- Flame-failure detector, 433
- Flicker, 252
- Fluorescent lamps, 19, 23
  - delay meter, 446
  - photometry, 274
- Fluorimetry, 280
- Flying-spot microscope, 381
- Flying-spot scanning, 368
- Flying-spot tube, 374
- Focal length, aperture, 162
  - electrostatic lens, 160
  - magnetic lens, 163
- Focal point, 160
- Food sorter, 441
- Fourier integral, 238
- Fourier series, 237
- Francium, 470
- Frequency band, facsimile, 354
  - television, 365
- Frequency modulation, 355
- Frequency response, gas phototube, 127
  - selenium photoconductive cell, 183
  - sound-reproduction system, 342
  - thallous sulfide cell, 186
  - vacuum phototube, 113
- Frequency spectrum, 238
- Front-wall cell, 198
- Gage, photoelectric, 443
- Galvanometer amplifier, 425
- Gamma rays, 12
- Gas amplification, 120, 131
- Gas analysis, 312
- Gas discharge counter, 263
- Gas dosage, 80
- Gas flame, 19
- Gas ionization, 122
- Gas mantle, 19, 22
- Gas phototube, 120
  - phase delay, 130
  - properties, 132
- Gas regulator tube, 247
- Gas tube, 233
- Gaseous sources, 19, 20
  - photometry, 274
- Geiger-Mueller counter, 263
- General Electric light-sensitive cell, 203, 212, 274
- Getters, 68, 141
- Glass-to-metal seals, 63
- Glasses, annealing point, 65
  - coefficient of expansion, 65
  - softening point, 65
  - transmission in ultraviolet, 99
- Gloss, 277
- Goniophotometer, 278
- Grid, vacuum tube, 222

- Grid-glow tube, 235
- Guidance device, 460
- Gun, electron, 370
- Hall effect, 180
- Hallwachs effect, 4
- Harmonics, 237
- Hefner lamp, 19, 24, 25
- Helium, 31, 79
- Hole conduction, 180
- Hololumen, 189
- Hot bodies, detection, 414
- House vacuum, 67
- Hydrogen, 31
  - firing, 66
  - introduction, 81
  - sensitizing, 92
- ICI standard observer, 284
- Iconoscope, 386
  - infrared, 418
- Illumination control, 421
- Illuminometer, 274
- Image dissector, 385
- Image iconoscope, 390
- Image multiplier or intensifier, 172, 468
- Image orthicon, 393
- Image tube, 155
  - accelerating-field tube, 155
  - cylindrical field, 173
  - disk of confusion, 156, 165, 167
  - infrared-sensitive, 171, 415
  - long magnetic field, 164
  - magnification, 167
  - multiple, 172
  - power supply, 416
  - short lens, 166
- Impurities, lattice, 179
- Incandescent lamps, 19
- Index of cooperation, 352
- Index of refraction, electron, 156, 157
- Industrial control, 434
- Industrial television, 403
- Infrared filters, 409
- Infrared iconoscope, 418
- Infrared radiation, 13
  - transmission by atmosphere, 407
- Infrared sources, 408
- Initial velocities, photoelectrons, 103
  - secondary electrons, 136
- Initial velocities, thermionic electrons, 221
- Inspection, automatic, 441
- Insulators, 179
- Integrating sphere, 271
- Interlaced scanning, 371
- Intrusion detection, 431
- Inverse feedback, 227
- Ion feedback, multiplier phototube, 148
- Ionization gage, 76
- Ionization in gases, 122
- Isotope, 31
- Johnson noise, 252
- Kerr cell, 243, 323
- Kinescope, 375
- Kinetic theory, 120
- Kovar, 64, 65
- Krypton, 80
- Lead glass, 62, 65
- Lead sulfide cell, 189
- Leak testing, 71, 76
- Leakage, electric, 87
  - multiplier phototube, 148
- Lenses, electrostatic, 157
  - magnetic, 162
- Light curtain, 434
- Light meter, portable, 275
- Light relay, 424
- Light sources, brightness, 19
  - efficiency, 19
  - measurement, 270
- Light valve, 324
- Lime glass, 62, 65
- Liquids, analysis, 313
- Lithium, 31, 82
  - introduction, 88
  - work function, 30
- Load line, 223
- Logarithmic meter, 286
- Lumen, 24
- Luminance, 293, 477
- Luminescent sources, 22
- Luminosity factor, 478
- Lux, 24
- Luxtron cell, 203, 209
- MKS system, 474
- Magnesium, work function, 30

- Magnetic field, motion in, 105  
Magnetic lenses, 162  
Magnetic multiplier, 142  
Magnetic regulator, 246  
Magnetic resistance, 164  
Map tracer, 426  
Materials for phototubes, 62  
McLeod gage, 74  
Mean free path, 121  
Mean square deviation, 250  
Mechanical equivalent of light, least, 25, 477  
Mechanical television, 366  
Mechanical units, 474  
Mercury arc lamp, 19, 20  
Mercury manometer, 74  
Metal industry, 439  
Metal tubes, 73  
Metals, coefficient of expansion, 65  
    melting point, 65  
    pretreatment, 66  
    vacuum firing, 67  
Meters, current, 217  
    vacuum-tube, 228  
Microphonic noise, 253  
Microphotometer, 298  
Microscope, electric, 405  
    flying-spot, 381  
    infrared, 417  
    scanning, 313  
Mirror image tube, 418  
Modulation, 239  
Molecular radii, 121  
Molecular-weight determination, 282  
Molybdenum-caesium phototube, 96  
Monatomic layer, 38  
Mosaic, 386  
Multiple image tube, 172  
Multiplier phototube, 136  
    beam spreading, 143  
    box-type, 146  
    circuits, 259  
    circular, 146  
    commercial, 152  
    cooling, 149  
    current-voltage relation, 153  
    dark current, 148  
    dynamic, 150  
    electrostatic, 144  
    for particle counting, 150, 316  
Multiplier phototube, for x-rays, 150, 314  
    gain, 152  
    magnetic, 142  
    measurement of low light level, 261  
    noise, 258  
    partition, 146  
    pinwheel, 375  
    power supplies, 260, 309  
    radiation detector, 316  
    screen-type, 144  
    single-stage, 144  
Neon, 80  
Neon lamp, 19, 20  
Neutron, 31  
Neutron detection, 316  
Night photography, aerial, 424  
Nipkow disk, 367  
Noise, 250  
    multiplier phototube, 258  
    photoconductive cell, 265  
    signal equivalent, 267  
Noise resistance, 252  
Odograph, 426  
Optophone, 457  
Organ, photoelectric, 455  
Orthicon, 391  
Outgassing, 67, 73  
Oxygen, adsorbed, 43  
    introduction, 81  
Packaging machine, 437  
Paville color printing, 295  
Pentane lamp, 19, 24  
Pentode, 225  
Penumbra recording, 326  
Periodic table, 474  
Phase delay, 130  
Philips gage, 77  
Phosphors, 22  
Photoconductive cells, 175, 469  
    cadmium sulfide, 193  
    lead sulfide, 189  
    noise, 265  
    selenium, 176, 181  
    silicon, 191  
    thallous sulfide, 184  
    vacuum-tube circuits, 231  
Photoconductive effect, 2, 180

- Photoeffect, normal, 42  
  selective, 39, 41, 42  
  surface, 33  
  volume, 33
- Photoelectric carrier, 6
- Photoelectric counter, 263
- Photoelectric organ, 455
- Photoelements, 196
- Photoemissive effect, 3, 25
- Photolight, high-speed, 421
- Photometric measurements, 23
- Photometric units, 476
- Photometry, 269
- Photomultiplier, *see* Multiplier photo-  
  tube
- Photon, 16
- Photosensitive surfaces, [Ag]-Cs<sub>2</sub>O-Cs, 47  
  [Ag]-Cs<sub>2</sub>O, Ag-Cs, 48, 114  
  [Ag]-K<sub>2</sub>O, Ag-K, 48  
  [Ag]-Na<sub>2</sub>O, Ag-Na, 48  
  [Ag]-O-Cs, 43  
  [Ag]-Rb<sub>2</sub>O, Ag-Rb, 48, 114  
  alloys, 55  
  barium-strontium oxide, 52  
  Bi, Cs, 55, 57, 114  
  Bi, K, 57  
  Bi, Li, 57  
  Bi, Na, 57  
  Bi, Rb, 57  
  Cs<sub>3</sub>Sb, 58, 114  
  dyes, effect on, 55  
  evaporation of metal, 49  
  K-KH-K, 45  
  K-K<sub>2</sub>O-K, 47  
  K-K<sub>2</sub>S-K, 55  
  K-K<sub>2</sub>Se-K, 55  
  K-K<sub>2</sub>Te-K, 55  
  Na-Na<sub>2</sub>S-Na, 55  
  Sb, Cs, 57, 114  
  Sb, K, 57  
  Sb, Li, 57  
  Sb, Na, 57  
  Sb, Rb, 57  
  sodium distilled in air, 54
- Phototube monitoring, 327
- Phototubes, alkali, 5  
  barium, 91  
  capacity, 116, 118, 152  
  central cathode, 86  
  cesium-magnesium, 90, 114
- Phototubes, commercial, 116, 118, 132,  
  152  
  copper oxide, 8  
  gas-filled, 120  
  geometry, 85, 116, 132  
  manufacturers, 116  
  materials, 62  
  maximum current, 116, 132, 152  
  molybdenum-cesium, 96  
  operating temperature, 118, 134  
  operating voltage, 116, 118, 132, 152  
  potassium hydride, 8, 44  
  preparation, 85  
  pure metal, 100, 118  
  sensitivity, 116, 118, 132, 153  
  silver-cesium oxide-cesium, 46, 93, 114  
  sodium, 101, 114  
  sodium amalgam, 5  
  strontium, 91  
  transparent cathode, 87, 95, 96  
  ultraviolet, 99, 114, 118, 153, 276  
  vacuum, 103  
  zinc amalgam, 8  
  zirconium, 276
- Photovision, 419
- Photovoltaic cells, 196  
  vacuum tube circuits, 231
- Photovoltaic effect, 1, 196
- Photronic cell, 202, 203, 204, 205, 206,  
  207, 208, 210, 213, 214, 231, 233
- Physical constants, 477
- Pickup, 351
- Pickup cameras, 398
- Picture element, 349
- Pinwheel multiplier, 375
- Pirani gage, 78
- Piston ring checker, 445
- Planck's constant, 16
- Plasma, 234
- Plate, vacuum tube, 222
- Plate characteristics, 224, 226
- Polarization, 39
- Potassium, 82  
  on platinum, 39  
  work function, 30
- Potassium hydride, 44, 93
- Potassium hydride phototube, 8, 44  
  preparation, 92
- Power conversion, barrier-layer cell, 209,  
  469

- Power supplies, image tube, 416
  - multiplier phototube, 260, 309
  - stabilized, 246
- Pressure, measurement of low, 74
- Pressweld, 63
- Principal plane, 160
- Projection kinescope, 376
- Projection receiver, 377
- Proton, 31
- Push-pull sound track, 325
- Pyrex, 62, 65
- Pyrometers, 291
- Q*, 244
- Quantum, 16
- Quantum efficiency, 465
- Quartz seals, 65
- r*-unit, 315
- R-F power measurement, 447
- Radiation, black-body, 14
  - infrared, 13
  - sources, 13, 19
  - spectrum, 10
  - ultraviolet, 10
- Radiation detector, photomultiplier, 316
- Radio waves, 13
- Railroad signals, 428
- Ray tracing, 158
- Rayleigh's formula, 16
- Reading machine, 456
- Receiver, television, 376
- Recorder, carbon paper, 359
  - electrolytic, 358
  - photographic, 357
- Rectifier, cuprous oxide, 197
  - vacuum tube, 222
- Redistribution, 389
- Reflectance, diffuse, 279
  - specular, 278
- Reflectometer, 277
- Refractive index, electron, 156, 157
- Refractometer, 283
- Refrigerants, 72
- Regenerative feedback, 244
- Regulation, 246
- Relay circuits, 230, 235
- Relays, 219
- Rerecording, 329
- Roentgen (unit), 315
- Rotameter, 435
- Rotary stabilizer, 333
- Rotation by magnetic field, 163
- Rubidium, 82
  - work function, 30
- Safety devices, 429
- Sawtooth wave, 371
- Scanners, facsimile, 352
- Scanning, 351
- Scanning microscope, 313
- Schmidt telescope, 415
- Schottky effect, 110
- Screen grid, 225
- Screen-type multiplier, 145
- Secondary currents, 181
- Secondary emission, 136
  - antimony-cesium, 137
  - dependence on angle, 137
  - dependence on voltage, 137
  - energy distribution, 136
  - mechanism, 139
  - noise, 251
  - silver-cesium oxide-cesium, 137
  - silver-magnesium, 140
- Secondary emission multiplier, *see* Multiplier phototube
- Secondary emitters, preparation, 140
- Selective effect, 39, 41, 42
- Selenium, 175
- Selenium barrier-layer cell, 201
  - capacity, 204
  - commercial, 214
  - current sensitivity, 207-209
  - dynamic response, 211
  - fatigue, 212
  - internal resistance, 205
  - power conversion, 209
  - spectral response, 202
  - temperature effect, 213
  - voltage sensitivity, 206
- Selenium photoconductive cell, 176, 180
  - spectral response, 182
- Semiconductors, impurity, 179
  - intrinsic, 180
- Sensitivity, cuprous oxide cell, 201
  - eye, 25, 466
  - gas phototubes, 132, 268
  - image orthicon, 397
  - lead sulfide cell, 266



- Sensitivity, multiplier phototubes, 266  
  relative, of photocells, 218  
  selenium barrier-layer cell, 206-209  
  selenium photoconductive cell, 182  
  thallous sulfide cell, 187  
  vacuum phototubes, 116, 466
- Sensitivity standard, 114
- Sensitization, argon, 94  
  evaporated metal, 49  
  hydrogen, 92
- Sensitrol relay, 219
- Sequential scanning, 351
- Shading signals, 389
- Sheen, 278
- Shot noise, 250
- Shutter tester, 446
- Side register control, 437
- Signal plate, 387
- Signaling, detection, 412  
  light sources, 408
- Silicon cell, 191
- Silver-magnesium, secondary emission,  
  140
- Smoke detector, 430
- Smoke recorder, 435
- Snell's law, 158
- Sniperscope, 417
- Snooperscope, 417
- Sodium, 82  
  distilled in air, 54  
  phototube, 101, 114  
  vapor lamp, 19, 22  
  work function, 30
- Sodium-amalgam phototube, 5
- Solenoid, field of, 163
- Sound recording, 323
- Sound reproduction, 334
- Sound reproduction system, frequency  
  response, 342
- Sound track, on projected film, 331  
  variable-area, 324  
  variable-density, 324
- Space charge, 105
- Space-charge grid, 255
- Space-charge limitation, 222
- Spectral response, 32
- Spectral response of photoconductive  
  cells, cadmium sulfide, 194  
  lead sulfide, 189  
  selenium, 183
- Spectral response of photoconductive  
  cells, silicon, 192  
  thallous sulfide, 187
- Spectral response of phototubes, [Ag]-  
   $\text{Cs}_2\text{O}$ , Ag-Cs, 48, 94, 102, 115  
  [Ag]- $\text{Cs}_2\text{O}$ , Ag, Cs-Cs, 50  
  [Ag]- $\text{Cs}_2\text{O}$ -Cs, 47  
  [Ag]- $\text{K}_2\text{O}$ , Ag-K, 48  
  [Ag]- $\text{Na}_2\text{O}$ , Ag-Na, 48  
  [Ag]-O-Cs, 43  
  [Ag]- $\text{Rb}_2\text{O}$ , Ag-Rb, 48, 115  
  alkali films on Pt-Ir, 41  
  alkali metals, 34  
  antimony-alkali metal, 57  
  antimony-cesium, 59, 98, 115  
  barium, 91  
  barium-strontium oxide, 51  
  bismuth-alkali metal, 57  
  bismuth-cesium, 57, 115  
  bismuth-cesium and [Ag]- $\text{Cs}_2\text{O}$ , Ag-Cs,  
    59  
  cadmium, 100  
  cesium-magnesium, 115  
  platinum, 119  
  potassium, 45  
  potassium hydride, 45, 56  
  potassium on platinum, 40  
  potassium sulfur, 56  
  S-1, S-3, S-4, S-5 (absolute values), 467  
  S-1, S-3, S-4, S-5, S-6, S-8, 115  
  S-1, S-4, for 2870° K light, 343  
  sodium, 115  
  sodium, distilled in air, 54  
  sodium-potassium alloy, 33  
  sodium-sulfur, 56  
  strontium, 91  
  tantalum, 119  
  thorium, 119  
  titanium, 100  
  uranium, 100  
  zinc, 100  
  zirconium, 100, 119
- Spectral response of photovoltaic cells,  
  cuprous oxide, 199  
  selenium, 203, 204
- Spectral response standard, 114
- Spectral selective effect, 39, 41, 42
- Spectrochemical analysis, 306
- Spectrophotometry, absorption, 299  
  exposure control, 297

- Spectrophotometry, luminescent materials, 303  
    recording, 298, 303  
    ultraviolet, 305  
Spectroscopy, electronic, 288  
Sperrschicht, 198  
Standard lamps, 24  
Star counter, 453  
Star-image stabilizer, 451  
Star-size determination, 454  
Stefan-Boltzmann constant, 14, 477  
Stoletow's law, 124  
Storage effect, 387  
Stroke, 353  
Strontium phototube, 91  
Subcarrier, 355  
Sunswitch, 421  
Superemitron, 390  
Supplementation of electrons, 53  
Suppressor grid, 225  
Surface photoeffect, 33  
Surface state, 200  
Synchronization, facsimile, 361  
    television, 401  
  
Tape facsimile, 362  
Telectroscope, 451  
Teledeltos, 358  
Telescope, infrared, 415  
Telescope drive, 450  
Television, 349  
    camera tubes, 385  
    cameras, 398  
    color, 377, 403  
    complete system, 400  
    electronic, 369, 385  
    film transmission, 399  
    industrial, 403  
    mechanical, 366  
    requirements, 365  
    viewing tubes, 375  
Temperature, effect on barrier-layer cells, 212  
    light sources, 19  
Temperature range, phototubes, 118, 134  
Test box, 274  
Tetrode, 225  
    gas, 235  
Textile applications, 438, 444  
Thallous sulfide cell, 184  
  
Thalofide cell, 184  
Thermal noise, 252  
Thermal sources, 13, 17, 19  
Thermionic emission, 220  
    initial velocities, 221  
    multiplier phototube, 148  
Thermocouple gage, 75  
Thickness gage, 443  
Threshold frequency, 28  
Threshold wave length, 28  
    for pure metals, 99  
Thyratron, 233  
Torching, 73  
Traffic control, 427  
Traffic counter, 429  
Transconductance, 224  
Transit time, 113  
Transmission, simultaneous, 350  
Transmitting typewriter, 425  
Triode, 222  
    gas, 234  
Tube noise, 252  
Tungsten, spectral emissivity, 18  
Turbidity comparator, 281  
  
Ultrafax, 378  
Ultraviolet radiation, 10  
    measurement, 276  
    phototubes, 99, 114, 118  
    recording, 326  
Unipotential lens, 161  
Units, 474  
  
Vacuum, production of high, 71  
Vacuum phototube, 103  
    properties, 116, 118  
Vacuum pumps, 67  
Vacuum tube, thermionic, 220  
Vacuum-tube regulator, 248  
Variable-area sound track, 324  
Variable-density sound track, 324  
Velocity distribution, photoelectrons, 103  
    secondary electrons, 136  
    thermionic electrons, 221  
Vernon-Harcourt pentane lamp, 24  
Vickers self-generating cell, 203, 211  
Viewing tube, 375  
Visagraph, 457  
Viscor filter, 202  
Vision, enhancement of, 466

- Visual correction filter, 202
- Visual sensitivity curve, 23, 204, 478
- Voltage amplification, 222
- Voltage range, phototubes, 116, 118, 132, 153
- Voltage regulation, 246
- Volume photoeffect, 33
  
- Water vapor, absorption, 407
  - in atmosphere, 310
- Wave length, electron, 161
- Weft straightening, 438
- Wet cells, 196
- Width gage, 444
- Wien's displacement law, 16
- Wien's formula, 16
  
- Work function, 28
  - pure metals, 30, 99
  
- X-rays, 12
  - absorption photometer, 318
  - detection, cadmium sulfide cell, 195
  - detection, multiplier phototube, 150, 314
  - inspection, 315
  - intensity measurement, 314
  - phototimer, 317
- Xenon, 80
  
- Zinc-amalgam phototube, 8
- Zinc sulfide, efficiency, 19
- Zirconium phototube, 118, 276





**For Reference  
Only.**